Friedrich-Schiller-Universität Jena

Chemisch-Geowissenschaftliche Fakultät

Poly(2-oxazoline)s and their derivatives:

A versatile polymer class with manifold application possibilities

Dissertation

(kumulativ)

zur Erlangung des akademischen Grades

doctor rerum naturalium (Dr. rer. nat.)

vorgelegt dem Rat der Chemisch-Geowissenschaftlichen Fakultät

der Friedrich-Schiller-Universität Jena

von Diplom-Chemiker Lutz Tauhardt

geboren am 10.07.1984 in Naumburg/Saale

Gutachter:

1. Prof. Dr. Ulrich S. Schubert, Friedrich-Schiller-Universität Jena
2. Prof. Dr. Dagmar Fischer, Friedrich-Schiller-Universität Jena

Tag der öffentlichen Verteidigung: 19.11.2014

Table of contents

Documentation of authorship 3

1. Introduction 11

2. Poly(2-oxazoline) modified surfaces – Attachment methods and applications 15

3. Poly(2-oxazoline)s as coating material for antifouling applications 19

4. Poly(2-oxazoline)s in systemic applications 23

   4.1. Poly(2-oxazoline)s as poly(ethylene glycol) alternative 23

   4.2. Zwitterionic poly(2-oxazoline)s 27

   4.3. Poly(2-oxazoline)s as potential anticancer drugs 31

5. Poly(2-oxazoline)-based cationic polymers for gene delivery 37

   5.1. Linear poly(ethylene imine)s and approaches to reduce their cytotoxicity 38

   5.2. Cationic poly(2-oxazoline)s 45

   5.3. High-throughput screening of pharmaceutical properties of cationic polymers 50

   5.4. Characterization of cationic polymers 51

   5.5. LPEI hydrogels for DNA capture and release 53

6. Summary 56

7. Zusammenfassung 60

8. References 64

List of abbreviations 70

Curriculum vitae 72

Publication list 73

Acknowledgements / Danksagung 77

Declaration of authorship / Selbstständigkeitserklärung 80

Publications P1-P13 81

Documentation of authorship

This section contains a list of individual authors' contributions to the publications reprinted in this thesis.

P1) "Poly(2-oxazoline) functionalized surfaces: From modification to application" L. Tauhardt,[1] K. Kempe,[2] M. Gottschaldt,[3] U. S. Schubert,[4] *Chem. Soc. Rev.* **2013**, *42*, 7998-8011.				
Autor	1	2	3	4
Conception of the manuscript	X			
Preparation of the manuscript	X			
Correction of the manuscript		X	X	X
Supervision of L. Tauhardt		X	X	X
Vorschlag Anrechnung Publikationsäquivalente	0.5			

P2) "Amine end-functionalized poly(2-ethyl-2-oxazoline) as promising coating material for antifouling applications" L. Tauhardt,[1] M. Frant,[2] D. Pretzel,[3] M. Hartlieb,[4] C. Bücher,[5] G. Hildebrand,[6] B. Schröter,[7] C. Weber,[8] K. Kempe,[9] M. Gottschaldt,[10] K. Liefeith,[11] U. S. Schubert,[12] *J. Mater. Chem. B* **2014**, *2*, 4883-4893.												
	1	2	3	4	5	6	7	8	9	10	11	12
Conceptual contribution	X							X		X		
Synthesis, characterization, and surface immobilization of PEtOx	X											
Synthesis of Fluo-PEtOx				X								
Extraction and surface immobilization of TEL					X							
Bioadhesion and microscopy studies		X										
Characterization of surface immobilized PEtOx						X	X					
Preparation of the manuscript	X	X										

Correction of the manuscript			X	X			X	X	X	X	X	X
Supervision L. Tauhardt									X	X		X
Project coordination			X									
Vorschlag Anrechnung Publikationsäquivalente	1.0											

P3) "Poly(2-ethyl-2-oxazoline) as alternative for the stealth polymer poly(ethylene glycol): Comparison of *in vitro* cytotoxicity and hemocompatibility"
M. Bauer,[1] C. Lautenschläger,[2] K. Kempe,[3] L. Tauhardt,[4] U. S. Schubert,[5] D. Fischer,[6] *Macromol. Biosci.* **2012**, *12*, 986-998.

	1	2	3	4	5	6
Synthesis and characterization of PEtOx			X	X		
Biological studies	X	X				
Preparation of the manuscript	X		X			
Correction of the manuscript		X		X	X	X
Supervision L. Tauhardt			X			X
Vorschlag Anrechnung Publikationsäquivalente				0.25		

P4) "*In vitro* hemocompatibility and cytotoxicity study of poly(2-methyl-2-oxazoline) for biomedical applications"
M. Bauer,[1] S. Schröder,[2] L. Tauhardt,[3] K. Kempe,[4] U. S. Schubert,[5] D. Fischer, *J. Polym. Sci., Part A: Polym. Chem.* **2013**, *51*, 1816–1821.

	1	2	3	4	5	6
Synthesis and characterization of PMeOx			X	X		
Biological studies		X				
Preparation of the manuscript	X		X			
Correction of the manuscript				X	X	X
Supervision L. Tauhardt				X		X
Vorschlag Anrechnung Publikationsäquivalente			0.5			

P5) "Zwitterionic poly(2-oxazoline)s as promising candidates for blood contacting applications" L. Tauhardt,[1] D. Pretzel,[2] K. Kempe,[3] M. Gottschaldt,[4] D. Pohlers,[5] U. S. Schubert,[6] *Polym. Chem.* **2014**, *5*, 5751-5764.						
	1	2	3	4	5	6
Conceptual contribution	X			X		
Synthesis and characterization of the polymers	X					
Biological studies		X			X	
Preparation of the manuscript	X	X				
Correction of the manuscript			X	X		X
Supervision L. Tauhardt			X	X		X
Vorschlag Anrechnung Publikationsäquivalente	1.0					

P6) "Synthesis and *in vitro* activity of platinum containing 2-oxazoline-based glycopolymers" L. Tauhardt,[1] D. Pretzel,[2] S. Bode,[3] J. Czaplewska,[4] K. Kempe,[5] M. Gottschaldt,[6] U. S. Schubert,[7] *J. Polym. Sci., Part A: Polym. Chem.* **2014**, *52*, 2703–2714.							
	1	2	3	4	5	6	7
Conceptual contribution						X	
Synthesis and characterization of the polymers	X						
Biological studies		X					
Synthesis of thiols			X	X			
Preparation of the manuscript	X	X					
Correction of the manuscript			X	X	X	X	X
Supervision L. Tauhardt					X	X	X
Vorschlag Anrechnung Publikationsäquivalente	1.0						

P7) "Rethinking the Impact of the Protonable Amine Density on Cationic Polymers for Gene Delivery: A Comparative Study of Partially Hydrolyzed Poly(2-ethyl-2-oxazoline)s and Linear Poly(ethylene imine)s" M. Bauer,[1] L. Tauhardt,[2] H. M. L. Lambermont-Thijs,[3] K. Kempe,[4] R. Hoogenboom,[5] U. S. Schubert,[6] D. Fischer,[7] in preparation.							
	1	2	3	4	5	6	7
Synthesis and characterization of starting POx			X	X			
Synthesis characterization of LPEI		X	X				
Synthesis and characterization of PHPEtOx		X					
Biological studies	X						
Preparation of the manuscript	X	X					
Correction of the manuscript				X	X	X	X
Supervision L. Tauhardt				X			X
Vorschlag Anrechnung Publikationsäquivalente		0.25					

P8) "Toward the design of LPEI containing block copolymers: Improved synthesis protocol, selective hydrolysis, and detailed characterization" L. Tauhardt,[1] K. Kempe,[2] U. S. Schubert,[3] *J. Polym. Sci., Part A: Polym. Chem.* **2012**, *50*, 4516-4523.			
	1	2	3
Synthesis and characterization	X		
Preparation of the manuscript	X		
Correction of the manuscript		X	X
Supervision L. Tauhardt		X	X
Vorschlag Anrechnung Publikationsäquivalente	1.0		

P9) "Dextran-graft-linear poly(ethylene imine)s for gene delivery: Importance of the linking strategy"

S. Ochrimenko,[1,#] A. Vollrath,[2,#] K. Kempe,[3] L. Tauhardt,[4] S. Schubert,[5] U. S. Schubert,[6] D. Fischer,[7] *Carbohydr. Polym.* **2014**, *113*, 597-606.

#Both authors contributed equally

	1	2	3	4	5	6	7
Conceptual development	X	X					
Synthesis and characterization of PEtOx			X				
Synthesis and characterization of LPEI				X			
Synthesis and characterization of Dex-*g*-LPEI		X					
Biological studies	X						
Preparation of the manuscript	X	X					
Correction of the manuscript			X	X	X	X	X
Vorschlag Anrechnung Publikationsäquivalente				0.25			

P10) "A cationic, non-toxic poly(2-oxazoline) with high *in vitro* transfection efficiency identified by a library approach"

A. C. Rinkenauer,[1,#] L. Tauhardt,[2,#] F. Wendler,[3] K. Kempe,[4] M. Gottschaldt,[5] A. Träger,[6] U. S. Schubert,[7] *Macromol. Biosci.*, accepted 07.10.2014.

[#]Both authors contributed equally

	1	2	3	4	5	6	7
Conceptual contribution				X			
Synthesis and characterization ButEnOx-based polymers		X					
Synthesis and characterization DecEnOx-based polymers		X	X				

Biological studies	X						
Preparation of the manuscript	X	X					
Correction of the manuscript				X	X	X	X
Supervision L. Tauhardt				X	X		X
Supervision F. Wendler		X		X			X
Vorschlag Anrechnung Publikationsäquivalente	1.0	1.0					

P11) "Parallel high-throughput screening of polymer vectors for nonviral gene delivery: Evaluation of structure–property relationships of transfection"

C. Rinkenauer,[1,#] A. Vollrath,[2,#] A. Schallon,[3] L. Tauhardt,[4] K. Kempe,[5] S. Schubert,[6] D. Fischer,[7] U. S. Schubert,[8] *ACS Comb. Sci.* **2013**, *15*, 475-482.

[#]Both authors contributed equally.

	1	2	3	4	5	6	7	8
Conceptual development	X	X	X				X	
Synthesis and characterization of PEtOx					X			
Synthesis and characterization of LPEI				X				
Polyplex preparation and DLS measurements		X						
Biological studies	X							
Preparation of the manuscript	X	X	X					
Correction of the manuscript				X	X	X	X	X
Vorschlag Anrechnung Publikationsäquivalente				0.25				

P12) "Characterization of cationic polymers by asymmetric flow field-flow fractionation and multi-angle light scattering – A comparison with traditional techniques"
M. Wagner,[1] C. Pietsch,[2] L. Tauhardt,[3] A. Schallon,[4] U. S. Schubert,[5] *J. Chromatogr. A* **2014**, *1325,* 195-203.

	1	2	3	4	5
Conceptual contribution				X	
Synthesis characterization of LPEI			X		
Synthesis and characterization of poly(methacrylate)s		X			
AF4, DLS and AUC investigations	X				
Preparation of the manuscript	X				
Correction of the manuscript		X	X	X	X
Vorschlag Anrechnung Publikationsäquivalente			0.25		

P13) "Linear poly(ethylene imine)-based hydrogels for effective binding and release of DNA"
C. Englert,[1] L. Tauhardt,[2] M. Hartlieb,[3] K. Kempe,[4] M. Gottschaldt,[5] U. S. Schubert,[6] *Biomacromolecules* **2014**, *15*, 1124–1131.

	1	2	3	4	5	6
Conceptual development		X	X			
Synthesis and characterization of LPEI	X	X				
Synthesis and characterization of the polymers and hydrogels	X					
Preparation of the manuscript	X					
Correction of the manuscript		X	X	X	X	X
Supervision of C. Englert		X		X	X	
Vorschlag Anrechnung Publikationsäquivalente		0.5				

Erklärung zu den Eigenanteilen des Promovenden/der Promovendin sowie der weiteren Doktoranden/Doktorandinnen als Koautoren an den Publikationen und Zweitpublikationsrechten bei einer kumulativen Dissertation

Für alle in dieser kumulativen Dissertation verwendeten Manuskripte liegen die notwendigen Genehmigungen der Verlage („Reprint permissions“) für die Zweitpublikation vor.

Die Co-Autoren der in dieser kumulativen Dissertation verwendeten Manuskripte sind sowohl über die Nutzung, als auch über die oben angegebenen Eigenanteile informiert und stimmen dem zu (es wird empfohlen, diese grundsätzliche Zustimmung bereits mit Einreichung der Veröffentlichung einzuholen bzw. die Gewichtung der Anteile parallel zur Einreichung zu klären).

Die Anteile der Co-Autoren an den Publikationen sind in der Anlage aufgeführt

Ich bin mit der Abfassung der Dissertation als publikationsbasiert, d.h. kumulativ, einverstanden und bestätige die vorstehenden Angaben. Eine entsprechend begründete Befürwortung mit Angabe des wissenschaftlichen Anteils des Doktoranden/der Doktorandin an den verwendeten Publikationen werde ich parallel an den Rat der Fakultät der Chemisch-Geowissenschaftlichen Fakultät richten.

Name Doktorand	Datum	Ort	Unterschrift
Name Erstbetreuer	Datum	Ort	Unterschrift

1. Introduction

The development of functional, well-defined materials for biological, pharmaceutical, and medicinal applications is one of the central challenges in current research. Due to their large diversity, polymers display an interesting class of compounds for this task. The development of living and controlled polymerization techniques enabled the possibility to synthesize well-defined polymers with tunable properties. Most commonly applied polymerization methods are: (1) Anionic polymerizations,[1, 2] (2) cationic polymerizations[2, 3] and (3) controlled radical polymerizations[4] (in particular reversible addition-fragmentation chain transfer (RAFT),[5, 6] atom transfer radical polymerization (ATRP)[5, 7] and nitroxide-mediation polymerization (NMP)[8, 9]). Prominent examples of biomedically used polymers obtained by controlled or living polymerization techniques are poly(*N,N*-dimethylaminoethyl methacrylate) (PDMAEMA) (radical)[6, 10] and poly(ethylene glycol) (PEG, anionic).[11, 12] In recent years, another class of biocompatible polymers, namely poly(2-oxazoline)s (POx), has gained increasing attention.[13-16] In particular the water soluble poly(2-methyl-2-oxazoline) (PMeOx) and poly(2-ethyl-2-oxazoline) (PEtOx) show similar features as PEG, such as antifouling behavior (Chapters 2 and 3), a high biocompatibility, and the so called "stealth effect" (Chapter 4), but at the same time exhibit some advantageous properties such as a lower viscosity,[17, 18] a higher stability on surfaces,[19, 20] and a less laborious synthesis. POx are obtained by the living cationic ring-opening polymerization (CROP) of 2-oxazolines (Scheme 1-1). By initiation with an electrophile (E), *e.g.* a functional triflate, tosylate, halide, or a strong protic or Lewis acid, a cationic oxazolinium species is formed. This leads to a weakening of the 2-oxazoline's C-O bond and facilitates the nucleophilic attack of another 2-oxazoline monomer. Thereupon, the C-O bond is broken and the ring opened repeating unit is obtained. Under appropriate conditions, no chain transfer or terminating reactions occur and the polymer chain growth propagates until all monomer is consumed. This allows the synthesis of block copolymers by sequential monomer addition. If a mixture of two or more monomers is polymerized, statistical or gradient copolymers are obtained, depending on the reactivity ratios of the respective monomers. Using microwave assisted synthesis, which

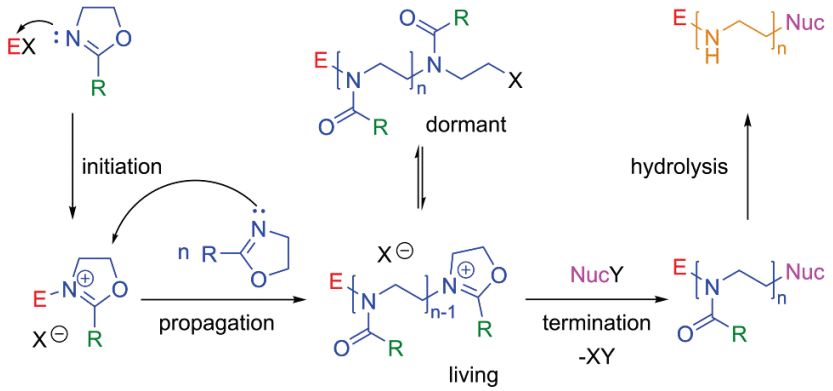

Scheme 1-1. Schematic representation of the synthesis of poly(2-oxazoline)s and the hydrolysis to LPEI.

enables reactions under pressurized conditions and, thus, at temperatures above the boiling point of the solvent, it was demonstrated that the polymerization time can be reduced from several days or times > 8 hours to a few hours or minutes, respectively.[21-24] To terminate the polymerization nucleophiles (Nuc) such as water, sodium azide, amines, or carboxylic acids, are added, which become the ω-end group of the final polymer. The existence of a broad range of functional 2-substituted-2-oxazoline monomers, initiators (E), and terminating agents (Nuc), enables the synthesis of highly functional, well-defined polymers with fine-tuned properties. The solubility and crystallinity of the polymer is mainly influenced by the substituent in 2-position of the monomer (R), which forms the side chain in the final polymer. While polymers with short side chains ($R \leq C_3$) are water soluble and amorphous, POx with aromatic or long aliphatic side chains ($R > C_4$) are water insoluble and semi-crystalline. An interesting aspect of the water soluble POx with R = C_2 (PEtOx) and R = C_3 (poly(2-*n*/*iso*/*cyclo*propyl-2-oxazoline)) is that they exhibit a lower critical solution temperature (LCST) behavior, *i.e.* their aqueous solutions show phase separation at elevated temperatures.[25] The temperature where phase separation occurs, the so called cloud point, depends on different parameters such as the degree of polymerization (DP), the polymer concentration, or the used buffer system. It can also be influenced by the type of comonomer.

Other interesting compounds are (co)polymers based on 2-(3-butenyl)-2-oxazoline (ButEnOx)[26-29] and 2-(9-decenyl)-2-oxazoline (DecEnOx).[30-34] Here, the double bonds can

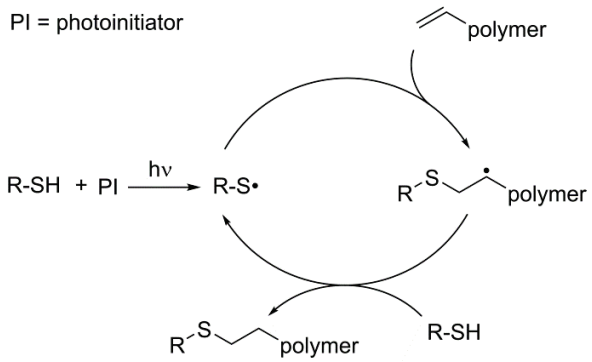

Scheme 1-2. Schematic representation of the radical-mediated thiol-ene photoaddition mechanism.

be used subsequently for the attachment of new functionalities in a post-polymerization modification step. A very efficient method for this purpose is the thiol-ene photoaddition reaction (Scheme 1-2).[35-37]

Applying UV light and a photoinitiator (PI) a thiyl radical is formed, which is prone to undergo a reaction with an alkene group, whereupon a carbon radical is obtained. By transfer of the radical to another thiol moiety a new thiyl radical is formed and the reaction proceeds. This approach enables the straightforward introduction of additional functional moieties into the polymer, *e.g.* amines (Chapters 4 and 5.2) as well as saccharides and terpyridine (Chapter 4.3). In this way, POx can be further fine-tuned for specific applications such as targeted drug delivery (Chapter 4.3) and gene delivery with cationic polymers (Chapter 5), both of significant interest in medical and pharmaceutical research. In particular cationic polymers are extensively studied, since they can be used as non-viral vectors, *i.e.* as carrier systems for genetic material (*e.g.* DNA, RNA).[38-41] One of the most prominent polymers for cationic gene delivery is linear poly(ethylene imine) (LPEI), a POx derivative that is obtained by acidic or basic hydrolysis (Scheme 1-1). However, LPEI suffers from an increasing cytotoxicity with increasing molar mass, while the transfection efficiency (TE) shows the contrary trend. Therefore, intensive efforts were made to synthesize polymers with high TE but low toxicity. A common method is the functionalization with biocompatible polymers, such as PEG or dextrans (Chapter 5.1). But also cationic polymers containing PEtOx or PMeOx as

biocompatible part, *e.g.* partially hydrolyzed PEtOx (PHPEtOx), PEtOx-*block*-LPEI, and amine functionalized POx, represent interesting compounds (Chapters 5.1 and 5.2).

As mentioned above, the usage of microwave synthesizers resulted in an accelerated synthesis of POx but also in a faster hydrolysis to LPEI. Using high-throughput (HT) synthesis approaches with automated synthesis robots and microwaves, it is possible to obtain large polymer libraries. Unfortunately, the HT characterization of the biomedical and pharmaceutical properties is so far only rudimentarily developed and, thus, represents a "bottleneck" on the way to a fast and efficient development and screening of new gene therapies based on cationic polymers. As a consequence, an automated combinatorial HT workflow was developed using branched and linear poly(ethylene imine)s and validated by comparison with results from literature and manually performed experiments (Chapter 5.3).

Another problem related to cationic polymers, besides the cytotoxicity, is the elucidation of structural information, in particular of high molar mass compounds. Here mass spectrometric methods, *e.g.* matrix-assisted laser/desorption ionization (MALDI) or electrospray ionization (ESI) time of flight (TOF) mass spectrometry (MS), often fail. Also molar mass determination by size exclusion chromatography (SEC) is problematic, due to strong interactions with the column material and missing calibration standards. Hence, it was investigated if asymmetric flow-field flow fractionation (AF4) can be used for the characterization of high molar mass cationic polymers (Chapter 5.4).

LPEIs are not only interesting for gene delivery applications but also for the synthesis of LPEI-based hydrogels. These water insoluble, three dimensional networks are capable of taking up water up to a multitude of their own mass. Moreover, LPEI-based hydrogels are able to capture and release genetic material. Therefore, they are investigated for DNA biochip applications, where a separation of genetic material, *e.g.* from blood or feces, is necessary (Chapter 5.5).

The goal of the thesis is the investigation of POx and their derivatives as versatile materials for life science applications.

2. Poly(2-oxazoline) modified surfaces – Attachment methods and applications

Parts of this chapter have been published in P1) L. Tauhardt, K. Kempe, M. Gottschaldt, U. S. Schubert, *Chem. Soc. Rev.* **2013**, *42*, 7998-8011.

Preventing the uncontrolled adhesion and adsorption of proteins, cells, bacteria, and other microorganisms onto surfaces, the so called fouling process, represents a major challenge for a wide range of applications such as medicine (*e.g.* medical devices, implants, drug delivery systems),[42, 43] mobility (*e.g.* ship hull coatings),[44, 45] food industry (*e.g.* packaging),[46] but also for membranes (*e.g.* in water purification systems),[47] microarrays, and (bio)sensors.[48] A widely used strategy for this task is the surface modification with poly(ethylene glycol) (PEG) and PEG-based copolymers.[19, 49] However, PEG suffers from a tense patent situation and is known to undergo degradation by (auto-)oxidation to form aldehydes and ethers, hampering its long-term application. Based on these issues, other polymer systems, such as poly(2-oxazoline)s (POx), in particular the water soluble poly(2-methyl-2-oxazoline) (PMeOx) and poly(2-ethyl-2-oxazoline) (PEtOx), are investigated as alternative antifouling coating materials. They show similar properties as PEG but exhibit several advantages such as higher stability on surfaces,[50] lower viscosity,[17, 19] and a less laborious synthesis.[22] Moreover, POx meet the following criteria, which were found to be common for all antifouling polymers: 1) The presence of hydrophilic (polar) functional groups and hydrogen bond accepting groups as well as 2) the absence of a net charge and hydrogen bond donating groups.[19, 49]

With regard to applications in coatings it is necessary to immobilize the POx on the surface. A weak binding onto the surface will lead to a loss of material over time. This will reduce the long term stability of the coating and is, thus, not sufficient. Therefore, the surface immobilization process plays an important role for the efficiency and stability of the coating. In general, there are three different methods to attach POx to a surface: 1) “Grafting onto”, 2) “grafting from” and 3) immobilization *via* electrostatic interactions.

"Grafting onto" can be accomplished in two different ways: 1) The coupling moiety is introduced to the polymer prior to surface attachment, *e.g.* by direct end-capping of the living polymer species with a silane coupling agent (Scheme 2-1A) or by applying the hydrosilation method reported by Chujo *et al.* at which a double bond is reacted with a trialkyloxysilane in the presence of chloroplatinic acid as catalyst.[51, 52] Also copper catalyzed 1,3-dipolar cycloaddition of triple bond containing POx to azide bearing surfaces was reported.[53, 54] 2) The coupling agent is attached to the surface first and the polymer is covalently bound in a next step, *e.g.* by photoinduced C-H insertion using benzophenon (Scheme 2-1B) or perfluorophenyl azide (Scheme 2-1C) derivatives.

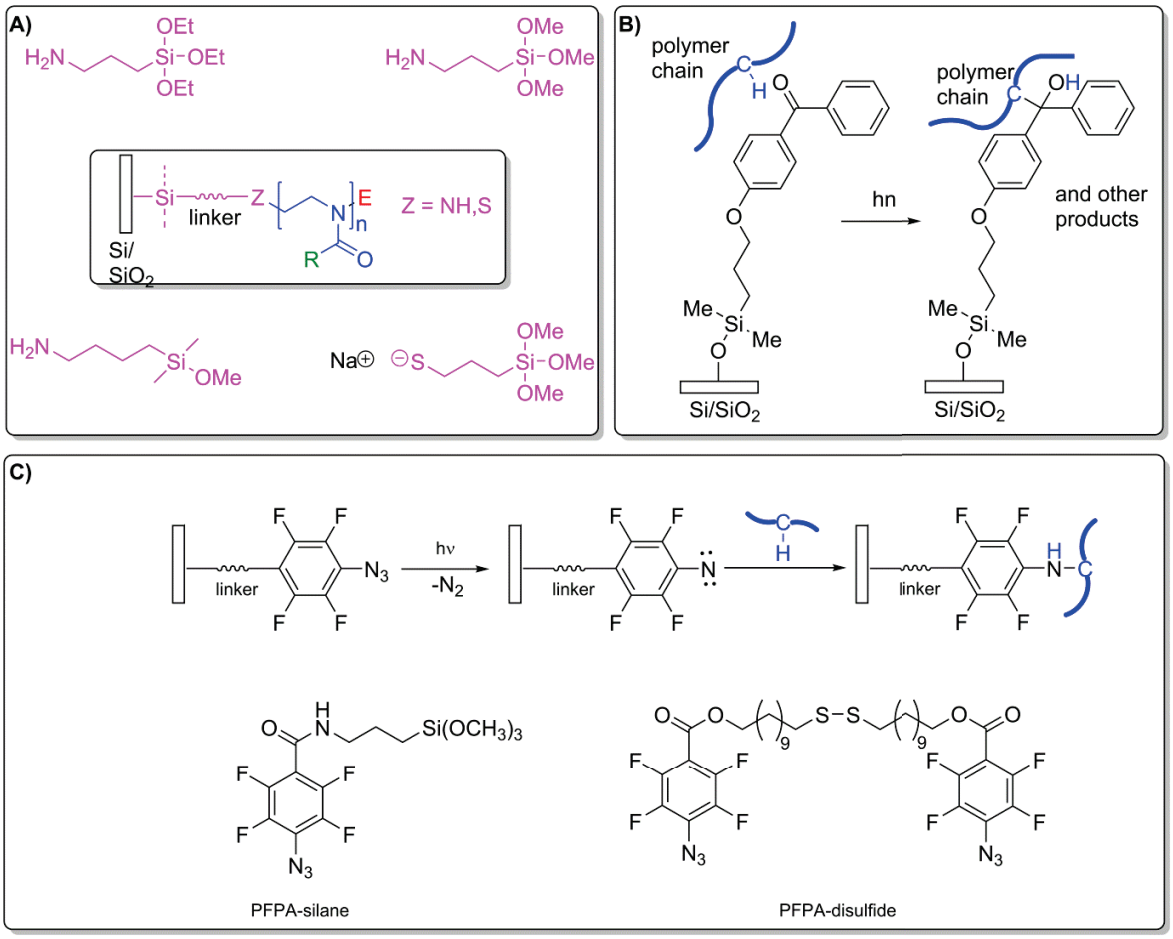

Scheme 2-1. Grafting onto approaches: A) End-capping with silane coupling agents, followed by surface attachment. Photoimmobilization *via* B) benzophenon and C) perfluorophenyl azide (PFPA) derivatives.

In the "grafting from" approach, the polymerization is started directly from the surface. To this end, suitable initiators (*e.g.* triflates and tosylates) have to be attached first (Scheme 2-2A, C). A special case is the self-initiated photografting and photopolymerization (SIPGP) of 2-*iso*propenyl-2-oxazoline followed by the CROP of another 2-oxazoline (Scheme 2-2B).[55]

The immobilization *via* electrostatic interactions is the weakest form of binding, and can be established, *e.g.* between negatively charged Nb_2O_5-coated silicon wafers and the positive charged poly(L-lysine)-*graft*-PMeOx as shown by Konradi and Pidhatika.[19, 20, 50, 56, 57] Investigations showed that these types of coatings are also able to withstand intensive washing processes and the attack of hydrogen peroxide solution.

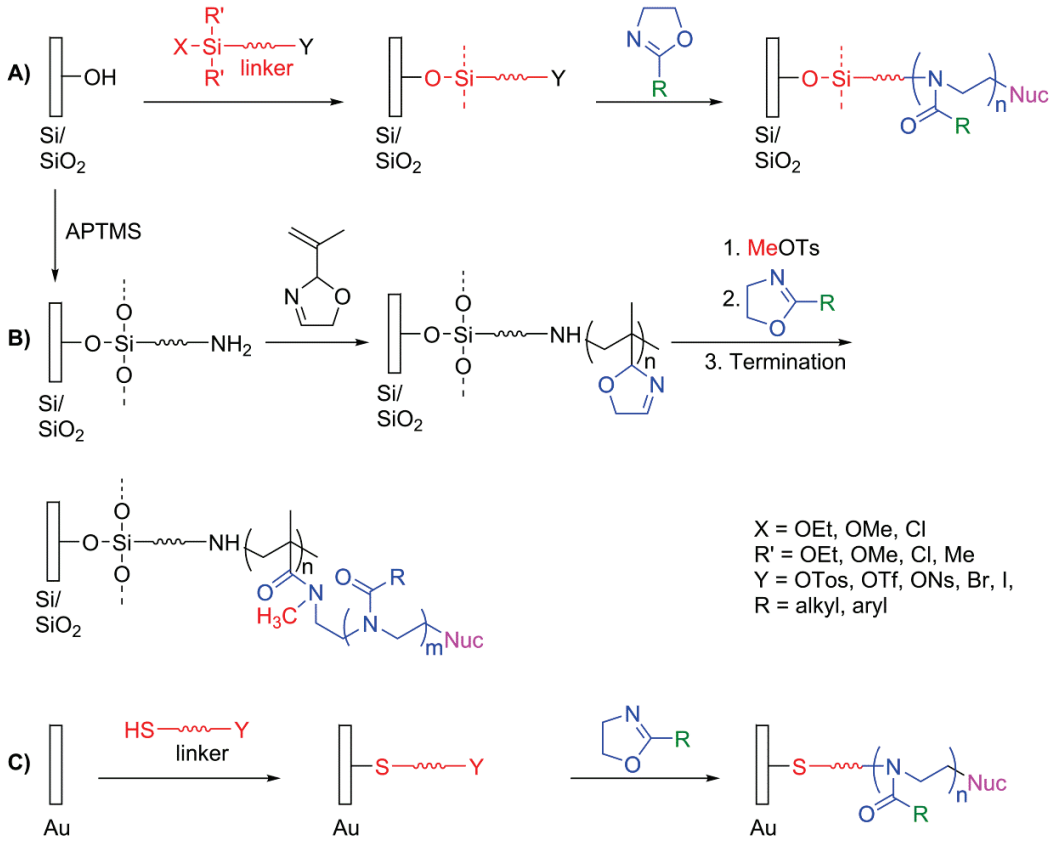

Scheme 2-2. Schematic representation of the surface initiated CROP of POx using A) different initiators, B) self-initiated photografting and photopolymerization of 2-isopropenyl-2-oxazoline followed by CROP of POx, and C) surface initiated CROP of POx on gold surfaces using different initiators.

Depending on the immobilization method and the structure of the used polymer, two types of POx coatings can be distinguished. First, linear, brush-like POx coatings, with only a single POx chain per surface grafting unit (Scheme 2-1, Scheme 2-2A,C), and second, POx-based comb polymer coatings, where more than one POx chain per grafting unit is attached to the surface *via* another polymer backbone (e.g. PLL) (Scheme 2-2B). The latter can exhibit a bottle brush-like structure, also referred to as molecular or cylindrical brushes, at high side chain grafting densities.

POx-modified surfaces are of significant interest for applications were the adhesion and adsorption of proteins, cells, bacteria, and microorganisms needs to be prevented, *e.g.* in medicine (*e.g.* for implants), microfluidic devices, and (bio)sensors. Different studies, using a single type of bacteria (e.g. *E. coli*),[19, 50, 57] cells (*e.g.* fibroblasts),[58, 59] or proteins (*e.g.* bovine serum albumin)[60-62] showed that POx exhibit good antifouling properties. An example is the nearly complete reduction of the fibronectin (Fn) adsorption (Figure 2-1) and HUVEC cell adhesion on PEtOx and PMeOx bottle brush-like coatings.[55] Moreover, POx-based coatings were found to be more stable against oxidation than PEG coatings, making them promising materials for antifouling applications, where a high long-term stability is essential.[19, 20]

However, POx-modified surfaces are not only interesting for controlling protein adsorption and cell adhesion, but also for other applications, *e.g.* dip-pen nanolithography. Here, PMeOx coatings on atomic force microscope tips helped in overcoming problems in direct-write patterning of viruses and cells.[63, 64]

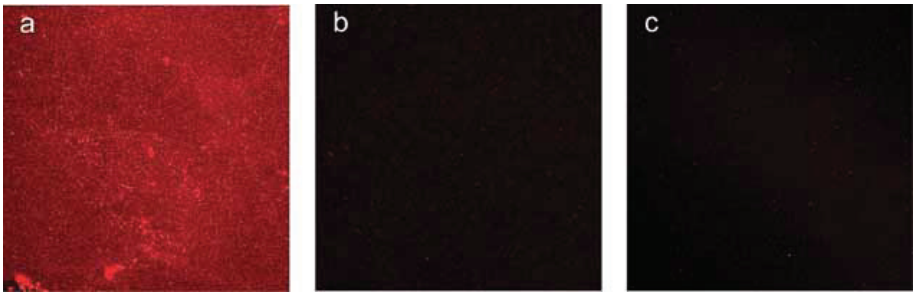

Figure 2-1 Fluorescence microscopy of fibronectin (Fn) adsorption on bottle brush-like POx coatings on glass reveals a good Fn adsorption on (a) poly(2-*n*-propyl-2-oxazoline) and no adsorption on (b) PEtOx, and (c) PMeOx. Fn adsorption was performed for 1 h in a 50 µg/mL solution of labeled Fn in PBS at pH = 7.4 and 37 °C. Reproduced with permission ref. 53. © 2012 John Wiley and Sons.

3. Poly(2-oxazoline)s as coating material for antifouling applications

Parts of this chapter have been published in P2) L. Tauhardt, M. Frant, D. Pretzel, M. Hartlieb, C. Bücher, G. Hildebrand, B. Schröter, C. Weber, K. Kempe, M. Gottschaldt, K. Liefeith, U. S. Schubert; *J. Mater. Chem. B* **2014**, *2*, 4883-4893.

As shown above, POx represent promising materials for antifouling coatings when exposed to certain proteins, cells, bacteria, or microorganisms. However, under real life condition more than one type of protein, cell, or bacteria will attack. Moreover, the long-term stability of POx coatings has not been investigated yet, but plays an important role when it comes to application, *e.g.* in water sensors or medical devices. On this account, the antifouling properties of PEtOx coatings and their stability has been studied under "real live"-mimicking conditions. To this end, PEtOx of different molar masses, bearing an amine end group for the surface attachment, were synthesized using a new, straight-forward approach *via* potassium phthalimide end-capping, followed by hydrazinolysis (Scheme 3-1, Table 3-1).

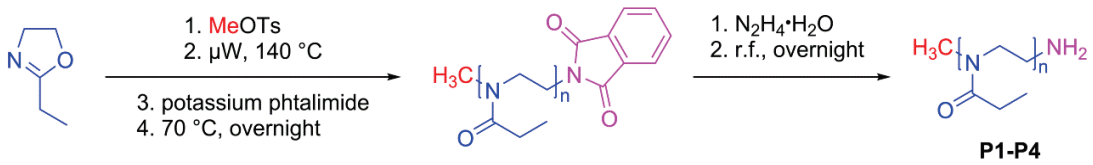

Scheme 3-1. Schematic representation of the synthesis of amine end-functionalized PEtOx.

Table 3-1. SEC data of the different PEtOx

Polymer	Monomer	DP	M_n (g/mol)[a)]	PDI[a)]
P1	EtOx	20	2,460	1.12
P2	EtOx	40	3,790	1.15
P3	EtOx	60	5,175	1.14
P4	EtOx	80	5,990	1.19

[a)]Determined by SEC (eluent: $CHCl_3$ + TEA + *i*PrOH (94:4:2), calibration: PS).

^{1}H NMR spectra revealed end-capping efficiencies of 100%. Moreover, no peaks for OH end groups, which are obtained when the reaction is quenched with water or air moisture, are visible in the MALDI-TOF mass spectra of both phthalimide and amine end-functionalized PEtOx (Figure 3-1).

For a stable and covalent attachment of the polymer to surface a "grafting onto" approach was used, which allows the detailed characterization of the polymer before attaching it to the surface and, thus, enables the discussion of structure-property relationships. As coupling agents a (3-glycidyloxypropyl)trimethoxysilane (GOPTMS) and cyanuric chloride modified tetraether lipid (TEL) were chosen. Covalent binding was achieved by reaction of the amine end group of PEtOx with the epoxy unit of the silane or with the cyanuric chloride of the TEL moiety, respectively (Scheme 3-2).

The suitability of the attachment method *via* GOPTMS and TEL, respectively, was proven using a fluorescein labeled PEtOx (Fluo-PEtOx) (Figure 3-2). The coating process was further monitored by means of X-ray photoelectron spectroscopy (XPS), showing the appearance of a nitrogen signal after the PEtOx coating process. Water contact angle measurements of air-dried and swollen coatings revealed a higher hydrophilicity of the swollen samples, ascribed to the formation of PEtOx hydrates.

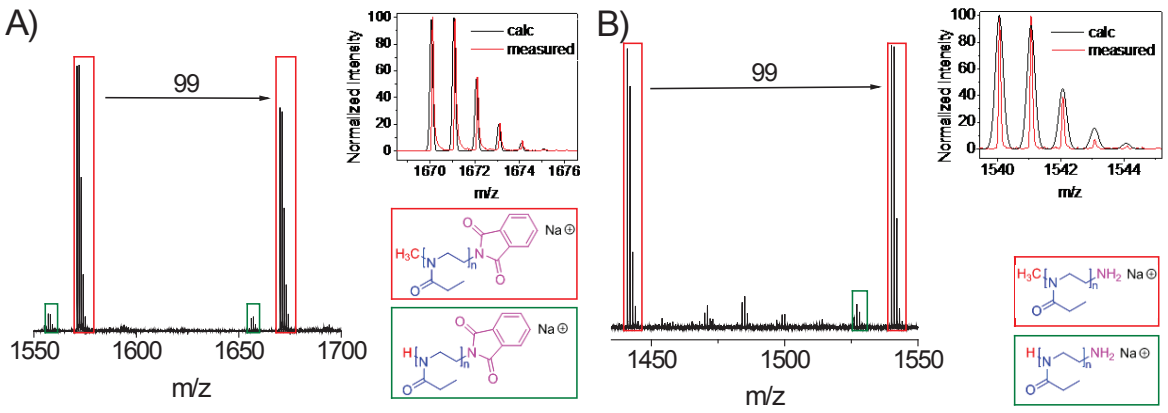

Figure 3-1. Expanded region of the MALDI-TOF mass spectrum of A) phthalimide end-capped $PEtOx_{20}$ and B) the amine end group bearing $PEtOx_{20}$.

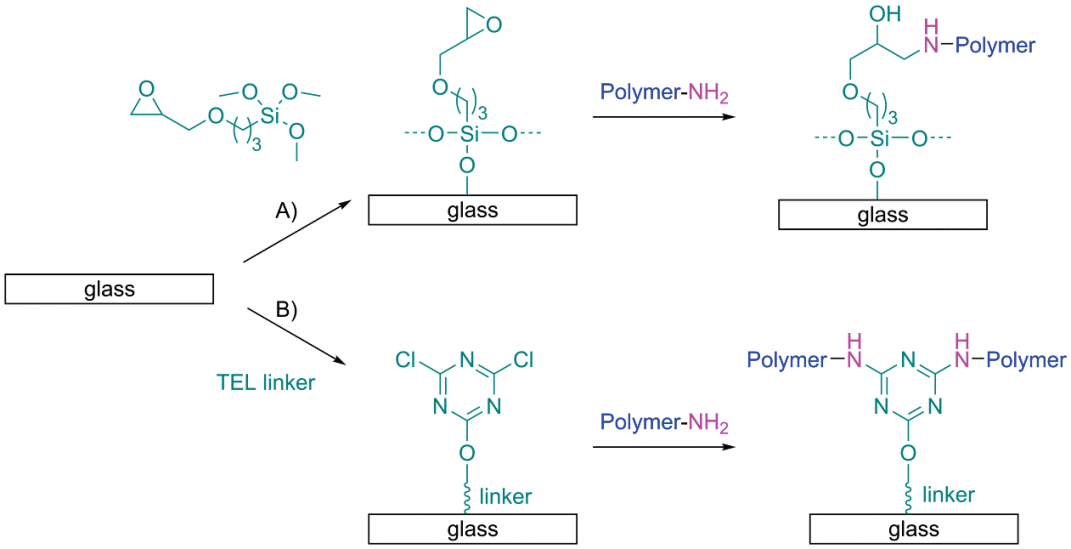

Scheme 3-2. Schematic representation of the PEtOx coating process using GOPTMS and a TEL linker.

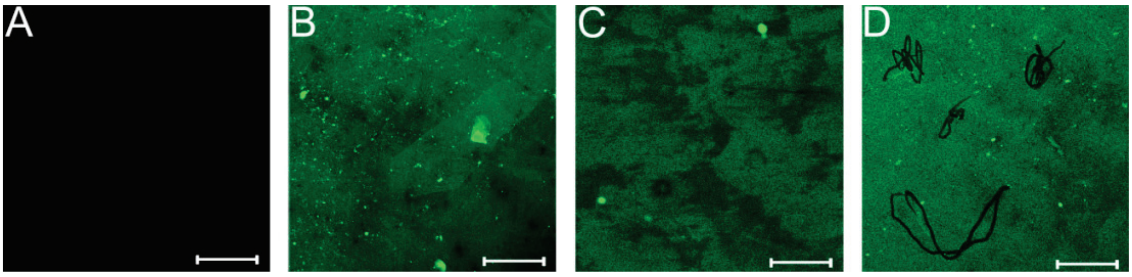

Figure 3-2. Fluorescence microscope images of A) uncoated glass, B) Fluo-PEtOx attached *via* GOPTMS, and C) Fluo-PEtOx attached *via* TEL and D) scratched sample of GOPTMS attached Fluo-PEtOx (scale bar: 100 µm).

Fouling studies were performed in a flow chamber under more "real-life" relevant conditions using a synthetic river water model containing five different bacteria. PEtOx modified glass samples exposed to this mixture for 15 h showed a reduction of the bioadhesion of up to 66% with no significant differences between the two different linkers (Figure 3-3). The best results were obtained applying a PEtOx with a DP of 20 attached *via* a tetraether lipid linker, which showed the lowest biofilm formation and the highest amount of dead bacteria. In addition, the

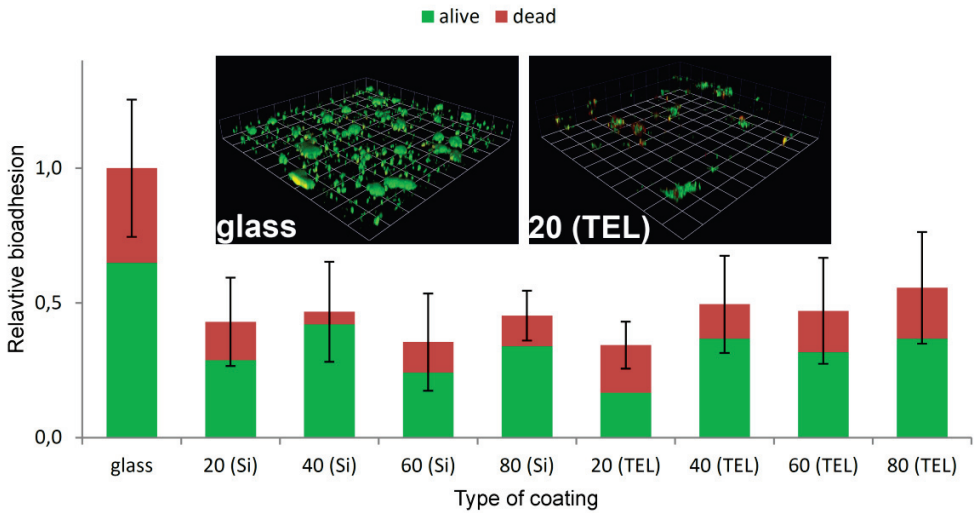

Figure 3-3. Bioadhesion on PEtOx coatings of different DP (20, 40, 60, and 80) to the glass slides *via* a silane (Si) and a tetraether lipid (TEL) linker (standard deviation is related to the total bioadhesion (sum of dead and vital bacteria)) as well as laser scanning images of the stained biofilms on glass and 20 (TEL) (1 unit = 42.59 µm).

stability of the PEtOx coatings against different types of stress has been investigated. The resistance against chemical stress, caused *e.g.* by fresh and salt water, was investigated over 12 weeks using dam and North Sea water, respectively. The durability of the coatings against abrasion in particle containing water is essential in the field of environmental monitoring. Based on environmental data a corresponding test solution containing aluminum oxide and silicon carbide particles was prepared. Mechanical stress was simulated by placing the glass slides into this solution and stirring for 8 hours a day over 1 week. In order to verify their thermal stability, the samples were exposed to a defined heating plan for 14 days with temperatures between 2 and 38 °C. No destruction of the polymer coatings was observed, demonstrating the capability of the films for long term applications.

In conclusion, POx represent a suitable class of polymers for antifouling coatings. They are able to reduce biofouling up to 66% and they are stable against thermal, mechanical, and chemical stress.

4. Poly(2-oxazoline)s in systemic applications

Parts of this chapter have been published in P3) M. Bauer, C. Lautenschläger, K. Kempe, L. Tauhardt, U. S. Schubert, D. Fischer; *Macromol. Biosci.* **2012**, *12*, 986-998. P4) M. Bauer, S. Schröder, L. Tauhardt, K. Kempe, U. S. Schubert, D. Fischer; *J. Polym. Sci., Part A: Polym. Chem.* **2013**, *51*, 1816–1821. P5) L. Tauhardt, D. Pretzel, K. Kempe, M. Gottschaldt, D. Pohlers, U. S. Schubert, *Polym. Chem.* **2014**, *5*, 5751-5764. P6) L. Tauhardt, D. Pretzel, S. Bode, J. Czaplewska, K. Kempe, M. Gottschaldt, U. S. Schubert, *J. Polym. Sci., Part A: Polym. Chem.* **2014**, *52*, 2703–2714.

4.1. Poly(2-oxazoline)s as poly(ethylene glycol) alternative

Besides being potential candidates for replacing PEG in antifouling coatings, POx are also investigated as PEG alternative for various (bio)medical and pharmaceutical applications. One of the major tasks in pharmacy is shielding drugs from degradation and rapid clearance from the body, but also improving the water solubility of hydrophobic drugs. Nowadays, the most frequently used polymer for this task is the "gold standard" PEG. It can be applied to encapsulate drugs or for the formation of water soluble drug conjugates. Moreover, PEG shows the so called "stealth effect", *i.e.* the suppression of nonspecific interactions with the blood components, which leads to a reduced blood clearance rate and results together with the enhanced permeability and retention (EPR) effect in a prolonged blood circulation time of the drug.[11] However, although only observed in a limited number of patients, concerns regarding immune responses,[65] formation of PEG-antibodies,[66] an accelerated blood clearance (ABC) phenomenon after multiple applications,[67] and non-biodegradability of PEG resulting in the body accumulation of high molar mass PEGs,[68] arose with an increasing number of clinical trials and a more profound experience with PEG in humans. Other drawbacks are the tendency of PEG to undergo degradation by (auto-)oxidation, resulting in the formation of ethers, peroxides, and aldehydes,[19, 20, 69-71] its high viscosity in water,[17, 18] and the possible contamination with toxic synthesis side products, *e.g.* 1,4-dioxane. Additionally, a tense patent situation regarding PEG complicates the introduction of new formulations to the market. As a

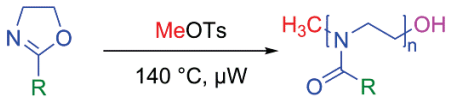

Scheme 4-1. Schematic representation of the synthesis of PMeOx and PEtOx.

consequence, intensive efforts have been made to look for alternative stealth polymers. One of the polymer classes investigated in this context are POx, in particular the water soluble PMeOx and PEtOx.[18] Their synthesis from low toxic MeOx and EtOx by CROP (Scheme 4-1) is less demanding than the preparation of PEG by anionic ring-opening polymerization of highly toxic and explosive ethylene oxide, and yields polymers with well-defined molar masses and narrow molar mass distributions (Table 4-1, Figure 4-1). Moreover, POx exhibit a high stability against oxidation[20] and have a lower viscosity in water.[17, 18]

To investigate their potential as PEG alternative, PMeOx and PEtOx of different molar masses have been synthesized. While self-synthesized PMeOx (**P5-P8**) and PEtOx (**P9-P11**, **P13-**

Table 4-1. SEC data of the different PMeOx and PEtOx samples.

Polymer	Monomer	DP[a)]	M_n (theo) (g/mol)[a)]	M_n (SEC) (g/mol)[b)]	PDI[b)]
P5	MeOx	23	2,000	3,700	1.17
P6	MeOx	47	4,000	6,700	1.20
P7	MeOx	118	10,000	12,300	1.39
P8	MeOx	236	20,000	19,000	1.44
P9	EtOx	4	400	-	-
P10	EtOx	21	2,080	3,700	1.11
P11	EtOx	41	4,060	6,500	1.11
P12[c)]	EtOx	50[d)]	8,456	20,100	2.37
P13	EtOx	103	10,200	12,800	1.15
P14	EtOx	207	20,500	22,900	1.18
P15	EtOx	379	37,500	41,000	1.25
P16[c)]	EtOx	504[d)]	17,939	74,100	4.13
P17[c)]	EtOx	2017[d)]	48,882	229,000	4.63

[a)]Determined by ^{1}H NMR spectroscopy; [b)]determined by SEC (eluent: DMAc + 0.21% LiCl, calibration: PS); [c)]commercial sample; [d)]DP calculated from the molar mass given by the supplier.

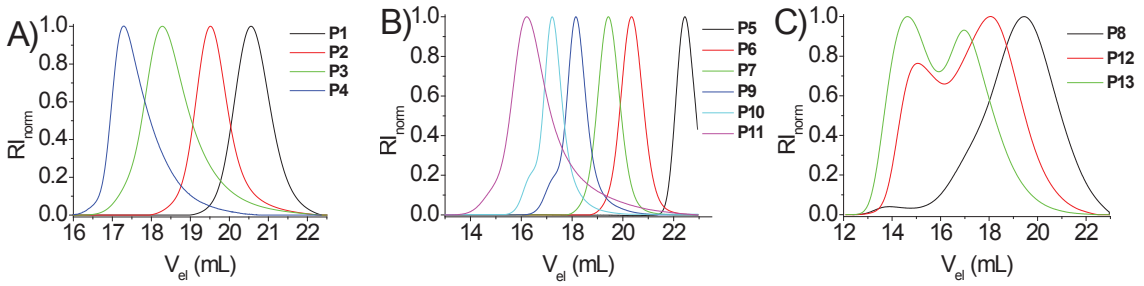

Figure 4-1. SEC curves of A) PMeOx, B) PEtOx and C) commercial PEtOx.

P15) exhibited monomodal distributions, commercially obtained PEtOx (**P12, P16, P17**) showed bimodal distributions with PDI values twice to four times higher as for self-synthesized polymers (Figure 4-1, Table 4-1), deriving from chain-transfer reactions.[72] Moreover, their molar masses revealed a large deviation from the declared values (Table 4-1), ascribed to the loss of reaction control, when the polymerization is aimed for high DPs, *i.e.* DP > 300 for PEtOx and DP > 100 for PMeOx.[22]

The biocompatibility studies of PMeOx and PEtOx in comparison to commercial PEGs of similar molar masses were performed under standardized conditions. Many of the polymers used in medical applications or as drug delivery system come into close contact with blood plasma and blood cells, in particular after systemic administration. Therefore, the influence of the polymers on the red blood cell hemolysis and aggregation was investigated. Independent of the pharmaceutical quality, incubation time, and polymer concentration, none of the PEGs and POx revealed values of hemolysis higher than 1.6%, indicating no detectable disturbance of the red blood cell membranes. According to the ASTM standard F756-00 a release of hemoglobin between 0 and 2% is regarded as non-hemolytic. Additionally, the potential of PMeOx, PEtOx, and PEG to aggregate red blood cells, an undesired phenomenon leading to circulatory side effects and even lethal toxicity, was studied. Neither the PEGs nor the PMeOx showed red blood cell aggregation even at the highest concentration of 80 mg/mL. For PEtOx a molar mass and concentration dependency was observed. PEtOx up to 50 kDa showed results comparable to PEG, with the exception of **P15** and **P16** at 80 mg/mL where a slight aggregation was observed. PEtOx of 200 kDa (**P17**) revealed the highest aggregating effect with no aggregation at 20 mg/mL, slight aggregation at 40 mg/mL, and high aggregation at

concentrations above 60 mg/mL. Cytotoxicity was investigated by means of lactate dehydrogenase (LDH) and 3-(4,5-dimethylthiazol-2-yl)-2,5-diphenyltetrazolium bromide (MTT) assay. LDH is released from the cell when the membrane is damaged. However, the LDH release of both the PEG and the POx treated cells was in the range from 0 to 8.5% even after 4 hours at the highest polymer concentration of 80 mg/mL. This is below the cytotoxic level of 10% and indicates that no damage of the cellular membranes occurred. For both, the PEG and the POx, the MTT assay revealed a moderate, time, concentration, and molar mass dependent cytotoxicity but only after long term treatment and at concentrations higher than the typically used dose (Figure 4-2). In conclusion, PMeOx and PEtOx exhibit similar properties as PEG and, therefore, represent good PEG alternatives.

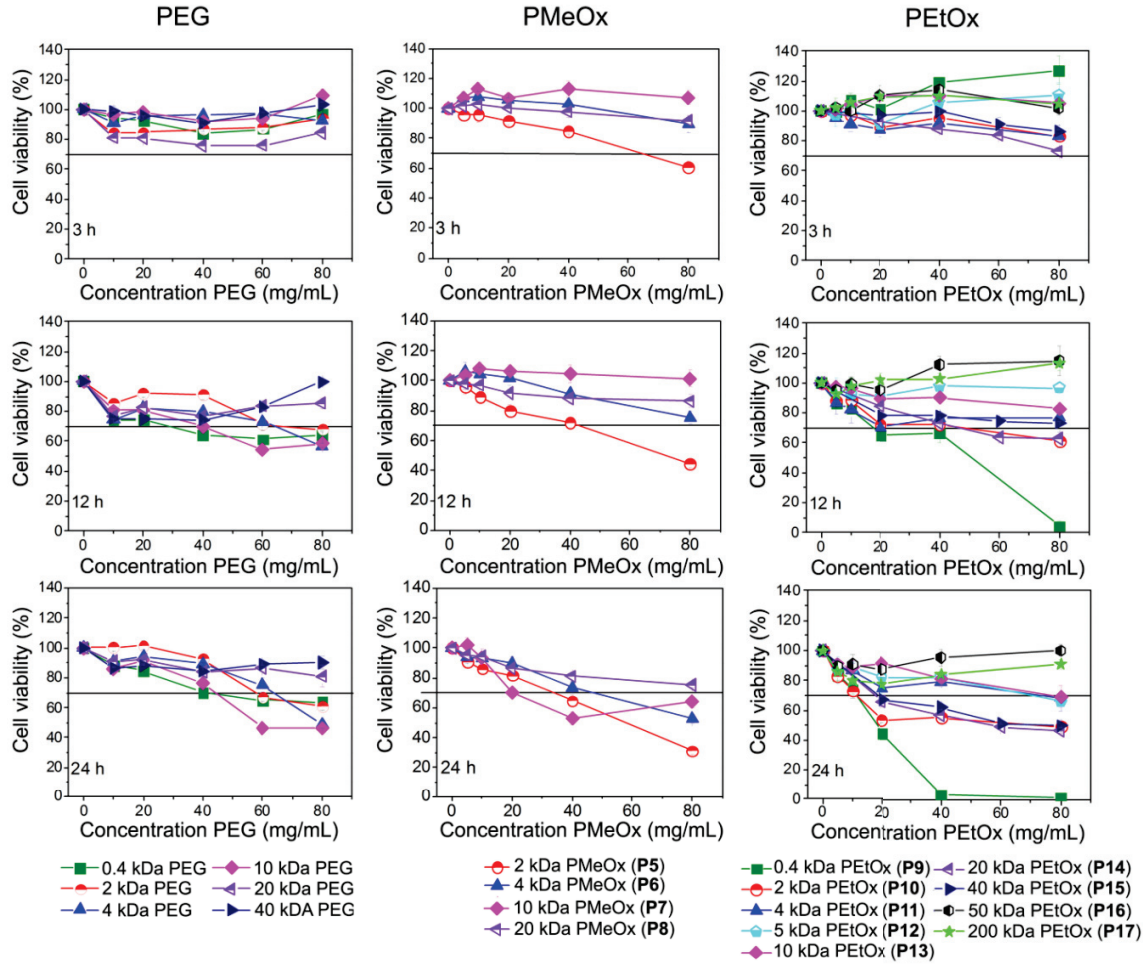

Figure 4-2. Cytotoxicity of PEG, PEtOx, and PMeOx in dependency of time, concentration, and molar mass. The cell viability was determined by MTT assay. Values below the marked line at 70% viability were regarded as cytotoxic according to ISO-10993-5. Data are presented as mean standard deviation of seven determinations.

4.2. Zwitterionic poly(2-oxazoline)s

Another class of materials that exhibits an excellent biocompatibility, but also antifouling behavior, are poly(betaine)s, *i.e.* polymers comprising a zwitterionic structure. In particular poly(2-methacryloyloxyethyl phosphorylcholine)s are of high interest as they are applied, *e.g.* for soft contact lenses. Other widely used zwitterionic polymers are poly(carboxybetaine)s and poly(sulfobetaine)s. An outstanding property of these polymers is their excellent blood compatibility which, in some cases, is going along with an anticoagulant activity, leading to a prolongation of the blood clotting time.[73-77] This is important with regard to medical applications, *e.g.* medical devices, implants, and drug delivery systems, where thrombogenicity is an issue. As a consequence, it was studied if POx based betaines show a similar behavior. To this end, a POx precursor, consisting of EtOx and ButEnOx, was synthesized and their polymerization kinetic under the conditions chosen was investigated. As already reported for the methyl triflate initiated copolymerization of EtOx and ButEnOx at 70 °C, the methyl tosylate initiated reaction at 140 °C showed a first-order kinetic behavior (Figure 4-3A).[29] However, due to the higher temperature, the polymerization proceeded much faster with polymerization constants of kp(EtOx) = 0.206 L mol^{-1} s^{-1} and kp(ButEnOx) = 0.188 L mol^{-1} s^{-1}(Table S1, Figure S1A). The similar conversions of both monomers are a reliable indication for the formation of a random copolymer. In addition, characterization by size exclusion chromatography (SEC) showed a growing molar mass with time (Figure 4-3B).

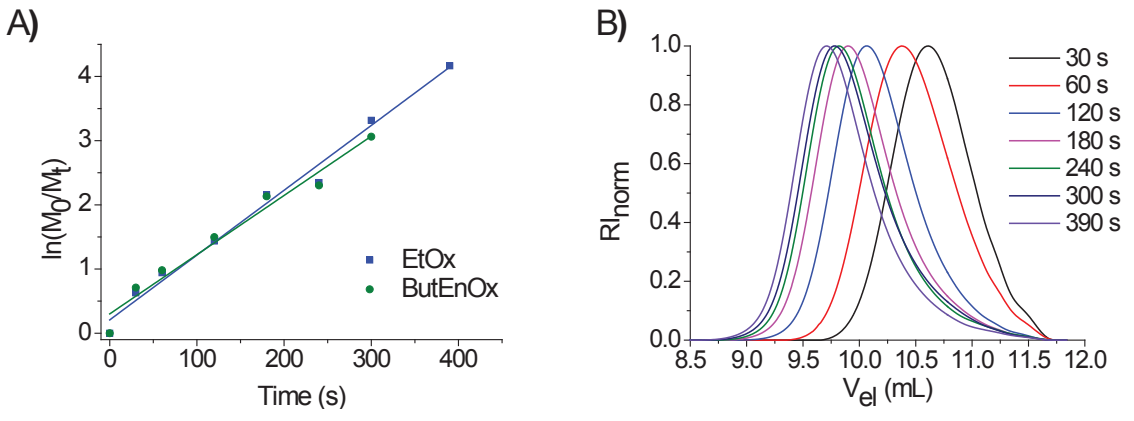

Figure 4-3. A) First-order kinetic plots of the copolymerization of EtOx (square) and ButEnOx (circle) at 140 °C with a total monomer concentration of 1 M in acetonitrile and a [MeOTs]/[EtOx]/[ButEnOx] ratio of 1:16:4 (conversions were determined by GC measurements). B) SEC curves of the kinetic study after different times.

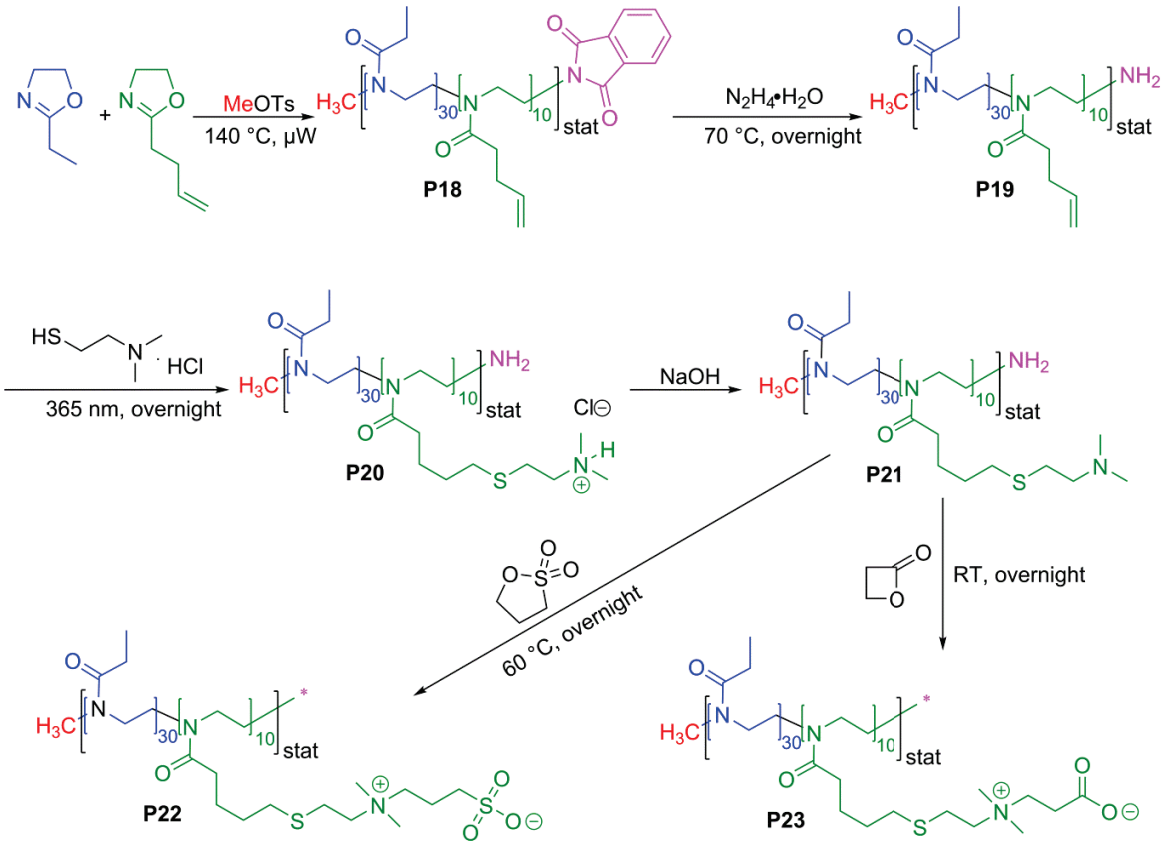

Scheme 4-2. Schematic representation of the synthesis of zwitterionic POx.

With the obtained kinetic data, an amine end-functionalized P($EtOx_{30}$-*stat*-$ButEnOx_{10}$) was prepared in a controlled way using the same synthesis route as described for the amine end-functionalized PEtOx (Chapter 3). The amine end group can be used for surface attachment, *e.g.* in antifouling coatings, or for labeling. Investigations by ^{1}H NMR spectroscopy revealed that the ButEnOx double bonds remained intact (Figure 4-4) and, hence, can be exploited for thiol-ene photoaddition of 2-dimethylaminoethanethiol hydrochloride (Scheme 4-2). The resulting polymer with tertiary amine groups (**P21**), was the basis for the betainization process using 1,3-propanesultone and *β*-propiolactone analog to the synthesis of poly(*N,N*-dimethylaminoethyl methacrylate) (PDMAEMA)-based betaines.[78, 79] The final zwitterionic polys(sulfobetaine)s and poly(carboxybetaine)s and the intermediates were investigated by means of ^{1}H NMR spectroscopy and SEC (Table 4-2), showing the success of the reactions.

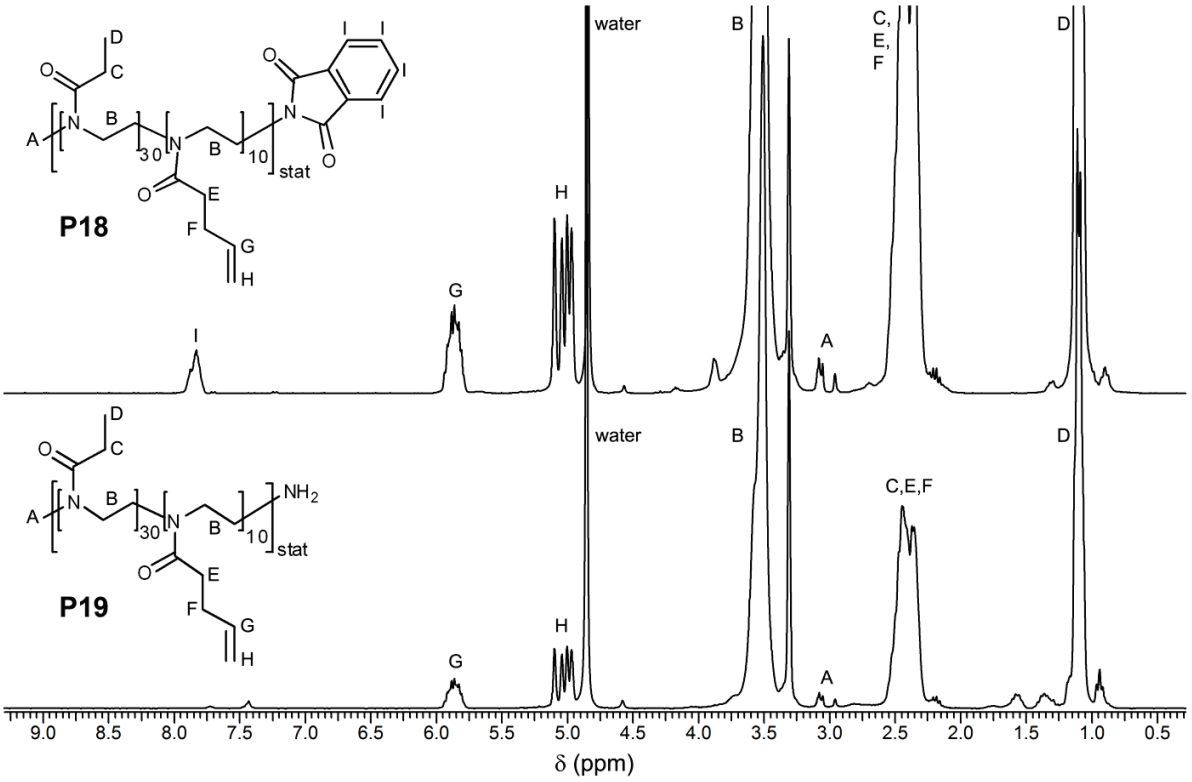

Figure 4-4. ^{1}H NMR spectrum of (top) phthalimide end-capped (**P18**) and (bottom) amine end-functionalized P($EtOx_{30}$-*stat*-$ButEnOx_{10}$) (**P19**) (300 MHz, CD_3OD).

Table 4-2. SEC data of the zwitterionic POx as well as the starting material and intermediates measured on different SEC systems.

Polymer	Composition (End group)	DMAc + 0.21% LiCl[a)]		$CHCl_3$ + TEA + *i*PrOH (94:4:2)[a)]	
		M_n (g/mol)	PDI	M_n (g/mol)	PDI
P18	$EtOx_{30}$:$ButEnOx_{10}$ (phthalimide)	6,860	1.16	4,590	1.16
P19	$EtOx_{30}$:$ButEnOx_{10}$ (NH_2)	6,980	1.19	3,920	1.16
P20	$EtOx_{30}$:tAmOx·HCl (NH_2)	7,740	1.20	4,820	1.18
P21	$EtOx_{30}$:$tAmOx_{10}$ (NH_2)	7,860	1.24	4,720	1.19
P22	$EtOx_{30}$:$SBOx_{10}$ (NH_2)	8,200	1.35	-[a)]	-[a)]
P23	$EtOx_{30}$:$CBOx_{10}$ (NH_2)	8,150	1.59	3,640	1.27
P24	$EtOx_{40}$ (NH_2)	6,600	1.21	4,830	1.15

[a)]Calibration against PS.

To evaluate the biocompatibility of the sulfobetaine POx (SB-POx, **P23**) and the carboxybetaine POx (CB-POx, **P24**), their influence on the erythrocyte aggregation, the blood viscosity, the platelet activation, the complement activation, and the blood coagulation were studied and compared to a PEtOx homopolymer (DP = 40). In addition, the cytotoxicity and hemolytic activity was investigated. Neither PEtOx nor the zwitterionic polymers revealed any cytotoxic or hemolytic effect at concentrations up to 10 $mg\,mL^{-1}$. Also no erythrocyte aggregation could be observed. Measurements showed a slightly increased blood viscosity, which was within the physiological tolerable range and could be fully attributed to the intrinsic viscosity of the added polymer. Therefore, no substantial interactions of the polymers with blood components, leading to changes of the blood viscosity itself, were observed. In a subsequent step, it was investigated if the polymers have any influence on the platelet activation, which is a very early event in the complex process of primary hemostasis, *i.e.* the process which causes bleeding to stop. A polymer induced malfunction of the platelets could either provoke excessive bleeding, or, in case of exceeding platelet activity, a life-threatening vessel clogging by spontaneous blood clot formation. It was found that both PEtOx and the zwitterionic POx had no influence on the platelet activation. In addition, no influence of the polymers on the activation of the complement system, as a part of the body's innate immune response, was observed. While all polymers did not influence the extrinsic blood coagulation pathway, anticoagulant activity *via* components of the intrinsic and/or the common coagulation pathway was observed for the CB-POx and to a lesser extent for the SB-POx. Pure PEtOx showed no anticoagulant behavior at all. Neither a prolongation nor a reduction of the blood clotting time was observed.

In conclusion, zwitterionic POx are potential candidates for materials that come in contact with blood or blood components. Possible applications are antithrombogenic membranes (*e.g.* for blood dialysis), targeted delivery approaches with the aim to increase the blood circulation time, but also the improvement of the hemocompatibility of biomaterials for *in vivo* diagnostics and implants.

4.3. Poly(2-oxazoline)s as potential anticancer drugs

Poly(2-oxazolines) are not only interesting as anticoagulant materials but also as basis for the development of other therapeutic agents, such as anticancer drugs. Anticancer drugs, such as the well-known cisplatin, often suffer from severe side effects such as renal toxicity, gastrointestinal toxicity, and neurotoxicity as well as acquired and intrinsic cisplatin resistance of various cancer types.[80-83] Owing to this, today's research focuses on the selective transport of the drug to the cancer cells by passive and active targeting. This can be achieved either exploiting the EPR effect (passive targeting) or by functionalization of the drug with bioactive substances such as proteins (*e.g.* transferrin), hormones (*e.g.* estrogen), amino acids, folic acid, and saccharides.[83-85] In particular the latter are interesting, as cancer cells commonly exhibit an altered sugar metabolism, *e.g.* a high glucose consumption for energy production.[83] Moreover, they possess specific saccharide receptors exclusively expressed by certain cancers. Wild *et al.* reported, that a poly(pentafluorostyrene) (PPFS) based glycopolymer, carrying galactose (Gal) as targeting unit and a terpyridine (tpy) chelated Pt(II) species as active agent, has a higher anticancer activity than cisplatin, even in cell growth/division inhibitor-resistant cells. The mechanism of action is apoptosis, *i.e.* programmed cell death, which is induced by DNA-intercalation and well-known for square-planar tpy-Pt(II) complexes.[86-88] However, due to the PPFS backbone, the polymer suffered from a poor water solubility. This problem can be overcome by using copolymers of the water soluble PEtOx and ButEnOx, whose double bonds can be exploited to attach sugar targeting units as well as the cytotoxic Pt(II) species (Scheme 4-3). To this end, P($EtOx_{30}$-*stat*-$ButEnOx_{10}$) (**P19**) was first partially functionalized with 6-([2,2':6',2''-terpyridin]-4'-yloxy)hexane-1-thiol, as platinum chelating moiety, using the thiol-ene photoaddition reaction. The success of the reaction was shown by a growing molar mass as measured by SEC (Table 4-3) and appearing tpy signals in the aromatic region of the ^1H NMR spectrum. Moreover, an absorption of the tpy unit was detected in the UV detector of the SEC, which was congruent with the RI signal of the polymer (Figure 4-5).

In a next step the targeting sugar units were attached to the polymer backbone by the reaction of the remaining double bonds with acetyl protected thioglucose (Ac_4GlcSH) and thiogalactose (Ac_4GalSH), respectively (Scheme 4-3). To ensure a full functionalization of the ButEnOx units an excess of thio-sugar was used and removed after reaction by preparative

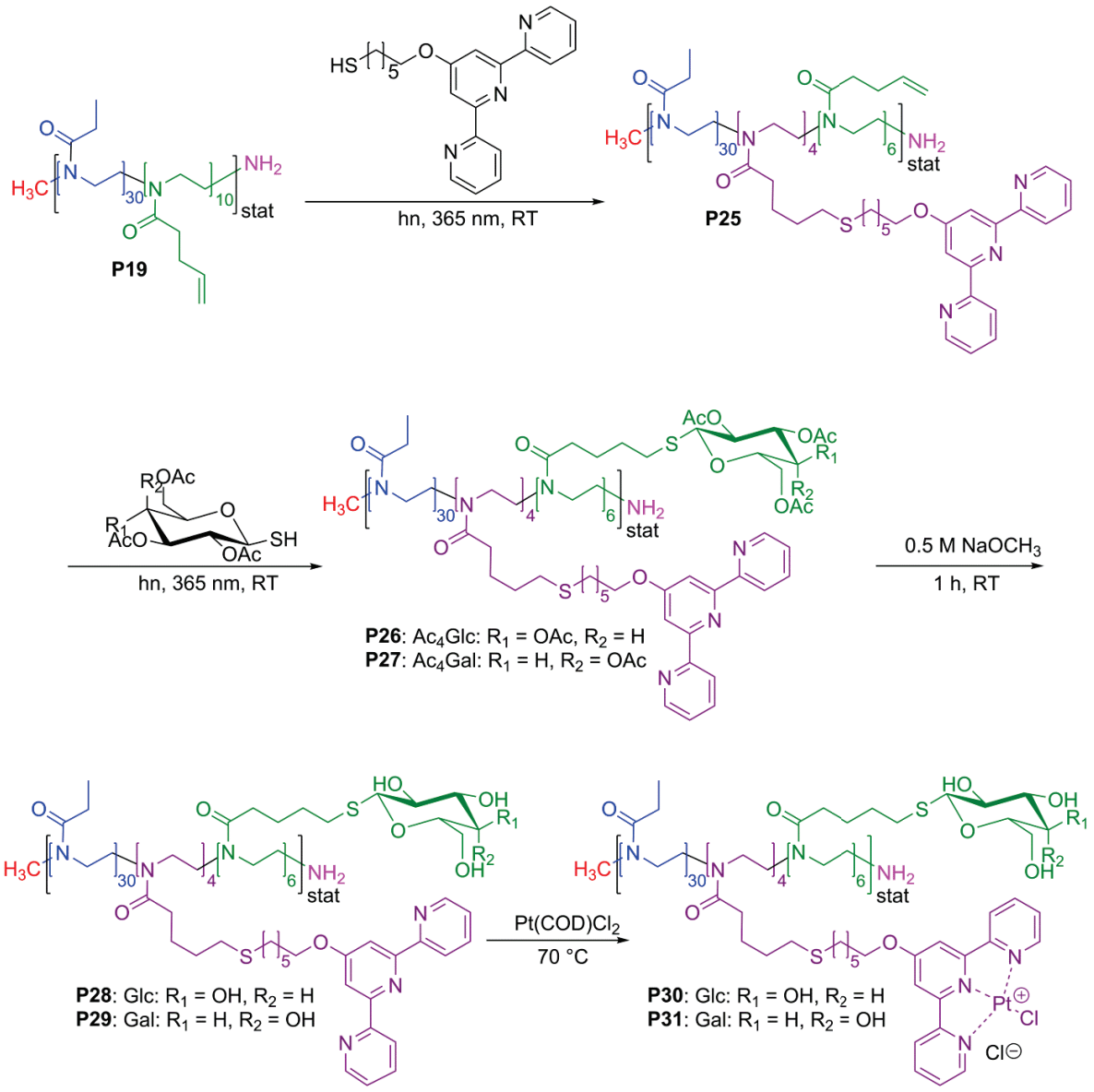

Scheme 4-3. Schematic representation of the synthesis of sugar and platinum containing POx.

size exclusion chromatography. Characterization by ^{1}H NMR spectrometry revealed the successful conversion, since all double bond signals disappeared, while new peaks, typical for acetylated sugars, were observed (for Glc see Figure 4-6).

SEC analysis revealed an increasing molar mass with no change of the PDI value in case of Glc and an insignificant change for Gal (Table 4-3).

Table 4-3. SEC data of the prepared poly(2-oxazoline)s.

Polymer	Composition	M_n (g/mol)[a)]	PDI[a)]
P19	$EtOx_{30}$:$ButEnOx_{10}$	6,980	1.19
P25	$EtOx_{30}$:$ButEnOx_6$:$tpyButOx_4$	8,000	1.21
P26	$EtOx_{30}$:$Ac_4GlcButOx_6$:$tpyButOx_4$	9,340	1.21
P27	$EtOx_{30}$:$Ac_4GalButOx_6$:$tpyButOx_4$	9,360	1.23
P28	$EtOx_{30}$:$GlcButOx_6$:$tpyButOx_4$	11,980	1.22
P29	$EtOx_{30}$:$GalButOx_6$:$tpyButOx_4$	11,800	1.23
P30	$EtOx_{30}$:$GlcButOx_6$:$PtButOx_4$	11,560	1.23
P31	$EtOx_{30}$:$GalButOx_6$:$PtButOx_4$	12,370	1.29

[a)]Determined by SEC (eluent: DMAc + 0.21% LiCl, calibration: PS).

Subsequent deprotection with sodium methoxide yielded free hydroxyl groups on the sugar moieties, which are important for targeting and good water solubility. The ^{1}H NMR spectra revealed a shift of the sugar signals, known from other sugar functionalized POx,[89, 90] and the disappearance of the peaks of the acetyl protecting groups at around 2 ppm (Figure 4-6). The tpy signals remained unchanged. Another proof for the successful deprotection was the disappearance of the C=O band of the acetyl protecting groups at 1,747 cm^{-1} (Glc) and 1,745 cm^{-1} (Gal), respectively, in the FT-IR spectra (for Glc see Figure 4-5B). SEC characterization revealed a change in molar mass (Table **4-3**). Although the theoretical molar masses are lower after the reaction, a shift to higher molar masses was observed. This finding was reported earlier for other sugar decorated POx and is ascribed to the increasing hydrodynamic volume in DMAc.[90]

In the last step the active Pt(II) species, which can induce cell death, was obtained by complexation reaction of tpy and platinum, using a very efficient and mild route with $Pt(COD)Cl_2$ in water. The side product cylcooctadiene was removed by washing the aqueous phase with diethyl ether. Characterization by ^{1}H NMR spectroscopy showed a broadening of the tpy signals, indicating the successful complexation (Figure 4-6).

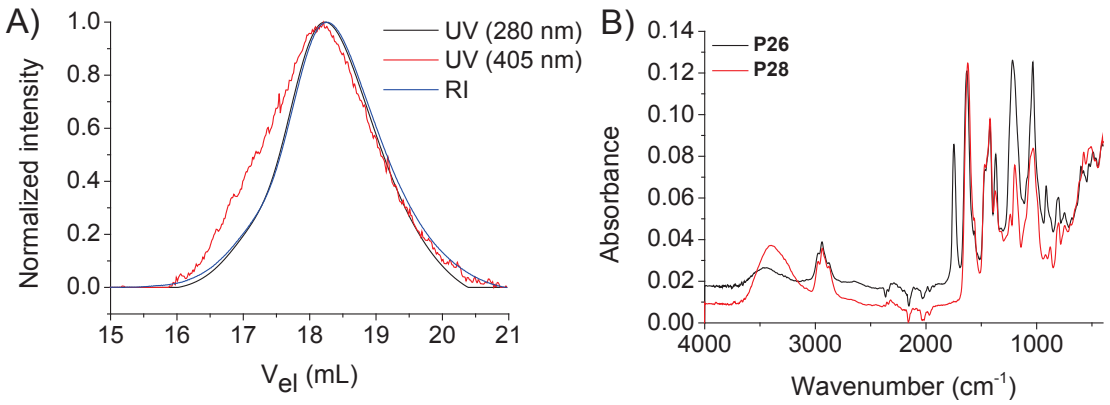

Figure 4-5. A) Overlay of the SEC curves of **P25** measured with an UV (280 nm and 405 nm) and a RI detector, respectively. B) ATR-FT-IR spectra of protected (**P26**) and deprotected (**P28**) galactose glycopolymers.

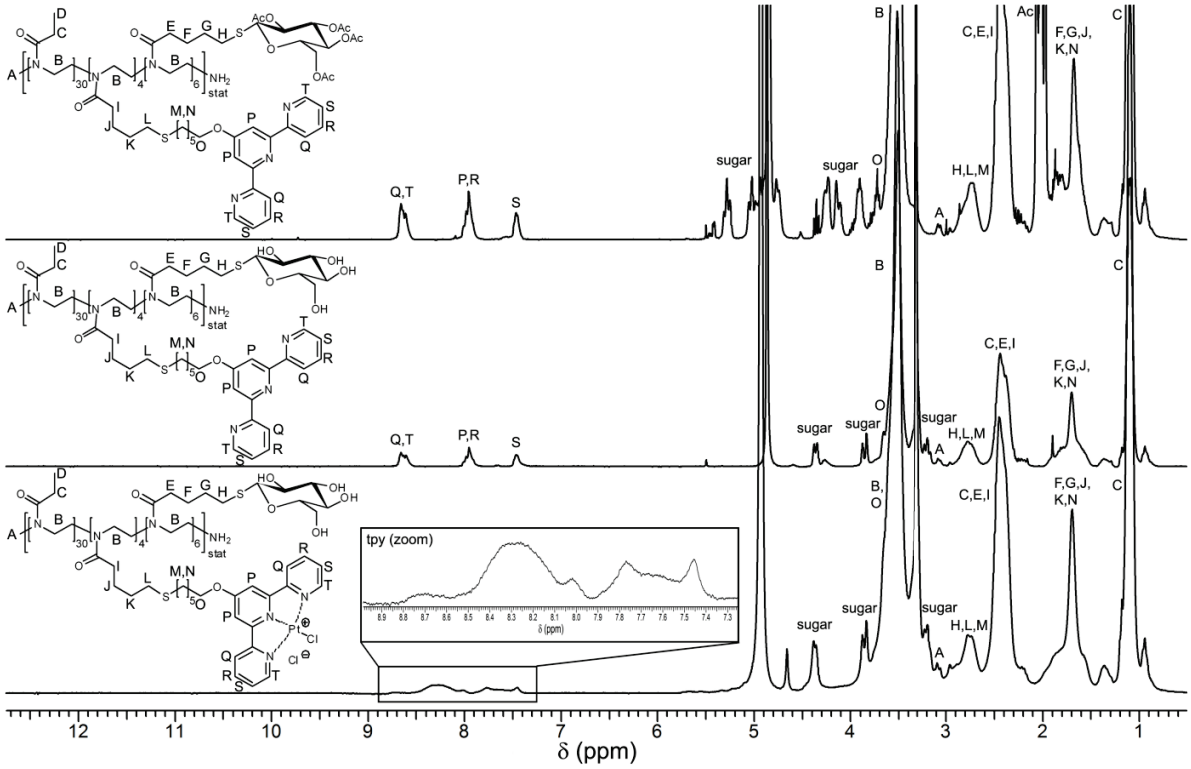

Figure 4-6. ^{1}H NMR spectra of (top) P(EtOx$_{30}$-*stat*-(Ac$_4$GlcButOx)$_6$-*stat*-tpyButOx$_4$) **P26**, (middle) P(EtOx$_{30}$-*stat*-GlcButOx$_6$-*stat*-tpyButOx$_4$) **P28**, and (bottom) P(EtOx$_{30}$-*stat*-GlcButOx-*stat*-PtButOx$_4$) **P30** (300 MHz, CD_3OD).

SEC analysis after complexation revealed a shoulder at lower elution volumes, *i.e.* higher molar mass, for glucose (**P30**) but to a higher extent for the galactose functionalized polymer (**P31**). Consequently, the PDI values are increasing, but do not exceed 1.30 (Table **4-3**). This finding might be ascribed to polymer-polymer coupling and led in case of fructose after deprotection (no Pt complexation) to the formation of a cross-linked hydrogel (data not shown).

Although having hydrophilic and hydrophobic domains, the polymers showed no self-assembly in water even at a concentration of 2 mg mL^{-1}. Dynamic light scattering (DLS) measurements gave only hydrodynamic radii of about 3 to 4 nm belonging to the free polymer chains.

To investigate the potential of the platinum containing glycopolymer as anti-cancer drug, their *in vitro* cytotoxicity and influence on blood integrity was studied and compared to cisplatin.

The hemolytic activity, *i.e.* the potential for damaging the cell membranes of erythrocytes, was investigated by photometrical determination of the hemoglobin release caused by the incubation with different concentrations of the glycopolymers and cisplatin (Figure 4-7A). Adverse hemolytic side reactions with red blood cells, representing the major cellular compartment of the blood, were observed in a concentration dependent manner.

The cytotoxicity was examined against mouse fibroblast L929 cells, human embryonic kidney cells HEK 293, and human hepatocytes HepG2 (Figure 4-7B). For both, cisplatin and the two glycopolymers, a dose dependent cytotoxicity was observed, with a higher activity of cisplatin at equimolar platinum amounts. However, cisplatin is a small molecule and, hence, *in vivo* the major part is excreted fast from the body (elimination half-life of 43 min),[91, 92] provoking the need for a high dosage which results in more severe side effects. In contrast, PEtOx-based polymers are known to show the so-called “stealth effect”, prolonging the blood circulation time, which can lead to an accumulation of the active compound in cancer tissue (EPR effect). Moreover, the attached sugar moieties might very likely promote the uptake by cancer cells, since neoplastic cells overexpressed sugar receptors on their cell surface. Therefore, it is assumed that the glycopolymers, although having a lower *in vitro* activity than cisplatin, might have a better performance *in vivo*. Assuming the need of a relatively low *in vivo* concentration necessary for cytotoxic performance and effectiveness, the observed hemolytic activity of the

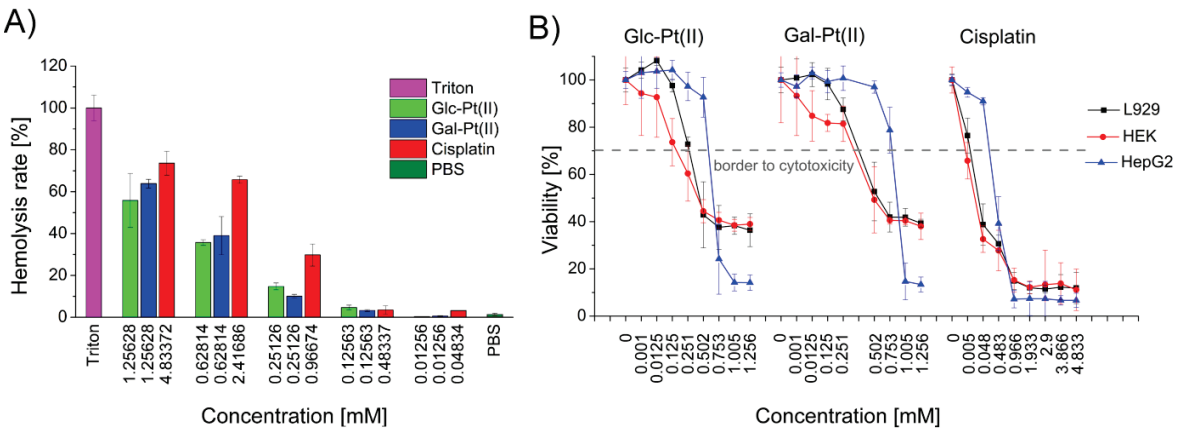

Figure 4-7. A) Photometric determination of hemolytic activity of cisplatin and the glycopolymers Glc-Pt(II) (**P30**) and Gal-Pt(II) (**P31**) after incubation for 1 h at 37 °C. Triton X-100 (1%) served as positive and PBS as negative control. Experiments were run in triplicate and were repeated once; data are presented as the mean percentage ± SD of hemolytic activity compared to the positive control set as 100%. B) Cell viability of L929 mouse fibroblasts, human embryonic kidney cells HEK 293, and human hepatocytes HepG2 after incubation with glycopolymers Glc-Pt(II) (**P30**) / Gal-Pt(II) (**P31**) and cisplatin at different concentrations for 24 hours. Cells incubated only with culture medium served as control. The cell viability was determined by XTT assay according to ISO 10993-5. Data are expressed as mean ± SD of six determinations

glycopolymers at higher concentrations as assessed *in vitro* might not be of clinical importance.

To conclude, platinum containing 2-oxazoline-based glycopolymers represent promising candidates for anticancer therapy, but a screening of their *in vivo* performance is necessary. In addition, the chosen synthetic approach allows the variation of the sugar/platinum content and with it the adjustment of the cytotoxic activity of the polymer.

5. Poly(2-oxazoline)-based cationic polymers for gene delivery

Part of this chapter have been / will be published in P7) M. Bauer, L. Tauhardt, H. M. L. Lambermont-Thijs, K. Kempe, R. Hoogenboom, U. S. Schubert, D. Fischer, in preparation. P8) L. Tauhardt, K. Kempe, U. S. Schubert, *J. Polym. Sci., Part A: Polym. Chem.* **2012**, *50*, 4516-4523. P9) S. Ochrimenko,[#] A. Vollrath,[#] K. Kempe, L. Tauhardt, S. Schubert, U. S. Schubert, D. Fischer, *Carbohydr. Polym.* **2014**, *113*, 597-606. P10) A. C. Rinkenauer,[#] L. Tauhardt,[#] F. Wendler, K. Kempe, M. Gottschaldt, A. Träger, U. S. Schubert, *Macromol. Biosci.*, accepted 07.10.2014. P11) A. C. Rinkenauer,[#] A. Vollrath,[#] A. Schallon, L. Tauhardt, K. Kempe, S. Schubert, D. Fischer, U. S. Schubert, *ACS Comb. Sci.* **2013**, *15*, 475-482. P12) M. Wagner, C. Pietsch, L. Tauhardt, A. Schallon, U. S. Schubert, *J. Chromatogr. A* **2014**, *1325*, 195-203. P13) C. Englert, L. Tauhardt, M. Hartlieb, K. Kempe, M. Gottschaldt, U. S. Schubert, *Biomacromolecules* **2014**, *15*, 1124–1131.

Gene delivery and gene knockdown/silencing using DNA or RNA drugs are alternative approaches investigated for anti-cancer therapy but also for the healing of other diseases caused by genetic disorders. However, due to rapid degradation by serum nucleases nucleic acids are unstable under *in vivo* conditions and, hence, need to be protected. This can be accomplished using cationic polymers as transport carriers (vectors). By electrostatic interactions with the phosphates of nucleic acids their primary, secondary, or tertiary amines are able to complex genetic material, forming the so called “polyplexes” (Figure 5-1). The protected genetic material enters the cells by endocytosis. The low intracellular pH value causes the protonation of the cationic polymer inside the endosome. The accumulation of protons, brought into the cell by the endosomal ATPase is accompanied by the influx of chloride counter ions, leading to a large increase of ion concentration and an osmotic swelling of the endosome. Moreover, the protonation causes internal charge repulsion, resulting in the expanding of the polymeric network. This volume increase leads to the rupture of the endosome membrane and the polyplex is released into the cytosol. This mechanism is often referred to as “proton-sponge-effect”[93] and is controversially discussed since also other ways

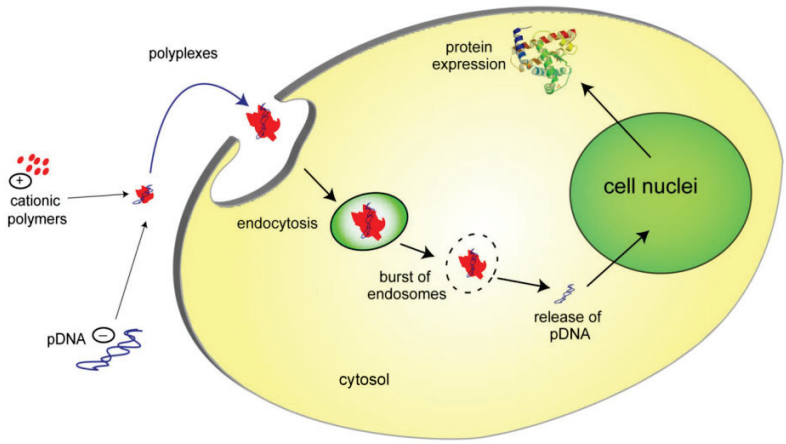

Figure 5-1. Schematic representation of a gene transfer using plasmid DNA and cationic polymers as non-viral vector.[94]

of uptake were discovered. After the release from the polyplex, the RNA remains in the cytosol, while plasmid DNA (pDNA) is taken up into the nucleus. Besides being used as non-viral vector for gene delivery, LPEI also represents an interesting starting material for the synthesis of hydrogels for DNA captures and release. Here, the synthesis, characterization, and pharmaceutical investigation of LPEI, LPEI modifications with biocompatible materials, and cationic poly(2-oxazoline)s are reported and will be discussed in the following subchapters

5.1. Linear poly(ethylene imine)s and approaches to reduce their cytotoxicity

The "gold standard" for gene delivery is linear poly(ethylene imine) (LPEI), a POx derivative obtained by acidic or basic hydrolysis of the amide bonds (Scheme 5-1). Using microwave reactors, it is possible to synthesize LPEIs in a highly reproducible manner, which is important with regard to pharmaceutical screenings and applications.[95, 96] Unfortunately, the harsh synthesis conditions are tolerated only by a limited number of end groups such as hydroxyl, amine, or azide.[96, 97] This fact diminishes the possibilities of a selective functionalization without destroying secondary amine groups, which are essential for the binding of the nucleic acids. However, the functionalization of LPEI is necessary, since it has not only a poor water solubility at temperatures below its melting point[95, 96] but also shows an increasing cytotoxicity with growing molar mass, while the transfection efficiency (TE) shows the

opposite trend.[98, 99] Investigations to overcome this problems aim at the modification with biocompatible, water soluble compounds such as PEG.[100-105] Another approach, that was investigated, is the usage of partially hydrolyzed POx, in particular partially hydrolyzed PEtOx (PHPEtOx) (Scheme 5-1). Using microwave synthesizers, the degree of hydrolysis (DH) can be accurately and easily adjusted *via* the hydrolysis time. In this way, PHPEtOx with an overall DP of 200 and different degrees of hydrolysis have been prepared (**P32-P35**, Table 5-1), and the influence of the charge density on different parameters, such as the polyplex size, the transfection efficiency, and the cytotoxicity, has been studied. For comparison, LPEIs (**P37-P42**) with DPs resembling the number of ethylene imine units in the PHPEtOx have been synthesized (Table 5-1).

Biological investigations revealed steadily decreasing cell viabilities with increasing molar mass for LPEI. While PHPEtOx and LPEIs with a DP < 175 were non-toxic even at a high polymer nitrogen to DNA phosphate (N/P) ratio of 50, LPEIs with a DP ≥ 175 reduced the cell viability below the critical value of 70% (Figure 5-2). However, although having similar or even lower polyplex sizes and comparable zeta potentials, the PHPEtOx showed significantly reduced transfection efficiencies compared to the corresponding LPEIs (Figure 5-2). This is ascribed to the reduced polyplex stability, leading to an insufficient protection of the DNA against enzymatic degradation. The poor DNA binding capacity of the PHPEtOx can be explained with the statistical distribution of the ethylene imine units within the copolymer. Some of the amine groups are not usable for an efficient DNA complexation, since the amine sequence is either too short or sterically blocked by the adjacent ethyl side chains. In addition, the antifouling character of the PEtOx hampers the interaction with the genetic material.

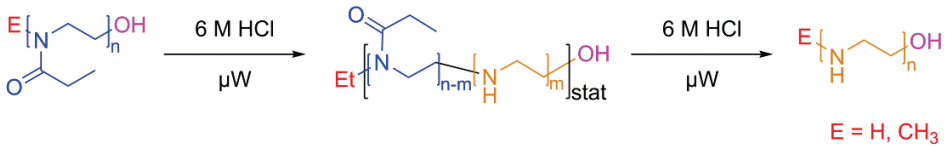

Scheme 5-1. Schematic representation of the synthesis of partially hydrolyzed poly(2-ethy-2-oxazoline) (PHPEtOx) and linear poly(ethylene imine) (LPEI).

Table 5-1. SEC data of the different synthesized PHPEtOx and LPEIs.

Polymer	EtOx:LPEI[a)]	Degree of hydrolysis (%)[a)]	M (^{1}H NMR) (g/mol)[a)]	M_n (SEC) (g/mol)[b)]	PDI[b)]
P32	158:42	21	17,500	33,010	1.38
P33	118:82	41	15,260	26,160	1.54
P34	88:112	56	13,580	19,290	1.73
P35	50:150	75	11,450	11,100	1.85
P36	28:172	86	10,220	13,810	1.64
P37	0:40	> 97	1,760	10,900	1.12
P38	0:80	> 97	3,480	16,800	1.22
P39	0:100	> 97	4,340	21,100	1.16
P40	0:150	> 97	6,490	27,400	1.27
P41	0:175	> 97	7,570	19,340	1.33
P42	0:200	> 97	8,650	17,450	1.57

[a)]Calculated from ^{1}H NMR spectroscopy, [b)]determined by SEC (eluent: hexafluoroisopropanol; calibration: PS).

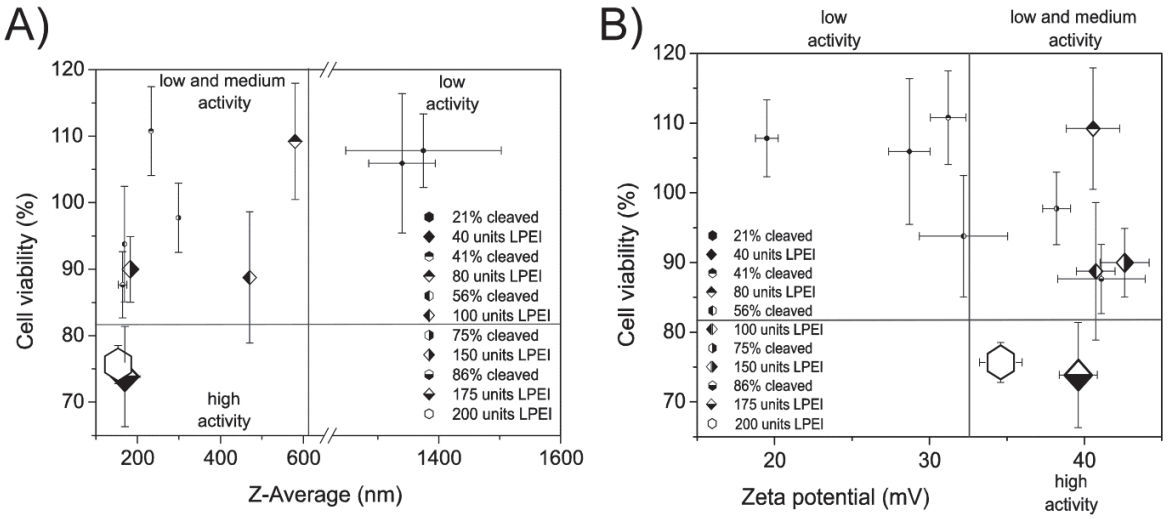

Figure 5-2. Comprehensive illustrations the relationships between the physicochemical and biological properties of PHPEtOx and LPEI polyplexes formed at N/P 25 (A) Z-average and (B) zeta potential of the polymers were plotted against the cell viability while transfection efficiency is illustrated by the icon size (the larger the icon size, the higher the transfection efficiency).

One possible approach to avoid the problem of sterically shielded ethylene imine units is the design of (well-defined) block copolymers of PEtOx and LPEI. As shown above, the acidic or basic hydrolysis of POx only yields statistically cleaved copolymers, making the synthesis of POx-LPEI block copolymers challenging. However, it has been reported that the sterical hindrance and, therefore, the type of side chain significantly influences the rate of hydrolysis.[95, 106] The more bulky the rest is, the slower the POx side chain is cleaved. This leads to the following order for the rate of hydrolysis: H > Me > Et > Ph. Since water solubility is a prerequisite for biological application, only polymers based on 2-*H*-2-oxazoline (HOx), MeOx, EtOx, or 2-*iso*propyl-2-oxazoline (*i*PrOx) are suitable as starting material. Unfortunately, the hydrolysis rates of PMeOx and PEtOx do not differ significantly for a selective hydrolysis. However, tests showed that poly(2-*H*-2-oxazoline) (PHOx) can be fully hydrolyzed to LPEI within 10 minutes using 3 M NaOH at 100 °C in a microwave synthesizer. Under the same conditions PEtOx is only hydrolyzed by 2% after 1 min, 6% after 5 min, and 8% after 10 min, respectively. When the reaction time was increased to 4 h the DH was about 12%. Based on this observation, it was investigated if PEtOx-*b*-LPEI can be obtained by selective basic hydrolysis of P(EtOx-*b*-HOx) (Scheme 5-2). To this end, the HOx monomer was synthesized applying an optimized procedure compared to earlier literature reports. Investigations of the homopolymerization kinetics revealed the living character of the polymerization, *i.e.* a linear first order kinetic plot was obtained. The polymerization rate was calculated to be kp = 0.0193 L mol^{-1} s^{-1}. PHOx was characterized by means of ^{1}H NMR spectroscopy and MALD-TOF-MS, showing the successful polymerization.

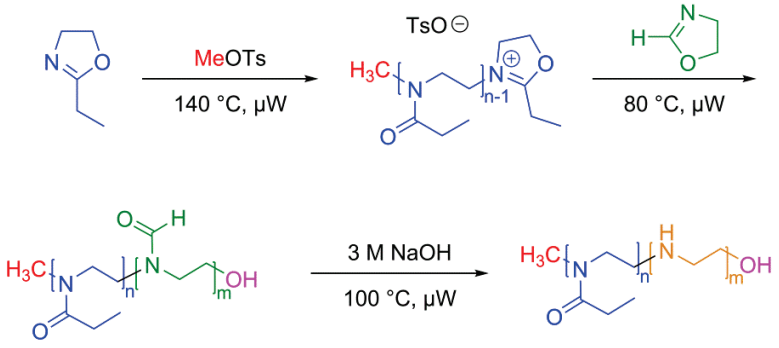

Scheme 5-2. Schematic representation of the synthesis of PEtOx-*block*-LPEI.

In the next step, P(EtOx-*b*-HOx) was prepared by sequential monomer addition. To determine the exact length of the starting block, always a reference PEtOx homopolymer was synthesized by reacting a part of the stock solution under the same conditions. A problem that arose during the polymerization of P(EtOx-*b*-HOx) is the precipitation during the polymerization, limiting the maximal length of the PHOx block. Moreover, the polymer becomes insoluble in anything but water, when the DP of the HOx block becomes too high. This was also observed for PHOx homopolymers and is ascribed to the formation of strong hydrogen bonds between the polymer molecules, due to interactions of the oxygen and hydrogen of the formyl side chains. This assumption is supported by infrared (IR) spectroscopy measurements on PHOx homopolymers, where a broad band at 3400 cm^{-1}, typical for hydrogen bonds, can be found. A good EtOx to HOx ratio was found to be n/m = 4/1. For this ratio the polymer is still soluble in other polar solvents such as methanol, DMSO, and *N,N*-dimethylacetamide. Three different P(EtOx-*b*-HOx) with a EtOx/HOx ratio of 4/1 and their corresponding PEtOx reference homopolymers were synthesized and characterized by ^{1}H NMR spectroscopy, MALDI-TOF-MS and SEC (Table 5-2), showing the formation of the copolymers.

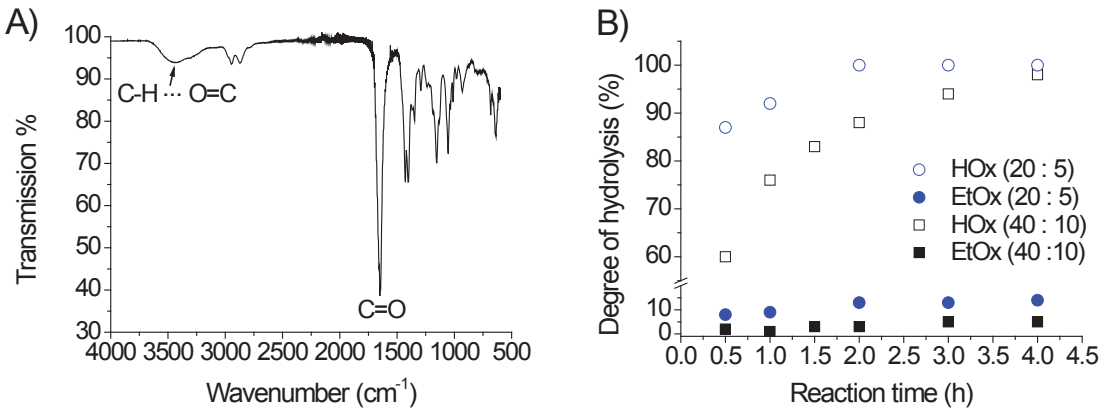

Figure 5-3. A) ATR-FT-IR of PHOx and B) kinetics of the hydrolysis of P(EtOx-*b*-HOx) (100 °C, 3 M NaOH). The degree of hydrolysis was determined by ^{1}H NMR spectroscopy.

Table 5-2. SEC data for the different P(EtOx-*b*-HOx) copolymers and the corresponding reference PEtOx homopolymers measured using different SEC systems.

Polymer	EtOx:HOx	DMAc + 2.1% LiCl		Water + 0.1% TFA + 0.05 M NaCl	
		M_n (g/mol)[a)]	PDI[a)]	Mn (g/mol)[a)]	PDI[a)]
P43	20 : 0	1,950	1.12	1,870	1.16
P44	20 : 5	3,100	1.27	1,980	1.23
P45	20 : 0	1,780	1.11	1,730	1.17
P46	20 : 5	2,280	1.17	1,850	1.29
P47	40 : 0	3,240	1.16	2,240	1.37
P48	40 : 10	4,660	1.26	2,420	1.40

[a)]Calibration against PEG.

In a last step, the hydrolysis kinetics of the different P(EtOx-*b*-HOx) under basic condition (3 M NaOH) at 100 °C were investigated. The degree of hydrolysis of each block was determined by ^{1}H NMR spectroscopy. The assumption that the PHOx block hydrolyzes much faster than the PEtOx block could be confirmed. The side chain cleavage in the PEtOx block was only about 5% for n/m = 40/10 and 14% for n/m = 20/5 when full cleavage of the PHOx side chain was achieved. This is in good agreement with the DH for the basic hydrolysis of the reference PEtOx homopolymers. Moreover, it was found that the copolymer with n/m = 20/5 hydrolyzed much faster than the copolymer with doubled block lengths. However, the block copolymer with n/m = 40/10 could be hydrolyzed much more selectively (Figure 5-3B). The obtained PEtOx-*b*-LPEI could be characterized by ^{1}H NMR spectroscopy and MALD-TOF-MS. Additional SEC measurements revealed a shift of the SEC curve after hydrolysis. However, due to missing standards, it was not possible to obtain reliable molar masses and PDI values for this type of cationic polymers. In addition, the synthetic problems caused by the PHOx block hamper the preparation of PEtOx-*b*-LPEIs with pharmaceutical relevant molar masses. Further investigations on developing alternative synthesis routes or the identification of suitable solvents for the polymerization of HOx are required.

Another approach to reduce the cytotoxicity of LPEI is its modification with dextrans. To this end, primary amine bearing LPEIs of different molar masses (860 and 1,720 g/mol) have been

prepared (Scheme 5-1) and coupled to dextran using: A) Reductive amination of aldehyde functionalized dextran (CHO-dex), B) EDC promoted coupling of LPEI to carboxymethylated dextran (CM-dex), and C) carbamate formation *via* activation of dextran with 4-nitrophenyl carbonate-substituted dextran (NPC-dex) followed by reaction with LPEI (Scheme 5-3).[107-109] While reductive amination and EDC coupling were found to be well-suited techniques for the synthesis of dextran-*graft*-linear poly(ethylene imine) (dex-*g*-LPEI), the carbamate formation method resulted in cross-linking during the reaction of 4-nitrophenyl carbonate-activated dextran with the LPEI, yielding insoluble products at higher DS. Therefore, this approach was not further investigated.

Applying the described methods, CM-dex-*g*-LPEIs and CHO-dex-*g*-LPEIs with varying degrees of substitution (DS) and varying LPEI chain lengths (n = 20, 40) have been prepared to investigate the influence of the linking strategy on the physicochemical properties (complex size, surface charge, DNA binding and stabilization), the transfection efficiency, and the biocompatibility. It was found that the method used to couple the LPEIs to dextran significantly affects the biological properties, while the physicochemical properties were only

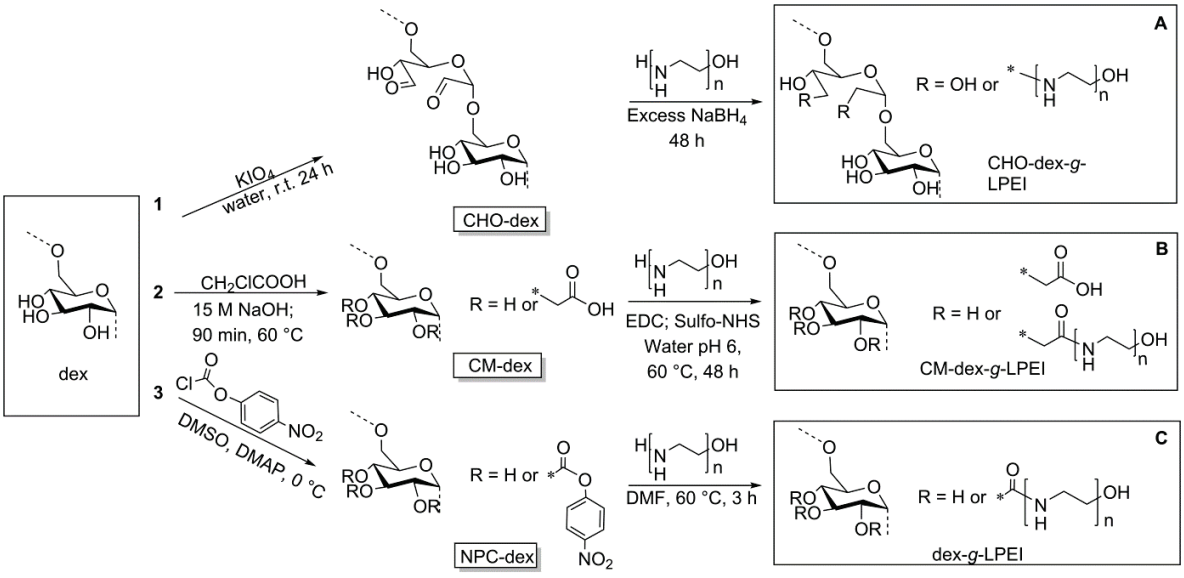

Scheme 5-3. Functionalization of dextran by (1) oxidation, (2) carboxymethylation, and (3) 4-nitrophenyl carbonate-activation and subsequent reaction with LPEIs *via* (A) reductive amination, (B) EDC coupling and (C) carbamate formation.

marginally affected. Independent from the linking strategy, the DS, and molar mass of LPEI, all polymers formed stable polyplexes with a positive surface charge and hydrodynamic diameters between 70 and 113 nm (in water). Moreover, all dex-*g*-LPEI/DNA polyplexes exhibited a good cyctocompatibility. However, a remarkable influence of the linking strategy on the transfection efficiency was observed. Despite a lower LPEI content, cationic dextrans obtained by EDC coupling exhibited a more than one order of magnitude increased transgene expression than the CHO-dex-*g*-LPEIs. In comparison, complexes formed from the low molar mass LPEIs showed almost no transgene expression. Blood compatibility tests revealed a higher red blood cell aggregation compared to the non-conjugated LPEIs, with CM-dex-*g*-LPEIs showing a lower erythrocyte aggregation activity than CHO-dex-*g*-LPEIs. The better hemocompatibility of the CM-dex-*g*-LPEIs is ascribed to their polyelectrolyte character and also known from other zwitterionic polymers (Chapter 4). The negatively charged carboxyl groups within the CM-dex backbone reduce the positive charge caused by the LPEI chains, accomplishing an overall charge that is advantageous for pDNA release and transfection efficiency.

In conclusion, the modification of LPEI with biocompatible compounds represents a suitable method to reduce its cytotoxicity. However, the TE might be reduced, due to the formation of less stable polyplexes and resulting enzymatic degradation.

5.2. Cationic poly(2-oxazoline)s

As reported, PHPEtOx show less cytotoxicity than LPEI but also display a lower TE with increasing PEtOx content.[110, 111] In addition, a decrease of the overall positive charge went along with a reduction of the polyplex stability and, hence, led to an inefficient cellular uptake and endosomal release. Moreover, the functionalization with PEG or hydrophilic POx (*e.g.* PMeOx, PEtOx) can result in an inefficient delivery, due to a reduced interaction with genetic material and the cellular membranes caused by the cell- and protein-repellent character of the polymers.[49, 56, 112-114] To overcome this drawback, additional polymer features have to be considered. Besides modifying polycations with "stealth" polymers,[11, 17] the introduction of more neutral or hydrophobic characteristics has been discussed for gene delivery applications.[115, 116] It is known from the development of antimicrobial POx that the

introduction of long alkyl groups leads to an enhanced membrane interaction.[117] Hence, it is assumed that the cellular uptake of modified cationic polymers, which is often reduced to the "stealth effect", can be improved by introducing hydrophobic moieties.

Based on this, the influence of hydrophobicity, amine type, and amine content on the transfection behavior was systematically investigated. To this end, cationic copolymers were prepared by thiol-ene photoaddition of primary and tertiary amines to POx copolymers of different side chain hydrophobicity, namely P(MeOx-*co*-ButEnOx) and P(MeOx-*co*-DecEnOx) (Scheme 5-4). MeOx was chosen as biocompatible comonomer to improve the water-solubility which is limited for P(EtOx-*co*-ButEnOx) and P(EtOx-*co*-DecEnOx) due to the LCST behavior of PEtOx.[118]

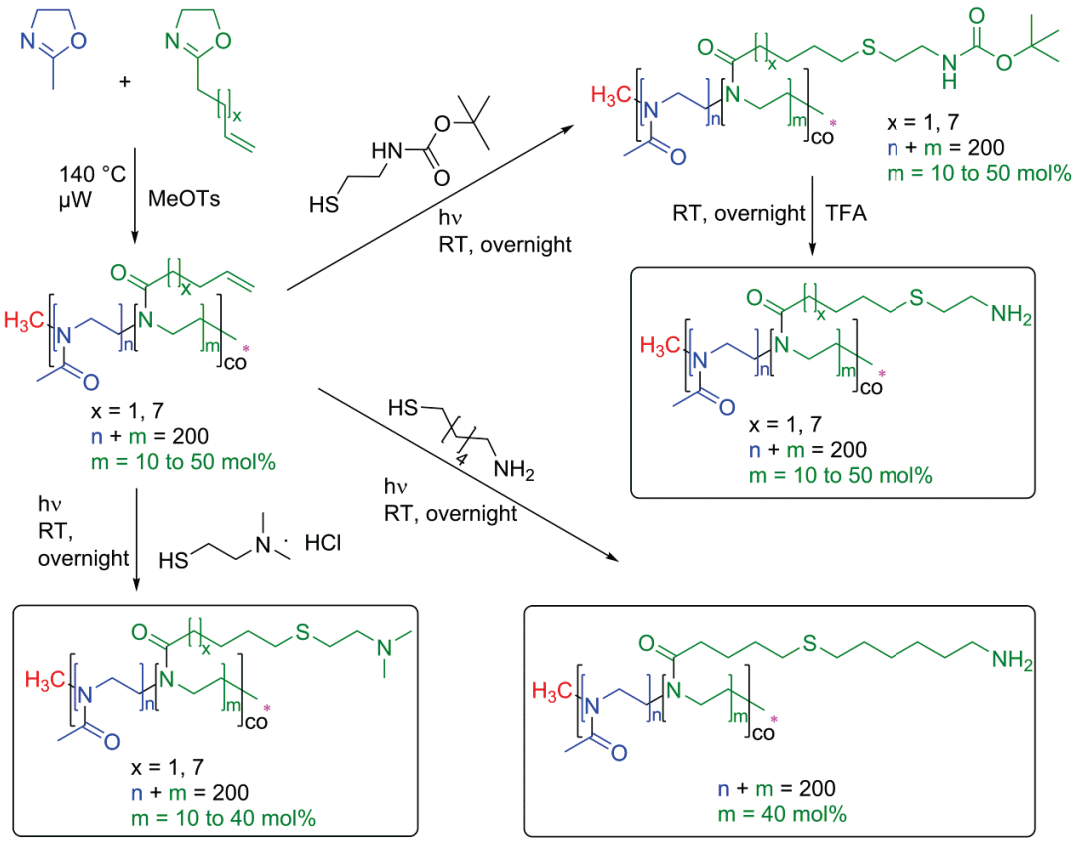

Scheme 5-4. Schematic representation of the synthesis of cationic POx.

First, the copolymerization kinetics of MeOx and ButEnOx were investigated at 140 °C with a [MeOTs]/[MeOx]/[ButEnOx] ratio of 1:90:10 and a total monomer concentration of 2 M in acetonitrile. Similar to the EtOx/ButEnOx (Chapter 4.2) copolymerization, first-order kinetic plots are obtained (Figure 5-4A). Having a higher polymerization rate, MeOx (k_p = 0.095 L mol^{-1} s^{-1}) is incorporated faster into the polymer chain than ButEnOx (k_p = 0.052 L mol^{-1} s^{-1}) indicative for the formation of a gradient copolymer. This is contrary to the copolymerization of EtOx and ButEnOx, where both monomers are incorporated with nearly the same rate. Characterization by size exclusion chromatography (SEC) revealed an increasing molar mass with increasing time (Figure 5-4B). The copolymerization kinetics of MeOx and DecEnOx were reported earlier by Dargaville *et al.*.[30]

The obtained results were used to prepare copolymers with a varying amount (10 to 50 mol%) of DecEnOx or ButEnOx, respectively, and an overall DP of 200 (Scheme 5-4). The polymers were obtained with acceptable PDI values for MeOx containing copolymers with DP > 100 (Table 5-3). In the next step, tertiary amine groups were introduced by thiol-ene photoaddition of 2-dimethylaminoethanethiol hydrochloride. Primary amines were obtained by thiol-ene reaction with 2-(Boc-amino)ethanethiol, followed by deprotection with trifluoroacetic acid. To investigate the influence of the side chain hydrophobicity and the sulfur position in more detail, the 40 mol% ButEnOx containing copolymer was reacted with 6-amino-1-hexanethiol

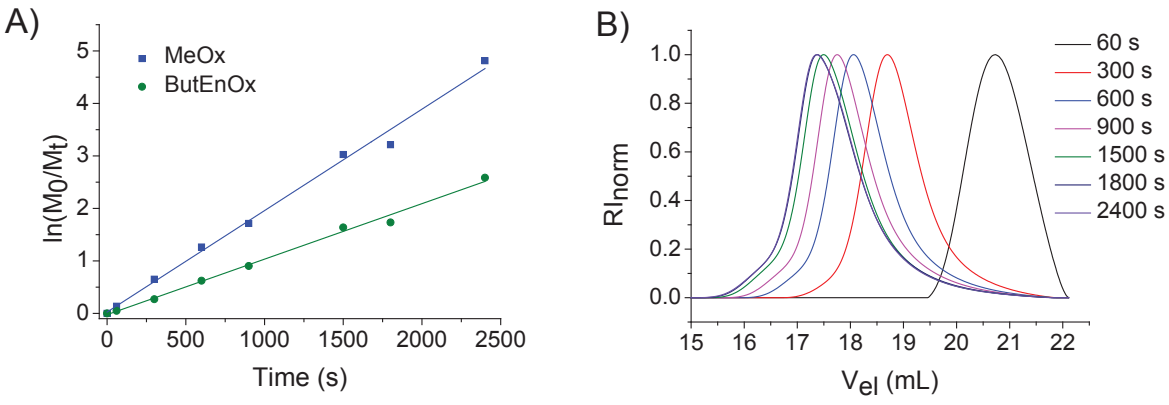

Figure 5-4. A) First-order kinetic plots of the copolymerization of MeOx and ButEnOx in acetonitrile at 140 °C with a total monomer concentration of 2 M and a [MeOTs]/[MeOx]/[ButEnOx] ratio of 1:90:10 (conversions were determined by GC measurements). B) SEC curves of the kinetic investigation.

Table 5-3. SEC data of the different cationic POx and their intermediates (Boc = protected primary amine, p = primary, t = tertiary, h = hexamethylene spacer).

MeOx-*co*-ButEnOx					MeOx-*co*-DecEnOx				
Polymer	**MeOx : ButEnOx**	**Amine**	**M_n[a] (g/mol)**	**PDI[a]**	**Polymer**	**MeOx : DecEnOx**	**Amine**	**M_n[a] (g/mol)**	**PDI[a]**
P49	180 : 20	-	22,800	1.43	**P69**	180 : 20	-	19,800	1.47
P50	160 : 40	-	23,300	1.46	**P70**	160 : 40	-	25,500	1.47
P51	140 : 60	-	23,300	1.49	**P71**	140 : 60	-	19,800	1.45
P52	120 : 80	-	22,200	1.56	**P72**	120 : 80	-	22,900	1.63
P53	100 : 100	-	20,300	1.48					
P54	180 : 20	Boc	26,000	1.43	**P73**	180 : 20	Boc	-	-
P55	160 : 40	Boc	29,000	1.46	**P74**	160 : 40	Boc	-	-
P56	140 : 60	Boc	29,500	1.47	**P75**	140 : 60	Boc	-	-
P57	120 : 80	Boc	32,000	1.50	**P76**	120 : 80	Boc	-	-
P58	100 : 100	Boc	27,700	1.47					
P59	180 : 20	p	24,100	1.44	**P77**	180 : 20	p	23,600	1.51
P60	160 : 40	p	23,200	1.40	**P78**	160 : 40	p	31,600	1.43
P61	140 : 60	p	27,400	1.40	**P79**	140 : 60	p	30,500	1.54
P62	120 : 80	p	29,100	1.52	**P80**	120 : 80	p	38,100	1.62
P63	100 : 100	p	28,500	1.26					
P64	180 : 20	t	20,440	1.43	**P81**	180 : 20	t	20,300	1.49
P65	160 : 40	t	19,560	1.43	**P82**	160 : 40	t	28,100	1.47
P66	140 : 60	t	18,120	1.45	**P83**	140 : 60	t	23,900	1.37
P67	120 : 80	t	20,180	1.35	**P84**	120 : 80	t	30,300	1.57
P68	120 : 80	p, h	34,200	1.31					

[a] Determined by SEC (eluent: DMAc + 0.21% LiCl, calibration: PS).

hydrochloride. The intermediates and the final products were characterized by means of ^{1}H NMR spectroscopy and SEC, confirming the successful synthesis. All in all, an 18-membered copolymer library was obtained and systematically investigated with regard to: 1) The ability of the copolymers to interact with pDNA and the cellular membrane, 2) their cellular uptake, 3) cytotoxicity, and 4) the transfection outcome.

The biological studies revealed that hydrophobic chains enhance the interaction with the cellular membrane. However, independent of the sulfur position polymers with long hydrophobic side chains (**P68-P84**) showed a high cytotoxicity, hemolysis, and LDH release, making them not suitable for gene delivery applications. POx with short side chains and tertiary amines were found to be biocompatible, but the interaction with the pDNA was too weak to efficiently protect the genetic material. Hence, the pDNA was released into the transfection media or inside the endosomes as demonstrated by heparin assay, and cellular uptake studies. For polymers with short side chains and primary amines, the optimal amine content was found to be at 40 mol%. While higher amine contents showed cytotoxic effects, polymers with a lower amine mol% revealed decreased TE values.

Table 5-4. Overview of all polymers with regard to the pharmaceutical characteristics and bottlenecks of the transfection process. Probable reasons for transfection failure or drawbacks are described as comments. Cytotoxicity (AlamarBlue), hemolysis and LDH were classified with 0 for no effect, 0.5 for middle occurrence, and 1 for high occurrence.

			EBA [%]	Size [nm]	ZP [mV]	Toxicity	Hemolysis	LDH	Uptake [%]	Heparin [U mg^{-1}]	TE [%]	comments
Short hydrophobic side chain (x = 1)	primary amines	10	80	255	-4	0	0	-	-	0	0	no polyplex formation
		20	72	178	22	0	0	-	-	3	8	labile polyplex
		30	72	110	40	0	0	-	-	10	6	?
		40	60	94	23	0	0	0	90	10	31	best performer!
		50	60	51	47	1	-	-	-	30	24	increased toxicity
	teriary amines	10	82	151	-6	0	0	-	-	0	1	no polyplex formation
		20	68	158	19	0	0	-	-	3	8	labile polyplex
		30	64	124	29	0	0	-	-	5	5	?
		40	57	105	29	0	0	0	60	5	3	inefficient uptake
x = 1		40	-	-	-	1	-	-	-	-	8	hexamethylene spacer, toxic
Long hydrophobic side chain (x = 7)	primary amines	10	69	152	-17	1	0	-	-	3	0	no polyplex formation
		20	46	105	28	1	1	-	-	10	6	toxic
		30	36	84	29	1	1	-	-	20	4	toxic
		40	30	97	34	1	1	1	80	50	6	toxic
	teriary amines	10	76	152	-9	0	0	-	-	0	0	no polyplex formation
		20	60	113	26	1	1	-	-	10	3	toxic
		30	50	84	30	1	1	-	-	20	6	toxic
		40	41	67	27	1	1	1	-	20	2	toxic
LPEI200			45	-	-	1	-	0	90	-	31	good performer but toxic

As a consequence **P62**, a polymer with a short ButEnOx based linker and a primary amine unit, was identified as material exhibiting superior properties to LPEI. It not only showed high transfection efficiencies similar to that of LPEI, but is non-toxic, even at high concentrations.

5.3. High-throughput screening of pharmaceutical properties of cationic polymers

As demonstrated, it is possible to synthesize large libraries of LPEI, PHPEtOx, and other cationic polymers, using synthetic robots and microwave synthesizers. A problem that arises from this large number of different polymers is the fast and efficient screening of their pharmaceutical properties. Commonly used techniques, such as the determination of binding affinity and polyplex stability by gel electrophoresis, are time-consuming and, hence, not suitable. However, the analysis and characterization of the biological and pharmaceutical properties of cationic polymers and their polyplexes in a high throughput (HT) manner is essential when polymer libraries with a large number of members are investigated. To this end, an automated combinatorial workflow was developed and validated by comparing the outcome with results of "classical" tests and literature values. Due to their wide-spread use and, hence, the excellent availability of data, linear (LPEI) and branched poly(ethylene imine)s (BPEI) of different DPs (n = 20, 200, and 600) were applied as model transfection agents. The automated formation of the polyplexes by complexation with pDNA was achieved using a liquid handling robot. The advantage of such a pipetting system is the possibility to systematically alter different parameters, such as the pH value, the buffer system, but also the polymer concentration. Polyplexes with different N/P ratios (N/P = 2.5, 5, and 10) were prepared and automatically distributed into different well plates for parallel analysis studies. The size of the polyplex was measured using a dynamic light scattering (DLS) plate reader, yielding average radii below the critical uptake size of 500 nm. Instead of using the elaborate and slow gel retardation assay, which is not suitable for the well plate format, the DNA binding and release properties were investigated using a fluorescence displacement assay with ethidium bromide (EB) and a heparin assay, respectively. Upon the formation of pDNA/polymer interelectrolyte complexes, EB is displaced from the DNA strand, leading to a decreased fluorescence signal. When heparin, a polyanion and a good competitor to negatively charged pDNA, is added to the polyplexes, the pDNA is released and EB can be intercalated again, leading to an increase in fluorescence intensity. The changes in fluorescence intensity

can be easily monitored using a fluorescence plate reader. In a similar manner the cytotoxicity of the polyplexes can be investigated. After seeding the cells into the well plate and incubation with polyplex suspension, the cell viability was detected by staining with the fluorescent dye Hoechst 33324, which crosses the cell membrane and stains the chromosomal DNA of the attached cells. The TE of the polyplexes was quantified using the enhanced green fluorescent protein (EGFP). Again a fluorescence plate reader was used for the determination of the fluorescence intensity. The measurements were complemented by microscope analysis, showing a good correlation between both methods.

The results obtained with the HT screening method corresponded well to results obtained by standard experiments and to literature values. Hence, the developed HT method is suitable for the investigation and characterization of large polymer libraries. Moreover, it enables the possibility to systematically vary different screening parameters, such as the pH value, the buffer system, N/P ratios, and concentrations.

5.4. Characterization of cationic polymers

A problem that arises for cationic polymers is their detailed characterization, in particular when they have a high molar mass. Determination of the molar mass distribution and the end groups by means of MALDI- and ESI-TOF-MS can only be done for polymers with a low DP and PDI, or even fail completely due to ionization issues. Moreover, the multiple charges can result in complex ESI spectra which are difficult to interpret. Molar mass determination by ^{1}H NMR spectroscopy can only be applied, if the polymer has a low DP so that the end groups, as reference for the mass calculation, are still visible. SEC characterization is also problematic, due to often strong column interactions of the positively charged polymers and the missing standards. The latter leads to large deviations between the calculated molar masses and values obtained from SEC measurements (*e.g.* Table 5-1). Viscosimetry is applicable, but suffer the drawback that the constants in the Kuhn-Mark-Houwink-Sakurada equation are not available for most cationic polymers. Techniques based on colligative phenomena are handicapped due to the required determination of the degree of protonation in water and with it the amount of species having counterions. Further important characterization methods like static light scattering (SLS) and analytical ultracentrifugation (AUC) only yield limited

information about the polydispersity index (PDI) of a sample. However, parameters like molar mass, radius, architecture, intermolecular interactions, and conformation strongly influence the resulting properties, and, hence, their knowledge is essential when structure-property relationships should be elucidated. A powerful tool with regard to the characterization of high molar mass samples is asymmetric flow-field flow fractionation (AF4), a technique where the polymers are separated in a trapezoidal channel according to their diffusion coefficient.[119] In contrast to chromatographic methods like SEC, the separation is achieved without any porous packing material but by applying a cross-flow perpendicular to the direction of the sample flow through a semipermeable membrane with a defined molar mass cut-off (MWCO). A detailed overview on AF4 is given elsewhere.[120] When coupled to UV/RI and multi angle laser light scattering (MALLS) detectors, AF4 can be used for the characterization of high molar mass LPEIs and other cationic polymers as validated by comparison with results obtained from analytical ultracentrifugation (AUC) and ^{1}H NMR. The values obtained from the AF4-MALLS (Figure 5-5) and the Zimm-plot, *e.g.* for $LPEI_{600}$ (M_n = 24.3 kg/mol, M_w = 32.0 kg/mol, PDI = 1.32), differed only slightly from the theoretical M_n, which was, in this case, calculated from the [M]/[I] ratio used for the synthesis of the PEtOx precursor. This slight difference probably derived from weighing errors, which are increased at high [M]/[I] ratios, since only a very small amount of initiator is required. With regard to the refractive index increment, which is essential for molar mass calculation by AF4, the studied PEIs reached the lower detection limit of the MALLS detector (low signal to noise ratio). In particular, low molar mass LPEIs (< 10 kg/mol) did not show a reliable light scattering signal, which can be distinguished from the baseline. A molar mass of 15 to 20 kg/mol was found to be the acceptable minimum for LPEI. For the low molar mass polymers the radius of gyration could not be obtained. Here, the minimum is around 8 to 10 nm.[121]

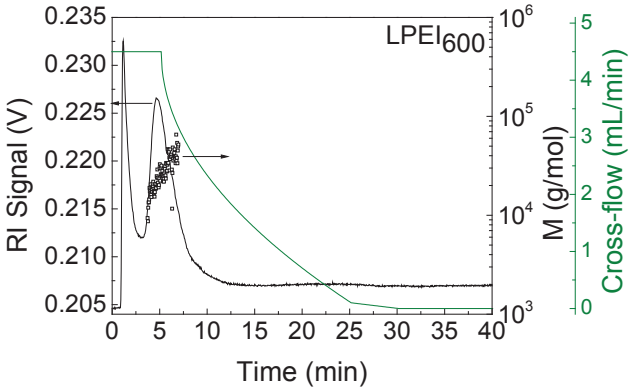

Figure 5-5. AF4 fractogram with the corresponding cross-flow rate and molar masses of $LPEI_{600}$ (solvent: water + 0.02% NaN_3).

5.5. LPEI hydrogels for DNA capture and release

Another field of application of LPEI, besides its use as vector in gene delivery, are DNA biochips. They play an important role in the analysis of genetic material and, hence, are interesting for applications in medicine and pharmacy as well as agriculture and food industry. In particular pathogens are of high interest. They can be detected by hybridization of their unique DNA/RNA sequences with DNA/RNA strands containing complementary nucleic acid sequences bound to the DNA chip. However, an essential prerequisite for a successful detection is the isolation, concentration, and purification of the nucleic acids from highly complex samples, such as blood and feces.[122] LPEI-based hydrogels are investigated as promising materials for this task, since they can bind and release DNA. Moreover, hydrogels have a higher loading capacity compared to two-dimensional systems, allowing the isolation of more genetic material.

The most common way to synthesize LPEI hydrogels is the cross-linking of the amine groups with difunctional compounds such as diisocyantes and diglycidyl ethers.[123-127] A major drawback of this method is that the amount of free secondary amine groups that remain after the cross-linking process cannot be determined, due to the insolubility of the product. However, knowing the exact amount of amine groups is essential for the calculation of the binding capacity. Therefore, the cross-linking has to be performed not *via* the amines but by

exploiting other functional groups. Widely-used functional moieties, *e.g.* for the synthesis of POx-based hydrogels, are double bonds. [30, 31, 128-130] Using dithiols they can be cross-linked *via* thiol-ene reaction. However, double bonds did not tolerate the harsh hydrolysis conditions of the LPEI synthesis and, hence, had to be introduced by post-hydrolysis modification. This was accomplished by the reaction of LPEI with *N*-succinimidyl-4-pentenate (Scheme 5-5). Appling this approach, it is possible to exactly calculate the amount of amine groups from the ^{1}H NMR spectrum of the obtained PButEnOx-*co*-LPEI precursors. PButEnOx-*co*-LPEIs with a total DP of 580 and degrees of functionalization (DF) between 15 and 95% have been prepared. Subsequent cross-linking *via* thiol-ene photoaddition using *bis*-functional 3,6-dioxaoctane-1,8-dithiol yielded stable hydrogels for DF above 18%. Their water uptake is 10 times more efficient from liquid phase than from the gas phase. Swelling values between 23 and 74% could be observed, dependent on the degree of cross-linking. The highest water uptake was shown by a hydrogel made from a PButEnOx-*co*-LPEI with a DF of 50%. However, for a fast DNA binding, the swelling values need to be improved, since DNA was taken up rather slowly, indicating a diffusion controlled process. Nevertheless, both the PButEnOx-*co*-LPEIs and nearly all hydrogels (exception: Hydrogels with 36% LPEI) were able to bind DNA, with a strong dependency on the LPEI content. Moreover, upon heparin addition the DNA was released up to 90% from the copolymers at room temperature after 32 min and up to 50% from the hydrogels at 90 °C after 80 min. The incomplete DNA release

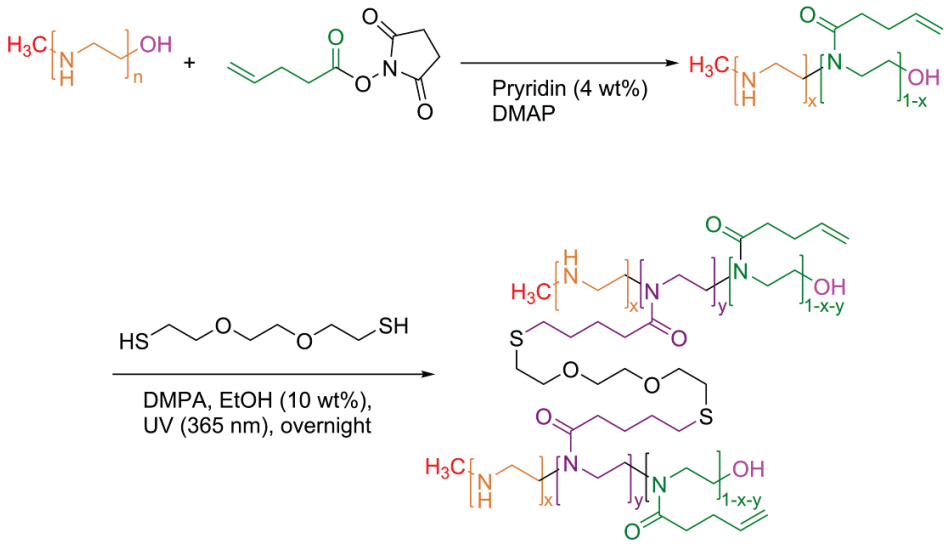

Scheme 5-5. Schematic representation of the synthesis of LPEI hydrogels.

from the hydrogels after 80 min can be ascribed to the slow, diffusion controlled process that was also observed for the DNA uptake. Since elevated temperatures accelerate the diffusion, a release within this period of time was only observed at elevated temperatures.

In conclusion, LPEI-based hydrogels, obtained by thiol-ene cross-linking of PButEnOx-*co*-LPEI, represent interesting compounds for the application in DNA biochips, since they are able to bind and release DNA. However, due to their low swelling values, the DNA uptake and release is rather slow and, hence, needs to be accelerated, *e.g.* by taking PHPEtOx instead of LPEI as starting materials.

6. Summary

Investigations within the scope of this thesis showed that poly(2-oxazolines) are promising alternatives for poly(ethylene glycol) (PEG), a polymer that is well-known and intensively used in many application fields, *e.g.* for drug delivery and antifouling coatings. Under conditions adopted to "real life" poly(2-ethy-2-oxazoline) (PEtOx) coatings attached to glass surfaces *via* a tetraether lipid and a silane linker, respectively, were able to reduce the biofilm formation on the substrate up to 66%. Moreover, the water soluble poly(2-methyl-2-oxazoline) (PMeOx) and PEtOx showed an excellent biocompatibility comparable to that of PEG. No hemolytic activity could be observed and cytotoxic effects only occurred after long term treatment at concentration much higher than the typically used therapeutic dose. By copolymerization with 2-(3-butenyl)-2-oxazoline (ButEnOx) and subsequent post-polymerization functionalization it was possible to synthesize zwitterionic, POx-based poly(sulfobetaine)s and poly(carboxybetaine)s, which showed a high biocompatibility and anticoagulant properties, *i.e.* they elongated the blood clotting time. Modified copolymers of EtOx and ButEnOx were further studied as potential materials for anticancer therapy. Thiol-ene photoaddition of terpyridine to the double bonds enabled the possibility for subsequent platinum complexation. In addition, the double bonds were exploited for the functionalization with sugars, *i.e.* glucose and galactose, as active targeting units. Investigation of the cytotoxicity of the final polymers against different cell lines showed the potential of the platinum containing glycopolymer as anticancer drugs.

Another important field for potential application of POx and their derivatives is gene delivery. In particular the "gold standard" linear poly(ethylene imine) (LPEI), a derivative obtained by acidic or basic hydrolysis of POx, is intensively investigated. To improve its water solubility and to reduce the cytotoxicity, while maintaining a high transfection efficiency (TE), a range of synthetic approaches for the modification with biocompatible compounds have been performed. Moreover, the influence of the structural changes on different parameters such as polyplex stability, cytotoxicity, and transfection efficiency has been investigated. In a first approach, partially hydrolyzed PEtOx (PHPEtOx) with different degrees of hydrolysis have

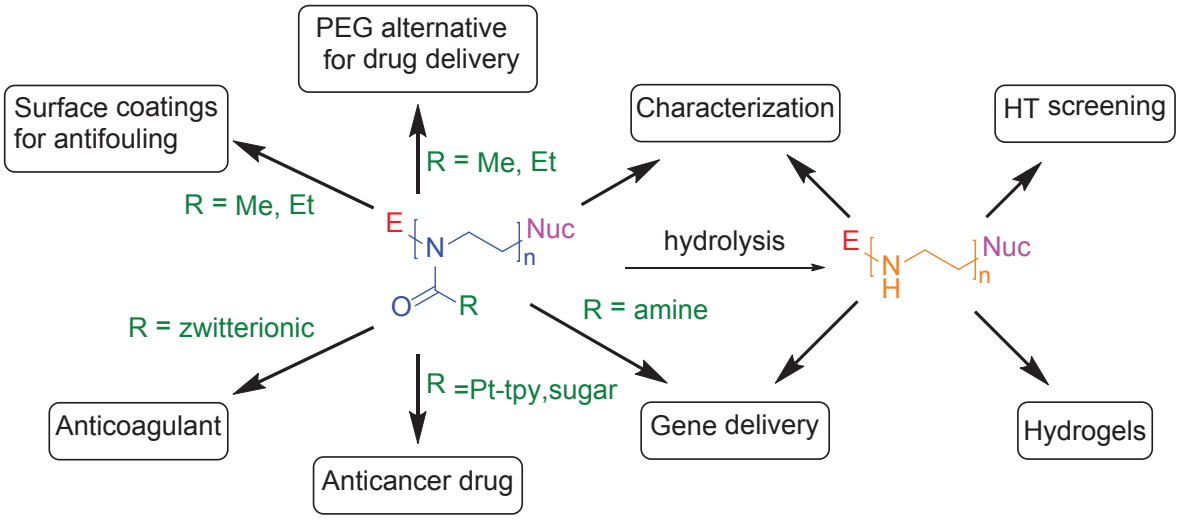

Figure 6-1. Overview of the versatility of poly(2-oxazoline)s and linear poly(ethylene imine) and the topics investigated within the thesis.

been prepared by adjusting the hydrolysis time. They were found to have a low cytotoxicity but showed a significantly decreased TE. The reason for this is the insufficient protection of the DNA against enzymatic degradation, due to the reduced polyplex stability. The latter is caused by the repellent character of PEtOx and the statistical distribution of the ethylene imine units within the copolymer, leading to sterically blocked amines and too short amine sequences for DNA binding. To overcome this problem, the synthesis of PEtOx-*b*-LPEI by selective, basic hydrolysis of P(EtOx-*b*-HOx) was investigated. Although a high selectivity for the HOx cleavage was observed, only polymers with short LPEI blocks and a maximal EtOx/LPEI ratio of 4/1 could be prepared. This was caused by the starting material P(EtOx-*b*-HOx), which precipitated during the polymerization when the degree of polymerization of the HOx block became larger. The resulting low molar masses of the PEtOx-*b*-LPEIs hampered the performance in pharmaceutical applications. Thus, the functionalization with another biocompatible compound, namely dextran, has been investigated. LPEIs of different molar masses bearing primary amine end groups were coupled to dextran applying different linking strategies. The best results were obtained from LPEIs attached to carboxymethylated dextran (CM-dex). These materials had a higher TE than the pure LPEIs and LPEIs coupled to aldehyde functionalized dextran (CHO-dex-*g*-LPEIs) and exhibited a lower erythrocyte

aggregation activity. This is ascribed to their polyelectrolyte character, which in general has a positive influence on the biocompatibility of compounds.

It was observed, and also reported in literature that the modification of LPEI with biocompatible, "stealth" polymers often decreases the polyplex stability. Due to the repellent character the interaction with the genetic material and the cell membranes is reduced. However, it is known from the development of antimicrobial POx that the introduction of alkyl groups enhances the interaction with the cellular membrane, a prerequisite an efficient for cell uptake and transfection. Therefore, an 18-member POx-based copolymer library with varying side chain lengths and hydrophobicity, varying amounts of amine (10 to 50%), and different types of amine (primary, tertiary) has been prepared and systematically investigated. It could be shown that polymers primary amines in the side chain are more efficient in protecting and delivering DNA. Moreover, it was found that polymers with longer alkyl side chains show an increased interaction with the cellular membrane. However, polymers with very long hydrophobic side chains had a high cytotoxicity, since they damaged the cellular membrane. The best compound was found to be a P(MeOx-*co*-ButEnOx)-based copolymer with primary amine groups and an amine content of 40 mol%. Here, no cytotoxicity but a TE similar to that of LPEI was observed.

The large number of synthesized polymers made it necessary to develop a high throughput (HT) method for the screening of the physicochemical and pharmaceutical properties. Using automated pipetting robots as well as fluorescence and DLS plate readers, different parameters, such as the pH value, the buffer system, the N/P ratio, and the concentration, could be systematically varied and their influence could be studied in a fast and efficient way. The obtained results corresponded well to results from "classical" experiments and to literature values.

A problem that occurred was the determination of the molar masses of the cationic polymers. Missing SEC standards and strong interactions with the columns, but also the failing of other methods, *e.g.* MALDI- and ESI-TOF-MS, due to multiple reasons, make their characterization challenging, in particular at high molar masses. Asymmetric flow-field flow fractionation (AF4) coupled to UV/RI and a multi angle laser light scattering detectors was found to be a suitable technique for this task.

Besides being investigated as vector for gene delivery, LPEIs were further used as starting materials for the synthesis of hydrogels. It could be shown, that LPEI-based hydrogels are capable to bind and release DNA, making them interesting compounds for DNA biochip applications.

To conclude, it could be shown that POx and its derivatives represent promising materials for a wide range of potential applications, such as antifouling coatings, drug and gene delivery. The presented results contribute to the understanding of structure-property relationships and will be the basis for the synthesis of further tailor-made polymers for various applications.

7. Zusammenfassung

Untersuchungen im Rahmen dieser Arbeit konnten zeigen, dass Poly(2-oxazoline) (POx) eine vielversprechende Alternative zu Poly(ethylenglycol) (PEG) darstellen. Letzteres Polymer findet in vielen Bereichen Verwendung, so zu Beispiel als Material für Antifouling-Beschichtungen und im Wirkstofftransport. Unter lebensnahen Versuchsbedingungen gelang es mit Hilfe von Poly(2-ethy-2-oxazolin) (PEtOx)-Beschichtungen die Bildung von Biofilmen auf Glasoberflächen um 66% zu reduzieren. Dafür wurden die PEtOx-Beschichtungen mittels eines Tetraetherlipides bzw. eines Silanhaftvermittlers kovalent an Glassubstrate gebunden. Es konnte weiterhin gezeigt werden, dass die wasserlöslichen Polymere Poly(2-methyl-2-oxazolin) und PEtOx eine ausgezeichnete Biokompatibilität, vergleichbar zu der von PEG, aufweisen. Auch wurde keine hemolytische Aktivität beobachtet und zytotoxische Effekte traten erst nach Langzeitbehandlung mit Konzentrationen oberhalb der normalerweise verwendeten therapeutischen Dosis auf. Durch Copolymerisation mit 2-(3-Butenyl)-2-oxazolin (ButEnOx) und anschließende Funktionalisierung wurden zwitterionische, POx-basierte Poly(sulfobetaine) und Poly(caboxybetaine) synthetisiert. Diese besaßen eine hohe Biokompatibilität und wirkten koagulanzhemmend, d.h. sie verlängerten die Blutgerinnungszeit. Modifizierte Copolymere aus EtOx und ButEnOx wurden weiterhin als potentielle Substanzen für die Krebstherapie untersucht. Durch Thiol-En-Photoaddition von Terpydridin an einen Teil der Doppelbindungen und anschließende Komplexierung von Platin konnte ein Antikrebswirkstoff erhalten werden. Um die Selektivität für Krebszellen zu erhöhen wurden die restlichen Doppelbindungen mit Zucker-Einheiten, d.h. Glukose bzw. Galaktose, funktionalisiert. Untersuchungen der zytotoxischen Wirkung auf verschiedene Zelllinien zeigten das therapeutische Potential der Platin-haltigen Glykopolymere.

Ein weiteres bedeutendes Anwendungsgebiet von POx und deren Derivate ist der Gentransfer. Insbesondere der „Goldstandard“ lineares Poly(ethylenimin) (LPEI), eine Verbindung welche durch saure oder basische Hydrolyse von POx entsteht, wird heutzutage intensiv untersucht. Um die Wasserlöslichkeit zu verbessern und die Zytotoxizität, unter Beibehaltung einer hohen Transfektionseffizienz (TE), zu verringern, wurde LPEI mit einer Reihe von biokompatiblen

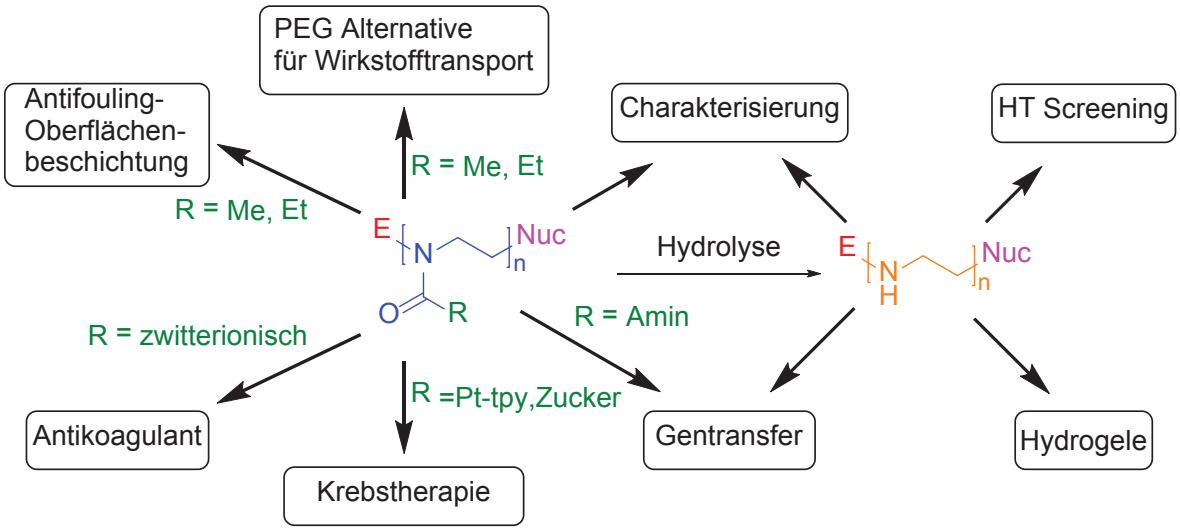

Figure 7-1. Übersicht über Vielfältigkeit von Poly(2-oxazolinen) und linearem Poly(ethylenimin) sowie über die Themen, welche im Rahmen der Arbeit untersucht wurden.

Verbindungen modifiziert. Anschließend wurde der Einfluss dieser strukturellen Veränderungen auf verschiedene Parameter, wie z.B. Polyplexstabilität, Zytotoxizität und TE, untersucht. In einem ersten Ansatz wurden partiell hydrolysierte PEtOx (PHPEtOx) hergestellt, deren Hydrolysegrad über die Reaktionszeit gesteuert wurde. Es zeigte sich, dass die PEtOx-Einheiten zwar die Zytotoxizität reduzierten, jedoch sank gleichzeitig die TE signifikant. Als Ursache dafür wurde eine reduzierte Polyplexstabilität ausgemacht, welch zu einem ungenügenden Schutz der DNA vor enzymatischen Abbau führte. Die schlechte DNA-Bindungskapazität der PHPEtOx beruht auf dem proteinabweisenden Charakter von der PEtOx-Bestandteile und der statistische Verteilung der Ethylenimine-Einheiten innerhalb der Copolymere. Letzteres erschwert eine stabile DNA-Bindung, da einige Amingruppen auf Grund ihrer kurzen Sequenz oder sterischer Abschirmung durch benachbarte PEtOx-Einheiten nicht für die DNA-Komplexierung zur Verfügung stehen. Um dieses Problem zu lösen, wurde die Synthese von PEtOx-LPEI-Blockcopolymeren durch selektive, basische Hydrolyse von P(EtOx-*b*-HOx untersucht. Obwohl eine hohe Selektivität für die Abspaltung der HOx-Seitenketten beobachtet wurde, konnten nur Polymere mit kurzen LPEI-Blöcken und einem maximalen EtOx/LPEI-Verhältnis von 4/1 hergestellt werden. Die Ursache dafür liegt in der Synthese des Ausgangsstoffs P(EtOx-*b*-HOx). Das Produkt fiel bei hohen Polymerisationsgraden des HOx-Blocks aus. Die daraus resultierende geringe Molmasse der

erhaltenen PEtOx-*b*-LPEIs verhinderte eine erfolgreiche pharmazeutische Anwendung. Aus diesem Grund wurde die Funktionalisierung mit einem anderen biokompatiblem Material, Dextran, untersucht. LPEIs unterschiedlicher Molmasse wurden über ihre primären Endgruppen auf verschiedene Arten an Dextran gekoppelt. Die besten Ergebnisse erzielten LPEIs, welche an carboxymethyliertes Dextran (CM-dex) gebunden waren. Diese CM-dex-*g*-LPEIs zeigten eine höhere TE als nichtfunktionalisierte LPEIs und LPEIs, welche an aldehydfunktionalisiertes Dextran gekoppelt wurden. Auch führten sie zu einer zu geringeren Erythrozyten Aggregation. Diese Beobachtung kann ihrem Polyelektrolytcharakter zugeschrieben werden, welcher oft einen positiven Einfluss auf die Biokompatibilität hat (siehe zwitterionische POx).

In den meisten Fällen reduzierte die Modifizierung von LPEI mit biokompatiblen „Stealth-Polymeren“ die Polyplexstabilität, da ihr abweisender Charakter die Wechselwirkung mit dem genetischen Material und den Zellmembranen verringerte. Von der Entwicklung antimikrobieller POx ist bekannt, dass das Einführen von Alkygruppen die Zellmembranwechselwirkung verbessern kann. Diese ist Voraussetzung für die erfolgreiche Aufnahme durch die Zelle und damit für die Transfektion. Aus diesem Grund wurde eine Bibliothek aus 18 Copolymeren hergestellt, wobei die Seitenkettenlänge und -hydrophobizität, der Amingehalt (10 bis 50%) und die Art des Amins (primär, tertiär) variiert wurden. Systematische Untersuchungen ergaben, dass primäre Amine eine höhere Effizienz beim Schutz und Transport der DNA aufweisen. Das Einführen von längeren Alkylseitenketten erhöhte die Wechselwirkung mit der Zellmembran. Jedoch zeigten Polymere mit sehr langen, hydrophoben Seitenketten eine hohe Zytotoxizität, da sie die Zellmembran zerstörten. Ein P(MeOx-*co*-ButEnOx)-basiertes Copolymer mit einem Amingehalt von 40 mol% lieferte die besten Resultate. Es war nicht zelltoxisch, wies jedoch eine TE vergleichbar zu LPEI auf.

Die große Anzahl an Polymer machte es notwendig eine Hochdurchsatzmethode für die Untersuchung der physikochemischen und pharmazeutischen Eigenschaften zu entwickeln. Durch die Verwendung von Fluoreszenz- und DLS-Analysemethoden sowie von Pipettierrobotern konnten verschiedene Parameter, wie der pH-Wert, das Puffersystem, das N/P-Verhältnis und die Konzentration, variiert und deren Einfluss studiert werden. Die erhaltenen Ergebnisse waren vergleichbar zur Literatur und zu Ergebnissen aus klassischen Experimenten.

Ein Problem stellte die Molmassenbestimmung der kationischen Polymere dar. Fehlende Standards für die Größenausschlusschromatographie und starke Wechselwirkungen mit dem Säulenmaterial, sowie das Versagen andere Methoden aus den verschiedensten Gründen, erschweren ihre Charakterisierung, insbesondere bei hohen Molmassen. Die an UV/RI- und Mehrwinkellaserlichtstreu-Detektoren gekoppelte asymmetrische Fluss-Feld-Fluss-Fraktionierung stellte sich als brauchbare Methode für diese Aufgabe heraus.

LPEIs wurden nicht nur als Gentransfervektoren untersucht, sie dienten auch als Ausgangsstoffe für die Synthese von Hydrogelen. Es konnte gezeigt werden, dass LPEI-basierte Hydrogele in der Lage sind DNA zu binden und wieder frei zu setzen, was sie zu interessanten Materialen für die Verwendung in DNA-Biochips macht.

Zusammenfassend konnte gezeigt werden, dass POx und ihre Derivate vielversprechende Materialien für ein großes Feld von Anwendungen darstellen, so z.B. für Antifouling-Beschichtungen, den Wirkstofftransport bzw. den Gentransfer. Die beschrieben Ergebnisse tragen zum besseren Verständnis von Struktur-Eigenschafts-Beziehungen bei und stellen die Grundlage für die Synthese weitere maßgeschneiderter Polymere für verschiedenste Anwendungen.

8. References

[1] C. Mangold, F. Wurm, H. Frey, *Polym. Chem.* **2012**, *3*, 1714-1721.
[2] O. Nuyken, S. Pask, *Polymers* **2013**, *5*, 361-403.
[3] S. Aoshima, S. Kanaoka, *Chem. Rev.* **2009**, *109*, 5245-5287.
[4] K. Matyjaszewski, *Curr. Opin. Solid St. M.* **1996**, *1*, 769-776.
[5] F. J. Xu, W. T. Yang, *Prog. Polym. Sci.* **2011**, *36*, 1099-1131.
[6] M. Ahmed, R. Narain, *Prog. Polym. Sci.* **2013**, *38*, 767-790.
[7] D. J. Siegwart, J. K. Oh, K. Matyjaszewski, *Prog. Polym. Sci.* **2012**, *37*, 18-37.
[8] R. B. Grubbs, *Polym. Rev.* **2011**, *51*, 104-137.
[9] J. Nicolas, Y. Guillaneuf, C. Lefay, D. Bertin, D. Gigmes, B. Charleux, *Prog. Polym. Sci.* **2013**, *38*, 63-235.
[10] S. Agarwal, Y. Zhang, S. Maji, A. Greiner, *Materials Today* **2012**, *15*, 388-393.
[11] K. Knop, R. Hoogenboom, D. Fischer, U. S. Schubert, *Angew. Chem. Int. Ed.* **2010**, *49*, 6288-6308.
[12] F. M. Veronese, G. Pasut, *Drug Discov. Today* **2005**, *10*, 1451-1458.
[13] N. Adams, U. S. Schubert, *Adv. Drug Deliv. Rev.* **2007**, *59*, 1504-1520.
[14] R. Hoogenboom, *Angew. Chem. Int. Ed.* **2009**, *48*, 7978-7994.
[15] R. Luxenhofer, Y. Han, A. Schulz, J. Tong, Z. He, A. V. Kabanov, R. Jordan, *Macromol. Rapid Commun.* **2012**, *33*, 1613-1631.
[16] H. Schlaad, C. Diehl, A. Gress, M. Meyer, A. L. Demirel, Y. Nur, A. Bertin, *Macromol. Rapid Commun.* **2010**, *31*, 511-525.
[17] M. Bauer, C. Lautenschlaeger, K. Kempe, L. Tauhardt, U. S. Schubert, D. Fischer, *Macromol. Biosci.* **2012**, *12*, 986-998.
[18] T. X. Viegas, M. D. Bentley, J. M. Harris, Z. Fang, K. Yoon, B. Dizman, R. Weimer, A. Mero, G. Pasut, F. M. Veronese, *Bioconjugate Chem.* **2011**, *22*, 976-986.
[19] R. Konradi, C. Acikgoz, M. Textor, *Macromol. Rapid Commun.* **2012**, *33*, 1663-1676.
[20] B. Pidhatika, M. Rodenstein, Y. Chen, E. Rakhmatullina, A. Muhlebach, C. Acikgoz, M. Textor, R. Konradi, *Biointerphases* **2012**, *7*, 1-15.
[21] R. Hoogenboom, M. W. M. Fijten, H. M. L. Thijs, B. M. van Lankvelt, U. S. Schubert, *Des. Monomers Polym.* **2005**, *8*, 659-671.
[22] F. Wiesbrock, R. Hoogenboom, M. A. M. Leenen, M. A. R. Meier, U. S. Schubert, *Macromolecules* **2005**, *38*, 5025-5034.
[23] F. Wiesbrock, R. Hoogenboom, M. Leenen, S. F. G. M. van Nispen, M. van der Loop, C. H. Abeln, A. M. J. van den Berg, U. S. Schubert, *Macromolecules* **2005**, *38*, 7957-7966.
[24] R. Hoogenboom, R. M. Paulus, Å. Pilotti, U. S. Schubert, *Macromol. Rapid Commun.* **2006**, *27*, 1556-1560.
[25] C. Weber, R. Hoogenboom, U. S. Schubert, *Prog. Polym. Sci.* **2012**, *37*, 686-714.
[26] C. Diehl, H. Schlaad, *Macromol. Biosci.* **2009**, *9*, 157-161.

[27] C. Diehl, H. Schlaad, *Chem. Eur. J.* **2009**, *15*, 11469-11472.
[28] A. Gress, PhD-Thesis thesis, University Potsdam (Potsdam), **2008**.
[29] A. Gress, A. Völkel, H. Schlaad, *Macromolecules* **2007**, *40*, 7928-7933.
[30] T. R. Dargaville, R. Forster, B. L. Farrugia, K. Kempe, L. Voorhaar, U. S. Schubert, R. Hoogenboom, *Macromol. Rapid Commun.* **2012**, *33*, 1695-1700.
[31] B. L. Farrugia, K. Kempe, U. S. Schubert, R. Hoogenboom, T. R. Dargaville, *Biomacromolecules* **2013**, *14*, 2724-2732.
[32] K. Kempe, R. Hoogenboom, M. Jaeger, U. S. Schubert, *Macromolecules* **2011**, *44*, 6424-6432.
[33] K. Kempe, R. Hoogenboom, U. S. Schubert, *Macromol. Rapid Commun.* **2011**, *32*, 1484-1489.
[34] K. Kempe, A. Vollrath, H. W. Schaefer, T. G. Poehlmann, C. Biskup, R. Hoogenboom, S. Hornig, U. S. Schubert, *Macromol. Rapid Commun.* **2010**, *31*, 1869-1873.
[35] C. E. Hoyle, C. N. Bowman, *Angew. Chem. Int. Ed.* **2010**, *49*, 1540-1573.
[36] N. B. Cramer, T. Davies, A. K. O'Brien, C. N. Bowman, *Macromolecules* **2003**, *36*, 4631-4636.
[37] A. B. Lowe, *Polym. Chem.* **2010**, *1*, 17-36.
[38] R. Duncan, *Nat. Rev. Drug Discov.* **2003**, *2*, 347-360.
[39] X. Gao, K.-S. Kim, D. Liu, *The AAPS Journal* **2007**, *9*, E92-E104.
[40] M. A. Mintzer, E. E. Simanek, *Chem. Rev.* **2008**, *109*, 259-302.
[41] M. Jäger, S. Schubert, S. Ochrimenko, D. Fischer, U. S. Schubert, *Chem. Soc. Rev.* **2012**, *41*, 4755-4767.
[42] V. K. Vendra, L. Wu, S. Krishnan, in *Nanotechnologies for the Life Sciences*, Wiley-VCH Verlag GmbH & Co. KGaA, **2007**.
[43] C. Blaszykowski, S. Sheikh, M. Thompson, *Chem. Soc. Rev.* **2012**, *41*, 5599-5612.
[44] S. Cao, J. Wang, H. Chen, D. Chen, *Chin. Sci. Bull.* **2011**, *56*, 598-612.
[45] P. Buskens, M. Wouters, C. Rentrop, Z. Vroon, *J. Coat. Technol. Res.* **2013**, *10*, 29-36.
[46] T. Mérian, J. M. Goddard, *J. Agric. Food Chem.* **2012**, *60*, 2943-2957.
[47] D. Rana, T. Matsuura, *Chem. Rev.* **2010**, *110*, 2448-2471.
[48] C. Zhao, L.-Y. Li, M.-M. Guo, J. Zheng, *Chem. Pap.* **2012**, *66*, 323-339.
[49] I. Banerjee, R. C. Pangule, R. S. Kane, *Adv. Mater.* **2011**, *23*, 690-718.
[50] B. Pidhatika, J. Möller, E. M. Benetti, R. Konradi, E. Rakhmatullina, A. Mühlebach, R. Zimmermann, C. Werner, V. Vogel, M. Textor, *Biomaterials* **2010**, *31*, 9462-9472.
[51] Y. Chujo, E. Ihara, H. Ihara, T. Saegusa, *Macromolecules* **1989**, *22*, 2040-2043.
[52] Y. Chujo, E. Ihara, S. Kure, T. Saegusa, *Macromolecules* **1993**, *26*, 5681-5686.
[53] C. Haensch, T. Erdmenger, M. W. M. Fijten, S. Hoeppener, U. S. Schubert, *Langmuir* **2009**, *25*, 8019-8024.
[54] F. Manzenrieder, R. Luxenhofer, M. Retzlaff, R. Jordan, M. G. Finn, *Angew. Chem. Int. Ed.* **2011**, *50*, 2601-2605.

[55] N. Zhang, T. Pompe, I. Amin, R. Luxenhofer, C. Werner, R. Jordan, *Macromol. Biosci.* **2012**, *12*, 926-936.
[56] R. Konradi, B. Pidhatika, A. Muhlebach, M. Textor, *Langmuir* **2008**, *24*, 613-616.
[57] B. Pidhatika, J. ller, V. Vogel, R. Konradi, *Chimia* **2008**, *62*, 264-269.
[58] N. Adden, A. Hoffmann, G. Gross, H. Windhagen, F. Thorey, H. Menzel, *J. Biomater. Sci., Polym. Ed.* **2007**, *18*, 303-316.
[59] J. U. Lind, C. Acikgöz, A. E. Daugaard, T. L. Andresen, S. Hvilsted, M. Textor, N. B. Larsen, *Langmuir* **2012**, *28*, 6502-6511.
[60] H. Wang, L. Li, Q. Tong, M. Yan, *ACS Appl. Mater. Interfaces* **2011**, *3*, 3463-3471.
[61] H. Wang, J. Ren, A. Hlaing, M. Yan, *J. Colloid Interf. Sci.* **2011**, *354*, 160-167.
[62] T. Lehmann, J. Rühe, *Macromol. Symp.* **1999**, *142*, 1-12.
[63] J. Kim, Y.-H. Shin, S.-H. Yun, D.-S. Choi, J.-H. Nam, S. R. Kim, S.-K. Moon, B. H. Chung, J.-H. Lee, J.-H. Kim, K.-Y. Kim, K.-M. Kim, J.-H. Lim, *J. Am. Chem. Soc.* **2012**, *134*, 16500-16503.
[64] Y.-H. Shin, S.-H. Yun, S.-H. Pyo, Y.-S. Lim, H.-J. Yoon, K.-H. Kim, S.-K. Moon, S. W. Lee, Y. G. Park, S.-I. Chang, K.-M. Kim, J.-H. Lim, *Angew. Chem. Int. Ed.* **2010**, *49*, 9689-9692.
[65] I. Hamad, A. C. Hunter, J. Szebeni, S. M. Moghimi, *Mol. Immunol.* **2008**, *46*, 225-232.
[66] T. Tagami, K. Nakamura, T. Shimizu, N. Yamazaki, T. Ishida, H. Kiwada, *J. Control. Release* **2010**, *142*, 160-166.
[67] H. Koide, T. Asai, K. Hatanaka, S. Akai, T. Ishii, E. Kenjo, T. Ishida, H. Kiwada, H. Tsukada, N. Oku, *Int. J. Pharm.* **2010**, *392*, 218-223.
[68] G. Pasut, F. M. Veronese, *Prog. Polym. Sci.* **2007**, *32*, 933-961.
[69] C. Crouzet, C. Decker, J. Marchal, *Makromol. Chem.* **1976**, *177*, 145-157.
[70] F. Kawai, T. Kimura, M. Fukaya, Y. Tani, K. Ogata, T. Ueno, H. Fukami, *Appl. Environ. Microbiol.* **1978**, *35*, 679-684.
[71] C. F. Gonzalez, W. A. Taber, M. A. Zeitoun, *Appl. Microbiol.* **1972**, *24*, 911-919.
[72] J. M. Warakomski, B. P. Thill, *J. Polym. Sci., Part A: Polym. Chem.* **1990**, *28*, 3551-3563.
[73] J. Cao, Y.-W. Chen, X. Wang, X.-L. Luo, *J. Biomed. Mater. Res., Part A* **2011**, *97A*, 472-479.
[74] Y. Chang, W.-Y. Chen, W. Yandi, Y.-J. Shih, W.-L. Chu, Y.-L. Liu, C.-W. Chu, R.-C. Ruaan, A. Higuchi, *Biomacromolecules* **2009**, *10*, 2092-2100.
[75] C. Rodriguez Emmenegger, E. Brynda, T. Riedel, Z. Sedlakova, M. Houska, A. B. Alles, *Langmuir* **2009**, *25*, 6328-6333.
[76] Y.-J. Shih, Y. Chang, *Langmuir* **2010**, *26*, 17286-17294.
[77] Y.-J. Shih, Y. Chang, A. Deratani, D. Quemener, *Biomacromolecules* **2012**, *13*, 2849-2858.
[78] H.-S. Han, J. D. Martin, J. Lee, D. K. Harris, D. Fukumura, R. K. Jain, M. Bawendi, *Angew. Chem. Int. Ed.* **2013**, *52*, 1414-1419.

[79] J.-T. Sun, Z.-Q. Yu, C.-Y. Hong, C.-Y. Pan, *Macromol. Rapid Commun.* **2012**, *33*, 811-818.
[80] K. J. Haxton, H. M. Burt, *J. Pharm. Sci.* **2009**, *98*, 2299-2316.
[81] H. Maeda, G. Y. Bharate, J. Daruwalla, *Eur. J. Pharm. Biopharm.* **2009**, *71*, 409-419.
[82] V. J. Venditto, F. C. Szoka Jr, *Adv. Drug Deliv. Rev.* **2013**, *65*, 80-88.
[83] X. Wang, Z. Guo, *Chem. Soc. Rev.* **2013**, *42*, 202-224.
[84] J. S. Butler, P. J. Sadler, *Curr. Opin. Chem. Biol.* **2013**, *17*, 175-188.
[85] C. Oerlemans, W. Bult, M. Bos, G. Storm, J. F. Nijsen, W. Hennink, *Pharm. Res.* **2010**, *27*, 2569-2589.
[86] S. D. Cummings, *Coord. Chem. Rev.* **2009**, *253*, 1495-1516.
[87] J. Moretto, B. Chauffert, F. Ghiringhelli, J. Aldrich-Wright, F. Bouyer, *Invest. New Drugs* **2011**, *29*, 1164-1176.
[88] K. Suntharalingam, O. Mendoza, A. A. Duarte, D. J. Mann, R. Vilar, *Metallomics* **2013**, *5*, 514-523.
[89] K. Kempe, C. Weber, K. Babiuch, M. Gottschaldt, R. Hoogenboom, U. S. Schubert, *Biomacromolecules* **2011**, *12*, 2591-2600.
[90] C. Weber, J. A. Czaplewska, A. Baumgaertel, E. Altuntas, M. Gottschaldt, R. Hoogenboom, U. S. Schubert, *Macromolecules* **2011**, *45*, 46-55.
[91] R. S. Go, A. A. Adjei, *J. Clin. Oncol.* **1999**, *17*, 409-422.
[92] P. Reece, I. Stafford, M. Davy, R. Morris, S. Freeman, *Cancer Chemother. Pharmacol.* **1989**, *24*, 256-260.
[93] J.-P. Behr, *Chimia* **1997**, *51*, 34-36.
[94] A. Schallon, *Untersuchung des nicht-viralen Gentransfers mit den Polymeren PEI und PDMAEMA*, Köster Berlin, Berlin, **2012**.
[95] H. M. L. Lambermont-Thijs, F. S. van der Woerdt, A. Baumgaertel, L. Bonami, F. E. Du Prez, U. S. Schubert, R. Hoogenboom, *Macromolecules* **2009**, *43*, 927-933.
[96] L. Tauhardt, K. Kempe, K. Knop, E. Altuntaş, M. Jäger, S. Schubert, D. Fischer, U. S. Schubert, *Macromol. Chem. Phys.* **2011**, *212*, 1918-1924.
[97] E. Altuntaş, K. Knop, L. Tauhardt, K. Kempe, A. C. Crecelius, M. Jäger, M. D. Hager, U. S. Schubert, *J. Mass Spectrom.* **2012**, *47*, 105-114.
[98] Z. Kadlecova, S. Nallet, D. L. Hacker, L. Baldi, H.-A. Klok, F. M. Wurm, *Macromol. Biosci.* **2012**, *12*, 628-636.
[99] M. Breunig, U. Lungwitz, R. Liebl, C. Fontanari, J. Klar, A. Kurtz, T. Blunk, A. Goepferich, *J. Gene Med.* **2005**, *7*, 1287-1298.
[100] Y. Akiyama, A. Harada, Y. Nagasaki, K. Kataoka, *Macromolecules* **2000**, *33*, 5841-5845.
[101] S. Bauhuber, R. Liebl, L. Tomasetti, R. Rachel, A. Goepferich, M. Breunig, *J. Control. Release* **2012**, *162*, 446-455.
[102] J. Dai, S. Zou, Y. Pei, D. Cheng, H. Ai, X. Shuai, *Biomaterials* **2011**, *32*, 1694-1705.
[103] R. Namgung, J. Kim, K. Singha, C. H. Kim, W. J. Kim, *Mol. Pharm.* **2009**, *6*, 1826-1835.

[104] L.-R. Tsai, M.-H. Chen, C.-T. Chien, M.-K. Chen, F.-S. Lin, K. M.-C. Lin, Y.-K. Hwu, C.-S. Yang, S.-Y. Lin, *Biomaterials* **2011**, *32*, 3647-3653.
[105] Z. Zhong, J. Feijen, M. C. Lok, W. E. Hennink, L. V. Christensen, J. W. Yockman, Y.-H. Kim, S. W. Kim, *Biomacromolecules* **2005**, *6*, 3440-3448.
[106] H. M. L. Lambermont-Thijs, J. P. A. Heuts, S. Hoeppener, R. Hoogenboom, U. S. Schubert, *Polym. Chem.* **2011**, *2*, 313-322.
[107] F. Vandoorne, D. Bruneel, R. Vercauteren, E. Schacht, *Makromolekulare Chemie-Macromolecular Chemistry and Physics* **1991**, *192*, 673-677.
[108] T. Azzam, H. Eliyahu, L. Shapira, M. Linial, Y. Barenholz, A. J. Domb, *J. Med. Chem.* **2002**, *45*, 1817-1824.
[109] Y.-X. Sun, X.-Z. Zhang, H. Cheng, S.-X. Cheng, R.-X. Zhuo, *J. Biomed. Mater. Res., Part A* **2008**, *84A*, 1102-1110.
[110] J. H. Jeong, S. H. Song, D. W. Lim, H. Lee, T. G. Park, *J. Control. Release* **2001**, *73*, 391-399.
[111] M. Thomas, J. J. Lu, Q. Ge, C. Zhang, J. Chen, A. M. Klibanov, *Proc. Natl. Acad. Sci. U. S. A.* **2005**, *102*, 5679-5684.
[112] L. Tauhardt, K. Kempe, M. Gottschaldt, U. S. Schubert, *Chem. Soc. Rev.* **2013**, *42*, 7998-8011.
[113] J. Blümmel, N. Perschmann, D. Aydin, J. Drinjakovic, T. Surrey, M. Lopez-Garcia, H. Kessler, J. P. Spatz, *Biomaterials* **2007**, *28*, 4739-4747.
[114] H. Hatakeyama, H. Akita, H. Harashima, *Adv. Drug Deliv. Rev.* **2011**, *63*, 152-160.
[115] J. A. Fortune, T. I. Novobrantseva, A. M. Klibanov, *J. Drug Deliv.* **2011**, *2011*, 204058.
[116] S. T. Kim, K. Saha, C. Kim, V. M. Rotello, *Acc. Chem. Res.* **2013**, *46*, 681-691.
[117] C. J. Waschinski, V. Herdes, F. Schueler, J. C. Tiller, *Macromol. Biosci.* **2005**, *5*, 149-156.
[118] K. Kempe, T. Neuwirth, J. Czaplewska, M. Gottschaldt, R. Hoogenboom, U. S. Schubert, *Polym. Chem.* **2011**, *2*, 1737-1743.
[119] A. Litzen, K. G. Wahlund, *J. Chromatogr.* **1991**, *548*, 393-406.
[120] K.-G. Wahlund, *J. Chromatogr. A* **2013**, *1287*, 97-112.
[121] A. Zattoni, D. C. Rambaldi, P. Reschiglian, M. Melucci, S. Krol, A. M. C. Garcia, A. Sanz-Medel, D. Roessner, C. Johann, *J. Chromatogr. A* **2009**, *1216*, 9106-9112.
[122] M. Wink, *An Introduction to Molecular Biotechnology: Molecular Fundamentals, Methods and Applications in Modern Biotechnology*, Wiley-VCH, Weinheim, Germany, **2006**.
[123] Y. Chujo, K. Sada, K. Matsumoto, T. Saegusa, *Polym. Bull.* **1989**, *21*, 353-356.
[124] Y. Chujo, K. Sada, K. Matsumoto, T. Saegusa, *Macromolecules* **1990**, *23*, 1234-1237.
[125] Y. Chujo, Y. Yoshifuji, K. Sada, T. Saegusa, *Macromolecules* **1989**, *22*, 1074-1077.
[126] A. M. Kelly, A. Hecke, B. Wirnsberger, F. Wiesbrock, *Macromol. Rapid Commun.* **2011**, *32*, 1815-1819.

[127] R. Goyal, S. K. Tripathi, S. Tyagi, A. Sharma, K. R. Ram, D. K. Chowdhuri, Y. Shukla, P. Kumar, K. C. Gupta, *Nanomedicine: Nanotechnology, Biology and Medicine* **2012**, *8*, 167-175.
[128] S. Grube, W. Oppermann, *Macromolecules* **2013**, *46*, 1948-1955.
[129] T. Yang, M. Malkoch, A. Hult, *J. Polym. Sci., Part A: Polym. Chem.* **2013**, *51*, 363-371.
[130] S. Mongkhontreerat, K. Oberg, L. Erixon, P. Lowenhielm, A. Hult, M. Malkoch, *J. Mater. Chem. A* **2013**, *1*, 13732-13737.

List of abbreviations

AF4	Asymmetric flow-field flow fractionation
ATR-FT-IR	Attenuated total reflection Fourier transform infrared
ButEnOx	2-(3-Butenyl)-2-oxazoline
CHO-dex	Aldehyde functionalized dextran
CM-dex	Carboxymethylated dextran
CROP	Cationic ring-opening polymerization
DecEnOx	2-(9-Decenyl)-2-oxazoline
DH	Degree of hydrolysis
DMAc	*N,N*-Dimethylacetamide
DMPA	2,2-Dimethoxy-2-phenylacetophenone
DNA	Deoxyribonucleic acid
DP	Degree of polymerization
ESI	Electrospray ionization
EtOx	2-Ethyl-2-oxazoline
Gal	Galactose
GC	Gas chromatography
Glc	Glucose
GOPTMS	(3-Glycidyloxypropyl)trimethoxysilane
HT	High-throughput
LPEI	Linear poly(ethylene imine)
MALDI	Matrix assisted laser desorption ionization
MALLS	Multi angle laser light scattering
MeOH	Methanol
MeOx	2-Methyl-2-oxazoline
MeOTs	Methyl tosylate
NMR	Nuclear magnetic resonance
[M]/[I]	[Monomer] / [initiator]
MS	Mass spectrometry
PDI	Polydispersity index
pDNA	Plasmid DNA
PEG	Poly(ethylene glycol)

PEtOx	Poly(2-ethyl-2-oxazoline)
PHOx	Poly(2-*H*-2-oxazoline)
PHPEtOx	Partially hydrolyzed poly(2-ethyl-2-oxazoline)
PMeOx	Poly(2-methyl-2-oxazoline)
POx	Poly(2-oxazoline)
PS	Poly(styrene)
RNA	Ribonucleic acid
RI	Refractive index
SEC	Size exclusion chromatography
TE	Transfection efficiency
TEL	Tetraether lipid
TOF	Time of flight
Tpy	Terpyridine
UV	Ultraviolet
µW	Microwave

Curriculum vitae

10.07.1984	Born in Naumburg/Saale, Germany
1991-06/2004	School education in Naumburg/Saale, Germany
25/06/2004	University entrance certification at Lepsius-Gymnasium in Naumburg/Saale, Germany
07/2004-03/2005	Military service at 7./PiBtl 701 and 2./PiBtl 722 in Gera, Germany
10/2005-10/2010	Study of chemistry at the Friedrich Schiller University Jena
11/2009-10/2010	Diploma thesis in the group of Prof. Dr. Ulrich Schubert at the Friedrich Schiller University Jena, Germany Topic: “Synthesis and characterization of functional linear poly(ethylene imine)s”
22/10/2010	Diploma
Since 11/2010	PhD student at the Laboratory of Macromolecular and Organic Chemistry (IOMC) at the Friedrich Schiller University Jena in the group of Prof. Dr. Ulrich S. Schubert

Jena, den 19.11.2014

_____

Lutz Tauhardt

Publication list

Peer-reviewed publications

[1] **L. Tauhardt**, K. Kempe, K. Knop, E. Altuntaş, M. Jäger, S. Schubert, D. Fischer, U. S. Schubert, "Linear polyethyleneimine: Optimized synthesis and characterization – on the way to "pharmagrade" batches", *Macromol. Chem. Phys.* **2011**, *212*, 1918-1924.

[2] E. Altuntaş, K. Knop, **L. Tauhardt**, K. Kempe, A. C. Crecelius, M. Jäger, M. D. Hager, U. S. Schubert, "Tandem mass spectrometry of poly(ethylene imine)s by electrospray ionization (ESI) and matrix-assisted laser desorption/ionization (MALDI)", *J. Mass Spectrom.* **2012**, *47,* 105-114

[3] M. Bauer, C. Lautenschlaeger, K. Kempe, **L. Tauhardt**, U. S. Schubert, D. Fischer, ´"Poly(2-ethyl-2-oxazoline) as alternative for the stealth polymer poly(ethylene glycol): Comparison of *in vitro* cytotoxicity and hemocompatibility", *Macromol. Biosci.* **2012**, *12*, 986-998.

[4] **L. Tauhardt**, K. Kempe, U. S. Schubert, "Toward the design of LPEI containing block copolymers: Improved synthesis protocol, selective hydrolysis, and detailed characterization", *J. Polym. Sci., Part A: Polym. Chem.* **2012**, *50*, 4516-4523.

[5] M. Bauer, S. Schröder, **L. Tauhardt**, K. Kempe, U. S. Schubert, D. Fischer, "*In vitro* hemocompatibility and cytotoxicity study of poly(2-methyl-2-oxazoline) for biomedical applications", *J. Polym. Sci., Part A: Polym. Chem.* **2013**, *51*, 1816–1821.

[6] A. C. Rinkenauer, A. Vollrath, A. Schallon, **L. Tauhardt**, K. Kempe, S. Schubert, D. Fischer, U. S. Schubert, "Parallel high-throughput screening of polymer vectors for nonviral gene delivery: Evaluation of structure–property relationships of transfection", *ACS Comb. Sci.* **2013**, *15*, 475-482.

[7] **L. Tauhardt**, K. Kempe, M. Gottschaldt, U. S. Schubert, "Poly(2-oxazoline) functionalized surfaces: From modification to application", *Chem. Soc. Rev.* **2013**, *42*, 7998-8011.

[8] M. Wagner, C. Pietsch, **L. Tauhardt**, A Schallon, U. S. Schubert, "Characterization of cationic polymers by asymmetric flow field-flow fractionation and multi-angle light scattering-A comparison with traditional techniques" *J. Chromatogr. A* **2014**, *1325*, 195-203.

[9] C. Englert, **L. Tauhardt**, M. Hartlieb, K. Kempe, M. Gottschaldt, U. S. Schubert, "Linear Poly(ethylene imine)-Based Hydrogels for Effective Binding and Release of DNA", *Biomacromolecules* 2014, 4, 1124-1131.

[10] **L. Tauhardt**, M. Frant, D. Pretzel, M. Hartlieb, C. Bucher, G. Hildebrand, B. Schroter, C. Weber, K. Kempe, M. Gottschaldt, K. Liefeith, U. S. Schubert, "Amine end-functionalized poly(2-ethyl-2-oxazoline) as promising coating material for antifouling applications", *J. Mater. Chem. B* **2014**, *2*, 4883-4893.

[11] **L. Tauhardt**, D. Pretzel, S. Bode, J. A. Czaplewska, K. Kempe, M. Gottschaldt, U. S. Schubert, "Synthesis and *in vitro* activity of platinum containing 2-oxazoline-based glycopolymers", *J. Polym. Sci., Part A: Polym. Chem.* **2014**, *52*, 2703–2714.

[12] **L. Tauhardt**, D. Pretzel, K. Kempe, M. Gottschaldt, D. Pohlers, U. S. Schubert, "Zwitterionic poly(2-oxazoline)s as promising candidates for blood contacting applications", *Polym. Chem.* **2014**, *5*, 5751-5764.

[13] S. Ochrimenko,[#] A. Vollrath,[#] K. Kempe, **L. Tauhardt**, S. Schubert, U. S. Schubert, D. Fischer, "Dextran-graft-linear poly(ethylene imine)s for gene delivery: Importance of the linking strategy", *Carbohydr. Polym.* **2014**, *113*, 597-606.

[14] A. C. Rinkenauer,[#] **L. Tauhardt**,[#] F. Wendler, K. Kempe, M. Gottschaldt, A. Träger, U. S. Schubert, "A cationic, non-toxic poly(2-oxazoline) with high *in vitro* transfection efficiency identified by a library approach", *Macromol. Biosci.*, accepted 07.10.2014.

Non-peer reviewed publications

[1] P. Prokop, O. Schewtschenko. D. Pretzel, **L. Tauhardt**, M. Gottschaldt, M. Hoffmann, "*In vivo* investigations on anti-fouling hydrogel coatings", *Biomed. Eng./Biomed. Tech.* **2013**, *58* (Suppl. 1).

[2] **L. Tauhardt**, D. Pretzel, M. Gottschaldt, U. S. Schubert, "Surface coating of sensor materials using poly(2-ethyl-2-oxazoline) based polymers for the prevention of biofilm formation", *Abstr. Pap. Am. Chem. Soc.* **2013**, *246*, COLL-459.

[3] U. S. Schubert, **L. Tauhardt**, M. Hartlieb, C. Englert, "Cationic poly(2-oxazoline)s", *Abstr. Pap. Am. Chem. Soc.* **2014**, *248*, POLY-217.

[4] S. Schubert, A. Vollrath, I. Perevyazko, A. Rinkenauer, **L. Tauhardt**, C. Pietsch, A. Träger, D. Fischer, U. S. Schubert, "High-throughput formulation of nanoparticles and polyplexes for structure-property investigations", *Abstr. Pap. Am. Chem. Soc.* **2014**, *248*, COLL-455.

Poster presentations

[1] M. Bauer, C. Lautenschläger, K. Kempe, **L. Tauhardt**, U. S. Schubert, D. Fischer, "*In vitro* comparative hemocompatibility study of poly(ethylene glycol) and poly(2-ethyl-2-oxazoline)" (***CRS**, German Local Chapter Annual Meeting 2011*,March 16th, **2011**, Jena, Germany)

[2] L. Tauhardt, K. Kempe, K. Knop, E. Altuntaş M. Jäger, S. Schubert, D. Fischer, U. S. Schubert, "On the way to 'pharmagrade' linear poly(ethylene imine)" (***Bayreuth Polymer Symposium***, September 11 - 13, **2011**, Bayreuth, Germany

[3] M. Bauer, H. Lambermont-Thijs, **L. Tauhardt**, K. Kempe, R. Hoogenboom, U. S. Schubert, D. Fischer, "Partially hydrolyzed poly(2-ethyl-2-oxazoline)s as linear poly(ethylene imine) derivatives for non-viral gene transfer" (***CRS**, German Local Chapter Annual Meeting 2012*, March 29 – 30, **2012**, Würzbug, Germany)

[4] S. Ochrimenko; A. Vollrath, K. Kempe, **L. Tauhardt**, S. Schubert, U. S. Schubert; D. Fischer, "Dextran-*graft*-linear poly(ethylene imine) for gene delivery – structure-activity relationship" (***CRS**, German Local Chapter Annual Meeting 2012*, March 29 – 30, **2012**, Würzbug, Germany)

[5] A. Vollrath, S. Ochrimenko, K. Kempe, **L. Tauhardt**, S. Schubert, D. Fischer, U. S. Schubert, "Dextran-*graft*-linear poly(ethylene imine) for gene delivery – structure - activity relationship" (***International Conference on Polymer Synthesis & Polymer Colloids***, July 08 – 12, **2012**, Warwick, United Kingdom)

[6] A. Vollrath, S. Ochrimenko, K. Kempe, **L. Tauhardt**, S. Schubert, D. Fischer, U. S. Schubert, "Dextran-*graft*-linear poly(ethylene imine) for gene – structure-activity relationship" (***Smart Polymers*** *– Biennial Meeting of the GDCh-Division of Macromolecular Chemistry*, October 07 – 09. 2012, Mainz, Germany)

[7] M. Wagner, C. Pietsch, **L. Tauhardt**, A. Schallon, U. S. Schubert, "Characterization of cationic polymers for gene delivery by AF4 and analytical ultracentrifugation" ***(6th International Symposium on the Separation and Characterization of Natural and Synthetic Macromolecules***, February 06 – 08, **2013**, Dresden, Germany)

[8] **L. Tauhardt**, D. Pretzel, M. Barthel, C. Bücher, G. Hildebrand, M. Frant, M. Gottschaldt, K. Liefeith, U. S. Schubert, "Surface coating of sensor materials using poly(2-ethyl-2-oxazoline) and poly(ethylene glycol) based polymers for the prevention of biofilm formation" (***Euro BioMAT*** 2013, April 23 – 24, **2013**, Weimar, Germany)

[9] C. Englert, **L. Tauhardt**, D. Pretzel, K. Kempe, U. S. Schubert, "PEI-based hydrogels for DNA binding" (***Euro BioMAT*** 2013, April 23 – 24, **2013**, Weimar, Germany)

[10] **L. Tauhardt**, D. Pretzel, M. Hartlieb, C. Bücher, G. Hildebrand, M. Frant, K. Liefeith, M. Gottschaldt, U. S. Schubert, "Surface coating of sensor materials using poly(2-ethyl-2-oxazoline) based polymers for the prevention of biofilm formation" (246th **ACS** National Meeting & Exposition, September 08 – 12, **2013**, Indianapolis, USA)

[11] P. Prokop, O. Schewtschenko. D. Pretzel, **L. Tauhardt**, M. Gottschaldt, M. Hoffmann, "*In vivo* investigations on anti-fouling hydrogel coatings", (***BMT*** 2013, September 19 – 21, **2013**, Graz, Austria)

Patents

[1] C. Englert, L. Tauhardt, M. Gottschaldt, U. S. Schubert
"Neue Poly(ethylenimin) basierte Copolymere zur Anbindung und Freisetzung von genetischem Material, insbesondere von DNA/RNA, sowie Verfahren zu deren Herstellung und Verwendung"
Deutsches Patent- und Markenamt, Aktenzeichen: 10 2013 016 750.7

[2] A. Schallon, A. C. Rinkenauer, L. Tauhardt, K. Kempe, U. S. Schubert
"Poly(2-oxazolines) for efficient and non-toxic gene delivery"
Patent application number: NL 1040674

Acknowledgements / Danksagung

An dieser Stelle wird es Zeit mich bei allen Leuten zu bedanken, ohne deren Hilfe und kontinuierlich Unterstützung diese Arbeit nicht möglich gewesen wäre. Mein erster Dank gilt meinem wissenschaftlichen Betreuer Prof. Dr. Ulrich S. Schubert für die Möglichkeit meine Doktorarbeit in dieser wunderbaren Arbeitsgruppe anfertigen zu dürfen. Danke auch für die vielen Möglichkeiten, die sich mir durch die gute Ausstattung mit Geräten geboten haben.

Der größte Dank gebührt meine beiden Betreuer Dr. Michael Gottschaldt und Dr. Kristian Kempe. Auch Dr. Christine Weber sei hier gedankt, da sie immer zur Stelle war, wenn einer der beiden mir nicht helfen konnte oder beide nicht da waren. Vielen, vielen Dank für eure Korrekturen, tollen Anregungen und die unzählige Diskussionen. Ohne eure kontinuierliche Unterstützung wäre diese Arbeit nicht möglich gewesen. Danke auch dafür, dass ihr mich immer wieder aufgebaut habt, wenn es mal nicht so lief oder es gewisse andere Probleme gab. Auch der ganzen „Wachstumskern BASIS“-Crew sei gedankt, vor allem Micha für das Schreiben des Antrags und Dr. David Pretzel für die ganze Koordination, es hat euch sicherlich jede Menge Nerven gekostet. Dafür habt ihr euch eine „Wachstumskern-Faust“ verdient. Passend zu BASIS möchte ich mich an dieser Stelle recht herzlich beim IBA für die gute Zusammenarbeit bedanken, vor allem Christian Bücher, Marion Frant und Prof. Dr. Klaus Liefheit. Mein Dank gilt auch dem BMBF für die Finanzierung des Projektes.

Weiterhin möchte ich allen (technischen) Angestellten danken. Cornelia Bader und Anette Kuse gebührt großer Dank für die „large-scale“ Synthese von Monomeren, ohne diese wären viele meiner Polymere nicht möglich gewesen. Danke auch an Frau Sentis und Dr. Günther für unzählige, auch aufwendige, NMR-Messungen. Bedanken möchte ich mich auch bei Dr. Grit Festag für zahlreiche Messungen und die vielen Mühen, die SECs, das GC und das GC/MS am Laufen zu halten. Ohne diese Geräte wäre ich aufgeschmissen gewesen. Mein Dank gilt weiterhin Dr. Anja Baumgärtel, Dr. Katrin Knop und Sarah Crotty für all die MALD-TOF-MS-Messungen. Special thanks go to Dr. Esra Altuntaş for all the ESI-Q-TOF-MS measurements (Danke, „Junge” ☺). Vielen Dank auch an Dr. Uwe Köhn, Sandra Köhn, Sylvia Pfeifer und Anette Kuse für die Bestellung von Chemikalien, Verbrauchsmaterialen, etc. Danke auch den Hausmeistern Gerry Weigand, Michael Schmäche und Igor Ponath für den

Transport von Chemikalien und Gasflaschen, sowie größere und kleiner Reparaturen. Auch den Glasbläsern, vor allem Uli Hempel und Marcel Markert, sei gedankt.

Weiterhin gilt ein Dank Prof. Dagmar Fischer und den Leuten der Pharmazeutischen Technologie, vor allem Marius Bauer und Susann Schröter. Durch diese interessante Kooperation habe ich viel über pharmazeutische und biologische Dinge gelernt. Auch möchte ich mich an dieser Stelle recht herzlich bei Sofia Ochrimenko, dem perfekten Bindeglied zwischen Prof. Fischers und Prof. Schuberts Gruppe, für die Charakterisierung der Dex-PEIs bedanken. In diesem Zusammenhang sei auch Dr. Antje Vollrath für die Synthese selbiger gedankt.

Weil wir gerade so schön bei „pharma“ und „bio“ sind: Ein sehr großer Dank geht an Alexandra Rinkenauer, Carolin Fritzsche und Dr. Anja Schallon. Ich hoffe, ich habe euch nicht zu sehr gestresst mit meiner riesigen Polymerbibliothek. Danke für die viele Geduld, die ihr hattet und auch für die sehr guten Erklärungen. Darauf ein „wuza/whooza“ (oder wie man das auch immer schreibt ☺). Auch David gebührt an dieser Stelle Dank für die biologische/pharmazeutische Charakterisierung meiner Polymere. Ich hoffe, ich bin dir die letzten Wochen nicht zu sehr auf die Nerven gegangen, aber der „Spaß“ musste fertig werden.

Mein Dank gilt auch dem Labor 213 (IOMC): Kempi, Christine, Chris. Ihr seid die Besten. Auch wenn Chris mir etwas zu sehr zu Chaos im Labor neigt, habe ich die sehr gute Atmosphäre in unserem Labor immer genossen. Ein hoch auch auf Radio Top40 und unsere Laborhymne „We found love“ von Rihanna ☺. Bedanken möchte ich mich außerdem bei Labor 128 (ZAF), auch wenn ich mich dort dank der vielen Schreibarbeit nur selten habe sehen lassen. In diesem Zusammenhang möchte ich noch mal Matthias dafür danken, dass er sich um die Hahnleisten, Glasgeräte, etc. gekümmert hat. Ohne dich wäre an Arbeiten wahrscheinlich immer noch nicht zu denken. Weiterer Dank gebührt meinen Büromitinsassen, vor allem aus dem IOMC, wo ich die meiste Zeit meiner Promotionszeit verbracht habe. Danke Bobby, Tobi, Krzysztof, Justyna und Thomas. Es war immer recht lustig mit euch. Einem Menschen möchte ich in diesem Zusammenhang besonders danken: Meinem „Halbbruder“ Andreas „Juri“ Wild. Was hätte ich nur ohne dich, die „Blöd“ und unsere gemeinsame Mudder gemacht?☺ Ein Dank geht auch an meine Büromithäftlinge in der

kleinen Zelle im bunkerartigen ZAF (kein oder sehr schlechter Handyempfang). Danke an: Christine, Grit, Christian, Pier und Ilknur.

Bardzo dziękuję moim przyjaciołom Justynie i Krzystofowi. Bardzo się cieszę z czasu spędzonego z wami. Specjalne podziękowania kieruje do Justyny (I... co nowego?) za cukry, interesujące rozmowy, imprezy, śmieszne prezenty, jedzenie ("Eat many, many, many!"), i tak dalej. Krzysztof dziękuję za wszytkie imprezy, spotkania, wycieczki itp., rozmowy i dyskusje oraz zabranie mnie po raz pierwszy do „Faß". Das bringt mich natürlich gleich zur „Faß-Gang", der an dieser Stelle herzlich gedankt sei: Krzysztof, Christine, Micha G., Tobi („Häufchen"), Berni, Esra, Stephanie H., „little" Christan (oder auch kurz CvdE), Pier (alias Herr Dr. Franz Peter von der Stuhlmann oder kurz „Opfi" ☺), Micha P., und alle die sonst noch ab und an mit waren, z.B. Alex „Breuler" Breul, Benedict, Jan und Kevin. Was wäre die Arbeit nur ohne mal bei „einem" Bierchen abschalten zu können, wobei ja auch viele gute Ideen im „Faß" entstanden sind (siehe z.B. tpy/Zucker-POx). Danke auch an Tobi, Rainer, Christian, Flo ("Fleurian") und Silvio für die vielen Kinoabende, Männertage und sonstige Unternehmungen. Danke auch an Tobi M. und vor ganz besonders an Chris für die großartigen Steiger-Parties. Es ist echt Wahnsinn was ihr für einen Aufwand betreibt um die Wohnung zu schmücken.

An dieser Stelle möchte ich noch mal ausdrücklich allen Koautoren und allen anderen Leuten, die ich hier vergessen habe, danken. Seid mir bitte nicht böse, wenn ich hier nicht jeden einzeln nennen kann, aber bei einer so großen, sich ständig ändernden Gruppe und so vielen Kooperationspartnern ist das nahezu unmöglich.

Bevor ich so langsam zum Ende komme, möchte ich noch allen meinen Freunden danken, die mich in all den Jahren unterstütz haben und immer für mich da sind. Danke, ihr seid die Besten. Dziękuję Wioli za wszystkie wspólne dni i miesiące razem.

Und nun zu den wichtigsten Personen, ohne die ich nicht dort wäre, wo ich heute bin: Meine Familie. Danke, dass ihr mich auf all meinen Wegen unterstützt und immer ein offenes Ohr für meine Probleme und Sorgen habt. Ohne euren Zuspruch und Rückhalt wäre vieles nicht möglich gewesen. Danke.

Declaration of authorship / Selbstständigkeitserklärung

Ich erkläre, dass ich die vorliegende Arbeit selbständig und unter Verwendung der angegebenen Hilfsmittel, persönlichen Mitteilungen und Quellen angefertigt habe.

I certify that the work presented here is, to the best of my knowledge and belief, original and the result of my own investigations, except as acknowledged, and has not been submitted, either in part or whole, for a degree at this or any other university.

Jena, den 19.11.2014

_____

Lutz Tauhardt

Publications P1-P13

P1: L. Tauhardt, K. Kempe, M. Gottschaldt, U. S. Schubert, *Chem. Soc. Rev.* **2013**, *42*, 7998-8011 – Reproduced by permission of The Royal Society of Chemistry.

P2: L. Tauhardt, M. Frant, D. Pretzel, M. Hartlieb, C. Bücher, G. Hildebrand, B. Schröter, C. Weber, K. Kempe, M. Gottschaldt, K. Liefeith, U. S. Schubert, *J. Mater. Chem. B* **2014**, *2*, 4883-4893 – Reproduced by permission of The Royal Society of Chemistry.

P3: M. Bauer, C. Lautenschläger, K. Kempe, L. Tauhardt, U. S. Schubert, D. Fischer, *Macromol. Biosci.* **2012**, *12*, 986-998 – Reproduced by permission of John Wiley & Sons Ltd., UK. Copyright © 2012 WILEY-VCH Verlag GmbH & Co. KGaA, Weinheim.

P4: M. Bauer, S. Schröder, L. Tauhardt, K. Kempe, U. S. Schubert, D. Fischer, *J. Polym. Sci., Part A: Polym. Chem.* **2013**, *51*, 1816-1821 – Reproduced by permission of John Wiley & Sons Ltd., UK. Copyright © 2013 Wiley Periodicals, Inc..

P5: L. Tauhardt, D. Pretzel, K. Kempe, M. Gottschaldt, D. Pohlers, U. S. Schubert, *Polym. Chem* **2014**, *5*, 5751-5764 – Reproduced by permission of The Royal Society of Chemistry.

P6: L. Tauhardt, D. Pretzel, S. Bode, J. Czaplewska, K. Kempe, M. Gottschaldt, U. S. Schubert, *J. Polym. Sci., Part A: Polym. Chem.* **2014**, *52*, 2703–2714 – Reproduced by permission of John Wiley & Sons Ltd., UK. Copyright © 2013 Wiley Periodicals, Inc..

P8: L. Tauhardt, K. Kempe, U. S. Schubert, *J. Polym. Sci., Part A: Polym. Chem.* **2012**, *50*, 4516-4523 – Reproduced by permission of John Wiley & Sons Ltd., UK. Copyright © 2012 Wiley Periodicals, Inc..

P9: Reprinted from Carbohydr. Polym., 113, S. Ochrimenko,[#] A. Vollrath,[#] K. Kempe, L. Tauhardt, S. Schubert, U. S. Schubert, D. Fischer, Dextran-graft-linear poly(ethylene imine)s for gene delivery: Importance of the linking strategy, Pages No. 597-606, Copyright (2014), with permission from Elsevier.

P10: A. C. Rinkenauer,[#] L. Tauhardt,[#] F. Wendler, K. Kempe, M. Gottschaldt, A. Träger, U. S. Schubert, *Macromol. Biosci.,* accepted 07.10.2014 – Reproduced by permission of John Wiley & Sons Ltd., UK. Copyright © 2012 WILEY-VCH Verlag GmbH & Co. KGaA, Weinheim.

P11: Reprinted with permission from *ACS Comb. Sci.* **2013**, *15*, 475-482. Copyright (2013) American Chemical Society.

P12: Reprinted from J. Chromatogr. A, 1325, M. Wagner, C. Pietsch, L. Tauhardt, A. Schallon, U. S. Schubert, Characterization of cationic polymers by asymmetric flow field-flow fractionation and MALS – A comparison with traditional techniques, Pages No. 195-203, Copyright (2014), with permission from Elsevier.

P13: Reprinted with permission from *Biomacromolecules* **2014**, *15*, 1124–1131. Copyright (2014) American Chemical Society.

#Both authors contributed equally.

Publication 1

“Poly(2-oxazoline) functionalized surfaces: From modification to application”

L. Tauhardt, K. Kempe, M. Gottschaldt, U. S. Schubert

Chem. Soc. Rev. **2013**, *42*, 7998-8011

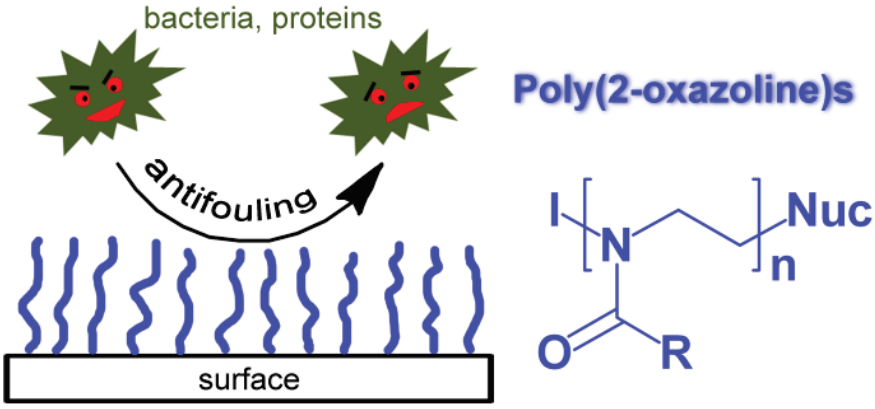

Chem Soc Rev

RSC Publishing

TUTORIAL REVIEW

View Article Online
View Journal | View Issue

Poly(2-oxazoline) functionalized surfaces: from modification to application

Cite this: *Chem. Soc. Rev.*, 2013, **42**, 7998

Received 23rd May 2013

DOI: 10.1039/c3cs60161g

www.rsc.org/csr

Lutz Tauhardt,[ab] Kristian Kempe,†[ab] Michael Gottschaldt[ab] and Ulrich S. Schubert*[abc]

Poly(2-oxazoline)s (POxs) are a versatile class of biocompatible polymers, which have been investigated as poly(ethylene glycol) (PEG) alternatives. In recent years, POxs have drawn significant attention as coatings for antifouling applications. In this tutorial review different approaches to immobilize POxs on surfaces as well as properties and applications of POx coated surfaces will be presented.

Key learning points
(1) Approaches to immobilize poly(2-oxazoline)s on surfaces
(2) Antifouling properties of poly(2-oxazoline) coated surfaces
(3) Parameters that influence the (antifouling) properties of poly(2-oxazoline) coated surfaces
(4) Applications of poly(2-oxazoline) coated surfaces

1. Introduction

Controlling the adhesion or adsorption of cells, proteins, bacteria and other microorganisms onto surfaces is of enormous importance for medicine (*e.g.* implants, medical devices, drug delivery carriers), the food industry (*e.g.* packaging), and mobility (*e.g.* ship hull coatings), but also for (bio)sensor and microarray applications.[1,2] Depending on the application either the promotion (*e.g.* osseointegration of implants) or the prevention of the adhesion (*e.g.* antifouling coatings) is desired. A widely used strategy for the latter is the surface modification with poly(ethylene glycol) (PEG) and PEG-based copolymers.[1,2] However, PEG suffers from a tense patent situation and is known to undergo degradation by (auto-)oxidation to form aldehydes and ethers.[1,2] Because of these problems poly(2-oxazoline)s (POxs), in particular the water soluble poly(2-methyl-2-oxazoline) (PMeOx) and poly(2-ethyl-2-oxazoline) (PEtOx), are investigated as alternative (coating) materials. POxs show similar properties to PEG (*e.g.* antifouling, ''stealth effect'')[3] but in addition they have several advantages such as higher stability,[4] lower viscosity,[1] and a less demanding synthesis.[5] Moreover, a broad variety of oxazoline monomers, as well as functional initiators and terminating agents, allows the synthesis of tailor-made POx.[6] With regard to coating applications, it is necessary to immobilize the POx on the surface. However, a weak binding onto the surface would reduce the long term stability of the coating and is thus not sufficient. Therefore, the surface immobilization process plays an important role in the efficiency and stability of the coating. Using different POxs for surface functionalization (''POxylation'') is an emerging field and immobilization methods have not been reviewed yet. Here, we provide an overview of general approaches to attach POxs to different surfaces, as well as the properties and applications of the POx coated surfaces.

[a] *Laboratory of Organic and Macromolecular Chemistry (IOMC), Friedrich Schiller University Jena, Humboldstraße 10, 07743 Jena, Germany. E-mail: ulrich.schubert@uni-jena.de; Web: http://www.schubert-group.com; Fax: +49-3641-948-202*
[b] *Jena Center for Soft Matter (JCSM), Friedrich Schiller University, Philosophenweg 7, 07743 Jena, Germany*
[c] *Dutch Polymer Institute (DPI), John F. Kennedylaan 2, 5612 AB, Eindhoven, The Netherlands*
† Current address: Department of Chemical and Biomolecular Engineering, The University of Melbourne, Victoria 3010, Australia.

2. Synthesis of poly(2-oxazoline)s and methods for their surface immobilization

2.1 Synthesis of poly(2-oxazoline)s

POxs can be synthesized by cationic ring-opening polymerization (CROP) (Scheme 1). The living character of the CROP allows the synthesis of well-defined polymers with low polydispersity index (PDI) values and adjustable molar masses. Moreover, a broad

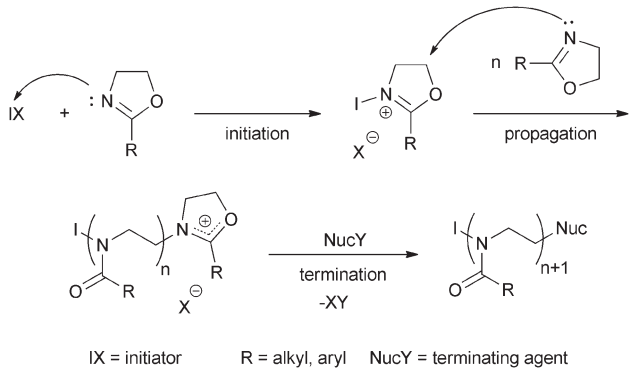

Scheme 1 Schematic representation of the polymerization of 2-oxazolines.

variety of different oxazoline monomers (defined by R), functional initiators (*e.g.* triflates, tosylates, organic iodides or bromides) and terminating agents (*i.e.* nucleophiles) is available and allows the tuning of the polymer properties. Often used POxs are PEtOx (R = Et), PMeOx (R = Me), and poly(2-isopropyl-2-oxazoline) (P*i*PrOx). The utilization of microwave-assisted synthesis procedures enables the polymerization in minutes to a few hours.[5]

2.2 Termination with coupling agents or amine functionalized surfaces ("grafting onto")

The oldest way to obtain POxs that can be attached to surfaces is the direct end-capping of the living polymer species with silane coupling agents such as (3-aminopropyl)triethoxysilane (APTES),[7,8] (3-aminopropyl)triethoxysilane (APTMS),[9,10] sodium (3-mercaptopropyl)trimethoxysilane (MPTMS),[11] and (4-aminobutyl)dimethylmethoxysilane (ABDMMS)[12,13] (Fig. 1).

Another way to introduce a silane functionality to POx is the hydrosilation method by Chujo *et al.*[7,9] Here, a double bond initiated (*e.g.* by allyl tosylate) or terminated (*e.g.* by diallylamine) POx is reacted with trialkyloxysilane in the presence of chloroplatinic acid as a catalyst (Scheme 2).

Multifunctional initiators or terminating agents enable the possibility to introduce more than one silane group.[7,8] The grafting

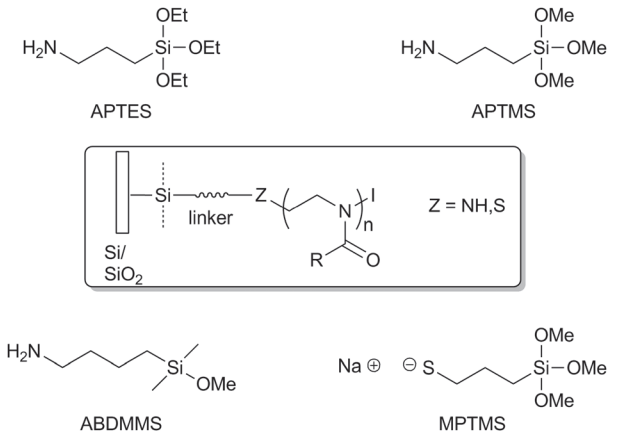

Fig. 1 Different coupling agents that can be used for the direct termination of the living oxazolinium species and the binding of such end-capped POxs onto the surface.

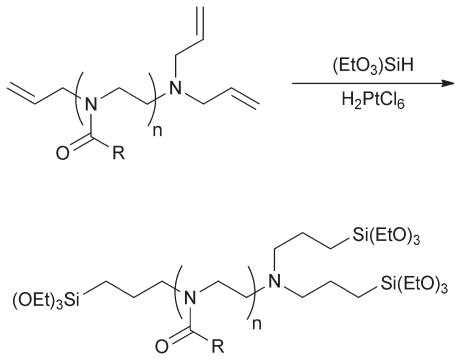

Scheme 2 Schematic representation of the hydrosilation of POx.

of the silane coupling agent functionalized POx onto the surface can be achieved by heating a solution of the polymer together with the particular object (*e.g.* silicon wafer, glass slide) that is supposed to be coated.[10–12]

Besides termination with a coupling agent, it is also possible to quench the living oxazolinium species directly with an amine functionalized surface (*e.g.* APTES modified surfaces). Yoshikawa and Tsubokawa *et al.* applied this method to graft PMeOx onto inorganic fibers,[14] such as glass, alumina, and carbon fibers, but also onto ultrafine silica[15] and carbon black.[16] In a similar approach, Fujiki *et al.*[17] and Yoshikawa *et al.*[18] first grafted poly(amidoamine) (PAMAM) dendrimers onto APTES functionalized glass fibers and silica using Michael addition. By amination of the terminal ester groups of PAMAM with ethylenediamine or hexamethylenediamine, amine end groups were obtained and used to terminate living PMeOx chains (Scheme 3).

The grafting of POxs onto gold surfaces can be achieved *via* disulfide or other sulfur bearing groups which can be introduced

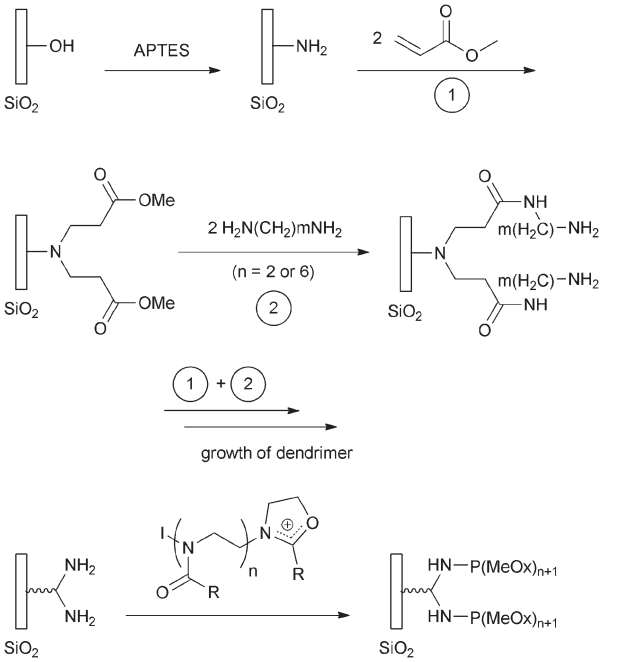

Scheme 3 Schematic representation of the preparation of PMeOx terminated PAMAM dendrimers on glass surfaces.

through the initiator. Lehmann and Rühe utilized tosylates of ω,ω′-dihydroxy alkyl disulfides for the initiation of the oxazoline polymerization and subsequently attached the POx onto the gold surface *via* chemisorption of the sulphur.[19]

2.3 "Clicking" onto the surface

Azide modified surfaces can be "POxylated" by means of copper-catalyzed azide–alkyne cycloaddition (CuAAC, "click" reaction). For this purpose, POx functionalized with an alkyne end group or side chain can be applied.

By means of CuAAC, Haensch *et al.* attached propargyl initiated PEtOx onto azide functionalized silicon wafers (Scheme 4).[20] In a similar manner, Lind *et al.* prepared micropatterned conductive devices on which the poly(styrene) azide ($PS–N_3$) surface was coated with PMeOx.[21]

Manzenrieder *et al.* used copolymers of 2-(pent-4-ynyl)-2-oxazoline (PynOx) and MeOx or EtOx (Fig. 2), but also alkyne initiated PMeOx and PEtOx to stabilize virus-like particles. The P(MeOx-*co*-PynOx) and P(EtOx-*co*-PynOx) were immobilized on azide functionalized particle surfaces *via* the alkyne side chain.

2.4 Surface initiated polymerization ("grafting from")

Besides grafting the POxs onto the surface by the introduction of terminal coupling groups (*e.g.* silanes or azides) or direct quenching of the living species with an amino group bearing surface, it is also possible to initiate the polymerization directly from the surface. For this so called "grafting from" approach an initiator has to be attached to the surface prior to the polymerization (Scheme 5). In the case of silica this can be accomplished by the reaction with silanes bearing initiating moieties like tosylate (OTos),[19] triflate (OTf), *p*-nitrobenzyl sulfonate (ONs),[22] and bromine[23] or iodine (Scheme 5a).[24–26] Gold surfaces can be "POxylated" using thiols with the same initiator groups (Scheme 5c).[27–29]

Another method exploits the self-initiated photografting and photopolymerization (SIPGP) of 2-isopropenyl-2-oxazoline (*i*PrEnOx) followed by the CROP of another oxazoline (Scheme 5b).[30]

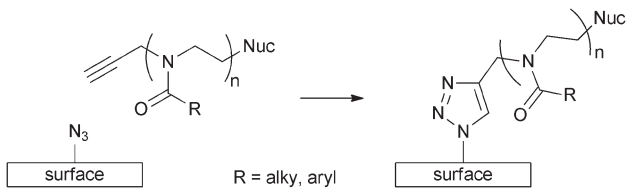

Scheme 4 Schematic representation of the immobilization of POx by "clicking" onto the surface.

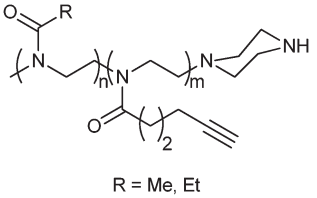

Fig. 2 Schematic representation of P(AlkylOx-*co*-PynOx).

First, *i*PrEnOx is photografted and photopolymerized onto the activated surface (*e.g.* with APTMS). The oxazoline ring of the resulting poly(2-isopropenyl-2-oxazoline) (P*i*PrEnOx) is subsequently attacked with an initiator (*e.g.* MeOTf). To the living oxazolinium species another oxazoline is added and polymerized by CROP. The SIPGP of *i*PrEnOx and the subsequent CROP lead to a bottle brush-like structure of the POx.

2.5 Photoimmobilization

A straightforward approach to obtain POx functionalized surfaces is the photoimmobilization. Two different ways are described in the literature, using either benzophenone (BP) or perfluorophenyl azide (PFPA) derivatives (Scheme 6).

In the case of BP derivatives the photoimmobilization occurs *via* a benzophenone diradical which is formed upon UV irradiation and can attack the polymer at the backbone but also at the side chain. A widely utilized method is the attachment of 4-(3′-chloro-dimethylsilyl)propyloxybenzophenone onto silicon or SiO_2 surfaces, followed by UV light initiated photoimmobilization of the POx (Scheme 3a).[31–35] This procedure was not only applied to immobilize POx, but also for a large variety of other polymers such as PEG, chitosan, and poly(ethylene imine). Besides modifying the surface with a benzophenone derivative it is also possible to use a benzophenone functionalized polymer. Samuel *et al.* attached benzophenone to the linear poly(ethylene imine) (LPEI) units of partially hydrolyzed PEtOx (PHPEtOx) (Scheme 3b).[36] The resulting copolymer of PEtOx, LPEI and poly(2-benzophenone-2-oxazoline) (PBPOx) was immobilized through the PBPOx units onto a poly(methyl methacrylate) (PMMA) film which was deposited on a gold coated lanthanum surface.

For the PFPA derivatives the photoimmobilization takes place by formation of a singlet perfluorophenyl nitren, which is created by the loss of N_2 under UV irradiation and can form covalent bonds with the POx *via* a CH insertion reaction (Scheme 3c). This reaction can also be triggered using heat instead of UV.[37] The "POxylation" of silicon, glass and gold surfaces can be achieved by using PFPA–silane and PFPA–disulfide, respectively.[37–43]

2.6 Other ways to attach POx onto a surface

Konradi and Pidhatika functionalized Nb_2O_5-coated silicon wafers with poly(L-lysine)-*graft*-P(MeOx) (PLL-*g*-PMeOx) copolymers, which have a bottle brush-like structure (Scheme 7a).[1,4,44–46] PLL-*g*-PMeOx copolymers of different side chain grafting densities were prepared by reaction of the PLL backbone with glutaric acid or ethyl piperidine-4-carboxylate end-capped PMeOx. The surface immobilization of the copolymers occurs *via* spontaneous self-assembly, caused by multiple electrostatic interactions between the negatively charged Nb_2O_5-coated silicon wafer and the polycationic PLL backbone. Although attached only by electrostatic interactions, the obtained POx monolayers are stable on the surface. They stand intensive washing processes and the attack of hydrogen peroxide solution.

Lehmann and Rühe reported the attachment of PHPEtOx onto surfaces bearing *N*-hydroxysuccinimide self-assembled

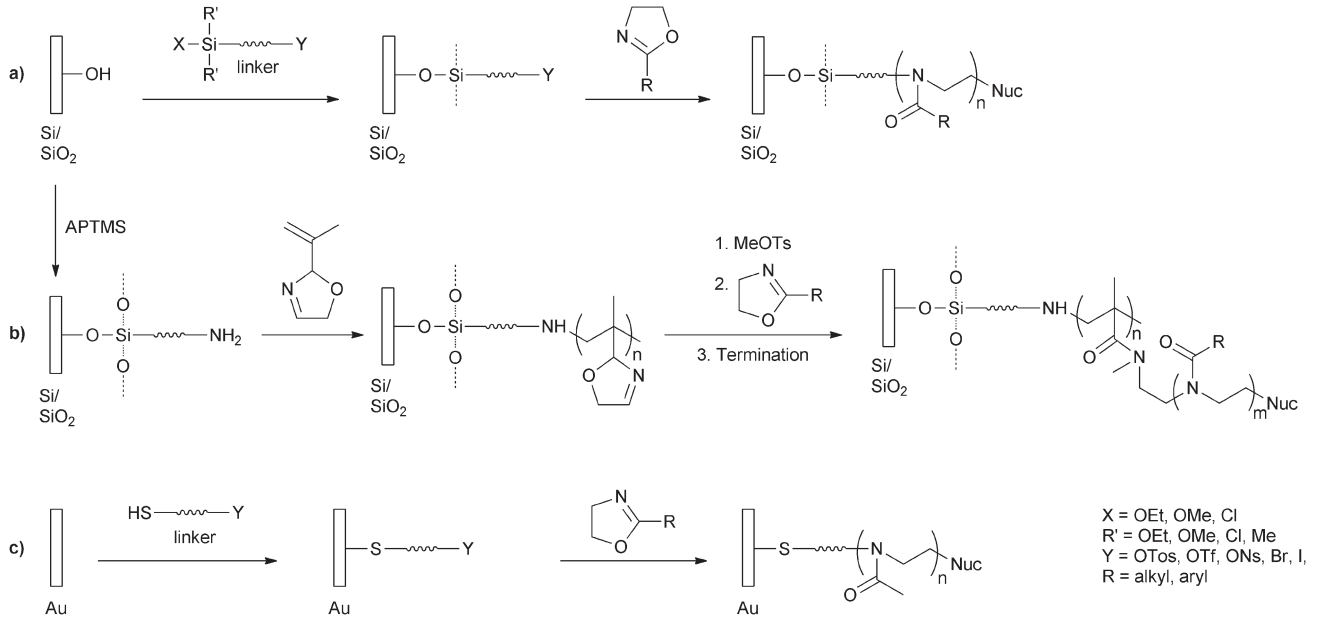

Scheme 5 Schematic representation of the surface initiated CROP of POx using (a) different initiators, (b) self-initiated photografting and photopolymerization of 2-isopropenyl-2-oxazoline followed by CROP of POx, and (c) surface initiated CROP of POx on gold surfaces using different initiators.

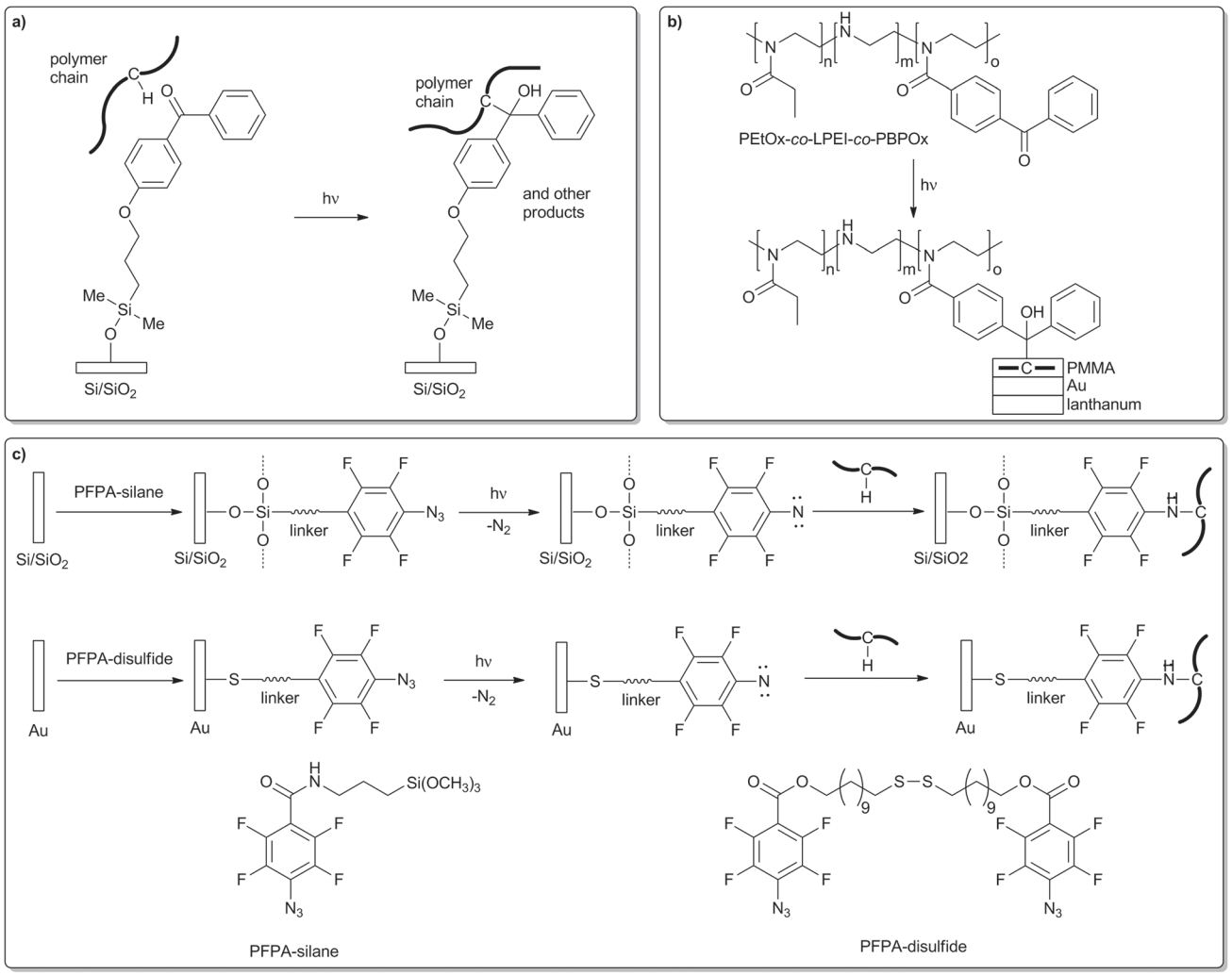

Scheme 6 Schematic representation of the photoimmobilization of POx by (a and b) benzophenone and (c) PFPA derivatives.

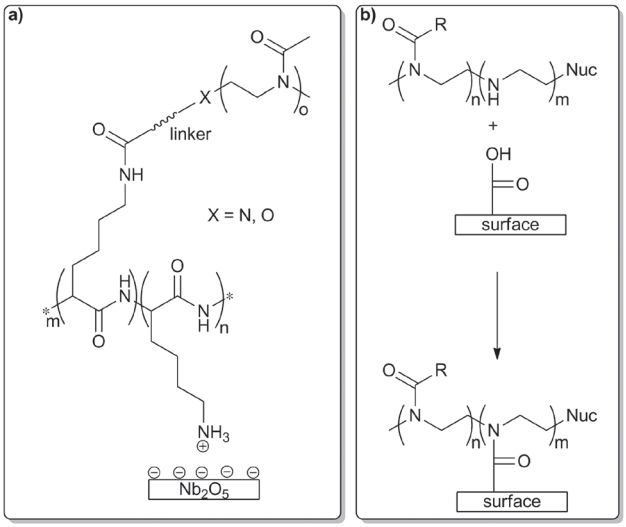

Scheme 7 Schematic representation of the surface immobilization of (a) bottle brush-like PLL-*g*-PMeOx and (b) partially hydrolyzed POx.

monolayers (SAMs).[19] Here, the binding occurred *via* the PEI units of the PHPEtOx. In a similar approach, carboxylic acid functionalized surfaces were ''POxlyated'' by amidation reaction of the COOH moieties with PEI units of partially hydrolyzed PMeOx (PHPMeOx) (Scheme 7b). Jeon *et al.* utilized this procedure to graft PMeOx onto multiwalled carbon nanotubes.[47]

Another ''POxylation'' method, using carboxylic acid functions as well, was introduced by Agrawal *et al.*[48] Copolymers of poly(2-carboxyethyl-2-oxazoline) (PCarbEtOx) and poly(2-isopropyl-2-oxazoline) (P*i*PrOx) (Fig. 3a) were grafted onto poly(glycidyl methacrylate) (PGMA)-coated silicon. The high reactivity of the epoxy groups of PGMA towards the COOH groups of the PCarbEtOx leads to the chemical attachment of the POx chains in a brush-like conformation.

The surface immobilization of POx *via* epoxy units cannot only be achieved with PGMA, but also by POx having epoxy groups.

Trumbo coated steel panels by cross-linking of side chain epoxidized poly(2-(dec-9-enyl)-2-oxazoline) (PDecEnOx) (Fig. 3b) with diamines or anhydrides.[49]

3. Properties and applications of POx modified surfaces

POx functionalized surfaces are of significant interest for applications where the adhesion and adsorption of proteins, cells, bacteria, and other microorganisms need to be controlled, *e.g.* in medicine (*e.g.* for implants), microfluidic devices, and (bio)sensors. In most applications, coating with POx aims to reduce or suppress the unwanted adsorption of proteins (*i.e.* protein fouling) or the undesired adhesion of cells, bacteria, and microorganisms (*i.e.* biofouling), respectively. For this purpose, the POxs used have to meet the following criteria, which were found to be common for all antifouling polymers: (1) the presence of hydrophilic (polar) functional groups and hydrogen bond accepting groups as well as (2) the absence of a net charge and hydrogen bond donating groups.[1,2] Hence, all antifouling investigations focused on water soluble POxs with short side chains (*e.g.* PEtOx, PMeOx) and their water soluble copolymers.

POx coatings are so called biopassive coatings, since most POxs do not actively kill the bacteria or cells but only prevent their adhesion. By introduction of end groups with a quaternary ammonium species, bioactive (*i.e.* actively killing) POx can be obtained.[50] To the best of our knowledge, no investigations on surface attached bioactive POx have been reported yet. Therefore, this chapter will focus on biopassive, anti-adhesive, and repellent coatings.

Depending on the immobilization method and the structure of the used polymer, two types of POx coatings can be distinguished. First, linear, brush-like POx coatings, with only a single POx chain per surface grafting unit (Fig. 4a), and second, POx-based comb polymer coatings, where more than one POx chain per grafting unit is attached to the surface *via* another polymer backbone (*e.g.* PLL) (Fig. 4b). The latter can exhibit a bottle brush-like structure, also referred to as molecular or cylindrical brushes, at high side chain grafting densities.

However, there are major issues which complicate the comparison of the published studies: (1) the diversity of POx attachment and, thus, the different surface architecture, (2) the applied test regimes, *i.e.* the use of different test conditions, different types of cells, bacteria, *etc.*, and (3) the usage of different analytical tools with different detection limits.

3.1 Properties of linear, brush-like POx coatings and their application for controlling cell adhesion and protein adsorption

In most cases of the above presented immobilization methods, the surface will be coated with a single, linear POx chain per grafting unit. Such POxylated surfaces exhibit a brush-like structure.

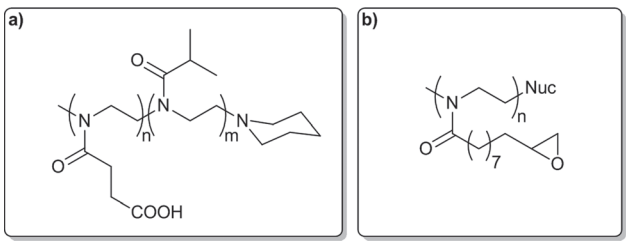

Fig. 3 (a) P(CarbEtOx-*co*-*i*PrOx) and (b) epoxidized PDecEnOx.

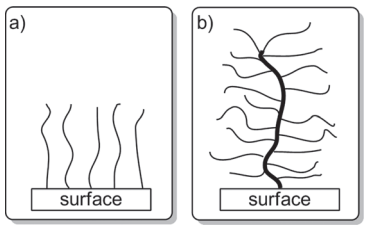

Fig. 4 (a) Linear, brush-like POx coatings and (b) bottle brush-like POx coatings.

The properties of POx functionalized surfaces are influenced in multiple ways. An important parameter of POx coatings is their swelling behavior, since it directly influences the anti-fouling properties. Theoretical calculations for hydrated PEG attached to a hydrophobic substrate showed that upon protein approach the PEG chains are compressed and water molecules are removed from the hydrated polymer.[2] This not only leads to a repulsive elastic force of the compressed chain but also to a thermodynamically unfavorable state. The magnitude of the resulting repulsive force was found to be influenced by the polymer chain length and the surface grafting density. An increased chain length causes greater protein repulsion. Coatings with water soluble POxs, *i.e.* PMeOx and PEtOx, are expected to show a similar behavior.

The swelling behavior of POx coated substrates can be investigated measuring either the weight change of the sample or the variation of the film thickness. Using the latter method a maximum swelling ratio ρ_{max} for POx coatings can be defined as the maximal swelling film thickness d_{max} divided by the initial dry film thickness d_0:

$$\rho_{max} = d_{max}/d_0 \quad (1)$$

Swelling measurements by Chujo *et al.* revealed that PEtOx-modified silica gel can absorb water up to 2.4-times of its own weight, depending on the DP.[8] For longer side chains (butyl, octyl) the water adsorption decreased. Other solvents, such as *N,N*-dimethylsulfoxid, *n*-propanol, or toluene, were adsorbed to a lower extent by all POxs.

Rehfeldt *et al.* investigated the static and dynamic swelling behavior of different chain lengths of APTMS end-capped PMeOx and PEtOx grafted onto SiO_2.[10] By measuring the equilibrium film thickness as a function of relative humidity (static swelling) and the change in film thickness as a function of time after abrupt change in the relative humidity (''osmotic shock'') (dynamic swelling), the authors observed that both the static and the dynamic swelling behavior are dependent on the polymer chain length but not on the type of side chain (Table 1).

Swelling behavior investigations by Lehmann and Rühe showed that the film thickness of PEtOx monolayers attached to gold can increase up to 50% upon exposure to humid air ($\rho_{max} \sim 1.45$).[19] The d_0 for these films (obtained by a ''grafting onto'' approach *via* thiol) increased with the degree of polymerization (DP = 5 to 150) but rapidly leveled off at about 3.5 nm (DP $\geq$ 50).

Table 1 Maximum swelling values of different POxs on different surfaces

Polymer	DP	End group	Spacer	Surface	d_0 (nm)	ρ_{max}
PMeOx	15	CH_3	APTMS	SiO_2	1.82–2.17[a]	2.7–3.4
PEtOx	15	CH_3	APTMS	SiO_2	1.24–2.08[a]	2.8–3.5
PEtOx	30	CH_3	APTMS	SiO_2	2.44–3.97[a]	1.6–1.8
PEtOx	150	Piperidine	$C_{11}H_{22}S$	Au	3.1[b]	$\sim$1.45
PEtOx	10	$N(C_{18}H_{37})_2$	$C_{11}H_{22}S$	Au	8.4–9.1[c]	1.2–1.35

[a] Determined at $\sim$4% relative humidity by ellipsometry.[10] [b] Determined at 0% relative humidity by surface plasmon resonance (SPR) spectroscopy.[19] [c] Determined by ellipsometry.[27]

Using a tosylate initiated ''grafting from'' approach on a silica substrate the authors were able to obtain PEtOx monolayers with d_0 = 20 to 30 nm for DPs > 600. The swelling ratio of this kind of POx coatings was higher ($\rho_{max} \sim 2$) than that observed for the ''grafting onto'' gold approach.

Jordan *et al.* grafted ABDMMS functionalised PEtOx with long alkyl end groups onto silica substrates (Fig. 1).[12] X-ray reflection studies showed that the obtained polymer film (total film thickness of 3.5 nm) was composed of two layers, a polymer sublayer of 1.75 nm and a polymer supported alkyl layer of 1.5 nm.[12,27] The values were obtained from water-swollen layers, where a phase separation of the amphiphilic ligands into a hydrophilic polymer layer and a layer of the tethered alkyl moieties occurred. In another approach Jordan and Ulman coated the gold substrate with PEtOx by surface initiated CROP using triflate of surface tethered 11-hydroxy-undecanethiolate (HUT) as an initiator.[27] The end-capping with *N,N*-dioctadecylamine resulted in a triple layer structure that is similar to the structure reported for the ''grafting onto'' of ABDMMS functionalized PEtOx. For a DP of 10 a film thickness of 9.1 nm was obtained. By swelling in water for 24 h, it increased to 11.3 nm. When rinsed with the poor solvent diethyl ether the film thickness decreased to 8.4 nm. Even after multiple cycles of swelling and deswelling, nearly identical values were obtained (ρ_{max} = 1.2 to 1.35). With $\sim$1.3 nm for the self-assembled monolayer of HUT and $\sim$1.5 nm for the terminal alkyl moiety, the polymer interlayer is 8.5 nm.

All these measurements show that the film thickness and the film quality, and with it the swelling ratio ρ_{max}, are dependent on the surface, the immobilization method, the used spacer, the polymer end group, and the DP. However, due to the diversity of the described systems and the different methods to analyze the films, it is not possible to draw some exact conclusions on how the DP influences the swelling behavior.

Another important parameter is the grafting density. It can be influenced by the concentration of the coupling agent[40] or the polymer,[39] respectively. A lower concentration of the coupling agent will lead to a lower grafting density due to less available binding sides on the surface. In a similar manner, a very low polymer concentration will reduce the grafting density, since not all binding sides will be saturated. However, a higher concentration of both, the coupling agent or the polymer, will increase the grafting density only to a certain point. If all binding sides on the substrate are covered, the excess of coupling agent or polymer cannot bind anymore. These assumptions are confirmed by investigations on the film thickness and grafting density of PEtOx films which were photoimmobilized using PFPA–silane. Bartlett and Yan[38] and Kim *et al.*[41] prepared spin coated PEtOx films of various thicknesses by adjusting the polymer solution concentration (1 to 20 mg mL^{-1}) (Fig. 5b). After removal of the excess polymer, the film thickness was always between 3.1 and 3.2 nm for PEtOx with M_w = 200 000 g mol^{-1}, and 2.8 nm for M_w = 50 000 g mol^{-1}. A similar film thickness (3 nm) was obtained by Prucker *et al.* when they immobilized PEtOx of the same molar mass (50 000 g mol^{-1}) on a benzophenone modified silicone

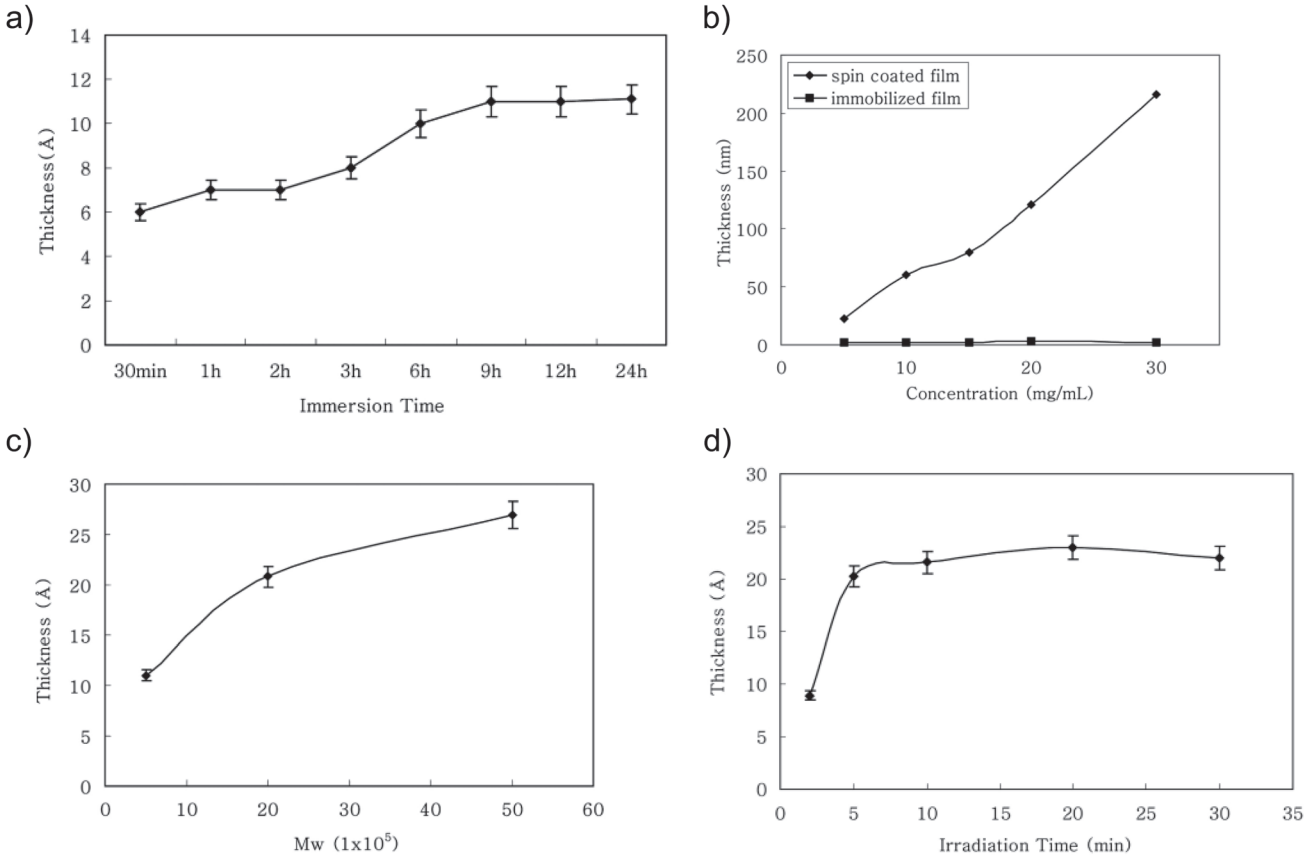

Fig. 5 (a) PFPA–silane film thickness as a function of soaking time. (b) Immobilized PEtOx (M_w = 200 000 g mol^{-1}) film thickness as a function of concentrations. (c) Immobilized PEtOx film thickness as a function of molar mass. Solutions of 10 mg mL^{-1} of PEtOx in chloroform were used. (d) Immobilized PEtOx film thickness as a function of UV irradiation time. Solutions of 10 mg mL^{-1} of PEtOx (M_w = 200 000 g mol^{-1}) in chloroform were used for spin coating. Reproduced with permission from ref. 40. © 2007 Elsevier.

surface.[35] This can be explained by the fact that the CH insertion reaction, which leads to the polymer binding, only occurs at the interface between the radical (benzophenone/nitrene) intermediate and the adjacent polymer chain. Therefore, excess polymer cannot bind and is washed away. However, investigations with PEtOx of different molar masses showed that the film thickness can be influenced by the DP.[37–42] It was observed that a higher molar mass (higher DP) leads to an increased film thickness (Fig. 5c).[38,42] Another parameter that influences the film thickness is the used solvent.[39] From a poor solvent more polymer can be adsorbed onto the substrate than from a good solvent when strong solvent–substrate interactions are absent. Due to the favorable solvation of the polymer in a good solvent, the repulsion between segments of the adsorbed polymer, but also between the adsorbed and the solvated polymer, is higher. This decreases the amount of polymer that is deposited at the surface and, thus, the grafting density and film thickness. Investigations by Wang *et al.* revealed that also the polarity of the used solvent influences the properties of the obtained film.[42] PEtOx was immobilized on PFPA functionalized surfaces using solutions in ethanol, water, and chloroform. The film prepared from chloroform solution had more hydrophobic domains exposed to the surface and was, therefore, slightly more hydrophobic than the films prepared from polar solvents, as revealed by contact angle measurements. In the case of photoimmobilization by benzophenone and PFPA derivatives the film thickness can also be influenced by the irradiation time (Fig. 5d).[35,40,41] Up to a certain point, a longer irradiation leads to an increasing film thickness. After this the film thickness does not increase anymore. The immobilization by PFPA–silane cannot only occur by UV irradiation but also by heating.[37] Here, the same effect of the heating time on the film texture can be observed. After an increase with heating time, the film thickness levels off to a constant value. As mentioned above, ''POxylated'' surfaces are investigated to control the adhesion or adsorption of cells. Depending on the field of interest either a promoted or a reduced cell adhesion is desired. An example for the former are medical implants (*e.g.* heart valves), where xenophobic reactions need to be suppressed and the implant integration has to be improved by controlled adhesion of the appropriate cells (*i.e.* osteoblasts, fibrocytes, *etc.*). In the case of implants in heart and vascular surgery, calcification is the major problem, causing aneurismatic degradation and vascular obliteration.[32–34] Hence, the patients have to be placed permanently on anticoagulation medication to prevent a thrombus. To inhibit the calcium binding the formation of a dense layer of healthy cells

Table 2 Different polymers photoimmobilized *via* benzophenone, their molar mass and film thickness as well as the seeding behavior of different cell lines according to microscopic appearance of the cell layer. Combined and adapted from ref. 31 and 33

Polymer	M_w (g mol^{-1})	d (nm)	Rat Fc	Sheep Fc	HUVEC	C3H10T1/2
PEtOx	380 000	6.0	2–3	2	1	—[a]
PEtOx	500 000	11.2	—[a]	—[a]	—[a]	4
PAA	4 000 000	26.2	3	4	3–4	—[a]
PAA	50 000	6.3	—[a]	—[a]	—[a]	3[b]
PHEMA	2 000 000	22.2	2	2	3–4	—[a]
PHEMA	250 000	3.0	—[a]	—[a]	—[a]	3[c]
Chitosan	400 000	6.1	2	1–2	2	—[a]
PMTA	30 000	4.1	2	2	1	—[a]
PMTA	—[a]	3.1	—[a]	—[a]	—[a]	3–4[c]
PEI	600 000	4.0	1–2	2	1	—[a]
PMAA	70 000	3.9	1	1	1	—[a]
PMAA	254 000	2.5	—[a]	—[a]	—[a]	1
PDMMA	270 000	9.9	3	4	3–4	—[a]
PDMAA	—[a]	11.3	—[a]	—[a]	—[a]	4
PAAm	5 800 000	10.3	4	2–3	4	—[a]
PVA	140 000	2.5	2	1	4	—[a]
PVBP	630 000	6.1	—[a]	—[a]	—[a]	1

[a] Not determined. [b] Inhomogeneous growth on some samples. [c] Some samples with clearly better cell growth. Fc = fibrocytes; HUVEC = human umbilical vein endothelial cells; C3H10T1/2 = murine mesenchymal precursor stem cells; PAA = poly(acrylic acid); PHEMA = poly(2-hydroxyethyl methacrylate); PMTA = poly[2-(methacryloyloxy)-ethyltrimethylammonium chloride]; PEI = poly(ethylene imine); PMAA = poly(methacrylic acid); PDMMA = poly(*N*,*N*-dimethyl acrylamide); PAAm = poly(acrylamide), PVA = poly(vinyl alcohol); PVBP = poly[diethyl(*p*-vinylbenzyl) phosphonate]. 1 = Excellent growth (comparable to the reference), 2 = growth less than on reference, 3 = less than 50% of the surface covered or small agglomerates, 4 = single cells or abnormal morphology.

on the implant needs to be accomplished. To this end, the groups of Rühe and Dahm investigated the suitability of several polymer coatings on glass to adhere rat and sheep fibrocytes as well as human umbilical vein endothelial cells (HUVEC) (Table 2).[32–34] Among these polymers, PEtOx (M_w = 380 000 g mol^{-1}) showed a promoted cell growth and a good adhesion of the cells, in particular for HUVECs. Sheep and rat fibroblast showed a slightly reduced cell growth compared to the glass reference. In a next step, a porcine heart valve was coated with PEtOx (Fig. 6) *via* benzophenone photoimmobilization.[34] A stable surface-attached hydrogel was obtained.

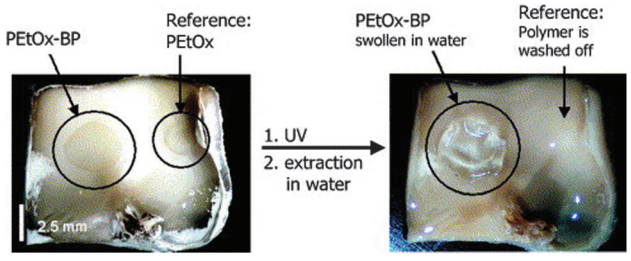

Fig. 6 Deposition of a surface-attached PEtOx on the tissue of a porcine heart valve. Both BP photoimmobilized PEtOx and pure PEtOx were deposited in different areas of the tissue. Only the polymer containing the photoreactive group underwent crosslinking during illumination with UV light and formed a stable surface-attached hydrogel. The reference polymer was washed off during the subsequent extraction of the sample in water. Reproduced with permission from ref. 34. © 2004 Elsevier.

In the case of bone implants small gaps between the bone and the implant remain, opening possibilities for an attack of particles and bacteria, which can cause a chronic inflammatory response followed by the loosening and failure of the implant.[31] Here, the coating needs to be repellent for the particles and bacteria, but at the same time has to promote the adhesion of osteoblasts directly after the implantation. Adden *et al.* studied a large number of benzophenone photoimmobilized polymer coatings on glass regarding their ability to support the adhesion and proliferation of murine mesenchymal precursor stem cells (C3H10T1/2), expressing human bone morphogenetic protein 2 (BMP2) (Table 2).[31] The cells were generated from mouse blastocyst and are able to differentiate into distinct mesenchymal lineages, depending on the stimulus. By the exogenous addition or recombinant expression of the BMP2, osteoblasts, chondrocytes, and adipocytes are developed. While poly(diethyl(*p*-vinylbenzyl)phosphonate) (PVBP) and poly(methacrylic acid) (PMAA) allowed an excellent cell growth, PEtOx (M_w = 500 000 g mol^{-1}) revealed only a weak cell adhesion, and was therefore not suitable to promote the integration of bone implants. The bad cell growth can be ascribed to the protein repellent character of PEtOx. Since the cell-surface adhesion is mediated by cell-adhesive proteins, a reduced protein adhesion will result in a poor cell growth.

The protein resistance of PEtOx was also reported by Wang *et al.*[42,43] Using fluorescence imaging, ellipsometry, and surface plasmon resonance (SPR) imaging, they studied the adsorption of bovine serum albumin (BSA) onto silicon wafers, glass slides, and gold surfaces coated with PFPA-photoimmobilized PEtOx of different molar masses (M_w = 5000 to 500 000 g mol^{-1}). The authors observed that the antifouling properties are influenced by the molar mass, the film thickness, and the used solvent. A higher molar mass and with it an increased film thickness, led to a higher polymer surface concentration and, hence, better protein repellency. Therefore, PEtOx with M_w = 500 000 g mol^{-1} had the best protein-resistance. In addition, it was shown that on PEtOx coatings prepared from chloroform solution, the BSA adsorption was slightly increased compared to films prepared from the polar solvents. This behavior was ascribed to the higher hydrophobicity of the film, caused by the formation of hydrophobic domains which are exposed on the surface. Based on these results, Wang *et al.* produced carbohydrate microarrays where PEtOx films were incorporated as antifouling coatings.[42] Binding studies with fluorescein isothiocyanate (FITC) labeled concanavalin A (FITC-Con A) on the different carbohydrates (mannose, glucose, *etc.*), revealed the reduction of the non-specific adsorption of FITC-Con A on the PEtOx coated samples. In this way the signal to noise ratio of the carbohydrate microarrays could be improved.

Lehmann and Rühe investigated the adsorption of fibrinogen on gold surfaces coated with PEtOx of different DP bound through a thioalkyl spacer.[19] By measuring the film thickness by SPR spectroscopy, the authors observed that the amount of adsorbed fibrinogen decreases with increasing DP, due to the decreasing influence of the relatively hydrophobic ω,ω′-dihydroxy alkyl spacer. At a DP of 150 the surface was almost

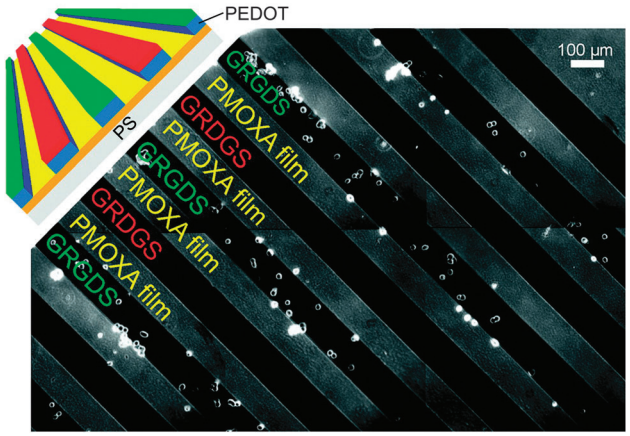

Fig. 7 Specific adhesion of 3T3 fibroblasts to PEDOT–N_3/PEDOT microelectrodes electroclicked with alkyne–PEG–GRGDS (green) *versus* corresponding PEDOT–N_3/PEDOT microelectrodes electroclicked with alkyne–PEG–GRDGS (red) as well as PMeOx–alkyne (red) re-exposed between the electrodes. Adapted and reproduced with permission from ref. 21. © 2012 American Chemical Society.

completely resistant against nonspecific adsorption, as demonstrated by minimal adsorption of fibrinogens (0 to 0.3 nm). The fibrinogen repellency of PEtOx coatings was also reported by Samuel *et al.* who photoimmobilized PHPEtOx-*co*-PBPOx on the surface of a microfluidic device *via* the benzophenone units attached to the polymer backbone.[36] Even when stored for several weeks in PBS buffer solution, the PEtOx coating remained stable and protein repellent.

Lind *et al.* produced micropatterned electronic devices for cell-capturing purposes (Fig. 7).[21] The conductive pattern consisted of poly(3,4-ethylenedioxythiophene) (PEDOT) on a PS–N_3 substrate. On top of the PEDOT pattern they placed peptide modified PEGs, which were coupled onto the PEDOT azide (PEDOT–N_3) surface *via* the alkyne initiator group of the PEGs. As peptides the amino acid sequence Gly-Arg-Gly-Asp-Ser (GRGDS), inducing specific cellular attachment *via* the RGD motif, and the scrambled sequence GRDGS, that does not induce specific cell attachment, have been used. The GRGDS–PEG and GRDGS–PEG were placed in an alternating manner. To reduce nonspecific cell-binding on the PS–N_3 substrate between the microelectrodes, a PMeOx layer was introduced by CuAAC. Cell adhesion studies with 3T3 fibroblasts, which were allowed to adhere for 1 h under stationary flow conditions in a microfluidic setup, followed by applying a defined flow for a specified time to detach and remove weakly bound cells, revealed a good cell adhesion on the GRGDS microelectrodes. As expected, the GRDGS functionalized electrodes as well as the PMeOx coated gaps between the microelectrodes, exhibited only a minor cell attachment (Fig. 7).

3.2 Bottle brush-like POx coatings and their (antifouling) properties

Unlike linear POx coatings with only a single polymer chain per surface grafting unit, POx-based comb polymers possess multiple POx chains linked to another polymer backbone which is attached to the surface. Such materials can be prepared in three different ways: (1) by grafting the POx chains *via* a reactive group onto another polymer backbone (“grafting onto”), (2) by initiating the oxazoline polymerization directly from the polymer backbone (“grafting from”), and (3) by using a POx-macroinitiator, *e.g.* PEtOx end-capped with methacrylic acid (“grafting through”).

An important parameter for comb polymers is the (POx) side chain grafting density (α) on the polymer backbone. It is defined as the number of POx-grafted backbone units divided by the total number of backbone units. The side chain grafting α can be influenced by the amount of initiator (“grafting from”), the addition of co-monomers (“grafting from” and “grafting through”) or the amount of POx that should be coupled to the other polymeric backbone (“grafting onto”). At high POx side chain grafting densities a bottle brush-like structure is formed. At low grafting densities, the POx side chains are too separated to form such a bottle brush-like structure (“mushroom” regime). In particular, the bottle brush-like structures were found to have high potential for antifouling applications. They share the structural motif with proteoglycans, which are a major component of the extracellular matrix and play an important role in cell adhesion.[30]

Zhang *et al.* reported the synthesis of surface attached POx bottle brushes by SIPGP of 2-isopropenyl-2-oxazoline followed by the surface initiated living CROP of different oxazolines, namely MeOx, EtOx, and 2-*n*-propyl-2-oxazoline (*n*PrOx) (Scheme 5b).[30] Using fluorescence microscopy, the authors investigated the influence of different parameters on the adsorption of the protein fibronectin (Fn) (Fig. 8). Variation of the side chain hydrophilicity revealed a comparable low Fn adsorption for the hydrophilic PEtOx and PMeOx ($\leq$6 ng cm^{-2}), near to the detection limit around 1 ng cm^{-2}. In contrast, a high Fn adsorption was observed for the more hydrophobic P*n*PrOx side chains (90 ng cm^{-2}). Moreover, the side chain length was found to have a significant influence. While very short PMeOx chains (m = 6) adsorbed about 45 ng cm^{-2} of Fn, the protein adsorption was effectively suppressed with longer side chain lengths ($\leq$11 ng cm^{-2} for m = 18). Variation of the POx side chain end group showed that its polarity has a very small influence on the protein repellency compared to other structural and compositional parameters. While ethyl isonipecotate and piperidine end-capped PMeOx had a low Fn adsorption, the value for *N*-Boc-piperazine end-capped PMeOx was slightly higher, due to the higher hydrophobicity of the terminal *tert*-butyl moiety.

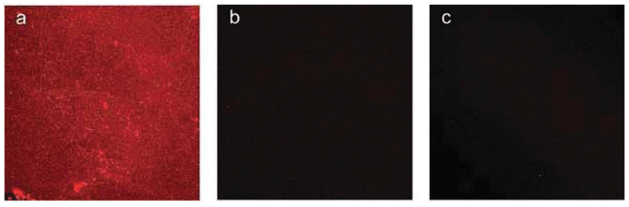

Fig. 8 Fluorescence microscopy of Fn adsorption on bottle brush-like POx coatings on glass reveals a good adsorption on (a) P*n*PrOx and no adsorption on (b) PEtOx and (c) PMeOx. Fn adsorption was performed for 1 h in a 50 µg mL^{-1} solution of labeled Fn in PBS at pH = 7.4 and 37 °C. Reproduced with permission from ref. 30. © 2012 John Wiley and Sons.

Although bearing the most hydrophilic end group (–OH), piperidinol end-capped PMeOx had the highest Fn adsorption. This finding is in accordance with the criteria for antifouling polymers. The hydrogen bonding donor properties of the hydroxy group decrease the protein repellency. In a next step, Zhang *et al.* investigated the adhesion behavior of HUVEC to POx bottle brush modified surfaces.[30] Since the attachment of cells to a solid surface is mediated by adsorbed proteins, the HUCEC seeding and cultivation was performed after the (attempted) Fn adsorption. It was found that even moderate Fn adsorption leads to cell adhesion. In contrast, on all surfaces that effectively suppressed the Fn attachment the adhesion or spreading of HUVEC was inhibited. The prevention of HUVEC adhesion shows that bottle brush-like POx coatings are better suitable for antifouling coatings, since photoimmobilized linear POx promoted the growth of HUVEC as shown by the groups of Rühe and Dahm.[32,33]

The higher efficiency of bottle brush-like structures can be ascribed to the higher POx amount per grafting unit, which effectively prevent the adsorption of proteins and, thus, the adhesion of cells.

Using another approach, Konradi and Pidhatika synthesized bottle brush-like POx by grafting PMeOx onto a PLL backbone.[1,4,44–46] The resulting PLL-*g*-PMeOx was attached onto negatively charged Nb_2O_5 through electrostatic interaction with the positively charged PLL backbone (Scheme 4). Polymers with PMeOx side chains of varying molar masses (M_w = 4000 to 8000 g mol^{-1}) and different side chain grafting densities (α = 0.05 to 0.77) were prepared. For comparison PLL-*g*-PEGs, having side chains with the same molar masses and comparable grafting densities as the PMeOx polymers, were synthesized. The coated Nb_2O_5 substrates were investigated in terms of their repellency of full human serum protein and *Escherichia coli* bacteria, as well as their stability. The adsorbed polymer, bacteria, and protein mass, as well as the average surface density of the PMeOx chains and the film thickness were quantified by means of optical waveguide lightmode spectroscopy (OWLS) and variable-angle spectroscopic ellipsometry (VASE). In OWLS the adsorbed mass is recorded as a function of time (Fig. 9). After the adsorption of the copolymer, the surface was rinsed with a buffer solution, exposed to full human serum, and rinsed again. The resistance towards the protein adsorption derives from a difference in the adsorbed mass before and after treatment with full human serum and rinsing with buffer solution. In this way, it was observed that the extent of polymer adsorption to the Nb_2O_5 substrate and, thus, the surface charge (zeta potential ζ) and the protein repellency, is dependent on the side chain grafting density α and the side chain molar mass. With increasing PMeOx grafting density the zeta potential of the PLL-*g*-PMeOx becomes more negative. The amount of adsorbed polymer mass as a function of α passes through a maximum and becomes zero at extremely high side chain grafting densities, whereas the bacteria and protein mass adsorption follows an inverse trend (Fig. 10). At low side chain grafting densities ($\alpha \approx 0.05$ to 0.1) the surface was positively charged due to the excess of lysine

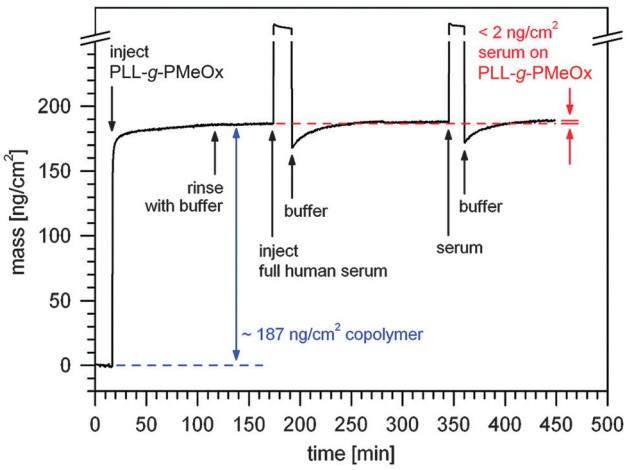

Fig. 9 Mass plot obtained by *in situ* optical waveguide lightmode spectroscopy (OWLS) showing the surface adsorption of PLL-*g*-PMeOx [PMeOx (5000 g mol^{-1})/Lys = 0.22] on Nb_2O_5 and its subsequent exposure to full human serum. Adapted and reproduced with permission from ref. 44. © 2008 American Chemical Society.

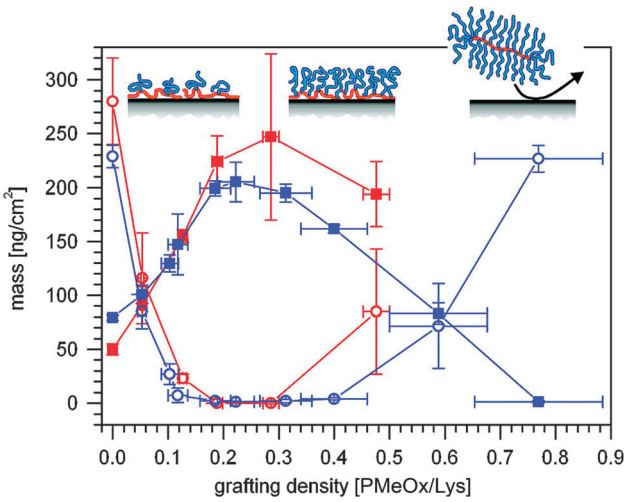

Fig. 10 Quantitative comparison of the PLL (20 kDa)-*g*-PmeOx (5 kDa) (blue squares) and PLL (20 kDa)-*g*-PEG (5 kDa) (red squares) adsorbed mass as a function of the side chain grafting density (number of PEG and PMeOx side chains per lysine unit, respectively). The adsorbed protein mass after subsequent exposure of PLL-*g*-PMOXA- (blue circles) and PLL-*g*-PEG-covered surfaces (red circles) to full human serum shows a minimum at the highest polymer coverage. Zero grafting density corresponds to the bare PLL backbone. Adapted and reproduced with permission from ref. 44. © 2008 American Chemical Society.

units. However, as a result of polymer adlayer defects, the adsorption of serum proteins could be observed. With increasing α, the amount of adsorbed polymer mass increased, whereas the serum adsorption decreased. The optimum was reached at medium side chain grafting densities ($\alpha \approx 0.22$ to 0.33), with the highest mass of the adsorbed polymer on the substrate, a zeta potential ζ that was close to neutral and a serum adsorption below the detection limit of the OWLS instrument of ~1 to 2 ng cm^{-2}. At higher POx side chain grafting densities ($\alpha \geq 0.56$), more and more positive charges of the PLL backbone are eliminated. Moreover, steric, energetic, and kinetic effects along with the reduced copolymer flexibility

led to an inhomogenously and incompletely covered surface and, subsequently, to a lower protein repellency. As a result of the incomplete coverage and the loss of positive charges, the ζ of the surface becomes more and more negative, with increasing PMeOx grafting density. At very high side chain grafting densities ($\alpha \geq 0.77$) nearly every lysine unit carries a PMeOx chain and the polymer adsorption to the negatively charged substrate was fully inhibited. Hence, a monolayer of serum proteins was adsorbed with a mass >200 ng cm^{-2} similar to blank Nb_2O_5.

Moreover, it was found that the optimal α depends on molar mass of the side chain (Fig. 11). The higher the side chain molar mass, the lower the optimal grafting density. As a result of this, the minimal number of side chain monomer units per surface area that is required to obtain fully resistant surfaces is lower for PLL-*g*-PMeOx than for PLL-*g*-PEG. PLL-*g*-PMeOx monolayers reach full repellency already at approximately 10 to 12 monomer units per nm^2 (n per nm^2), whereas for PLL-*g*-PEG approximately twice the amount is necessary (≥ 20 n_{EG} per nm^2), since an ethylene glycol monomer unit has only half the molar mass of a MeOx repeating unit. However, an exact α is not decisive to obtain highly protein-repellent surfaces, since the minimum in serum adsorbed mass is rather broad.

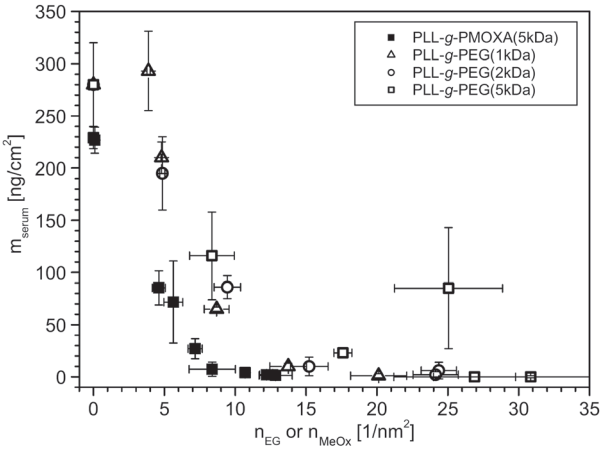

Fig. 11 Serum adsorbed mass as a function of the side chain monomer surface density for PLL-*g*-PMeOx (5 kDa) (black full squares), PLL-*g*-PEG (1 kDa) (open triangles), PLL-*g*-PEG (2 kDa) (open circles), and PLL-*g*-PEG (5 kDa) (open squares). Adapted and reproduced with permission from ref. 45. © 2008 Swiss Chemical Society.

In addition to the serum protein adsorption behavior, Pidhatika *et al.* investigated the adhesion of *E. coli* K12 bacteria at varying ionic strengths of the solution.[1,4,45] The *E. coli* strains were genetically engineered either to lack or to express type 1 fimbriae. Fimbriae are thin, hair-like proteinaceous appendages of the bacterial cell membrane, which can interact with surfaces through specific and non-specific interactions and, therefore, can mediate non-specific adhesion. Both used *E. coli* strains had a net negative charge at all investigated ionic strength.

Non-fimbriated bacteria behaved like hard, negatively charged particles and their adhesion seemed to be mainly driven by electrostatic interactions (Fig. 12a). Therefore, at low ionic strength the bacterial adhesion was high for low α (''mushroom'' type) and pure PLL (positive ζ). At high side chain grafting densities and pure Nb_2O_5 the bacteria adhesion was suppressed due to the repulsion between the negatively charged surface and the negative bacteria surface. At physiologically relevant salt concentrations (160 mM) the influence of electrostatic interactions is reduced and, hence, the adhesion is mostly governed by PMeOx surface density. Here, bacteria adhesion followed a similar trend as described for the protein adsorption. Independent of the ionic strength a medium side chain grafting density (α = 0.3) showed the best antifouling properties.

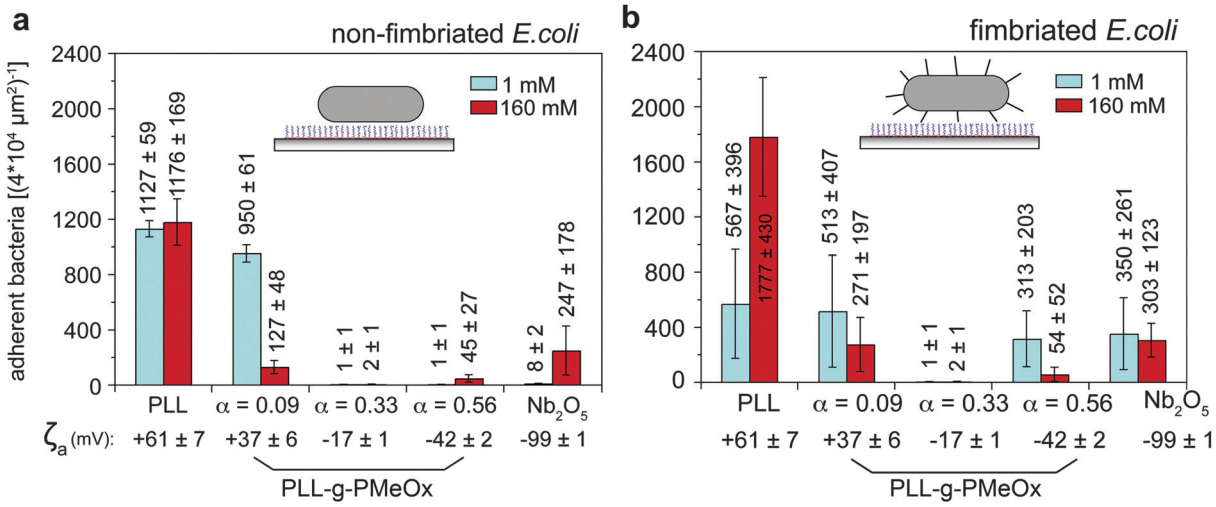

Fig. 12 Average numbers of (a) non-fimbriated and (b) fimbriated *E. coli* bacteria adhered on 4 × 104 µm^2 area after incubation in a protein-free buffer medium of either 1 mM or 160 mM ionic strength present on the different model surfaces: bare Nb_2O_5 and Nb_2O_5 coated with PLL and PLL-*g*-PMeOx with different grafting densities (α = 0.09, 0.33, and 0.56). Adapted and reproduced with permission from ref. 4. © 2010 Elsevier.

However, fimbriated *E. coli* revealed a different behavior (Fig. 12b). Due to the high length of the *E. coli* fimbriae (up to a micron), interactions between the negative bacterial body net charge and the surface can be neglected. Instead, the bacterial adhesion mainly occurs through fimbrial tip protein adhesion, which is driven by van der Waals, electrostatic, and in particular by hydrophobic interactions. Since the latter is the main driving force for the adhesion of fimbriated *E. coli*, all charged surfaces, *i.e.* pure PLL and Nb_2O_5 as well as PLL-*g*-PMeOx with a low or high α, showed bacterial fouling.

At low ionic strength primary (directly at the Nb_2O_5 surface) and secondary (on top of the polymer adlayer) adsorptions, caused by electrostatic interactions, play a role, whereas only primary adsorption occurs at high ionic strength. Hence, the behavior is again similar to that of non-fimbriated bacterial and serum proteins. For both ionic strengths, only dense brush monolayers, consistent with a medium α, effectively inhibited bacterial adhesion by reducing primary and secondary adsorption of the fimbrial tip proteins by preventing short-range van der Waals and hydrophobic interactions between the bacteria and the surface, and shielding attractive electrostatic forces. Both PLL-*g*-PMeOx and PLL-*g*-PEG of optimal grafting density were found to reduce *E. coli* adhesion to $<1\%$ compared to the blank Nb_2O_5 substrate.[45]

Pidhatika *et al.* further investigated PLL-*g*-PMeOx and PLL-*g*-PEG bottle brush coatings as to their long time stability which is an important parameter for antifouling coatings.[1,46] The authors prepared a solution containing 10 mM hydrogen peroxide, 10 mM 4-(2-hydroxyethyl)-1-piperazine ethane sulfonic acid (HEPES), and 150 mM NaCl at a pH of 7.4. This mixture mimics a physiological solution in the presence of an oxidative substance secreted by cells and bacteria.

When treated with this mixture, the PLL-*g*-PMeOx coatings only degenerated to less than 20%, while the PLL-*g*-PEG film thickness decreased up to 60%. Subsequent exposure to full human serum showed that the PLL-*g*-PMeOx remained largely protein repellent, in contrast to PLL-*g*-PEG where a strong protein adsorption was observed.

3.3 Other applications

"POxylated" surfaces are not only interesting for controlling protein adsorption and cell adhesion, but also for other applications.

POx coatings can be applied in dip-pen nanolithography (DPN). DPN is a direct-write scanning probe method which uses "ink"-coated atomic force microscope (AFM) tips to transport ink materials, such as dissolved proteins or peptides, to a surface. The driving force for the material transport is molecular diffusion through a water meniscus formed between the tip and the substrate surface. Unfortunately, for larger (bio)-materials, such as viruses and bacteria, the transport and deposition through the water meniscus is a challenging task. However, the group of Lim demonstrated that PMeOx-coated tips are suitable to overcome this problem and can be applied for the direct-write patterning of adeno-associated viruses (AAVs)[25] and bacteria cells (*E. coli* JM 109)[24] by DPN (Fig. 13).

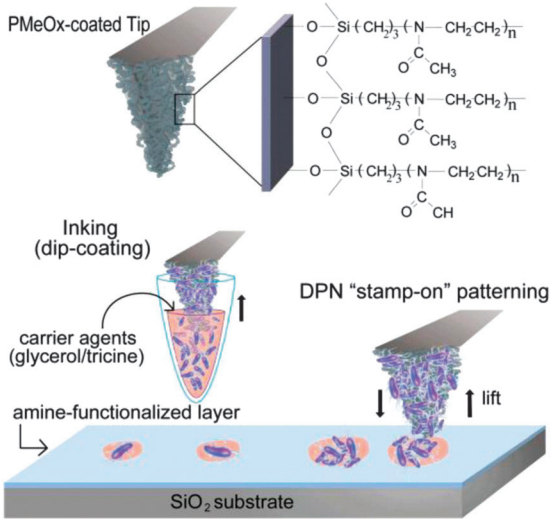

Fig. 13 Representation of "stamp-on" DPN of bacterial cells on modified surfaces. Reproduced with permission from ref. 24. © 2012 American Chemical Society.

By adsorbing the ink, the surface immobilized PMeOx forms a swollen hydrogel, which reduces the denaturation and desiccation of the ink as well as the associated viruses or bacteria. When brought into contact with an amine-functionalized surface, the ink solution diffuses out of the nanoporous hydrogel on the tip and onto the surface. Compared to classical DPN, where the ink diffusion is meniscus mediated, the diffusion barrier within the PMeOx-hydrogel is very small and, therefore, allows the transport of larger bioparticles. A further beneficial effect of PMeOx is the already described biomolecule repellency, which enhances the diffusion from the hydrogel. In addition, the diffusion is driven by electrostatic interactions between the positive amine-functionalized surface of the substrate and the negatively charged surface of the AAVs or bacteria, respectively. However, upon patterning the *E. coli* bacteria died. This behavior was attributed to cell membrane damage that occurred during the drying step of the patterning process. By means of fluorescence microscopy it was shown that the bacteria coated to the AFM tip were still alive after 40 min, when a mixture of glycerol and tricine was used as carrier ink. This mixture not only protects *E. coli* bacteria from drying and denaturing while on the tip, but also increases the viscosity and interaction of the ink solution and, thus, facilitates the bacterial cell delivery during the patterning process. As a result of this, the cell death has to take place by denaturation on the surface rather than the DPN itself. The problem of cell death was overcome by coating the amine-functionalized surface with lysogeny broth (LB) agar, which is commonly used for growing cells. Using this method, all bacteria remained alive even when a high contact force was applied for the deposition.

Another application of "POxylated" surfaces is the immobilization and stabilization of nanoparticles (NPs). Agrawal *et al.* reported P(CarbEtOx-*co*-*i*PrOx) (Fig. 3a) layers which were obtained by reacting the epoxy groups of PGMA coated on silica with the carboxyl groups of the PCarbEtOx units.[48] A brush-like

conformation of the POx chains was obtained and used for the stabilization of Au NPs. Compared to other conventional surface modification techniques, such as self-assembled monolayers (SAMs), the usage of such P(CarbEtOx-*co*-*i*PrOx) brushes has some advantages: (1) the easy and controllable introduction of the polymer, (2) a high polymer surface density, (3) a high stability and robustness of the grafted layers, (4) biocompatibility, (5) temperature responsiveness due to the P*i*PrOx, and (6) the presence of numerous polar functionalities, *i.e.* unreacted carboxyl groups, amino groups in the backbone, and carbonyl groups in the POx side chain, which can be exploited to bind the NPs. In addition the immobilized Au NPs show excellent catalytic and optical properties. Therefore, the developed system has great application potential in areas such as catalysis, sensors, medicine, and optics.

4. Conclusions

Poly(2-oxazoline)s are a highly interesting class of polymers for many applications. The first two members of the aliphatic homologue series, namely poly(2-methyl-2-oxazoline) and poly(2-ethyl-2-oxazoline), do not only show the so called ''stealth effect'' and exhibit similar antifouling properties to PEG, but also have other beneficial properties such as a higher stability and a lower viscosity. Moreover, they are less demanding in their synthesis and a broad range of different oxazoline monomers, functional initiators and terminating agents is available, allowing the synthesis of tailor-made polymers by CROP with adjustable properties.

An emerging application field of POxs is their use as antifouling coatings. However, POx coatings cannot only be applied for the control of cell adhesion and protein adsorption, but also for the stabilization of inorganic nanoparticles, such as Au NPs, and in nanolithography. POx coatings can be prepared using different approaches, such as ''grafting from'', ''grafting onto'', photoimmobilization or immobilization by electrostatic interactions. Different parameters influence the properties of POx coatings, namely: the surface and side chain grafting density, the film thickness, the type of (co)polymer and related to this their hydrophobicity and swelling behavior. Depending on the immobilization method and the structure of the used polymer, two types of POx coatings can be distinguished: (1) linear POx coatings with only a single chain per surface grafting unit, and (2) bottle brush-like POx coatings which exhibit multiple POx chains per grafting unit and are attached to the surface *via* another polymer backbone. Both coating types can endow surfaces with antifouling properties. However, as reported to date, in particular POx bottle brushes show excellent antifouling properties.

Acknowledgements

KK is grateful to the Alexander von Humboldt-foundation for financial support. USS thanks the Dutch Polymer Institute (DPI, technology area HTE) for financial support. The authors would like to thank the Bundesministerium für Bildung und Forschung (Germany) for funding (project: BASIS, 03WKCB01C).

Notes and references

1 R. Konradi, C. Acikgoz and M. Textor, *Macromol. Rapid Commun.*, 2012, **33**, 1663–1676.
2 I. Banerjee, R. C. Pangule and R. S. Kane, *Adv. Mater.*, 2011, **23**, 690–718.
3 N. Adams and U. S. Schubert, *Adv. Drug Delivery Rev.*, 2007, **59**, 1504–1520.
4 B. Pidhatika, J. Möller, E. M. Benetti, R. Konradi, E. Rakhmatullina, A. Mühlebach, R. Zimmermann, C. Werner, V. Vogel and M. Textor, *Biomaterials*, 2010, **31**, 9462–9472.
5 F. Wiesbrock, R. Hoogenboom, M. A. M. Leenen, M. A. R. Meier and U. S. Schubert, *Macromolecules*, 2005, **38**, 5025–5034.
6 B. Guillerm, S. Monge, V. Lapinte and J.-J. Robin, *Macromol. Rapid Commun.*, 2012, **33**, 1600–1612.
7 Y. Chujo, E. Ihara, S. Kure and T. Saegusa, *Macromolecules*, 1993, **26**, 5681–5686.
8 Y. Chujo, E. Ihara, K. Suzuki and T. Saegusa, *Polym. Bull.*, 1993, **31**, 317–322.
9 Y. Chujo, E. Ihara, H. Ihara and T. Saegusa, *Macromolecules*, 1989, **22**, 2040–2043.
10 F. Rehfeldt, M. Tanaka, L. Pagnoni and R. Jordan, *Langmuir*, 2002, **18**, 4908–4914.
11 T. Loontjens and L. Rique-Lurbet, *Des. Monomers Polym.*, 1999, **2**, 217–229.
12 R. Jordan, K. Graf, H. Riegler and K. K. Unger, *Chem. Commun.*, 1996, 1025–1026.
13 R. Jordan, K. Martin, H. J. Räder and K. K. Unger, *Macromolecules*, 2001, **34**, 8858–8865.
14 S. Yoshikawa, N. Tsubokawa, K. Fujiki and M. Sakamoto, *Compos. Interfaces*, 1998, **6**, 395–407.
15 N. Tsubokawa and S. Yoshikawa, *J. Polym. Sci., Part A: Polym. Chem.*, 1995, **33**, 581–586.
16 S. Yoshikawa and N. Tsubokawa, *Polym. J.*, 1996, **28**, 317–322.
17 K. Fujiki, M. Sakamoto, S. Yoshikawa, T. Sato and N. Tsubokawa, *Compos. Interfaces*, 1998, **6**, 215–226.
18 S. Yoshikawa, T. Satoh and N. Tsubokawa, *Colloids Surf., A*, 1999, **153**, 395–399.
19 T. Lehmann and J. Rühe, *Macromol. Symp.*, 1999, **142**, 1–12.
20 C. Haensch, T. Erdmenger, M. W. M. Fijten, S. Hoeppener and U. S. Schubert, *Langmuir*, 2009, **25**, 8019–8024.
21 J. U. Lind, C. Acikgöz, A. E. Daugaard, T. L. Andresen, S. Hvilsted, M. Textor and N. B. Larsen, *Langmuir*, 2012, **28**, 6502–6511.
22 K. Yoshinaga and Y. Hidaka, *Polym. J.*, 1994, **26**, 1070–1079.
23 J.-H. Lee, Y.-C. An, D.-S. Choi, M.-J. Lee, K.-M. Kim and J.-H. Lim, *Macromol. Symp.*, 2007, **249–250**, 307–311.
24 J. Kim, Y.-H. Shin, S.-H. Yun, D.-S. Choi, J.-H. Nam, S. R. Kim, S.-K. Moon, B. H. Chung, J.-H. Lee, J.-H. Kim,

K.-Y. Kim, K.-M. Kim and J.-H. Lim, *J. Am. Chem. Soc.*, 2012, **134**, 16500–16503.
25 Y.-H. Shin, S.-H. Yun, S.-H. Pyo, Y.-S. Lim, H.-J. Yoon, K.-H. Kim, S.-K. Moon, S. W. Lee, Y. G. Park, S.-I. Chang, K.-M. Kim and J.-H. Lim, *Angew. Chem., Int. Ed.*, 2010, **49**, 9689–9692.
26 J. Ueda, W. Gang, K. Shirai, T. Yamauchi and N. Tsubokawa, *Polym. Bull.*, 2008, **60**, 617–624.
27 R. Jordan and A. Ulman, *J. Am. Chem. Soc.*, 1998, **120**, 243–247.
28 R. Jordan, N. West, A. Ulman, Y.-M. Chou and O. Nuyken, *Macromolecules*, 2001, **34**, 1606–1611.
29 M. Rusa, J. K. Whitesell and M. A. Fox, *Macromolecules*, 2004, **37**, 2766–2774.
30 N. Zhang, T. Pompe, I. Amin, R. Luxenhofer, C. Werner and R. Jordan, *Macromol. Biosci.*, 2012, **12**, 926–936.
31 N. Adden, A. Hoffmann, G. Gross, H. Windhagen, F. Thorey and H. Menzel, *J. Biomater. Sci., Polym. Ed.*, 2007, **18**, 303–316.
32 B.-J. Chang, O. Prucker, E. Groh, A. Wallrath, M. Dahm and J. Rühe, *Colloids Surf., A*, 2002, **198–200**, 519–526.
33 M. Dahm, B.-J. Chang, O. Prucker, M. Pierkes, T. Alt, E. Mayer, J. Rühe and H. Oelert, *Ann. Thorac. Surg.*, 2001, **71**, S437–S440.
34 H. Murata, B. J. Chang, O. Prucker, M. Dahm and J. Rühe, *Surf. Sci.*, 2004, **570**, 111–118.
35 O. Prucker, C. A. Naumann, J. Rühe, W. Knoll and C. W. Frank, *J. Am. Chem. Soc.*, 1999, **121**, 8766–8770.
36 J. D. J. S. Samuel, T. Brenner, O. Prucker, M. Grumann, J. Ducree, R. Zengerle and J. Rühe, *Macromol. Chem. Phys.*, 2010, **211**, 195–203.
37 M. Yan and J. Ren, *Chem. Mater.*, 2004, **16**, 1627–1632.
38 M. A. Bartlett and M. Yan, *Adv. Mater.*, 2001, **13**, 1449–1451.
39 J. P. Gann and M. Yan, *Langmuir*, 2008, **24**, 5319–5323.
40 J. Y. Kim, Y. H. Park, J. S. Kim, K. T. Lim and Y. T. Jeong, *J. Ind. Eng. Chem.*, 2007, **13**, 1023–1028.
41 J. Y. Kim, Y. H. Park, J. S. Kim, K. T. Lim, M. Yan and Y. T. Jeong, *J. Ind. Eng. Chem.*, 2007, **13**, 781–785.
42 H. Wang, L. Li, Q. Tong and M. Yan, *ACS Appl. Mater. Interfaces*, 2011, **3**, 3463–3471.
43 H. Wang, J. Ren, A. Hlaing and M. Yan, *J. Colloid Interface Sci.*, 2011, **354**, 160–167.
44 R. Konradi, B. Pidhatika, A. Muhlebach and M. Textor, *Langmuir*, 2008, **24**, 613–616.
45 B. Pidhatika, J. ller, V. Vogel and R. Konradi, *Chimia*, 2008, **62**, 264–269.
46 B. Pidhatika, M. Rodenstein, Y. Chen, E. Rakhmatullina, A. Muhlebach, C. Acikgoz, M. Textor and R. Konradi, *Biointerphases*, 2012, **7**, 1–15.
47 J.-H. Jeon, S.-H. Lee, J.-H. Lim and K.-M. Kim, *J. Appl. Polym. Sci.*, 2010, **116**, 2937–2943.
48 M. Agrawal, J. C. Rueda, P. Uhlmann, M. Müller, F. Simon and M. Stamm, *ACS Appl. Mater. Interfaces*, 2012, **4**, 1357–1364.
49 D. Trumbo, *J. Coat. Technol. Res.*, 2006, **3**, 87–88.
50 C. P. Fik, C. Krumm, C. Muennig, T. I. Baur, U. Salz, T. Bock and J. C. Tiller, *Biomacromolecules*, 2012, **13**, 165–172.

Publication 2

“Amine end-functionalized poly(2-ethyl-2-oxazoline) as promising coating material for antifouling applications”

L. Tauhardt, M. Frant, D. Pretzel, M. Hartlieb, C. Bücher, G. Hildebrand, B. Schröter, C. Weber, K. Kempe, M. Gottschaldt, K. Liefeith, U. S. Schubert

J. Mater. Chem. B **2014**, *2*, 4883-4893

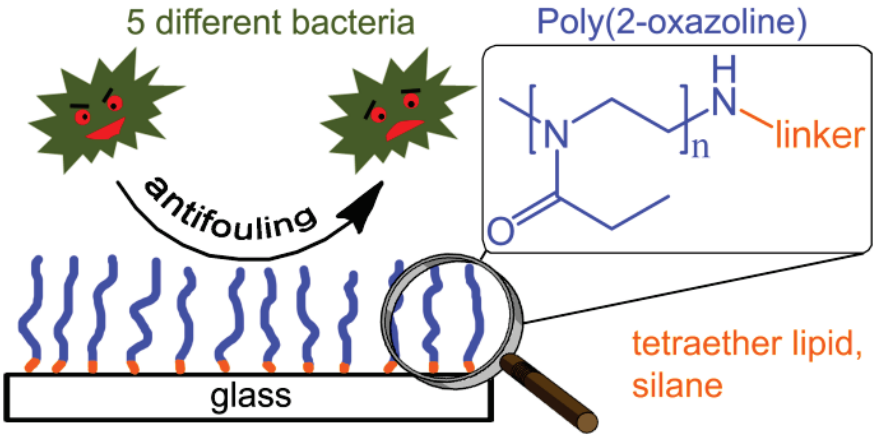

Journal of Materials Chemistry B

PAPER

View Article Online
View Journal | View Issue

Cite this: *J. Mater. Chem. B*, 2014, **2**, 4883

Amine end-functionalized poly(2-ethyl-2-oxazoline) as promising coating material for antifouling applications†

Lutz Tauhardt,[ab] Marion Frant,[c] David Pretzel,[ab] Matthias Hartlieb,[ab] Christian Bücher,[c] Gerhard Hildebrand,[c] Bernd Schröter,[d] Christine Weber,[ab] Kristian Kempe,‡[ab] Michael Gottschaldt,[ab] Klaus Liefeith[c] and Ulrich S. Schubert*[abe]

Received 5th February 2014
Accepted 27th May 2014

DOI: 10.1039/c4tb00193a

www.rsc.org/MaterialsB

The antifouling behavior of different poly(2-ethyl-2-oxazoline) (PEtOx) coatings was investigated under "real live" conditions. Amine end-functionalized PEtOx of different molar masses have been prepared using a new and straightforward, two step synthesis method. Subsequently, the PEtOx were attached to glass surfaces *via* a tetraether lipid and a common silane, respectively. The polymers and coatings were characterized using techniques such as ^{1}H NMR spectroscopy and MALDI-TOF-MS as well as XPS and contact angle measurements. In a next step, the coatings were exposed to the simultaneous attack of five different bacteria in synthetic river water. A clear reduction of the biofilm formation was observed. In addition, the stability of the coatings against thermal, mechanical, and chemical stress was studied.

Introduction

Preventing the uncontrolled adhesion and adsorption of proteins, cells, bacteria, and other microorganisms onto surfaces, the so called fouling process, represents a major challenge for a wide range of applications such as medicine (*e.g.* medical devices, implants, drug delivery systems),[1,2] mobility (*e.g.* ship hull coatings),[3,4] food industry (*e.g.* packaging),[5] but also for membranes (*e.g.* in water purification systems),[6] microarrays, and (bio)sensors.[7]

In principle one can distinguish between two types of antifouling coatings: (1) bioactive coatings that cause a direct or indirect inactivation of adherent microorganisms or biofilms by either releasing an antifouling agent (*e.g.* biocides), or by killing the cells, bacteria, or microorganisms on contact using specific molecules (*e.g.* quarternized polymers), and (2) biopassive coatings, which reduce fouling due their protein and cell repellent character without interfering with the proliferation cycle or the cell metabolism.[8–10] However, coatings that are bioactive or release antifouling agents suffer from a loss of activity over time. In case of bioactive coatings self-deactivation occurs due to the fact that dead cells or microorganisms adhere to the active layer, cover it and, therefore, allow the adhesion and proliferation of new cells on the cell debris.[10] Coatings that release antifouling agents lose their activity when all antifouling agent (*e.g.* biocide) is consumed. Moreover, they are harmful to the environment, since the released antifouling agents are not only active on the surface that should be protected and, hence, can kill in a nonselective way or accumulate in microorganisms, animals (*e.g.* fish), and plants.[11,12] An approach to overcome these issues is the covalent binding of the antifouling coatings onto the surface. In particular biopassive coatings are promising, since they are not self-deactivating and do not release toxic and polluting compounds. Recently published studies have led to the conclusion that materials for biopassive coating have to meet the following criteria: (1) the presence of hydrogen bond accepting and hydrophilic (polar) groups, and (2) the absence of hydrogen bond donating groups and net charges.[8,13] If we otherwise accept, that the formation of a hydration layer (water barrier) is a vital prerequisite to build up anti-adhesive surfaces with non-fouling properties hydrogen bond accepting groups are of the same importance as hydrogen bond donating groups.[14] Based on the possibility to tune their properties, polymers can be adapted to a wide range of requirements and, thus, represent an interesting class of compounds for such surface tethered antifouling coatings. A widely used polymer for biopassive and repellent coatings is poly(ethylene glycol)

[a]*Laboratory of Organic and Macromolecular Chemistry (IOMC), Friedrich Schiller University Jena, Humboldtstr. 10, 07743 Jena, Germany. E-mail: ulrich.schubert@uni-jena.de; Fax: +49 3641 948 202*

[b]*Jena Center for Soft Matter (JCSM), Friedrich Schiller University Jena, Philosophenweg 7, 07743 Jena, Germany*

[c]*Institute for Bioprocessing and Analytical Measurement Techniques e.V. (IBA), Rosenhof, 37308 Heilbad Heiligenstadt, Germany*

[d]*Institute for Solid State Physics, Friedrich Schiller University Jena, Helmholtzweg 5, 07743 Jena, Germany*

[e]*Dutch Polymer Institute (DPI), John F. Kennedylaan 2, 5612 AB Eindhoven, The Netherlands*

† Electronic supplementary information (ESI) available. See DOI: 10.1039/c4tb00193a

‡ Current address: Department of Chemical and Biomolecular Engineering, The University of Melbourne, Victoria 3010, Australia.

(PEG).[8,15–18] However, PEG is known to undergo degradation by (auto-)oxidation to form ethers and aldehydes, hampering its long-term application.[13,19–22] On this account, poly(2-oxazoline)s (POx), in particular the water soluble poly(2-methyl-2-oxazoline)s (PMeOx) and poly(2-ethyl-2-oxazoline)s (PEtOx), are investigated as alternative coating materials.[13,19,23–31] Compared to the synthesis of PEG by anionic polymerization, the preparation of POx by cationic ring-opening polymerization (CROP) is less labor demanding, but also yields well-defined polymers with controlled molar masses and low polydispersity index (PDI) values. Moreover, a broad variety of functional electrophilic initiators, nucleophilic terminating agents, and 2-oxazoline monomers allows the synthesis of well-defined (co)polymers and the tuning of the polymer properties.[32] It was shown that POx coatings have similar antifouling properties as PEG, but are stable in an oxidizing environment.[13,19] However, up to now all antifouling investigations on POx surfaces were performed under laboratory conditions using only a single type of protein (*e.g.* fibronectin,[29,30] bovine serum albumin[27,28]), cell (*e.g.* fibroblasts[24]), or bacterium (*e.g. E. coli*[13,25,26]). A review on methods to attach POx to surfaces as well the properties and applications of POx functionalized surfaces was published recently.[33]

The chemical long-term stability of antifouling coatings is mandatory and can be greatly improved by covalent tethering of the polymers to the surface *via* linker molecules. Recently, tetraether lipids (TEL), *i.e.* bipolar membrane spanning lipids from thermoacidophilic archaea, were presented as an interesting new class of linker molecules.[34–39] By a simple self-assembling process, a stable, highly ordered impermeable TEL monolayer (~4 nm) with biomembrane-like properties is formed. The covalent immobilization of this thin lipid layer on surfaces can be achieved easily when the lipid headgroups are functionalized with cyanuric chloride.[35–37,39] An outstanding property of TELs is their excellent stability against oxidation, acidic and basic hydrolysis as well as biodegradation, which is based on the fully saturated character of the methyl branched alkyl chains.[34] Moreover, biocompatibility analyses revealed that TELs are both nontoxic and immunologically inert and, additionally, exhibit antifouling activity.[35–38] Hence, the usage of TEL linkers to attach POx to surfaces is highly interesting.

Here, we report the antifouling behavior of amine end-functionalized PEtOx, covalently bound to glass substrates using two different methods: (1) attachment *via* epoxide ring-opening reaction of a common glycidyl ether silane tethered to the surface as described in literature, *e.g.* for PEG,[15,40] and (2) immobilization *via* the cyanuric chloride functionalized headgroups of a TEL linker. To this end, a new approach to synthesize amine end-functionalized POx was developed. PEtOx of different chain lengths were prepared and characterized by ^{1}H NMR spectroscopy, matrix-assisted laser desorption/ionization time of flight laser mass spectrometry (MALDI-TOF-MS), and size exclusion chromatography (SEC). The PEtOx coatings were analyzed by contact angle measurements and X-ray photoelectron spectroscopy (XPS). The subsequent antifouling investigations were performed in synthetic river water using a microbiological mixed culture consisting of five different types of bacteria. Biofilm formation and the stability of the coatings were studied using confocal laser scanning microscopy.

Methods and materials

General methods and surface characterization

Used chemicals, instruments, and characterization methods are described in the ESI.†

Synthesis of phthalimide end-capped PEtOx (1)

A solution of initiator (MeOTs), monomer (EtOx), and solvent (acetonitrile) was prepared with a total monomer to initiator ratio of [M]/[I] = 20, 40, 60, and 80, respectively. The total monomer concentration was adjusted to 4 M. The solution was heated at 140 °C in a microwave synthesizer for a predetermined time. After cooling to room temperature a 2-fold excess of potassium phthalimide was added and the reaction mixture was stirred overnight at 70 °C. The reaction mixture was filtered and the solvent removed. The residue was dissolved in chloroform and washed twice with a saturated aqueous solution of $NaHCO_3$ and once with brine. The organic phase was dried over sodium sulfate. After filtration, the polymer was concentrated under reduced pressure, precipitated into ice-cold diethyl ether, and dried at 40 °C under reduced pressure.

Synthesis of amine end-capped PEtOx (2)

Phthalimide end-capped PEtOx was dissolved in ethanol and a 10-fold excess of hydrazine monohydrate was added. The reaction mixture was heated under reflux overnight. After cooling to room temperature, a concentrated hydrochloric acid was added to adjust the pH value to 2–3. The precipitate was removed by filtration and the ethanol was evaporated. The residue was dissolved in water and aqueous sodium hydroxide solution until the pH value reached 9–10. The aqueous solution was extracted thrice with chloroform. The organic phase was dried over sodium sulfate, concentrated, and precipitated into ice-cold diethyl ether. The white precipitate was filtered off and dried at 40 °C under reduced pressure.

Synthesis of fluoresceine labeled P(EtOx-*stat*-AmOx) (Fluo-PEtOx) (5)

The starting material P($EtOx_{36}$-*stat*-$AmOx_4$) (**4**) was synthesized as reported earlier.[41]

P($EtOx_{36}$-*stat*-$AmOx_4$) (1 g, 242 mmol) was dissolved in DMSO (50 mL). 5(6)-Carboxyfluorescein *N*-hydroxysuccin-imide ester (114.5 mg, 242 mmol, 1 eq. per polymer chain) and TEA (2.5 mL) were added to the solution and the reaction was stirred for 3 h. Subsequently, the product was precipitated in cold diethyl ether (700 mL), filtered off, dissolved in methanol (20 mL) and precipitated again into diethyl ether (200 mL). The polymer was obtained as orange solid (1.039 g, 95%).

Coating procedure for silane on borofloat® 33 glass slides

Prior to use, each side of the glass slides was cleaned in oxygen plasma for 15 min. In a glove box, the glass slides were treated

with (3-glycidyloxypropyl)trimethoxysilane for 1 h and subsequently rinsed with dry DMF. One side of the glass slide was covered with the respective polymer solution in DMF (200 mg mL^{-1}) at a concentration of 3 mL cm^{-2} (64 mg cm^{-2}). Then, a second glass slide was put on top (face-to-face assembly). After 2 days at room temperature, the slides were separated, intensely rinsed with deionized water and air-dried.

Coating procedure for tetraether lipid on borofloat® 33 glass slides

Preparation of TEL vesicle emulsion. The main phospholipid included in dried biomass of *Sulfolobus acidocaldarius* was isolated and purified as described earlier.[39] The head-groups of the extracted tetraether lipid were activated by refluxing with cyanuric chloride over 1 week in dry chloroform/methanol (1 : 1).

The activated lipids were dissolved in dry chloroform/methanol 1 : 1, sodium bicarbonate (1.5 g per 100 mg lipid) was added and a thin lipid layer at the sides of the flask was formed. Subsequently, the solvents were removed completely under reduced pressure. The lipid film was hydrated with pure water at a final lipid concentration of about 2 mg mL^{-1}. Further treatment in an ultrasonic bath at 50 °C for 15 minutes yielded a cloudy lipid emulsion consisting of large multilamellar vesicles. Afterwards, the emulsion was extruded through a polycarbonate membrane (pore diameter 100 nm).

Coating. The glass substrates were purified as follows: (1) sonication in diluted detergent solution (Blanchipon®, Optical II), (2) incubation in ethanol and 35% nitric acid, and (3) storing in de-ionised water. Subsequently, the surfaces were activated with nitric acid and by exposure to UV irradiation. After amino silanization using 3-(ethoxydimethylsilyl)propylamine the substrates were cleaned with chloroform, methanol, and water. TEL coating was performed *via* liposome spreading in a PTFE reaction chamber by incubation with a freshly prepared lipid emulsion at 70 °C overnight.[39] Finally, the coated substrates were sonicated in chloroform for 10 minutes and dried with pressurized air. In a next step, the PEtOx were immobilized on the TEL-coated glass by coupling the amine end group of the polymer with the cyanuric chloride moiety of the TEL. The reaction was performed in borate buffer solution (10 mg PEtOx per mL, pH = 8.5) at 60 °C overnight. Subsequently, the glass slides were extensively rinsed with distilled water and dried under ambient conditions.

Preparation of synthetic river water medium

The synthetic river water was prepared by dissolving calcium chloride dihydrate (34.6 mg L^{-1}), magnesium sulfate heptahydrate (112.3 mg L^{-1}), sodium bicarbonate (126.0 mg L^{-1}), monopotassium phosphate (4.35 mg L^{-1}), sodium nitrate (85.0 mg L^{-1}), glucose (6.6 mg L^{-1}), and pepton (2.0 mg L^{-1}) in distilled water.

Five typical microorganisms with a high potential of biofilm formation were isolated from the river Ruhr near Mühlheim (Germany): *Aeromonas hydrophila/caviae*, *Sphingomonas paucimobilis*, *Pasteurella* spp., *Aeromonas salmonicida*, and *Leuconostoc* spp. The microorganisms were precultivated at 30 °C overnight on a shaker (100 rpm) in a special water medium (pH 7) consisting of: yeast extract (0.5 g mL^{-1}), peptone (0.5 mg mL^{-1}), casein hydrolysate (0.5 mg mL^{-1}), glucose (0.5 mg mL^{-1}), sodium pyruvate (0.3 mg mL^{-1}), starch (0.5 mg mL^{-1}), dipotassium hydrogenphosphate (0.3 mg mL^{-1}), and monopotassium phosphate (0.05 mg mL^{-1}). Bacteria were harvested by centrifugation at 4000*g* for 15 min. The pellet was washed twice with synthetic river medium to remove other particle-like components that may have an impact on the kinetic process. A constant cell concentration of 2×10^6 cells per mL synthetic river water was adjusted.

Investigation of the biofilm formation

Polymer coated sterilized glass slides were incubated in flow chambers. Prior to use, all probes were sterilized using ethanol (70%). Subsequently, the coated glass slides were placed in a flow chamber running with bacteria containing synthetic river water at a flow rate of 0.3 mL min^{-1} at room temperature. After incubating for 15 hours, a rinsing cycle with pure cultivation medium was performed to remove non-adhered microorganisms from the surface. The bioadhesion was evaluated by means of confocal laser scanning microscopy. To this end, the adherent microorganisms were stained using a LIVE/DEAD® *Bac*Light™ Bacterial Viability Kit (MoBiTec, Germany). At each sample ten images of biofilms were taken at different positions in the flow channel by confocal laser scanning microscopy (LSM710, Zeiss microscopy, Germany, Plan Apochromat 5×/0.16). The surface area covered by microorganisms was quantified by software supported analysis of the microscopy images (Volocity improvision®). Bioadhesion experiments were performed in triplicate.

Stability tests

Stability tests were performed on Fluo-PEtOx coated glass slides attached *via* TEL and silane linker, respectively.

Investigation of the resistance against chemical stress. Samples were incubated at room temperature over 12 weeks in an upright position in closed boxes on a shaker (75 rpm) filled with sterile filtrated water of a drinking water dam (Neustadt/Ilm, Germany) and salt water from the North sea, respectively. Media were changed weekly.

Investigation of the resistance against mechanical stress. Resistance against mechanical stress was investigated using aluminum oxide and silicon carbide particles in distilled water, based on environmental data. The test solution comprised 150 mg particles per liter. The particle size was distributed as follows: Ø 320 μm = 0.4%, Ø 120 μm = 41%, Ø 20 μm = 31.8%, Ø 9 μm = 26.8%. Samples were incubated at room temperature in a closed beaker glass with stirring (750 rpm) corresponding to a streaming of 2 m s^{-1}. Over 1 week a permanent change between 8 h rotation time and 16 h resting time without rotation was realized.

Investigation of the resistance against thermal stress. In order to investigate thermal stability the samples were placed in distilled water and exposed to a defined temperature protocol

with 25 cycles between 2 and 38 °C and an incubation period of 14 days. Dwell time at each temperature was 1 h.

Image analysis. After each stress procedure fluorescence image data of the Fluo-PEtOx coated samples were recorded by confocal laser scanning microscopic method (LSM710, Zeiss microscopy, Germany, Plan Apochromat 5×/0.16). The recordings were made with uniform measurement parameters (gain, offset, pinhole, average, *etc.*) to allow a comparison of results among each other but also to untreated coatings as a proof of the layer stability.

Results and discussion

Synthesis and characterization of amine end-capped poly(2-ethyl-2-oxazoline)s

PEtOx of different molar masses were synthesized with the aim to covalently bind the polymer to the surface *via* an epoxide bearing silane and a cyanuric chloride functionalized tetraether lipid (TEL), respectively. Since it is known that both epoxides and cyanuric chloride can react quite easily with amines, PEtOx bearing an amine end group were prepared using a new synthesis route.

The synthesis of an amine end-functionalized poly(2-oxazoline) (POx) was already described in literature. Lin *et al.* terminated the living oxazolinium species directly with ammonia in acetonitrile.[42] However, the authors only obtained a degree of functionalization of about 80%. As an alternative three step method, Park *et al.* quenched the reaction mixture with a methanolic NaOH solution.[43] The resulting hydroxyl end group was then reacted with phthalimide in the presence of triphenylphosphine and diethyl azodicarboxylate to yield a POx with a phthalimide end group. In a final step, the amine end group was obtained by treatment with hydrazine monohydrate. However, this procedure led only to an amine end group functionalization efficiency of 62%. An additional problem, reducing the efficiency of this method, is the possible formation of ester end groups instead of hydroxyl end groups, when the reaction is quenched.[44–46] These esters need to be hydrolyzed to hydroxyl groups before the polymer can be further functionalized. To overcome the drawbacks of these methods, a new synthesis route to synthesize amine end-functionalized PEtOx was developed (Scheme 1). In this approach the living cationic species is quenched directly with an excess of potassium phthalimide, saving one step compared to the method described by Park *et al.* Moreover, the end-capping efficiency is quantitative according to ^{1}H NMR spectroscopy and MALDI-TOF-MS.

The ^{1}H NMR spectrum of **1** (Fig. 1 top) shows a broad signal around 7.76 ppm deriving from the aromatic protons of the phthalimide unit (4 protons). By correlation with the signals at about 3 ppm, which are associated with the CH_3 α-end group (3 protons), the quantitative functionalization with the desired ω-end group is confirmed. The broad peak at 3.44 ppm derives from the polymer backbone. The side chain signals can be found at 1.11 ppm (CH_3) and 2.32 ppm (CH_2), respectively. Due to a different chemical environment, the backbone CH_2 group adjacent to the phthalimide is shifted to 3.83 ppm.

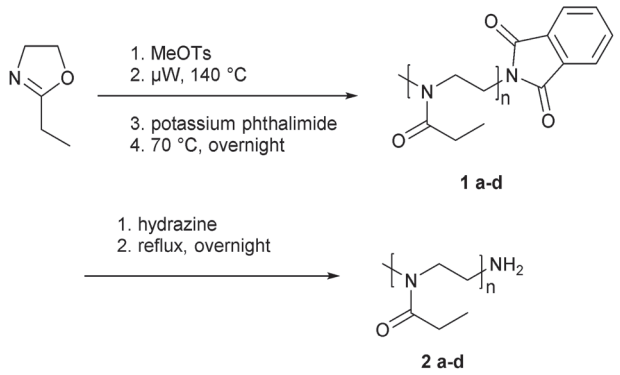

Scheme 1 Schematic representation of the synthesis of amine end-functionalized PEtOx.

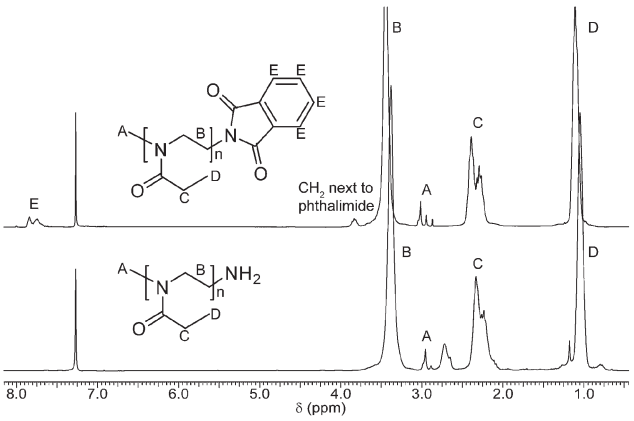

Fig. 1 ^{1}H NMR spectra of phthalimide (**1a**, top) and amine (**2a**, bottom) end-functionalized PEtOx (300 MHz, solvent $CDCl_3$).

The MALDI-TOF mass spectrum of **1** shows two distributions that can be assigned to the sodium adduct of phthalimide end-capped PEtOx (Fig. 2). The methyl-initiated species derives from the initiation of the polymerization with methyl tosylate. The proton-initiated species is formed by chain transfer reactions occurring during the polymerization.[47,48] A hydroxyl end group bearing species could not be observed. This fact further underlines the complete functionalization and is in accordance with the results from ^{1}H NMR analysis. Moreover, the measured isotopic patterns match with the calculated isotopic patterns of the assigned species.

The phthalimide end-capped PEtOx **1** were subsequently treated with hydrazine monohydrate to obtain the amine functionalized polymers (**2**).[43,49] Characterization of the product by ^{1}H NMR spectrometry revealed the success of the reaction (Fig. 1 bottom). After the hydrazinolysis, the signals of the aromatic phthalimide end group and the CH_2 group adjacent to the phthalimide disappeared quantitatively.

The MALDI-TOF mass spectrum of **2** shows two major distributions which belong to the sodium adducts of methyl and proton initiated PEtOx bearing an amine end group (Fig. 3). The initial phthalimide-bearing species could not be detected

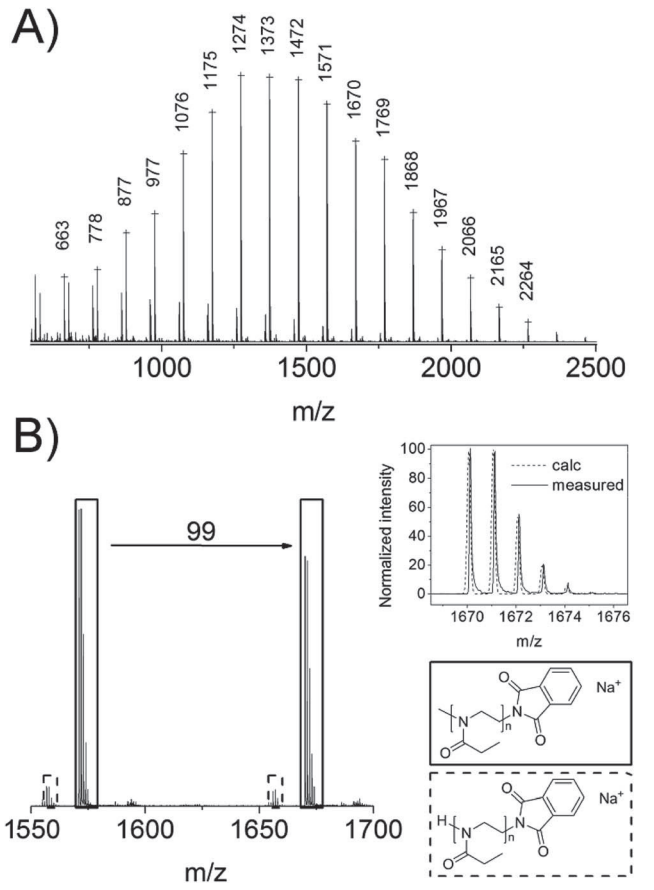

Fig. 2 (A) MALDI-TOF mass spectrum of phthalimide end-capped PEtOx. (B) An expanded region of the spectrum (right), the structural assignments for the different distributions as well as the calculated and measured isotopic pattern of the peak at $m/z = 1670$ (left).

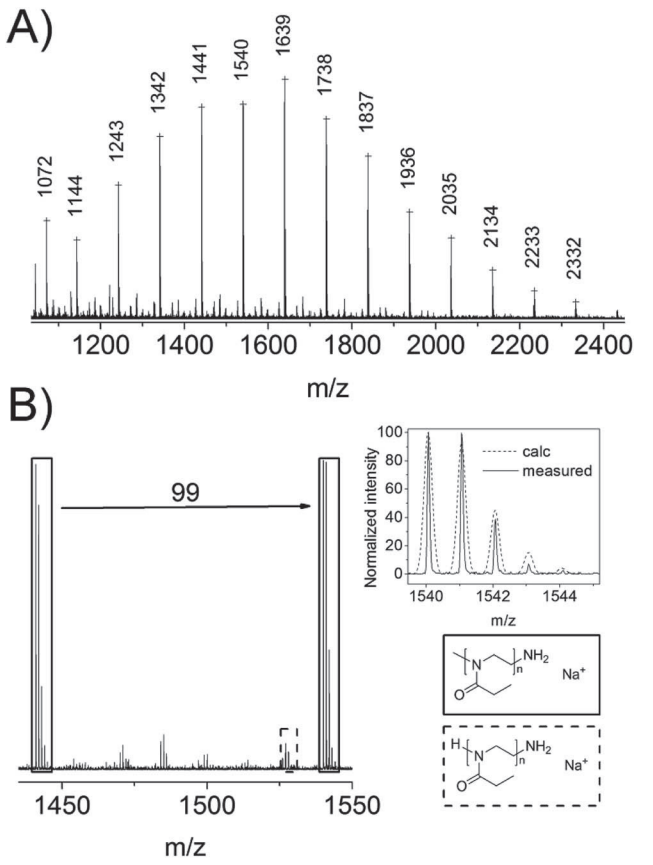

Fig. 3 (A) MALDI-TOF mass spectrum of amine functionalized PEtOx. (B) An expanded region of the spectrum (right), the structural assignments for the different distributions as well as the calculated and measured isotopic pattern of the peak at $m/z = 1540$ (left).

anymore. In addition, the measured and the calculated isotopic pattern coincide.

The presented synthesis route was used to prepare amine functionalized PEtOx (**2**) with different molar masses, namely 2000, 4000, 6000, and 8000 g mol^{-1} (n = 20, 40, 60, and 80), which can be achieved simply by variation of the [M]/[I] ratio applied for the CROP. Characterization by size exclusion chromatography (SEC) revealed PDI values between 1.12 and 1.19 (Table 1).

Table 1 SEC-data of the different POx

Sample	EtOx : BocOx : AmOx : F	M_n[a] (g mol^{-1})	PDI[a]
2a	20 : 0 : 0 : 0	2460	1.12
2b	40 : 0 : 0 : 0	3790	1.15
2c	60 : 0 : 0 : 0	5175	1.14
2d	80 : 0 : 0 : 0	5990	1.19
3	36 : 4 : 0 : 0	5300	1.08
4	36 : 0 : 4 : 0	5400	1.12
5	36 : 0 : 3 : 1	5500	1.18

[a] Determined by SEC (eluent: $CHCl_3$/2-propanol/TEA, calibration with a PS standard).

Fluorescein labeled PEtOx

To prove the suitability of the attachment methods and to investigate the stability of the obtained PEtOx layers against different types of stress, a fluorescein labeled PEtOx (Fluo-PEtOx, **5**) was used. To this end, a copolymer with an amine monomer content of 10% and an overall degree of polymerization (DP) of 40 (P($EtOx_{36}$-*stat*-$AmOx_4$), **4**) was synthesized by copolymerization of EtOx and a *tert*-butyloxycarbonyl (Boc)-protected amine group containing 2-oxazoline followed by deprotection (Scheme 2).[41] In a next step one amine group was labeled using a fluorescein-NHS ester derivative. The reaction of this activated acid with amine groups is highly efficient under basic conditions and was, therefore, performed with triethylamine (TEA) as a base. Purification was accomplished by repeated precipitation into diethyl ether to eliminate traces of unreacted fluorescein. The successful labeling of the copolymer was confirmed by SEC, which provided congruent UV (485 nm) and RI-detector traces (Table 1 and Fig. S1†). Moreover, no signal of unreacted fluorescein was detected. In addition, ^{1}H NMR spectroscopy shows the characteristic peaks of fluorescein with broadening attributed to the attachment to the polymer chain (Fig. S2†).

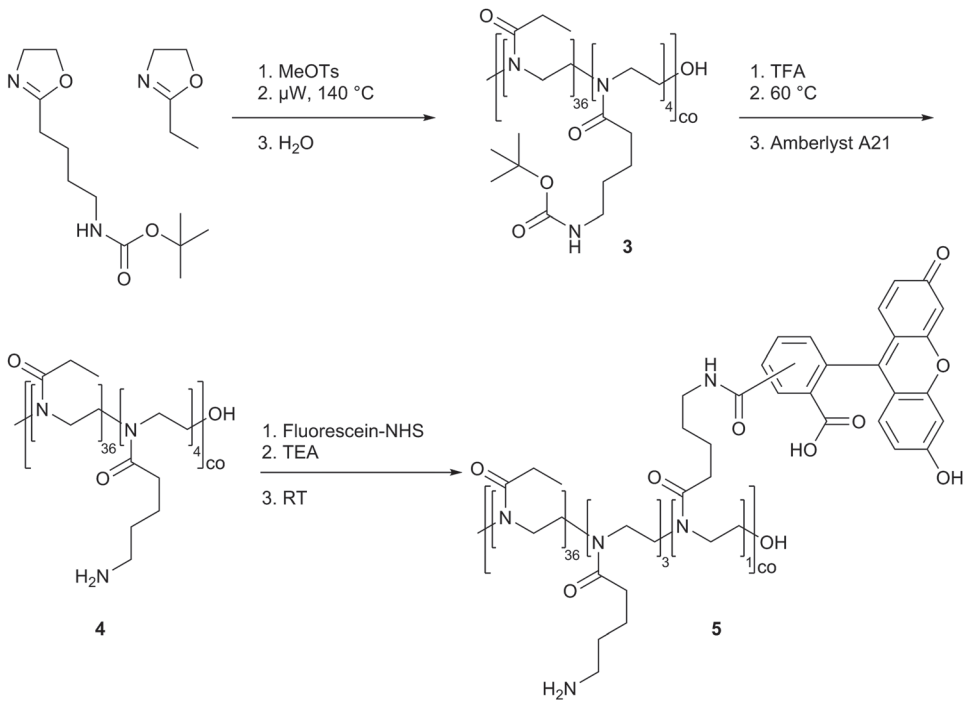

Scheme 2 Schematic representation of the synthesis of amine containing POx and labeling of the polymer with fluorescein.

Coating of glass slides with PEtOx of different molar masses using different spacers

To investigate their suitability for the prevention of bioadhesion, the PEtOx polymers (**2a–d**) were immobilized on borofloat® 33 glass employing either (1) a silane based linker or (2) a TEL linker (Scheme 3). In case of coupling *via* a silane based linker, the glass slides were first treated with (3-glycidyloxypropyl)trimethoxysilane (GOPTMS). Subsequently, PEtOx of different molar masses were attached by reaction of the epoxide unit of GOPTMS with the end group of the polymer (Scheme 3A route 1). For the coupling *via* a TEL linker (Scheme 3B) the terminal hydroxyl groups of the lipid were modified with cyanuric chloride to enable the covalent coupling to the glass surfaces as well as the covalent binding of PEtOx on top of the lipid membrane (Scheme 3A route 2). The TEL functionalized glass slides were coated with PEtOx with the same molar masses as for route 1.

Characterization of the polymer thin films

In order to examine the suitability of the attachment methods and the quality of the PEtOx coatings, fluorescein labeled PEtOx was grafted to the different linker molecules in the same way as the PEtOx homopolymers. By means of laser scanning microscopy it could be shown that homogenous Fluo-PEtOx films are obtained for both the GOPTMS and the TEL linker (Fig. 4).

The coating process with the PEtOx homopolmyers was further monitored by means of X-ray photoelectron spectroscopy (XPS). Using this method information on the chemical composition of surface layers, which are only a couple of nanometers thick, can be obtained. A comparison of the nitrogen 1s signal of pure borofloat glass, the different linkers, and the different PEtOx films showed the successful coating (Fig. 5). While on pure glass and GOPTMS treated substrate, no nitrogen was found, the TEL coated glass shows a nitrogen signal due the cyanuric chloride moieties. Moreover, the nitrogen signal intensity increased significantly after attaching the PEtOx.

Water contact angle measurements on air-dried and hydrated polymer coatings were performed with the aim to investigate the wetting behavior of the surface tethered PEtOx films (Fig. 6). Both, samples that were coated with GOPTMS and TEL linker, respectively, displayed an increased water contact angle compared to the reference borosilicate glass (after treatment with argon plasma). Subsequent PEtOx grafting further increased the water contact angles for GOPTMS attached samples. In case of TEL linked PEtOx only for a DP of 20, referred to as 20(TEL), an increased contact angle could be observed when compared to pure TEL. For all other chain lengths the contact angle is in the same range as for pure TEL or even decreased. These changes in wettability indicate a successful coating of the substrates with the linkers and PEtOx, respectively.

In the air-dried state, surfaces that were coated with PEtOx *via* a GOPTMS linker display water contact angles in a rather wide range between 57° and 85°. The variations for surfaces that were coated with PEtOx *via* TEL linkers are narrower, ranging from 53° to 70°. While for coatings attached through TEL decreasing contact angles with increasing chain lengths could be observed, no trend could be found for GOPTMS attached PEtOx.

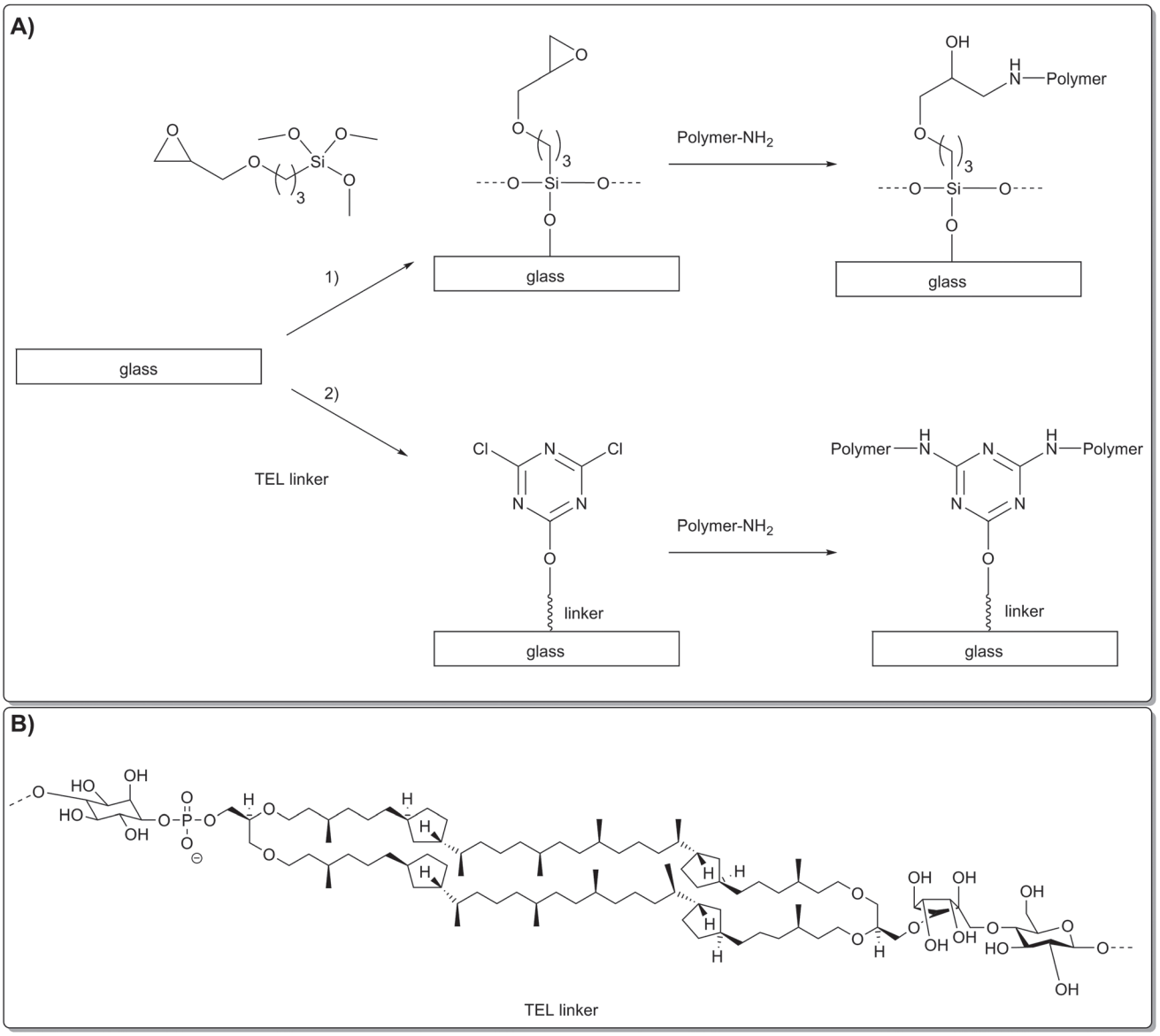

Scheme 3 (A) Schematic representation of the PEtOx coating process using GOPTMS (route 1) and a TEL (route 2) linker, respectively, and (B) of the TEL linker structure.

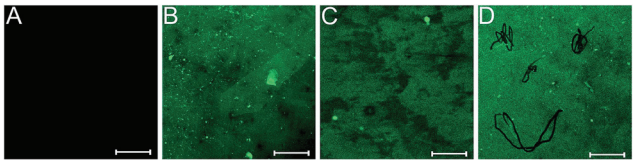

Fig. 4 Confocal laser scanning microscopy images of (A) uncoated glass, (B) Fluo-PEtOx attached *via* GOPTMS, (C) Fluo-PEtOx attached *via* TEL, and (D) scratched sample of Fluo-PEtOx attached *via* GOPTMS (scale bar: 100 μm).

After swelling in water, the coatings display reduced contact angles. This finding is ascribed to the hydration of the hygroscopic, hydrophilic PEtOx. Again a clear trend to reduced contact angles for longer polymer chains can be found for TEL attached coatings. Moreover, the difference in contact angles between air-dried and hydrated state ($\Delta\theta$) increases with the chain length from 0.7° for $n = 20$(TEL) to 18.1° for $n = 80$(TEL). This observation indicates that longer polymers can bind/absorb more water molecules and, thus, should have a higher antifouling potential. This is in accordance with theoretical calculation for PEG.[8] For GOPTMS tethered films such tendency could not be observed. Here, a constant $\Delta\theta$ of ~10° was determined.

An important parameter with regard to the antifouling properties is the grafting density,[33] which is in general calculated either from the film thickness[28,50] or the weight loss of the sample upon heating.[51,52] However, due to technical reasons (*e.g.* monolayer, glass substrate) the determination of these parameters was not possible. To ensure the highest possible grafting density an excess of polymer was used.

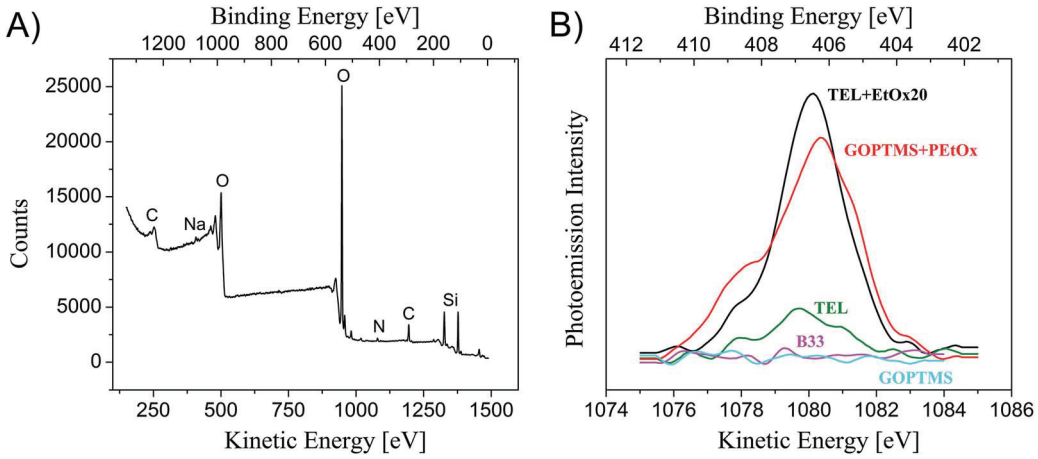

Fig. 5 (A) Typical XPS spectrum of a TEL-PEtOx coating. (B) Overlay of the nitrogen 1s signals of bare borofloat glass as well as the different linkers and coatings.

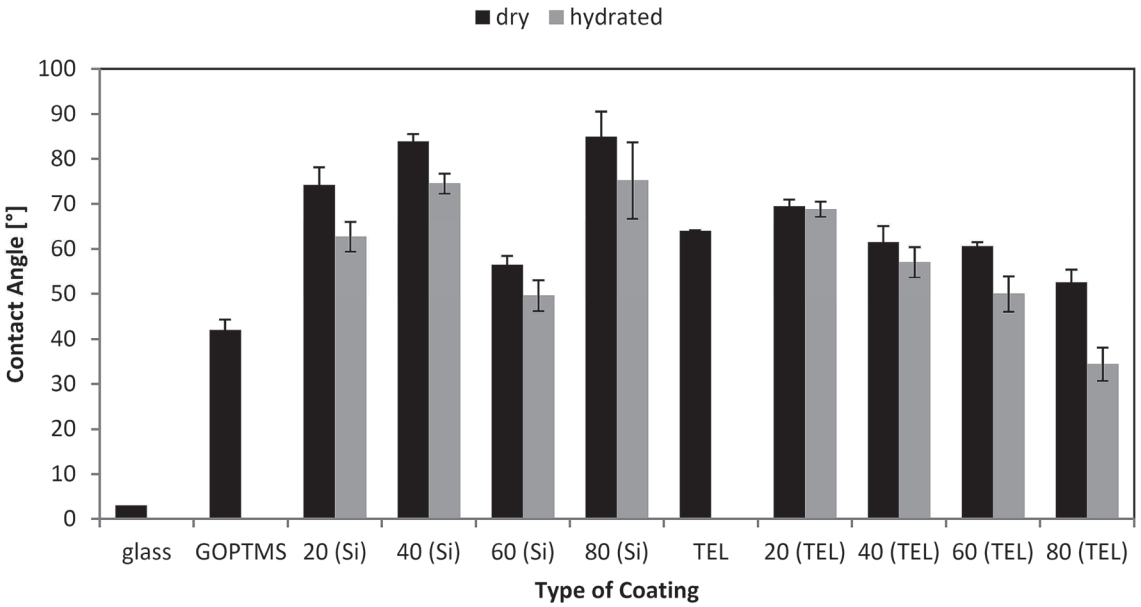

Fig. 6 Water contact angles of the different PEtOx-coatings in dry and hydrated state (data are presented as mean ± standard deviation for $n = 45$). The numbers indicate the different DPs of PEtOx (20, 40, 60 and 80), linkers are given in brackets.

Antifouling properties of the different PEtOx coatings

The antifouling properties of the different PEtOx-coated glass slides were investigated in flow-through chambers that allow a continuous cross flow of synthetic river water under reproducible conditions over an arbitrary period of time. Based on the water composition of the river Ruhr near Mühlheim (Germany), five different microorganisms with a high potential of biofilm formation were chosen, namely: *Aeromonas hydrophila/caviae*, *Sphingomonas paucimobilis*, *Pasteurella* spp., *Aeromonas salmonicida*, and *Leuconostoc* spp. After 15 hours incubation the adherent microorganisms were stained using a LIVE/DEAD® *Bac*Light™ Bacterial Viability Kit and investigated by means of confocal laser scanning microscopy. A clear reduction of the bioadhesion, induced by the PEtOx coatings, was detected (up to 66% compared to uncoated glass), with no significant differences between films attached *via* GOPTMS and TEL, respectively, suggesting that similar grafting efficiencies are reached (Fig. 7). Although in case of TEL linkers the hydrophilicity of swollen PEtOx samples increased with the chain length and longer chains should, therefore, have a higher antifouling potential, an influence of the molar mass on the cell adhesion could not be observed. Also the bacterial viability rate was hardly affected. Only the samples 40(Si) and 20(TEL) showed higher deviations. While on 40(Si) nearly no dead cells could be found, the 20(TEL) coating showed a reduced cell viability. In addition, 20(TEL) shows the lowest overall bioadhesion, making it the best coating produced within this study. However, from an

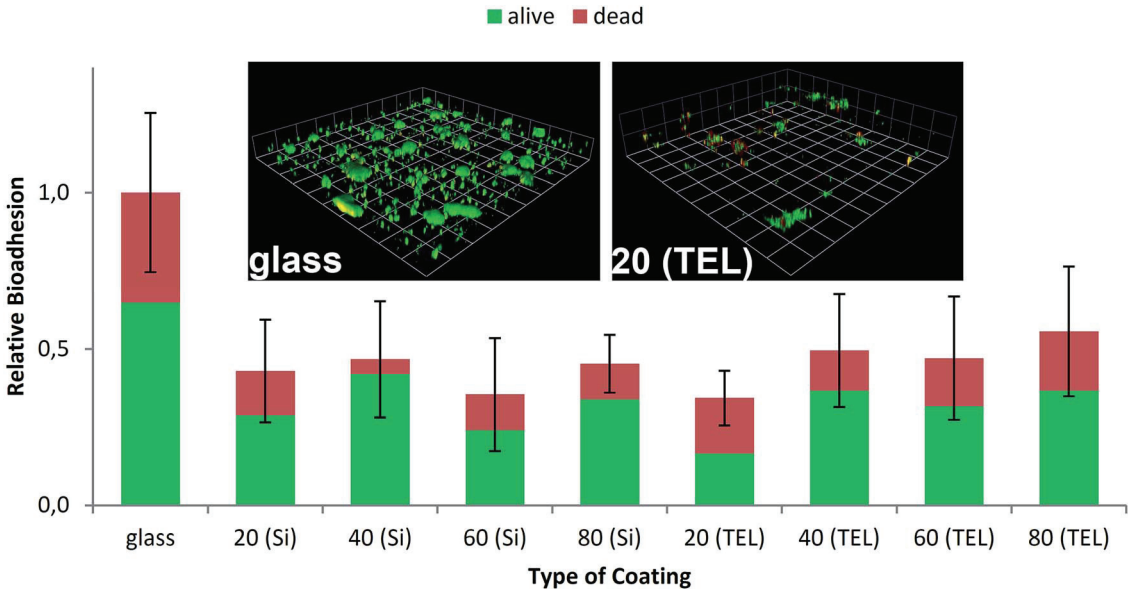

Fig. 7 Bioadhesion on PEtOx coatings of different DP (20, 40, 60, and 80) to the glass slides *via* a silane (Si) and a tetraether lipid (TEL) linker (standard deviation is related to the total bioadhesion (sum of dead and vital bacteria)) as well as confocal laser scanning microscopy images of the stained biofilms on glass and 20 (TEL).

use-oriented point of view, *i.e.* for large scale applications, the attachment *via* GOPTMS is favored, since similar results are obtained and the coating process is easier. Moreover, GOPTMS, in contrast to TEL, is easily available in large amounts.

Antifouling properties of immobilized PEG- and POx-based coatings have been widely reported in the literature.[8,14–20] Due to the different, more real life test conditions, *e.g.* attack of multiple bacteria and synthetic river water medium, a comparison of the obtained results to other POx or PEG coatings, reported in literature, is difficult.

Stability of the PEtOx coatings

An important parameter with regard to their application, *e.g.* as sensor coatings, is the stability of the PEtOx films. To this end, Fluo-PEtOx coated glass slides, attached through GOPTS and TEL spacer, respectively, were exposed to three different types of stress: (1) chemical stress, (2) mechanical stress and (3) thermal stress. The resistance against chemical stress, caused *e.g.* by fresh and salt water, was investigated over 12 weeks using dam and North Sea water, respectively. The durability of the coatings against abrasion in particle containing water is essential in the field of environmental monitoring. Based on environmental data a corresponding test solution containing aluminum oxide and silicon carbide particles was prepared. Mechanical stress was simulated by placing the glass slides into this solution and stirring for 8 hours a day over 1 week. In order to verify their thermal stability, the samples were exposed to a defined heating profile for 14 days with temperatures between 2 and 38 °C. Subsequent analysis by means of confocal laser scanning microscopy showed that the coatings withstood the different types of stress (Fig. 8).

Conclusion

The potential of PEtOx coatings to prevent bioadhesion under "real life" conditions was investigated. To this end, amine end-functionalized PEtOx of four different molar masses have been prepared applying a new and straightforward synthesis method. The polymers obtained were characterized by MALDI-TOF mass spectrometry, ^{1}H NMR spectroscopy, and size exclusion chromatography, which showed the successful introduction of ω-amine groups. PEtOx were attached to glass surfaces through silane and tetraether lipid based linkers. The surface immobilization of PEtOx was investigated by fluorescence microscopy measurements of surfaces modified with fluorescently labeled PEtOx as well as by XPS investigations, which showed the presence of nitrogen signals after the PEtOx coating process. Contact angle measurements of air-dried and swollen coatings revealed a higher hydrophilicity of the swollen samples, ascribed to the formation of PEtOx hydrates. Fouling studies were performed in a flow-through chamber under "real-life" relevant conditions using a synthetic river water model containing five different bacteria. PEtOx modified glass samples exposed to the synthetic river water for 15 h showed a bioadhesion reduction of up to 66% with no significant differences between the two different linkers. The best results were obtained by PEtOx with 20 repeating units attached *via* a tetraether lipid linker, which revealed the lowest biofilm formation and the highest amount of dead bacteria. In addition, the stability of the PEtOx coatings towards chemical, mechanical, and thermal stress was investigated. No significant destruction of the polymer layer was observed, demonstrating the capability of the films for long term applications.

The present study underlines the potential of POx for antifouling coatings and is in agreement with other studies.[33]

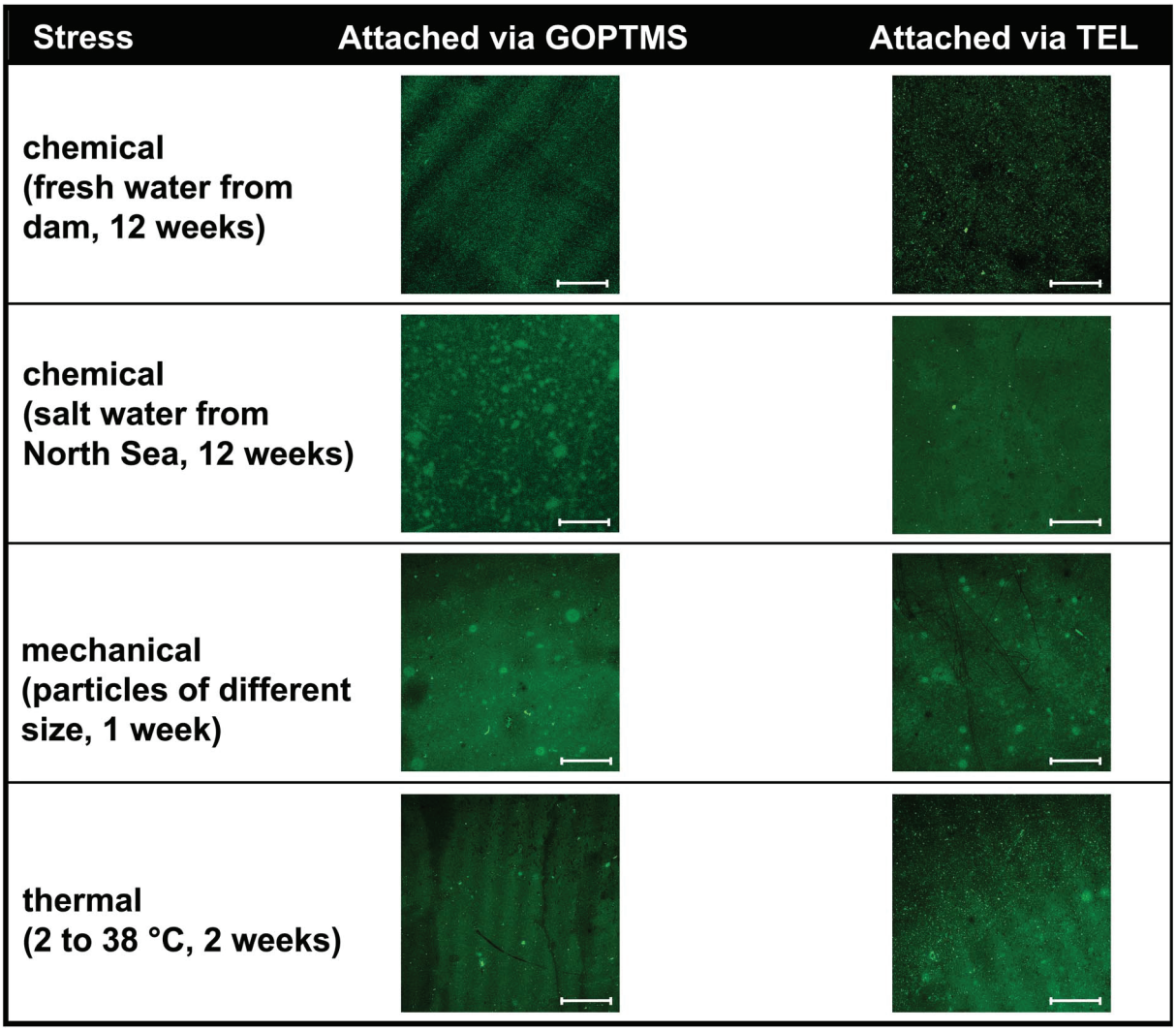

Fig. 8 Confocal laser scanning microscopy images of the Fluo-PEtOx coatings after stress tests (scale bar: 100 μm).

However, at the chosen, more realistic conditions, a complete reduction of biofilm formation could not be observed. Further investigations have to be performed and will aim at the application of mixtures of PEtOx with different molar masses as well as PEtOx of different architectures to result in a denser packing of the polymer chains on the surface. Another interesting aspect is probably the grafting of polyhydrophilic and polyzwitterionic entities to form a stable superficial water barrier. Future tests will have to show whether the presented coatings are able to maintain their antifouling behavior under real life conditions, *i.e.* the simultaneous acting of bacteria and stresses.

Acknowledgements

The authors would like to thank the Bundesministerium für Bildung und Forschung (Germany) funding (project: BASIS, 03WKCB01C) and 4H Jena Engineering for the stability tests. CW acknowledges the Carl-Zeiss foundation. KK is grateful to the Alexander von Humboldt-foundation for financial support. We also thank the Dutch Polymer Institute (DPI, technology area HTE).

Notes and references

1 V. K. Vendra, L. Wu and S. Krishnan, in *Nanotechnologies for the Life Sciences*, Wiley-VCH Verlag GmbH & Co. KGaA, 2007.
2 C. Blaszykowski, S. Sheikh and M. Thompson, *Chem. Soc. Rev.*, 2012, **41**, 5599–5612.
3 S. Cao, J. Wang, H. Chen and D. Chen, *Chin. Sci. Bull.*, 2011, **56**, 598–612.
4 P. Buskens, M. Wouters, C. Rentrop and Z. Vroon, *J. Coat. Technol. Res.*, 2013, **10**, 29–36.
5 T. Mérian and J. M. Goddard, *J. Agric. Food Chem.*, 2012, **60**, 2943–2957.
6 D. Rana and T. Matsuura, *Chem. Rev.*, 2010, **110**, 2448–2471.
7 C. Zhao, L.-Y. Li, M.-M. Guo and J. Zheng, *Chem. Pap.*, 2012, **66**, 323–339.
8 I. Banerjee, R. C. Pangule and R. S. Kane, *Adv. Mater.*, 2011, **23**, 690–718.

9 M. Charnley, M. Textor and C. Acikgoz, *React. Funct. Polym.*, 2011, **71**, 329–334.
10 F. Siedenbiedel and J. C. Tiller, *Polymers*, 2012, **4**, 46–71.
11 F. A. Guardiola, A. Cuesta, J. Meseguer and M. A. Esteban, *Int. J. Mol. Sci.*, 2012, **13**, 1541–1560.
12 J.-P. Maréchal and C. Hellio, *Int. J. Mol. Sci.*, 2009, **10**, 4623–4637.
13 R. Konradi, C. Acikgoz and M. Textor, *Macromol. Rapid Commun.*, 2012, **33**, 1663–1676.
14 K. Liefeith, H. Rothe, M. Frant and R. Schade, in *Biofunctional Surface Engineering*, ed. M. Scholz, Pan Stanford Publishing Pte. Ltd, Singapore, 2014, pp. 71–120.
15 J. Blümmel, N. Perschmann, D. Aydin, J. Drinjakovic, T. Surrey, M. Lopez-Garcia, H. Kessler and J. P. Spatz, *Biomaterials*, 2007, **28**, 4739–4747.
16 A. Rosenhahn, S. Schilp, H. J. Kreuzer and M. Grunze, *Phys. Chem. Chem. Phys.*, 2010, **12**, 4275–4286.
17 A. Roosjen, H. C. van der Mei, H. J. Busscher and W. Norde, *Langmuir*, 2004, **20**, 10949–10955.
18 E. Ostuni, R. G. Chapman, R. E. Holmlin, S. Takayama and G. M. Whitesides, *Langmuir*, 2001, **17**, 5605–5620.
19 B. Pidhatika, M. Rodenstein, Y. Chen, E. Rakhmatullina, A. Muhlebach, C. Acikgoz, M. Textor and R. Konradi, *Biointerphases*, 2012, **7**, 1–15.
20 C. Crouzet, C. Decker and J. Marchal, *Makromol. Chem.*, 1976, **177**, 145–157.
21 F. Kawai, T. Kimura, M. Fukaya, Y. Tani, K. Ogata, T. Ueno and H. Fukami, *Appl. Environ. Microbiol.*, 1978, **35**, 679–684.
22 C. F. Gonzalez, W. A. Taber and M. A. Zeitoun, *Appl. Microbiol.*, 1972, **24**, 911–919.
23 R. Konradi, B. Pidhatika, A. Muhlebach and M. Textor, *Langmuir*, 2008, **24**, 613–616.
24 J. U. Lind, C. Acikgöz, A. E. Daugaard, T. L. Andresen, S. Hvilsted, M. Textor and N. B. Larsen, *Langmuir*, 2012, **28**, 6502–6511.
25 B. Pidhatika, J. ller, V. Vogel and R. Konradi, *Chimia*, 2008, **62**, 264–269.
26 B. Pidhatika, J. Möller, E. M. Benetti, R. Konradi, E. Rakhmatullina, A. Mühlebach, R. Zimmermann, C. Werner, V. Vogel and M. Textor, *Biomaterials*, 2010, **31**, 9462–9472.
27 H. Wang, L. Li, Q. Tong and M. Yan, *ACS Appl. Mater. Interfaces*, 2011, **3**, 3463–3471.
28 H. Wang, J. Ren, A. Hlaing and M. Yan, *J. Colloid Interface Sci.*, 2011, **354**, 160–167.
29 N. Zhang, T. Pompe, I. Amin, R. Luxenhofer, C. Werner and R. Jordan, *Macromol. Biosci.*, 2012, **12**, 926–936.
30 N. Zhang, T. Pompe, R. Luxenhofer, C. Werner and R. Jordan, *Polym. Prepr. (Am. Chem. Soc., Div. Polym. Chem.)*, 2012, **53**, 301–302.
31 N. Zhang, M. Steenackers, R. Luxenhofer and R. Jordan, *Macromolecules*, 2009, **42**, 5345–5351.
32 B. Guillerm, S. Monge, V. Lapinte and J.-J. Robin, *Macromol. Rapid Commun.*, 2012, **33**, 1600–1612.
33 L. Tauhardt, K. Kempe, M. Gottschaldt and U. S. Schubert, *Chem. Soc. Rev.*, 2013, **42**, 7998–8011.
34 M. Hanford and T. Peeples, *Appl. Biochem. Biotechnol.*, 2002, **97**, 45–62.
35 M. Frant, in *Zentrum für Ingenieurwissenschaften* Martin-Luther-Universität Halle-Wittenberg, Halle, 2008.
36 M. Frant, P. Stenstad, H. Johnsen, K. Dölling, U. Rothe, R. Schmid and K. Liefeith, *Materialwiss. Werkstofftech.*, 2006, **37**, 538–545.
37 A. Sateesh, J. Vogel, E. Dayss, B. Fricke, K. Dölling and U. Rothe, *J. Biomed. Mater. Res., Part A*, 2008, **84A**, 672–681.
38 S. Vidawati, J. Sitterberg, U. Bakowsky and U. Rothe, *Colloids Surf., B*, 2010, **78**, 303–309.
39 C. Bücher, X. Grosse, H. Rothe, A. Fiethen, H. Kuhn and K. Liefeith, *Biointerphases*, 2014, **9**, 011002.
40 J. Piehler, A. Brecht, R. Valiokas, B. Liedberg and G. Gauglitz, *Biosens. Bioelectron.*, 2000, **15**, 473–481.
41 M. Hartlieb, D. Pretzel, K. Kempe, C. Fritzsche, R. M. Paulus, M. Gottschaldt and U. S. Schubert, *Soft Matter*, 2013, **9**, 4693–4704.
42 C. P. Lin, Y. C. Sung and G. H. Hsiue, *J. Med. Biol. Eng.*, 2012, **32**, 365–372.
43 J.-S. Park, Y. Akiyama, F. M. Winnik and K. Kataoka, *Macromolecules*, 2004, **37**, 6786–6792.
44 A. Baumgaertel, E. Altuntaş, K. Kempe, A. Crecelius and U. S. Schubert, *J. Polym. Sci., Part A: Polym. Chem.*, 2010, **48**, 5533–5540.
45 A. Baumgaertel, C. Weber, N. Fritz, G. Festag, E. Altuntaş, K. Kempe, R. Hoogenboom and U. S. Schubert, *J. Chromatogr. A*, 2011, **1218**, 8370–8378.
46 S. Kobayashi, E. Masuda, S. Shoda and Y. Shimano, *Macromolecules*, 1989, **22**, 2878–2884.
47 M. Litt, A. Levy and J. Herz, *J. Macromol. Sci., Part A: Pure Appl. Chem.*, 1975, **9**, 703–727.
48 A. Levy and M. Litt, *J. Polym. Sci., Part A-1: Polym. Chem.*, 1968, **6**, 1883–1894.
49 P. Mongondry, C. Bonnans-Plaisance, M. Jean and J. F. Tassin, *Macromol. Rapid Commun.*, 2003, **24**, 681–685.
50 M. Agrawal, J. C. Rueda, P. Uhlmann, M. Müller, F. Simon and M. Stamm, *ACS Appl. Mater. Interfaces*, 2012, **4**, 1357–1364.
51 C. Bartholome, E. Beyou, E. Bourgeat-Lami, P. Chaumont and N. Zydowicz, *Macromolecules*, 2003, **36**, 7946–7952.
52 J. P. Gann and M. Yan, *Langmuir*, 2008, **24**, 5319–5323.

Electronic Supplementary Material (ESI) for Journal of Materials Chemistry B.

Supporting Information

Amine end-functionalized poly(2-ethyl-2-oxazoline) as promising coating material for antifouling applications

Lutz Tauhardt,[1,2] Marion Frant,[3] David Pretzel,[1,2] Matthias Hartlieb,[1,2] Christian Bücher,[3] Gerhard Hildebrand,[3] Bernd Schröter,[4] Christine Weber,[1,2] Kristian Kempe,[1,2,6] Michael Gottschaldt,[1,2] Klaus Liefeith,[3] Ulrich S. Schubert*[1,2,5]

[1]Laboratory of Organic and Macromolecular Chemistry (IOMC), Friedrich Schiller University Jena, Humboldtstr. 10, 07743 Jena, Germany.

[2]Jena Center for Soft Matter (JCSM), Friedrich Schiller University Jena, Philosophenweg 7, 07743 Jena, Germany.

[3]Institute for Bioprocessing and Analytical Measurement Techniques e.V. (IBA), Rosenhof, 37308 Heilbad Heiligenstadt, Germany.

[4]Institute for Solid State Physics, Friedrich Schiller University Jena, Helmholtzweg 5, 07743 Jena.

[5]Dutch Polymer Institute (DPI), John F. Kennedylaan 2, 5612 AB Eindhoven, The Netherlands.

Corresponding author footnote: Fax. +49 3641 948 202; Email: ulrich.schubert@uni-jena.de

[6]Current address: Department of Chemical and Biomolecular Engineering, The University of Melbourne, Victoria 3010, Australia.

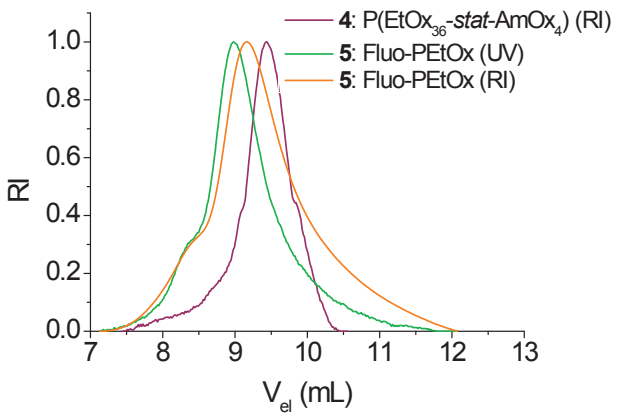

Fig. S1. SEC curves of amine containing POx **4** and Fluo-PEtOx **5 (**eluent: $CHCl_3$/2-propanol/TEA).

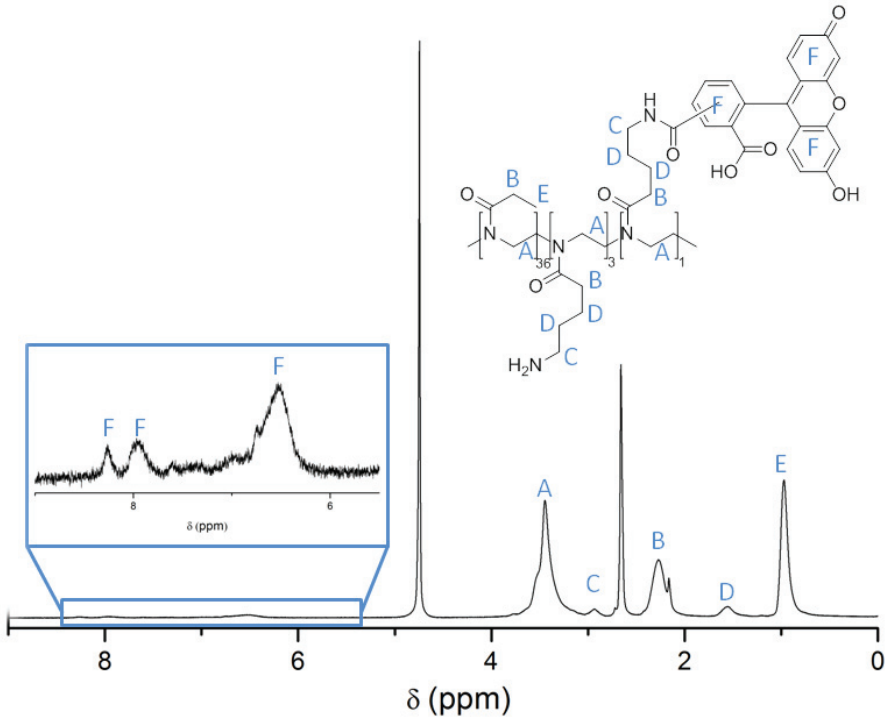

Fig. S2 ^{1}H NMR spectrum of PEtOx-FITC (300 MHz, solvent CD_3OD).

Methods and materials

General

Dry acetonitrile, MeOx and methyl tosylate (MeOTs) were obtained from Acros Organics, distilled to dryness over barium oxide (BaO), and stored under nitrogen. Dry *N,N*-dimethylformamide (DMF) was purchased from Acros Organics, (3-glycidyloxypropyl)-trimethoxysilane from ABCR, hydrazine monohydrate and potassium phthalimide from Fluka. Triethylamine was distilled over calcium hydride prior use.
Borofloat 33 glass slides were purchased from Schott (Jena, Germany) and cleaned using a low-pressure oxygen plasma instrument from Diener Electronic (Nagold, Germany). The Initiator Sixty single-mode microwave synthesizer from Biotage, equipped with a noninvasive IR sensor (accuracy: ±2%), was used for polymerizations under microwave irradiation. Prior to use, the microwave vials were heated at 110 °C overnight and allowed to cool to room temperature under a nitrogen atmosphere. Proton (^{1}H) nuclear magnetic resonance (NMR) spectra were recorded on a Bruker AC 300 MHz at 298 K. Chemical shifts are reported in parts per million (ppm, δ scale) relative to the residual signal of the deuterated solvent. Size exclusion chromatographies (SEC) of the PEtOx were measured on a Shimadzu system equipped with a SCL-10A VP system controller, a DGU-14A degasser, a LC-10AD VP pump, a RID-10A refractive index detector and a PSS SDV column running with chloroform, triethylamine (TEA), and 2-propanol (94:4:2) as eluent. The Techlab column oven was set to 50 °C. Molar masses were calculated using a polystyrene (PS) standard. The MALDI-TOF-MS spectra were recorded utilizing an Ultraflex III TOF/TOF (Bruker Daltonics GmbH, Bremen, Germany), equipped with a frequency-tripled Nd:YAG laser, operating at a wavelength of 355 nm. All spectra were measured in the positive reflector mode using *trans*-2-[3-(4-*tert*-butylphenyl)-2-methyl-2-propenylidene]malononitrile (DCTB) with sodium iodide as matrix. XPS measurements were performed on an EA200-ESCA-system (SPECS Surface Nano Analysis GmbH, Berlin, Germany).

X-ray photoelectron spectroscopy (XPS)

XPS investigations were carried out with an EA200-ESCA-system (SPECS) using nonmonochromatic Al Kα radiation (hν = 1486 eV). The samples have been measured as received under constant conditions (ϑ = 0°). The nitrogen 1s photoemission signals have been background subtracted and smoothed.

Contact angle measurements

Determination of water contact angles has been carried out with a computer controlled contact angle measuring system (DCA20, dataphysics, Germany) using the sessile drop technique (drops of 3 µL). In order to evaluate expected hydration effects of the PEtOx-layers, both dry and swollen samples were characterized. To obtain the latter, the coated glass slides were swollen in distilled water for 30 min. Prior to the determination, excess of water on the surface was removed with pressurized air. The presented contact angles are an average from 15 measurements at 5 different surface points (n = 45).

Publication 3

”Poly(2-ethyl-2-oxazoline) as alternative for the stealth polymer poly(ethylene glycol): Comparison of *in vitro* cytotoxicity and hemocompatibility”

M. Bauer, C. Lautenschläger, K. Kempe, L. Tauhardt, U. S. Schubert, D. Fischer

Macromol. Biosci. **2012**, *12*, 986-998

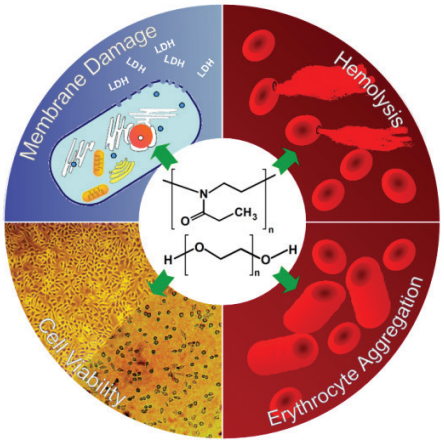

Poly(2-ethyl-2-oxazoline) as Alternative for the Stealth Polymer Poly(ethylene glycol): Comparison of in vitro Cytotoxicity and Hemocompatibility

Marius Bauer, Christian Lautenschlaeger, Kristian Kempe, Lutz Tauhardt, Ulrich S. Schubert, Dagmar Fischer*

Limitations of PEG in drug delivery have been reported from clinical trials. PEtOx (0.4–40 kDa) as alternative is synthesized by a living, microwave-assisted polymerization, and is directly compared to PEG of similar molar mass regarding cytotoxicity and hemocompatibility. In short-term treatments, both types of polymers are well tolerated even at high concentrations. Moderate concentration and molar mass dependent cytotoxic effects occurred only after long-term incubation at concentrations higher than therapeutic doses. PEtOx possesses not only an easy route of synthesis and beneficial physicochemical characteristics such as low viscosity and high stability, which are advantageous over PEG, but additionally in vitro toxicology comparable to PEG.

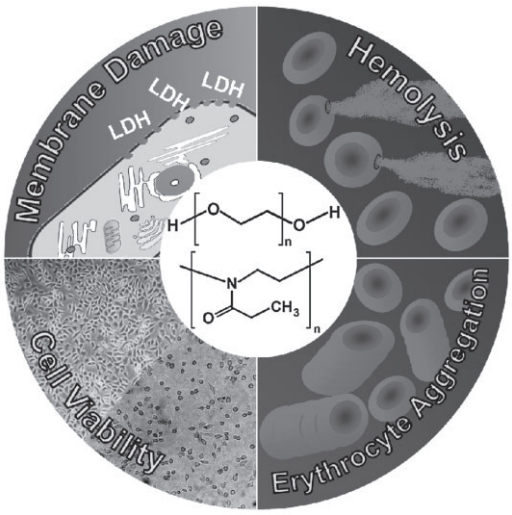

1. Introduction

Poly(ethylene glycol) (PEG) currently represents the gold standard for stealth polymers in drug delivery and is to date the only stealth polymer that made it to the market.[1,2] The success story began about 20 years ago, when the first PEGylated drug Adagen® received approval. Many others, mostly PEG-protein conjugates followed.[2] However, although only observed for a limited number of patients, concerns regarding immune responses,[3] formation of PEG-antibodies,[4] an accelerated blood clearance (ABC) phenomenon after multiple applications,[5] and non-biodegradability of PEG resulting in body accumulation of high-molar-mass PEGs[6] arose with an increasing number of clinical trials and a more profound experience with PEG in humans. In addition, a tense patent situation regarding PEG complicates the introduction of new formulations to the market. Hence, intensive efforts were made to search for alternative stealth polymers.

M. Bauer, C. Lautenschlaeger, Prof. D. Fischer
Department of Pharmaceutical Technology, Institute of Pharmacy, Friedrich-Schiller University Jena, Otto-Schott-Strasse 41, 07745 Jena, Germany
E-mail: dagmar.fischer@uni-jena.de
Dr. K. Kempe, L. Tauhardt, Prof. U. S. Schubert
Laboratory of Organic and Macromolecular Chemistry (IOMC), Friedrich-Schiller-University Jena, Humboldtstr. 10, 07743 Jena, Germany
Prof. U. S. Schubert, Prof. D. Fischer
Jena Center for Soft Matter (JCSM), Friedrich-Schiller-University Jena, Humboldtstr. 10, 07743 Jena, Germany

DOI: 10.1002/mabi.201200017

In recent years poly(2-oxazoline)s (POx) which were already discovered in the 1960s have been discussed as potential alternatives for PEG as stealth polymers.[7] They can be synthesized easily by the living cationic ring-opening polymerization (CROP) of 2-substituted 2-oxazolines, thus offering the advantage of a straightforward control of the degree of polymerization and the polymer architecture, and to obtain polymers with low polydispersity indices (PDI) in high quality. Since classical bulk polymerizations took several hours to several days, the commercial spreading of POx was limited. In the last years, the introduction of microwave-assisted polymerization techniques increased the synthesis speed by a factor of up to 350 while allowing at the same time to improve the livingness of the polymerization, making poly(2-oxazolines) easily[8] available and more attractive for commercialization. For the use as stealth polymers, poly(2-methyl-2-oxazoline) (PMeOx) and poly(2-ethyl-2-oxazoline) (PEtOx) were investigated. Physicochemical properties such as the non-ionic character, a broad solubility in hydrophilic and lipophilic solvents, and a high flexibility of the main chain were found to be comparable to PEG.[9] Even though only available to a limited extent, biopharmaceutical studies revealed that pharmacokinetics of POx-modified drug delivery systems are comparable to PEG. PMeOx and PEtOx conjugated liposomes showed a prolonged blood circulation time with preferential distribution comparable to PEGylated liposomes in liver, spleen, and kidney after 24 h.[7] PEtOx conjugates of biomolecules like uricase, catalase, ribonuclease, insulin, and albumin demonstrated the stealth effect of POx.[10] The safety of 10 and 20 kDa POx was shown in vivo in rats after intravenous administration with maximum tolerated doses higher than $2\,g \cdot kg^{-1}$ and without any signs of toxicity.[10]

Although, many studies have been published dealing with the cyto- and hemocompatibility of PEG, only few publications have dealt with such experiments regarding PEtOx.[9,11–13] POx with varying alkyl chains, and molar masses were shown to have no significant cytotoxic effects up to $5\,mg \cdot mL^{-1}$ on RAT-2 cells and did not induce immunological effects.[12] POx block copolymers of different architectures were well tolerated by mammalian cells.[13] Nonetheless, any systematic investigation of PEtOx in particular in direct comparison to PEG under standardized conditions is still missing. Comprehensive hemocompatibility studies of PEtOx were not yet reported. Additionally, already published studies are difficult to compare since they used different test conditions, different cell types, and polymers of different origin and purity. Therefore, in the present study, a large set of PEtOx was systematically analyzed in a comprehensive cyto- and hemotoxicity study in direct comparison to PEG, aiming at a systematic analysis of the influence of polymer molar mass, polymer concentration, incubation time, polymer purity, and source of the polymers.

2. Experimental Section

2.1. Commercial Polymers

Six commercial PEGs with molar masses of 0.4, 2, 4, and 20 kDa (Carl Roth, Karlsruhe, Germany), 10 kDa (Merck, Darmstadt, Germany), and 40 kDa (Serva, Heidelberg, Germany) were selected. All PEGs were purchased in pharmaceutical grade according to the European Pharmacopeia 6.8 (Ph. Eur. 6.8) except 10 kDa PEG, which was only available as chemical grade. Commercially available PEtOxs were obtained from Polysciences Europe GmbH (Eppelheim, Germany) (5 kDa) and Sigma-Aldrich (Deisenhofen, Germany) (50 and 200 kDa).

2.2. Synthesis of Poly(2-ethyl-2-oxazoline)

The initiator 60 single-mode microwave synthesizer from Biotage, equipped with a non-invasive infrared sensor (accuracy: ±2%), was used for polymerizations under microwave irradiation.[8] Microwave vials were heated to 110 °C overnight and allowed to cool to room temperature under an argon atmosphere before usage. All polymerizations were carried out with temperature control. Methyl tosylate and 2-ethyl-2-oxazoline (EtOx) (Acros Organics, Geel, Belgium) were distilled to dryness over barium oxide (BaO) and stored under argon. A stock solution of acetonitrile (Sigma-Aldrich), initiator (methyl tosylate), and monomer EtOx was prepared. The total monomer concentration was adjusted to 4 M with a total monomer-to-initiator ratio of 4, 20, 40, 100, 200, and 400, respectively. The stock solutions were divided into 4–5 vials, which were heated to 140 °C in the microwave synthesizer for a pre-determined time. After cooling, a sample for the determination of the monomer conversion by ^{1}H NMR spectroscopy was prepared.

The following purification procedure was applied for all PEtOx samples. A 15-fold excess of aqueous sodium carbonate (Sigma-Aldrich) was added to the polymerization mixture, which was stirred at 100 °C overnight. Subsequently, the two-phase solution was diluted with dichloromethane; the organic phase was washed three times with water and saturated sodium chloride solution and dried over $MgSO_4$. The polymer was concentrated in vacuo and precipitated into ice-cold diethyl ether. The PEtOx samples with a molar mass of 0.4 and 2 kDa were re-dissolved in water and stirred with amberlite (basic loaded) for 24 h. After filtration and washing of the resin the water was evaporated under reduced pressure. The polymer was re-dissolved in dichloromethane and precipitated into ice-cold diethyl ether. All polymer samples were kept under reduced pressure at 40 °C for 4 d. Subsequently, the polymers were lyophilized.

2.3. Physicochemical Characterization of the Polymers

Molar masses and polydispersity indices were determined for all commercial and non-commercial polymers. Size exclusion

chromatography (SEC) measurements were performed using an Agilent system equipped with a SCL-10A system controller, a LC-10AD pump, a RID-10A refractive index detector, and both a PSS Gram30 and a PSS Gram1000 column in series, whereby, *N,N*-dimethylacetamide with 2.1 mg · mL^{-1} LiCl was applied as an eluent at 1 mL · min^{-1} flow rate and the column oven was set to 40 °C. The system was calibrated with PEG (0.4–1000 kDa) and polystyrene (0.4–44.7 kDa) standards (Polymer Standard Service, Mainz, Germany) using a third order polynomial fit. ^{1}H NMR spectra were recorded on a Bruker AC 300 MHz spectrometer at room temperature with deuterated chloroform as solvent. The chemical shifts were given in ppm relative to the signal from residual non-deuterated solvent.

2.4. Preparation of Polymer Stock Solutions

PEG solutions were prepared by dissolving the polymer in highly purified water with a concentration twice as high as the required final concentration and sterilized by autoclaving. To reach the final concentration they were mixed with double concentrated Roswell Park Memorial Institute 1640 culture medium (RPMI 1640, PAA, Pasching, Austria). PEtOx solutions were directly prepared in RPMI 1640 culture medium and sterilized by filtration (0.2 μm, VWR International, Darmstadt, Germany). Filterability was tested by gravimetric measurement of aqueous stock solutions at highest concentrations of 80 mg · mL^{-1}. Therefore, 1 mL stock solution and 1 mL filtrate were transferred into tare glass vials and lyophilized in a Alpha 1-2/LD Plus freeze dryer (Martin Christ, Osterode Germany) at a pressure of 0.006 mbar for 48 h. Samples were weighed on a Sartorius RC 210 P semi-micro balance (Sartorius, Goettingen, Germany). Serial dilutions with concentrations between 5 and 80 mg · mL^{-1} were prepared. pH and osmolarity of the polymer solutions were routinely measured with a pH meter 1140 (Mettler Toledo, Giessen, Germany) and a semi-microosmometer (Knauer, Berlin, Germany), respectively.

2.5. Cell Culture

L929 mouse fibroblasts (German Collection of Microorganisms and Cell Cultures, Braunschweig, Germany) were incubated in RPMI 1640 culture medium containing 10% fetal calf serum Gold (FCS Gold, PAA) and 2×10^{-3} M glutamine at 37 °C, 5% CO_2, and 95% relative humidity. Cells were routinely tested with standard test kits for absence of squirrel monkey retrovirus (QIAamp® DNA Mini kit, Qiagen, Hilden, Germany) and mycoplasma (Venor®GeM, Minerva Biolabs, Berlin, Germany).

2.6. 3-(4,5-Dimethylthiazol-2-yl)-2,5-diphenyltetrazolium bromide (MTT) Assay

The MTT assay was performed according to a modified method of Mosmann[14] and Fischer et al.[15] L929 mouse fibroblasts (8500 per well) were seeded into 96-well microtiter plates (Greiner Bio-One, Frickenhausen, Germany) and incubated for 24 h. Subsequently, the culture medium was replaced by 100 μL serial dilutions of the polymers. After 3, 12, and 24 h polymer solutions were removed and 200 μL MTT solution (0.5 mg · mL^{-1}, Sigma), prepared in RPMI 1640 without FCS, were added for 4 h. MTT solution was aspirated and the formazane crystals were dissolved in 200 μL dimethyl sulfoxide (Carl Roth). Absorbance was measured at 570 nm wavelength in a microplate reader (Fluostar OPTIMA, BMG Labtech, Offenburg, Germany). Culture medium without cells was used to calibrate the zero absorbance (blank). For the determination of 0% viability (positive control), cells were treated with a 0.02% thiomersal solution (Synopharm, Barsbüttel, Germany) in culture medium. For 100% viability (negative control), cells were kept only in cell culture medium. After subtracting the blank from all values, the cell viability (%) was calculated as absorbance of test polymer divided by absorbance of negative control times 100%. According to ISO 10993-5[16], a cell viability lower than 70% in comparison to the negative control was regarded as cytotoxic. All experiments were run in seven parallel experiments and were repeated once. Additionally, changes in cell morphology and detachment of cells from the dish were observed with a Leica inverse phase contrast microscope (Leica DM IL, Leica, Germany) equipped with an objective (Achromat 10/0.20 Phaco 1a, Leica, Germany) of ×100 magnification. The results were classified according to the staging system of ISO 10993-5.

2.7. Lactate Dehydrogenase (LDH) Assay

L929 mouse fibroblasts (100 000 per well) were cultured in 12-well cell culture plates (Greiner Bio-One) in RPMI 1640 with 10% FCS. After 48 h incubation, the cell culture medium was removed and replaced by 2 mL · well^{-1} polymer solution. Serial polymer dilutions with concentrations of 40, 60, and 80 mg · mL^{-1} were prepared in RPMI 1640 cell culture medium without FCS and phenol red (PAA). Aliquots of 120 μL per well were collected from the supernatant after 0, 1, 2, and 4 h of exposure. The LDH concentration was determined by using a commercial LDH cytotoxicity assay kit (Cayman, Ann Arbor, USA) according to the manufacturer's protocol. The LDH release (%) is defined as the ratio of LDH released by the test compounds over total LDH in treated cells. For determination of total LDH positive controls were performed using a 0.1% Triton X-100 solution (Ferak, Berlin, Germany). Cells only treated with culture medium were used as negative control. A LDH release of less than 10% was regarded as non-toxic effect level.[17]

2.8. Hemolysis of Erythrocytes

The hemolytic activity of the polymers was investigated according to a modified method of Parnham and Wetzig.[18] Blood was collected in heparinized-tubes from sheep. Plasma was removed by centrifugation at 4500*g* for 5 min (Eppendorf Centrifuge 5804R, Eppendorf, Hamburg, Germany). The pellet was washed three times with cold 1.5×10^{-3} M phosphate-buffered saline pH = 7.4 (PBS) by centrifugation at 4500*g* for 5 min and was resuspended in the same buffer. The red blood cell suspensions were used within 24 h after collection. For the experiments, stock solutions were diluted with PBS in a ratio of 1:6.67 to receive the necessary number of erythrocytes. Polymer solutions were prepared in PBS buffer with concentrations of 40, 60, and 80 mg · mL^{-1}. They were mixed 1:1 with erythrocytes and incubated in a water bath at 37 °C for 60 min. Hemoglobin release was determined by spectrophotometric

analysis of the supernatant at 544 nm after centrifugation at 2400*g* for 5 min (Eppendorf mini spin, Eppendorf). As positive control, 1% Triton X-100 solution was used. The negative control was received by treating erythrocytes with PBS. The percentage of hemolysis was calculated according to

$$\text{Hemolysis}(\%) = \frac{(\text{Absorption}_{\text{sample}} - \text{Blank}_{\text{sample}}) - (\text{Absorption}_{\text{negative control}} - \text{Blank}_{\text{negative control}})}{\text{Absorption}_{\text{positive control}} - \text{Blank}_{\text{positive control}}} \times 100\% \quad (1)$$

Hemoglobin release of 0–2, 2–5, or >5% of the total release was classified as non-hemolytic, slightly hemolytic, or hemolytic, respectively, according to the ASTM F756-08 standard.[19] Experiments were run in triplicate and were repeated once.

2.9. Erythrocyte Aggregation Assay

A modified method from Ogris et al.[20] was applied for testing the erythrocyte aggregation of the polymers by microscopy. Polymers were dissolved in PBS buffer with concentrations up to 80 mg · mL^{-1}. The erythrocytes were isolated as described above. Erythrocyte suspensions (100 μL) containing 9.4×10^6 erythrocytes · mL^{-1} were mixed with the same volume of test compounds in a 24-well plates (Nunc, Roskilde, Denmark). Cells were incubated at 37 °C for 2 h. Erythrocyte aggregation was evaluated by microscopic observations (Leica DM IL, Achromat 10/0.20 Phaco 1a objective, 200× magnification) classifying the results in three stages. At stage 1, the erythrocytes stayed discrete in suspension, no aggregation was detectable. Stage 2 showed a moderate aggregation with rouleau formation but the majority of erythrocytes were discrete. In stage 3, almost all erythrocytes were aggregated in clusters. For determination of stage 1, erythrocytes were treated with PBS as negative control. Positive controls were treated with 30 μg · mL^{-1} 25 kDa branched poly(ethylene imine) (bPEI, kind gift of BASF corporation, Ludwigshafen, Germany) and were classified as stage 3.[21] The experiments were run in duplicate and were repeated once. Each data point is presented as the mean of four experiments.

2.10. Photometric Erythrocyte Aggregation Assay

Erythrocyte aggregation of two selected polymers 0.4 and 200 kDa PEtOx as well as 25 kDa bPEI were additionally tested using a photometric method according to Cardoso et al.[22] Test polymer solutions were prepared in dilutions ranging from 10 to 80 mg · mL^{-1}. 25 kDa bPEI as positive control was tested up to a maximum concentration of 40 μg · mL^{-1}. Each polymer dilution with a volume of 50 μL was mixed with 50 μL of erythrocyte suspension (9.4×10^6 erythrocytes · mL^{-1}) in a clear flat bottomed 96-well plate (Greiner Bio-One). Cells were incubated under vigorous shaking at 37 °C for 2 h. Absorbance was measured at 645 nm in a microplate reader. Negative controls were cells only treated with PBS. Blank values were determined with PBS and subtracted from the sample values. Absorbances of the test solutions lower than the negative control were regarded as aggregation. Results were additionally checked by microscopic observation after the measurement. Tests were run in triplicate and repeated once.

3. Results

3.1. Synthesis and Physicochemical Characterization of the Polymers

In the following experiments, PEGs with molar masses in the range from 0.4 to 40 kDa (corresponding to 8–900 repeating units) were investigated, representing polymers that are typically used in pharmaceutical and medical applications. With exception of PEG 10 kDa, all PEGs were purchased in pharmaceutical grade with defined limited concentrations of impurities like dioxane (max. 0.0001%), ethylene oxide (max. 0.0001%), and formaldehyde (max. 0.0015%). PEG 10 kDa was not tested according to the specifications of Ph. Eur. because no monograph is available for this particular polymer length. The theoretical molar masses of PEG given by the suppliers correlated well with the weight-average ($\overline{M}_w$) and number-average ($\overline{M}_n$) molar mass determined by SEC (Figure 1a and Table 1a). The molar mass distribution of PEG was found to be low, with a maximum of 1.09 for polymers ≤4 kDa up to 1.19 for PEG >5 kDa.

For comparison to PEG, six PEtOx with molar masses in the same range as the PEGs (0.4–40 kDa consistent with 4, 20, 40, 100, 200, and 400 repeating units) were synthesized by living CROP. PEtOxs were soluble in water, ethanol, methanol, acetonitrile, tetrahydrofuran, chloroform, dichloromethane, and *N,N*-dimethylacetamide. For the synthesis of a set of PEtOxs, a series of stock solutions containing MeOT (initiator), EtOx (monomer), and acetonitrile (solvent) were prepared and polymerized under microwave irradiation at 140 °C for pre-determined times yielding clear and colorless polymer solutions. The degree of polymerization was adjusted by choosing different monomer-to-initiator ratios. In order to guarantee the same chemical structure of all polymers as well as to remove initiator traces, the reaction mixture was treated with aqueous sodium carbonate at 100 °C after microwave polymerization, resulting in the formation of a hydroxy end group. The quenching of the polymerization with water would lead to two different end groups (hydroxyl and ester), which could have an influence on the properties, in particular of the shorter polymers.[23] In order to remove residual monomer and solvents, the polymers were purified

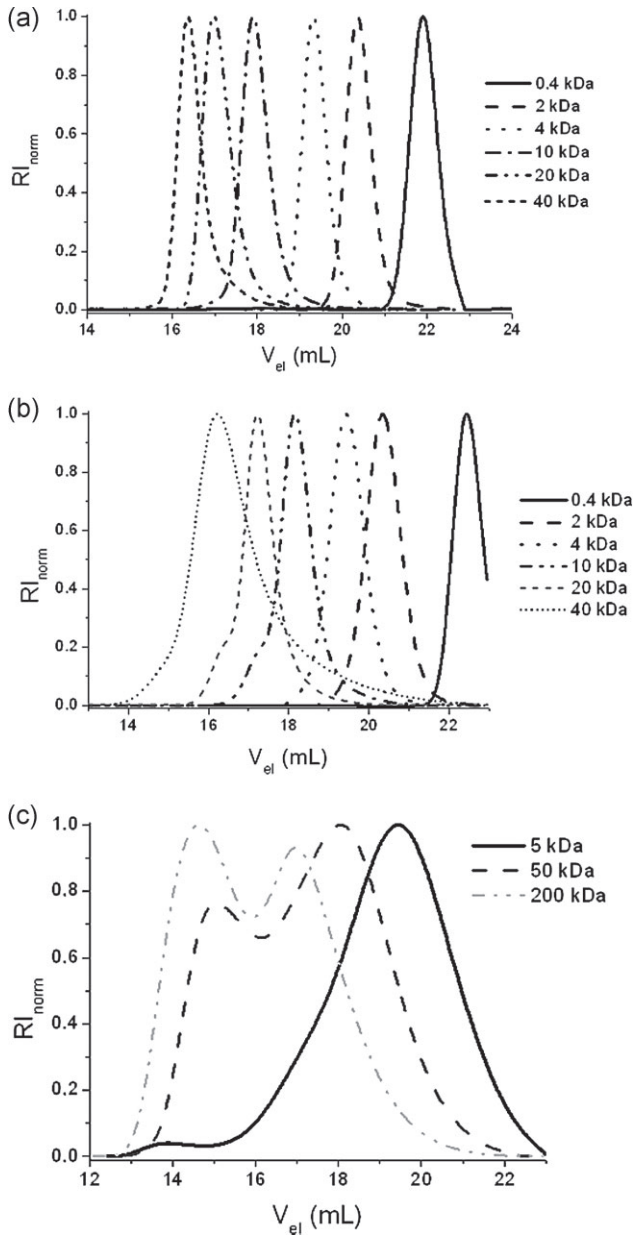

Figure 1. SEC traces of commercial PEG (0.4 kDa–40 kDa; a), synthesized PEtOx (0.4–40 kDa; b), and commercial PEtOx (5, 50, and 200 kDa; c). Synthesized PEtOx was obtained by microwave-assisted living CROP at 140 °C in acetonitrile with methyl tosylate as initiator.

by several washing steps, precipitation in ice-cold diethyl ether, drying in vacuo, and lyophilization. PEtOx with shorter chain length (<20 repeating units) were additionally treated with amberlite in aqueous solution to remove residual tosylate. The purified 0.4 kDa PEtOx was clear, semi-solid, and colorless, whereas polymers with higher molar masses were white powders. The purity of all polymers was tested by ^{1}H NMR spectroscopy, which additionally revealed a good agreement of the theoretical and experimental molar masses (Table 1b). The analysis by SEC confirmed that the PEtOx homopolymers were synthesized with narrow molar mass distributions (Table 1b and Figure 1b) comparable to commercial PEG (Table 1a). $\overline{M}_n$, $\overline{M}_w$, and PDI of 0.4 kDa PEtOx could not be determined by SEC because of the overlap of the polymer and the solvent signal. In addition, three commercial PEtOx with 5, 50, and 200 kDa were investigated. In these cases, the obtained molar masses showed a large deviation from the declared values with PDI values twice to four times higher as for non-commercial PEtOx (Figure 1c).

3.2. Preparation of Polymer Solutions

For cell culture experiments, sterile solutions of the polymers were required. PEG solutions were autoclaved under standard conditions according to Ph. Eur. 6.8 at 121 °C and 2 bar for 15 min. After sterilization, the PEG solutions were clear, colorless, and particle-free. Autoclaving was chosen as sterilization technique for PEG since the viscosity of the high molar mass PEG stock solutions inhibited a quantitative sterile filtration. Additionally, this high viscosity limited also the biological test of polymer concentrations higher than 80 mg · mL^{-1}. PEtOx solutions were sterilized by filtration using a 0.2 μm cellulose acetate filter. The filtered and afterwards freeze dried 0.4 and 200 kDa PEtOx solutions showed a recovery of 101 and 102% in the filtrate, respectively, demonstrating the filterability of PEtOx. Osmolarity and pH value of the polymer dilutions in cell culture medium were routinely measured to avoid unspecific cytotoxic effects. Both types of polymers had no influence on the pH value of the cell culture medium. In the case of the serial dilutions in PBS, all values were in physiological range between 7.2 and 7.6. The osmolarity of the polymer solutions was measured by freezing point depression. Cell culture medium alone has an average osmolarity of 280 mosmol · kg^{-1}. Previous experiments have shown that osmolarities up to 400 mosmol · kg^{-1} were well tolerated by L929 cells without a decrease in cell viability or morphological changes (data not shown). Osmolarities higher than 400 mosmol · kg^{-1} were only detected for 0.4 kDa PEG and 0.4 kDa PEtOx at 60 and 80 mg · mL^{-1} as well as for 2 kDa PEG at a concentration of 80 mg · mL^{-1}. For all other polymers and investigated concentrations, osmolarities in the range from 280 to 390 mosmol · kg^{-1} were measured.

3.3. Influence of Polymer Concentration, Molar Mass, Incubation Time, and Polymer Purity on Metabolic Cell Activity

The MTT assay was chosen as a test for the influence of the polymers on the metabolic activity of L929 mouse fibroblasts, which were used as target cells since they are

Table 1. Physicochemical characterization of weight-average ($\overline{M}_w$) and number-average ($\overline{M}_n$) molar mass and PDI values of PEG and PEtOx.

Sample	Expt. molar mass[a)] [Da]	$\overline{M}_n$[b)] [Da]	$\overline{M}_w$[b)] [Da]	PDI[b)]
0.4 kDa PEG		345	378	1.09
2 kDa PEG		1845	2009	1.09
4 kDa PEG		3994	4182	1.05
10 kDa PEG		9776	10 801	1.10
20 kDa PEG		19 002	21 595	1.14
40 kDa PEG		31 612	37 741	1.19
0.4 kDa PEtOx	400	–	–	–
2 kDa PEtOx	2 080	3660	4063	1.11
4 kDa PEtOx	4 060	6460	7171	1.11
5 kDa PEtOx[c)]	8 456	20 082	47 594	2.37
10 kDa PEtOx	10 200	12 750	14 663	1.15
20 kDa PEtOx	20 500	22 900	27 022	1.18
40 kDa PEtOx	37 500	41 000	51 250	1.25
50 kDa PEtOx[c)]	17 939	74 074	305 926	4.13
200 kDa PEtOx[c)]	48 882	229 010	1 071 767	4.68

[a)]Determined by means of ^{1}H NMR spectroscopy; [b)]Determined by means of SEC [*N,N*-dimethylacetamide containing 2.1 mg · mL^{-1} LiCl; PEG standards for PEG samples, polystyrene standards for PEtOx samples]; [c)]Commercial PEtOx samples.

recommended by many standard institutions like the International Organization for Standardization (ISO) or ASTM International (formerly known as American Society for Testing and Materials) as reference cell line for biomaterial testing.[16,24] In preliminary experiments, MTT assays performed with pure polymer solutions without the addition of cells showed that the presence of test polymers up to 80 mg · mL^{-1} had no influence on the chemical reaction of the assay and the spectrophotometric measurement (data not shown). L929 mouse fibroblasts were incubated with the polymers for 3, 12, and 24 h (Figure 2). According to ISO 10993-5, a cell viability ≥70% was regarded as non-toxic.

Untreated cells were used as negative control and were set as 100% viable cells. Thiomersal solution (0.02%) as positive control reduced the mean cell viability to 3.5% (data not shown). None of the PEGs caused any cytotoxic effect on cell viability (>70%) after 3 h, as shown in Figure 2a. After 12 h (Figure 2b) and 24 h (Figure 2c), a concentration- and molar mass-dependent effect on cell viability could be observed. Low molar mass PEGs (0.4, 2, and 4 kDa) as well as the 10 kDa PEG of non-pharmaceutical quality revealed only moderate cytotoxic effects at ≥60 mg · mL^{-1} after 12 h. In contrast, high molar mass PEGs (20 and 40 kDa) were found to be non-toxic, with cell viabilities being above 70%. Comparable profiles were received after 24 h. Up to 40 mg · mL^{-1}, all PEGs were found to be non-toxic. At higher concentrations for 0.4–4 kDa PEGs, only a slight decrease of cell viability between 0.5% (0.4 kDa PEG) and 8.4% (4 kDa PEG) could be detected compared to 12 h. Again, 10 kDa PEG demonstrated the highest toxicity of all PEGs tested.

After 3 h, the biocompatibility of PEtOx was found to be comparable to PEG. Treatment of L929 cells with PEtOx up to 80 mg · mL^{-1} did not change their metabolic activity (>70%). After longer incubation times, the cell viability was influenced by PEtOx in a concentration, time, and molar mass dependent manner as also observed for PEG. Up to 40 mg · mL^{-1} all other polymers revealed no cell damaging effect after 12 h except 0.4 kDa PEtOx. At higher concentrations, the two low molar mass PEtOx (0.4 and 2 kDa) as well as 20 kDa PEtOx decreased the cell viability below 70%, whereas all other polymers were found to be non-toxic. This was more pronounced after 24 h than after 12 h. In contrast to 0.4 kDa PEG, the 0.4 kDa PEtOx caused a complete loss of cell viability at 80 mg · mL^{-1} after 12 h and 40 mg · mL^{-1} after 24 h. PEtOx with the highest molar mass (50 and 200 kDa) were well tolerated. The 5 and 10 kDa polymers reduced the activity of the cells to <70% only at 80 mg · mL^{-1}, whereas 2, 20, and 40 kDa PEtOx revealed moderate cytotoxic effects starting at 20 mg · mL^{-1}.

Additionally, L929 mouse fibroblasts were microscopically investigated before and after treatment with the polymers. Untreated L929 fibroblasts are adhesive, spindle-

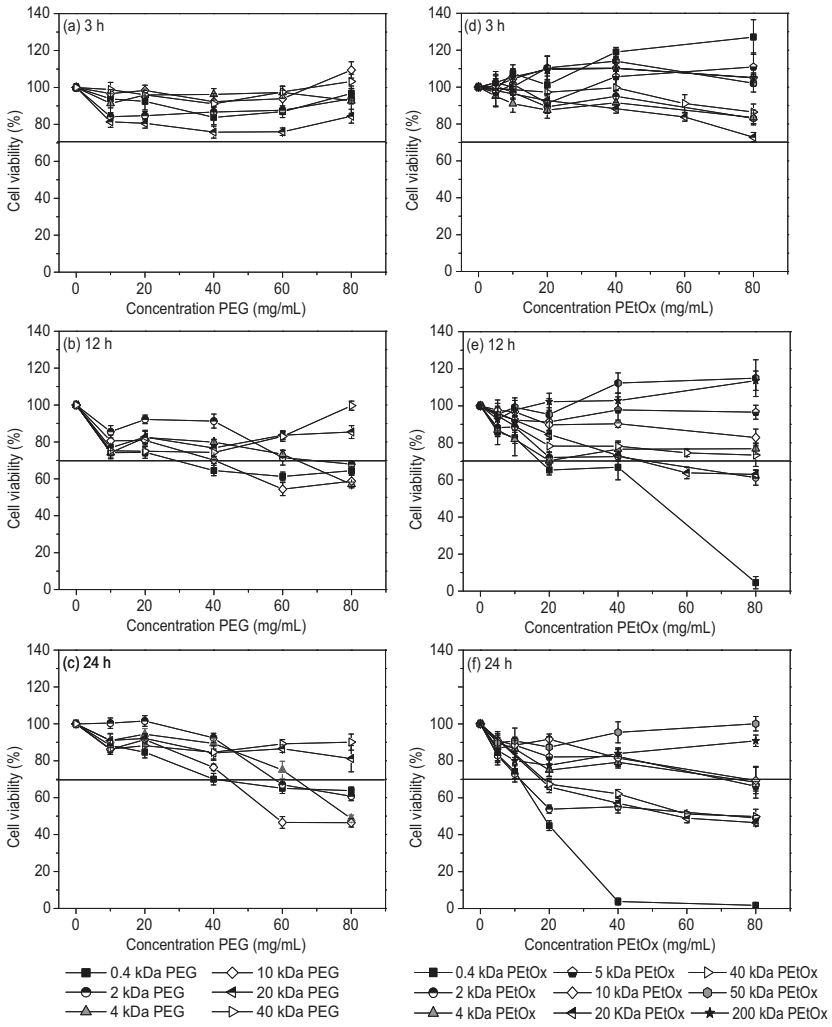

Figure 2. Cell viability of L929 mouse fibroblasts after treatment with PEG (a-c) and PEtOx (d–f) up to 80 mg · mL^{-1} after 3, 12, and 24 h incubation. Values below the marked line at 70% viability were regarded as cytotoxic according to ISO 10993-5. The cell viability was determined by means of an MTT assay. Data are presented as mean ± SD of seven determinations.

shaped cells growing to confluent monolayers (Figure 3a). For the classification of the toxic effects were treated with thiomersal as positive control. A reduction of the total cell number (Figure 3b) could be observed. Microscopic observations correlated well with the results of the quantitative MTT assay. An intact monolayer or only slight changes in morphology were detectable for non-toxic polymers. Examples of 40 kDa PEtOx and 40 kDa PEG were shown in Figure 3c and d. Cell detachment from the dish bottom, reduced growth and an increased number of spherically shaped cells as shown for 10 kDa PEG and 20 kDa PEtOx in Figure 3e and f as well as for 0.4 kDa PEtOx (Figure 3g and h) were detected in the case of the toxic effect levels determined in the MTT assay.

3.4. PEG and PEtOx Show No Membrane-Damaging Effect

Membrane damaging effects of PEG and PEtOx were quantified by the LDH assay as an indicator for early toxicity. Polymers were tested at the three-highest concentrations (40, 60, and 80 mg · mL^{-1}) of the MTT assay for a maximum incubation time of 4 h (Figure 4). Pure polymer solutions up to 80 mg · mL^{-1}, which were analyzed in the same manner as preparations with cells, confirmed that the LDH assay was not affected by the presence of the test polymers. Absorbances were comparable to the blank values determined with cell culture medium without FCS (data not shown). At the beginning of the experiment (0 h), samples were drawn for confirmation of the intactness of the L929 mouse fibroblasts. LDH release of these samples was in the range from 0 to 8.5%, that is, lower than 10%, which is regarded as cytotoxic effect level indicating that the cells were intact at the beginning of the experiment. After 1–4 h incubation (Figure 4), the mean LDH release for all PEGs and PEtOx was not higher than 10% indicating that PEG and PEtOx did not damage the cellular membranes and both were found to be comparable. For comparison, spontaneous LDH release of untreated cells was in the range of 0.1–4.5%.

3.5. Blood Compatibility of PEG and PEtOx

The interactions of the PEG and PEtOx polymers with erythrocytes as major blood components and one of the first contact partners after systemic administration were investigated with regard to red blood cell hemolysis and aggregation. The release of hemoglobin was used to quantify the erythrocyte membrane damaging effect of the polymers. The treatment of red blood cells with PBS buffer and 1% Triton X-100 solution provided 0 and 100% hemolysis, respectively. Erythrocytes were incubated with 40, 60, and 80 mg · mL^{-1} polymer solution for 1 h. Independent of the polymer type, pharmaceutical quality, incubation time, and polymer concentration, none of the PEG and PEtOx polymers showed values of hemolysis higher than 0.6% indicating no detectable disturbance of the red blood cell membranes (data not shown). According to the ASTM standard F756-00,

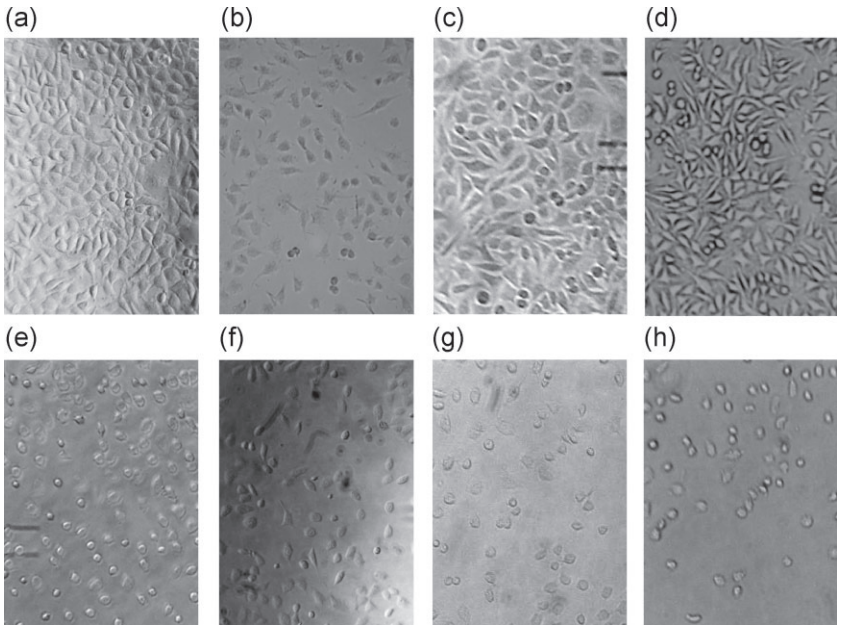

Figure 3. Microscopic analysis of L929 mouse fibroblasts after treatment with PEG and PEtOx compared to untreated (negative control) (a) and 0.02% thiomersal treated (positive control) (b) cells (100 ×). Cells treated with test polymers in non-toxic effect levels were comparable with the negative control as shown for 40 kDa PEG (c) and 40 kDa PEtOx (d) at 40 mg · mL^{-1} after 12 h incubation. Changes in cell detachment and morphology were observed for toxic polymer concentrations. The observable effects were similar for all tested polymers as exemplarily shown for 10 kDa PEG (e), 20 kDa PEtOx (f) at 80 mg · mL^{-1} as well as 0.4 kDa PEtOx at 40 and 80 mg · mL^{-1} (g and h) after 24 h incubation.

a hemoglobin release between 0 and 2% was regarded as non-hemolytic. For comparison negative controls had a mean hemolysis of 1.02%.

Additionally, the potential of PEG and PEtOx to aggregate red blood cells as an undesired phenomenon leading to circulatory side effects and even lethal toxicity was microscopically visualized after 2 h incubation (Figure 5). For classification of the intensity of the effects a three-stage classification system was applied (Table 2) as described in the Section 2. PBS buffer was used as negative control and did not show any sign of cluster formation (stage 1, Figure 5a). Treatment with 25 kDa bPEI at 30 μg · mL^{-1} as positive control caused the formation of aggregates (stage 3, Figure 5b). None of the PEGs showed any red blood cell aggregation even at the highest concentration of 80 mg · mL^{-1}. As representative examples, the results for PEGs with the lowest (0.4 kDa) and highest (40 kDa) molar mass are shown in Figure 5c and d, respectively. Therefore, PEG polymers were tested only at the highest concentrations of 60 and 80 mg · mL^{-1}, whereas PEtOx polymers were investigated from 20 to 80 mg · mL^{-1} (Table 2b). No aggregates (stage 1) were visible with all PEtOx polymers at 20 mg · mL^{-1}. PEtOx up to 40 kDa showed results comparable to PEG (Figure 5e), with one exception; the treatment of erythrocytes with 40 kDa PEtOx at 80 mg · mL^{-1} caused slight aggregation at stage 2 (Figure 5g). PEtOx 50 kDa was tolerated up to 60 mg · mL^{-1} (Figure 5f) but represented a stage 2 at 80 mg · mL^{-1} (Figure 5h). In case of 200 kDa PEtOx which showed the highest aggregating effect, a concentration dependent potential to aggregate erythrocytes could be detected (Figure 5i–l), starting at 40 mg · mL^{-1} (stage 2, Figure 5j) and reached the maximum at 60 and 80 mg · mL^{-1} (stage 3, Figure 5k and l) with formation of large clusters.

To receive additionally quantitative information, we established an assay to quantify erythrocyte aggregation by absorbance measurements with a standard plate reader and report for the first time its use for the biological characterization of polymers. Light emitted through sample suspensions is scattered by erythrocytes and reduces the amount of light reaching the detector. The higher the amount of free erythrocytes, the higher is the determined absorbance of the suspension. When erythrocytes aggregate to clusters and sediment, the total absorption area of free erythrocytes is reduced, resulting in a lower light scattering and, consequently, a lower detectable absorption. To avoid interferences with the absorbance of hemoglobin, measurements were performed at a wavelength of 645 nm. Negative controls treated with PBS were used to determine the absorbance of non-aggregating erythrocytes. Preliminary experiments confirmed that sample suspensions with an absorbance below the negative control could be regarded as aggregating (data not shown). Data are shown for a serial dilution of the positive control 25 kDa bPEI with a maximum concentration of 40 μg · mL^{-1} as well as for PEtOx polymers with the highest (200 kDa) and the lowest (0.4 kDa) molar mass tested in serial dilutions up 80 mg · mL^{-1} (Figure 6). Erythrocyte suspensions treated with 25 kDa bPEI showed a concentration dependent decrease of absorbance (Figure 6a) starting at 5 μg · mL^{-1} and correlated with an increasingly strong cluster formation by microscopy. The erythrocyte aggregation of bPEI concentrations <5 μg · mL^{-1} were rated as stage 1 while concentrations ≥ 5 μg · mL^{-1} were rated as stage 3. The absorbance of 0.4 kDa PEtOx up to 80 mg · mL^{-1} was comparable to the values of the negative control (Figure 6b) indicating that no aggregation occurred. This correlates well with the results of microscopic observations (Table 2b). For 200 kDa PEtOx, a concentration dependent

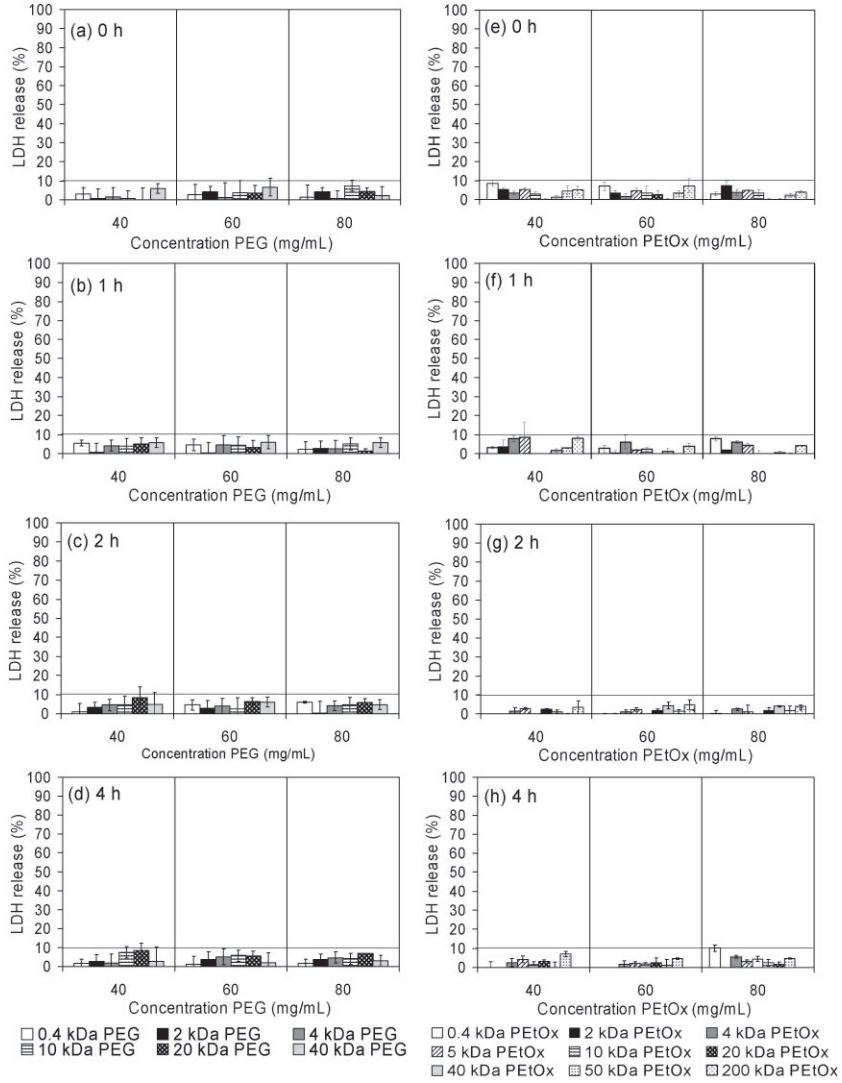

Figure 4. Time- and concentration-dependent membrane damaging effect of PEG (a–d) and PEtOx (e–h) on L929 mouse fibroblasts after 0, 1, 2, and 4 h. The membrane damaging potential was determined by quantification of cytosolic LDH released into the cell culture medium after treatment with 40, 60, and 80 mg · mL^{-1} polymer solution. A LDH release higher than 10% (plotted line) was regarded as cytotoxic effect level.

decrease in the absorbance was detected (Figure 6c), which follows a linear regression ($R^2 = 0.9899$). Only the absorbances at concentrations of 10 and 20 mg · mL^{-1} were comparable to the negative control. Higher concentrations revealed an absorbance below the negative control, corresponding to an increased erythrocyte aggregation. Although the positive control PEI and 200 kDa PEtOx (80 mg · mL^{-1}) were both ranked as stage 3 by microscopy, PEI was characterized by a higher decrease of absorption values with higher concentrations in the quantitative assay, which correlates with the formation of larger erythrocyte clusters compared to PEtOx.

4. Discussion

Several disadvantages of PEG, such as the demanding polymerization process with undesired impurities in the product, formation of peroxides, limited stability, high viscosity, and accumulation in some organs with formation of vacuoles because of the desiccant nature of PEG,[2] have triggered the investigation of PEtOx as alternative to PEG. In the present study, various PEtOx were systematically analyzed as potential alternative for PEG in direct comparison with regard to cyto- and hemocompatibility.

Polymers with molar masses from 0.4 to 40 kDa were selected, representing biomedically and pharmaceutically relevant sizes for PEG applications. PEG with molar masses below 0.4 kDa were reported to be not suitable for medical applications due to degradation to toxic diacid and hydroxyacid metabolites by alcohol and aldehyde dehydrogenase in humans.[25] Whereas PEGs below 10 kDa are mainly used to shield particulate drug carriers or antibodies against opsonization, high molar mass PEGs (>10 kDa) were typically bound to smaller drug molecules to decrease their renal excretion.[26] In our study, several PEtOx were synthesized by a fast and highly controlled polymerization procedure forming chemically well-defined polymers with low PDI values and a high purity similar to commercially available PEtOx. With the exception of 5 kDa PEtOx, only molecules with molar masses (50 and 200 kDa) higher than that used for PEG are commercially available. Special attention was directed toward the extensive purification of the polymers in order to exclude any side effects of byproducts. Differences in cyto- and hemotoxicity between the commercial and the non-commercial PEtOx were not obvious although the commercial polymers showed a significantly broader molar mass distribution as it is obvious from the bimodal SEC traces. The upper concentrations for the PEtOx testing varied between different publications from 5 to 20 mg · mL^{-1}.[12,13] In the present study, 80 mg · mL^{-1} was selected as the highest possible concentration limited by the high viscosity of PEG solutions, whereas PEtOx was still low viscous under these conditions. The lower viscosity of 20–40 kDa PEtOx compared to PEG was also demonstrated

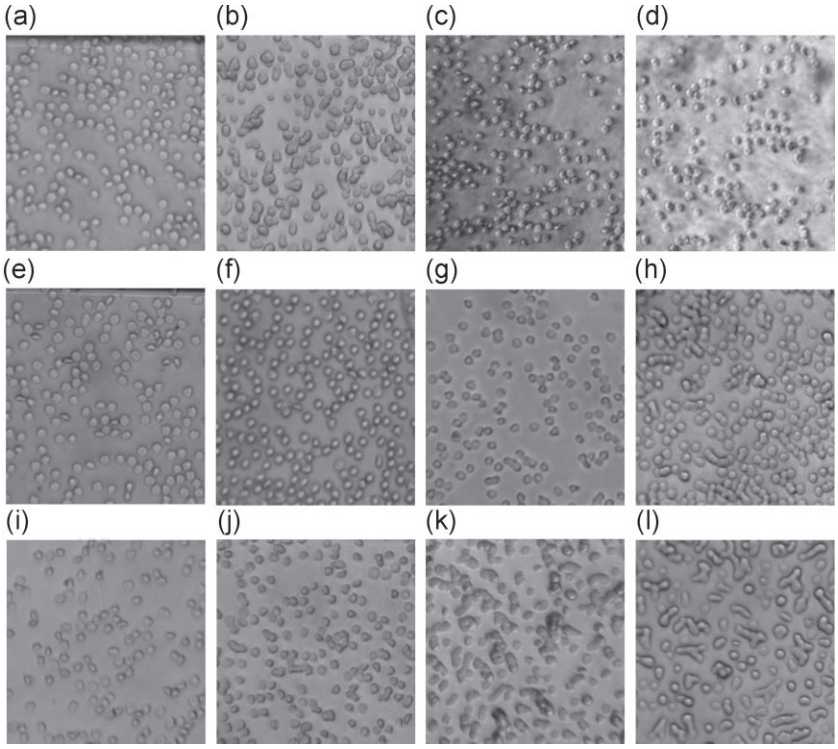

Figure 5. Representative micrographs of red blood cell aggregation of PEG and PEtOx at 37°C after 2 h incubation (200 ×), (a) negative control (PBS); (b) positive control (30 μg · mL^{-1} 25 kDa bPEI); (c) 0.4 kDa PEG (80 mg · mL^{-1}); (d) 40 kDa PEG (80 mg · mL^{-1});); (e) 40 kDa PEtOx (60 mg · mL^{-1}; (f) 50 kDa PEtOx (60 mg · mL^{-1}); (g) 40 kDa PEtOx (80 mg · mL^{-1}); (h) 50 kDa PEtOx (80 mg · mL^{-1}); (i–l) 200 kDa PEtOx (20, 40, 60, and 80 mg · mL^{-1}).

by Viegas et al.,[10] thus allowing easier pharmaceutical formulation, filterability, and syringeability of PEtOx even at higher concentrations. The selected concentrations up to 80 mg · mL^{-1} are higher than therapeutically used doses and represent a worst case scenario, which could be reached, for example, by overdosing or repeated administration and accumulation of the polymers in the body. Up to now, the concentration of PEG in commercially used drug conjugates for systemic administration is lower than 1 mg · mL^{-1} per dose. To avoid unspecific cytotoxic effects, all polymer solutions were adjusted to physiological pH and tolerable osmolarity. Although an osmolarity above 300 mosmol · kg^{-1} is considered as cytotoxic, our preliminary experiments showed that osmolarities up to 400 mosmol · kg^{-1} were well tolerated by L929 cells, comparable with literature data on the investigation of bovine aortic endothelium cells.[27]

After short incubation times, results of different assays such as MTT and LDH assay correlated well. More specifically, after 3 h (MTT) and 4 h (LDH) no changes in metabolic activity and LDH release could be detected for both types of polymers, independent of molar mass or polymer concentration. The comparison of the results of the hemolysis assay and the LDH assay, which both analyze membrane damaging effects, showed comparable results despite the differences between fibroblasts and erythrocytes regarding membrane composition and glycocalyx.[28,29]

PEG as well as PEtOx were found to be highly biocompatible polymers in MTT and LDH assays. For both types of polymers, cytotoxicity was found to be dependent on time, concentration, molar mass, and purity of the polymers. While PEG was found to be non-toxic up to 40 mg · mL^{-1} even after 24 h, PEtOx showed some inhibition of cell proliferation at 20–40 mg · mL^{-1}. These moderate cytotoxic effects occurred only after long-term treatments of 12 and 24 h. Prolonging the incubation time from 12 to 24 h slightly increased the effects. Furthermore, the cytotoxicity was strongly dependent on the molar masses. Low molar mass polymers of both polymer groups up to 10 kDa as well as 20 and 40 kDa PEtOx, affected the cell viability more profoundly than polymers with higher molar mass. The 10 kDa PEG demonstrated the highest cytotoxicity of all tested PEGs, which might be related to a higher amount of impurities due to the non-pharmaceutical quality. At this point, it should be noted that long-term toxicity of concentrations >40 mg · mL^{-1} of 0.4 kDa PEG and 0.4 kDa PEtOx as well as of 80 mg · mL^{-1} of 2 kDa PEG could also be caused by osmolarity values higher than the well tolerated 400 mosmol · kg^{-1}. As single reason, however, this explanation is insufficient since 0.4 kDa PEtOx caused a higher reduction of the cell viability than 0.4 kDa PEG despite comparable osmolarities. For PEtOx, comparable toxicity data were reported by Kronek et al.[12] testing polymers with 2–67.3 kDa up to 5 mg · mL^{-1} in rat RAT-2 cells over 48 h. Macrophages challenged by 67.3 kDa PEtOx did not exert decreased functionality.[12] In agreement with our data, Kronek et al.[12] reported a slightly higher toxicity of PEtOx with molar masses lower than 1.6 · 10^4 g · mol^{-1} which was ascribed to the cytotoxic activity of EtOx monomer traces, thus emphasizing the necessity of purification. Here, during the extensive purification steps of the non-commercial PEtOx, the monomer was completely removed and it can thus be excluded as a reason for cytotoxic reactions. However, the experiments showed a reduction of cell viability although no membrane damage was observed.

Table 2. Classification (1: no erythrocyte aggregation, 2: slight aggregation with rouleau formation, 3: severe aggregation with three-dimensional cluster formation) of the erythrocyte aggregation of PEG and PEtOx after 2 h incubation. The experiments were run in duplicate and were repeated once. Each data point is presented as the mean of four experiments.

Sample	Erythrocyte aggregation			
	20 mg mL^{-1}	40 mg mL^{-1}	60 mg mL^{-1}	80 mg mL^{-1}
0.4 kDa PEG			1	1
2 kDa PEG			1	1
4 kDa PEG			1	1
10 kDa PEG			1	1
20 kDa PEG			1	1
40 kDa PEG			1	1
0.4 kDa PEtOx	1	1	1	1
2 kDa PEtOx	1	1	1	1
4 kDa PEtOx	1	1	1	1
5 kDa PEtOx	1	1	1	1
10 kDa PEtOx	1	1	1	1
20 kDa PEtOx	1	1	1	1
40 kDa PEtOx	1	1	1	2
50 kDa PEtOx	1	1	1	2
200 kDa PEtOx	1	2	3	3

Luxenhofer et al.[13] could show that POxs were generally taken up by endocytosis while uptake rate and efficiency increased with increasing hydrophobicity. To be taken up by 50% of the target cells the required concentration of a PEtOx homopolymer was 180-fold higher than the concentration of the most efficient block copolymer consistent of a PEtOx and poly(2-butyl-2-oxazoline) block.[13] The data confirmed our results since very high concentrations of hydrophilic PEtOx were required to enter the cells and in our case causing a reduction of the cell viability. Additionally, the polymer concentration was found to play a key role in toxicity since PEtOx accumulation within cells was found to be dependent on the polymer concentration.[12]

The low cytotoxicity of PEG as compared to other polymers such as poly(L-lysine), dextran, etc. was shown by several authors.[30,31] PEG is generally regarded as safe and non-toxic. But comparable with our results in the cell viability experiments different studies showed that the biocompatibility of PEG is strongly related to the molar mass. Independent of the chosen test animal or application route in vivo studies revealed that with a decreasing molar mass the lethal doses of PEG decrease.[32] Similar results were obtained in in vitro experiments for PEGs with varying molar masses investigated for the use as cell protector against mechanical damage. Under the chosen conditions 0.4 kDa PEG inhibited the cell growth >50%. In contrast for PEG > 1.4 kDa no negative effects or even an increased cell growth was observed.[33] Although, the concentrations used in these studies were lower than 1% ($m \cdot V^{-1}$), comparable data were obtained in our experiments even at higher concentrations.

Hemolytic activity could be observed neither for PEG nor for PEtOx at 0.4–200 kDa up to 80 mg $\cdot$ mL^{-1} demonstrating a comparable behavior. This correlates well with the erythrocyte compatibility up to 10 mg $\cdot$ mL^{-1} reported for PEtOx by Viegas et al.,[10] who suggested a protective effect of the non-ionic, hydrophilic polymers on cell membranes in the same way as plasma proteins act in providing hemocompatibility against stress and exogenous influences.[34] For low molar mass PEG (<1 kDa), a relationship between hemolysis, polymer concentration, and polymer molar mass was reported by several authors.[35,36] The lower the molar mass and the higher the polymer concentration, the higher was the damage of the erythrocytes which was suggested to be caused by an increase in osmolarity.[37] This effect was more pronounced for PEGs with a molar mass <400 Da than for PEGs with larger sizes.[36] Our results correlated well with these findings.

To date no studies on erythrocyte aggregation have been published for PEtOx. Up to 40 kDa and 80 mg $\cdot$ mL^{-1}, erythrocyte aggregation was comparable for PEG und PEtOx, with the exception of 40 kDa PEtOx starting to form moderate aggregates at the highest concentration. Higher molar mass PEtOx (50–200 kDa) demonstrated concentration- and molar mass-dependent effects on erythrocytes. For PEG, the data correlate well with observations by

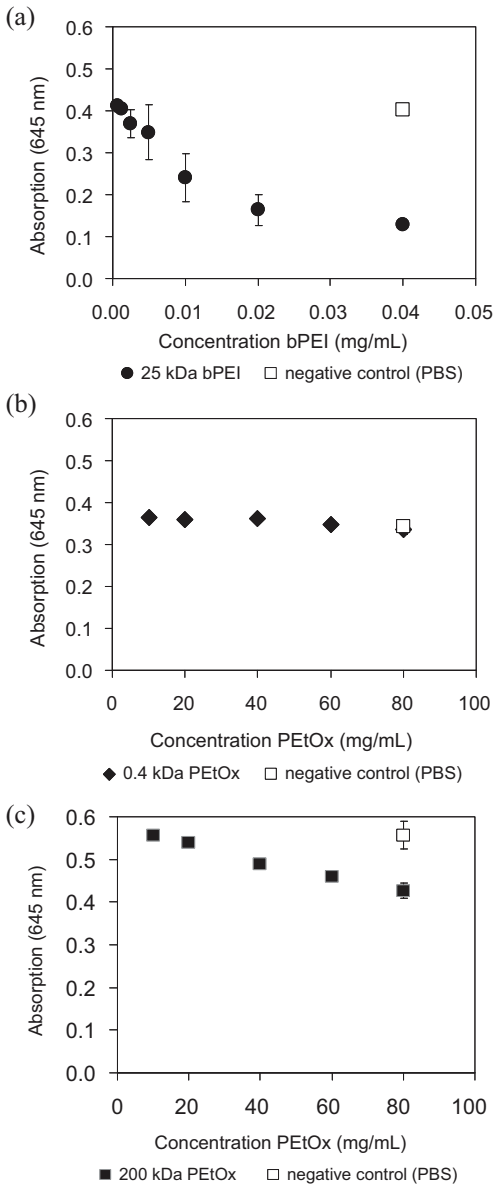

Figure 6. Determination of erythrocyte aggregation of 25 kDa bPEI (a), 0.4 kDa (b), and 200 kDa (c) PEtOx by UV/Vis spectroscopy. Erythrocytes were incubated under shaking for 2 h. Absorbance was measured at 645 nm. Data are presented as the mean ± SD ($n = 3$).

Geller et al.[38] and Levtov et al.,[39] reporting concentration- and molar mass-dependent effects on erythrocyte aggregation. Aggregating effects could be observed only for PEGs with very low (<1 kDa) or very high molar masses (>20 kDa). In Viaspan, which is a solution for preservation and storage of organ transplants, 20–35 kDa PEGs reduced the deformation and sedimentation of erythrocytes and inhibited the aggregation of red blood cells compared to hydroxyethyl starch.[40] Armstrong et al.[41] suggested that the influence of a non-ionic polymer on red blood cell aggregation is the consequence of its hydrodynamic radius and that the specific type of a given macromolecule is of only minor importance. When added to whole blood, 6 kDa PEG inhibited erythrocyte aggregation whereas 20 kDa PEG promoted aggregation.[38] These findings could not be confirmed in our experiments since no aggregation was detected with all PEGs independent of molar mass and concentration. Possible explanations were given by differences in the experimental settings, especially the use of full blood by Geller et al.[38] compared to PBS in our experiments.

5. Conclusion

In a directly comparative study, PEGs and PEtOxs with pharmaceutically relevant molar mass were tested regarding cytotoxicity and hemocompatibility under standardized conditions. PEG and PEtOx were well tolerated by mouse fibroblasts as well as by red blood cells. Both types of polymers showed comparable properties in the therapeutically relevant dose range demonstrating the potential of PEtOx as an adequate candidate to substitute PEG with regard to biological compatibility. Moderate cytotoxic effects occurred only in the MTT assay after long-term incubation (12 and 24 h) at higher concentrations and were dependent on polymer concentration, molar mass, and polymer purity. Compared to PEG, PEtOxs could be synthesized without toxic side products with comparable molar mass ranges, and PDI values as well as additional beneficial physicochemical properties like high stability and low viscosity. Referring to our results we can conclude that PEtOx could be a promising alternative for PEG.

Acknowledgements: The authors thank the Thuringian Ministry for Education, Science, and Culture (Grant #B514-09051, NanoConSens) for financial support. K. K. is grateful for financial support from the Landesgraduiertenförderung Thüringen.

Received: January 16, 2012; Published online: May 30, 2012; DOI: 10.1002/mabi.201200017

Keywords: biocompatibility; hydrophilic polymers; poly(2-oxazoline)s; poly(ethylene glycol)s; stealth effect

[1] S. Grund, M. Bauer, D. Fischer, *Adv. Eng. Mater.* **2011**, *13*, B61.
[2] K. Knop, R. Hoogenboom, D. Fischer, U. S. Schubert, *Angew. Chem., Int. Ed.* **2010**, *49*, 6288.
[3] I. Hamad, A. C. Hunter, J. Szebeni, S. M. Moghimi, *Mol. Immunol.* **2008**, *46*, 225.
[4] T. Tagami, K. Nakamura, T. Shimizu, N. Yamazaki, T. Ishida, H. Kiwada, *J. Controlled Release* **2010**, *142*, 160.

[5] H. Koide, T. Asai, K. Hatanaka, S. Akai, T. Ishii, E. Kenjo, T. Ishida, H. Kiwada, H. Tsukada, N. Oku, *Int. J. Pharm.* **2010**, *392*, 218.
[6] G. Pasut, F. M. Veronese, *Prog. Polym. Sci.* **2007**, *32*, 933.
[7] M. C. Woodle, C. M. Engbers, S. Zalipsky, *Bioconjugate Chem.* **1994**, *5*, 493.
[8] F. Wiesbrock, R. Hoogenboom, C. H. Abeln, U. S. Schubert, *Macromol. Rapid Commun.* **2004**, *25*, 1895.
[9] A. Mero, G. Pasut, L. D. Via, M. W. M. Fijten, U. S. Schubert, R. Hoogenboom, F. M. Veronese, *J. Controlled Release* **2008**, *125*, 87.
[10] T. X. Viegas, M. D. Bentley, J. M. Harris, Z. Fang, K. Yoon, B. Dizman, R. Weimer, A. Mero, G. Pasut, F. M. Veronese, *Bioconjug. Chem.* **2011**, *22*, 976.
[11] S. Cheon Lee, C. Kim, I. Chan Kwon, H. Chung, S. Young Jeong, *J. Controlled Release* **2003**, *89*, 437.
[12] J. Kronek, Z. Kroneková, J. Lustoň, E. Paulovičová, L. Paulovičová, B. Mendrek, *J. Mater. Sci.: Mater. Med.* **2011**, *22*, 1725.
[13] R. Luxenhofer, G. Sahay, A. Schulz, D. Alakhova, T. K. Bronich, R. Jordan, A. V. Kabanov, *J. Controlled Release* **2011**, *153*, 73.
[14] T. Mosmann, *J. Immunol. Methods* **1983**, *65*, 55.
[15] D. Fischer, Y. Li, B. Ahlemeyer, J. Krieglstein, T. Kissel, *Biomaterials* **2003**, *24*, 1121.
[16] "Biological evaluation of medical devices Part 5: Tests for in vitro cytotoxicity", 2nd edition, International Organization for Standardization/ANSI;ISO ISO 10993-5, Geneva, Switzerland: **2009**.
[17] S. Choksakulnimitr, S. Masuda, H. Tokuda, Y. Takakura, M. Hashida, *J. Controlled Release* **1995**, *34*, 233.
[18] M. J. Parnham, H. Wetzig, *Chem. Phys. Lipids* **1993**, *64*, 263.
[19] ASTM F756, 2000 (2008), "Standard Practice for Assessment of Hemolytic Properties of Materials", in *Annual Book of ASTM Standards*, Vol. 13. 01, ASTM, Philadelphia **2008**.
[20] M. Ogris, S. Brunner, S. Schuller, R. Kircheis, E. Wagner, *Gene Ther.* **1999**, *6*, 595.
[21] H. Petersen, P. M. Fechner, A. L. Martin, K. Kunath, S. Stolnik, C. J. Roberts, D. Fischer, M. C. Davies, T. Kissel, *Bioconjug. Chem.* **2002**, *13*, 845.
[22] A. V. Cardoso, M. H. Pereira, G. d. A. Marcondes, A. R. Ferreira, P. R. d. Araújo, *Mater. Res.* **2007**, *10*, 31.
[23] S. Kobayashi, E. Masuda, S. Shoda, Y. Shimano, *Macromolecules* **1989**, *22*, 2878.
[24] ASTM F0813, 1996 (2007), "Standard Practice for Direct Contact Cell Culture Evaluation of Materials for Medical Devices", in *Annual Book of ASTM Standards*, Vol. 13.01, ASTM, Philadelphia **2008**.
[25] D. A. Herold, K. Keil, D. E. Bruns, *Biochem. Pharmacol.* **1989**, *38*, 73.
[26] L. Scott, J. Yao, A. Benson, A. Thomas, S. Falk, R. Mena, J. Picus, J. Wright, M. Mulcahy, J. Ajani, T. Evans, *Cancer Chemother. Pharmacol.* **2009**, *63*, 363.
[27] E. H. Luh, S. R. Shackford, M. A. Shatos, J. A. Pietropaoli, *J. Surg. Res.* **1996**, *60*, 122.
[28] F. Schroeder, *J. Membr. Biol.* **1982**, *68*, 141.
[29] R. F. A. Zwall, B. Roelofsen, C. Michael Colley, *Biochim. Biophys. Acta, Rev. Biomembr.* **1973**, *300*, 159.
[30] D. Sgouras, R. Duncan, *J. Mater. Sci.: Mater. Med.* **1990**, *1*, 61.
[31] X. Y. Liu, J.-M. Nothias, A. Scavone, M. Garfinkel, J. M. Millis, *ASAIO J.* **2010**, *56*, 241.
[32] H. F. Smyth, C. P. Carpenter, C. S. Weil, *J. Am. Pharm. Assoc.* **1950**, *39*, 349.
[33] J. D. Michaels, E. T. Papoutsakis, *J. Biotechnol.* **1991**, *19*, 241.
[34] R. Barbucci, S. Lamponi, A. M. Aloisi, *J. Biomed. Mater. Res.* **1999**, *46*, 186.
[35] J. F. Krzyzaniak, D. M. Raymond, S. H. Yalkowsky, *Int. J. Pharm.* **1997**, *152*, 193.
[36] B. L. Smith, D. E. Cadwallader, *J. Pharm. Sci.* **1967**, *56*, 351.
[37] J. Farrant, A. E. Woolgar, *Cryobiology* **1970**, *7*, 56.
[38] N. M. Geller, V. A. Kropachev, V. A. Levtov, I. V. Potapova, *Polym. Med.* **1981**, *11*, 83.
[39] V. A. Levtov, V. N. Shuvaeva, N. Shustova, A. T. Matchanov, T. V. Kim, *Fiziol Zh SSSR Im I M Sechenova* **1991**, *77*, 72.
[40] I. B. Mosbah, R. Franco-Gou, H. B. Abdennebi, R. Hernandez, G. Escolar, D. Saidane, J. Rosello-Catafau, C. Peralta, *Transplant. Proc.* **2006**, *38*, 1229.
[41] J. K. Armstrong, R. B. Wenby, H. J. Meiselman, T. C. Fisher, *Biophys. J.* **2004**, *87*, 4259.

Publication 4

"*In vitro* hemocompatibility and cytotoxicity study of poly(2-methyl-2-oxazoline) for biomedical applications"

M. Bauer, S. Schröder, L. Tauhardt, K. Kempe, U. S. Schubert, D. Fischer

J. Polym. Sci., Part A: Polym. Chem. **2013**, *51*, 1816–1821

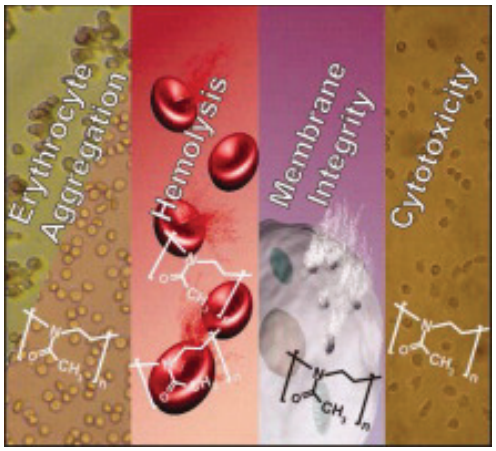

In Vitro Hemocompatibility and Cytotoxicity Study of Poly(2-methyl-2-oxazoline) for Biomedical Applications

Marius Bauer,[1] Susann Schroeder,[1] Lutz Tauhardt,[2,3] Kristian Kempe,[2,3] Ulrich S. Schubert,[2,3] Dagmar Fischer[1,3]

[1]Department of Pharmaceutical Technology, Institute of Pharmacy, Friedrich-Schiller University Jena, Otto-Schott-Str. 41, 07745 Jena, Germany
[2]Laboratory of Organic and Macromolecular Chemistry (IOMC), Friedrich-Schiller-University Jena, Humboldtstr. 10, 07743 Jena, Germany
[3]Jena Center for Soft Matter (JCSM), Friedrich-Schiller-University Jena, Philosophenweg 7, 07743 Jena, Germany
Correspondence to: D. Fischer (E-mail: dagmar.fischer@uni-jena.de)

Received 28 December 2012; accepted 11 January 2013; published online 7 February 2013
DOI: 10.1002/pola.26564

ABSTRACT: Since poly(2-methyl-2-oxazolines) (PMeOx) attract high attention for the potential use in drug delivery, cytotoxicity, and hemocompatibility of a set of PMeOxs with molar masses in the range from 2 to 20 kDa are systematically investigated under standardized conditions in terms of molar mass, concentration and time dependency. PMeOx polymers are well tolerated in red blood cell aggregation and hemolysis assays without any damaging effects even at high concentrations up to 80 mg/mL. Only in long term cytotoxicity tests PMeOx polymers moderately influence cell viability in a time, concentration, and molar mass dependent manner. Referring to these results it can be concluded that PEtOx could be promising nonionic hydrophilic polymers for many biomedical applications without any cyto- and hemotoxic effects at typically used therapeutic doses. © 2013 Wiley Periodicals, Inc. J. Polym. Sci., Part A: Polym. Chem. **2013**, *51*, 1816–1821

KEYWORDS: biocompatibility; hemocompatibility; hydrophilic polymer; poly(2-methyl-2-oxazoline); ring-opening polymerization

INTRODUCTION The use of the hydrophilic, nonionic poly(2-methyl-2-oxazoline) (PMeOx) in biomedical and pharmaceutical applications has enormously evolved during the last years.[1,2] On the one hand, PMeOx can be considered chemically as a poly(ethylene imine) (bPEI) backbone with amide-bonded side groups. On the other hand, these polymers were also described as pseudopeptides or bioinspired polymers due to their structural relation to polypeptides. In contrast to peptides, the tertiary amine groups of PMeOx cannot be recognized by enzymes for hydrolytic cleavage which provides high stability in the biological environment.[3]

Since the early 90s several studies are available reporting the use and importance of PMeOx as a component of drug delivery systems such as peptide, protein, and lipid conjugates as well as for liposomes and micelles (for reviews, see e.g., refs. 1 and 2). Miyamoto et al.[4] demonstrated that the covalent binding of PMeOx to liver catalase influenced the enzyme activity dependent on polymer molar mass and degree of conjugation. Furthermore, it was possible to preserve the enzymatic activity in organic solvents due to an increase of solubility provided by the conjugated PMeOx.[4] Amphiphilic block copolymers of PMeOx and poly(2-butyl-2-oxazoline)s were tested as micellar carrier systems for the delivery of hydrophobic drugs such as paclitaxel. The results revealed a low intrinsic toxicity of the micelles and a high micellar drug uptake without loss of drug activity.[5] Similar results were received for micelles formed of block copolymers with hydrophobic poly(L-lactide) or poly(ε-caprolactone) and PMeOx.[6,7]

Many of the observed effects were found to be comparable to the beneficial properties of poly(ethylene glycol) (PEG) with regard to stealth behavior, biodistribution, and biocompatibility. PMeOx can induce a stealth effect in a similar way as PEG when grafted on liposomes or surfaces.[8,9] Clearance from the blood was similar for PEG and PMeOx, whereas for instance the more lipophilic poly(2-ethyl-2-oxazoline) (PEtOx) was removed somewhat faster.[10] Liposomes decorated with PMeOx were characterized by a prolonged blood circulation time and a preferential organ distribution in liver, spleen, and kidney after 24 h.[8,10] Protein-repellent and non-fouling, antimicrobial effects after coating of PMeOx to surfaces, for example, of implants, biosensors or nanoparticles quantitatively reached the excellent properties of PEG.[9,11]

Additional Supporting Information may be found in the online version of this article.

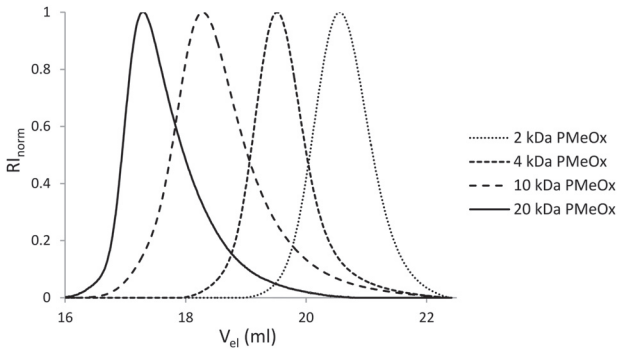

FIGURE 1 SEC diagram, showing the refraction index (RI) depending on eluted polymer volume (V_{el}) of the PMeOx synthesized by microwave-assisted living cationic ring-opening polymerization at 140 °C with methyl tosylate as initiator and acetonitrile as solvent.

A requirement for the administration of PMeOx in patients is the biocompatibility of PMeOx which was first demonstrated *in vivo* by Goddard et al.[12] after intravenous injection in mice. It was reported that PMeOx did not accumulate in organs and can be rapidly cleared from the blood stream.[13] Only some high molar mass PMeOx polymers were found in skin and muscle tissue.[12] However, *in vitro* hemocompatibility data are not available for PMeOx to the best of our knowledge and *in vitro* cytotoxicity data are limited. Kronek et al.[14] investigated only one PMeOx polymer with 8.5 kDa in a [3-(4,5-dimethylthiazol-2-yl)-2,5-diphenyl tetrazolium bromide] (MTT) assay and found no cytotoxic effects up to a concentration of 5 mg/mL after 24 and 48 h. Luxenhofer et al.[15] used only two PMeOx derivatives of about 4 kDa, however modified with piperazine and Boc-piperazine, to demonstrate the biocompatibility of PMeOx in a cytotoxicity (MTT) assay over up to 24 h. More information is only available for copolymers with PMeOx.[15]

Consequently, in the present study *in vitro* cytotoxicity and hemocompatibility of pure PMeOx polymers with a wide range of molar masses from 2 to 20 kDa were systematically investigated under standardized conditions to close the gaps. In particular, the influence of polymer molar mass, polymer concentration and incubation time was investigated.

RESULTS AND DISCUSSION

Four PMeOx polymers with pharmaceutical and biomedical relevant molar masses from 2 to 20 kDa were synthesized as described in the Supporting Information. All PMeOxs were obtained as white crystalline powders. Identity and purity of the polymers were proven by means of ^{1}H NMR spectroscopy and size exclusion chromatography analysis which confirmed that the PMeOx polymers were synthesized with defined molar masses and acceptable molar mass distribution [polydispersity index (PDI) values < 1.45] (Fig. 1 and Supporting Information Table S1).

Before administration of the PMeOxs to cells, potential non-specific effects of the polymer solutions falsifying the results of the toxicity tests were excluded. Polymer loss due to incomplete passage of PMeOx through the sterile filter could be excluded by comparing the mass of unfiltered and filtered stock solutions after freeze drying (data not shown). pH values and osmolarities of all stock solutions were routinely measured before application to the cells. The pH values of all polymer solutions were comparable to the corresponding pure medium. Osmolarities of the stock solutions ranged from 335 to 420 mosmol/kg (Supporting Information Table S2). Differences were attributed to varying polymer molar mass and type of medium. A MTT assay using culture medium of different osmolarities (280–650 mosmol/kg) demonstrated that osmolarities up to 490 mosmol/kg were well tolerated by L929 cells without morphological changes or decrease in cell viability up to 24 h (Supporting Information Fig. S1). Only the highest osmolarity of 650 mosmol/kg showed a reduction of the cell viability to 34% after 24 h which correlates well with reports for other cell types.[16]

Many of the polymers used in medical applications or as drug delivery system come into close contact with blood plasma and blood cells, in particular after systemic administration. Therefore, the influence of PMeOx polymers on the aggregation behavior and hemolysis of sheep erythrocytes was investigated. Erythrocyte aggregation of PMeOx was qualitatively visualized by microscopy and quantitatively measured by UV/Vis spectrophotometry. Quantitative measurements determined the changes in absorbance based on different light scattering of aggregated and non-aggregated erythrocytes as described by Cardoso et al.[17] who showed that with increasing degree of aggregation the sample absorbance decreased. Serial dilutions of the four PMeOx polymers (20–80 mg/mL) without addition of erythrocytes showed absorbances (maximum $A = 0.083$) comparable to phosphate buffered saline (PBS) blank values ($A = 0.039$). Consequently, a polymer related error of the measurement could be excluded. The selection of polymer concentrations was based on the reported concentrations of previous studies of other non-ionic hydrophilic polymers.[18] These concentrations represent the worst case scenario such as overdosing or polymer accumulation in the body. As negative control red blood cells were treated only with PBS showing no signs of aggregation. A 25 kDa branched bPEI solution (30 μg/mL) was used as positive control causing strong aggregation with formation of three-dimensional clusters due to its high cationic charge as described before.[19]

In quantitative measurements no signs of aggregation could be observed for any of the PMeOx polymers. Regardless of the used concentration or molar mass of all four polymers no erythrocyte aggregation dependent decline of absorption could be detected (Fig. 2). Values were found to be in the range of PBS as negative control with a mean value of 0.589 $\pm$ 0.081. All values of the polymer solutions were higher than that of 25 kDa bPEI as positive control (0.228 $\pm$ 0.123). The results were verified qualitatively by microscopic observation. Erythrocyte aggregation was classified with a three stage classification system as described in the Supporting Information. Stage 3 was determined with 25 kDa bPEI

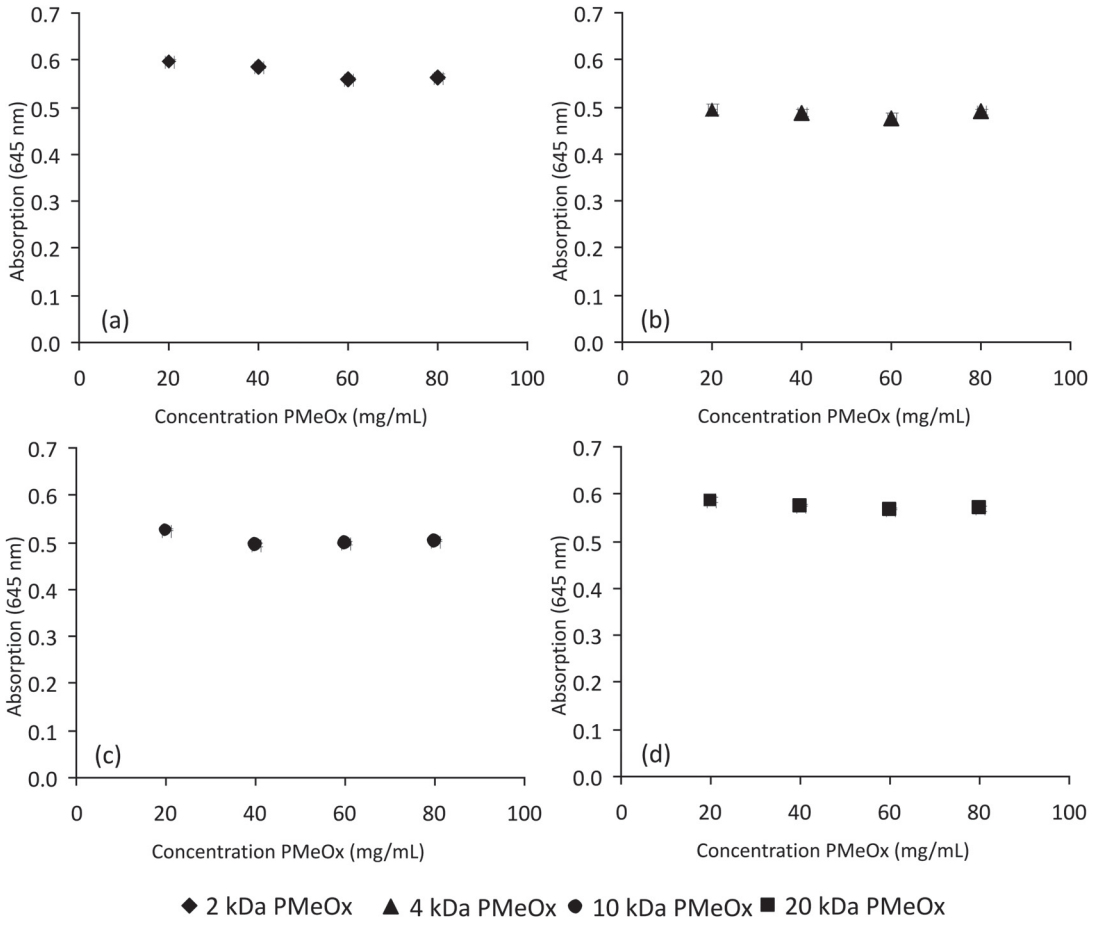

FIGURE 2 Concentration dependent spectrophotometric quantification of erythrocyte aggregation after PMeOx polymer treatment at 37 °C for 2 h. Absorbance was measured at 645 nm. Data are presented as mean ± SD ($n = 3$).

[Supporting Information Fig. S2(a)] whereas erythrocytes suspended in PBS were classified as stage 1 [Supporting Information Fig. S2(b)]. Independent of polymer molar mass and concentration all tested PMeOx solutions did not show any aggregation and were therefore classified as stage 1 [Supporting Information Fig. S2(c–f)]. These data confirmed the results of the spectrophotometric measurements.

Hemolysis caused by PMeOx polymers was quantified by the release of hemoglobin as an indicator for erythrocyte membrane damage. Erythrocytes were incubated with PMeOx solutions at 20–80 mg/mL for 1 h as well as with PBS buffer as negative control and 1% Triton X-100 as positive control (100%). Release of hemoglobin between 0 and 2% was regarded as non-hemolytic as defined in the ASTM (American Society for Testing and Materials) standard F756-08.[20] All PMeOxs did not show values higher than 1.06% regardless of their molar mass and concentration indicating that they did not disturb the erythrocyte membranes (data not shown). For comparison, the mean hemolysis of the negative control was 0.31%.

Taken the hemocompatibility data together, the 2–20 kDa PMeOx polymers demonstrated an excellent blood compatibility comparable to other non-ionic hydrophilic polymers such as PEG,[18] PEtOx,[18,21] and polyglycerol.[22]

For further investigations of the influence of PMeOx polymers on the membrane integrity as an early indicator for toxicity, short term incubations were performed with fibroblast cell cultures using a lactate dehydrogenase (LDH) assay. The release of LDH into culture medium was detected after 0–4 h polymer treatment using concentrations of 40, 60, and 80 mg/mL (Fig. 3). According to official guidelines L929 mouse fibroblasts were used as cell line for the cytotoxicity experiments.[23,24] As described by Choksakulnimitr et al.[25] a LDH release > 10% was regarded as cytotoxic. Assays performed with polymer solutions up to 80 mg/mL without the addition of cells showed that the test polymers itself had no influence on the chemical reactions of the assay and the spectrophotometric measurement (data not shown). The membrane integrity of L929 mouse fibroblasts at the beginning of the experiment was determined by drawing samples directly after the addition of the test polymers. Up to 4 h treatment with PMeOx polymers up to 20 kDa LDH values ranged from 0.1 to 8.1% (Fig. 3), confirming the intactness of the cells even at the highest concentration of

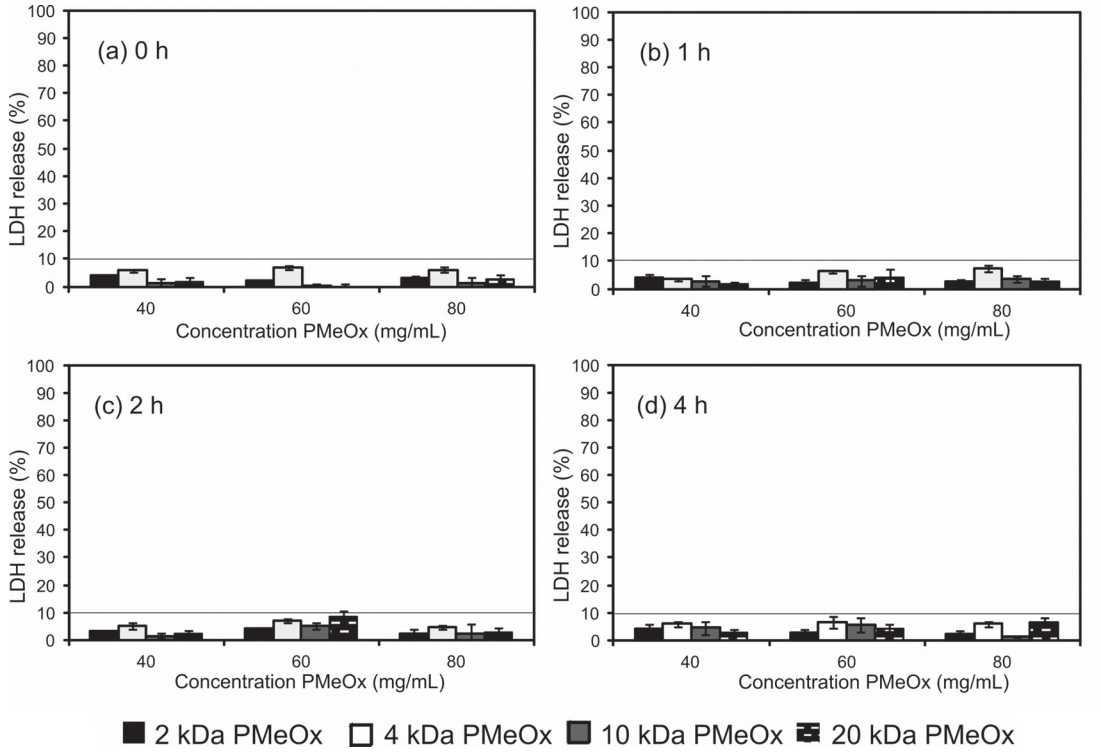

FIGURE 3 Concentration dependent LDH release of PMeOx polymers after treatment for 0 h (a), 1 h (b), 2 h (c), 4 h (d). LDH levels lower than 10% (plotted line) were regarded as non-toxic. Results are presented as mean ± SD of three determinations.

80 mg/mL. Spontaneous LDH release of the negative control ranged in comparison from 1.5 to 1.9%. Results of the experiments correlated well with data of the hemolysis tests and demonstrated that under the chosen conditions the presence of PMeOx polymers had no influence on the membrane integrity of sheep erythrocytes and L929 mouse fibroblasts independent of the polymer molar mass.

Long-term treatments were investigated via MTT tests with incubation times of 3, 12, and 24 h, respectively (Fig. 4). A preliminary experiment performed with the PMeOx solutions without cells confirmed that the presence of test polymers up to 80 mg/mL did not affect the chemical reaction of the assay and the spectrophotometric measurement (data not shown). Cell viability of 100% was obtained from cells treated only with culture medium (negative control). As positive control a 0.02% thiomersal solution which reduced the average cell viability to 0.23%, was used. According to the specifications of ISO 10993-5, cell viability <70% was regarded as cytotoxic.

As shown in Figure 4(a,b), after 3 and 12 h incubation 4, 10, and 20 kDa PMeOx had no influence on the cell viability of L929 cells. Only 2 kDa PMeOx at the highest concentration of 80 mg/mL reduced the cell viability to about 60 and 44%, after 3 and 12 h, respectively. After 24 h a concentration, time, and molar mass dependent increase in cytotoxicity could be detected. At the highest concentration only 20 kDa PMeOx showed a cell viability higher than 70%. From the results of the MTT assay it could by concluded that the molar mass of the polymers seems to play an important role for the biocompatibility of PMeOx. Microscopic observations made before and after the polymer treatment confirmed the results of the MTT assay. L929 fibroblasts treated with culture medium or non-toxic polymer solutions were adhesive, grew as confluent monolayers and were typically spindle-shaped. Cells treated with thiomersal solution and toxic polymer solutions showed a reduction of the total cell number as well as changes in morphology such as rounding and detachment from the dish bottom.

The high biocompatibility at concentrations < 40 mg/mL is comparable with data from the literature. PMeOx with molar masses of 4 and 8.5 kDa tested at maximum concentrations of 20 and 5 mg/mL, respectively, showed no reduction of cell viability.[14,15]

CONCLUSION

Concluding the *in vitro* toxicity studies, no toxic effects of the PMeOx polymers of molar masses up to 20 kDa could be detected in red blood cells and short term L929 cell (LDH) assays. Only in long term treatments (MTT assay) at concentrations higher than typically used in biomedical applications, polymers were found to moderately influence the viability of cells in a time, concentration, and molar mass dependent manner. Unspecific effects such as changes of pH

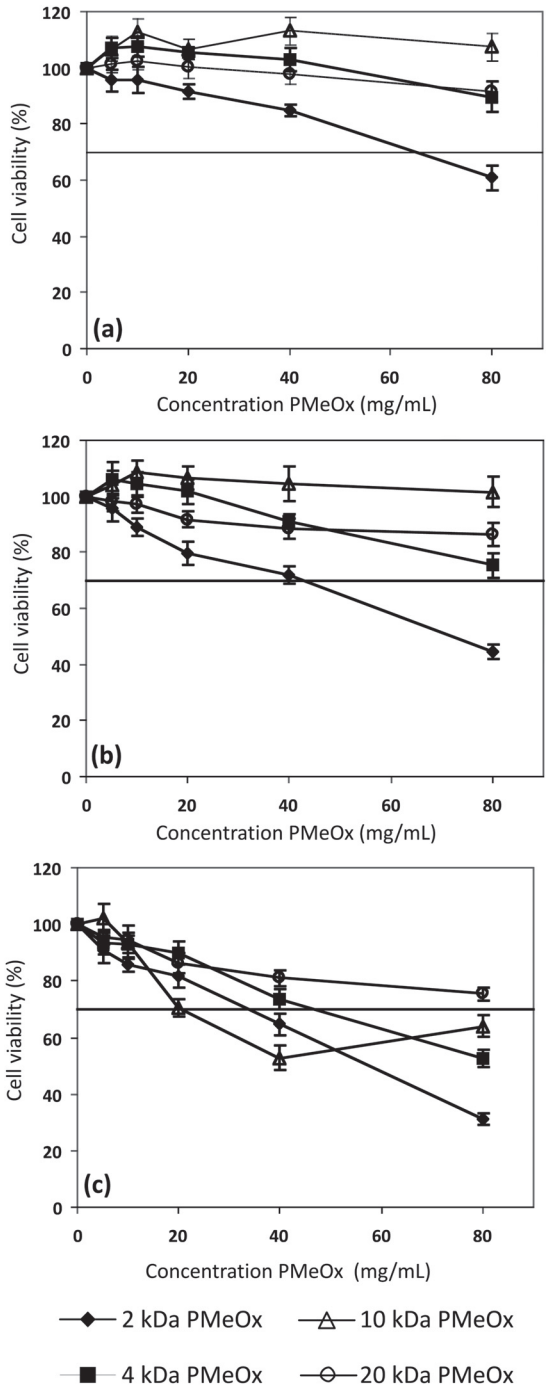

FIGURE 4 Time-, concentration, and molar mass dependent cytoxicity of PMeOx polymers after 3 h (a), 12 h (b), and 24 h (c) incubation of L929 cells. Cell viability was determined by MTT assay and specified according to ISO 10993-5. Results are presented as mean ± SD of seven determinations.

value or osmolarity of the medium by the polymer solutions could be excluded. Therefore, PMeOx represents a promising polymer for many biomedical applications, since it possesses not only an easy synthetic access and beneficial physicochemical characteristics like low viscosity and high stability, but additionally excellent *in vitro* toxicological features.

EXPERIMENTAL

Experimental details including polymerization procedure, physicochemical properties, and biological investigations are provided in the Supporting Information.

ACKNOWLEDGMENTS

The authors gratefully acknowledge the Thuringian Ministry for Education, Science, and Culture (Grant #B514-09051, Nano ConSens) for financial support. K. K. is grateful to the Landesgraduiertenfoerderung Thueringen for financial support.

REFERENCES AND NOTES

1 N. Adams, U. S. Schubert, *Adv. Drug Deliv. Rev.* **2007,** *59*, 1504–1520.

2 R. Hoogenboom, *Angew. Chem. Int. Ed. Engl.* **2009,** *48*, 7978–7994.

3 R. Hoogenboom, H. Schlaad, *Polymers* **2011,** *3*, 467–488.

4 M. Miyamoto, K. Naka, M. Shiozaki, Y. Chujo, T. Saegusa, *Macromolecules* **1990,** *23*, 3201–3205.

5 R. Luxenhofer, A. Schulz, C. Roques, S. Li, T. K. Bronich, E. V. Batrakova, R. Jordan, A. V. Kabanov, *Biomaterials* **2010,** *31*, 4972–4979.

6 G. H. Hsiue, C. H. Wang, C. L. Lo, C. H. Wang, J. P. Li, J. L. Yang, *Int. J. Pharm.* **2006,** *317*, 69–75.

7 S. Cheon Lee, C. Kim, I. Chan Kwon, H. Chung, S. Young Jeong, *J. Controlled Release* **2003,** *89*, 437–446.

8 M. C. Woodle, C. M. Engbers, S. Zalipsky, *Bioconjugate Chem.* **1994,** *5*, 493–496.

9 R. Konradi, B. Pidhatika, A. Muhlebach, M. Textor, *Langmuir* **2008,** *24*, 613–616.

10 S. Zalipsky, C. B. Hansen, J. M. Oaks, T. M. Allen, *J. Pharm. Sci.* **1996,** *85*, 133–137.

11 B. Pidhatika, J. Möller, E. M. Benetti, R. Konradi, E. Rakhmatullina, A. Mühlebach, R. Zimmermann, C. Werner, V. Vogel, M. Textor, *Biomaterials* **2010,** *31*, 9462–9472.

12 P. Goddard, L. E. Hutchinson, J. Brown, L. J. Brookman, *J. Controlled Release* **1989,** *10*, 5–16.

13 F. C. Gaertner, R. Luxenhofer, B. Blechert, R. Jordan, M. Essler, *J. Controlled Release* **2007,** *119*, 291–300.

14 J. Kronek, Z. Kroneková, J. Lustoň, E. Paulovičová, L. Paulovičová, B. Mendrek, *J. Mater. Sci. Mater. Med.* **2011,** *22*, 1725–1734.

15 R. Luxenhofer, G. Sahay, A. Schulz, D. Alakhova, T. K. Bronich, R. Jordan, A. V. Kabanov, *J. Controlled Release* **2011,** *153*, 73–82.

16 E. H. Luh, S. R. Shackford, M. A. Shatos, J. A. Pietropaoli, *J. Surg. Res.* **1996,** *60*, 122–128.

17 A. V. Cardoso, M. H. Pereira, G. D. A. Marcondes, A. R. Ferreira, P. R. D. Araújo, *Mater. Res.* **2007,** *10*, 31–36.

18 M. Bauer, C. Lautenschlaeger, K. Kempe, L. Tauhardt, U. S. Schubert, D. Fischer, *Macromol. Biosci.* **2012,** *12*, 986–998.

19 P. Petersen, P. M. Fechner, A. L. Martin, K. Kunath, S. Stolnik, C. J. Roberts, D. Fischer, M. C. Davies, T. Kissel, *Bioconjugate Chem.* **2002,** *13*, 845.

20 ASTM F756-08, 2000 (2008). In Annual Book of ASTM Standards. ASTM: Philadelphia; **2012;** Vol. 13.01.

21 T. X. Viegas, M. D. Bentley, J. M. Harris, Z. Fang, K. Yoon, B. Dizman, R. Weimer, A. Mero, G. Pasut, F. M. Veronese, *Bioconjugate Chem*. **2011,** *22*, 976–986.

22 D. Motlagh, J. Yang, K. Y. Lui, A. R. Webb, G. A. Ameer, *Biomaterials* **2006,** *27*, 4315–4324.

23 Biological evaluation of medical devices Part 5: Tests for in vitro cytotoxicity. Geneva (Switzerland): International Organization for Standardization/ANSI;ISO ISO 10993–5:2009 second edition, Geneva, **2009**.

24 ASTM F813-07, 1996 (2012). In Annual Book of ASTM Standards; ASTM: Philadelphia; **2008;** Vol. 13.01.

25 S. Choksakulnimitr, S. Masuda, H. Tokuda, Y. Takakura, M. Hashida, *J. Controlled Release* **1995,** *34*, 233–241.

Supporting Information

for, DOI: 10.1002/POLA.(xxx)

In Vitro Hemocompatibility and Cytotoxicity Study of Poly(2-methyl-2-oxazoline) for Biomedical Applications

Susann Schroeder, Marius Bauer, Lutz Tauhardt, Kristian Kempe, Ulrich S. Schubert, Dagmar Fischer**

Experimental Section

Synthesis and Physicochemical Characterization of Poly(2-methyl-2-oxazoline)

Prior to use, the microwave vials were heated at 110 °C overnight and allowed to cool down to room temperature under an argon atmosphere. All polymerizations were performed under controlled temperature in an initiator sixty single-mode microwave synthesizer from Biotage, equipped with a non-invasive IR sensor (accuracy: ±2%). Methyl tosylate and 2-methyl-2-oxazoline (MeOx, Acros Organics, Geel, Belgium) were distilled to dryness over barium oxide (BaO) and stored under argon. A stock solution of dry acetonitrile (Acros Organics, Geel Belgium), 2-methyl-2-oxazoline (MeOx) (monomer), and methyl tosylate (initiator) was prepared with a total monomer concentration of 4 M. As total monomer-to-initiator ratios 23, 47, 118, and 236 were chosen. The stock solutions were divided over 4 to 5 vials and heated in the microwave synthesizer at 140 °C for a predetermined time. After cooling to room temperature, samples for the determination of the molar mass (distribution) by size exclusion chromatography and the monomer conversion by ^{1}H NMR spectroscopy were prepared. Subsequently, the solvent was removed. The polymers were re-dissolved in dichloromethane and precipitated in ice-cold diethyl ether. After drying under reduced pressure at 40 °C, the polymers were dissolved in water and stirred with basic loaded amberlite for 24 h. The resin

was filtered off, the polymer was washed with water, and the solvent was evaporated under reduced pressure. The polymer samples were dried for several days at 40 °C *in vacuo,* followed by lyophilization.

Molar masses and polydispersity indices were determined by size-exclusion chromatography (SEC) on an Agilent Technologies 1200 Series size-exclusion chromatography system equipped with a G131A isocratic pump, G1329A autosampler, G1362A refractive index detector as well as a PSS Gram 30 and a PSS Gram 1000 columns both placed in series. As eluent a 2.1% lithiumchloride solution in *N,N*-dimethylacetamide, running at 1 mL/min flow rate and a column oven temperature of 40 °C, was used. Molar masses were calculated against polystyrene standards. ^{1}H NMR spectra were recorded on a Bruker AC 300 MHz spectrometer at room temperature with deuterated chloroform as solvent. The chemical shifts were given in ppm relative to the signal from residual non-deuterated solvent.

Aggregation Behavior of Red Blood Cells

Erythrocyte aggregation of poly(2-methyl-2-oxazoline) (PMeOx) polymers was quantitatively determined by a modified spectrophotometric method according to Cardoso et al.[1] and qualitatively by light microscopy with a modified method of Ogris et al.[2] Sheep blood was collected in heparinized-tubes. Erythrocytes were separated by centrifugation at 2880 g for 5 min (Eppendorf Centrifuge 5804R, Eppendorf, Hamburg, Germany) and washed three times with ice cold phosphate buffered saline (PBS) (8 mM disodium hydrogen phosphate, 1.5 mM potassium dihydrogen phosphate, 137 mM sodium chloride and 2.7 mM potassium chloride) via centrifugation at 2,880 g for 5 min. Finally, erythrocytes were resuspended in PBS (9.4 million erythrocytes/mL). PMeOx solutions were prepared in PBS and sterilized by filtration (0.2 µm, VWR international, Darmstadt, Germany). To test the filterability of PMeOx gravimetric measurements of aqueous polymer stock solutions (80 mg/mL) before and after filtration were performed.

Osmolarity and pH of the PMeOx stock solutions were routinely measured with a Φ350 pH meter (Beckman Coulter, Krefeld, Germany) and a semi-micro osmometer (Knauer, Berlin, Germany). Negative controls were obtained by incubating the erythrocytes with buffer solution. Branched poly(ethylene imine) (30 µg/mL 25 kDa bPEI, kind gift of BASF corporation, Ludwigshafen, Germany) was used as positive control. For the experiments, polymer solutions or the controls each in a volume of 50 µL were placed in a clear flat bottomed 96-well culture plate (Greiner Bio-One, Frickenhausen, Germany). Afterwards, 50 µL erythrocyte suspension were added to each well and the plates were incubated under vigorous shaking at 37 °C for 2 h. Absorbance was measured at 645 nm in a Fluostar OPTIMA microplate reader (BMG Labtech, Offenburg, Germany). Blank values were obtained by measuring pure PBS and the received values were substracted from the sample values. Two different parameters of the curves were evaluated. Firstly, the curve progression with increasing polymer concentrations and, secondly, the differences between the absorbance values of the samples, the negative and positive control. Simultaneously, qualitative erythrocyte aggregation was investigated with a Leica inverse phase contrast microscope (Leica DM IL, Leica, Wetzlar, Germany) equipped with an objective (Achromat 20/0.30 Phaco 1a objective, Leica) at 200× magnification. The degree of aggregation was classified with a three-stage system. Discrete erythrocytes staying free in suspension were rated as stage 1 and corresponded to the treatment with PBS. Low aggregation with the formation of few rouleaux but with the majority of cells still discrete was ranked as stage 2. Stage 3 was determined with 25 kDa bPEI causing almost all erythrocytes to aggregate in large clusters. All experiments were run in triplicate and repeated once.

Quantification of Red Blood Cell Hemolysis

A modified spectrophotometric method of Parnham and Wetzig was used to detect the hemolytic activity of PMeOx.[3] Erythrocyte suspensions and polymer dissolutions were

prepared as described above. Spontaneous hemolysis was determined by the treatment with PBS (negative control). Erythrocytes treated with 1% Triton X-100 (Ferak, Berlin, Germany) provided the 100% hemolysis value (positive control). Polymer or control solutions (500 µL) were placed in a 96-deepwell plate (Nunc, Roskilde, Denmark) and mixed with 500 µL erythrocyte suspension followed by an incubation under shaking at 37 °C for 1 h and a centrifugation at 2,250 g for 5 min (Eppendorf Centrifuge 5804R). One hundred µL supernatant were sampled and transferred in a clear flat bottomed 96-well culture plate (Greiner Bio-One). Solutions of all samples and controls were additionally added on the same plate to determine the blank values. Hemoglobin released in the supernatant was quantified at 544 nm with a Fluostar Optima plate reader and the percentage hemolysis was calculated according to the following equation:

Equation 1:

$$Hemolysis(\%) = \frac{((Absorption_{Sample} - Blank_{Sample}) - (Absorption_{\substack{Negative \\ control}} - Blank_{\substack{Negative \\ control}}))}{(Absorption_{\substack{Positive \\ control}} - Blank_{\substack{Positive \\ control}})} \times 100$$

Results were evaluated according to specifications of the ASTM (American Society for Testing and Materials) F756-08 standard which describes a hemoglobin release of >5%, 2% to 5%, 0% to 2%, of the total release as hemolytic, slightly hemolytic, non-hemolytic, respectively.[4] Experiments were run in triplicate and were repeated once.

Lactate Dehydrogenase (LDH) Assay

L929 mouse fibroblasts were received from the German Collection of Microorganisms and Cell Cultures (DSMZ, Braunschweig, Germany). The cells were incubated at 37 °C, 5% CO_2 and 95% relative humidity (r.h.) in Roswell Park Memorial Institute 1640 culture medium (RPMI 1640) (PAA, Pasching, Austria) containing 10% fetal bovine serum Gold (FBS Gold) (PAA) and 2 mM glutamine. L929 cells (100,000/well) were seeded in 12-well cell culture plates (Greiner Bio-One) in RPMI 1640 with 10% FBS and incubated for 48 h. Afterwards,

culture medium was aspirated and sample solutions were added (2 mL/well). Polymer solutions (40, 60, 80 mg/mL, respectivly) were prepared in RPMI 1640 medium without FBS and phenol red (PAA) and sterilized by filtration. After 0, 1, 2 and 4 h incubation 120 µL aliquots were drawn from the supernatant. Released LDH was determined by a LDH dependent dye conversion using a commercial cytotoxicity assay kit (Cayman, Ann Arbor, USA) for spectrophotometric quantification at 490 nm. Spontaneous LDH release was obtained by treatment of the cells with culture medium (negative control). Complete cell lysis and 100% LDH release was determined with 0.1% Triton X-100 solution (positive control). Blanks were obtained from the measurement of pure culture medium. As described by Choksakulnimitr et al.[5] a percental LDH release > 10% was regarded as cytotoxic and calculated with the following equation:

Equation 2. $$LDHrelease_{Sample} = \frac{[A]_{Sample}}{[A]_{Positivecontrol}} * 100$$

Cell Viability Assay

The (3-(4,5-dimethylthiazol-2-yl)-2,5-diphenyl tetrazolium bromide) (MTT) assay was performed according to a modified method of Fischer et al.[6] and Mosmann.[7] Briefly, PMeOx stock solutions were prepared in RPMI 1640 with 10% FBS and sterilized by filtration. L929 cells (8,500 cells/well) were seeded into 96-well plates (Greiner Bio-One) and incubated at 37 °C in RPMI 1640 with 10% FBS for 24 h. Afterwards, culture medium was replaced by 100 µL PMeOx solutions (5 to 80 mg/mL). Samples were aspirated after 3, 12 and 24 h, and 200 µL MTT (0.5 mg/mL, Sigma) in RPMI 1640 without FBS were added. After further 4 h incubation the MTT solution was aspirated and the formazane crystals were dissolved in 200 µL dimethyl sulfoxide (Carl Roth, Karlsruhe, Germany). Samples were analyzed with a Fluostar Optima microplate reader at 570 nm. Zero absorbance (blank) was obtained by the measurement of pure culture medium. Cells incubated with culture medium

served as negative control (100% viability). Thiomersal (0.02%) in culture medium was used as positive control decreasing the cell viability to 0%. Cell viability (%) was calculated after subtracting the blank from all values with the following equation:

Equation 3. $$Viability(\%) = \frac{[A]_{test\ polymer}}{[A]_{negativecontrol}} \times 100$$

Results were evaluated as given in the ISO 10993-5 which describe cell viability below 70% in comparison to the negative control as cytotoxic.[8] Experiments were run in 7 parallel experiments and were repeated once. Morphological changes of the fibroblasts were additionally investigated with an inverse phase contrast microscope with an Achromat 10/0.20 Phaco 1a objective (Leica) at 100x magnification. Evaluation was performed using the staging system of ISO 10993-5.

References

1. Cardoso, A. V.; Pereira, M. H.; Marcondes, G. d. A.; Ferreira, A. R.; Araújo, *Mat.* P. R. d. *Res.* **2007**, *10*, 31-36.
2. Ogris, M.; Brunner, S.; Schuller, S.; Kircheis, R. Wagner, E. *Gene Ther.* **1999**, *6*, 595-605.
3. Parnham, M. J.; Wetzig, H. *Chem. Phys. Lipids* **1993**, *64*, 263-274.
4. ASTM F756, 2000 (2008). Standard Practice for Assessment of Hemolytic Properties of Materials. In: Annual Book of ASTM Standards, Vol. 13.01. Philadelphia: ASTM; **2008**.
5. Choksakulnimitr, S.; Masuda, S.; Tokuda, H.; Takakura, Y.; Hashida, M. *J. Control. Release* **1995**, *34*, 233-241.
6. Fischer, D.; Li, Y.; Ahlemeyer, B.; Krieglstein, J.; Kissel, T. *Biomaterials* **2003**, *24*, 1121-1131.
7. Mosmann, T. *J. Immunol. Methods* **1983**, *65*, 55-63.
8. Biological evaluation of medical devices Part 5: Tests for *in vitro* cytotoxicity. Geneva (Switzerland): International Organization for Standardization/ANSI;ISO, ISO 10993-5:**2009** second edition", Geneva, **2009**.

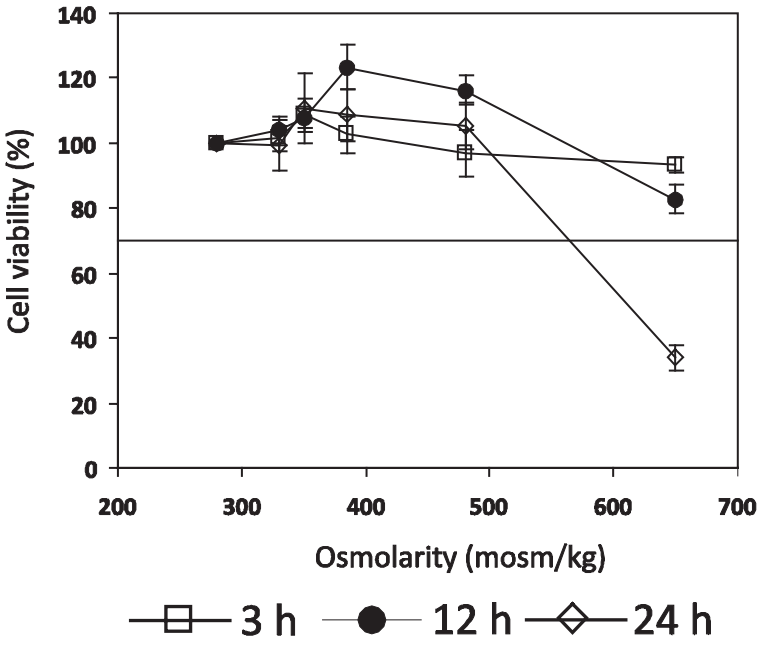

Figure S1. Influence of osmolarity on the cell viability of L929 mouse fibroblasts after 3 h, 12 h and 24 h incubation testing cell culture medium of osmolarities up to 650 mosmol/kg. Cell viability was determined by MTT assay. Data are presented as mean ± SD of seven determinations.

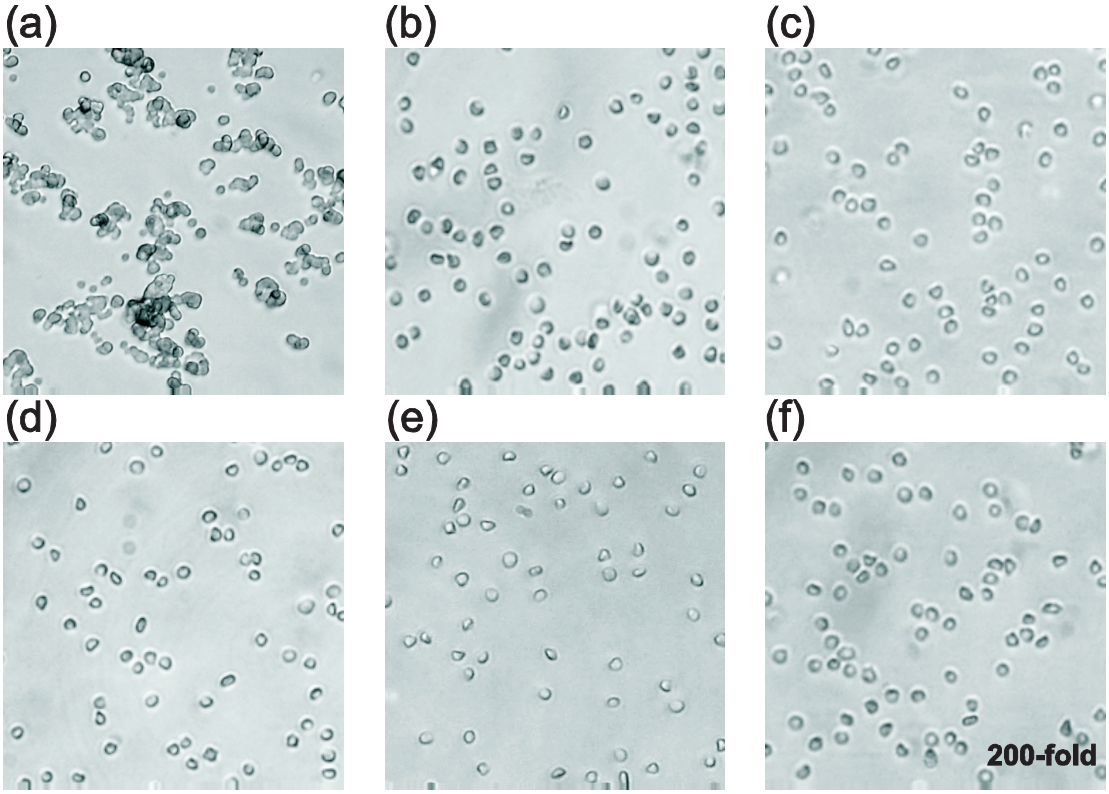

Figure S2. Representative light microscopic photographs (magnification: 200x) of erythrocyte aggregation induced by PMeOx at the highest concentration of 80 mg/mL after 2 h incubation. (a) Positive control (30 µg/mL 25 kDa bPEI); (b) negative control (PBS buffer); (c) 2 kDa PMeOx; (d) 4 kDa PMeOx; (e) 10 kDa PMeOx; (f) 20 kDa PMeOx.

Table S1 Physicochemical characteristics of the PMeOx polymers. The experimental molar mass was calculated by ^{1}H NMR spectroscopy, number average (Mn) and polydispersity index (PDI) values were determined by SEC (eluent: *N,N*-dimethylacetamide containing 2.1 g/L LiCl; polystyrene standards).

Polymer	Experimental molar mass (Da)	Mn (kDa)	PDI
2 kDa PMeOx	2,000	3,700	1.17
4 kDa PMeOx	4,000	6,700	1.20
10 kDa PMeOx	10,000	12,300	1.39
20 kDa PMeOx	20,000	19,000	1.44

Table S2 Osmolarities of PMeOx polymer stock solutions at 80 mg/mL in PBS buffer and RPMI culture medium with 10% FCS (for MTT assay) and without FCS (for LDH assay).

Polymer	PBS buffer (mosmol/kg)	RPMI with 10% FCS (mosmol/kg)	RPMI without FCS (mosmol/kg)
Reference (pure buffer or medium without PMeOx)	280	280	280
2 kDa PMeOx	365	420	335
4 kDa PMeOx	365	400	345
10 kDa PMeOx	366	360	335
20 kDa PMeOx	358	340	335

Publication 5

“Zwitterionic poly(2-oxazoline)s as promising candidates for blood contacting applications”

L. Tauhardt, D. Pretzel, K. Kempe, M. Gottschaldt, Dirk Pohlers, U. S. Schubert

Polym. Chem. **2014**, *5*, 5751-5764

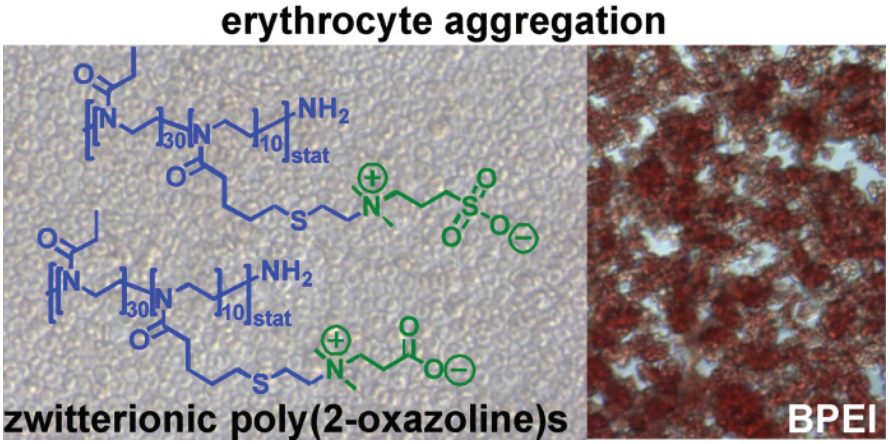

Polymer Chemistry

PAPER

View Article Online
View Journal | View Issue

Cite this: *Polym. Chem.*, 2014, **5**, 5751

Zwitterionic poly(2-oxazoline)s as promising candidates for blood contacting applications†

Lutz Tauhardt,[ab] David Pretzel,[ab] Kristian Kempe,‡[ab] Michael Gottschaldt,[ab] Dirk Pohlers[c] and Ulrich S. Schubert*[abd]

Received 26th March 2014
Accepted 15th May 2014

DOI: 10.1039/c4py00434e

www.rsc.org/polymers

We report the synthesis of highly hemo- and cytocompatible zwitterionic 2-oxazoline-based poly(sulfobetaine)s and poly(carboxybetaine)s, which demonstrate beneficial anticoagulant activity. The polymers were obtained by thiol–ene photoaddition of a tertiary amine-containing thiol onto an alkene-containing precursor copoly-(2-oxazoline), followed by betainization with 1,3-propansultone and β-propiolactone. The polymers and their intermediates were characterized by means of ^{1}H NMR spectroscopy and size exclusion chromatography. The influence of the zwitterionic polymers on the aggregation and hemolysis of erythrocytes, the whole blood viscosity, the platelet and complement activation as well as the blood coagulation has been studied in detail. In addition, the cytotoxicity of the materials has been evaluated. It was found that the zwitterionic POx show no negative interactions with blood. Moreover, anticoagulant activity *via* the intrinsic and/or the common coagulation pathway was observed. The high hemocompatibility and the low cytotoxicity as well as the beneficial anticoagulant activity of the presented zwitterionic poly(2-oxazoline)s demonstrate their potential for the use in biomedical applications.

Introduction

Zwitterionic polymers, also known as poly(betaine)s, are of significant interest as coating materials for medical devices, implants and drug delivery systems. Due to their hydrophilic, protein repellent character, they have been investigated as antifouling coatings for the reduction of non-specific adhesion and adsorption of proteins, microorganisms and eukaryotic cells.[1–4] The most prominent zwitterionic polymer is poly-(2-methacryloyloxyethyl phosphorylcholine). It can be obtained by the controlled radical polymerization of the commercially available 2-methacryloyloxyethyl phosphorylcholine[5,6] and is used as coating material, *e.g.*, in contact lenses.[7,8] Other widely-used zwitterionic polymers are poly(sulfobetaine)s and poly-(carboxybetaine)s. Generally, they are obtained either by controlled radical polymerization of appropriate zwitterionic monomers, which are usually based on 2-(*N*,*N*-dimethylamino)-ethyl methacrylate (DMAEMA),[1–4,9–12] or by post-polymerization modification of poly(DMAEMA) (co)polymers.[13,14] An outstanding property of these polymers is their excellent blood compatibility which, in some cases, is going along with an anticoagulant activity leading to a prolongation of the blood clotting time.[10–12,15,16] This is important within medical applications where thrombogenicity is undesired.

In a dissolved state, anticoagulant polymers are of particular interest as heparin mimetics. Heparin, a well-known polysaccharide with multiple negative charges per repeating unit, is a widely used anticoagulant reagent for the treatment and prevention of thrombosis, which can result from operations, blood transfusions, or dialysis. However, being obtained from animal tissues sources, the use of heparin comes along with some problems, *e.g.* contaminations, a heterogeneous effectiveness depending on the isolated batches, and most importantly, heparin can lead to autoimmune diseases in long term treated patients.[17] Therefore, biocompatible anticoagulant polymers, which can be synthesized in a standardized procedure yielding products with identical chemical and functional characteristics, display a promising alternative to heparin salts.

Anticoagulant polymers are also of interest for drug delivery and diagnostic approaches. Here, the prevention of non-specific and immunologic interactions of the carriers (nanoparticles, micelles, vesicles, *etc.*) with the various blood components (*e.g.* cells, proteins), represents an important task.

By using biocompatible, anticoagulant "stealth" polymers an improved stability and blood circulation time can be reached, promoting the diagnostic or therapeutic functions.[18]

[a]*Laboratory of Organic and Macromolecular Chemistry (IOMC), Friedrich Schiller University Jena, Humboldtstr. 10, 07743 Jena, Germany. E-mail: ulrich.schubert@uni-jena.de; Fax: +49 3641 948 202*

[b]*Jena Center for Soft Matter (JCSM), Friedrich Schiller University Jena, Philosophenweg 7, 07743 Jena, Germany*

[c]*Centre for Diagnostic at the Clinic of Chemnitz, Flemmingstraße 2, 09116 Chemnitz, Germany*

[d]*Dutch Polymer Institute (DPI), John F. Kennedylaan 2, 5612 AB Eindhoven, The Netherlands*

† Electronic supplementary information (ESI) available. See DOI: 10.1039/c4py00434e

‡ Current address: Department of Chemical and Biomolecular Engineering, The University of Melbourne, Victoria 3010, Australia.

If such anticoagulant polymers can be additionally attached to solid surfaces, the application field is further enlarged and includes the biomedically relevant area of implant material functionalization. Existing synthetic biomaterials introduced into the human body, *e.g.* as implantable devices, often suffer from problems associated with surface-induced thrombosis, clot formation, and infection. Implants coated with non-thrombogenic, biocompatible materials would not only reduce the need for aggressive anticoagulant therapies, they would also be beneficial for cardiovascular applications, where the blood response to artificial materials, including thrombosis and platelet deposition, limits the long-term efficacy. The surface modification of these devices with anticoagulant polymers could increase their working life span due to an increased biocompatibility.[19]

Furthermore, zwitterionic, anticoagulant polymers are promising materials for extracorporeal blood contacting applications, in particular dialysis membranes, which are massively used to separate metabolites from blood of patients with nephrologic diseases. Here the blocking of the membrane pores by blood clot formation and biofouling needs to be prevented.

A class of polymers with a high biocompatibility and anti-fouling properties are poly(2-oxazoline)s (POx), in particular the water soluble (co)polymers based on 2-methyl-2-oxazoline (MeOx) and 2-ethyl-2-oxazoline (EtOx).[20–28] They exhibit similar properties as poly(ethylene glycol) (PEG),[29] but have some additional advantages such as a lower viscosity[23,30] and a less demanding synthesis, since no gaseous and highly toxic starting materials have to be used. Although having excellent blood compatibility, there are no reports on anticoagulant POx to the best of our knowledge. In contrast, a study published recently showed that POx-based copolymers have no impact on the blood clotting time.[31] The synthesis of POx by living cationic ring-opening polymerization (CROP) and the broad variety of functional 2-oxazoline monomers, initiators, and terminating agents, enable the preparation of tailor-made polymers, with adjustable molar masses, narrow molar mass distributions, and tunable properties.[32–37] Previously, well-defined (co)polymers based on 2-(3-butenyl)-2-oxazoline (ButEnOx)[38–40] and 2-(9-decenyl)-2-oxazoline (DecEnOx)[41–45] have been reported, which provide a platform for efficient post-polymerization modifications *via* thiol–ene photoaddition and, thus, enable the introduction of further functionalities.

Here we report the synthesis of zwitterionic POx and the evaluation of their blood compatibility with the focus on blood clotting. To this end, a double bond containing copolymer of ButEnOx and EtOx was prepared. Modification with 2-dimethylaminoethanethiol hydrochloride by thiole–ene addition resulted in the introduction of tertiary amine pendant groups. Subsequent functionalization with 1,3-propansultone and β-propiolactone yielded zwitterionic POx, a sulfobetaine POx (SB-POx) and a carboxybetaine POx (CB-POx), respectively. For comparison, a PEtOx homopolymer was prepared. All polymers were characterized by ^{1}H NMR spectroscopy and size exclusion chromatography (SEC). The influence of the polymers on the aggregation and hemolysis of erythrocytes, the whole blood

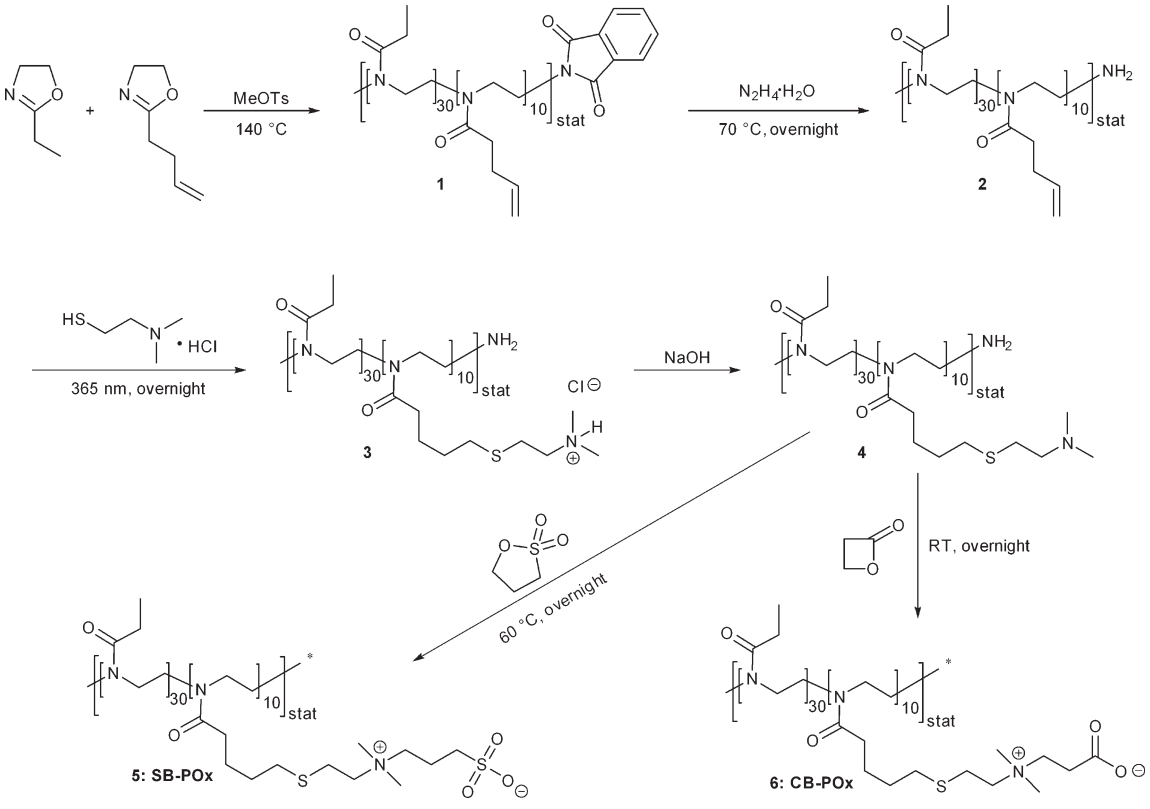

Scheme 1 Schematic representation of the synthesis of zwitterionic POx.

viscosity, the platelet and complement activation as well as the blood coagulation was studied. Moreover, their cytotoxic activity was investigated.

Results and discussion

Synthesis of amine end-functionalized P($EtOx_{30}$-*stat*-$ButEnOx_{10}$) and $PEtOx_{40}$

The synthesis of water-soluble zwitterionic POx was accomplished *via* the post-polymerization modification of ButEnOx-based copolymers. First, the kinetics of the copolymerization of EtOx and ButEnOx has been investigated. As already reported for the methyl triflate initiated copolymerization at 70 °C, also the methyl tosylate initiated reaction at 140 °C shows a first-order kinetic behavior (Fig. S1A†).[40] The observed linear increase of $\ln([M]_0/[M]_t)$ with time, demonstrates a constant concentration of propagating species indicative of a living polymerization mechanism. However, due to the higher temperature, the polymerization proceeded much faster with polymerization constants of $k_p(EtOx) = 0.206$ L mol^{-1} s^{-1} and $k_p(ButEnOx) = 0.188$ L mol^{-1} s^{-1} (Table S1, Fig. S1A†). The similar conversions of both monomers indicate the formation of a random copolymer. In addition, characterization by size exclusion chromatography (SEC) showed an increasing molar mass with time and narrow molar mass distributions (Table S1, Fig. S1B†).

For the intended synthesis of zwitterionic POx, amine end-functionalized P($EtOx_{30}$-*stat*-$ButEnOx_{10}$) (**2**) was prepared as a starting material in an easy, two-step procedure (Scheme 1). To this end, the living species of the CROP was quenched with potassium phthalimide. The end-capping efficiency was calculated to be 100% according to ^{1}H NMR spectroscopy (Fig. S1†). Subsequent hydrazinolysis yielded a terminal amine group, which can be used for further reactions, *e.g.* labeling or surface attachment. While the double bond signals at 5.87 ppm and 5.04 ppm remained unchanged, the signal of the phthalimide end-group disappeared in the ^{1}H NMR spectrum, indicating the success of the reaction (Fig. S1†). Characterization by SEC revealed a narrow molar mass distribution for both phthalimide and amine end-functionalized polymers (Table S1†) with monomodal distributions (Fig. S2†). For comparison an amine end-functionalized PEtOx homopolymer with a degree of polymerization of 40 has been prepared using the same procedure.

Thiol–ene photoaddition and betainization

In the next step the double bonds of the ButEnOx repeating units were functionalized with 2-dimethylaminoethanethiol hydrochloride by thiol–ene photoaddition reaction. The resulting tertiary amine group is essential for the subsequent betainization with 1,3-propansultone and β-propiolactone, respectively. The hydrochloride, which hampered the direct betainization under various conditions, was neutralized by dissolving the polymer in water and adding aqueous NaOH up to a pH of 14. After removing the water, the polymer was separated from the resulting salt by extraction with chloroform. The structure of the obtained P($EtOx_{30}$-*stat*-*t*$AmOx_{10}$) (**3**) resembles that of poly(DMAEMA), a well-known starting material for the synthesis of zwitterionic polymers. Characterization by ^{1}H NMR spectroscopy did not only show the success of the thiol–ene photoaddition, *i.e.* the disappearance of the double bond signals, but

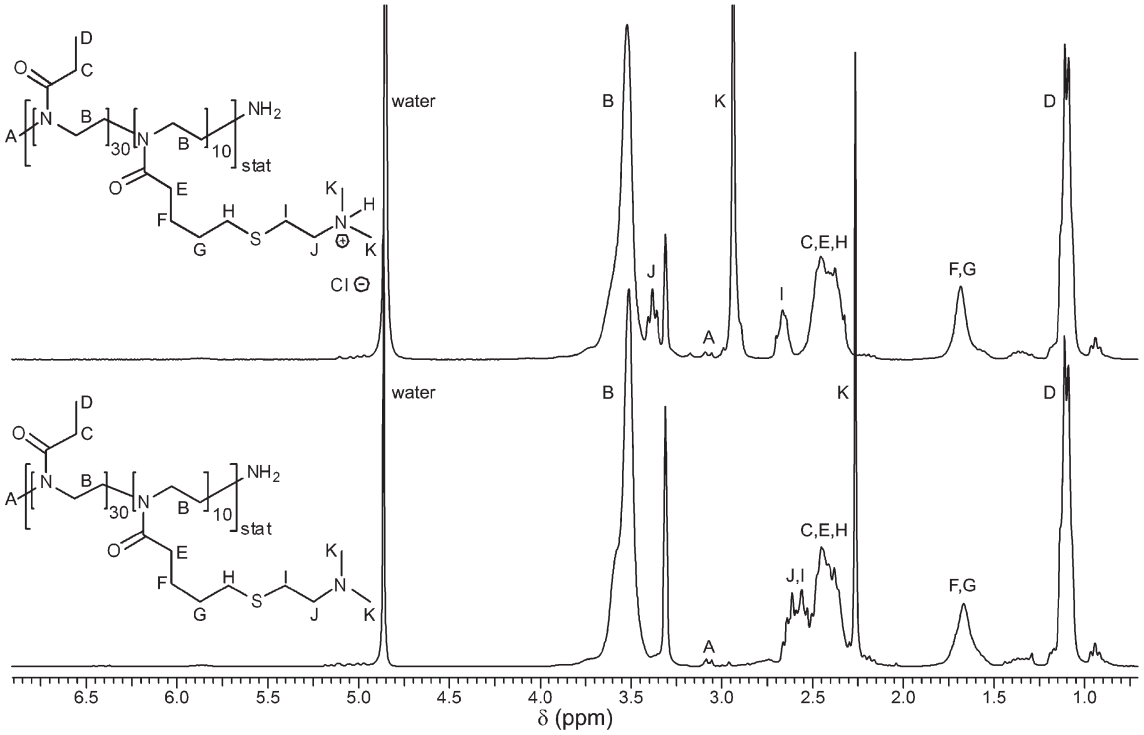

Fig. 1 ^{1}H NMR spectra of P($EtOx_{30}$-*stat*-*t*$AmOx_{10}$) (top) before and (bottom) after treatment with aqueous NaOH (300 MHz, CD_3OD).

also a shift of the signals of the CH_3 groups of the tertiary amine and the adjacent CH_2 group to lower ppm values after treatment with aqueous NaOH (Fig. 1). SEC measurements revealed an increasing molar mass after the photoaddition (Table S2†).

In the last step, the zwitterionic structures were formed by reacting P($EtOx_{30}$-*stat*-*t*$AmOx_{10}$) with 1,3-propansultone (60 °C) and *β*-propiolactone (room temperature), respectively, in acetonitrile for one day. The successful quaternization of the tertiary amine group was proven by ^{1}H NMR spectroscopy (Fig. 2). The signals for the methyl groups attached to the amine group were shifted to higher ppm values. Moreover, new peaks, deriving from the methylene groups between the quaternized nitrogen and the head groups of the betaines, are visible. Depending on the system, characterization by SEC showed either an increasing (solvent: DMAc + 0.21% LiCl) or a decreasing ($CHCl_3$ + TEA + *i*PrOH (94 : 4 : 2)) molar mass when compared to the PEG standards. On the SEC system running with DMAc + 0.21% LiCl both polymers show a shoulder at lower elution volumes, *i.e.* higher molar masses. The shoulders were observed neither for the starting materials on both systems nor for the sulfobetaine POx (SB-POx) when measured on a SEC system running with $CHCl_3$+ TEA + *i*PrOH (94 : 4 : 2). They probably derive from strong interactions of the zwitterionc polymers with the particular column, since chain coupling is very unlikely. The carboxybetaine POx (CB-POx) was only soluble in DMAc so that a direct comparison was not possible.

In vitro cytotoxicity

To prove the applicability of the prepared zwitterionic polymers for biomedical applications, the *in vitro* biocompatibility was investigated. Therefore, the cytocompatibility of the polymers was studied following a standardized protocol.

The *in vitro* cytotoxicity was evaluated on the basis of an XTT assay using mouse fibroblast L929 cells and human hepatocytes HepG2 (Fig. 3A). Neither PEtOx nor the zwitterionic polymers revealed any cytotoxic effect after 24 h incubation at different concentrations (ranging from 0.1 to 10 mg mL^{-1}). A detailed live/dead microscopy study of the polymer treated cells confirmed their membrane integrity (exclusion of red fluorescent propidium iodide (PI) from cell nuclei) and their excellent viability (strong green fluorescence of fluorescein diacetate (FDA) in cytoplasm) (Fig. 3B). In summary, no cytotoxic effect caused by the zwitterionic polymers was observed. These results confirm the low cytotoxicities previously reported for POx homopolymers and copolymers[20–24,26,27,34,46–48] as well as zwitterionic materials.[49–51]

Erythrocyte aggregation and hemolysis

As blood is the first contact partner within the human body during intravenous administration, the polymers were tested for their general blood compatibility.

Adverse side reactions with red blood cells were evaluated in terms of erythrocyte aggregation and hemolysis upon polymer incubation. To assess the influence of the zwitterionic polymers on the red blood cell membrane, the hemolytic activity was measured photometrically by means of hemoglobin release after potential damage of erythrocytes. The polymers were investigated at different concentrations (1, 5, and 10 mg mL^{-1}) in comparison to phosphate buffered saline (PBS) as negative and Triton-X100 as positive control. Both, the PEtOx and the zwitterionic polymers revealed a hemoglobin release below 2%, proving that they do not damage the erythrocyte membrane (Fig. 4A). Furthermore, the induction of erythrocyte aggregation was investigated to assess the blood compatibility of the polymers. Formation of aggregates, which could lead to an impeded

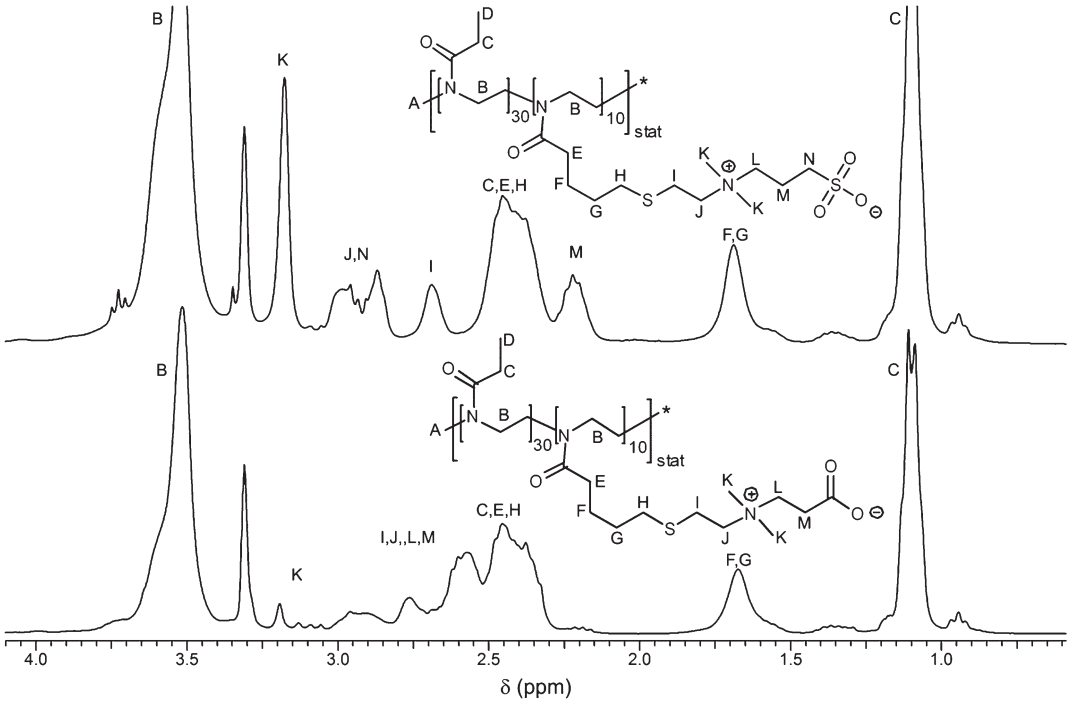

Fig. 2 ^{1}H NMR spectra of the POx-based (top) poly(sulfobetaine) and (bottom) poly(carboxybetaine) (300 MHz, CD_3OD).

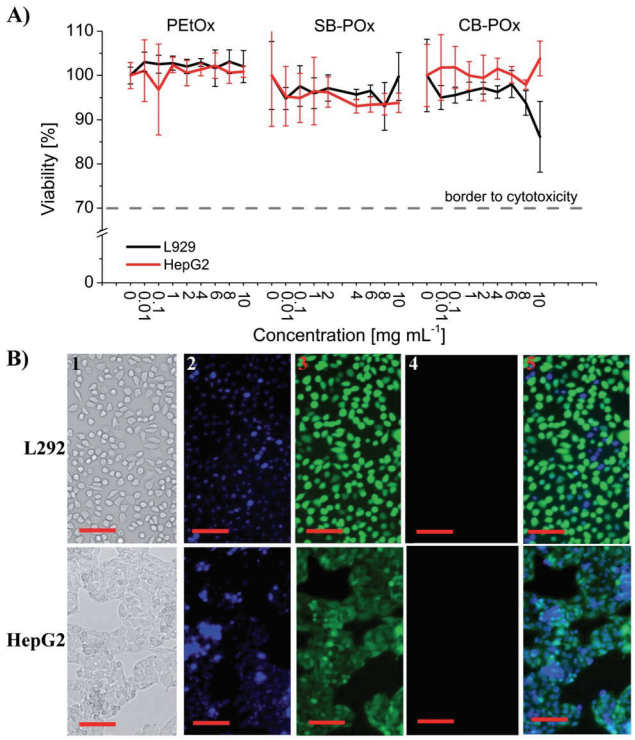

Fig. 3 (A) Cell viability of L929 mouse fibroblasts and human hepatocytes HepG2 after incubation with zwitterionic polymers up to 10 mg mL^{-1} for 24 hours. Cells incubated with polymer free culture medium served as control. The cell viability was determined by XTT assay according to ISO 10993-5. Data are expressed as mean ± SD of six determinations. (B) Representative bright field and fluorescence micrographs of Hoechst 33342/FDA/PI stained L929 mouse fibroblast cells (upper panel) and human hepatocytes HepG2 (lower panel) cultured for 24 hours in the presence of 10 mg mL^{-1} of CB-POx (identical results for SB-POx and PEtOx). (1) Light field image, (2) blue fluorescent Hoechst 33342 dye labels nuclei of all cells present, (3) green fluorescent FDA dye indicates cytoplasm of vital cells, (4) red fluorescent PI signals tag nuclei of dead cells, and (5) overlay of Hoechst 33342 dye fluorescence and green fluorescence of the FDA dye.

blood flow, was analyzed by UV/Vis absorption measurements for different polymer concentrations (1, 5, and 10 mg mL^{-1}) in comparison to phosphate buffered saline (PBS) as negative and branched poly(ethylene imine) (bPEI) as positive control (Fig. 4B). No cluster formation was observed photometrically in the polymer treated samples and the negative control. In contrast, the positive control clearly exhibited a cell cluster formation. These results could be confirmed microscopically (Fig. 4C).

To conclude, no adverse side reactions with red blood cells, representing the major cellular compartment of the blood, were observed for the two zwitterionic polymers and the PEtOx reference polymer. On that basis, all three polymers were submitted to an even more detailed blood compatibility analysis. This included the analysis of possible impacts on undesired alterations of the blood viscosity, platelet activation, complement factor activation, and finally a detailed look at possible modulations of the coagulation pathways.[52]

Blood viscosity

Polymers entering the blood stream could possibly interfere with different blood components, such as plasma proteins and cellular membrane structures of blood cells, leading to a critical change of the whole blood viscosity. Since an appropriate blood viscosity is crucial for the proper function of blood, alterations would have a severe impact on the cardiovascular system and heart function. Measuring the blood viscosity following incubation with polymers allows the unspecific estimation of strong mutual reactions of the polymers with whole blood components.

The whole blood viscosity was measured after the addition of the polymers in different concentrations (1, 5, and 10 mg mL^{-1}, respectively). To distinguish between a change in viscosity caused by the intrinsic viscosity of the polymer and a polymer mediated interaction or aggregation of blood components, the viscosities of the blood/polymer solutions as well as the corresponding solutions containing only polymer (in PBS) at equivalent concentrations were compared. It turned out that the concentration dependent increase of the blood viscosity can be fully attributed to the intrinsic viscosity of the added polymer (Fig. 5). As a consequence, no substantial interactions of the polymers with blood components leading to an increase or decrease of the blood viscosity were observed. The slightly increased values obtained by the addition of highly concentrated polymer solutions are in the physiological tolerable range.[53] Besides, it is rather unlikely, that a biomedically used polymer will be administered to the blood flow at such high concentrations.

Platelet activation

The activation of platelets at sites of damaged blood vessels displays a very early event in the complex process of primary hemostasis, which is finally leading to the plug like coagulation of blood *via* the formation of fibrin stabilized platelet aggregates. By introducing a polymeric material this sensitive system can be fatally destabilized. A malfunction of platelets could provoke excessive bleeding, whereas an exceeding platelet activity would cause spontaneous blood clot formation resulting in a life-threatening clogging of vessels.

Immunologically, platelets can be distinguished from other blood cells by the constitutive expression of the surface antigen CD42. Additionally, the CD62p (P-selectin) membrane glycoprotein is exclusively induced on activated platelets. The latter marker was used to identify the status of activation in human platelets upon incubation with the polymers. The measurement of the CD42/CD62p co-expression in platelet samples treated with the polymers at different concentrations (1, 5, and 10 mg mL^{-1}) and incubation times (10 and 30 min) revealed that there was no effect of the zwitterionic polymers as well as the PEtOx control polymer on the CD62p expression in CD42 positive cells. The percentage of activated platelet phenotype in terms of CD62p positive cells stayed at the constant low level of the control sample treated only with PBS.

To exclude measurement errors, platelets of the positive control were treated with thrombin, an endogenous inducer of platelet activation. Within 10 min an immediate up-regulation of up to 95% of the CD62 expression was observed, indicating the sensitivity and proper setup of the assay (Fig. 6).

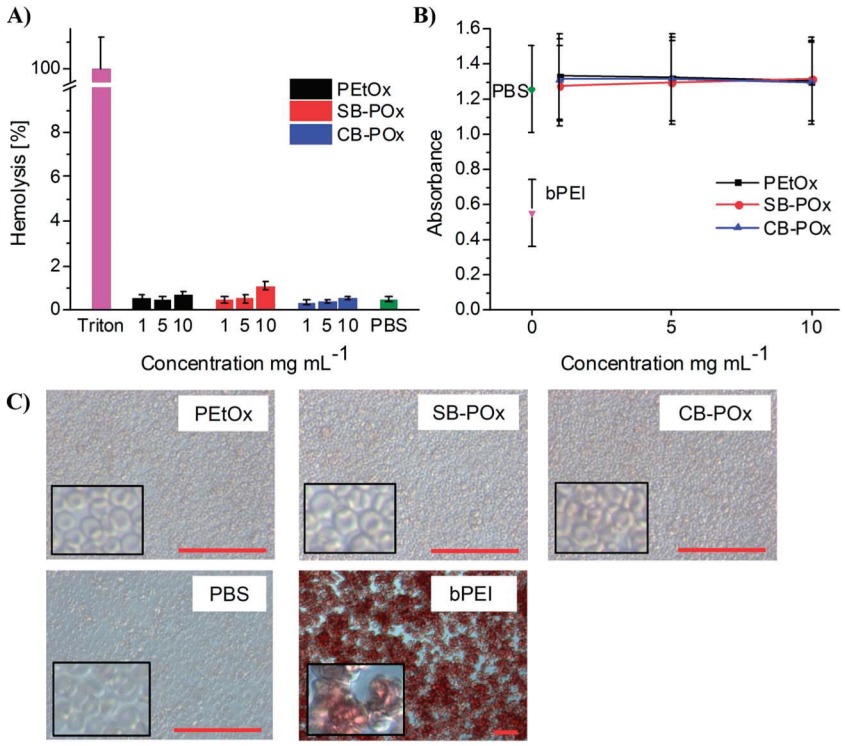

Fig. 4 Blood compatibility of PEtOx and zwitterionic POx-based polymers. (A) Photometric determination of hemolytic activity after incubation with different polymer concentrations for 1 h at 37 °C. Triton X-100 (1%) served as positive and PBS as negative control. Experiments were run in triplicate and were repeated once; data are presented as the mean percentage ± SD of hemolytic activity compared to the positive control set as 100%. (B) Photometric determination of the erythrocyte aggregation after 2 h incubation at 37 °C with polymers. 25 kDa bPEI (50 μg mL^{-1}) served as positive and PBS as negative control. Experiments were run in triplicate and were repeated once; data are presented as the mean measured absorbance ± SD. (C) Representative micrographs of red blood cell aggregation after 2 h incubation at 37 °C with polymers. PBS served as negative and 25 kDa bPEI (50 μg mL^{-1}) as positive control.

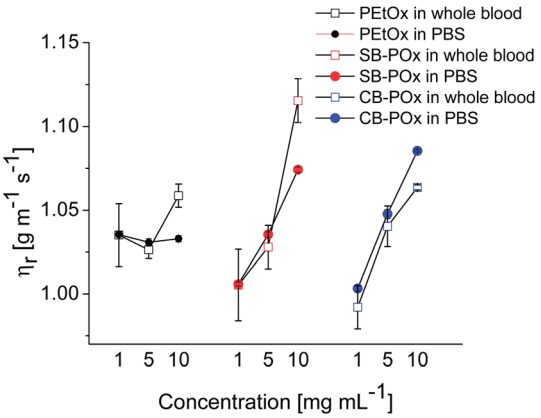

Fig. 5 Blood compatibility of PEtOx and zwitterionic POx-based polymers concerning their influence on the whole blood viscosity: relative viscosity of the polymer solutions in PBS and in whole blood. Experiments were run in quadruplicate at three inclination angles, data are presented as the mean percentage ± SD.

Complement activation

A polymer introduced into the human organism is very likely to be recognized as a foreign substance by the interaction with the complement system, which plays a crucial role in the detection, opsonization and clearance of the host components, microorganisms and cells. Complement factors are a group of proteins acting in different cascade like activation pathways, including the interaction of complement factors with antibody–antigen complexes and bacterial carbohydrates as well as the binding to foreign surfaces. As a consequence, either macrophages recognize and phagocytose these elements or so called membrane attack complexes lead to a lysis of opsonized cells.[54] Even though the complement activation pathways are very complex they share the generation of the enzyme C3-convertase, which is able to activate complement component C3 creating C3b and C3a. Hence the anaphylatoxin C3a was used within a commercial immunoassay kit to detect the general activation of the complement system upon interaction with the zwitterionic polymers.[52,55] C3a levels were measured after incubation for 10, 30, and 60 min with different concentrations of the polymers (1, 5, and 10 mg mL^{-1}) and compared to a saline control and C3a low/high standards (Fig. 7). No activation of the complement system was observed following the incubation with the zwitterionic polymers and the PEtOx control. In all cases the C3a levels remained on the level of the negative control containing only saline.

Similar results were found in a previous study analyzing the effect of zwitterionic structures on blood compatibility issues where only a slight increase of the C3a concentration occurred compared to the negative control.[56]

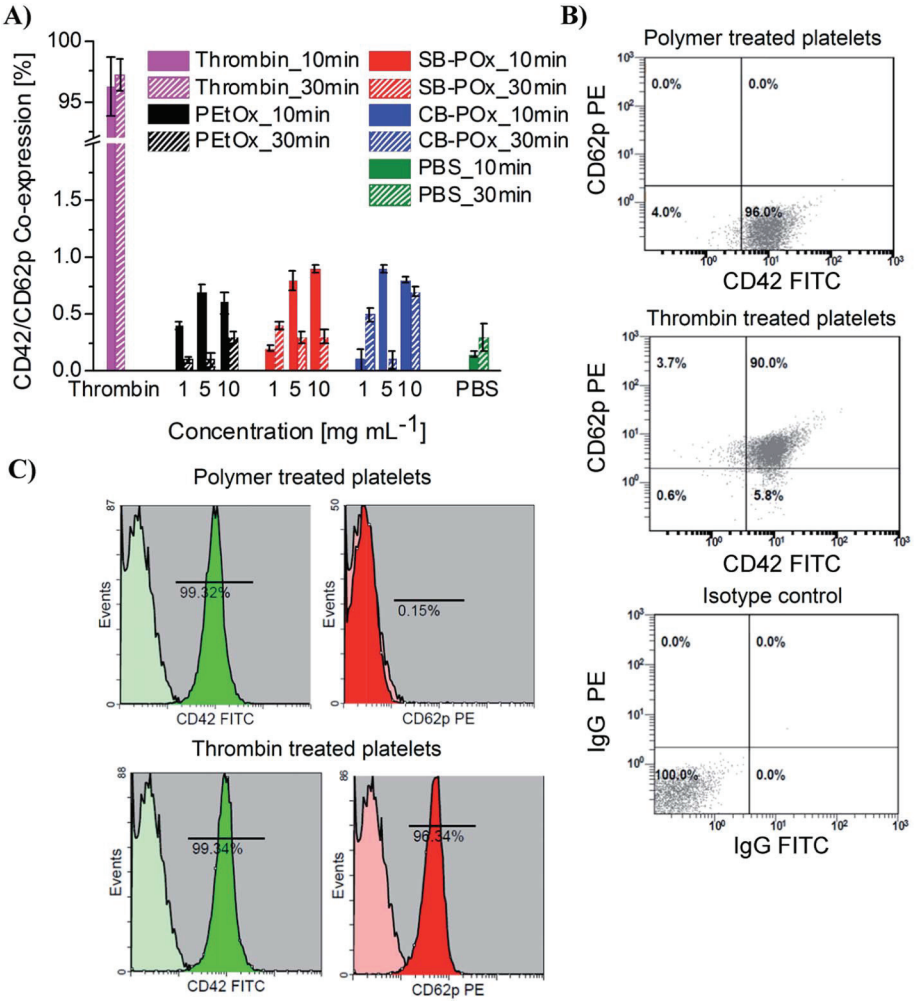

Fig. 6 (A) FACS analysis of polymer mediated platelet activation measured by determination of CD62p/CD42 co-expression after 10 min incubation. Experiments were run in triplicate, data are presented as percentage of platelets positive for both CD62p and CD42 epitopes ± SD. (B) Representative dot-plots for the expression of CD62p and CD42 of a CB-POx treated sample and a thrombin treated positive control after 10 min incubation and, additionally, staining pattern of the isotype control. Non activated cells are in the lower right panel and only positive for CD42, cells in the upper right panel of the dot plot diagrams are double positive for CD62p and CD42, indicating an activated platelet phenotype. The absence of non-specific binding of the antibodies is proven by the very low fluorescence signal of the platelets in the isotype control, where all cells are located in the lower left panel. (C) Histogram plots. The faint colored graphs indicate the value of the isotype control and green/red graph of the sample stained with the specific CD42 and CD62p antibodies.

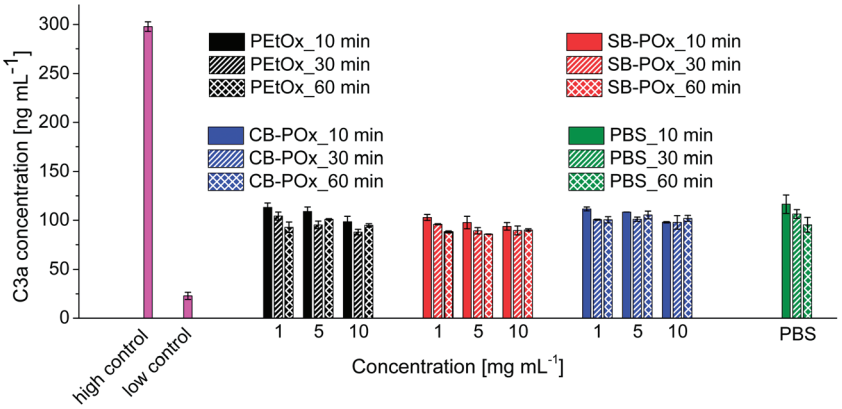

Fig. 7 Complement activation by the polymers measured by determination of C3a levels after 10 min, 30 min, and 60 min incubation. Experiments were run in triplicate and data are presented as the mean measured absorbance ± SD of three determinations.

Regarding the complement activation by POx-based materials, the literature reports divergent properties ranging from an inert behavior to a slight or clear activation of the complement system. In all cases, POx with different ratios of hydrophilic and hydrophobic domains have been investigated.[31,57,58] Their amphiphilic character resembles the structural setup of biological membranes which are, amongst others, a prominent target of complement factors and thus might explain the complement activation by these materials. In contrast, the POx-based zwitterions in the present study are composed of a copolymer with a clear hydrophilic character, which very likely leads to the absence of any complement system activation.

Blood coagulation

The viscosity measurements of polymer treated whole blood samples already proved that there was no significant induction of blood coagulation mediated by the zwitterionic polymers. A deeper insight into possible interactions with the blood coagulation system and a possibly altered coagulation ability of the blood was gained by measuring parameters for the intrinsic (*in vivo* triggered by contact to collagen exposed in damaged tissue) and the extrinsic (*in vivo* activated by tissue factor released from damaged tissue) pathway, which are both activating the final common coagulation pathway (conversion of fibrinogen into fibrin).[59] In the secondary hemostasis reaction, the coagulation factors mediate the strengthening of the platelet plug formed in the primary hemostasis reaction. An aberration of the cascade-like activation of the coagulation factors, which are mainly proteases and glycoprotein cofactors, could lead to pathologies such as uncontrolled bleeding or thromboembolism. Even though the division of coagulation into two pathways is originating from the substances used in the laboratory to initiate the clotting (silica for the intrinsic and thromboplastin for the extrinsic pathway) and, hence, is almost an artificial division, the activated partial thromboplastin time (APTT) and the prothrombin time (PT) are routinely used to examine mainly the intrinsic and extrinsic pathways, respectively. Since they both end up in the final common pathway, they indirectly demonstrate the status of that pathway.

The PT assay revealed that for both the zwitterionic POx and the PEtOx reference but also for the saline control, all PT values were *ca.* 10 s, fitting into the clinically normal range of 7 to 10 s (Fig. 8A). It has to be mentioned at that point, that the PT assay, which is using thromboplastin (a mixture of tissue factor and phospholipids) as coagulation initiator, is preferentially sensitive to coagulation factors II, V, VII and X and fibrinogen.[60,61] Hence, the results suggest that an interaction of the zwitterionic polymers with these components of the extrinsic and common blood coagulation pathway can be excluded.

In contrast, the APTT values for the zwitterionic polymers show a clear elongation of the time, which is required to form a fibrin clot in the plasma. As measured with the Pathrombin SL activator (Fig. 8B), the APTTs for the CB-POx at all concentrations

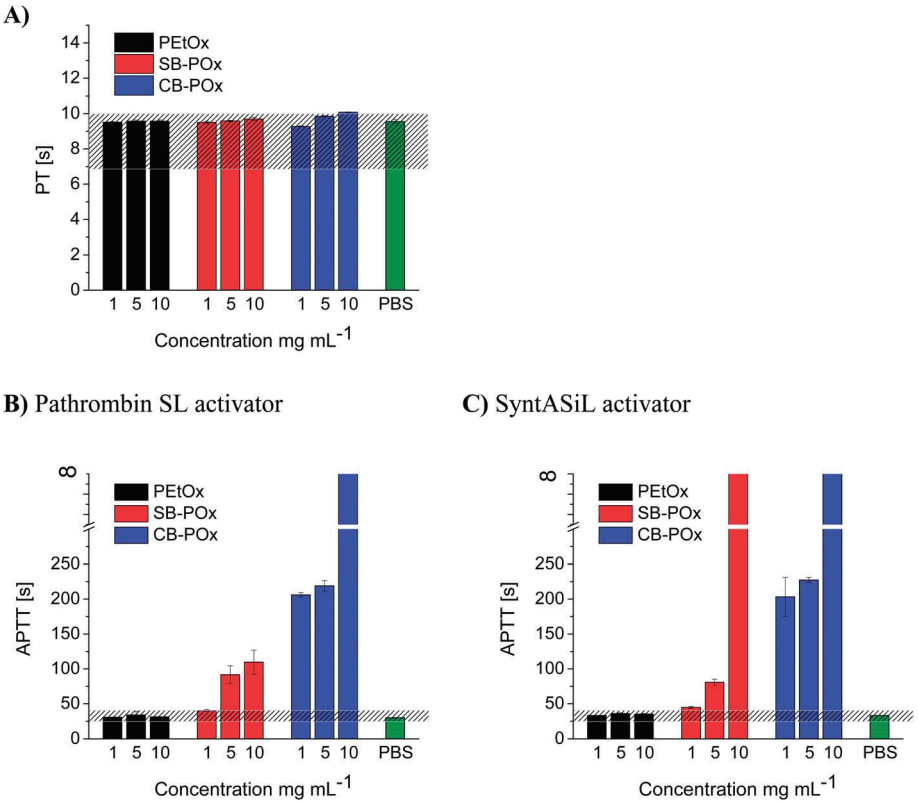

Fig. 8 Effects of the polymers on the coagulation detected by (A) the prothrombin time (PT) and (B and C) the activated partial thromboplastin time (APTT); after 5 min incubation. Experiments were run in triplicate and data are presented as the mean measured ± SD. Hatched area indicates the range of values judged as clinically normal.

were much longer than the clinical range of 26 to 42 s [206 s (1 mg mL^{-1}); 220 s (5 mg mL^{-1}); $\gg$240 s (10 mg mL^{-1})]. Also the SB-POx induced a retarded, but less pronounced, coagulation time depending on the used concentration [40 s (1 mg mL^{-1}); 92 s (5 mg mL^{-1}); 109 s (10 mg mL^{-1})]. Interestingly, PEtOx without zwitterionic groups showed no influence on the coagulation characteristics (all APTT around 30 s), proving its completely inert properties in this assay. These results were confirmed by using a second APTT activator (SyntASiL), known to be sensitive to even more coagulation factors (Fig. 8C).

The elongation in coagulation times, mediated by the zwitterionic polymers, indicates an anticoagulant activity most probably *via* the intrinsic pathway and/or the common coagulation pathway. This assumption is based on the fact that an activation of extrinsic pathway components (as detectable by the applied PT assay) was not observed and the APTT assays utilized in this study are sensitive to a broad range of coagulation factors from all three pathways (factors II, V, VIII, IX, X, XI and XII).[62–65]

However, due to the partially overlapping specificity of the assays and the many coagulation factors involved in the different pathways, one can only speculate about the interactions of the investigated polymers with specific coagulation factors. It is very likely that the sulfobetaine/carboxybetaine groups interact with one or more of the downstream clotting factors, but due to the above mentioned complexity of the coagulation system, our preliminary study on the coagulation pathways does not give sufficient information to speculate on the mechanism of coagulation factor–polymer interactions. Nevertheless, it is known that zwitterionic polymers based on carboxy- and sulfobetaine functionalities exhibit anticoagulant activity, mainly attributed to the high hydrophilicity and the overall charge neutrality of the structures.[9–12,15,16,56,66]

From a methodological point of view, it might also be taken into account that the tested zwitterionic polymers interfere with the activation agents (silica particles and phospholipids), which are necessary for the induction of the coagulation *in vitro*. It is imaginable that, *e.g.*, the surface of the silica particles could be shielded by the polymers creating an interfacial hydration layer around these particles attenuating the activation reaction.

Conclusion

The blood compatibility of zwitterionic POx has been investigated with special focus on the anticoagulant activity. Therefore, a 2-oxazoline-based poly(carboxybetaine) (CB-POx) and a poly(sulfobetaine) (SB-POx) have been prepared by post-polymerization modification of P($EtOx_{30}$-*b*-$ButEnOx_{10}$). For comparison a PEtOx homopolymer with the same overall degree of polymerization (DP = 40) has been synthesized. The polymers were characterized by means of ^{1}H NMR spectroscopy and SEC, showing the suitability of the used synthesis route *via* thiol–ene photoaddition with a tertiary amine-containing thiol species followed by betainization. *In vitro* experiments revealed an excellent cytocompatibility of both the PEtOx and the zwitterionic POx-based polymers, since no viability reduction occurred in L929 mouse fibroblasts and human hepatocytes HepG2 after incubation with the polymers. Moreover, no adverse reactions with human blood occurred in terms of alterations of the whole blood viscosity. Also, no harmful effects were observed for the zwitterionic polymers and PEtOx in terms of an induction of erythrocyte aggregation or lysis accompanied by the absence of undesired platelet activation.

Additionally, no interference with the immune activation *via* the complement system was detected. Exceedingly, an anticoagulant activity *via* the components of the intrinsic and/or the common coagulation pathway was observed for the poly(carboxybetaine)s and to a lesser extent for the poly(sulfobetaine)s, but not for the PEtOx reference.

The presented properties of the zwitterionic polymers make them promising alternatives to the widely used antithrombogenic heparin and further investigations concerning the possible mode of action and *in vivo* activity should be performed. Moreover, the zwitterionic polymers display promising candidates for blood contacting materials, such as antithrombogenic membranes (*e.g.*, for blood dialysis) and implants. In addition, their excellent biocompatibility combined with their anticoagulant activity could be useful for diagnostic and targeted delivery systems with the aim to reduce unspecific interactions with blood components and thereby increase their blood circulation time.

Experimental section

Chemicals and instrumentation

1,3-Propanesultone was obtained from Sigma Aldrich. Dry acetonitrile, 2-dimethylaminoethanethiol hydrochloride, β-propiolactone, EtOx, and methyl tosylate (MeOTs) were purchased from Acros Organics. ButEnOx was prepared as described earlier.[40] EtOx, ButEnOx, and MeOTs were distilled to dryness over barium oxide (BaO), and stored under nitrogen. The synthesis of P(EtOx) homopolymer is described elsewhere.[23] The amine end-functionalization was performed according to the here reported procedure.

^{1}H NMR spectra were recorded on a Bruker AC 300 MHz at 298 K. Chemical shifts are reported in parts per million (ppm, δ scale) relative to the residual signal of the deuterated solvent.

Size exclusion chromatography (SEC) investigations of the polymers were measured on two systems: (1) an Agilent Technologies 1200 Series gel permeation chromatography system equipped with a G1329A autosampler, a G131A isocratic pump, a G1362A refractive index detector, and both a PSS Gram 30 and a PSS Gram 1000 column placed in series. As eluent a 0.21% LiCl solution in *N*,*N*-dimethylacetamide (DMAc) was used at 1 mL min^{-1} flow rate and a column oven temperature of 40 °C. (2) A Shimadzu system equipped with a SCL-10A VP system controller, a DGU-14A degasser, a LC-10AD VP pump, a RID-10A refractive index detector and a PSS SDV column running with chloroform, triethylamine (TEA), and 2-propanol (94 : 4 : 2) as eluent. The Techlab column oven was set to 50 °C. For both systems, molar masses were calculated against poly(styrene) standards.

For the photometric absorbance measurement, a TECAN Infinite M200 PRO plate reader (TECAN, Crailsheim, Germany)

was used to measure the absorption of samples from (a) the XTT cytotoxicity assay (570 nm with a background correction of the optical density (OD) at 690 nm), (b) the hemolysis of erythrocytes (540 nm with a background correction of the OD at 690 nm), (c) the photometric evaluation of erythrocyte aggregation (645 nm), and (d) the activation of complement factors C3a and SC5b-9 (450 nm). Each well containing the sample was measured in four different spots each with 10–25 flashes per scan. The evaluation of platelet activation was performed by flow cytometry (FC) measured on a Beckmann Coulter Cytomics FC-500 equipped with Uniphase Argon ion laser, 488 nm, 20 mW output and analyzed with the Cytomics CXP software. The blood coagulation time was spectroscopically determined with the clinical coagulation analyzer BCS XP 1.1 (Siemens Healthcare Diagnostics, Marburg, Germany). Viscosity measurements were conducted on an AMVn rolling ball viscometer (Anton Paar, Graz, Austria) and the density of the solutions was measured by a densitometer (DMA 4100, Anton Paar, Graz, Austria). To visualize the viability of cells after incubation with the polymers, the blue/red/green fluorescence signal of cells cultured in a 96 well plate and stained with Hoechst 33342/fluorescein diacetate (FDA)/propidium iodide (PI) was observed on a fluorescence microscope (Cell Observer Z1, Carl Zeiss, Jena, Germany) equipped with a mercury arc UV lamp and the appropriate filter combinations for excitation and detection of emission. Images of a series were captured with a 10 objective using identical instrument settings (*e.g.* UV lamp power).

Erythrocyte aggregation was observed microscopically using an inverse light microscope (Zeiss AX 10 Vert A1, 100 and 400× magnification).

Synthesis of phthalimide end-capped P(EtOx$_{30}$-*stat*-ButEnOx$_{10}$) (1)

A solution of initiator (MeOTs), solvent (acetonitrile), and monomers (EtOx, ButEnOx) was prepared with a [EtOx]/[ButEnOx]/[I] ratio of 30 : 10 : 1. The total monomer concentration was adjusted to 3 M. The solution was heated at 140 °C in a microwave synthesizer for a predetermined time and subsequently cooled to room temperature. A 2-fold excess of potassium phthalimide was added and the reaction mixture was stirred at 70 °C overnight. After filtration, the solvent was removed. The residue was dissolved in dichloromethane and washed with water, a saturated aqueous solution of $NaHCO_3$, and brine. The organic phase was dried over sodium sulfate, filtered, and concentrated. After precipitation into ice-cold diethyl ether, the polymer was dried at 40 °C.

^{1}H NMR (300 MHz, CD_3OD): δ 7.78–7.91 (br, C*H* of phthalimide), 5.79–5.95 (m, C*H*=CH_2), 4.92–5.13 (br, CH=CH_2), 3.35–4.00 (br, CH_2 backbone), 2.91–3.15 (m, initial CH_3), 2.07–2.78 (br, CH_2 side chains), 0.82–1.39 (br, CH_3 side chain).

Synthesis of amine end-functionalized P(EtOx$_{30}$-*stat*-ButEnOx$_{10}$) (2)

Phthalimide end-capped P(EtOx$_{30}$-*stat*-ButEnOx$_{10}$) was dissolved in ethanol and refluxed overnight with a 10-fold excess of hydrazine monohydrate. After cooling to room temperature, the pH was adjusted to 2–3 using concentrated HCl. The precipitate filtered off and the ethanol was evaporated. After dissolving the residue in water, aqueous NaOH was added up to pH 9 to 10. The aqueous phase was extracted thrice with chloroform. The combined organic layers were dried over sodium sulfate, concentrated, and precipitated into ice-cold diethyl ether. The white precipitate was filtered off and dried at 40 °C under reduced pressure.

^{1}H NMR (300 MHz, CD_3OD): δ 5.79–5.95 (m, C*H*=CH_2), 4.91–5.12 (br, CH=CH_2), 3.39–3.99 (br, CH_2 backbone), 2.92–3.15 (m, initial CH_3), 2.10–2.68 (br, CH_2 side chains), 0.83–1.81 (br, CH_3 side chain).

Functionalization with 2-dimethylaminoethanethiol hydrochloride (3)

A 5% solution of P(EtOx$_{30}$-*stat*-ButEnOx$_{10}$), 0.1 mol% 2,2-dimethoxy-2-phenylacetophenone (DMPA) per double bond, and a 2-fold excess per double bond of 2-dimethylaminoethanethiol hydrochloride in methanol was degassed with nitrogen for 30 min. Subsequently, the reaction mixture was stirred in a UV chamber (λ = 365 nm) overnight. The solvent was evaporated. The polymer was dissolved in water and aqueous NaOH was added up to pH 14. After evaporation of the water, chloroform was added and the salt removed by filtration. The organic phase was dried over sodium sulfate, filtered, concentrated under reduced pressure, and precipitated into ice-cold diethyl ether. The product was dried under reduced pressure at 40 °C for three days.

^{1}H NMR (300 MHz, CD_3OD): δ 3.30–3.72 (br, CH_2 backbone), 2.83–3.04 (m, initial CH_3), 2.20–2.77 (br, CH_2 side chains), 2.04–2.20 (br, N–CH_3 side chains), 0.72–1.37 (br, CH_3 side chain).

Betainization with 1,3-propanesultone (4)

To a 5% solution of P(EtOx$_{30}$-*stat*-*t*AmOx$_{10}$) in dry acetonitrile a 2-fold excess of 1,3-propanesultone per tertiary amine group was added. The reaction mixture was stirred at 60 °C overnight. Subsequently, the solvent was concentrated and the polymer precipitated into ice-cold diethyl ether. The product was dried under reduced pressure at 40 °C for three days. At last, the product was dissolved in a small amount of water and lyophilized.

^{1}H NMR (300 MHz, CD_3OD): δ 3.39–3.99 (br, CH_2 backbone), 3.09–3.27 (br, N–CH_3), 2.11–3.08 (br, CH_2 side chains), 1.47–1.87 (br, CH_2 side chain), 0.81–1.46 (br, CH_3 side chain).

Betainization with β-propiolactone (5)

To a 4.5% solution of P(EtOx$_{30}$-*stat*-*t*AmOx$_{10}$) in dry acetonitrile a 1.1-fold excess of 1,3-propanesultone per tertiary amine group was added. The reaction mixture was stirred at room temperature for one day. After evaporation of the solvent, the polymer was purified by preparative size exclusion chromatography (Sephadex® SX-1, solvent: dichloromethane). The product was dried under reduced pressure at 40 °C for three days. At last, the product was dissolved in a small amount of water and lyophilized.

^{1}H NMR (300 MHz, CD_3OD): δ 3.35–3.95 (br, CH_2 backbone), 3.03–3.23 (br, N–CH_3), 2.12–3.03 (br, CH_2 side chains), 1.47–1.93 (br, CH_2 side chain), 0.81–1.44 (br, CH_3 side chain).

Polymer cytotoxicity

For the cytotoxicity experiments, the mouse fibroblast cell line L929 and the human hepatocyte cell line HepG2 were purchased from a commercial cell bank (Cell line service, Eppelheim, Germany). The cells were routinely cultured as follows: Cell culture media [Dulbecco's modified eagle's medium (DMEM) for L929 cells and DMEM/F-12 for HepG2 cells] were supplemented with 10% fetal calf serum, 100 U mL^{-1} penicillin, and 100 μg mL^{-1} streptomycin (all components from Biochrom, Berlin, Germany) at 37 °C in a humidified atmosphere with 5% (v/v) CO_2. The cytotoxicity was determined with a XTT assay following the ISO/EN 10993 part 5 protocol: Cells (L929 and HepG2) were seeded in 96-well plates at a density of 1×10^4 cells per well and grown as monolayer cultures for 24 h. The cells were then incubated separately with different polymer concentrations (from 0.01 to 10.00 mg mL^{-1} ($n = 6$)) for 24 h. Control cells were incubated with fresh culture medium. After incubation, 50 μL of a XTT solution prepared according to the manufacturer's instructions were added to each well. After 4 h at 37 °C, 100 μL of each solution were transferred to a new microtiter plate and the optical density (OD) was measured photometrically. The negative control was standardized as 0% of metabolism inhibition and referred as 100% viability. Experiments were run in sextuplicate.

In addition, the viability of the cells after exposure to the polymers was examined microscopically using a modified fluorescein diacetate (FDA)/propidium iodide (PI) viability assay.[67]

Hemolysis of erythrocytes

For testing the hemolytic activity of the polymer solutions, blood from three unmedicated and healthy donors was collected (Institute for Transfusion Medicine, Friedrich Schiller University Jena) and stabilized by sodium citrate. After centrifugation at 4.500 × *g* for 5 min, the pellet was washed three times with cold 1.5 mM phosphate buffered saline pH 7.4 (PBS). After dilution with PBS in a ratio of 1 : 7 (number of erythrocytes approx. 2×10^6 mL^{-1}), aliquots of the erythrocyte suspension were mixed 1 : 1 with the polymer solutions (final polymer concentrations in the erythrocyte suspension of 10 mg mL^{-1}, 5 mg mL^{-1} and 1 mg mL^{-1}) and incubated in a water bath at 37 °C for 60 min. After centrifugation at 2400*g* for 5 min the hemoglobin release into the supernatant was determined spectrophotometrically using a microplate reader at 544 nm wavelength. Complete hemolysis was achieved using 1% Triton X-100 reflecting the 100% value. PBS served as negative control. Less than 5% hemolysis rate were taken as non-hemolytic. Experiments were run in triplicate and were repeated once.

Erythrocyte aggregation

Erythrocyte aggregation induced by the polymers were tested using a photometric and microscopic method according to literature.[68] Erythrocytes were isolated as described above. Erythrocyte suspensions (100 μL) containing 2 Mio erythrocytes per mL were mixed with the same volume of polymer solutions (20, 10 and 2 mg mL^{-1} diluted in PBS buffer) in a clear flat bottomed 96-well plate. The cells were incubated under vigorous shaking at 37 °C for 2 h, and the absorbance was measured at 645 nm in a microplate reader. 25 kDa bPEI (50 μg mL^{-1}) was used as positive control. As negative controls, cells were only treated with PBS. Blank values were determined with PBS and subtracted from the sample values. Absorbance values of the test solutions lower than the negative control were regarded as aggregation. Experiments were run in triplicate and were repeated once.

Additionally, erythrocyte aggregation was evaluated by microscopic observations using 10× diluted samples from the above described photometric determinations.

Blood viscosity

The influence of the polymers on blood viscosity was tested according to a formerly published setup.[31] The pooled blood of three unmedicated and healthy donors was collected (Institute for Transfusion Medicine, Friedrich Schiller University Jena) and stabilized by sodium citrate. Within 4 hours after collection, 200 μL of PBS or polymer solution (50 mg mL^{-1}, 10 mg mL^{-1} and 5 mg mL^{-1} to obtain final polymer concentrations in the whole blood of 10 mg mL^{-1}, 5 mg mL^{-1} and 1 mg mL^{-1}) were added to 800 μL of whole blood and incubated for 30 min at 37 °C. In a parallel setup, PBS was used instead of the whole blood sample to measure the dynamic viscosity of PBS and the corresponding polymer solutions. Viscosity measurements were conducted at 20 °C using an AMVn (Anton Paar, Graz, Austria) rolling ball viscometer at three inclination angles (50°/70°/85°) of the capillary. For normalization, the dynamic viscosity values of the polymers diluted in whole blood or phosphate buffered saline were divided by the viscosity value of the pure blood or PBS, respectively, and results are expressed as relative dynamic viscosity.

Platelet activation

The blood of three unmedicated and healthy donors was collected (Institute for Transfusion medicine, Friedrich Schiller University Jena) and stabilized by sodium citrate. The platelet rich plasma (PRP) was isolated by centrifugation, pooled, and used immediately. To 240 μL of PRP 60 μL of PBS or polymer solution (50 mg mL^{-1}, 10 mg mL^{-1} and 5 mg mL^{-1} to obtain final polymer concentrations in the PRP of 10 mg mL^{-1}, 5 mg mL^{-1} and 1 mg mL^{-1}) were added and incubated for 10 min or 30 min at 37 °C. To activate platelets 0.5 U mL^{-1} of bovine thrombin (Sigma, Taufkirchen, Germany) were added to the positive control instead of the polymer solution. Aliquots containing 50 μL of the incubated mixture were removed and fixed for 10 min at room temperature using 4% paraformaldehyde in PBS. After washing and centrifugation a double immuno-staining was performed using 20 μL of FITC labeled monoclonal antibody directed against CD42 and 20 μL of phycoerythrin (PE) labeled monoclonal antibody directed

against CD62P. Isotype controls were incubated with mouse IgG antibodies conjugated with fluorescein isothiocyanate (FITC) or PE dye, respectively (all antibodies were purchased from BD Biosciences, Heidelberg, Germany). After 30 min incubation at room temperature the activation state of the platelets was determined using fluorescence flow cytometry. Expression of the platelet activation marker CD62P and the constitutively present platelet marker CD42 were detected using a Beckmann Coulter Cytomics FC-500 equipped with Uniphase Argon ion laser, 488 nm, 20 mW output. Overall 100 000 platelets were measured per sample and analyzed with the Cytomics CXP software. The experiment was repeated three times.

Complement activation

The complement activation was measured on the basis of C3a anaphylatoxins with the appropriate ELISA kit (Quidel, San Diego, USA). The blood of three unmedicated and healthy donors was collected (Institute for Transfusion Medicine, Friedrich Schiller University Jena) and stabilized by sodium citrate. The plasma was isolated by centrifugation, pooled, and used immediately. 40 μL of plasma were mixed with 10 μL PBS or polymer solution (50 mg mL^{-1}, 10 mg mL^{-1} and 5 mg mL^{-1} to obtain final polymer concentrations in the plasma of 10 mg mL^{-1}, 5 mg mL^{-1} and 1 mg mL^{-1}) and incubated for 10, 30, and 60 min. Subsequently, samples, standards, and controls were diluted in the ratio 1 : 200 with sample buffer provided by the supplier and applied to a 96 well plate precoated with an antibody directed against C3a epitopes. Further incubation steps were performed according to the instructions of the supplier. The C3a concentrations were measured as absorption (at 450 nm) of the chromogenic substrate added during performance of the assay. Experiments were run in triplicate.

Blood coagulation

The blood of three unmedicated and healthy donors was collected (Institute for Transfusion Medicine, Friedrich Schiller University Jena) and stabilized by sodium citrate. The plasma was isolated by centrifugation at 4000*g* for 3 min at room temperature and used within 3 hours. The prothrombin time (PT) and the activated partial thromboplastin time (APTT) were spectroscopically determined with the clinical coagulation analyzer BCS XP 1.1 (Siemens Healthcare Diagnostics, Marburg, Germany). To 240 μL of plasma 60 μL of PBS or polymer solution (50 mg mL^{-1}, 10 mg mL^{-1} and 5 mg mL^{-1} to obtain final polymer concentrations in the plasma of 10 mg mL^{-1}, 5 mg mL^{-1} and 1 mg mL^{-1}) were added and incubated for 5 min. Experiments were run in triplicate. For the APTT determination, the intrinsic and common coagulation pathways were activated by adding 100 μL Pathrombin SL activator (Siemens Healthcare Diagnostics, Marburg, Germany) to 100 μL of the probe. After 2 min incubation at 37 °C, the coagulation was triggered by calcium chloride addition (100 μL, 0.025 M) and followed spectroscopically for up to 240 s at 671 nm. Additional samples were treated identically but with 100 μL of SyntASiL activator (Instrumentation Laboratory, Kirchheim, Germany) instead of Pathrombin SL activator. The PT was determined by addition of 100 μL of Dade Innovin activator (Siemens Healthcare Diagnostics, Marburg, Germany) to 50 μL of the plasma-polymer. The coagulation reaction was followed spectroscopically for 120 s at 671 nm. Each experiment was repeated three times.

Acknowledgements

The authors want to thank the Dutch Polymer Institute (DPI, Technology Area HTE). LT wants to thank Cornelia Bader for large-scale synthesis of ButEnOx monomer. KK is grateful to the Alexander von Humboldt foundation for financial support.

References

1 H.-W. Chien, C.-C. Tsai, W.-B. Tsai, M.-J. Wang, W.-H. Kuo, T.-C. Wei and S.-T. Huang, *Colloids Surf., B*, 2013, **107**, 152–159.
2 N. Y. Kostina, C. Rodriguez-Emmenegger, M. Houska, E. Brynda and J. Michálek, *Biomacromolecules*, 2012, **13**, 4164–4170.
3 Z. Zhang, T. Chao, S. Chen and S. Jiang, *Langmuir*, 2006, **22**, 10072–10077.
4 Z. Zhang, J. A. Finlay, L. Wang, Y. Gao, J. A. Callow, M. E. Callow and S. Jiang, *Langmuir*, 2009, **25**, 13516–13521.
5 A. Lewis, Y. Tang, S. Brocchini, J.-W. Choi and A. Godwin, *Bioconjugate Chem.*, 2008, **19**, 2144–2155.
6 Y. Asanuma, Y. Inoue, S.-I. Yusa and K. Ishihara, *Colloids Surf., B*, 2013, **108**, 239–245.
7 T. Goda and K. Ishihara, *Expert Rev. Med. Devices*, 2006, **3**, 167–174.
8 T. Shimizu, T. Goda, N. Minoura, M. Takai and K. Ishihara, *Biomaterials*, 2010, **31**, 3274–3280.
9 W.-H. Kuo, M.-J. Wang, H.-W. Chien, T.-C. Wei, C. Lee and W.-B. Tsai, *Biomacromolecules*, 2011, **12**, 4348–4356.
10 C. R. Emmenegger, E. Brynda, T. Riedel, Z. Sedlakova, M. Houska and A. B. Alles, *Langmuir*, 2009, **25**, 6328–6333.
11 Y.-J. Shih and Y. Chang, *Langmuir*, 2010, **26**, 17286–17294.
12 Y.-J. Shih, Y. Chang, A. Deratani and D. Quemener, *Biomacromolecules*, 2012, **13**, 2849–2858.
13 H.-S. Han, J. D. Martin, J. Lee, D. K. Harris, D. Fukumura, R. K. Jain and M. Bawendi, *Angew. Chem., Int. Ed.*, 2013, **52**, 1414–1419.
14 J.-T. Sun, Z.-Q. Yu, C.-Y. Hong and C.-Y. Pan, *Macromol. Rapid Commun.*, 2012, **33**, 811–818.
15 J. Cao, Y.-W. Chen, X. Wang and X.-L. Luo, *J. Biomed. Mater. Res., Part A*, 2011, **97A**, 472–479.
16 Y. Chang, W.-Y. Chen, W. Yandi, Y.-J. Shih, W.-L. Chu, Y.-L. Liu, C.-W. Chu, R.-C. Ruaan and A. Higuchi, *Biomacromolecules*, 2009, **10**, 2092–2100.
17 Y. I. Oh, G. J. Sheng, S.-K. Chang and L. C. Hsieh-Wilson, *Angew. Chem., Int. Ed.*, 2013, **52**, 11796–11799.

18 Z. Cao and S. Jiang, *Nano Today*, 2012, **7**, 404–413.
19 A. G. Kidane, H. Salacinski, A. Tiwari, K. R. Bruckdorfer and A. M. Seifalian, *Biomacromolecules*, 2004, **5**, 798–813.
20 N. Adams and U. S. Schubert, *Adv. Drug Delivery Rev.*, 2007, **59**, 1504–1520.
21 R. Luxenhofer, Y. Han, A. Schulz, J. Tong, Z. He, A. V. Kabanov and R. Jordan, *Macromol. Rapid Commun.*, 2012, **33**, 1613–1631.
22 H. Schlaad, C. Diehl, A. Gress, M. Meyer, A. L. Demirel, Y. Nur and A. Bertin, *Macromol. Rapid Commun.*, 2010, **31**, 511–525.
23 M. Bauer, C. Lautenschlaeger, K. Kempe, L. Tauhardt, U. S. Schubert and D. Fischer, *Macromol. Biosci.*, 2012, **12**, 986–998.
24 M. Bauer, S. Schroeder, L. Tauhardt, K. Kempe, U. S. Schubert and D. Fischer, *J. Polym. Sci., Part A: Polym. Chem.*, 2013, **51**, 1816–1821.
25 L. Tauhardt, K. Kempe, M. Gottschaldt and U. S. Schubert, *Chem. Soc. Rev.*, 2013, **42**, 7998–8011.
26 J. Kronek, J. Lustoň, Z. Kroneková, E. Paulovičová, P. Farkaš, N. Petrenčíková, L. Paulovičová and I. Janigová, *J. Mater. Sci.: Mater. Med.*, 2010, **21**, 879–886.
27 J. Kronek, E. Paulovičová, L. Paulovičová, Z. Kroneková and J. Lustoň, *J. Mater. Sci.: Mater. Med.*, 2012, **23**, 1457–1464.
28 V. R. de la Rosa, *J. Mater. Sci.: Mater. Med.*, 2014, **25**, 1211–1225.
29 K. Knop, R. Hoogenboom, D. Fischer and U. S. Schubert, *Angew. Chem., Int. Ed.*, 2010, **49**, 6288–6308.
30 T. X. Viegas, M. D. Bentley, J. M. Harris, Z. Fang, K. Yoon, B. Dizman, R. Weimer, A. Mero, G. Pasut and F. M. Veronese, *Bioconjugate Chem.*, 2011, **22**, 976–986.
31 K. Knop, D. Pretzel, A. Urbanek, T. Rudolph, D. H. Scharf, A. Schallon, M. Wagner, S. Schubert, M. Kiehntopf, A. A. Brakhage, F. H. Schacher and U. S. Schubert, *Biomacromolecules*, 2013, **14**, 2536–2548.
32 R. Hoogenboom, *Angew. Chem., Int. Ed.*, 2009, **48**, 7978–7994.
33 A. Makino and S. Kobayashi, *J. Polym. Sci., Part A: Polym. Chem.*, 2010, **48**, 1251–1270.
34 O. Sedlacek, B. D. Monnery, S. K. Filippov, R. Hoogenboom and M. Hruby, *Macromol. Rapid Commun.*, 2012, **33**, 1648–1662.
35 B. Guillerm, S. Monge, V. Lapinte and J.-J. Robin, *Macromol. Rapid Commun.*, 2012, **33**, 1600–1612.
36 K. Aoi and M. Okada, *Prog. Polym. Sci.*, 1996, **21**, 151–208.
37 E. Rossegger, V. Schenk and F. Wiesbrock, *Polymers*, 2013, **5**, 956–1011.
38 C. Diehl and H. Schlaad, *Macromol. Biosci.*, 2009, **9**, 157–161.
39 C. Diehl and H. Schlaad, *Chem.–Eur. J.*, 2009, **15**, 11469–11472.
40 A. Gress, A. Völkel and H. Schlaad, *Macromolecules*, 2007, **40**, 7928–7933.
41 T. R. Dargaville, R. Forster, B. L. Farrugia, K. Kempe, L. Voorhaar, U. S. Schubert and R. Hoogenboom, *Macromol. Rapid Commun.*, 2012, **33**, 1695–1700.
42 B. L. Farrugia, K. Kempe, U. S. Schubert, R. Hoogenboom and T. R. Dargaville, *Biomacromolecules*, 2013, **14**, 2724–2732.
43 K. Kempe, R. Hoogenboom, M. Jaeger and U. S. Schubert, *Macromolecules*, 2011, **44**, 6424–6432.
44 K. Kempe, R. Hoogenboom and U. S. Schubert, *Macromol. Rapid Commun.*, 2011, **32**, 1484–1489.
45 K. Kempe, A. Vollrath, H. W. Schaefer, T. G. Poehlmann, C. Biskup, R. Hoogenboom, S. Hornig and U. S. Schubert, *Macromol. Rapid Commun.*, 2010, **31**, 1869–1873.
46 J. Kronek, Z. Kroneková, J. Lustoň, E. Paulovičová, L. Paulovičová and B. Mendrek, *J. Mater. Sci.: Mater. Med.*, 2011, **22**, 1725–1734.
47 J. Kronek, E. Paulovičová, L. Paulovičová, Z. Kroneková and J. Lustoň, in *Practical Applications in Biomedical Engineering*, ed. A. A. Pereira, A. O. Andrade, E. L. M. Naves and A. B. Soares, InTech, Rijeka, Croatia, 2013, pp. 257–284.
48 R. Luxenhofer, G. Sahay, A. Schulz, D. Alakhova, T. K. Bronich, R. Jordan and A. V. Kabanov, *J. Control. Release*, 2011, **153**, 73–82.
49 X. Wang, X. Sun, G. Jiang, R. Wang, R. Hu, X. Xi, Y. Zhou, S. Wang and T. Wang, *J. Appl. Polym. Sci.*, 2013, **128**, 3289–3294.
50 M. Sun, L. Yang, P. Jose, L. Wang and J. Zweit, *J. Mater. Chem. B*, 2013, **1**, 6137–6146.
51 W. Lin, Z. Wang and S. Chen, *Functional Polymers for Nanomedicine*, The Royal Society of Chemistry, 2013, pp. 227–244.
52 R. K. Kainthan, S. R. Hester, E. Levin, D. V. Devine and D. E. Brooks, *Biomaterials*, 2007, **28**, 4581–4590.
53 C. Lenz, A. Rebel, K. F. Waschke, R. C. Koehler and T. Frietsch, *Transfus. Altern. Transfus. Med.*, 2008, **9**, 265–272.
54 C. A. Janeway, P. Travers and M. Walport, in *Immunobiology: The Immune System in Health and Disease*, Garland Science, New York, 5th edn, 2001.
55 R. K. Kainthan, J. Janzen, E. Levin, D. V. Devine and D. E. Brooks, *Biomacromolecules*, 2006, **7**, 703–709.
56 X. Wang, X. Chen, L. Xing, C. Mao, H. Yu and J. Shen, *J. Mater. Chem. B*, 2013, **1**, 5036–5044.
57 R. Luxenhofer, A. Schulz, C. Roques, S. Li, T. K. Bronich, E. V. Batrakova, R. Jordan and A. V. Kabanov, *Biomaterials*, 2010, **31**, 4972–4979.
58 R. Donev, N. Koseva, P. Petrov, A. Kowalczuk and J. Thome, *The World Journal of Biological Psychiatry*, 2011, **12**, 44–51.
59 C. Pallister, A. Garner and M. S. Watson, *Haematology*, Scion Publishing Limited, 2010.
60 R. Bader, P. M. M. Mannucci, A. Tripodi, J. Hirsh, F. Keller, E. M. Solleder, P. Hawkins, M. Peng, H. Pelzer, L. M. Teijidor, I. F. Ramirez and H. J. Holde, *Thromb. Haemost.*, 1994, **71**, 292–299.
61 R. Gosselin, W. Dager, A. Roberts, L. Freeman, L. Gandy, J. Gregg and D. Dwyre, *Am. J. Clin. Pathol.*, 2011, **136**, 848–854.
62 D. C. Turi and E. I. Peerschke, *Am. J. Clin. Pathol.*, 1986, **85**, 43–49.
63 E. A. Vandervelde and L. Poller, *Thromb. Haemost.*, 1995, **73**, 73–81.

64 J. T. Brandt, D. A. Triplett, W. A. Rock, E. G. Bovill and C. F. Arkin, *Arch. Pathol. Lab. Med.*, 1991, **115**, 109–114.
65 A. Bowyer, S. Kitchen and M. Makris, *Int. J. Lab. Hematol.*, 2011, **33**, 154–158.
66 S.-H. Chen, Y. Chang, K.-R. Lee, T.-C. Wei, A. Higuchi, F.-M. Ho, C.-C. Tsou, H.-T. Ho and J.-Y. Lai, *Langmuir*, 2012, **28**, 17733–17742.
67 H. Ahrem, D. Pretzel, M. Endres, D. Conrad, J. Courseau, H. Müller, R. Jaeger, C. Kaps, D. O. Klemm and R. W. Kinne, *Acta Biomater.*, 2014, **10**, 1341–1353.
68 A. Vollrath, D. Pretzel, C. Pietsch, I. Perevyazko, S. Schubert, G. M. Pavlov and U. S. Schubert, *Macromol. Rapid Commun.*, 2012, **33**, 1791–1797.

Electronic Supplementary Material (ESI) for Polymer Chemistry.

Supporting Info

Zwitterionic poly(2-oxazoline)s as promising candidates for blood contacting applications

Lutz Tauhardt,[1,2] David Pretzel,[1,2] Kristian Kempe,[1,2,#] Michael Gottschaldt,[1,2] Dirk Pohlers,[4] Ulrich S. Schubert*[1,2,3]

[1]Laboratory of Organic and Macromolecular Chemistry (IOMC), Friedrich Schiller University Jena, Humboldtstr. 10, 07743 Jena, Germany.

[2]Jena Center for Soft Matter (JCSM), Friedrich Schiller University Jena, Philosophenweg 7, 07743 Jena, Germany.

[3]Dutch Polymer Institute (DPI), John F. Kennedylaan 2, 5612 AB Eindhoven, The Netherlands.

[4]Centre for Diagnostic at the Clinic of Chemnitz, Flemmingstraße 2, 09116 Chemnitz, Germany

[#]Current address: Department of Chemical and Biomolecular Engineering, The University of Melbourne, Victoria 3010, Australia.

Corresponding author footnote: Fax. +49 3641 948 202; Email: ulrich.schubert@uni-jena.de

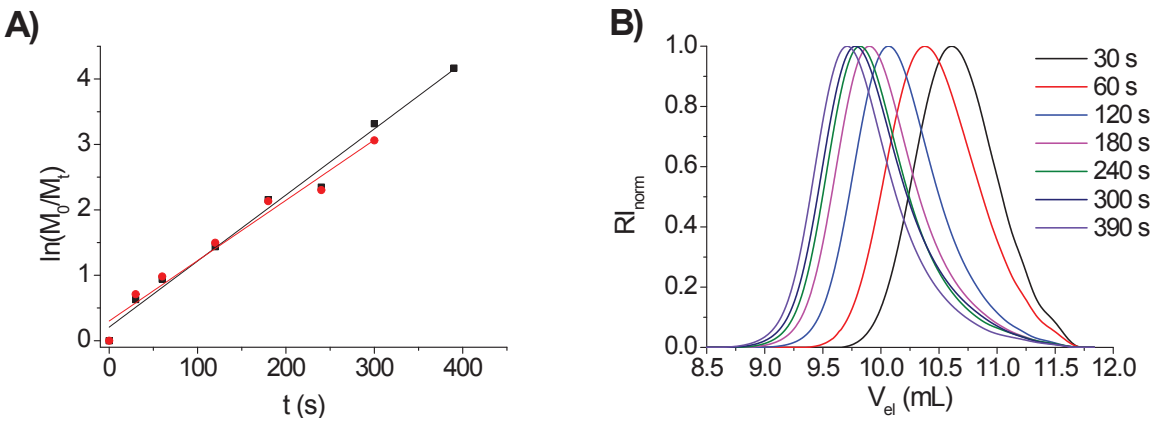

Figure S1. A) First-order kinetic plots of the copolymerization of EtOx (square) and ButEnOx (circle) at 140 °C with a total monomer concentration of 1 M and a [EtOx]:[ButEnOx]:[MeOTs] ratio of 16:4:1. B) SEC curves kinetic study after different times.

Table S1. Data of the kinetic study.

Time	Conversion of EtOx:ButEnOx (%)[a)]	M_n (g/mol)[b)]	PDI[b)]
30	47:51	900	1.22
60	61:63	1,115	1.25
120	76:78	1,590	1.22
180	88:88	1,850	1.23
240	90:90	1,980	1.23
300	96:95	2,020	1.24
390	98:100	2,250	1.23

[a)]Determined by GC. [b)]Determined by SEC (chloroform/TEA/2-propanol 94:4:2, calibration against PS).

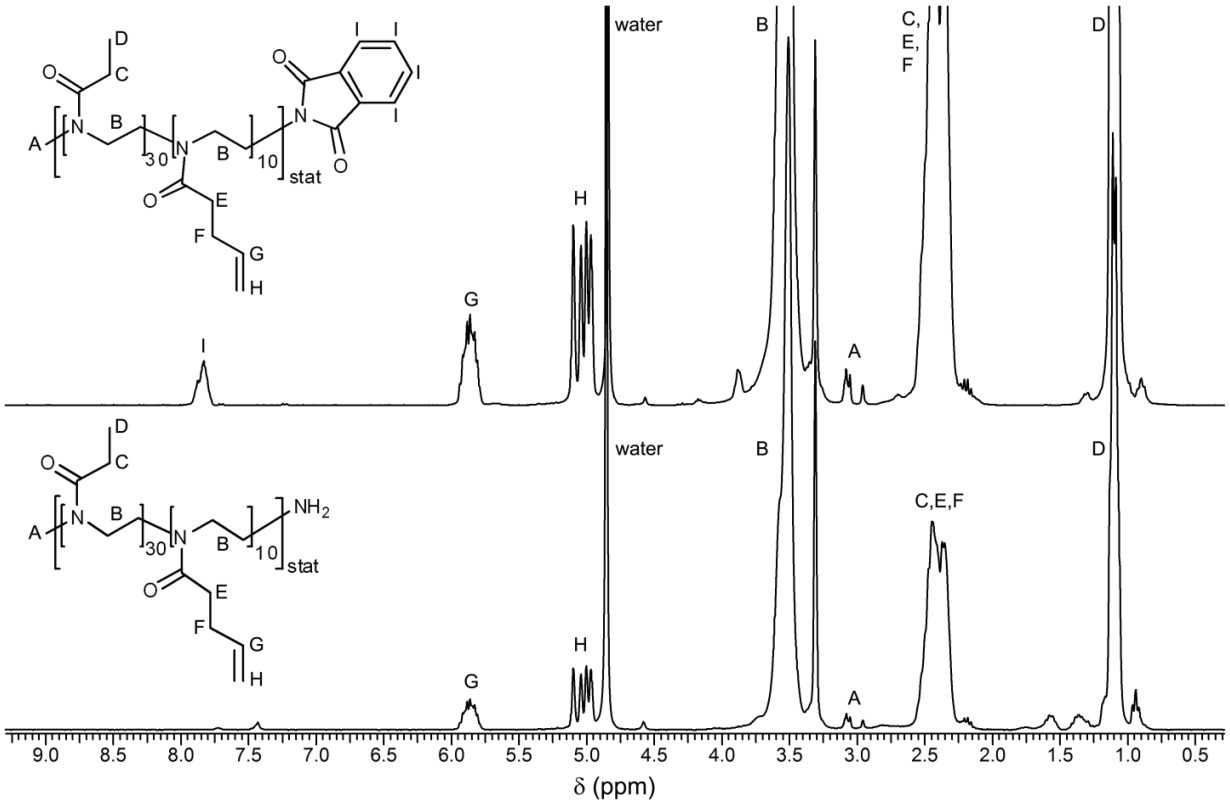

Figure S2. ^{1}H NMR spectra of (top) phthalimide end-capped and (bottom) amine end-functionalized polymer (300 MHz, CD_3OD).

Table S2. SEC data of the different polymers.

Compound	DMAc + 0.21% LiCl		$CHCl_3$ + TEA + iPrOH (94:4:2)	
	M_n (g/mol)[b]	PDI[b]	M_n (g/mol)[b]	PDI[b]
1	6,860	1.16	4,590	1.16
2	6,980	1.19	3,920	1.16
3	7,740	1.20	4,820	1.18
4	7,860	1.24	4,720	1.19
5	8,200	1.35	-[a]	-[a]
6	8,150	1.59	3,640	1.27
PEtOx	6,600	1.21	4,830	1.15

[a] Insoluble in the solvent. [b] Calibration against PS.

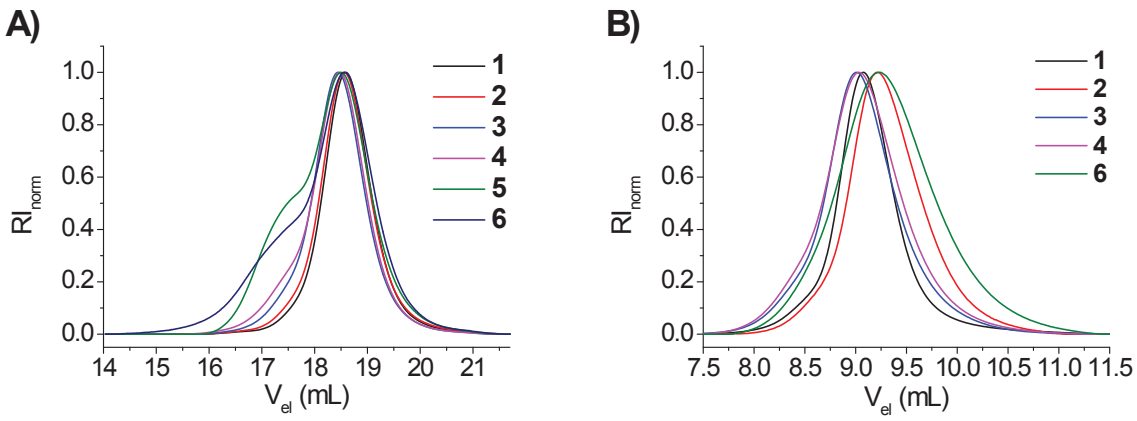

Figure S3. SEC curves of the different polymers. SEC running with A) DMAc + 0.21% LiCl, and B) $CHCl_3$ + TEA + iPrOH (94:4:2).

Publication 6

"Synthesis and *in vitro* activity of platinum containing 2-oxazoline-based glycopolymers"

L. Tauhardt, D. Pretzel, S. Bode, J. Czaplewska, K. Kempe, M. Gottschaldt, U. S. Schubert

J. Polym. Sci., Part A: Polym. Chem. **2014**, *52*, 2703–2714

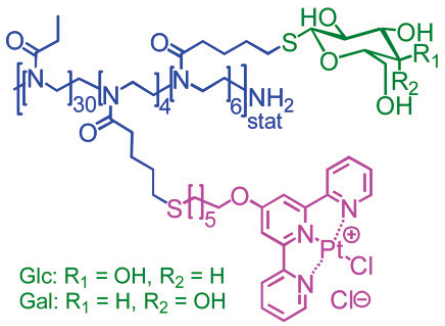

Synthesis and *In Vitro* Activity of Platinum Containing 2-Oxazoline-Based Glycopolymers

Lutz Tauhardt,[1,2] David Pretzel,[1,2] Stefan Bode,[1,2] Justyna A. Czaplewska,[1,2] Kristian Kempe,[1,2*] Michael Gottschaldt,[1,2] Ulrich S. Schubert[1,2,3]

[1]Laboratory of Organic and Macromolecular Chemistry (IOMC), Friedrich Schiller University Jena, Humboldtstr. 10, 07743 Jena, Germany

[2]Jena Center for Soft Matter (JCSM), Friedrich Schiller University Jena, Philosophenweg 7, 07743 Jena, Germany

[3]Dutch Polymer Institute (DPI), John F. Kennedylaan 2, 5612 AB Eindhoven, The Netherlands

Correspondence to: U. S. Schubert (E-mail: ulrich.schubert@uni-jena.de)

Received 27 March 2014; accepted 15 May 2014; published online 9 July 2014

DOI: 10.1002/pola.27290

ABSTRACT: We report the synthesis of glyco(poly(2-oxazoline)s) functionalized with Pt(II) units for targeted tumor applications. To this end, poly(2-ethyl-2-oxazoline-*block*-2-(3-butenyl)-2-oxazoline) is modified with thiol-modified acetyl protected glucose and galactose, respectively, and terpyridine (tpy) units using thiol-ene photoaddition. Deprotection of the sugars with sodium methoxide and treatment with $Pt(COD)Cl_2$ applying a mild synthesis route yields polymers with monosaccharide targeting moieties and cytotoxic Pt(II) units. The polymers and intermediates are characterized by ^1H nuclear magnetic resonance spectroscopy and size exclusion chromatography. Subsequently, the hemolytic activity, induction of erythrocyte aggregation as well as the cytotoxicity against mouse fibroblast L929 cells, human embryonic kidney cells HEK 293, and human hepatocytes HepG2 are studied. The comparison to cisplatin, the standard for cancer therapy, demonstrates the potential of the presented system. © 2014 Wiley Periodicals, Inc. J. Polym. Sci., Part A: Polym. Chem. **2014**, *52*, 2703–2714

KEYWORDS: biological applications of polymers; cationic polymerization, copolymerization; functionalization of polymers; glycopolymer; poly(2-oxazoline); ring-opening polymerization

INTRODUCTION Platinum-based drugs are of high interest for anticancer applications. The most prominent example is *cis*-$[PtCl_2(NH_3)_2]$ (cisplatin), a chemotherapeutic drug that induces apoptosis, that is, programmed cell death, by inter- and intrastrand DNA-crosslinking processes.[1–3] However, severe side effects such as renal toxicity, gastrointestinal toxicity, and neurotoxicity as well as acquired and intrinsic cisplatin resistance of various cancer types have led to the search for alternatives.[2–5] Modern drugs aim for selective transport to the cancer cells by active and passive targeting.[1–3,5–10] The latter can be achieved by exploiting the so called enhanced permeability and retention (EPR) effect, that is the preferred accumulation of molecules of a certain size in tumor tissue. Such molecules can be, for example, drug-loaded nanoparticles, nanospheres, liposomes, carbon nanotubes, and polymeric dendrimers or micelles. Particularly, polymer-based systems are of high interest.[2,3,9,10] Their broad diversity makes them ideal materials for drug complexation or encapsulation. In this context, an often used material is oligo- or poly(ethylene glycol) (PEG), since it is nontoxic, water soluble, and shows the so called "stealth effect."[11] However, to not only rely on a possible EPR effect and to increase the drug selectivity, active targeting has previously attracted increasing interest. Since certain receptors are often overexpressed in tumor cells, this can be achieved by functionalization with bioactive substances such as proteins (e.g., transferrin), hormones (e.g., estrogen), amino acids, folic acid, and saccharides.[5,6,9,12] In particular the latter are interesting, as cancer cells commonly display an altered sugar metabolism, for example, a high glucose consumption for energy production.[5] Moreover, they possess specific saccharide receptors exclusively expressed by certain cancers. It was shown by Stenzel et al. that micellar gold-glycopolymer complexes display a high activity against OVCAR-3 human ovarian carcinoma cells.[13] Recently, Wild et al. reported, a poly(pentafluorostyrene)-based glycopolymer, carrying galactose as targeting unit and a terpyridine (tpy) complexed Pt(II) species as active agent, which revealed a higher activity against cisplatin-resistant Nalm-6 leukemia cells than cisplatin.[14] Hence, it showed a higher

*Present address: Department of Chemical and Biomolecular Engineering, The University of Melbourne, Victoria 3010, Australia

Additional Supporting Information may be found in the online version of this article.

apoptotic activity, even in cells resistant to common chemotherapeutic agents. The mechanism of action, which causes apoptosis, is most probably the DNA-intercalation and is well known for square-planar tpy-Pt(II) complexes.[15–17] Although the chosen synthesis method by thiol-*p*-fluorine "click" allowed the synthesis of tailor-made polymers with the possibility to tune the amount of sugar and platinum, the use of PPFS as backbone resulted in poor water solubility. This problem can be overcome by using poly(2-oxazoline)s (POx), a versatile class of polymers, which can be prepared with a narrow molar mass distribution by the living cationic ring-opening polymerization (CROP) of 2-oxazolines. Moreover, the broad variety of initiators, terminating agents, and monomers enable the preparation of tailor-made polymers whose functional groups can be exploited for post-polymerization reactions. The most prominent examples are the water soluble poly(2-methyl-2-oxazoline) and poly(2-ethyl-2-oxazoline) (PEtOx). They are investigated as PEG alternatives, since they not only show similar positive properties as PEG (e.g., "stealth effect,"[18,19] "antifouling" properties[20,21]) but also exhibit some advantageous features such as higher stability,[22] lower viscosity,[18,23] and a less demanding synthesis. The copolymerization with other 2-oxazolines, namely 2-(3-butenyl)-2-oxazoline (ButEnOx) and 2-(9-decenyl)-2-oxazoline), enables the post-polymerization functionalization or hydrogel formation via thiol-ene photoaddition.[24–31] Applying this approach, it is possible to attach sugar units as targeting moieties.[25,26,28–30] In the same manner, it is possible to incorporate anticancer active units by photoaddition of tpy-thiols (tpy-SH) and subsequent platinum complexation. Tpy-thiols are described in literature but have not been attached to POx so far.[32,33] Here we describe the synthesis of Pt(II) containing, water soluble, 2-oxazoline based glycopolymers. To this end, a copolymer of EtOx and ButEnOx was synthesized and partially functionalized with tpy via thiol-ene photoaddition. In a next step acetyl protected galactose (Ac_4Gal) and glucose (Ac_4Glc), respectively, were attached using the same approach. After deprotection of the sugars, the active anticancer agent was formed by complexation of the platinum under mild conditions. The resulting polymer architecture is advantageous, since the covalent binding of the tpy-Pt complex prevents its uncontrolled release. All polymers were characterized structurally and their *in vivo* activity has been investigated.

EXPERIMENTAL

Chemicals and Instrumentation

Dry acetonitrile, dry methanol, EtOx, and methyl tosylate (MeOTs) were purchased from Acros Organics. ButEnOx was prepared as described earlier.[28] EtOx, ButEnOx, and MeOTs were distilled to dryness over barium oxide (BaO), and stored under nitrogen. Dichloro(1,5-cyclooctadiene)platinum(II) (Pt(COD)Cl_2), sodium methoxide in methanol (0.5 M), and 2,2-dimethoxy-2-phenylacetophenone (DMPA) were obtained from Sigma Aldrich. 2,3,4,6-Tetra-*O*-acetyl-*β*-D-1-thioglucopyranoside (Ac_4GlcSH) and 2,3,4,6-tetra-*O*-acetyl-*β*-D-1-thioglacatopyranoside (Ac_4GalSH) were prepared according to the literature.[34] 6-([2,2′:6′,2″′-Terpyridin]-4′-yloxy)hexane-1-thiol was synthesized analogically to other known terpyridine thiols (Supporting Information).[35]

For the polymerizations, an Initiator Sixty single-mode microwave synthesizer from Biotage, equipped with a noninvasive IR sensor (accuracy: ±2%) was used. ^{1}H nuclear magnetic resonance (NMR) spectra were recorded on a Bruker AC 300 and 250 MHz at 298 K. Chemical shifts are reported in parts per million (ppm, δ scale) relative to the residual signal of the deuterated solvent.

Size exclusion chromatographies (SEC) of the polymers were measured on an Agilent Technologies 1200 Series gel permeation chromatography system equipped with a G1329A autosampler, a G131A isocratic pump, a G1362A refractive index detector, and both a PSS Gram 30 and a PSS Gram 1000 column placed in series. As eluent a 0.21% LiCl solution in *N,N*-dimethylacetamide (DMAc) was used at 1 mL min^{-1} flow rate and a column oven temperature of 40 °C. Molar masses were calculated against poly(styrene).

Synthesis of Phthalimide End-Functionalized P($EtOx_{30}$-*stat*-$ButEnOx_{10}$) (1)

Prior to the reaction the kinetics of the copolymerization of EtOx and ButEnOx have been investigated (see Supporting Information).

A solution of initiator (MeOTs), solvent (acetonitrile), and monomers (EtOx, ButEnOx) was prepared with a [EtOx]/[ButEnOx]/[I] ratio of 30:10:1 and a total monomer concentration of 3 M. The solution was heated at 140 °C in a microwave synthesizer for a predetermined time. After cooling to room temperature a twofold excess of potassium phthalimide was added and the reaction mixture was stirred at 70 °C overnight. The reaction mixture was filtered and the solvent was removed under reduced pressure. Subsequently, the residue was dissolved in dichloromethane and washed with water, a saturated aqueous solution of $NaHCO_3$, and brine. The organic phase was dried over sodium sulfate, filtered, and concentrated. After precipitation into ice-cold diethyl ether, the polymer was dried at 40 °C.

^{1}H NMR (300 MHz, $CDCl_3$, δ): 7.59–7.94 (br, C*H* of phthalimide), 5.55–5.99 (m, C*H*═CH_2), 4.64–5.19 (br, CH═CH_2), 3.07–4.02 (br, CH_2 backbone), 2.81–3.07 (m, initial CH_3), 1.98–2.68 (br, CH_2 side chains), 0.68–1.39 (br, CH_3 side chain).

Synthesis of Amine End-Functionalized P($EtOx_{30}$-*stat*-$ButEnOx_{10}$) (2)

Phthalimide end-capped P($EtOx_{30}$-*stat*-$ButEnOx_{10}$) was dissolved in ethanol, a 10-fold excess of hydrazine monohydrate was added, and the reaction mixture was refluxed overnight. After cooling to room temperature, concentrated HCl was added up to pH = 2–3. The precipitate was removed by filtration. The ethanol was evaporated and the residue was dissolved in water. Aqueous NaOH was added up to pH = 9–10 and the aqueous solution was extracted thrice with

chloroform. The combined organic layers were dried over sodium sulfate, concentrated, and precipitated into ice-cold diethyl ether. The white precipitate was filtered off and dried at 40 °C under reduced pressure.

^{1}H NMR (300 MHz, $CDCl_3$, δ): 5.65–5.97 (m, C*H*═CH_2), 4.81–5.18 (br, CH═CH_2), 3.06–4.17 (br, CH_2 backbone), 2.75–3.05 (m, initial CH_3), 1.87–2.65 (br, CH_2 side chains), 0.54–1.43 (br, CH_3 side chain).

Thiol-ene Functionalization of P(EtOx$_{30}$-*stat*-ButEnOx$_{10}$) with 6-([2,2′:6′,2″-terpyridin]-4′-yloxy)hexane-1-thiol (3)

To a 5 mass% solution of **2** in THF/methanol (1:0.2) the photocatalyst DMPA (0.04 equiv. per double bond) and tpy-SH (0.4 equiv. per double bond) were added. After degassing with nitrogen for 30 min, the reaction mixture was exposed to UV light (365 nm) overnight. The solvent was evaporated, the residue dissolved in chloroform, and washed twice with a 0.1 M EDTA solution, followed by washing with a saturated aqueous solution of $NaHCO_3$ and brine. The organic layer was dried over sodium sulfate, concentrated, and precipitated into ice-cold diethyl ether. The polymer was filtered off and dried under reduced pressure at 40 °C.

^{1}H NMR (300 MHz, $CDCl_3$, δ): 8.47–8.79 (C*H* of tpy), 7.72–7.91 (C*H* of typ), 7.17–7.48 (C*H* of typ), 5.64–5.97 (m, C*H*═CH_2), 4.87–5.17 (br, CH═CH_2), 4.12–4.34 (—CH_2—O—typ), 3.09–4.10 (br, CH_2 backbone), 2.83–3.09 (m, initial CH_3), 2.64–2.83 (br, —CH_2—S—CH_2—), 2.01–2.64 (br, CH_2 side chains), 1.40–2.00 (br, CH_2 side chains), 0.73–1.39 (br, CH_3 side chain).

Thiol-ene Functionalization with Ac_4GlcSH (4) and Ac_4GalSH (5)

To a 5 mass% solution P(EtOx$_{30}$-*stat*-ButEnOx$_6$-*stat*-tpyButOx$_4$) (**3**) in THF the photocatalyst DMPA (0.1 equiv. per double bond), and Ac_4GlcSH or Ac_4GalSH (4 equiv. per double bond), respectively, were added. After degassing with nitrogen for 30 min, the reaction mixture was exposed to UV light (365 nm) overnight. The solvent was concentrated *in vacuo* and the polymer was isolated by preparative SEC (Bio-Beads® S-X1, THF). The solvent was evaporated and the polymer was dried at 40 °C under reduced pressure.

4 (Glc): ^{1}H NMR (300 MHz, CD_3OD, δ): 8.52–8.79 (C*H* of tpy), 7.81–8.12 (C*H* of typ), 7.35–7.61 (C*H* of typ), 4.62–5.54 (m, sugar), 3.77–4.45 (m, sugar), 3.69–3.76 (m, CH_2—O—tpy), 3.20–3.69 (br, CH_2 backbone), 2.94–3.15 (m, initial CH_3), 2.60–2.93 (br, —CH_2—S—), 2.14–2.59 (br, CH_2 side chains), 1.91–2.12 (—OAc), 1.45–1.91 (br, CH_2 side chains), 0.80–1.45 (br, CH_3 side chain).

5 (Gal): ^{1}H NMR (300 MHz, CD_3OD, δ): 8.50–8.83 (C*H* of tpy), 7.80–8.13 (C*H* of typ), 7.35–7.61 (C*H* of typ), 4.47–5.64 (m, sugar), 3.79–4.44 (m, sugar), 3.70–3.78 (m, CH_2—O—tpy), 3.19–3.78 (br, CH_2 backbone), 2.94–3.18 (m, initial CH_3), 2.62–2.94 (br, —CH_2—S—), 2.24–2.61 (br, CH_2 side chains), 1.91–2.23 (—OAc), 1.45–1.90 (br, CH_2 side chains), 0.81–1.45 (br, CH_3 side chain).

Deprotection of Glucose and Galactose (6, 7)

The respective sugar functionalized polymer was dissolved in dry methanol. A 0.5 M solution of sodium methoxide (1 equiv. per sugar) in methanol was added and the reaction mixture was stirred at room temperature for 1 h. The solvent was removed and the residue was dissolved in water. Subsequently, the polymer was purified by dialysis against water. The water was evaporated and the product was dried under reduced pressure at 40 °C.

6 (Glc): ^{1}H NMR (300 MHz, CD_3OD, δ): 8.49–8.74 (C*H* of tpy), 7.81–8.08 (C*H* of typ), 7.29–7.55 (C*H* of typ), 4.15–4.49 (m, C*H* sugar), 3.80–3.98 (m, C*H* sugar), 3.25–3.79 (br, CH_2 backbone), 3.13–3.25 (m, C*H* sugar), 3.02–3.13 (m, initial CH_3), 2.61–3.01 (br, —CH_2—S—), 2.10–2.62 (br, CH_2 side chains), 1.45–2.10 (br, CH_2 side chains), 0.79–1.44 (br, CH_3 side chain).

7 (Gal): ^{1}H NMR (300 MHz, CD_3OD, δ): 8.51–8.75 (C*H* of tpy), 7.82–8.07 (C*H* of typ), 7.34–7.59 (C*H* of typ), 4.13–4.45 (br, C*H* sugar), 3.83–3.98 (br, C*H* sugar), 3.66–3.81 (m, —CH_2—O—tpy), 3.17–3.66 (br, CH_2 backbone), 3.01–3.13 (m, initial CH_3), 2.62–2.98 (br, —CH_2—S—), 2.06–2.62 (br, CH_2 side chains), 1.45–2.02 (br, CH_2 side chains), 0.79–1.44 (br, CH_3 side chain).

Complexation with Platinum (8, 9)

The deprotected polymer was dissolved in water. After addition of Pt(COD)Cl_2 (1 equiv. per tpy unit) the reaction mixture was heated at 70 °C until all Pt compound was dissolved (35–40 min). A color change to yellow could be observed. Subsequently, the water phase was washed five times with diethyl ether. The water was evaporated and the yellow product was dried at 40 °C under reduced pressure.

8 (Glc): ^{1}H NMR (300 MHz, CD_3OD, δ): 7.32–8.87 (C*H* of tpy), 3.81–4.75 (m, C*H* sugar), 3.25–3.80 (br, CH_2 backbone), 3.14–3.26 (m, C*H* sugar), 3.03–3.14 (m, initial CH_3), 2.64–3.03 (br, —CH_2—S—), 2.10–2.62 (br, CH_2 side chains), 1.47–2.10 (br, CH_2 side chains), 0.82–1.47 (br, CH_3 side chain).

9 (Glc): ^{1}H NMR (300 MHz, CD_3OD, δ): 7.35–8.89 (C*H* of tpy), 3.81–4.65 (m, C*H* sugar), 3.67–3.81 (m, CH_2—O—tpy), 3.15–3.67 (br, CH_2 backbone), 3.00–3.15 (m, initial CH_3), 2.65–3.00 (br, —CH_2—S—), 2.10–2.65 (br, CH_2 side chains), 1.45–2.10 (br, CH_2 side chains), 0.71–1.45 (br, CH_3 side chain).

Polymer Cytotoxicity

For the cytotoxicity screening, the mouse fibroblast cell line L929, the human embryonic kidney cell line HEK 293, and the human hepatocyte cell line HepG2 were purchased from a commercial cell bank (Cell line service, Eppelheim, Germany). The cells were routinely cultured as follows: Cell culture media [Dulbecco's modified eagle's medium (DMEM) for L929 cells, Eagle's Minimum Essential Medium (EMEM) for HEK 293 cells, and DMEM/F-12 for HepG2 cells] were supplemented with 10% fetal calf serum, 100 U mL^{-1} penicillin, and 100 μg mL^{-1} streptomycin (all components from

Biochrom, Berlin, Germany) at 37 °C in a humidified atmosphere with 5% (v/v) CO_2. The cytotoxicity was determined with a XTT assay following the ISO/EN 10993 part 5 protocol: Cells (L929, HEK 293, and HepG2) were seeded in 96-well plates at a density of 1×10^4 cells/well and grown as monolayer cultures for 24 h. The cells were then incubated separately with different concentrations of the glycopolymers (from 0.0012 to 1.256 mM) or cisplatin (from 0.005 to 4.833 mM) for 24 h. The chosen glycopolymer and cisplatin concentrations were comparable in terms of an equimolar concentration of platinum moieties in the final solutions. Control cells were incubated with fresh culture medium. After incubation, 50 μL of a XTT solution prepared according to the manufacturer's instructions were added to each well. After 4 h at 37 °C, 100 μL of each solution were transferred to a new microtiter plate and the optical density (OD) was measured photometrically. The negative control was standardized as 0% of metabolism inhibition and referred as 100% viability. Experiments were run in sextuplicate.

In addition, the viability of the cells after exposure to the polymers was examined microscopically using a modified fluorescein diacetate (FDA)/propidium iodide (PI) viability assay.[36]

Hemolysis of Erythrocytes

For testing the hemolytic activity of the glycopolymer and cisplatin solutions, blood from three unmedicated and healthy donors was collected (Institute for Transfusion Medicine, Friedrich Schiller University Jena) and stabilized by sodium citrate. After centrifugation at 4500 g for 5 min, the pellet was washed three times with cold 1.5 mM phosphate buffered saline pH 7.4 [phosphate buffered saline (PBS)]. After dilution with PBS in a ratio of 1:7 (number of erythrocytes $\sim 2 \times 10^6$ mL^{-1}), aliquots of the erythrocyte suspension were mixed 1:1 with the glycopolymer or cisplatin solutions (final concentrations in the erythrocyte suspension: 1.25628, 0.62814, 0.25126, 0.12563, and 0.01256 for both glycopolymers and 4.83372, 2.41686, 0.96674, 0.48337, and 0.04834 mM for cisplatin) and incubated in a water bath at 37 °C for 60 min. After centrifugation at 2400 g for 5 min the hemoglobin release into the supernatant was determined spectrophotometrically using a microplate reader at 544 nm wavelength. Complete hemolysis was achieved using 1% Triton X-100 reflecting the 100% value. PBS served as negative control. Less than 5% hemolysis rate were taken as non-hemolytic. Experiments were run in triplicates and were repeated once.

Erythrocyte Aggregation

Erythrocyte aggregation induced by the polymers was tested according to literature using a photometric and a microscopic method.[37] Erythrocytes were isolated as described above. Erythrocyte suspensions (100 μL) containing 2×10^6 erythrocytes per mL were mixed with the same volume of polymer solutions (final concentrations in the erythrocyte suspension: 1.25628, 0.62814, 0.25126, 0.12563, and 0.01256 for both glycopolymers and 4.83372, 2.41686, 0.96674, 0.48337, and 0.04834 mM for cisplatin) in a clear flat bottomed 96-well plate. The cells were incubated under vigorous shaking at 37 °C for 2 h. A 25 kDa bPEI (50 μg mL^{-1}) was used as a positive control. As negative controls, cells were only treated with PBS. The erythrocyte aggregation was evaluated by microscopic observations using 10-times diluted samples. Experiments were run in triplicates and were repeated once.

RESULTS AND DISCUSSION

Synthesis of Amine End-Functionalized P(EtOx$_{30}$-*stat*-ButEnOx$_{10}$)

The synthesis of P(EtOx-*stat*-ButEnOx) was previously described in literature.[28] The methyl triflate initiated copolymerization at 70 °C showed first-order kinetic behavior. The same behavior was found when methyl tosylate was used as initiator and the reaction was performed at 140 °C in acetonitrile (Supporting Information Fig. S1A). However, due to the higher temperature, the polymerization proceeded much faster with polymerization constants of k_p(EtOx) = 0.206 L mol^{-1} s^{-1} and k_p(ButEnOx) = 0.188 L mol^{-1} s^{-1}. The similar conversions of both monomers are a reliable indication of the formation of a random copolymer. Investigations by SEC showed an increasing molar mass with increasing time (Supporting Information Fig. S1B and Table S1).

The data obtained from the kinetic investigations were used to synthesize amine end-functionalized P(EtOx$_{30}$-*stat*-ButEnOx$_{10}$) (**2**), a multifunctional copolymer, which enables post-polymerization modifications, for example, labeling with dyes. The living cationic species of the polymerization reaction was quenched with potassium phthalimide (**1**, Scheme 1).

The quantitative end-capping with phthalimide was proven by ^{1}H NMR spectroscopy. Subsequent reaction with hydrazine yielded the free amine end-group (**2**) as can be seen by the disappearance of the phthalimide signal at 7.8 ppm (Fig. 1). The ButEnOx double bonds remained intact under these reaction conditions with no changes in the integral intensities in the ^{1}H NMR spectrum. Consequently, the double bonds were exploited for thiol-ene photoadditions to introduce tpy and monosaccharides. Characterization by SEC revealed a narrow molar mass distribution for both, phthalimide and amine end-functionalized, polymers with no or only a minor change of the polydispersity index (PDI) after hydrazinolysis, depending on the used SEC system (Fig. 2 and Table 1; Supporting Information Table S2).

Thiol-ene Functionalization of P(EtOx$_{30}$-*stat*-ButEnOx$_{10}$) with Monosaccharides and Terpyridine Moieties as well as Platinum Complexation

In order to incorporate platinum complexing ligands into copolymer **2**, four of the ButEnOx side chains of P(EtOx$_{30}$-*stat*-ButEnOx$_{10}$) were functionalized with 6-([2,2′:6′,2″-terpyridin]-4′-yloxy)hexane-1-thiol (tpy-SH) by thiol-ene photoaddition (**3**, Scheme 1). The success of the reaction was shown by ^{1}H NMR spectroscopy (Fig. 1). Peaks for the tpy

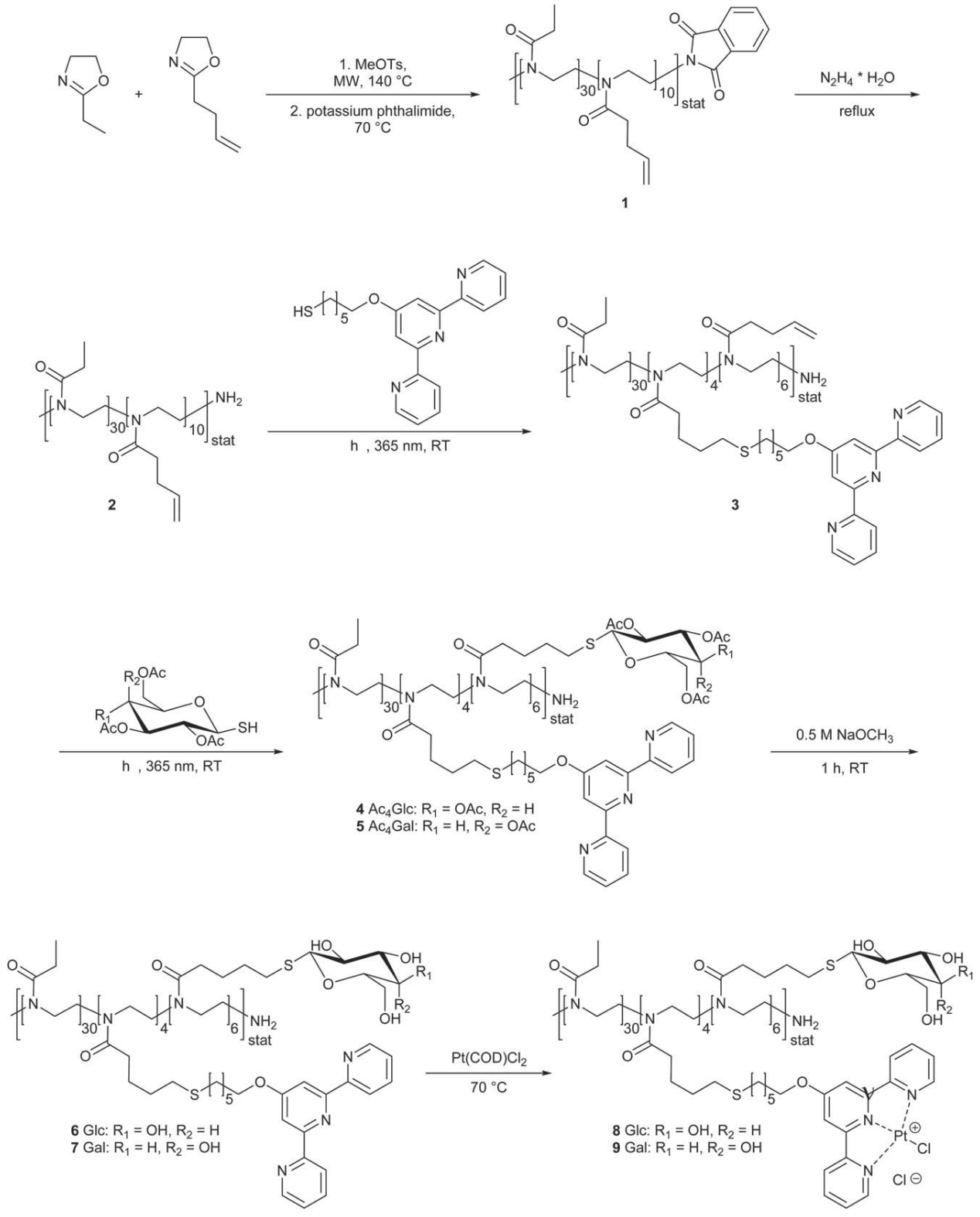

SCHEME 1 Schematic representation of the synthesis of platinum and sugar functionalized POx.

units appeared between 7 and 9 ppm. The signals of the hexamethylene linker can be found between 1.5 and 2 ppm. Further evidence for the successful photoaddition of the tpy units was provided by SEC (Table 1 and Fig. 2; Supporting Information Table S2). A growing molar mass compared with the starting material P($EtOx_{30}$-*stat*-$ButEnOx_{10}$) was observed,

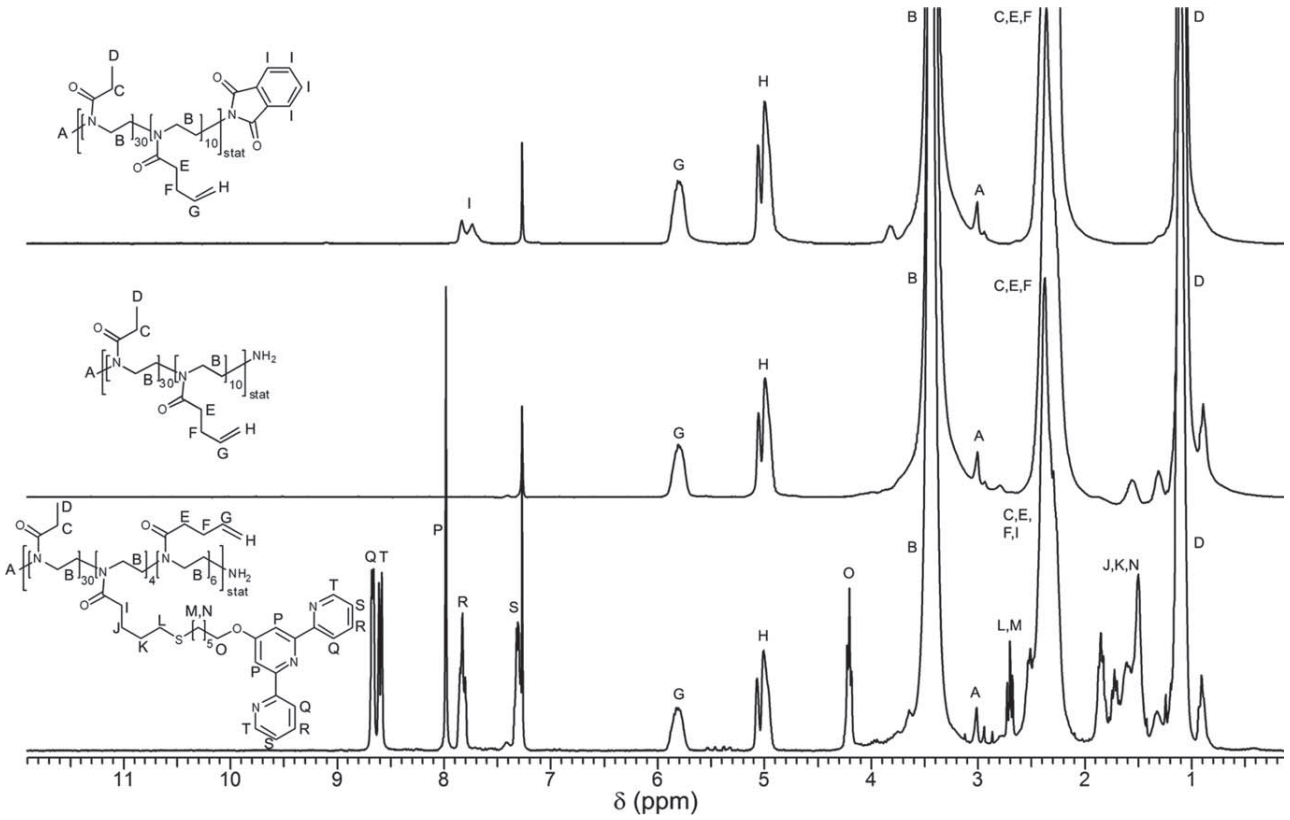

FIGURE 1 ^{1}H NMR spectra of (**top**) phthalimide (**1**) and (**middle**) amine (**2**) end-functionalized P(EtOx$_{30}$-*stat*-ButEnOx$_{10}$) as well as (**bottom**) P(EtOx$_{30}$-*stat*-ButEnOx$_{6}$-*stat*-typButOx$_{4}$) (**3**) (300 MHz, $CDCl_3$).

while the PDI changed only slightly. Moreover, absorption of the tpy unit can be detected in the UV detector of the SEC, which is congruent with the RI signal of the polymer (Supporting Information Fig. S2). In addition, no SEC signal of unreacted tpy-SH was detected. The slight shoulder at lower elution volume, that is, higher molar mass, might derive from polymer–polymer coupling and could not be removed by preparative SEC.

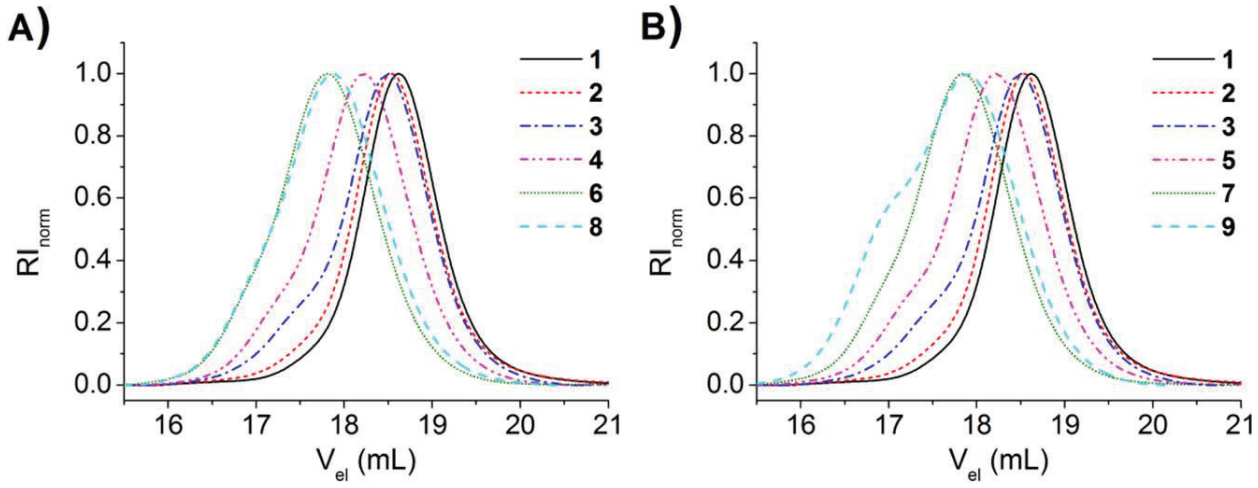

FIGURE 2 SEC curves of the different polymers: (**A**) Starting material and glucose functionalized polymers, (**B**) starting material and galactose functionalized polymers. [Color figure can be viewed in the online issue, which is available at wileyonlinelibrary.com.]

TABLE 1 SEC Data of the Different Polymers

Compound	M_n (g mol^{-1})[a]	PDI[a]
1	6,860	1.16
2	6,980	1.19
3	8,000	1.21
4	9,340	1.21
5	9,360	1.23
6	11,980	1.22
7	11,800	1.23
8	11,560	1.23
9	12,370	1.29

[a] Determined by SEC: DMAc + 0.21% LiCl, calibration against PS.

In the next step the targeting sugar units were attached to the polymer backbone by a second thiol-ene photoaddition (Scheme 1). To this end, the remaining ButEnOx were reacted with acetyl protected thioglucose (Ac_4GlcSH) and thiogalactose (Ac_4GalSH), respectively. To ensure a full functionalization of the ButEnOx units an excess of thio-sugar was used and removed after reaction by preparative SEC. Characterization by ^{1}H NMR spectroscopy revealed the quantitative consumption of the double bond and the appearance of signals typical for acetylated sugars (Fig. 3; Supporting Information Fig. S3). The obtained spectra resemble spectra of other sugar functionalized POx.[38,39] SEC analysis revealed an increasing molar mass with no change of the PDI value in case of Glc and an insignificant change for Gal (Fig. 2 and Table 1). In addition, no traces of unreacted sugar could be detected by SEC.

Deprotection of the sugar moieties was achieved by treatment with sodium methoxide (Scheme 1). After deprotection, a shift of the sugar signals in the ^{1}H NMR spectrum was observed as already described for other sugar bearing POx (Fig. 3; Supporting Information Fig. S3).[38,39] In particular, the peaks at around 5 ppm are shifted to lower ppm. However, the most obvious change is the disappearance of the peaks of the acetyl protecting groups at around 2 ppm. The tpy signals remained unchanged. Another proof for the successful deprotection is the disappearance of the C═O band of the acetyl protecting groups at 1747 cm^{-1} (Glc) and 1745 cm^{-1} (Gal), respectively, in the Fourier transform infrared (FT-IR) spectra (Supporting Information Fig. S4). SEC characterization revealed a change in molar mass (Table 1 and Fig. 2). Although the theoretical molar masses are lower after the deprotection reaction, a shift to higher molar masses was observed. This finding was reported earlier for other sugar

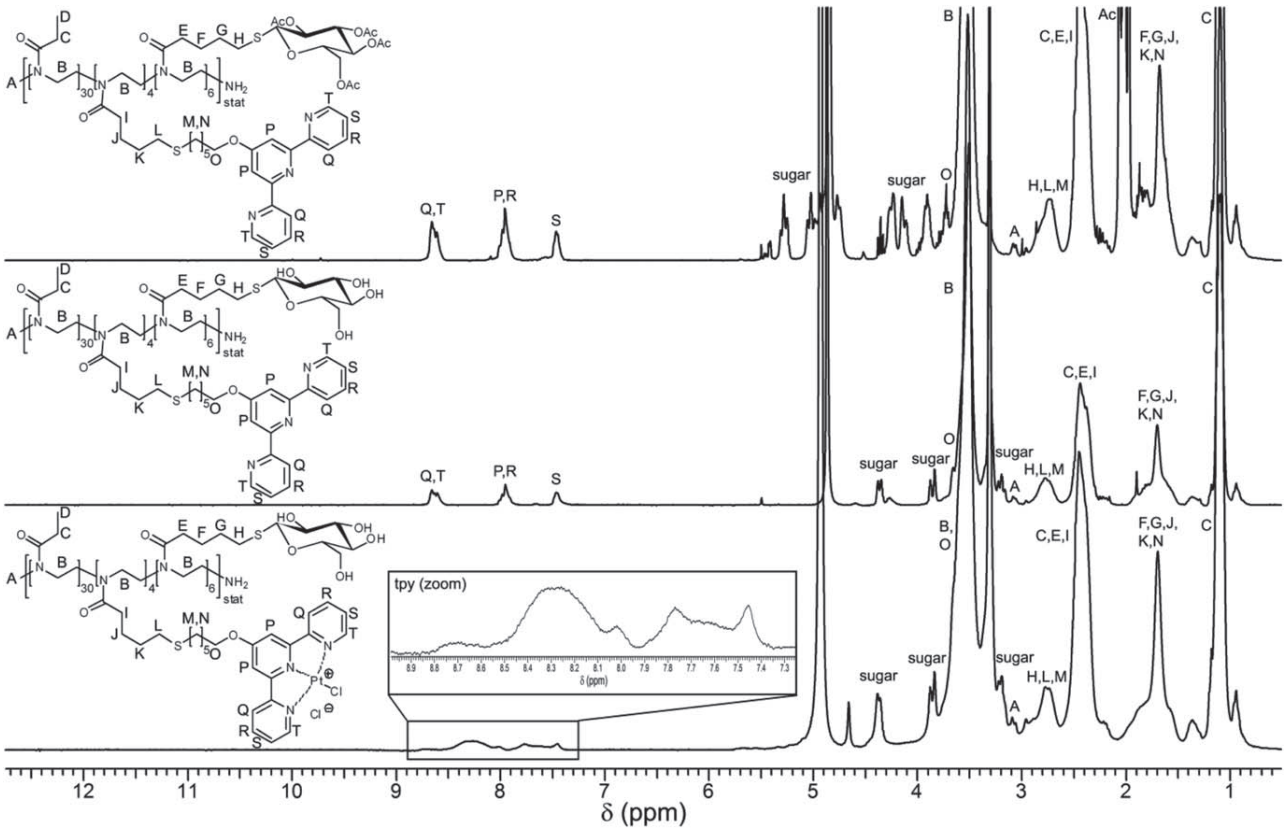

FIGURE 3 ^{1}H NMR spectra of (**top**) P(EtOx$_{30}$-*stat*-(Ac$_4$GlcButOx)$_6$-*stat*-tpyButOx$_4$) (**4**), (**middle**) P(EtOx$_{30}$-*stat*-GlcButOx$_6$-*stat*-tpyButOx$_4$) (**6**), and (**bottom**) P(EtOx$_{30}$-*stat*-GlcButOx-*stat*-PtButOx$_4$) (**8**) (300 MHz, CD_3OD).

decorated POx and is ascribed to the increasing hydrodynamic volume in DMAc.[39] However, PDI values remained low with no significant change in the shape of the SEC curves, which confirms that the rest of the polymer, for example, the tpy units, is not affected by the deprotection.

To obtain an active agent, which can induce cell death, the tpy moieties were complexed with platinum. For this purpose, the very efficient and mild route, using $Pt(COD)Cl_2$ in water, of Annibale et al. was applied.[14,40] Since $Pt(COD)Cl_2$ is insoluble in water and only dissolves upon complexation of the Pt, the reaction progress can be monitored easily. A color change to orange/yellow, known from other tpy complexation reactions,[14,40,41] was observed. When an excess of platinum compound was used, as reported by Wild et al.,[14] a black compound, insoluble in common organic solvents and water, was obtained. Hence, a tpy:Pt ratio of 1:1 was chosen. The side product cylco-octadiene was removed by washing the aqueous phase with diethyl ether.

Characterization by ^1H NMR spectroscopy showed a broadening of the tpy signals, indicating the successful complexation (Fig. 3; Supporting Information Fig. S3). SEC analysis after complexation revealed a shoulder at lower elution volumes, that is, higher molar mass, for glucose (**8**) but to a higher extent for the galactose functionalized polymer (**9**) (Table 1 and Fig. 2). Consequently, the PDI values are increasing, but do not exceed 1.3 (Table 1). This finding might be ascribed to polymer–polymer coupling.

Although having hydrophilic and hydrophobic domains, the polymers showed no self-assembly in water even at a concentration of 2 mg mL^{-1}. Dynamic light scattering (DLS) measurements gave only hydrodynamic radii of about 3–4 nm belonging to the free polymer chain (Supporting Information Fig. S5).

In vitro Cytotoxicity

The potential of the platinum modified glycopoly(2-oxazoline)s as anticancer agents was examined *in vitro* against mouse fibroblast L929 cells, human embryonic kidney cells HEK 293, and human hepatocytes HepG2. The *in vitro* cytotoxicity was evaluated following a standardized XTT assay protocol, in which a reduction of cell viability below 70% is defining the tested substance as cytotoxic. The cells were incubated with different polymer concentrations for 24 h. A significant reduction of the metabolic activity was already observed at glycopolymer concentrations in the range of 0.502 and 0.753 mM, depending on the analyzed cell type [Fig. 4(A)]. HEK 293 and L929 cells tended to be slightly more sensitive to the cytotoxic moieties of the glycopolymers than HepG2 cells. However, a specific effect of the type of conjugated sugar on the cytotoxicity could not be observed, since for both, glucose and galactose functionalized polymers, the viability rates of the particular cell types were in most cases on similar levels. The absence of an enhanced effectiveness of galactose functionalized polymers in HepG2 cells is unexpected since literature reports a galactose-mediated targeting of polymeric substances to liver cells via the asialoglycoprotein receptors.[42,43] Possibly, the uptake of the platinum containing glycopolymers was accomplished preferentially via non-receptor–mediated endocytosis. Thus, the role of the type of sugar conjugated was not evident. Compared with free cisplatin, the glycopolymers exhibited lower activities at same molar concentrations of platinum, e.g. cisplatin is clearly cytotoxic at 0.483 mM, whereas the glycopolymers, having four active platinum units per molecule, are still cytocompatible at an equimolar platinum content ($c_{Polymer} = 0.125$ mM).

A detailed live/dead microscopy study of the glycopolymer and cisplatin treated cells confirmed the dose dependent cytotoxic potential. At relatively low concentrations (0.005–0.048 mM for cisplatin and 0.001–0.251 mM for both glycopolymers), an excellent cell viability (strong green fluorescence of FDA in cytoplasm) and the integrity of the cell membranes (exclusion of red fluorescent PI from cell nuclei) could be observed, proving the absence of cytotoxic effects of the substances. In contrast, at higher concentrations (from 0.483 mM for cisplatin and from 0.502 mM for both glycopolymers), all cells were killed by both the platinum containing glycopolymers and the cisplatin reference [Fig. 4(B); Supporting Information Figs. S6–S8].

The lower *in vitro* cytotoxic activity of the glycopolymers when compared with cisplatin at equimolar amounts of platinum can be ascribed to the molecular structure of the components. While cisplatin with a relatively low molar mass of 300 g mol^{-1} is considered to enter the cell mostly by passive diffusion,[44] the uptake of the macromolecular glycopolymeric platinum complexes might be retarded due to their high molar mass of around 8000 g mol^{-1}. Hence, the internalization of the glycopolymers is rather accomplished by endocytosis as well as receptor-mediated endocytosis promoted by the attached sugar targeting moieties.

Even though the *in vitro* experiments revealed a higher efficiency of cisplatin compared with the glycopolymer conjugated platinum, it is very likely that *in vivo* the latter is more efficient and shows less side effects. As cisplatin is characterized by a relatively low molar mass, the better part of the drug is excreted from the body within short time (elimination half-life of 43 min).[45,46] Hence, the higher antitumor activity of cisplatin cannot be fully exploited *in vivo*. This provokes the need of an increased dosage of cisplatin, leading to more serious side effects for the patient. In contrast, for both investigated glycopolymers, excretion from the body might be decelerated due to their high molar mass and the "stealth effect" of the PEtOx units. A prolonged blood circulation time would be beneficial for the accumulation in cancerous tissue (EPR effect). Moreover, the attached sugars might support the specific uptake by neoplastic cells since they exhibit overexpressed sugar receptors on their cell surface.[47,48] These effects could argue for a more cytotoxic potential of the glycopolymers *in vivo* than observed *in vitro* and could, in turn, decrease the overall drug dosage necessary for disease treatment. The mode of action of platinum based anticancer agents is based on the electrophilic

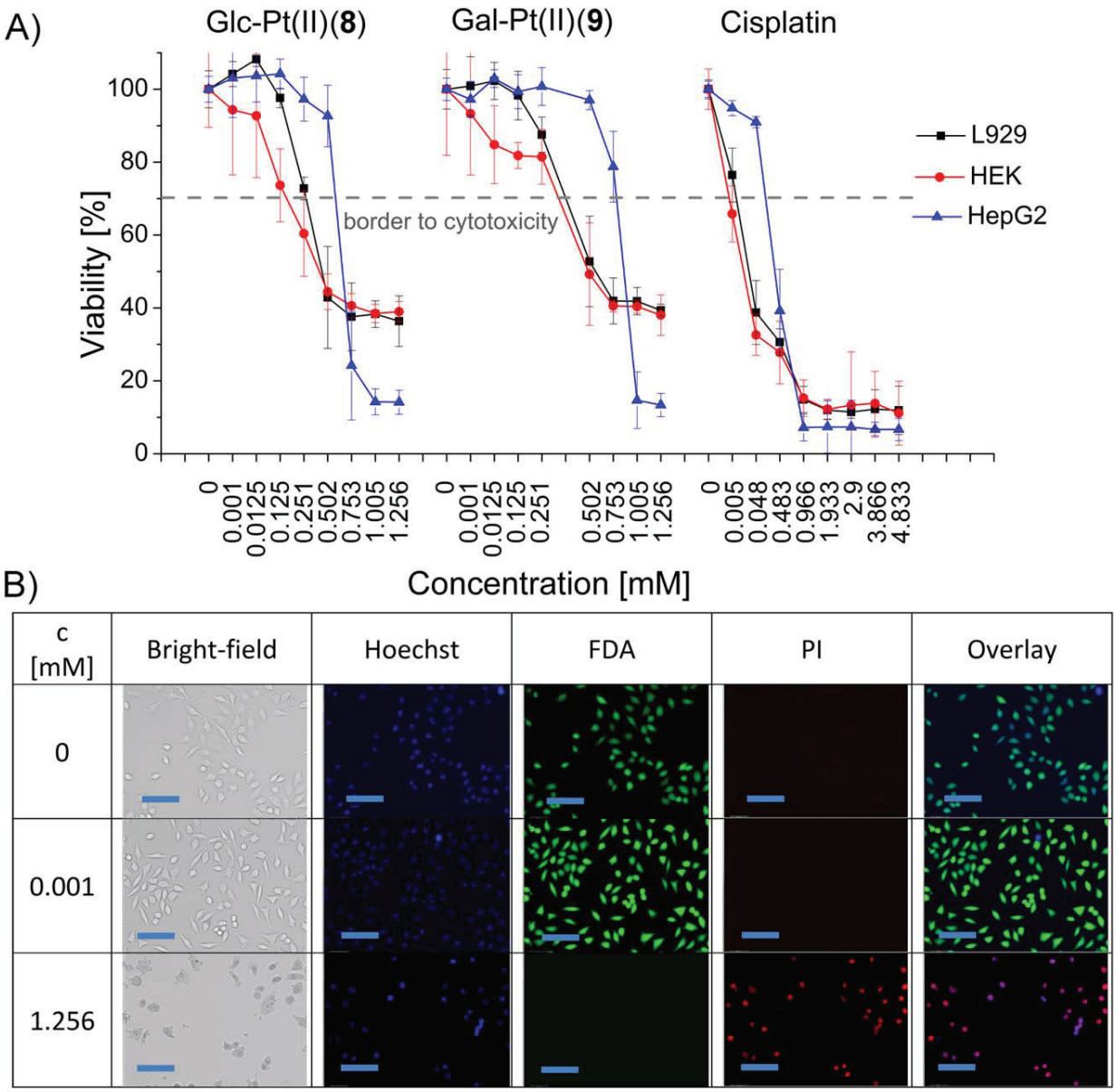

FIGURE 4 (**A**) Cell viability of L929 mouse fibroblasts, human embryonic kidney cells HEK 293, and human hepatocytes HepG2 after incubation with glycopolymers Glc-Pt(II) (**8**)/Gal-Pt(II) (**9**) and cisplatin at different concentrations for 24 h. Cells incubated only with culture medium served as control. The cell viability was determined by XTT assay according to ISO 10993-5. Data are expressed as mean ± SD of six determinations. (**B**) Representative light field and fluorescence micrographs of Hoechst 33342/FDA/PI stained L929 mouse fibroblast cells cultured for 24 h in the presence of high and low concentrations of Glc-Pt(II) (identical results for Gal-Pt(II) and cisplatin). (1) Bright field image, (2) blue fluorescent Hoechst 33342 dye labels nuclei of all cells present, (3) green fluorescent FDA dye indicates cytoplasm of vital cells, (4) red fluorescent PI signals tag nuclei of dead cells, and (5) overlay of Hoechst 33342 dye fluorescence and green fluorescence of the FDA dye. Scale bar = 100 μm. [Color figure can be viewed in the online issue, which is available at wileyonlinelibrary.com.]

properties of platinum and implies the crosslinking of DNA strands, induction of DNA mutations as well as the suppression of DNA repair mechanisms. Hence, another possible reason for the attenuated effectiveness of the glycopolymers compared with cisplatin could be a hindered accessibility of the active platinum species within the polymeric backbone or an altered or shielded electrophilic capacity of the platinum complexes.

Hemolysis and Erythrocyte Aggregation

As blood is the first contact partner within the human body during intravenous administration, the platinum conjugated

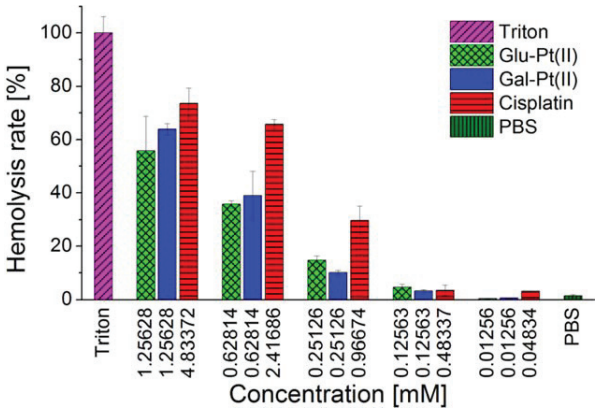

FIGURE 5 Photometric determination of the hemolytic activity of cisplatin and the glycopolymers Glc-Pt(II) (**8**) and Gal-Pt(II) (**9**) after incubation for 1 h at 37 °C. Triton X-100 (1%) served as positive and PBS as negative control. Experiments were run in triplicates and were repeated once; data are presented as the mean percentage ± SD of hemolytic activity compared with the positive control set as 100%. [Color figure can be viewed in the online issue, which is available at wileyonlinelibrary.com.]

glycopolymers as well as the cisplatin reference were tested for their interaction with human blood.

In detail, adverse side reactions with red blood cells were evaluated in terms of erythrocyte aggregation and hemolysis upon glycopolymer and cisplatin incubation. To assess their influence on the red blood cell membrane, the hemolytic activity was measured photometrically by means of hemoglobin release after potential damage of the erythrocyte membrane (Fig. 5). The test substances were investigated at different concentrations (both glycopolymers: 1.25628, 0.62814, 0.25126, 0.12563, and 0.01256 mM; cisplatin: 4.83372, 2.41686, 0.96674, 0.48337, and 0.04834 mM) in comparison to PBS as negative and Triton-X100 as positive control. A hemoglobin release of greater than 5% of the total release was classified as hemolytic according to the ASTM F756-08 standard.[49]

At low concentrations (between 0.01256 to 0.12563 mM for glycopolymers and 0.04834 to 0.4834 mM for cisplatin), both glycopolymers and cisplatin induced only a slight and negligible hemoglobin release. It has to be mentioned, that these glycopolymer concentrations are not within the cytotoxic range, as assessed *in vitro* using the XTT assay. Nevertheless, the required dosage for *in vivo* effectiveness was not evaluated within this study.

Increasing the concentrations of glycopolymers (0.25126–1.25628 mM) and cisplatin (0.96674–4.83372 mM) led to a dose dependent damage of the erythrocyte membrane with a remarkable release of hemoglobin from the cell plasma. Interestingly, this effect was more pronounced in cisplatin treated blood cells, indicating a higher hemolytic activity of cisplatin than glycopolymer conjugated platinum. A major difference between the glucose and galactose functionalized polymers could not be observed.

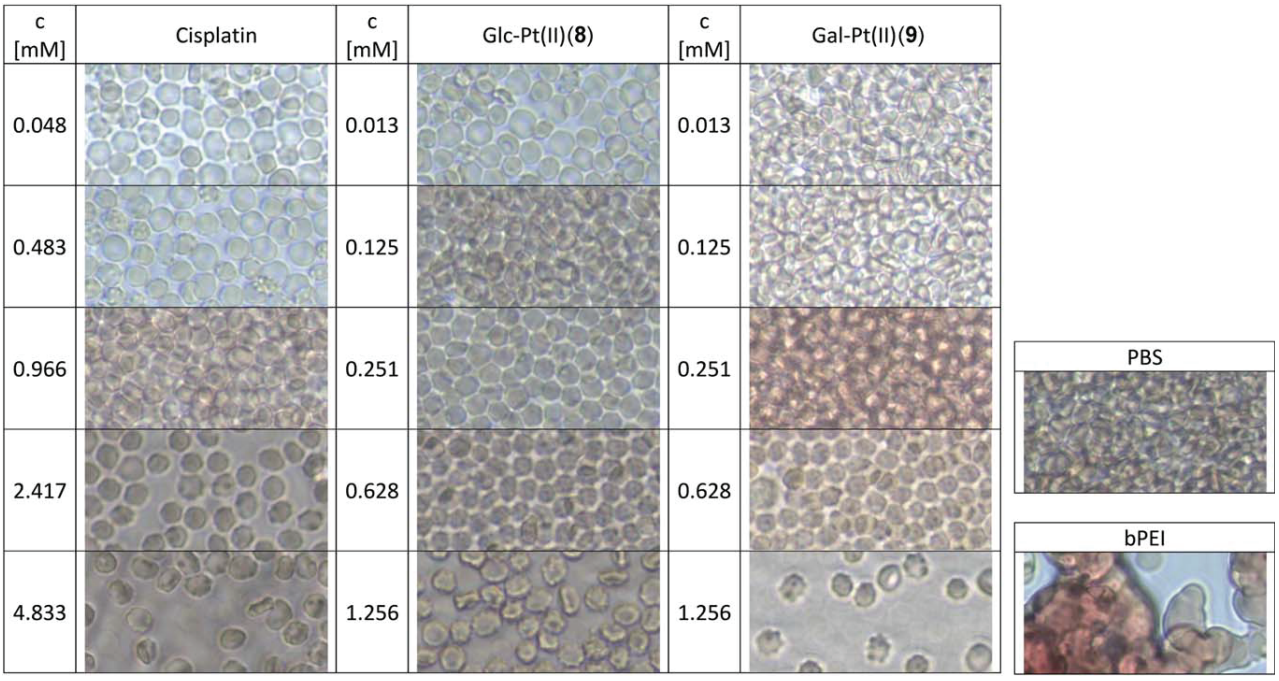

FIGURE 6 Representative micrographs of red blood cells after 2 h incubation at 37 °C with cisplatin, and the glycopolymers Glc-Pt(II) (**8**) and Gal-Pt(II) (**9**). PBS served as negative and 25 kDa bPEI (50 μg mL^{-1}) as positive control. [Color figure can be viewed in the online issue, which is available at wileyonlinelibrary.com.]

In addition, the induction of erythrocyte aggregation was investigated microscopically. The formation of aggregates, which could lead to an impeded blood flow, was analyzed for different test substance concentrations (both glycopolymers: 1.25628, 0.62814, 0.25126, 0.12563, and 0.01256 mM; cisplatin: 4.83372, 2.41686, 0.96674, 0.48337, and 0.04834 mM) in comparison to PBS as negative and branched poly(ethylene imine) (bPEI) as positive control. Microscopic analysis revealed that no clear cell cluster formation occurred with exception of the positive control (bPEI). In contrast, it could be shown that a partial lysis of erythrocytes occurred at the highest concentrations of cisplatin and both glycopolymers visible in a reduction of the total cell density (Fig. 6). This assumption is supported by the measurement of the hemolytic activity of both glycopolymers and cisplatin shown before.

To conclude, adverse hemolytic side reactions with red blood cells, representing the major cellular compartment of the blood, were observed in a concentration dependent manner for the two glycopolymeric platinum complexes but also for the cisplatin reference, which is in clinical application for many years. Interpreting these results, one has to keep in mind that after intravenous injection the local drug concentration in the blood stream of the patient is usually an order of magnitude lower (for cisplatin maximum 2 mg L^{-1} which equates to 0.013 mM)[50] than tested in our *in vitro* experiments (for cisplatin between 7 and 1450 mg L^{-1}/0.48–4.83 mM; for glycopolymers between 1000 and 10,000 mg L^{-1}/0.012–1.256 mM). Due to this, the potential hemolytic activity of the glycopolymers at high concentrations is not of clinical relevance since such high concentration levels will not be reached in the circulating human blood *in vivo* when the anticancer drug is administered in a highly diluted solution.

CONCLUSIONS

We herein describe for the first time the synthesis of platinum containing 2-oxazoline-based glycopolymers which were obtained by attaching terpyridine (tpy) as well as acetyl protected glucose and galactose, respectively, to poly(2-ethyl-2-oxazoline-*block*-2-(3-butenyl)-2-oxazoline) using thiol-ene photoaddition. Subsequent deprotection of the sugars with sodium methanolate and treatment with $Pt(COD)Cl_2$ applying a mild synthetic route in water, yielded polymers with both, sugar units for active tumor targeting as well as cytotoxic Pt(II) units. This synthetic approach allows the variation of the sugar/platinum content and with it the fine-tuning of the polymer properties.

To investigate the potential of the platinum containing glycopolymer as anticancer drug, their *in vitro* cytotoxicity and influence on blood integrity has been studied and the results have been compared with cisplatin as reference.

The cytotoxicity was examined against mouse fibroblast L929 cells, human embryonic kidney cells HEK 293, and human hepatocytes HepG2. For both, cisplatin and the two glycopolymers, a dose dependent cytotoxicity was observed, with a higher activity of cisplatin at equimolar platinum amounts. However, the overexpression of sugar receptors on neoplastic cells and the possible EPR effect, often observed for hydrophilic polymers, might lead to a better *in vivo* performance of the glycopolymers.

In conclusion, we demonstrated a straightforward route for the synthesis of platinum containing 2-oxazoline-based glycopolymers as promising candidates for anticancer therapy, whose potential will be exploited in our upcoming work.

ACKNOWLEDGMENTS

We thank the Dutch Polymer Institute (DPI, Technology Area HTE) for financial support. LT wants to thank Cornelia Bader for large-scale synthesis of the ButEnOx monomer and Caroline Fritzsche for performing cell biological experiments. KK is grateful to the Alexander von Humboldt foundation for financial support. S.B. is grateful to the Fonds der Chemischen Industrie (FCI) for a generous Ph.D. fellowship.

REFERENCES AND NOTES

1 B. W. Harper, A. M. Krause-Heuer, M. P. Grant, M. Manohar, K. B. Garbutcheon-Singh, J. R. Aldrich-Wright, *Chem. Eur. J.* **2010**, *16*, 7064–7077.

2 K. J. Haxton, H. M. Burt, *J. Pharm. Sci.* **2009**, *98*, 2299–2316.

3 H. Maeda, G. Y. Bharate, J. Daruwalla, *Eur. J. Pharm. Biopharm.* **2009**, *71*, 409–419.

4 V. J. Venditto, F. C. Szoka Jr, *Adv. Drug Deliv. Rev.* **2013**, *65*, 80–88.

5 X. Wang, Z. Guo, *Chem. Soc. Rev.* **2013**, *42*, 202–224.

6 J. S. Butler, P. J. Sadler, *Curr. Opin. Chem. Biol.* **2013**, *17*, 175–188.

7 L. Kelland, *Nat. Rev. Cancer* **2007**, *7*, 573–584.

8 C. R. Maldonado, L. Salassa, N. Gomez-Blanco, J. C. Mareque-Rivas, *Coord. Chem. Rev.* **2013**, *257*, 2668–2688.

9 C. Oerlemans, W. Bult, M. Bos, G. Storm, J. F. Nijsen, W. Hennink, *Pharm. Res.* **2010**, *27*, 2569–2589.

10 M. J. Vicent, R. Duncan, *Trends Biotechnol.* **2006**, *24*, 39–47.

11 K. Knop, R. Hoogenboom, D. Fischer, U. S. Schubert, *Angew. Chem. Int. Ed.* **2010**, *49*, 6288–6308.

12 W. Scarano, H. T. T. Duong, H. Lu, P. L. De Souza, M. H. Stenzel, *Biomacromolecules* **2013**, *14*, 962–975.

13 S. Pearson, W. Scarano, M. H. Stenzel, *Chem. Commun.* **2012**, *48*, 4695–4697.

14 A. Wild, K. Babiuch, M. Konig, A. Winter, M. D. Hager, M. Gottschaldt, A. Prokop, U. S. Schubert, *Chem. Commun.* **2012**, *48*, 6357–6359.

15 S. D. Cummings, *Coord. Chem. Rev.* **2009**, *253*, 1495–1516.

16 J. Moretto, B. Chauffert, F. Ghiringhelli, J. Aldrich-Wright, F. Bouyer, *Invest. New Drugs* **2011**, *29*, 1164–1176.

17 K. Suntharalingam, O. Mendoza, A. A. Duarte, D. J. Mann, R. Vilar, *Metallomics* **2013**, *5*, 514–523.

18 M. Bauer, C. Lautenschlaeger, K. Kempe, L. Tauhardt, U. S. Schubert, D. Fischer, *Macromol. Biosci.* **2012**, *12*, 986–998.

19 M. Bauer, S. Schroeder, L. Tauhardt, K. Kempe, U. S. Schubert, D. Fischer, J. *Polym. Sci., Part A: Polym. Chem.* **2013**, *51*, 1816–1821.

20 R. Konradi, C. Acikgoz, M. Textor, *Macromol. Rapid Commun.* **2012**, *33*, 1663–1676.

21 L. Tauhardt, K. Kempe, M. Gottschaldt, U. S. Schubert, *Chem. Soc. Rev.* **2013**, *42*, 7998–8011.

22 B. Pidhatika, M. Rodenstein, Y. Chen, E. Rakhmatullina, A. Muhlebach, C. Acikgoz, M. Textor, R. Konradi, *Biointerphases* **2012**, *7*, 1–15.

23 T. X. Viegas, M. D. Bentley, J. M. Harris, Z. Fang, K. Yoon, B. Dizman, R. Weimer, A. Mero, G. Pasut, F. M. Veronese, *Bioconjugate Chem.* **2011**, *22*, 976–986.

24 T. R. Dargaville, R. Forster, B. L. Farrugia, K. Kempe, L. Voorhaar, U. S. Schubert, R. Hoogenboom, *Macromol. Rapid Commun.* **2012**, *33*, 1695–1700.

25 C. Diehl, H. Schlaad, *Macromol. Biosci.* **2009**, *9*, 157–161.

26 C. Diehl, H. Schlaad, *Chem. Eur. J.* **2009**, *15*, 11469–11472.

27 B. L. Farrugia, K. Kempe, U. S. Schubert, R. Hoogenboom, T. R. Dargaville, *Biomacromolecules* **2013**, *14*, 2724–2732.

28 A. Gress, A. Völkel, H. Schlaad, *Macromolecules* **2007**, *40*, 7928–7933.

29 K. Kempe, R. Hoogenboom, M. Jaeger, U. S. Schubert, *Macromolecules* **2011**, *44*, 6424–6432.

30 K. Kempe, R. Hoogenboom, U. S. Schubert, *Macromol. Rapid Commun.* **2011**, *32*, 1484–1489.

31 K. Kempe, A. Vollrath, H. W. Schaefer, T. G. Poehlmann, C. Biskup, R. Hoogenboom, S. Hornig, U. S. Schubert, *Macromol. Rapid Commun.* **2010**, *31*, 1869–1873.

32 F.-P. Sun, T. Darbre, *Helv. Chim. Acta* **2002**, *85*, 3002–3018.

33 U. S. Schubert, C. Eschbaumer, O. Hien, P. R. Andres, *Tetrahedron Lett.* **2001**, *42*, 4705–4707.

34 D. A. Fulton, J. F. Stoddart, *J. Org. Chem.* **2001**, *66*, 8309–8319.

35 T. B. Norsten, B. L. Frankamp, V. M. Rotello, *Nano Lett.* **2002**, *2*, 1345–1348.

36 H. Ahrem, D. Pretzel, M. Endres, D. Conrad, J. Courseau, H. Müller, R. Jaeger, C. Kaps, D. O. Klemm, R. W. Kinne, *Acta Biomater.* **2014**, *10*, 1341–1353.

37 A. Vollrath, D. Pretzel, C. Pietsch, I. Perevyazko, S. Schubert, G. M. Pavlov, U. S. Schubert, *Macromol. Rapid Commun.* **2012**, *33*, 1791–1797.

38 K. Kempe, C. Weber, K. Babiuch, M. Gottschaldt, R. Hoogenboom, U. S. Schubert, *Biomacromolecules* **2011**, *12*, 2591–2600.

39 C. Weber, J. A. Czaplewska, A. Baumgaertel, E. Altuntas, M. Gottschaldt, R. Hoogenboom, U. S. Schubert, *Macromolecules* **2011**, *45*, 46–55.

40 G. Annibale, M. Brandolisio, B. Pitteri, *Polyhedron* **1995**, *14*, 451–453.

41 S. D. Cummings, *Coord. Chem. Rev.* **2009**, *253*, 449–478.

42 K. Babiuch, D. Pretzel, T. Tolstik, A. Vollrath, S. Stanca, F. Foertsch, C. R. Becer, M. Gottschaldt, C. Biskup, U. S. Schubert, *Macromol. Biosci.* **2012**, *12*, 1190–1199.

43 Y. Watanabe, X. Liu, I. Shibuya, T. Akaike, J. *Biomater. Sci., Polym. Ed.* **2000**, *11*, 833–848.

44 P. A. Andrews. In Platinum-Based Drugs in Cancer Therapy; Kelland, L., Farrell, N., Eds.; Humana Press: Totowa, **2000**; pp 89–113.

45 R. S. Go, A. A. Adjei, *J. Clin. Oncol.* **1999**, *17*, 409–422.

46 P. Reece, I. Stafford, M. Davy, R. Morris, S. Freeman, *Cancer Chemother. Pharmacol.* **1989**, *24*, 256–260.

47 R. S. Brown, R. L. Wahl, *Cancer* **1993**, *72*, 2979–2985.

48 A. Godoy, V. Ulloa, F. Rodríguez, K. Reinicke, A. J. Yañez, M. d. l A. García, R. A. Medina, M. Carrasco, S. Barberis, T. Castro, F. Martínez, X. Koch, J. C. Vera, M. T. Poblete, C. D. Figueroa, B. Peruzzo, F. Pérez, F. Nualart, *J. Cell. Physiol.* **2006**, *207*, 614–627.

49 ASTM F756, Standard practice for assessment of hemolytic properties of materials. In Annual Book of ASTM Standards; ASTM: Philadelphia, **2008**.

50 S. B. Salas, C. Mercier, J. Ciccolini, B. Pourroy, B. Tranchand, S. Monjanel-Mouterde, M. Baciuchka-Palmaro, C. Dupuis, C. G. Yang, M. Balti, B. Lacarelle, F. Duffaud, A. Durand, R. Favre, *Ther. Drug Monit.* **2006**, *28*, 532–539.

SUPPORTING INFO

Synthesis and *In Vivo* Activity of Platinum containing 2-Oxazoline-based Glycopolymers

Lutz Tauhardt,[1,2] David Pretzel,[1,2] Stefan Bode,[1,2] Justyna A. Czaplewska,[1,2] Kristian Kempe,[1,2,#] Michael Gottschaldt,[1,2] Ulrich S. Schubert*[1,2,3]

[1]Laboratory of Organic and Macromolecular Chemistry (IOMC), Friedrich Schiller University Jena, Humboldtstr. 10, 07743 Jena, Germany.

[2]Jena Center for Soft Matter (JCSM), Friedrich Schiller University Jena, Philosophenweg 7, 07743 Jena, Germany.

[3]Dutch Polymer Institute (DPI), John F. Kennedylaan 2, 5612 AB Eindhoven, The Netherlands.

[#]Current address: Department of Chemical and Biomolecular Engineering, The University of Melbourne, Victoria 3010, Australia.

Correspondence to: Ulrich S. Schubert (E-mail: *ulrich.schubert@uni-jena.de*)

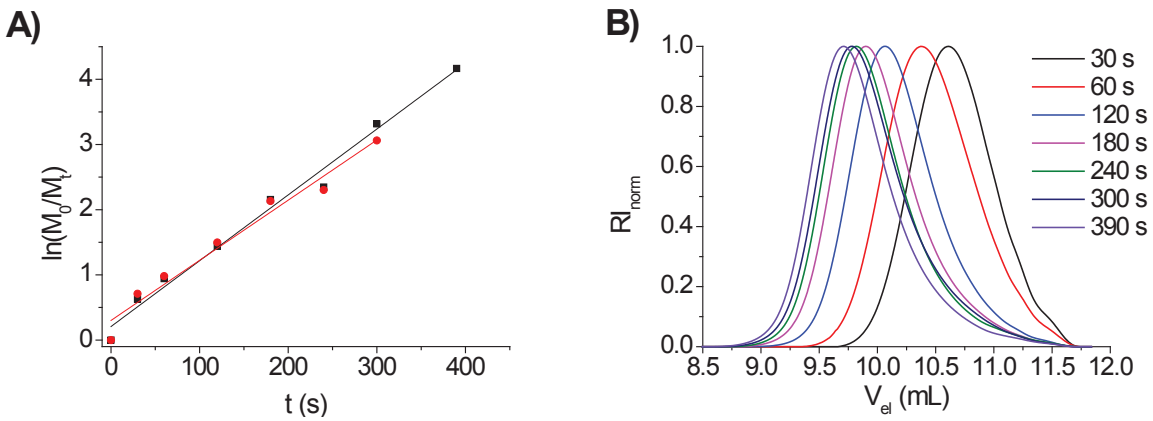

FIGURE S1 A) First-order kinetic plots of the copolymerization of EtOx (square) and ButEnOx (circle) at 140 °C with a total monomer concentration of 1 M and a [EtOx]:[ButEnOx]:[MeOTs] ratio of 16:4:1. B) SEC curves kinetic study after different times.

TABLE S1. Data of the kinetic study.

Time (s)	Conversion of EtOx:ButEnOx (%)[a)]	M_n (g mol^{-1})[b)]	PDI[b)]
30	47:51	900	1.22
60	61:63	1,115	1.25
120	76:78	1,590	1.22
180	88:88	1,850	1.23
240	90:90	1,980	1.23
300	96:95	2,020	1.24
390	98:100	2,250	1.23

[a)]Determined by GC. [b)]Determined by SEC (chloroform/TEA/2-propanol 94:4:2, calibration against PS).

TABLE S2. SEC data of the different polymers.

Compund	M_n (g mol^{-1})[a)]	PDI[a)]
1	4,590	1.16
2	3,920	1.16
3	7,590	1.14

[a)]Determined by SEC (chloroform/TEA/2-propanol 94:4:2, calibration against PS).

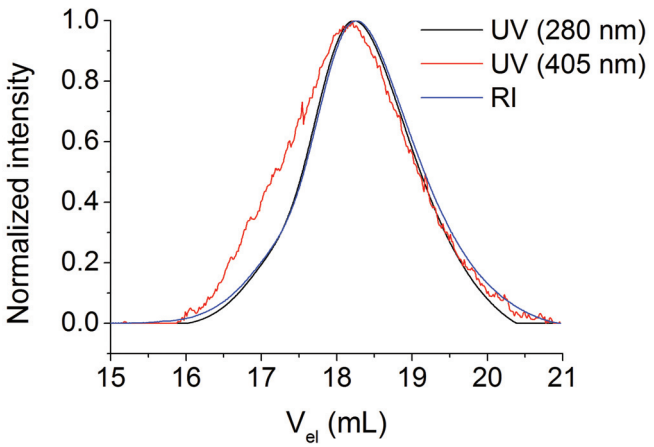

FIGURE S2. Overlay of the SEC curves of polymer 3 measured with an UV (280 nm and 405 nm) and an RI detector, respectively.

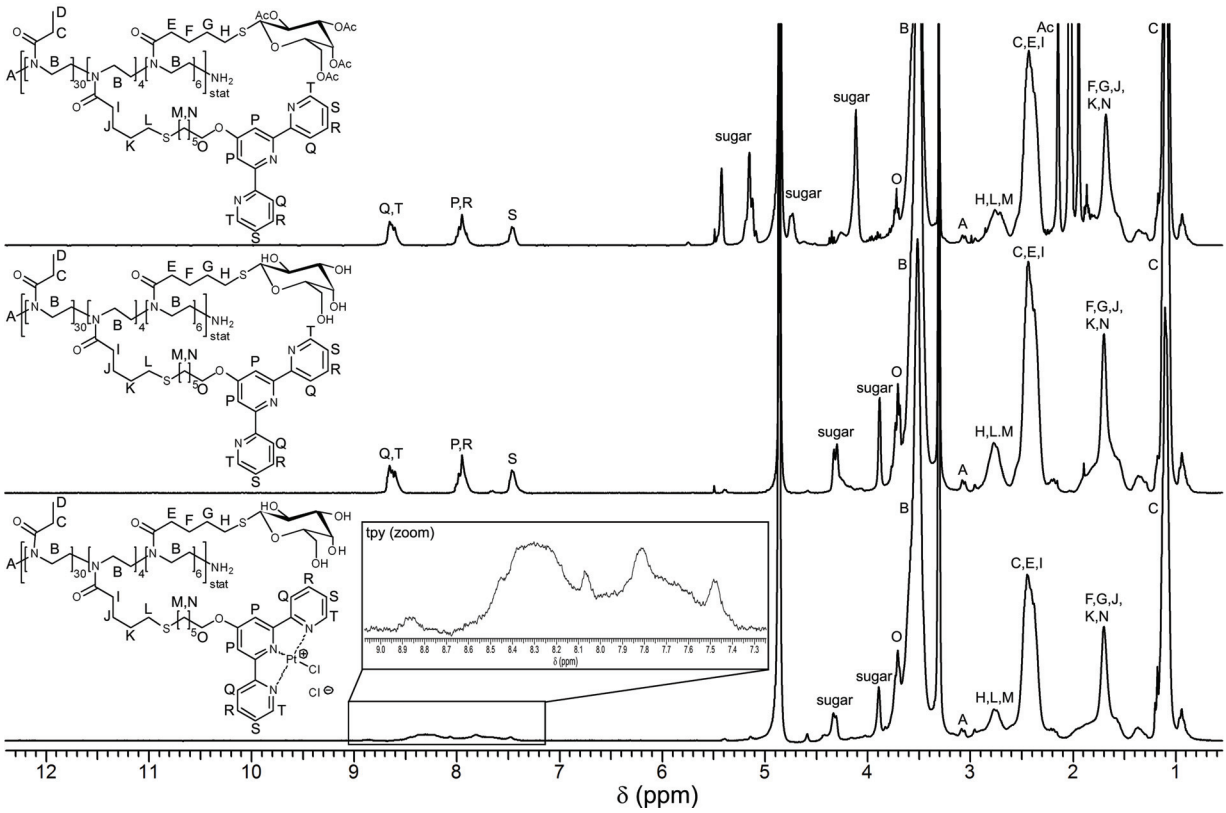

FIGURE S3 ^{1}H NMR spectra of P(EtOx$_{30}$-*stat*-(Ac$_4$GalButOx)$_6$-*stat*-tpyButOx$_4$), P(EtOx$_{30}$-*stat*-GalButOx$_6$-*stat*-tpyButOx$_4$), and P(EtOx$_{30}$-*stat*-GalButOx-*stat*-PtButOx$_4$) (300 MHz, CD_3OD).

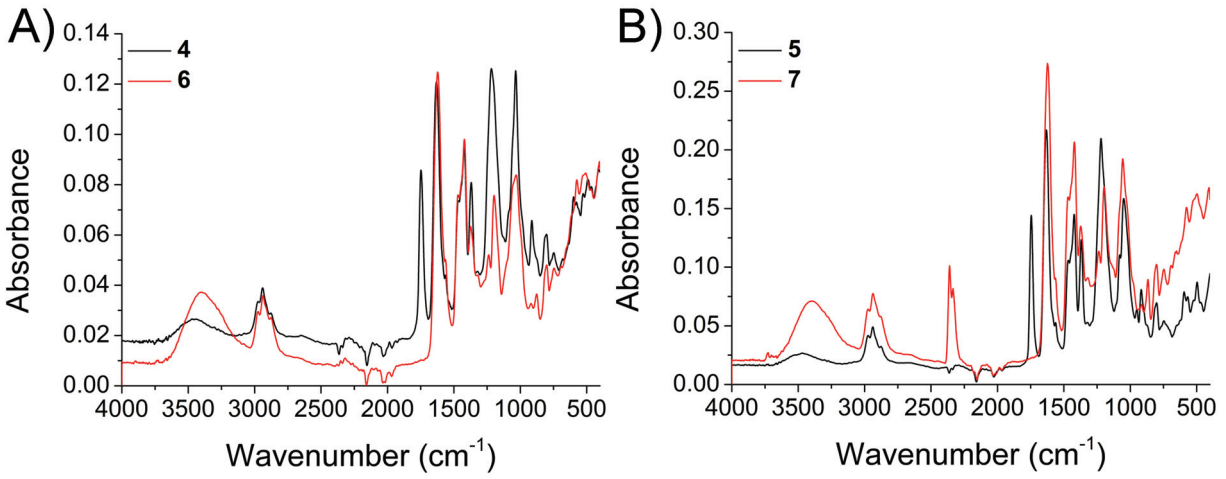

FIGURE S4 ATR-FT-IR spectra of A) glucose and B) fructose functionalized glycopolymers before (**4, 5**) and after (**6, 7**) deprotection.

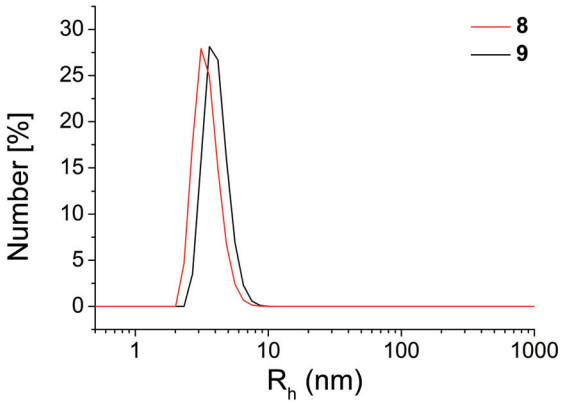

FIGURE S5 Dynamic light scattering (DLS) plot of the glycopolymers **8** and **9**.

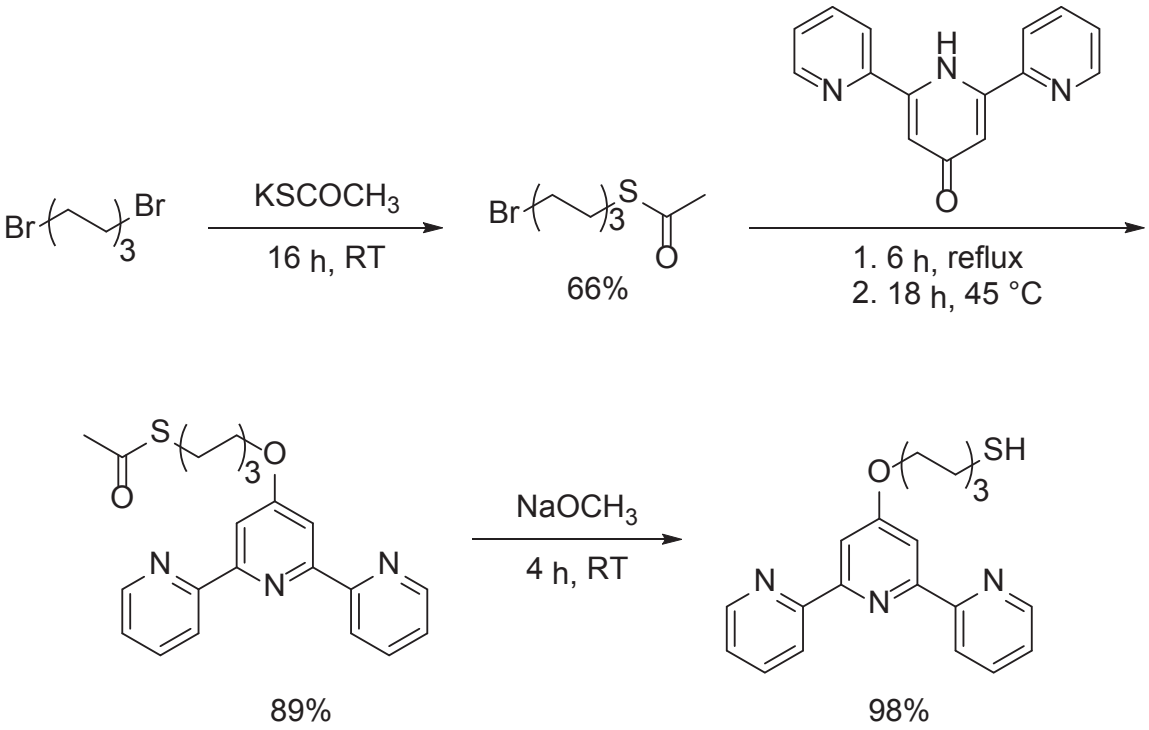

SCHEME S1. Schematic representation of the synthesis of 6-([2,2':6',2''-terpyridin]-4'-yloxy)hexane-1-thiol. The shown reaction pathway is known in literature for other terpyridine thiols and was applied for a C6-linker between the terpyridine moiety and the thiol function.[1-3]

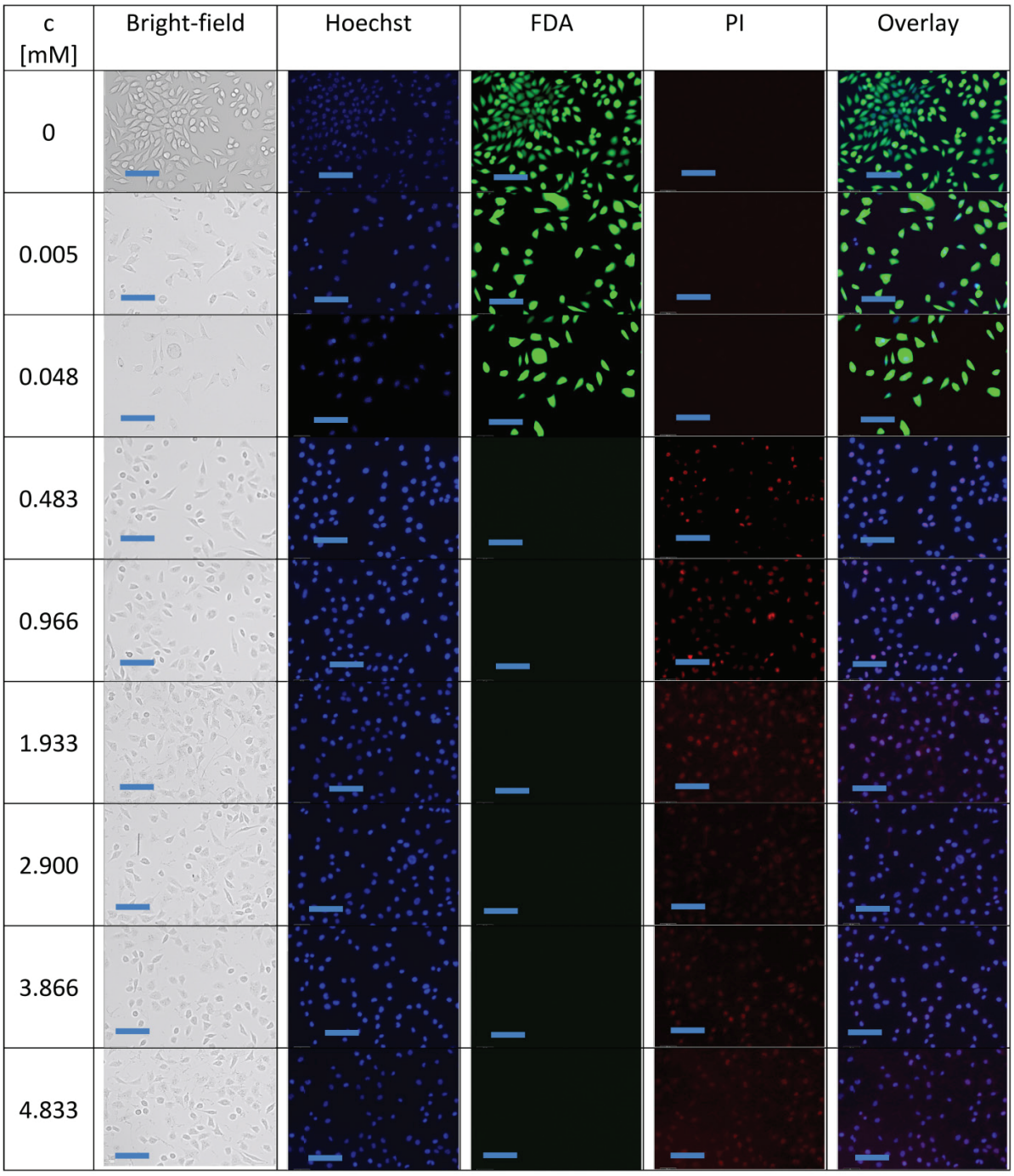

FIGURE S6 Microscopy study on the cell viability of L929 mouse fibroblasts after incubation with cisplatin at different concentrations for 24 hours. Cells incubated only with culture medium served as control. Representative bright field images and fluorescence micrographs from different channels: The blue fluorescent Hoechst 33342 dye labels nuclei of all cells present, the green fluorescent FDA dye indicates cytoplasm of vital cells, and the red fluorescent PI signals tag nuclei of dead cells. Identical results were obtained for human embryonic kidney cells HEK293 and human hepatocytes HepG2 (not shown). Scale bar = 100 µm.

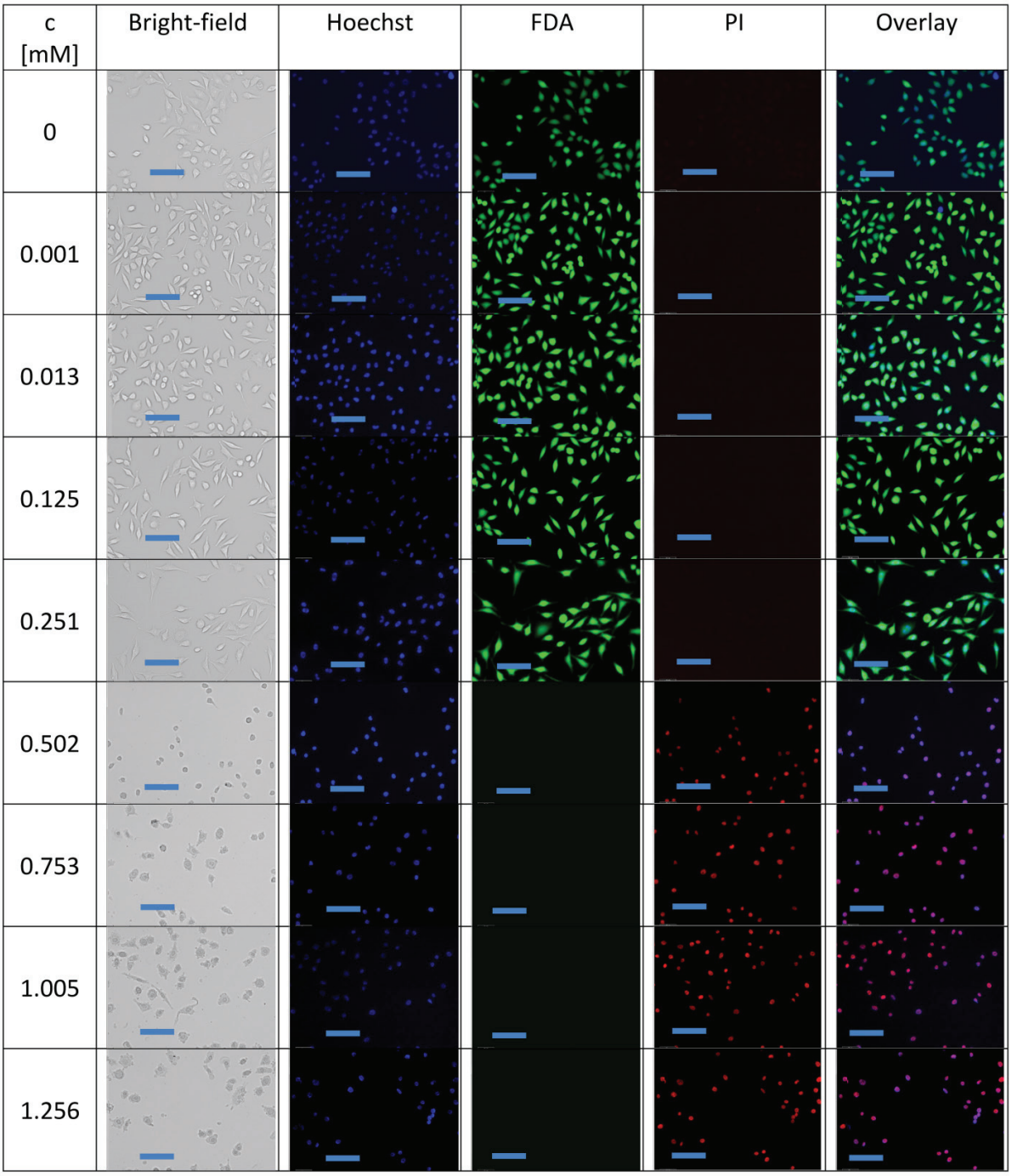

FIGURE S7 Microscopy study on the cell viability of L929 mouse fibroblasts after incubation with Glc-Pt(II) (**8**) at different concentrations for 24 hours. Cells incubated only with culture medium served as control. Representative bright field images and fluorescence micrographs from different channels: The blue fluorescent Hoechst 33342 dye labels nuclei of all cells present, the green fluorescent FDA dye indicates cytoplasm of vital cells, and the red fluorescent PI signals tag nuclei of dead cells. Identical results were obtained for human embryonic kidney cells HEK293 and human hepatocytes HepG2 (not shown). Scale bar = 100 µm.

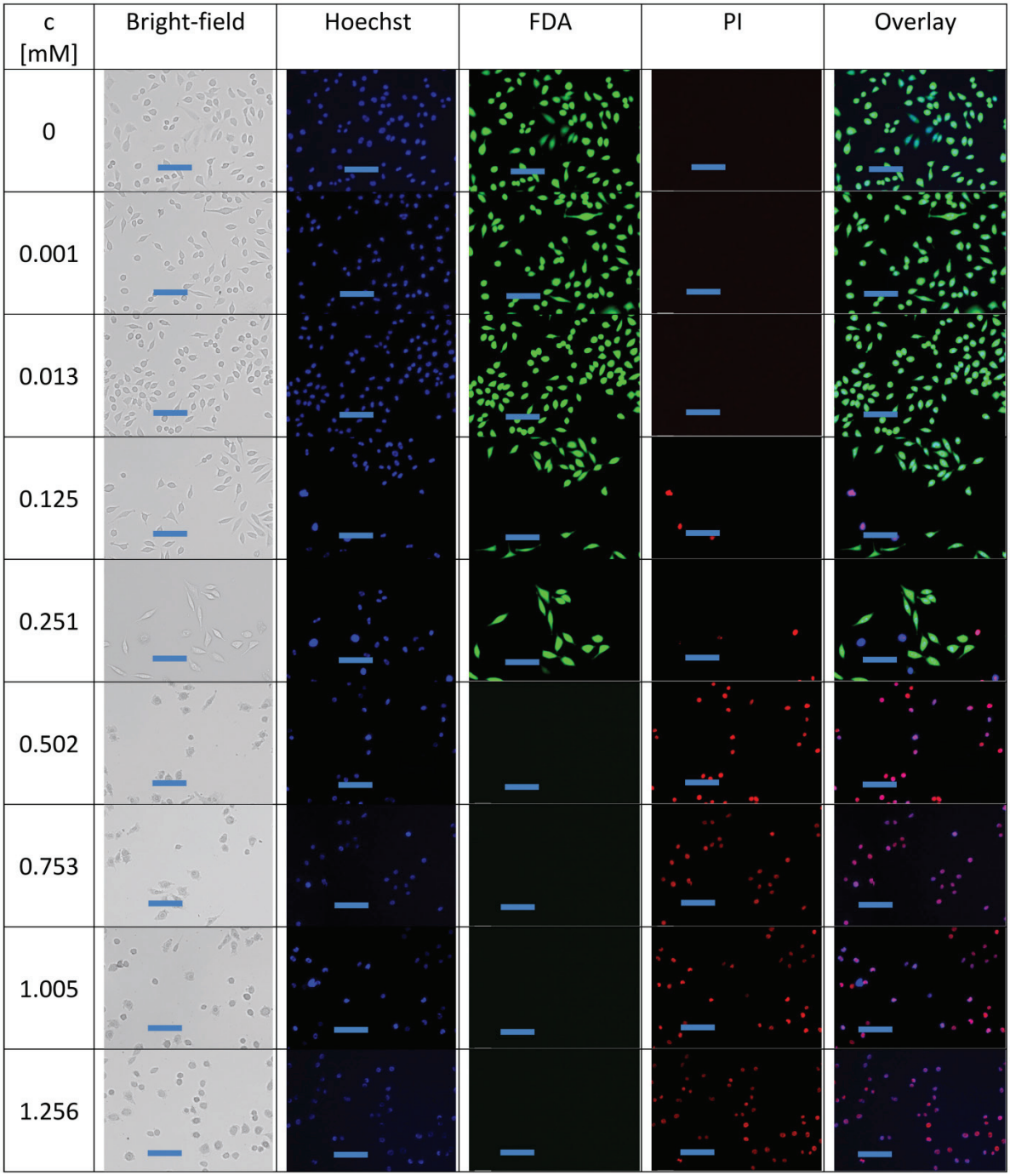

FIGURE S8 Microscopy study on the cell viability of L929 mouse fibroblasts after incubation with Gal-Pt(II) (**9**) at different concentrations for 24 hours. Cells incubated only with culture medium served as control. Representative bright field images and fluorescence micrographs from different channels: The blue fluorescent Hoechst 33342 dye labels nuclei of all cells present, the green fluorescent FDA dye indicates cytoplasm of vital cells, and the red fluorescent PI signals tag nuclei of dead cells. Identical results were obtained for human embryonic kidney cells HEK293 and human hepatocytes HepG2 (not shown). Scale bar = 100 µm.

EXPERIMENTAL

Chemicals and instrumentation

THF was dried and distilled over sodium, aceton over calcium chloride. Size exclusion chromatography (SEC) investigations of the kinetic study were measured on a Shimadzu system equipped with a SCL-10A VP system controller, a DGU-14A degasser, a LC-10AD VP pump, a RID-10A refractive index detector and a PSS SDV column running with chloroform, triethylamine (TEA), and 2-propanol (94 : 4 : 2) as eluent. The Techlab column oven was set to 50 °C. Molar masses were calculated against polystyrene (PS) standards. Gas chromatography (GC) measurements of the kinetic study were performed on a Shimadzu GC2010 equipped with a Restek Rtx-5 column (30 m length, 0.25 mm ID, 0.25 µm film thickness [5% diphenyl, 95% dimethyl polysiloxane] (carrier gas: helium) and a FID detector (carrier gases: H_2, combustion: air). ATR-FT-IR spectra were measured on a Nicolet Avatar 370 DTGS from Thermo Electron Corporation. Dynamic light scattering (DLS) was performed on a Zetasizer Nano ZS (Malvern Instruments, Herrenberg, Germany). After an equilibration time (25°C) of 180 s, 3 x 30 runs were carried out at 25°C (λ = 633 nm). The counts were detected at an angle of 173°. Polymer concentration was 2 mg/mL. Each measurement was performed in triplicate. Apparent hydrodynamic radii, R_h, were calculated according to the Stokes–Einstein equation.

S-(6-Bromohexyl) ethanethioate[2,3]

Under nitrogen atmosphere 1.7 mL dibromohexane (11.22 mmol) were dissolved in 20 mL dichloromethane. A solution of 760 mg potassium thioacetate (6.66 mmol) in 25 mL ethanol was added dropwise to the reaction mixture and a white precipitate formed. Subsequently the reaction mixture was stirred at room temperature for 16 hours.

After this the solvents were evaporated and the residue was dissolved in dichloromethane. The solution was washed with deionized water and the organic phase was dried over Na_2SO_4. The solution was concentrated and the compound purified by a silica gel chromatography (*n*-hexane/chloroform 2:1).

Yield: 1.046 g of a yellow liquid, 66%

^{1}H NMR (250 MHz, $CDCl_3$): δ = 1.25 – 1.64 (m, 6H, *H-alkyl*), 1.85 (q, *J* = 6.75 Hz, 2H, CH_2-CH_2Br), 2.32 (s, 3H, -CH_3), 2.86 (t, *J* = 7.25 Hz, 2H, CH_2-S), 3.41 (t, *J* = 6.75 Hz, 2H, CH_2-Br) ppm.

^{13}C NMR (62.5 MHz, $CDCl_3$): δ = 27.6 (C_γ), 27.9 (C_δ), 28.9 (C_β), 29.3 (C_ε), 30.6 (*C*H_2-S), 32.6(-*C*H_3), 33.7 (*C*H_2-Br), 195.9 (*C*=O) ppm.

ESI-TOF MS (HR): m/z = $[C_8H_{15}OSBr+Na]^+$: calcd.: 260.9919; found: 260,9923; error: 1.6 ppm

_S_-(6-([2,2':6',2''-Terpyridin]-4'-yloxy)-hexyl) ethanethioate

510 mg S-(6-Bromohexyl) ethanethioate (2.13 mmol), 810 mg potassium carbonate, and 525 mg 2,6-bis-(pyrid-2-yl)-4-pyridone (2.11 mmol) were dissolved in 60 mL dry acetone. The solution was stirred under reflux for 6 hours. After this the mixture was stirred at 45 °C for 18 hours.

Subsequently, the solvent was evaporated and the residue was dissolved in dichloromethane. After washing with water (300 mL) the organic layer was dried over Na_2SO_4 and concentrated. The product was obtained by silica gel chromatography ($CHCl_3$).

Yield: 763 mg of a white solid, 89%

^{1}H NMR (250 MHz, $CDCl_3$): δ = 1.45 – 1.65 (m, 6H, $H_{\gamma,\delta,\varepsilon}$), 1.86 (q, *J* = 7.00 Hz, 2H, CH_2-CH_2S), 2.33 (s, 3H, -CH_3), 2.90 (t, *J* = 7.00 Hz, 2H, CH_2-S), 4.22 (t, *J* = 6.25 Hz, 2H, O-CH_2), 7.33 (dd, *J* = 4.75 Hz, J = 1.50 Hz , 2H, $H_{5,5''}$), 7.85 (td, *J* = 8.00 Hz, *J* = 1.50 Hz, 2H, $H_{4,4''}$), 8.01 (s, 2H, $H_{3',5'}$), 8.62 (d, *J* = 8.00 Hz, 2H, $H_{3,3''}$), 8.69 (d, *J* = 4.75 Hz, 2H, $H_{6,6''}$) ppm.

^{13}C NMR (62.5 MHz, $CDCl_3$): δ = 25.5 (C_δ), 28.4 (C_γ), 28.9 (C_ε), 29.0 (C_β), 29.4 (*C*H_2-S), 30.6 (-*C*H_3), 68.0 (O-*C*H_2), 107.4 ($C_{5,5''}$), 121.3 ($C_{4,4''}$), 123.8 ($C_{3,3''}$), 136.8 ($C_{3',5'}$), 148.9 ($C_{6,6''}$), 156.1 ($C_{2,2''}$), 157.0 ($C_{2',6'}$), 167.3 ($C_{4'}$), 195.9 (*C*=O) ppm.

Elemental analysis:

$C_{23}H_{25}N_3O_2S$	calcd.:	C	67.79%	H	6.18%	N	10.31%	S	7.86%
(407.518)	found:	C	67.84%	H	6.14%	N	10.20%	S	7.54%

6-([2,2':6',2''-Terpyridin]-4'-yloxy)hexane-1-thiol (tpy-SH)

In a three neck flask 503 mg of **6a** (1.23 mmol) were dissolved in 40 mL dry THF. The solution was degassed with nitrogen for 30 minutes and then 6 mL of a 0.5 M solution of sodium methoxide in methanol was slowly added. The reaction mixture was stirred for 4 hours at room temperature. Subsequently, the reaction was quenched by the addition of 60 mL of a saturated aqueous ammonium chloride solution. The solvents were evaporated and the residue was dissolved in water and dichloromethane. The aqueous phase was extracted with dichloromethane (300 mL) and the combined organic phases were dried over Na_2SO_4. The solvent was evaporated and the product was used without further purification.

Yield: 440 mg of a white solid, 98%

^{1}H NMR (250 MHz, $CDCl_3$): δ = 1.26 – 1.64 (m, 9H, -S*H*, $H_{\beta,\gamma,\delta,\varepsilon}$), 2.53 (t, *J* = 7.25 Hz, 2H, H_α), 4.23 (t, *J* = 6.25 Hz, 2H, H_ζ), 7.33 (dd, *J* = 2.00 Hz, 4.75 Hz , 2H, $H_{5,5''}$), 7.85 (td, *J* = 2.00 Hz, 8.00 Hz, 2H, $H_{4,4''}$), 8.01 (s, 2H, $H_{3',5'}$), 8.62 (d, *J* = 8.00 Hz, 2H, $H_{3,3''}$), 8.79 (d, *J* = 4.75 Hz, 2H, $H_{6,6''}$) ppm.

^{13}C NMR (62.5 MHz, $CDCl_3$): δ = 24.5 (C_γ), 25.6 (C_δ), 28.0 (C_β), 28.9(C_ε), 33.9 (C_α), 68.0 (C_ζ), 107.4 ($C_{5,5''}$), 121.4 ($C_{4,4''}$), 123.8 ($C_{3,3''}$), 136.8 ($C_{3',5'}$), 149.0 ($C_{6,6''}$), 156.1 ($C_{2,2''}$), 157.0 ($C_{2',6'}$), 167.3 ($C_{4'}$) ppm.

ESI-TOF MS (HR): m/z = $[M+Na]^+$: calcd.: 388.1460; found: 388.1456; error: 1.03 ppm

$[M+H]^+$: calcd.: 366.1640; found: 366.1634; error: 1.64 ppm

Kinetic study of the copolymerization of EtOx and ButEnOx

For the kinetic studies, a stock solution containing methyl tosylate (initiator), acetonitrile (solvent) EtOx and ButEnOx was prepared. The total monomer concentration was adjusted to 1 M with a

[EtOx]/[ButEnOx]/[I] ratio of 16:4:1. The stock solution was divided over seven microwave vials and capped under nitrogen. To calculate the conversion, t_0 samples were taken. The vials were heated to 140 °C for different times in the microwave synthesizer. After cooling to room temperature, the reaction was quenched, and the conversion of the monomers was determined by GC. As internal standard the polymerization solvent was used.

REFERENCES

1 T. B. Norsten; B. L. Frankamp; V. M. Rotello, *Nano Lett.* **2002**, *2*, 1345-1348.

2 F.-P. Sun; T. Darbre, *Helv. Chim. Acta* **2002**, *85*, 3002-3018.

3 T. K. Tran; M. Oçafrain; S. Karpe; P. Blanchard; J. Roncali; S. Lenfant; S. Godey; D. Vuillaume, *Chem. Eur. J.* **2008**, *14*, 6237-6246.

Publication 7

“Rethinking the Impact of the Protonable Amine Density on Cationic Polymers for Gene Delivery: A Comparative Study of Partially Hydrolyzed Poly(2-ethyl-2-oxazoline)s and Linear Poly(ethylene imine)s”

M. Bauer, L. Tauhardt, H. M. L. Lambermont-Thijs, K. Kempe, R. Hoogenboom, U. S. Schubert, D. Fischer

in preparation

Rethinking the Impact of the Protonable Amine Density on Cationic Polymers for Gene Delivery: A Comparative Study of Partially Hydrolyzed Poly(2-ethyl-2-oxazoline)s and Linear Poly(ethylene imine)s

Marius Bauer,[a] Lutz Tauhardt,[b] Hanneke M. L. Lambermont-Thijs,[c] Kristian Kempe,[c,#] Richard Hoogenboom,[d] Ulrich S. Schubert, [b, c, e], Fischer, D.[a, e *]

[a]Department of Pharmaceutical Technology, Friedrich-Schiller-University Jena, Jena, Germany

[*]Corresponding Author: Friedrich Schiller University Jena, Institute of Pharmacy, Department of Pharmaceutical Technology, Otto-Schott-Strasse 41, 07745 Jena. Tel.: (+49)3641 9-49941; Fax: (+49)3641 9-49942;

Email address: dagmar.fischer@uni-jena.de

[b]Laboratory of Organic and Macromolecular Chemistry (IOMC), Friedrich Schiller University Jena, Humboldtstrasse 10, 07743 Jena, Germany

[c]Laboratory of Macromolecular Chemistry and Nanoscience, Eindhoven University of Technology, Eindhoven, The Netherlands

[d]Department of Organic Chemistry, Gent University, Gent, Belgium

[e]Jena Center for Soft Matter (JCSM), Friedrich-Schiller-University Jena, Philosophenweg 7, 07743 Jena, Germany

[#]Current address: Department of Chemical and Biomolecular Engineering, The University of Melbourne, Victoria, Australia.

Keywords:

Gene delivery, Poly(ethylene imine), Poly(2-ethyl-2-oxazoline), Transfection, Polymer, Nonviral vector

Abstract

To receive a more profound insight on the impact of the number and the density of protonable amines on the performance of polycations as non-viral vectors, a series of linear poly(ethylene imine)s (LPEIs) with different numbers of ethylene imine (EI) units was compared to partially hydrolyzed poly(2-ethyl-2-oxazoline)s (PHPEtOxs) with corresponding numbers of EI-units but with varying densities. PHPEtOxs synthesized from 20 kDa PEtOx with hydrolysis degrees between 21 and 86% as well as the corresponding LPEIs were able to form polyplexes with DNA and their cyto- and hemotoxicity increased with increasing numbers of EI units. Since PHEtOxs were only slightly better tolerated it was considered that the total number of EI units per polymer had a higher impact on the biocompatibility than the density of EI units. In addition it could be shown that the transfection efficiency of PHPEtOxs was much lower than that of their corresponding LPEIs leading to the assumption that the presence of high numbers of EI numbers in close juxtaposition to each other is a key parameter for the high transfection rate of LPEI and that the reduction of the EI density is a modification technique which should, with regard to the cost-benefit ratio, be critically scrutinized.

Abbreviations:

MTT, 3-(4,5-dimethylthiazol-2-yl)-2,5-diphenyl tetrazolium bromide; BCA, bicinchoninic acid; BSA, bovine serum albumin; CHO-K1, Chinese hamster ovary cells; CROP, cationic ring opening polymerization; DH, degree of hydrolysis; DP, degree of polymerization; EI, ethylene imine; FBS, fetal bovine serum; HFIP, hexafluoroisopropanol; LPEI, linear poly(ethylene imine); PHPEtOx, partially hydrolyzed poly(2-ethyl-2-oxazoline); PBS, phosphate buffered saline; pDNA, plasmid DNA; PEtOx, poly(2-ethyl-2-oxazoline); POx, poly(2-oxazoline); PMeOx, poly(2-methyl-2-oxazoline); PS, poly(styrene); PDI, polydispersity index; RLU, relative light unit; RPMI 1640, Roswell Park Memorial Institute 1640; SEC, Size exclusion chromatography; SI, supporting information; Tris, tris(hydroxymethyl)aminomethane.

1. Introduction

The use of DNA and RNA is a promising approach in therapy, especially for applications aiming at the treatment of acquired and hereditary genetic defects, chronic heart insufficiency as well as infectious, neurological, and tumor diseases.[1] More and more nucleic acid formulations move from the preclinical development to the clinical trials, and several gene therapies are or will soon be in late-stage human trials.[2] Polycationic polymers are successful non-viral vectors, and a plethora of agents is already available for in vitro applications.[3] However, only a limited number of such polymers made their way to the clinical testing.[2] Limited efficacies as well as biocompatibility and safety issues are the most challenging reasons that hamper their therapeutic use so far.[4]

To improve their benefit-to-risk ratio, many studies to understand structure-property relationships have been performed.[5-8] Molar mass, three-dimensional architecture and molecular flexibility as well as type, number and density of cationic charges were identified as relevant parameters.[6, 9-10] High molar masses, number and density of the cationic residues were found to allow a more efficient electrostatic interaction with the nucleic acids, resulting in the formation of small sized and enzymatically stable polyplexes with enhanced cell uptake and transfection efficacy.[11] However, electrostatic interactions with negatively charged cell membranes caused membrane damaging effects, metabolic impairments, and

hemotoxic effects.[6, 12] This so called charge dilemma forced various strategies to reduce the number and density of charges. For poly(ethylene imine) (PEI), the most successful non-viral vector polymer, several approaches to address these shortcomings were investigated such as using low molar mass PEIs, [13-14] PEI copolymers with “stealth effect” to mask the surface charge, [15] biodegradable [16] and zwitterionic PEIs.[17] While for branched PEI the importance of the structural parameters was already shown in extenso, [11, 18-20] for linear PEIs (LPEI) the data base is comparatively limited.

LPEIs can be obtained by the complete hydrolysis of poly(2-oxazoline)s (POxs) that are synthesized by cationic ring opening polymerization (CROP).[21] An increasing time of hydrolysis directly correlates with a higher number of ethylene imine units and cationic charges. High transfection efficacy and cytotoxicity were shown to be mediated by an increasing degree of hydrolysis (DH).[22] Preferentially, a DH between 70-88 % was identified as suitable due to moderate cytotoxicity and acceptable transfection rates.[22-23] The molar mass of the starting POx material defines the number of EI units of the resulting LPEI. Using partially hydrolyzed high molar mass poly(2-ethyl-2-oxazoline)s (PEtOxs, 50 and 200 kDa) Jeong et al. suggested that beside the charge density a high molar mass also seems to play a critical role for high transfection.[22] Fernandes et al. [23] used lower molar mass 10 kDa PEtOx, forming polyplexes with comparably lower zeta potentials and siRNA transfection rates. In these studies, the performance of the polymers was compared to PEIs with a totally different structure such as 25 kDa branched PEI [22] or only to one fully hydrolyzed LPEI.[23]

In the present study, five PHPEtOxs were synthesized from a 20 kDa PEtOx with a wide range of degrees of hydrolysis between 21% and 86% resulting in a series of polymers with different numbers of EI units separated by randomly distributed 2-ethyl-2-oxazoline groups. In contrast to previous studies, a 20 kDa PEtOx was selected as starting material forming hydrolyzed polymers with molar masses that demonstrated in previous studies to be

the most relevant size range for efficacy as non-viral vector.[13-14] The PHPEtOxs were compared to six fully hydrolyzed LPEIs with a comparable number of EI units to be able to clearly identify the different importance of the number and the density of EI units. The influence of the different polymer structures on DNA binding, enzymatic polyplex stability, cyto- and hemotoxicity as well as transfection efficacy was investigated

2. Material and methods

2.1 Synthesis of linear poly(ethylene imine) and partially hydrolyzed poly(2-ethyl-2-oxazoline)

The synthesis and characterization of the LPEIs has been reported in detail elsewhere.[21, 24-25] PHPEtOx synthesis was performed as follows: Twenty kDa PEtOx (4 g) were dissolved in 6 M HCl (12 mL). The mixture was heated in an Initiator Sixty single-mode microwave synthesizer (Biotage, Uppsala, Sweden) equipped with a non-invasive infrared sensor (accuracy: ±2), at 100 °C for different times. The solvent was removed under reduced pressure, and the residue was dissolved in water. Further purification was performed using two different approaches. For the DH below 75% (21, 41, 56%), the solution was neutralized to pH 7 with 3 M NaOH solution and dialyzed against water. After dialysis, the water was removed under reduced pressure. For a DH of 75% and higher, 3 M NaOH solution was added until a white precipitate occurred. The precipitate was filtered off and re-crystallized from water. All polymers were dried at 40 °C for 5 days under vacuum.

2.2 Characterization of the polymers

^{1}H NMR spectra were recorded on a Bruker AC 300 MHz spectrometer (Bruker BioSpin GmbH, Rheinstetten, Germany) at room temperature. As solvent deuterated methanol was used. The chemical shifts were given in ppm relative to the signal from residual non-

deuterated solvent. The degree of hydrolysis (DH) was calculated by correlating the methyl proton signal of the uncleaved side chain (1.13 ppm) and the protons of the LPEI backbone (2.73 ppm). Size exclusion chromatography (SEC) of the LPEIs and the PHPEtOxs was measured at 40 °C on a system equipped with a Shimadzu LC-10AD pump (Shimadzu Europe GmbH, Duisburg, Germany), a Waters 2414 refractive index detector (35 °C), a Spark Holland MIDAS injector (Spark Holland, Emmen, the Netherlands) a Polymer Standards Service GmbH (PSS) PFG guard column, and two PFG-linear-XL (7 µm, 8 x 300 mm) columns placed in series (PSS, Mainz, Germany). As eluent hexafluoroisopropanol (HFIP, Apollo Scientific Limited, Stockport, United Kingdom) with potassium trifluoroacetate (3 g/L) was used at a flow rate of 0.8 mL/min. In all cases, the molar masses were calculated against poly(styrene) standards.

2.3 Formation of polyplexes

Polymer stock solutions were prepared with a PEI content of 0.9 mg/mL in highly purified water at pH 7.4. After sterile filtration (0.2 µm, VWR International, Darmstadt, Germany), the PEI concentration was determined spectrophotometrically by Cu^{2+} chelation according to Perrine et al.[26] using a microplate reader (Fluostar OPTIMA, BMG Labtech, Offenburg, Germany) at a wavelength of 645 nm. Only the stock solutions for the hemocompatibility experiments required a maximum concentration of 3 mg/mL and were prepared in 1.5 mM phosphate buffered saline pH 7.4 (PBS). Polyplexes were prepared as described previously[14] with different N/P ratios (polymer nitrogen (N)) per DNA phosphate (P)). The required volumes of polymer stock solution (0.9 mg/mL) and 5 µg DNA were each diluted in 150 mM NaCl (Roth, Karlsruhe, Germany) solution (pH 7.4) to a total volume of 125 µL, vortexed for 10 seconds and incubated for 10 minutes at room temperature. Afterwards, the polymer solution was pipetted to the DNA solution, vortexed for 10 seconds and incubated for further 10 minutes before use. Dependent on the experiment, herring testis

DNA (1 mg/mL tris(hydroxymethyl)aminomethane (Tris) buffered stock solution, type XIV, Sigma Aldrich, Deisenhofen, Germany) or plasmid DNA (pDNA) (pGL3, Promega, Madison, WI, USA) were used. Amplification of the pGL3 plasmid encoding the luciferase reporter gene was performed in competent E. coli TG1 (Hans-Knoell Institute, Jena, Germany) followed by isolation with a standard kit according to the manufacturer's protocol (Plasmid Maxi Kit E.Z.N.A®, OMEGA bio-tek, Norcross, GA, USA).

2.4 Horizontal gel retardation assay

Fifty µL aliquots of the polyplex solutions containing 1 µg herring testis DNA were mixed with 5 µL loading buffer (40 mM Tris, 50% (v/v) glycerol 85%, 1 mM EDTA (ethylenediaminetetraacetic acid), pH 7.4, all from Roth) and applied on a 1% agarose gel (peqGold Universal Agarose, Peqlab Biotechnology GmbH, Erlangen, Germany) loaded with ethidium bromide. Free DNA and free polymer solutions were used as controls. Bromphenolblue was applied in a separate pocket as running control. Electrophoretic separation was carried out in an electrophoresis chamber (Biometra, Goettingen, Germany) at 80 V for 1 h with TAE running buffer (40 mM Tris, 1% acetic acid, 1 mM EDTA, all from Roth). Gels were photographed under UV transillumination (Intas GmbH, Goettingen Germany) at 312 nm with a gel documentation system (Digit Store UNO, Intas GmbH).

2.5 Laser light scattering experiments

Hydrodynamic diameter and zeta potential of pGL3 polyplexes were measured with the Zetasizer nano ZS (4 mW HeNe Laser, 633 nm) (Malvern Instruments, Worcestershire, United Kingdom) in 50 mM NaCl solution. The hydrodynamic diameter was determined by photon correlation spectroscopy in six measurement cycles in a ZEN 0112 low volume sizing cuvette (Brand, Wertheim, Germany) at a scattering angle of -173° at 25 °C. For data analysis the refractive index (1.33) and the viscosity (0.88 mPa·s) of distilled water at 25 °C were

used. Results were calculated with the CONTIN algorithm using the Malvern Zetasizer software 6.20. Zeta potential was determined by measuring the electrophoretic mobility at 25 °C in DTS1060 capillary cells (Malvern) in five measurement cycles. Results were calculated by the Malvern software 6.20. All experiments were repeated once.

2.6 Stability testing of polyplexes

Polyplexes with 5 µg pDNA were prepared as described above and treated with 10 µL DNase I (5 Kunitz units/µg plasmid), diluted in 150 mM NaCl solution supplemented with 20 mM $MgCl_2$ solution, pH 7.4 (Amersham Biosciences, Piscataway, USA), at 37 °C for 45 minutes. Afterwards the enzyme was inactivated by heating of the samples to 70 °C for 35 minutes. To release pDNA from the polyplexes, 50 µL dextran sulfate solution (10 mg/mL) (5 kDa, *Leuconostoc species pluralis*, Sigma) were added at 37 °C for 20 minutes. Untreated free pDNA and free pDNA equally treated as the polyplexes, but without the addition of DNase I represented the negative controls. Non-complexed pDNA treated with DNase I was used as positive control. Separation by gel electrophoresis was performed as described in the section above.

2.7 In vitro transfection of eukaryotic cells

Transfection efficiency was tested on CHO-K1 (Chinese hamster ovary cells, German Collection of Microorganisms and Cell Cultures, DSMZ, Braunschweig, Germany) cells cultured in Ham's F12 medium (PAA, Pasching, Austria) containing 1 mM L-glutamine and 10% fetal bovine serum Gold (FBS Gold, PAA) at 37 °C, 5% CO_2 and 95% relative humidity. Polyplexes were freshly prepared before each experiment as described above in 150 mM NaCl containing 4 µg pGL3 plasmid in a total volume of 200 µL. Cells (50.000/well) were seeded in 12-well plates (Greiner bio one) with each well containing 2 mL medium. After 24 h medium was changed, and polyplexes or controls were added in serum-containing

medium. Cells only treated with 200 µL physiological saline served as negative control while polyplexes formed with a commercial LPEI (2.5 kDa, Polysciences Europe GmbH, Eppelheim, Germany) at N/P 25 were used as positive control. Additionally, the minimum transfection rate was determined by the use of non-complexed plasmid DNA. After 4 h incubation medium was changed again, and the cells were incubated for further 44 h. Afterwards cells were lysed, and luciferase activity was determined using a commercial kit (Luciferase assay system, Promega) according to the manufacturer's protocol using an onboard dispensing system for the direct application of the assay reagent on the samples in the microplate reader (Fluostar OPTIMA microplate reader, BMG Labtech, Offenburg, Germany). The protein content of the samples was quantified with a standard bicinchoninic acid (BCA) assay kit (Thermo Scientific, Rockford, USA) as instructed by the manufacturer with minor changes. To inactivate dithiothreitol of the lysis reagent, 25 µL cell lysate were treated with 10 µL 0.05 M iodacetamide solution (Applichem, Darmstadt, Germany) at 37 °C for 20 min. Afterwards, 200 µL BCA assay reagent were added and incubated at 37 °C for 40 minutes. Absorption was measured using a microplate reader at a wavelength of 570 nm and compared to a bovine serum albumin (BSA) standard curve. The transfection efficiency is presented as relative light units (RLUs)/µg protein.

2.8 Biocompatibility assays

To investigate the cytotoxicity of the polyplexes the 3-(4,5-dimethylthiazol-2-yl)-2,5-diphenyl tetrazolium bromide (MTT) assay was performed as described before [27] using L929 mouse fibroblasts (DSMZ) grown in clear flat bottomed 96-well plates (Greiner bio one) in Roswell Park Memorial Institute 1640 culture medium (RPMI 1640, PAA) supplemented with 10% FBS Gold and 2 mM L-glutamine at 37 °C, 5% CO_2 and 95% relative humidity. To obtain the same polyplex to cell ratios as used in the transfection experiments polyplexes at N/P 25 and 50 were formed by mixing 3.2 µg DNA and the

required polymer stock solution each diluted with 150 mM physiological saline to a total volume of 60.5 µL as described in the section above. Afterwards, the polyplex solutions were diluted with 1089 µL medium. Aliquots of 110 µL were added to the cells and incubated for 4 h. Polyplex solutions were replaced by 200 µL RPMI 1640 medium, and cells were incubated for further 20 h. Experiments were run in seven parallel experiments and repeated once.

Hemocompatibility testing of non-complexed LPEIs and PHPEtOxs was performed by erythrocyte aggregation and hemolysis assays. The collection of sheep erythrocytes and the assay procedures were described in detail by Bauer et al.[27] For light microscopic determination of erythrocyte aggregation, polymer dilutions with five different concentrations up to a minimum concentration of 1.875 µg/mL were prepared. As negative and positive controls erythrocytes were treated with PBS or 25 kDa branched poly(ethylene imine) (30 µg/mL, kind gift of BASF corporation, Ludwigshafen, Germany). Test polymers as well as controls were incubated with erythrocytes for 2 h followed by the evaluation of the erythrocyte aggregating potential with a three staged classification system as described in [27].

For hemolysis experiments five different polymer concentrations were investigated ranging from 0.1875 to 3 mg/mL compared to the negative control consisting of PBS. Positive control (100%) was achieved by treatment of red blood cells with a 1% Triton X-100 solution (Ferak, Berlin, Germany). Polymer solutions as well as controls were mixed with the erythrocyte suspension at ratio 1:1, and incubated at 37 °C for 1 h. Measurements and evaluation were described in detail elsewhere.[27]

3. Results and discussion

3.1 Synthesis and structural characterization of the polymers

LPEIs (Fig. 1 a) with molar masses from 1.76 to 8.65 kDa (corresponding to 40–200 repeating units) have been synthesized (Table 1) by acidic hydrolysis of both poly(2-methyl-2-oxazoline) (PMeOx) and PEtOx. The starting poly(2-oxazoline)s were obtained by CROP.[24, 27] For the synthesis of the PHPEtOx (Fig 1 b) with different amounts of ethylene imine units, the 20 kDa PEtOx [polydispersity index (PDI) = 1.35, Mn (SEC) = 12,000 Da] was partially hydrolyzed under acidic conditions. With increasing hydrolysis time, the DH increased from 21, 41, 56 and 75 to 86% (corresponding to 42, 82, 112, 150, and 172 ethylene imine repeating units) (Table 2). Analysis of the LPEIs and PHPEtOxs by means of ^{1}H NMR spectroscopy confirmed their purity and identity. The DHs of the PHEtOxs were calculated by correlating the methyl proton signal of the uncleaved side chain (1.13 ppm) and the protons of the LPEI backbone (2.73 ppm). Size exclusion chromatography revealed that the LPEIs were synthesized with a narrow molar mass distribution (Table 1). The high PDI values of some PHPEtOx (Table 2) can be ascribed to the statistical character of the hydrolysis, resulting in polymer chains with different amounts of positively charged ethylene imine units and slightly varying molar masses and, hence, different interactions with the used SEC column. The differences between the calculated molar masses and the measured values can be explained with the usage of the neutral PS as calibration standard, while the LPEIs and PHPEtOx are positively charged, varying with the amount of ethylene imine units. All polymer stock solutions could be spectrophotometrically quantified by copper chelate complex formation. Preliminary experiments using polymer concentrations up to 2 mg/mL confirmed that the presence of 2-oxazoline units did not interfere with the quantification of the ethylene imine units (data not shown).

3.2 Determination of DNA binding by agarose gel electrophoresis

A qualitative insight into the DNA binding capacity of LPEIs and PHPEtOxs resulting from electrostatic interactions between the oppositely charged binding partners was obtained by agarose gel electrophoresis. Based on previous experiments with LPEIs, N/P ratios from 0.25 to 9 were selected to form polyplexes.[13] DNA was classified as complexed when its movement in the electric field was completely inhibited either by increase in size due to the formation of nanoassemblies and/or by masking its anionic charge. Free herring testes DNA that was used as model DNA [28], migrated into the gel without any hindrance and showed a broad fluorescent band corresponding to its broad molar mass distribution (Fig. 1 SI and 2 SI, "untreated"). Free polymers were used as controls to exclude unspecific polymer/dye interactions and exhibited no signals (Fig. 1 SI and 2 SI, "free polymer").

Although all cationic polymers spontaneously formed polyplexes with herring testes DNA (Fig. 1 SI and 2 SI, "N/P 0.25-9"), differences between LPEIs and PHPEtOx were obvious. For the LPEIs a molar mass dependent binding profile could be observed in accordance to earlier reports [13], resulting from the increase of EI units. While for LPEIs with $\geq$ 60 monomer units (Table 1, Fig. 1 SI d-h) a complete retardation of DNA was apparent already at N/P 1 representing charge balance, for LPEIs with lower molar masses higher N/P ratios of 2 or 3 were necessary, indicating a weaker DNA binding capacity (Fig. 1 SI a-c).

The formation of interpolyelectrolyte polyplexes of the PHPEtOxs was found to be dependent on the degree of hydrolysis. Only PHPEtOx-86 (Table 2, Fig. 2 SI e) was able to fully complex DNA at N/P ratio 1 whereas all other partially hydrolyzed polymers started to form polyplexes at N/P ratio 2 (Table 2, Fig. 1 SI a - d). Comparable data were reported by others [22-23, 29] showing a more efficient neutralization of DNA phosphate groups with increasing DH. The direct comparison of LPEIs and PHPEtOxs revealed that despite having the same number of ethylene imine units, a higher N/P ratio was necessary for the PHPEtOxs to fully retard DNA which might be related to the lower density of ethylene imine units of the

PHPEtOx, the protein repellent character of the PEtOx units, and a possible steric hindrance caused by the 2-ethyl-2-oxazoline side chains.

3.3 Polyplex stability against enzymatic treatment

The formation of stable polymer/DNA nanoassemblies by electrostatic interactions is not only a prerequisite to facilitate cell uptake but also for the protection of DNA against enzymatic digestion in the blood stream and the endosome. The enzymatic stability of plasmid DNA was tested by agarose gel electrophoresis with a DNase I concentration of 96.2 U mL-1 which is approximately 270-times higher than the normal level in human blood [30], representing a worst case scenario. Afterwards, the enzyme was inactivated by heat treatment and the DNA released by dissociation of the polyplexes with dextran sulfate. For the experiments two different N/P ratios (25 and 100) were selected that represent conditions with fully condensed DNA based on preliminary experiments (data not shown) and reports.[13-14]

Untreated DNA showed two characteristic bands for the supercoiled and the open circular form (Fig. 2 a-d, lane 1, “untreated"). The same pattern was obtained for plasmid treated according to the same procedure as the complexed DNA but without enzyme (Fig. 2 a-d, lane 2, “treated”). It was found to be stable and served as control to exclude non-specific degradation. DNase treated free plasmid was highly prone to enzymatic degradation to low molar mass products with higher mobility, and the bands disappeared (Fig. 2 a-d, lane 3, “DNase I”).

The DNA protection by the polyplexes was found to be strongly dependent on the physicochemical characteristics of the polymers and the polyplex composition that correlated well with the observations of the binding studies described above. After interaction with the LPEIs, plasmid was stabilized not only with increasing polyplex N/P ratios but also an increasing number of the ethylene imine units per polymer. While at N/P ratio 25 (Fig. 2 a,

lane 10) 150 monomers were necessary to stabilize the DNA, at N/P ratio 100 already 50 units (Fig. 2 b, lane 6) were found to be effective. PHPEtOxs started to form stable polyplexes at a degrees of hydrolysis of 86% and 75% at N/P ratios 25 (Fig. 2 c, lane 8) and 100 (Fig. 2 d, lane 7), respectively. The direct comparison of LPEIs and PHPEtOxs with the same number of EI units revealed an increased stability against the degradative mechanisms by the fully cleaved LPEIs that might reflect the stronger intermolecular associations and a more effective shielding of DNA described in the section before. Changes in the topology of the plasmids were observed in some cases as reported earlier.[28, 31] For the following experiments only the PHPEtOxs and LPEIs with a comparable number of ethylene imine monomers were selected and tested.

3.4 Size and zeta potential of the polyplexes

Measurements of the hydrodynamic radius (Fig. 3 a) und the zeta potential (Fig. 3 b) were performed with plasmid DNA polyplexes at N/P ratios 25 and 100. Polyplexes consisting of plasmid and commercial 2.5 kDa LPEI at N/P ratio 25 were used as control since they showed a high transfection efficiency and an acceptable toxicity in preliminary experiments (data not shown). They were characterized by a particle size of 169 nm and a zeta potential of 35.4 mV.

None of the polymers with 40 EI units was able to form small sized (hydrodynamic radius > 1000 nm) monodisperse particles (Fig. 3 a). For the LPEIs from 40 to 150 EI units a decrease of particle size from 1340 nm to 153 nm, respectively, could be detected with increasing polymer chain length at N/P 25 (Fig. 3 a), whereas LPEI-150 to LPEI-200 gave comparable results. The decrease was found to be more pronounced at N/P 100 where already the lower molar mass LPEIs with 80 and 100 EI units formed polyplexes ≤ 264 nm. The tendency of the PDIs and the monomodality of the LPEI polyplexes were found to be directly correlated with the hydrodynamic diameters. Comparable data were obtained by

characterization of the LPEIs using ultracentrifugation.[32] The influence of the density of EI units on particle size was found to be comparatively lower as demonstrated by the PHPEtOx polyplexes. With exception of the PHPEtOx-21, all polyplexes were found to be in a size range from 112 to 299 nm. Not only the hydrodynamic diameters but also the PDIs and the monomodality were widely independent of the N/P ratio and the degree of hydrolysis.

Due to the excess of the cationic polymer at N/P ratios 25 and 100, all polyplexes were positively charged with zeta potentials between 19.5 and 47.3 mV (Fig. 3 b). The large hydrodynamic diameter and the strong tendency to aggregate of the 40 EI unit polyplexes with both types of polymers were related to the lowest surface charges and, thus, minimal charge-charge repulsion. A comparison of fully and partially cleaved polymers revealed higher cationic zeta potentials for LPEIs compared to PHPEtOxs despite a comparable amount of EI units. The LPEIs with 80 ethylene imine units already reached the maximum zeta potentials with minor changes at higher N/P ratios or more monomer units. For the PHEtOxs structure dependent changes were detectable. At N/P 25 the zeta potential increased from 19.5 mV for 21% to 41.1 mV for 86% whereas at N/P 100 the increase was only detectable from 21% to 56% followed by a plateau phase for higher degrees of hydrolysis.

The physicochemical characteristics of the polyplexes were reasonably consistent with the earlier findings reporting a dependency of both parameters on the number of EI units. Jeong et al. compacted pDNA by 88% hydrolyzed PHPEtOx to about 150 nm with a zeta potential of 28.4 mV.[22] Fernandes et al. also reported a correlation of size and surface charge with the degree of hydrolysis, the formation of PHPEtOx/DNA polyplexes with comparable particle sizes but only moderate cationic zeta potential.[23] This might be related to the lower molar masses of 10 kDa used for the synthesis of PHPEtOx.

3.5 In vitro cyto- and hemotoxicity testing

To evaluate the influence of the polymer characteristics on the cell viability, a MTT assay (Fig. 4) was performed after 24 h incubation using L929 mouse fibroblasts according to the recommendations of different standard organizations.[33-35] To be able to directly compare the results with the transfection experiments the same N/P ratios, incubation times, and polyplex/cell ratios were used. Positive control cells treated with a 0.02% thiomersal solution showed a reduced cell viability of 2.8% mean.

Although at N/P 25 a slight trend to a reduced cell viability with an increase in the number of EI units could be observed (Fig. 4 a), all polyplexes could be classified as non-toxic based on the recommendations of the DIN ISO 10993-5 that categorizes cell viabilities higher than 70% as non-toxic.[35] The comparison of partially and fully cleaved compounds up to 175 EI units did not reveal relevant differences, indicating that the ethylene imine density had no substantial impact on cytotoxicity of the polyplexes at N/P 25. Increasing the N/P ratio from 25 to 50 elicited in a decline of the metabolic activity of the cells that might be related to the larger amount of unbound polymer in the polyplexes (Fig. 4 b). Cell viabilities below 70% could be observed for partially and fully cleaved polymers with ≥ 175 EI units. The increase of the N/P ratio was found to be associated with larger differences of cytotoxicity between both types of polymers with PHPEtOxs being slightly better tolerated than their fully cleaved counterparts (Fig. 4 b).

Since the polyplexes are intended for systemic administration a high hemocompatibility is essential. Therefore, aggregation and hemolysis of sheep erythrocytes were analyzed after treatment with LPEIs and PHPEtOxs at different concentrations. To simulate a worst case scenario possibly caused by polyplex dissociation, overdosing or general wrong use, the polymers were investigated in the free form. In the screenings of the red blood cell aggregation, the negative control was represented by erythrocytes only treated with PBS, classified as stage 1 (data not shown). In contrast, strong rouleau and cluster

formation could be observed for the positive control cells incubated with 25 kDa BPEI (30 µg/mL) that was classified as stage 3 (data not shown).

None of the polymers induced changes (stage 1) of the red blood cells at the lowest concentration (1.875 µg/mL) tested (Fig. 5). This was also valid for PHPEtOx-21 and -41 as well as for LPEI-40 up to the highest concentration of 30 µg/mL. In contrast, LEI ≥ 150 ethylene imine units and PHEtOx-86 already formed clusters (stage 3) at 3.75 µg/mL. All polymers in between demonstrated an increased aggregation of the erythrocytes with increasing polymer concentration. A direct comparison of LPEI and PHPEtOx with comparable number of ethylene imine units demonstrated a more pronounced effect on red blood cells for LPEIs than for PHPEtOxs indicating a more important role of the number than of the density of the ethylene imine units.

To exclude any influence of the polymers on the membrane integrity of erythrocytes under the chosen conditions the hemoglobin release was spectrophotometically quantified. Completely lysed erythrocytes treated with 1% Triton X-100 solution represented 100% hemolysis, while negative controls incubated in PBS reached values of about 0.6%. Limits for the evaluation of hemolysis were taken from ASTM F756-13 that describes a relative hemolysis below 2% as non-hemolytic. [36] Neither LPEIS nor PHPEtOxs caused hemolysis higher than 1.9%, demonstrating the low membrane damaging potential of both types of polymers under the chosen conditions (data not shown).

As mentioned above in the discussion of the so called charge dilemma, the cationic charge of the polymers is not only the key parameter for the electrostatic interaction with the DNA, but also responsible for the electrostatic attachment of the polymers to negatively charged cell membranes, plasma proteins and connective tissues, leading to unwanted side effects or rapid elimination from the blood.[37] In accordance to our observations, with an increasing number of cationic charges, the deposition of LPEIs on the cell surface was found to be increased impairing the plasma membrane functions and leading to cell death.[12] In

accordance, for HEEI-copolymers higher ratios of EI in the copolymers correlated with increasing degree of protonation, allowing more efficient interactions with membranes.[11] In agreement with previous outcomes, the cytotoxic effects of the LPEI polyplexes were comparably lower than that of the non-complexed polymers.[6]

Additionally, a reduced charge density was identified as advantageous for the biocompatibility of cationic polymers.[6, 22] In accordance to our results, for PHEtOxs the cell viability was described to decline as the DH increased.[22-23] However, Fernandes et al. reported a 70% hydrolyzed PHPEtOx still to be low toxic which might be related to the lower molar mass of their starting materials.[23] The biocompatibility of PEtOx itself has been widely studied in *in vitro* experiments showing that this polymer is well tolerated by mouse fibroblasts and red blood cells.[27]

When comparing the influence of the number and density of the EI units on the biocompatibility, the number of EI units seems to have a slightly higher impact on the cytotoxicity of polyplexes than their density. In red blood cell experiments, for LPEIs and PHPEtOxs with corresponding EI units < 40 units and ≥ 150 units both parameters cannot be ranked since the minimum or maximum of toxicity has been reached. For polymers with numbers of EI units in between can be suggested that the total amount of EI units has a more profound effect on the aggregation of red blood cells than their density. Differences to former investigations are possibly related to different study designs using free polymers for cytotoxicity test, only small ranges or numbers of hydrolyzed polymers or missing fully cleaved counterparts with comparable EI units.[22-23, 38]

3.6 In vitro transfection efficiency

For the quantification of the transfection efficacy, CHO-K1 cells were transfected with polyplexes containing pGL3 pDNA that encodes the luciferase gene driven by a SV40 promoter. Reporter gene expression efficiency was presented as relative light units (RLUs)/µg

protein and calculated by dividing the total RLUs determined by bioluminescence measurements by the total protein mass. Based on preliminary experiments, N/P ratios 25 (Fig. 6 a) and 50 (Fig. 6 b) of the polyplexes were found to be suitable and were selected for the following experiments. Non-complexed DNA and untreated cells served as controls and failed to produce detectable levels of transgene expression (Fig. 6).

LPEI/DNA polyplexes mediated an increase of the transgene expression with a higher number of EI units and increasing N/P ratios. A minimum of 80 and 40 EI units at N/P ratio 25 and 50 were necessary to achieve detectable transfections. LPEI-175 and LPEI-200 reached transfection efficiencies higher than the commercial 2.5 kDa LPEI at both N/P ratios tested, presumably due to their higher molar mass. The slightly lower transfection rate of the LPEI-200 compared to LPEI-175 might be related to its higher cytotoxicity as observed by BCA assay which showed a reduced protein content (data not shown).

The PHEtOxs were able to transfect the CHO-K1 cells, but with a comparably lower rate of expression compared to the LPEIs. A trend to higher transfection with increasing N/P ratios and higher degrees of hydrolysis could be observed. While at N/P ratio 25 PHPEtOx-86 was found to be the most efficient partially hydrolyzed polymer, at N/P 50 no difference could be observed between PHPEtOx-75 and PHPEtOx-86 that correlated with a reduced protein content. Accordingly, PHPEtOx polymers with DHs between 70 and 85% were reported to be the most efficient PHPEtOx.[22-23, 38] However, only PHPEtOx hydrolyzed from PEtOx with a higher molar mass of 50 kDa reached efficacies comparable to 22 kDa LPEI [38] and 25 kDa branched PEI.[22]

Generally/In general, for both types of polymer low transfection rates correlated well with large polyplex sizes, the formation of aggregates and low zeta potentials which was reported before for many classes of polycations.[39] The lower gene transfer of PHPEtOx compared to LPEI, although having a similar number of EI units could not be explained by an impaired endosomal release since the addition of the lysosomotropic agent chloroquine did

not improve the transfection efficacy (data not shown). PHPEtOx polyplexes performed less efficient in transfection, although they exhibited smaller or even comparable polyplex diameters, similar zeta potentials and similar or even preferred biocompatibility profiles compared to the LPEI polyplexes under the chosen conditions. Excluding all these parameters as explanation, the weaker DNA binding and lower protective effect of PHPEtOxs against enzymatic degradation of pDNA, as shown in the gel electrophoresis experiments, seem to be the conclusive reason for the poorer performance. Since all transfection experiments were performed in serum containing culture medium, DNA degradation could be partially caused by heat resistant DNases that are present in fetal bovine serum.[40]

4. Conclusion

Partially hydrolyzed poly(2-ethyl-2-oxazoline)s (PHPEtOxs) with a degree of polymerization of 200 and different degrees of hydrolysis (21 to 86%) have been prepared by acidic hydrolysis. They have been compared to LPEIs with an equivalent number of EI units regarding the physicochemical and biological characteristics of their polyplexes with DNA. PHPEtOxs revealed a lower DNA binding capacity and enzymatic polyplex stability leading conclusively, to a reduced transfection efficacy compared to LPEIs. The biocompatibility profile was found to be more preferred only for the free polymers, but comparable for the polyplexes. The direct comparison of both polymer types revealed that the total amount of EI units is not the most important parameter but their density within the polymer backbone. The LPEIs with EI units in close juxtaposition with each other demonstrated a dramatically higher increase in transfection with increasing number of EI units compared to the PHPEtOx with a lower density of protonable amines in the backbone. Conclusively, the reduction of EI density to generate more biocompatible polyplexes has to be carefully discussed since the effect on toxicity is dramatically lower than the loss of transfection capability.

Acknowledgements

The authors would like to thank the Thuringian Ministry for Education, Science, and Culture (Grant #B514-09051, NanoConSens) for financial support. KK is grateful to the Alexander von Humboldt foundation for financial support.

References

[1] F. Schlenk, S. Grund, D. Fischer, Recent developments and perspectives on gene therapy using synthetic vectors, Therapeutic Delivery, 4 (2012) 95-113.
[2] www.wiley.com/legacy/wileychi/genmed/clinical
[3] A. Aied, U. Greiser, A. Pandit, W. Wang, Polymer gene delivery: overcoming the obstacles, Drug Discovery Today, 18 (2013) 1090-1098.
[4] O.M. Merkel, T. Kissel, Quo vadis polyplex?, Journal of Controlled Release, in press, (2014), DOI: 10.1016/j.jconrel.2014.06.009
[5] S. Bauhuber, R. Liebl, L. Tomasetti, R. Rachel, A. Goepferich, M. Breunig, A library of strictly linear poly(ethylene glycol)–poly(ethylene imine) diblock copolymers to perform structure–function relationship of non-viral gene carriers, Journal of Controlled Release, 162 (2012) 446-455.
[6] D. Fischer, Y. Li, B. Ahlemeyer, J. Krieglstein, T. Kissel, In vitro cytotoxicity testing of polycations: influence of polymer structure on cell viability and hemolysis, Biomaterials, 24 (2003) 1121-1131.
[7] R. Tang, R.N. Palumbo, L. Nagarajan, E. Krogstad, C. Wang, Well-defined block copolymers for gene delivery to dendritic cells: Probing the effect of polycation chain-length, Journal of Controlled Release, 142 (2010) 229-237.
[8] D. Schaffert, C. Troiber, E. Wagner, New sequence-defined polyaminoamides with tailored endosomolytic properties for plasmid DNA delivery, Bioconjugate Chemistry, 23 (2012) 1157-1165.
[9] H. Yin, R.L. Kanasty, A.A. Eltoukhy, A.J. Vegas, J.R. Dorkin, D.G. Anderson, Non-viral vectors for gene-based therapy, Nature Review Genetics, 15 (2014) 541-555.
[10] E.V.B. van Gaal, R. van Eijk, R.S. Oosting, R.J. Kok, W.E. Hennink, D.J.A. Crommelin, E. Mastrobattista, How to screen non-viral gene delivery systems in vitro?, Journal of Controlled Release, 154 (2011) 218-232.
[11] D. Fischer, A. von Harpe, K. Kunath, H. Petersen, Y. Li, T. Kissel, Copolymers of ethylene Imine and N-(2-hydroxyethyl)-ethylene Imine as tools to study effects of polymer structure on physicochemical and biological properties of DNA complexes, Bioconjugate Chemistry, 13 (2002) 1124-1133.
[12] L. Parhamifar, A.K. Larsen, A.C. Hunter, T.L. Andresen, S.M. Moghimi, Polycation cytotoxicity: a delicate matter for nucleic acid therapy-focus on polyethylenimine, Soft Matter, 6 (2010) 4001-4009.
[13] M. Breunig, U. Lungwitz, R. Liebl, C. Fontanari, J. Klar, A. Kurtz, T. Blunk, A. Goepferich, Gene delivery with low molecular weight linear polyethylenimines, The Journal of Gene Medicine, 7 (2005) 1287-1298.
[14] D. Fischer, T. Bieber, Y. Li, H.-P. Elsässer, T. Kissel, A novel non-viral vector for DNA delivery based on low molecular weight, branched polyethylenimine: Effect of molecular weight on transfection efficiency and cytotoxicity, Pharmaceutical Research, 16 (1999) 1273-1279.

[15] Y.-Y. Liu, X.-Y. Yang, Z. Li, Z.-L. Liu, D. Cheng, Y. Wang, X.-J. Wen, J.-Y. Hu, J. Liu, L.-M. Wang, H.-J. Wang, Characterization of polyethylene glycol-polyethyleneimine as a vector for alpha-synuclein siRNA delivery to PC12 cells for parkinson's disease, CNS Neuroscience & Therapeutics, 20 (2014) 76-85.
[16] D.K. Bonner, X. Zhao, H. Buss, R. Langer, P.T. Hammond, Crosslinked linear polyethylenimine enhances delivery of DNA to the cytoplasm, Journal of Controlled Release, 167 (2013) 101-107.
[17] W.Y. Seow, K. Liang, M. Kurisawa, C.A.E. Hauser, Oxidation as a facile strategy to reduce the surface charge and toxicity of polyethyleneimine gene carriers, Biomacromolecules, 14 (2013) 2340-2346.
[18] M. Breunig, U. Lungwitz, J. Klar, A. Kurtz, T. Blunk, A. Goepferich, Polyplexes of polyethylenimine and per-N-methylated polyethylenimine-cytotoxicity and transfection efficiency, J Nanosci Nanotechnol, 4 (2004) 512-520.
[19] R.K. Oskuee, A. Philipp, A. Dehshahri, E. Wagner, M. Ramezani, The impact of carboxyalkylation of branched polyethylenimine on effectiveness in small interfering RNA delivery, J Gene Med, 12 (2010) 729-738.
[20] A.M. Doody, J.N. Korley, K.P. Dang, P.N. Zawaneh, D. Putnam, Characterizing the structure/function parameter space of hydrocarbon-conjugated branched polyethylenimine for DNA delivery in vitro, Journal of Controlled Release, 116 (2006) 227-237.
[21] L. Tauhardt, K. Kempe, K. Knop, E. Altuntaş, M. Jäger, S. Schubert, D. Fischer, U.S. Schubert, Linear polyethyleneimine: Optimized synthesis and characterization – on the way to "pharmagrade" batches, Macromol Chem Physic, 212 (2011) 1918-1924.
[22] J.H. Jeong, S.H. Song, D.W. Lim, H. Lee, T.G. Park, DNA transfection using linear poly(ethylenimine) prepared by controlled acid hydrolysis of poly(2-ethyl-2-oxazoline), Journal of Controlled Release, 73 (2001) 391-399.
[23] J.C. Fernandes, X. Qiu, F.M. Winnik, M. Benderdour, X. Zhang, K. Dai, Q. Shi, Linear polyethylenimine produced by partial acid hydrolysis of poly(2-ethyl-2-oxazoline) for DNA and siRNA delivery in vitro, Int J Nanomedicine, 8 (2013) 4091-4102.
[24] H.M.L. Lambermont-Thijs, F.S. van der Woerdt, A. Baumgaertel, L. Bonami, F.E. Du Prez, U.S. Schubert, R. Hoogenboom, Linear poly(ethylene imine)s by acidic hydrolysis of poly(2-oxazoline)s: Kinetic screening, thermal properties, and temperature-induced solubility transitions, Macromolecules, 43 (2009) 927-933.
[25] E. Altuntaş, K. Knop, L. Tauhardt, K. Kempe, A.C. Crecelius, M. Jäger, M.D. Hager, U.S. Schubert, Tandem mass spectrometry of poly(ethylene imine)s by electrospray ionization (ESI) and matrix-assisted laser desorption/ionization (MALDI), J. Mass Spectrom., 47 (2012) 105-114.
[26] T.D. Perrine, W.R. Landis, Analysis of polyethylenimine by spectrophotometry of its copper chelate, Journal of Polymer Science Part A-1: Polymer Chemistry, 5 (1967) 1993-2003.
[27] M. Bauer, C. Lautenschlaeger, K. Kempe, L. Tauhardt, U.S. Schubert, D. Fischer, Poly(2-ethyl-2-oxazoline) as alternative for the stealth polymer poly(ethylene glycol): Comparison of in vitro cytotoxicity and hemocompatibility, Macromolecular Bioscience, 12 (2012) 986-998.
[28] D. Fischer, H. Dautzenberg, K. Kunath, T. Kissel, Poly(diallyldimethylammonium chlorides) and their N-methyl-N-vinylacetamide copolymer-based DNA-polyplexes: role of molecular weight and charge density in complex formation, stability, and in vitro activity, International Journal of Pharmaceutics, 280 (2004) 253-269.
[29] B. Brissault, C. Leborgne, C. Guis, O. Danos, H. Cheradame, A. Kichler, Linear topology confers in vivo gene transfer activity to polyethylenimines, Bioconjugate Chemistry, 17 (2006) 759-765.

[30] S.N. Tamkovich, A.V. Cherepanova, E.V. Kolesnikova, E.Y. Rykova, D.V. Pyshnyi, V.V. Vlassov, P.P. Laktionov, Circulating DNA and DNase activity in human blood, Annals of the New York Academy of Sciences, 1075 (2006) 191-196.
[31] C.L. Gebhart, S. Sriadibhatla, S. Vinogradov, P. Lemieux, V. Alakhov, A.V. Kabanov, Design and formulation of polyplexes based on pluronic-polyethyleneimine conjugates for gene transfer, Bioconjugate Chemistry, 13 (2002) 937-944.
[32] I.Y. Perevyazko, M. Bauer, G.M. Pavlov, S. Hoeppener, S. Schubert, D. Fischer, U.S. Schubert, Polyelectrolyte complexes of DNA and linear PEI: Formation, composition and properties, Langmuir, 28 (2012) 16167-16176.
[33] Biological reactivity tests, in vitro, United States Pharmacopeia Convention <87>, United States Pharmacopeia and National Formulary (USP36- NF31), Rockville, 2013.
[34] ASTM Standard F813, 2012 (2007), ‘‘Standard practice for direct contact cell culture evaluation of materials for medical devices’’, ASTM International, West Conshohocken, PA, 2012, DOI: 10.1520/F0813-07R12, www.astm.org
[35] ‘‘Biological evaluation of medical devices Part 5: Tests for in vitro cytotoxicity’’, 2nd edition, International Organization for Standardization/ANSI;ISO ISO 10993-5, Geneva, Switzerland: 2009.
[36] ASTM Standard F756, 2013, ‘‘Standard practice for assessment of hemolytic properties of materials’’, ASTM International, West Conshohocken, PA, 2013, DOI: 10.1520/F0756, www.astm.org
[37] S. Grund, M. Bauer, D. Fischer, Polymers in rug Delivery—State of the art and future trends, Advanced Engineering Materials, 13 (2011) B61-B87.
[38] B. Brissault, A. Kichler, C. Guis, C. Leborgne, O. Danos, H. Cheradame, Synthesis of linear polyethylenimine derivatives for DNA transfection, Bioconjugate Chemistry, 14 (2003) 581-587.
[39] M.A. Mintzer, E.E. Simanek, Nonviral vectors for gene delivery, Chemical Reviews, 109 (2008) 259-302.
[40] M. von Köckritz-Blickwede, O.A. Chow, V. Nizet, Fetal calf serum contains heat-stable nucleases that degrade neutrophil extracellular traps, Blood, 114 (2009) 5245-5246.

Figures

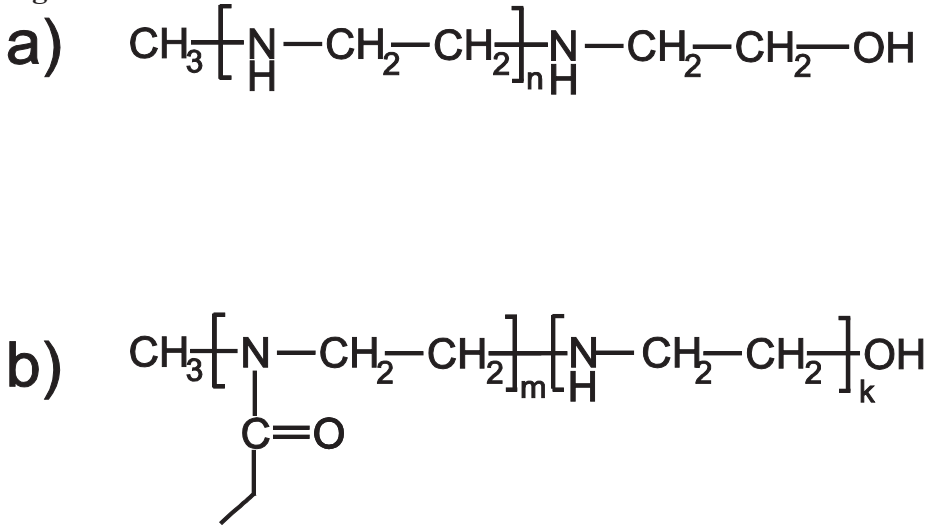

Fig 1. Schematic drawing of linear PEI (a) and partially hydrolyzed PEtOx (b)

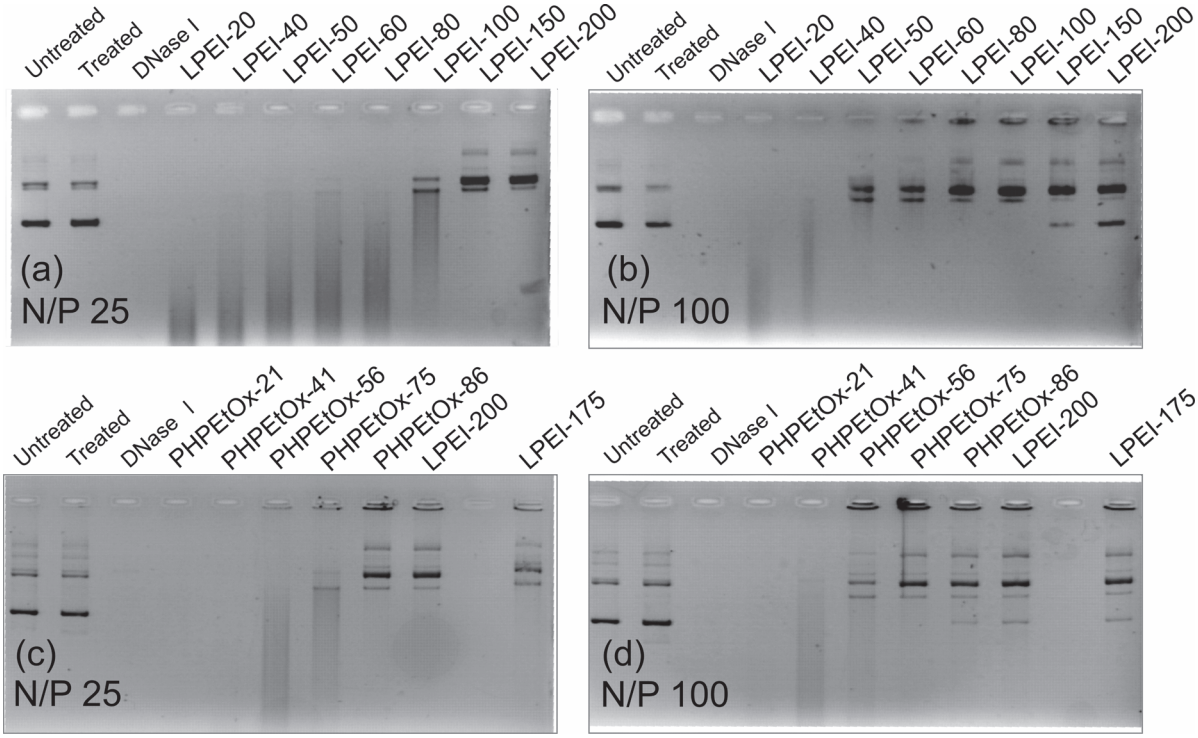

Fig. 2. Stability of LPEI (a, b) and PHPEtOx (c, d) polyplexes with plasmid DNA against enzymatic degradation by DNase I at N/P ratios 25 (a, c) and 100 (b, d). Controls: lane 1: untreated free plasmid; lane 2: free plasmid treated in the same way as polyplexes but without enzyme; lane 3: free plasmid treated with enzyme.

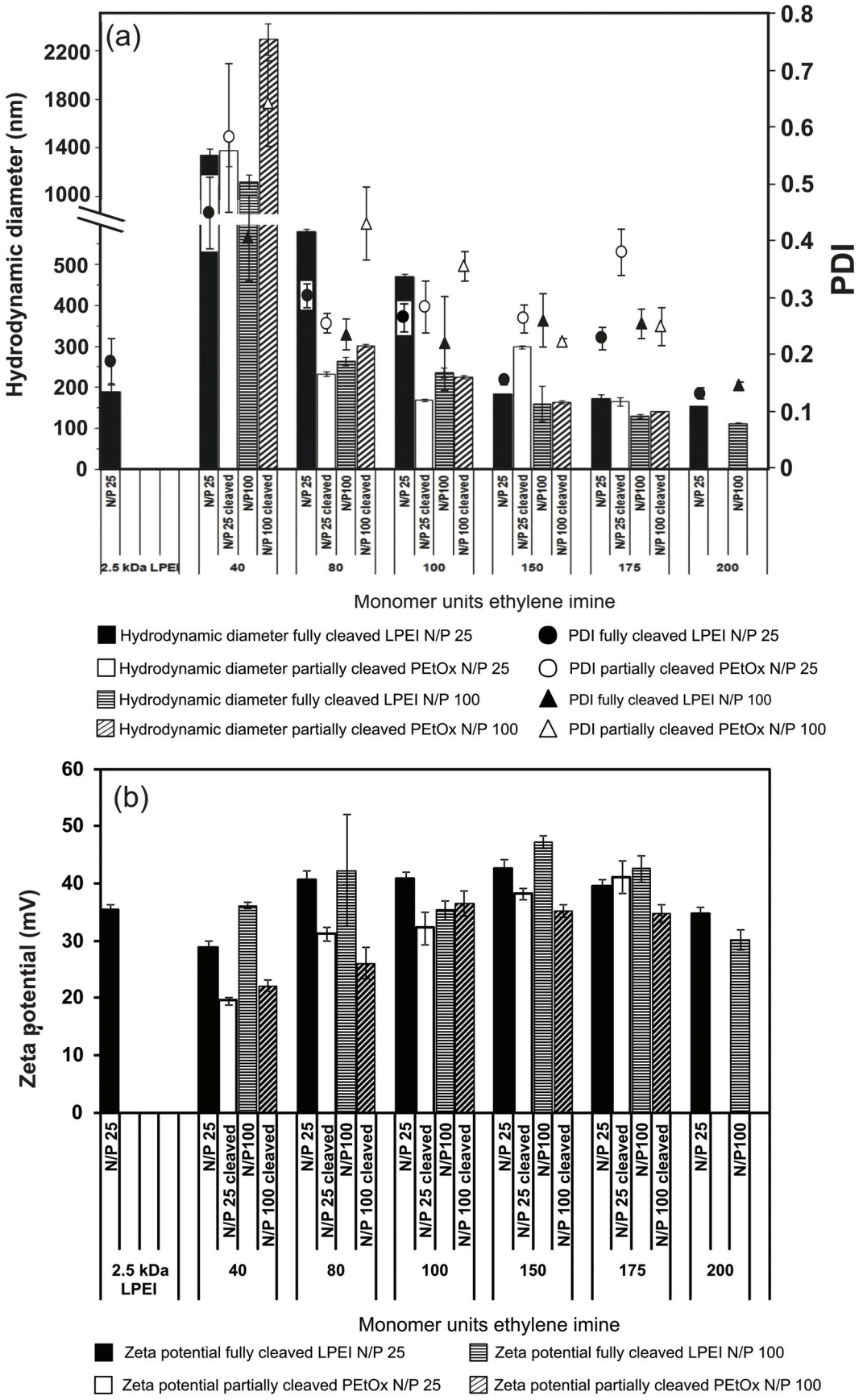

Fig. 3. Hydrodynamic diameter (a) and zetapotential (b) of polyplexes formed at N/P ratio 25 and 100. Results are shown as the mean of at least 5 measurements ± SD.

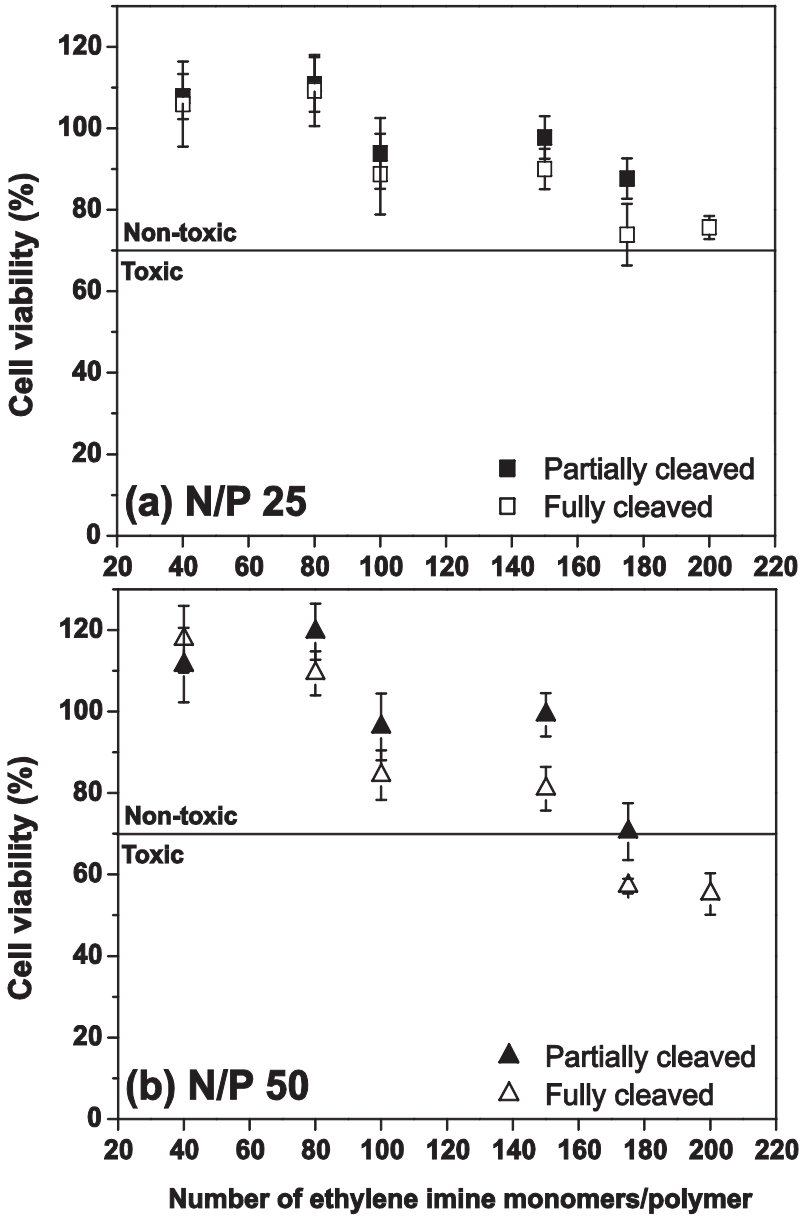

Fig. 4. Cytotoxicity of PHPEtOx and LPEI polyplexes with herring testes DNA at N/P 25 (a) and N/P 50 (b) as a function of the number of ethylene imine monomers. Tests were performed with L929 mouse fibroblasts using the MTT assay after 24 h incubation. According to ISO 10993-5 values below 70% viability (see plotted line) were regarded as cytotoxic. Each data point represented the mean ± SD of seven determinations.

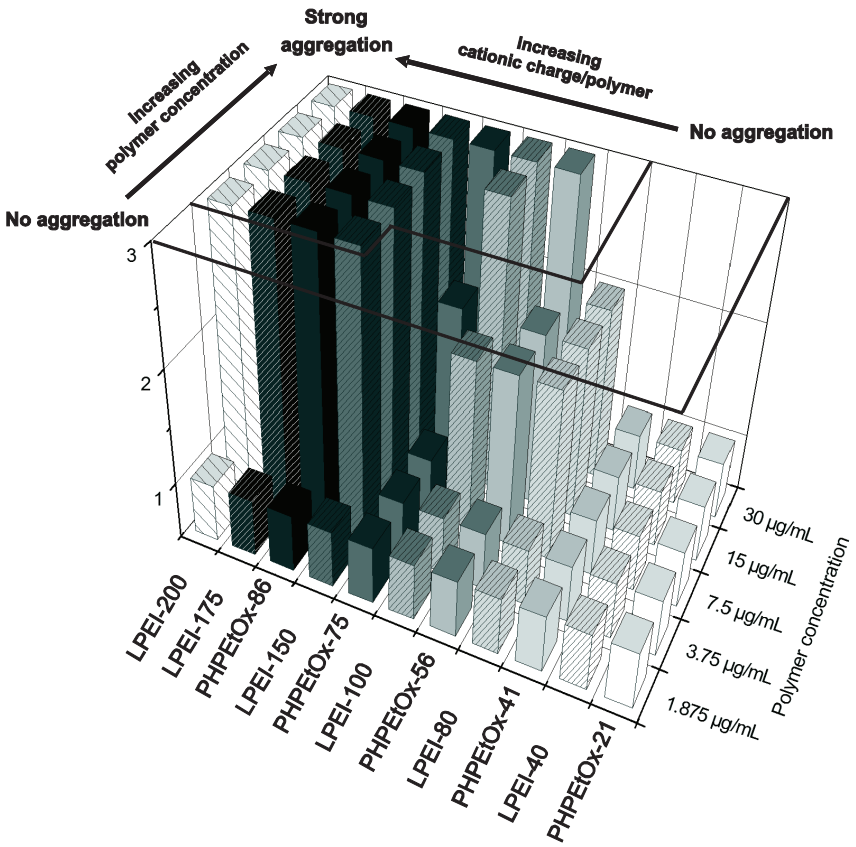

Fig. 5. Dependency of the erythrocyte aggregation of PHPEtOx and LPEI polymers on polymer concentration, number of EI units, and degree of hydrolysis, Aggregation was classified from stage 1 (no aggregation) over stage 2 (slight rouleau formation) to stage 3 (strong aggregation with cluster formation). Each bar shows the mean value of three determinations.

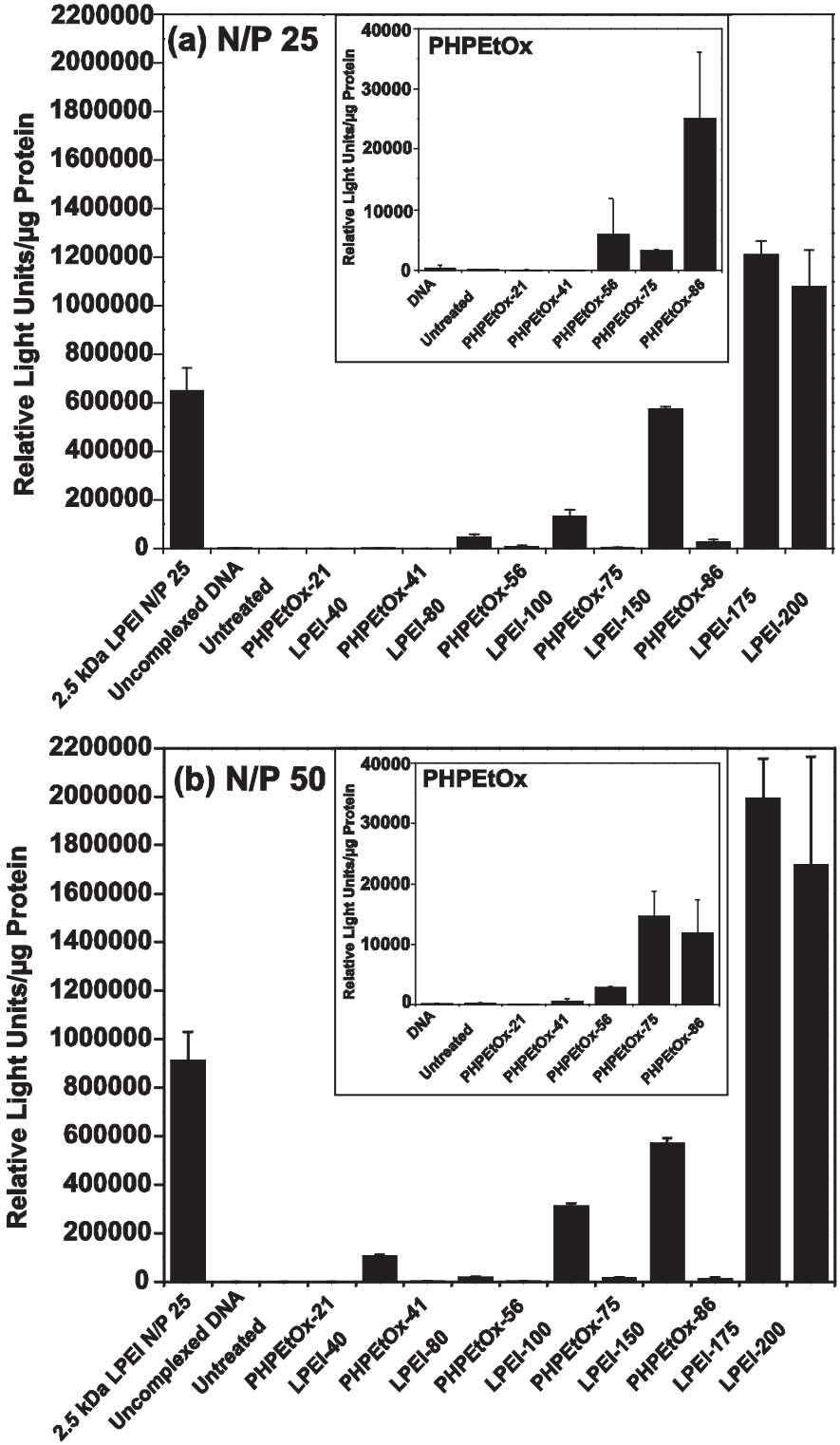

Fig. 6. Transfection efficiency of polyplexes tested on CHO-K1 cells with a luciferase assay. Polyplexes were formed with pGL3 at N/P 25 (a) and N/P 50 (b). Luciferase reporter gene expression is shown as relative light units/µg. Polyplexes with commercial 2.5 kDa LPEI at N/P 25 were used as positive control. Cells treated with 150 mM NaCl solution or non-complexed DNA represented controls. The inserts give a more detailed view on the results of the negative controls and PHPEtOxs.

Tables

Table 1 Physicochemical and DNA-binding characteristics of LPEIs

Polymer	LPEI-20	LPEI-40	LPEI-50	LPEI-60	LPEI-80	LPEI-100	LPEI-150	LPEI-175	LPEI-200
DP	20	40	50	60	80	100	150	175	200
M_w, calculated (Da)[a)]	877	1,755	2,186	2,616	3,478	4,339	6,493	7,569	8,646
M_n (Da)[b)]	6,800	10,900	13,900	15,200	16,800	21,100	27,400	19,340	17,450
PDI[b)]	1.09	1.12	1.12	1.15	1.22	1.16	1.27	1.33	1.57
N/P ratio of DNA complexation[c)]	3	2	2	1	1	1	1	1	1

[a)]calculated for CH_3-$(C_2H_5N)_n$-OH;

[b)]determined by SEC (eluent: hexafluoroisopropanol (HFIP); calibration against poly(styrene) (PS) standards);

[c)]determined by horizontal gel electrophoresis.

Table 2 Physicochemical and DNA-binding characteristics of PHPEtOx.

PHPEtOx	PHPEtOx-21	PHPEtOx-41	PHPEtOx-56	PHPEtOx-75	PHPEtOx-86
Degree of hydrolysis (%)[a)]	21	41	56	75	86
Corresponding number of ethylene imine units	42	82	112	150	172
M_w (calculated) (Da)[b)]	17,503	15,261	13,579	11,449	10,216
M_n (SEC) (Da)[c)]	33,010	26,160	19,290	11,100	13,810
PDI (SEC)[b)]	1.38	1.54	1.73	1.85	1.64
N/P ratio of DNA complexation[d)]	2	2	2	2	1

[a)]determined by ^{1}H NMR spectroscopy;

[b)]calculated for CH_3-$[(C_5H_9NO)_m$-*stat*-$(C_2H_5N)_k]$-OH;

[c)]determined by SEC (eluent: HFIP; calibration against PS standards);

[d)]determined by horizontal gel electrophoresis.

Publication 8

"Toward the Design of LPEI Containing Block Copolymers: Improved Synthesis Protocol, Selective Hydrolysis, and Detailed Characterization"

L. Tauhardt, K. Kempe, U. S. Schubert

J. Polym. Sci., Part A: Polym. Chem. **2012**, *50*, 4516-4523

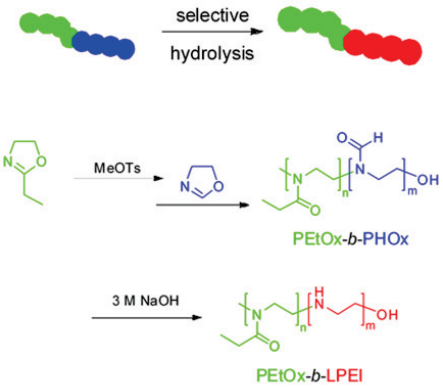

Toward the Design of LPEI Containing Block Copolymers: Improved Synthesis Protocol, Selective Hydrolysis, and Detailed Characterization

Lutz Tauhardt,[1,2] Kristian Kempe,[1,2] Ulrich S. Schubert[1,2,3*]

[1]Laboratory of Organic and Macromolecular Chemistry (IOMC), Friedrich-Schiller-University Jena, Humboldtstr. 10, 07743 Jena, Germany
[2]Jena Center for Soft Matter (JCSM), Friedrich-Schiller-University Jena, Philosophenweg 7, 07743 Jena, Germany
[3]Dutch Polymer Institute (DPI), John F. Kennedylaan 2, 5612 AB Eindhoven, The Netherlands
Correspondence to: U. S. Schubert (E-mail: ulrich.schubert@uni-jena.de)

Received 28 May 2012; accepted 5 July 2012; published online 6 August 2012
DOI: 10.1002/pola.26261

ABSTRACT: The synthesis of poly(2-ethyl-2-oxazoline)-*b*-linear poly(ethylenimine) (PEtOx-*b*-LPEI) copolymers by selective basic hydrolysis of PEtOx-*b*-poly(2-*H*-2-oxazoline) (PEtOx-*b*-PHOx) is described. For this purpose, an easy method for the preparation of the 2-*H*-2-oxazoline (HOx) monomer was developed. Based on the microwave-assisted polymerization kinetics for this monomer, PEtOx-*b*-PHOx copolymers were prepared. Subsequently, the block copolymers were selectively hydrolyzed to PEtOx-*b*-LPEI under basic conditions. The success of the polymerizations and subsequent post-polymerization reactions was demonstrated by ^{1}H NMR spectroscopy and MALDI-TOF-MS investigations of the obtained polymers. © 2012 Wiley Periodicals, Inc. J Polym Sci Part A: Polym Chem 50: 4516–4523, 2012

KEYWORDS: block copolymer; cationic polymerization; linear poly(ethylenimine); poly(2-*H*-2-oxazoline); ring-opening polymerization

INTRODUCTION Linear poly(ethylenimine)s (LPEIs) are of high interest in pharmaceutical research. As they can interact with negatively charged macromolecules like DNA, RNA, and si-RNA they are investigated as polymeric vectors for gene delivery.[1] However, their *in vivo* and clinical administrations are limited due to cytotoxic effects and a low hemocompatibility.[2] To overcome these drawbacks as well as the poor water solubility of LPEI, chemical modifications with biocompatible compounds have been performed. In this context, poly(ethylene glycol) (PEG) represents a suitable polymer with beneficial properties. It has good water solubility and exhibits the so-called "stealth effect."[3] A large number of PEG-LPEI copolymers are already described in literature.[4–6] They can be synthesized, for example, by grafting acryl terminated-PEG to LPEI via Michael addition[5] or using tosylated PEG as initiator for the cationic ring-opening polymerization (CROP) of poly(2-oxazoline)s (POxs), which are subsequently hydrolyzed to LPEI.[6] As a promising alternative to PEG, POxs,[7–12] particularly poly(2-ethyl-2-oxazoline) (PEtOx)[13,14] and poly(2-methyl-2-oxazoline) (PMeOx),[15,16] have shown comparable features like PEG, but have additional advantageous properties such as low viscosity and high stability in the therapeutically relevant dose. Jeong et al.[17] could show that statistical copolymers of LPEI and PEtOx, obtained by partial hydrolysis of PEtOx, have a reduced cytotoxicity and a transfection efficiency similar to branched poly(ethylenimine). Hsiue et al.[18] reported the synthesis of PEtOx-*b*-LPEI by coupling PEtOx with LPEI in a thiol-disulfide exchange reaction between sulfhydryl and pyridyl disulfide terminated groups. These polymers also showed a low cytotoxicity and high transfection efficiency. However, the block copolymer synthesis via thiol-disulfide exchange includes multiple reaction steps and is rather time-consuming. Conversely, statistical copolymers of LPEI and PEtOx suffer from the problem that they are not well-defined, since only an overall degree of hydrolysis can be determined, but not the exact lengths of the LPEI blocks. Moreover, some free nitrogens of the LPEI units might not be usable for DNA complexation, since the LPEI units are either too short or sterically blocked by the adjacent ethyl side chains. Hence, well-defined block copolymers of PEtOx and LPEI are of interest for pharmaceutical research. Unfortunately, the synthesis of well-defined POx-LPEI block copolymers is demanding. As LPEI is prepared by acid[19–21] or basic[22,23] hydrolysis of POx, usually statistical cleaved copolymers of LPEI and POx are obtained, when POx homo- or copolymers are hydrolyzed. However, it is known that the sterical hindrance, and therefore, the type of the side chain significantly influence the rate of hydrolysis.[19,24] The more bulky the rest is the slower the POx side chain is cleaved. This leads to the following order for the rate of hydrolysis: H > Me > Et > Ph. The selective hydrolysis of PMeOx-*b*-PPhOx to LPEI-*b*-PPhOx is already reported.[24] Basic

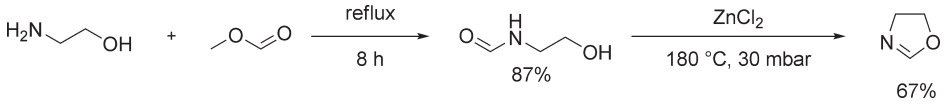

SCHEME 1 Schematic representation of the synthesis of HOx.

hydrolysis conditions were found to have a much slower hydrolysis rate, but also a higher selectivity, so that the poly(2-phenyl-2-oxazoline) (PPhOx) block remained almost unhydrolyzed. Litt et al.[25] described the selective hydrolysis of poly[2-(4-*t*-butylbenzoyl)-2-oxazoline]-*b*-PEtOx, where only the PEtOx block is hydrolyzed to LPEI with the help of methanesulfonic acid. A similar behavior is expected for block copolymers of 2-*H*-2-oxazoline (HOx) and 2-ethyl-2-oxazoline (EtOx). Saegusa et al.[23] reported that LPEI can be prepared by basic hydrolysis of PHOx within 3 h at 98 °C, whereas the basic hydrolysis of PEtOx proceeds much slower. Only 12% of the side chains are cleaved after 2 h at 130 °C.[21]

Here, we report the preparation of PEtOx-*b*-LPEI based on a significant improved and straightforward method for the large scale synthesis of the HOx monomer. Most of the preparation methods described so far suffer from problems like low overall yields due to instable intermediates and multiple reaction steps, or they use expensive or highly toxic starting material. Moreover, polymerization kinetics of HOx, the synthesis of PEtOx-*b*-PHOx and its subsequent hydrolysis to PEtOx-*b*-LPEI were performed. All polymers were characterized by in detail by ^{1}H NMR spectroscopy and MALDI-TOF-MS investigations.

RESULTS AND DISCUSSION

Synthesis of HOx

For the detailed kinetic studies, the preparation of different PEtOx-*b*-PHOx copolymers, as well as for the subsequent hydrolysis, larger amounts of HOx are required. HOx was first synthesized by Wenker in 1938.[26] With minor changes, Wenker's way is the most common method to obtain HOx. Starting from *N*-(2-hydroxyethyl)formamide, *N*-(2-chloroethyl)formamide is prepared by chlorination with thionyl chloride. Subsequent addition of a base, for example, KOH,[23,26–30] $NaHCO_3$,[29] or NaH,[27,31] leads to the formation of the oxazoline ring. However, the intermediate *N*-(2-chloroethyl)formamide is very unstable and tends to decompose to carbon monoxide and chloroethylamine, resulting in a low overall yield and a contaminated product. By performing the reactions under inert condition with prepurified educts, and using solvents such as 1-methyl-2-porrolidone,[27,31] triglyme,[27] and tertiary amines or amides,[23,27] the yield could be improved. Another drawback of the "Wenker method" is the ring closure by means of a base/water system, which increases the chance of uncontrolled polymerization or the decomposition of the reactive HOx, and therefore decreases the yield.

Other methods to synthesize HOx either use highly toxic and expensive compounds, like AgCN[32] and *t*-butyl isocyanide,[32,33] or they suffer from bad overall yields.[34–38] Therefore, they are not suitable for a large scale synthesis. However, HOx can also be prepared by dehydration of *N*-(2-hydroxyethyl)formamide, heating it with a Lewis acid under reduced pressure. When Al_2O_3 and Fe_2O_3 are used as catalyst the product yield is low, due to decomposition to 2-ethanolamine.[39] However, when zinc chloride is used as catalyst the decomposition does not occur, and the product can be obtained in a high yield accompanied by the formation of water.[40] This method was used for the synthesis of HOx in multigram scale (Scheme 1). Before the polymerization the water had to be removed. As HOx tends to autopolymerize when heated, and has also a high fugacity, water could not be removed by fractionized distillation under heating as stated by the Kaiser.[40] However, Saegusa described a method to dry the HOx, obtained from the instable *N*-(2-chloroethyl)formamide, by distillation over crushed KOH under reduced pressure into a cooling trap.[23] This procedure turned out to be the most suitable drying method, since no heating or extraction is needed, and hence, no autopolymerization or the presence of impurities from extraction solvents are observed. Also, the fugacity could be overcome, since the product is collected in a cooling trap. Additional distillation over BaO gave dry HOx in an excellent purity and good yield (67%), suitable for the subsequent application in the CROP. By combining the $ZnCl_2$ catalyzed dehydration method with Saegusa's drying method, it is possible to obtain HOx in only two reaction steps with a high purity. Moreover, the observed overall yield (67%) starting from *N*-(2-hydroxyethyl)formamide is much higher than for other synthesis approaches, for example, 42% for Saegusa's approach, and the reaction can be easily upscaled to synthesize multiple grams of HOx. No instable, expensive, smelly, or toxic compounds have to be used. The intermediate *N*-(2-hydroxyethyl)formamide can be easily prepared by heating 2-ethanolamine with methyl formate, followed by fractionized distillation. It can be stored in a freezer without decomposition for more than a year.

Polymerization and Characterization of HOx

The CROP of HOx, its polymerization kinetics and polymerization mechanism, was first studied by Saegusa et al. in the beginning of the 1970s.[23,41–44] The polymerization kinetics were only recorded at 24, 31, and 40 °C, respectively, and polymerizations were performed in general for 5 h at 80 °C. However, no polymerization kinetic for that temperature was reported. Since Saegusa et al. already showed that methyl tosylate (MeOTs) is the most suitable initiator, and that *N,N*-dimethylformamide (DMF) and acetonitrile are the best solvents for the CROP of HOx, the polymerization kinetics have been studied in acetonitrile with MeOTs as initiator. The polymerization was performed in a microwave synthesizer at 80 °C, with a $[M]/[I]$ ratio of 20 and a monomer

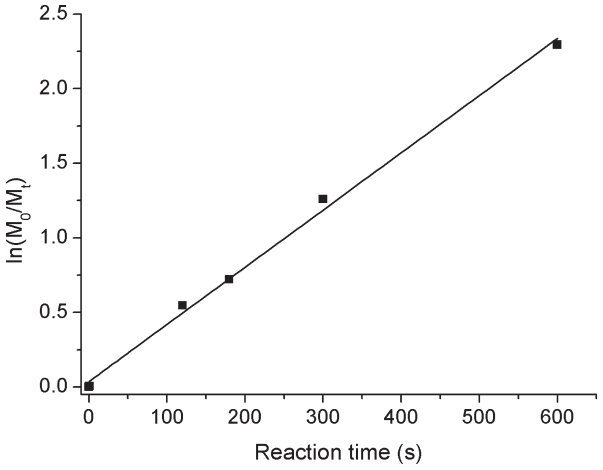

FIGURE 1 First order polymerization kinetics for the microwave-assisted polymerization of HOx in acetonitrile at 80°C using MeOTs as initiator.

concentration of 4 M; the monomer conversion was determined by GC. The linearity of the first order kinetic plots shows the living character of the polymerization (Fig. 1). A polymerization rate of $k_p = 0.0193$ L mol^{-1} s^{-1} was calculated. As expected, the reactions proceeds much faster compared to Saegusa's results for 24, 31, and 40 °C.[43] In every case, the product precipitated during the polymerization, as was already noted by Saegusa. This behavior is ascribed to the formation of strong hydrogen bonds between the polymer molecules, due to interactions of the oxygen and hydrogen of the formyl side chains. A broad band at 3400 cm^{-1}, typical for hydrogen bonds, can be found in the IR spectrum (Fig. 2). The obtained PHOx is soluble only in water at room temperature and dimethyl sulfoxide (DMSO) at temperatures above 120 °C. In DMSO, unfortunately no polymerization could be observed. To overcome the drawback, different polar ionic liquids have been investigated as solvent, for example, 1-ethyl-3-methylimidazolium chloride, 1-butyl-3-methylimidazolium chloride, and 1-allyl-3-methylimidazolium chloride. Some dissolved the PHOx, but they were too hygroscopic to be used as polymerization solvent. Because of dissolution problems and unsuitable columns, on which the polymer adhered, size exclusion chromatography (SEC) characterization of the samples from the kinetic study could not be performed.

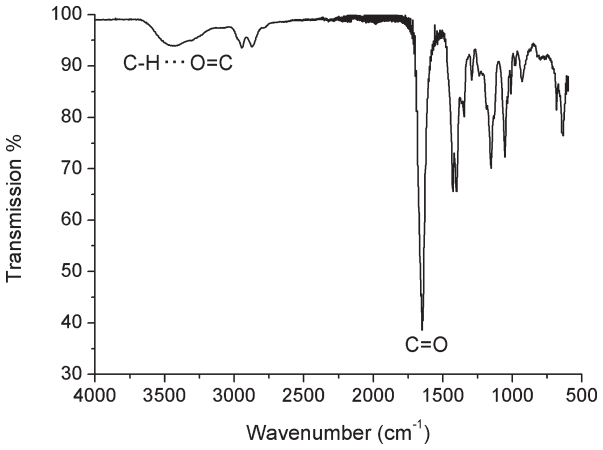

FIGURE 2 ATR-FT-IR spectrum of PHOx.

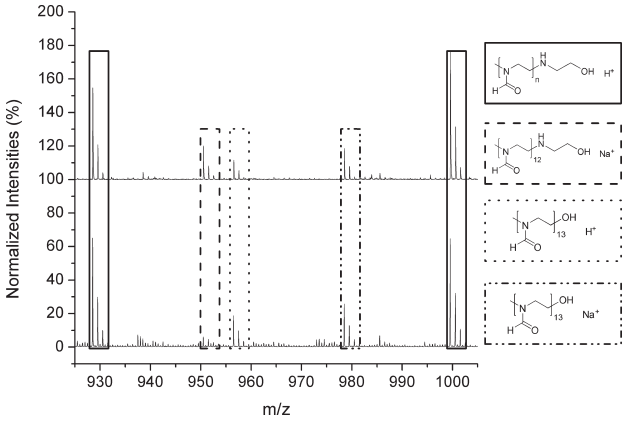

FIGURE 3 Expanded region of the MALDI- (top) and the ESI-TOF-MS (bottom) spectra as well as structural assignments for the different distributions of PHOx.

The PHOx was characterized by MALDI-TOF- and ESI-Q-TOF-MS (Fig. 3), showing similar results. This is the first report of PHOx mass spectra. Distributions for hydroxyl and ethylenimine-terminated species can be found. The two different end groups originate from the varying possible ring-opening reactions when the reaction is quenched with water (Scheme 2). Either a hydroxyl group or a formyl ester is formed and subsequently hydrolyzed. The ester formation also occurs for other POxs.[45,46]

Synthesis of PEtOx-*b*-PHOx

PEtOx-*b*-PHOx was prepared by the sequential monomer addition method (Scheme 3). The concentration of EtOx in the solvent acetonitrile was adjusted to 4 M and MeOTs was used as initiator. As reference, always an aliquote of the stock solution was polymerized under the same conditions, but without addition of the second monomer. Three block copolymers with EtOx/HOx ratios of 20/5 (**1b, 2b**) and 40/10 (**3b**) were synthesized using this approach (Table 1).

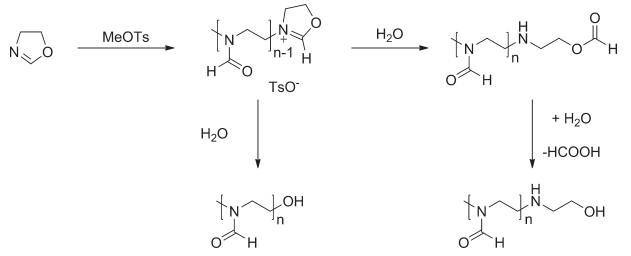

SCHEME 2 Schematic representation of the different ring-opening possibilities leading to different end groups of PHOx.

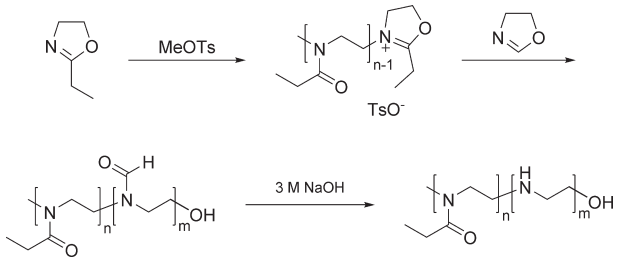

SCHEME 3 Schematic representation of the synthesis of PEtOx-*b*-LPEI.

Characterization by SEC revealed the growth of the polymer chain and therewith the increase of the molar mass. Compared to the reference PEtOx homopolymer, the SEC curve is shifted to higher molar masses after the addition of the second monomer (HOx, Fig. 4). Furthermore, in the ^{1}H NMR spectra an additional peak at $\delta = 8.02$ ppm, deriving from the formyl side chain, can be found (Fig. 5). Similar as for pure PHOx the polymer precipitated during the polymerization of the second block. When the PHOx block becomes too long, the copolymer is only soluble in water. A good ratio for EtOx and HOx was found to be $n/m = 4/1$. For this ratio, the polymer is still soluble in polar solvents like methanol, DMSO, and *N,N*-dimethylacetamide.

Characterization by MALDI-TOF-MS revealed a PEtOx with one HOx unit (PEtOx$_n$-*b*-PHOx$_1$) as main distribution. Also, other distributions were found, but they were hardly visible. This is ascribed to a mass discrimination effect, which often occurs in MALDI-TOF-MS measurements. Hence, the copolymer was fractionated by preparative SEC using a Sepahdex LH20 column with methanol as eluent. The obtained fractions showed a complex pattern of overlapping peaks in the expected molar mass region, but allowed a detailed interpretation. In all fractions, both monomers were incorporated, but with different ratios and chain lengths. An example MALDI-TOF-MS spectrum and the assignment of all the peaks is shown below (Fig. 6). Based on the results of ^{1}H NMR spectroscopy, this fraction contains an EtOx/HOx ratio of 4/1. The difference between the ratio calculated from ^{1}H NMR spectroscopy and the ratio in the MALDI-TOF mass spectrum can also be explained with the mass discrimination occurring in MALDI-TOF-MS.

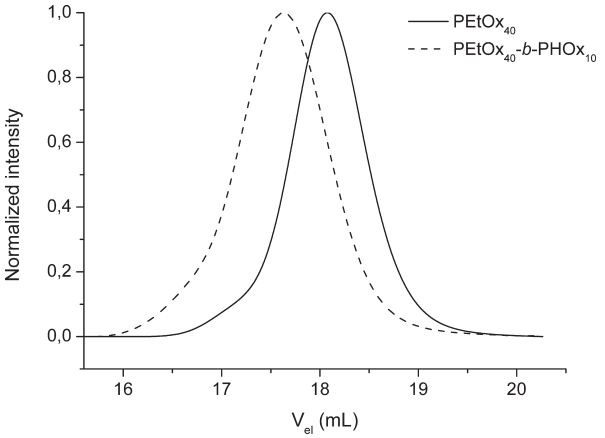

FIGURE 4 Comparison of the SEC curves of the PEtOx-*b*-PHOx **3b** (dashed) and the reference PEtOx homopolymer **3a** (straight) (SEC eluent: DMAc + 0.21% LiCl).

Hydrolysis of PHOx, PEtOx, and PEtOx-*b*-PHOx Under Basic Conditions

As already reported by Saegusa, PHOx can be easily hydrolyzed under basic conditions at 98 °C within 3 h.[23] When the hydrolysis of PHOx with 3 M NaOH was performed at 100 °C in a microwave synthesizer, the degree of hydrolysis was 93% after 1 min, and 99% after 5 min as determined by ^{1}H NMR spectroscopy. After 10 min full hydrolysis was observed. This shows that the formyl side chain can be very easily cleaved off. Under the same conditions, PEtOx was only hydrolyzed for 2% after 1 min, 6% after 5 min, and 8% after 10 min, respectively. When the reaction time was increased to 4 h the degree of hydrolysis was about 12%. As the PHOx can be hydrolyzed much easier and faster than the PEtOx, it is assumed that PEtOx-*b*-PHOx can be selectively hydrolyzed to PEtOx-*b*-LPEI. For the investigation of the hydrolysis conditions, 25 mg of PEtOx-*b*-PHOx were heated with 1 mL of 3 M NaOH in a microwave synthesizer at 100 °C for different times. The solvent was removed under vacuum. The degree of hydrolysis was determined by ^{1}H NMR spectroscopy by correlating the proton signal of the uncleaved PHOx side chain ($\delta = 8.02$ ppm) and the

TABLE 1 SEC Data for the Different PEtOx-b-PHOx Copolymers and Reference PEtOx Homopolymers

		DMAc + 2.1% LiCl (PEG calibration)			Water + 0.1% TFA + 0.05 M NaCl (PEG calibration)		
Sample	EtOx:HOx	M_n (g mol^{-1})	M_w (g mol^{-1})	PDI	M_n (g mol^{-1})	M_w (g mol^{-1})	PDI
1a	20:0	1,950	2,180	1.12	1,870	2,170	1.16
1b	20:5	3,100	3,950	1.27	1,980	2,440	1.23
2a	20:0	1,780	1,970	1.11	1,730	2,020	1.17
2b	20:5	2,280	2,680	1.17	1,850	2,390	1.29
3a	40:0	3,240	3,750	1.16	2,240	3,080	1.37
3b	40:10	4,660	5,850	1.26	2,420	3,380	1.40

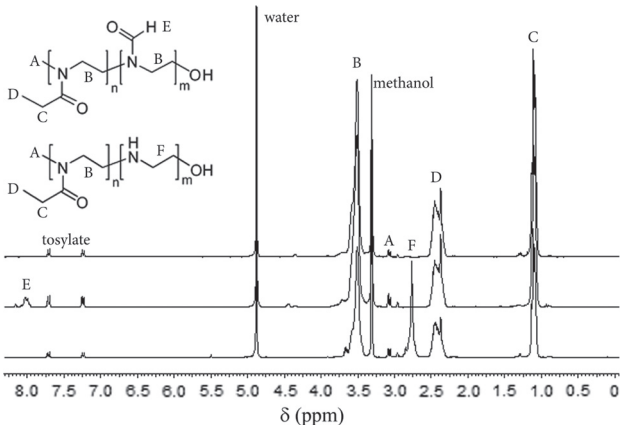

FIGURE 5 ^{1}H NMR spectra of the reference PEtOx **2a** (top), PEtOx-*b*-PHOx **2b** (middle), and PEtOx-*b*-LPEI (bottom) (solvent: CD_3OD).

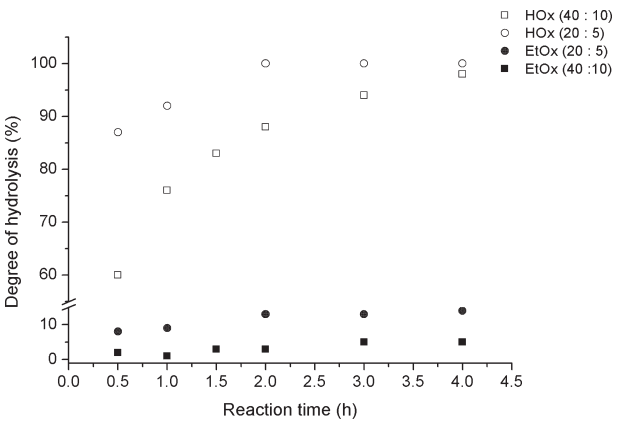

FIGURE 7 Degree of hydrolysis of **2b** (circle) and **3b** (square) against hydrolysis time as determined by ^{1}H MNR spectroscopy.

resulting formiate ($\delta = 8.53$ ppm). The determination of the degree of hydrolysis of the PEtOx block by ^{1}H NMR spectroscopy was challenging since the broad signals of LPEI ($\delta = 2.76$ ppm) and CH_2 group of PEtOx ($\delta = 2.42$ ppm) overlap. Also, the signals of the CH_2 group of the resulting propionate ($\delta = 2.20$ ppm) and CH_2 groups of PEtOx were not clearly separated. Nevertheless, reproducible results could be obtained. The degree of hydrolysis of PEtOx is about 5% for $n/m = 40/10$ and 14% for $n/m = 20/5$ when full cleavage of the PHOx side chain is achieved. This is in good agreement with the degree of hydrolysis for the basic hydrolysis of the reference PEtOx homopolymers. It was found that the copolymer with $n/m = 20/5$ hydrolyzed much faster than the copolymer with doubled block lengths; however, the block copolymer with $n/m = 40/10$ is hydrolyzed more selectively (Fig. 7).

Unlike LPEI, the PEtOx-*b*-LPEI copolymer with a m/n ratio of 4/1 is soluble in chloroform and dichloromethane. This allows the purification of the copolymer, since it can be easily extracted from the salt residues (NaOH, formiate) after removal of the solvent. The comparison of the ^{1}H NMR spectra before and after the hydrolysis shows that the peak of the formiate side chain of the PHOx block totally disappeared (Fig. 5). Instead a new peak for LPEI can be found at 2.76 ppm. Moreover, no signals for formiate or propionate can be found anymore, showing that extracting the block copolymer with dichloromethane represents a suitable purification method. SEC was measured on a PSS SUPREMA-MAX column, which is applicable for cationic polymers and does not only separate by size, but also by charge. Consequently, the SEC curve of the PEtOx-*b*-LPEI is shifted to a lower elution volume although the molar mass is lower compared to the starting material PEtOx-*b*-PHOx (Fig. 8), confirming that the PHOx block is hydrolyzed and the cationic LPEI is formed. Unfortunately, there are no suitable available standards for the determination of the molar masses and PDI values of the PEtOx-*b*-LPEI.

The MALDI-TOF mass spectrum showed a complex pattern of overlapping peaks, making the interpretation nearly

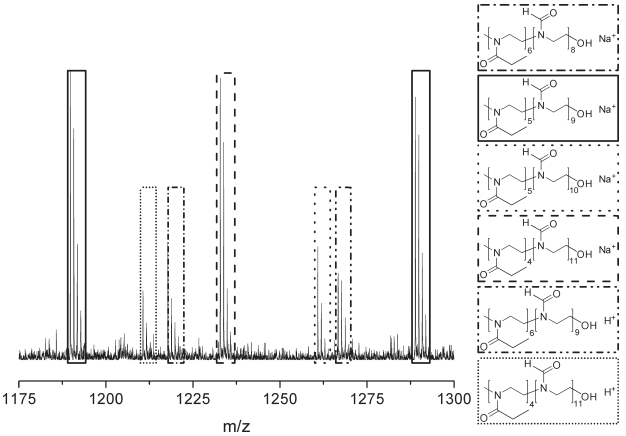

FIGURE 6 Expanded region of the MALDI-TOF mass spectrum of PEtOx-*b*-PHOx **1b** and assignments of the different distributions (matrix: DHB).

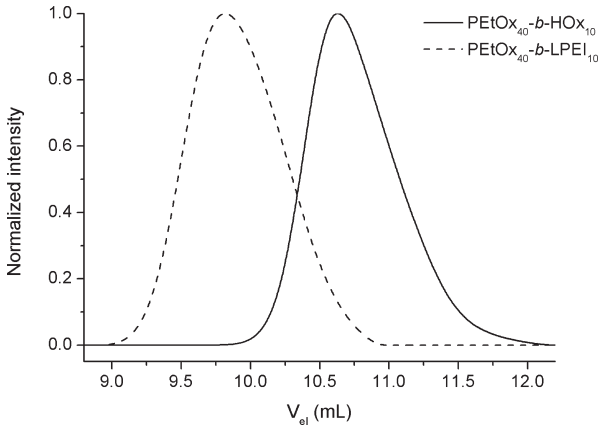

FIGURE 8 SEC curve of PEtOx-*b*-PHOx **3b** before (straight) and after hydrolysis (dashed) (SEC eluent: water + 0.1% TFA + 0.05 M NaCl).

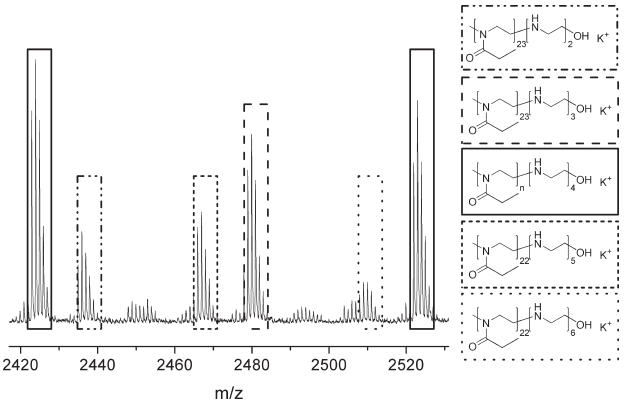

FIGURE 9 Expanded region of the MALDI-TOF mass spectrum of PEtOx-*b*-LPEI and assignments of the different distributions (matrix: DHB).

impossible. Therefore, analog to the PEtOx-*b*-PHOx, the copolymer was fractionated by preparative SEC using a Sephadex LH20 column (eluent methanol). After fractionation, fractions with different EtOx and EI chain lengths and ratios, but interpretable MALDI-TOF mass spectra were obtained. Both EtOx and EI repeating units can be assigned, demonstrating that the PHOx block is successfully hydrolyzed to LPEI (Fig. 9).

EXPERIMENTAL SECTION

Chemicals and Instrumentation

Dry acetonitrile and methyl formate were purchased from Acros Organics and 2-ethanolamine from Sigma Aldrich. EtOx and MeOTs were obtained from Acros Organics, distilled to dryness over barium oxide (BaO), and stored under argon.

The Initiator Sixty single-mode microwave synthesizer from Biotage, equipped with a noninvasive IR sensor (accuracy: ±2%), was used for polymerizations and hydrolyses under microwave irradiation. Before usage, the microwave vials were heated to 110 °C overnight and allowed to cool down to room temperature under an argon atmosphere. Proton (^{1}H) and carbon (^{13}C) nuclear magnetic resonance (NMR) spectra were recorded on a Bruker AC 300 MHz at 298 K. Chemical shifts are reported in parts per million (ppm, δ scale) relative to the residual signal of the deuterated solvent. SEC of PEtOx and PEtOx-*b*-PHOx was measured on an Agilent Technologies 1200 Series gel permeation chromatography system equipped with a G131A isocratic pump, a G1329A autosampler, a G1362A refractive index detector, and both a PSS Gram 30 and a PSS Gram 1000 column placed in series. A 0.21% LiCl solution in *N,N*-dimethylacetamide (DMAc) was used as eluent at 1 mL min^{-1} flow rate and a column oven temperature of 40 °C. Molar masses were calculated against PEG. SECs of PEtOx-*b*-PHOx and PEtOx-*b*-LPEI were measured on a Jasco SEC system equipped with a PU-980 pump, a AS-1555 autosampler, a DG-980-50 degasser, a RI930 refractive index detector, and a PSS SUPREMA-MAX column. As eluent, a solution of 0.1% trifluoroacetic acid (TFA) and 0.05 M NaCl in water, running at a flow rate of 1 mL min^{-1} and a column oven temperature of 30 °C, was used. Molar masses were calculated against PEG. The MALDI-TOF-MS spectra were recorded using an Ultraflex III TOF/TOF (Bruker Daltonics GmbH, Bremen, Germany), equipped with a frequency-tripled Nd:YAG laser, operating at a wavelength of 355 nm. All spectra were measured in the positive reflector mode using 2,5-dihydroxybenzoic acid (DHB) as matrix. ESI-Q-TOF-MS measurements were performed with a micrOTOF Q-II (Bruker Daltonics) mass spectrometer. The ESI-Q-TOF mass spectrometer was operating at 4.5 kV at a desolvation temperature of 180 °C. The mass spectrometer was operating in the positive ion mode. As solvent methanol/water mixtures were used. The ESI-Q-TOF-MS instrument was calibrated in the *m/z* range of 50–3000 using an internal calibration standard (Tunemix solution), which was supplied from Agilent. The electron impact MS spectra were measured with a Finnigan MAT SSQ710 spectrometer. The IR spectra were recorded on a FT-IR spectrometer IRAffinity-1 (Shimadzu).

Synthesis of *N*-(2-Hydroxyethyl)formamide

Methyl formate (107 mL, 1.72 mol) was heated with a 25% excess 2-ethanolamine (130 mL, 2.15 mol) for 8 h under reflux. The resulting methanol was removed by distillation at normal pressure and the residue was purified by vacuum distillation. A colorless liquid was obtained (bp. 110–112 °C, 0.01 mbar). Yield: 132.93 g (87%).

^{1}H NMR (300 MHz, CD_3OD, δ, ppm): 8.09 (s, trans, 1H), 8.01 (s, cis, 1H), 3.57–3.64 (m, 2H), 3.28–3.37 (m, 2H). ^{13}C NMR (300 MHz, CD_3OD, δ, ppm): 166.36 (cis), 162.68 (trans), 61.60 (cis), 60.00 (trans), 43.94 (cis), 40.11 (trans). IR (ATR-FT-IT, cm^{-1}): 3278 (OH/NH), 2877 (CH), 1651 (C=O), 1531 (NH), 1060 (C—O).

Synthesis of the HOx Monomer

A flask equipped with a Claisen condenser was charged with $ZnCl_2$ (1.412 g, 10 mmol) and *N*-(2-hydroxyethyl)formamide (10.026 g, 112 mmol). The reaction mixture was heated at 180 °C and 30 mbar. The product was collected in a cooling trap together with the resulting water. Crushed KOH (8.38 g) was added and the crude product was distilled into a cooling trap at 30 mbar. To the distillate, crushed KOH (6.24 g) was added, and the product was distilled again under reduced pressure (30 mbar) into a cooling trap. Repeated addition of KOH (3.22 g) was followed by distillation under reduced pressure (30 mbar) into a cooling trap. At last, the product was distilled over BaOH under reduced pressure (30 mbar) into a cooling trap. The product was stored under argon over mol sieve 4 Å. Yield: 5.38 g (67%).

^{1}H NMR (300 MHz, CD_3OD, δ, ppm): 6.71 (s, 1H), 4.08 (t, ^3J = 9.71 Hz, 2H), 3.71 (td, ^3J = 9.71 Hz, ^4J = 1.88 Hz, 2H). ^{13}C NMR (300 MHz, $CDCl_3$, δ, ppm): 155.16 (CH), 65.39 (CH_2), 53.37 (CH_2). (ATR-FT-IT, cm^{-1}): 2978 (CH), 1627 (C=N), 1080 (C—O—C), 918 (=CH). MS (EI, *m/z*, %): 71 (41) [M$^+$], 41 (45) [M—CH_2O]$^+$, 40 (12) [M—C_2H_3N]$^+$, 32 (100).

Kinetic Investigation of the Polymerization of HOx

For the kinetic studies, a stock solution containing MeOTs (initiator), HOx (monomer), and acetonitrile (solvent) was

prepared. The monomer concentration was adjusted to 4 M, and a monomer to initiator ratio ($[M]/[I]$) of 20 was used. The stock solution was divided over six microwave vials that were capped under argon. For the calculation of the conversion, t_0 samples were taken. The vials were heated to 80 °C for different times in the microwave synthesizer. After cooling, the reaction was quenched and GC samples were prepared to determine the monomer conversion. The polymerization solvent was used as internal standard.

^{1}H NMR (300 MHz, D_2O, δ, ppm): 7.90 (m, N—CHO), 3.42 (m, N—CH_2), 2.84 (m, CH_3—N). IR (ATR-FT-IR, cm^{-1}): 2939 (CH), 2870 (CH), 1651 (C=O), 1427 (CH_2/CH_3), 1400 (CH_2/CH_3), 1153 (C—O—C), 1053 (C—O—C).

Synthesis of the PEtOx-*b*-PHOx Copolymers

A stock solution containing MeOTs (initiator), 2-ethyl-2-oxazoline (monomer), and acetonitrile (solvent) was prepared. The EtOx concentration was adjusted to 4 M, with a monomer to initiator ration of $[M]/[I] = 20$ and $[M]/[I] = 40$, respectively. An aliquot of the stock solution was taken and polymerized as reference for the PEtOx block. Both, the remaining stock solution and reference sample were heated in a microwave synthesizer at 140 °C for a predetermined time. After cooling to room temperature, the second monomer (HOx) was added to the polymerization mixture through the septum with a syringe and heated in a microwave synthesizer at 80 °C for a predetermined time. The reaction mixture was cooled to room temperature. The precipitate was dissolved in methanol, precipitated in ice-cold diethyl ether and dried under reduced pressure at 40 °C.

^{1}H NMR (300 MHz, CD_3OD, δ, ppm): 8.02 (m, N—CHO), 3.54 (m, N—CH_2), 3.08 (m, CH_3—N), 2.42 (m, C—CH_2—C), 1.11 (m, C—CH_3).

Kinetic Investigations of the Basic Hydrolysis of PHOx and PEtOx

PHOx and PEtOx (40 ± 1 mg), respectively, were dissolved in 3 M NaOH (2 mL) in a microwave vial. The reaction mixture was heated at 100 °C for different times in a microwave synthesizer. After cooling to room temperature, the solvent was removed under reduced pressure. The residue was dissolved in deuterated methanol and the degree of hydrolysis was determined by ^{1}H NMR spectroscopy.

Kinetic Investigations of the Basic Hydrolysis of PEtOx-*b*-PHOx

PEtOx-*b*-PHOx (**2b, 3b**) (25 ± 1 mg) was dissolved in 3 M NaOH (1 mL). The reaction mixture was heated in a microwave synthesizer for different times at 100 °C. After cooling to room temperature, the solvent was removed under reduced pressure. The residue was dissolved in deuterated methanol, and the degree of hydrolysis was determined by ^{1}H NMR spectroscopy.

Synthesis of PEtOx-*b*-LPEI

PEtOx-*b*-PHOx **2b** (216 mg) was heated in 3 M NaOH (4 mL) at 100 °C for 4 h in a microwave synthesizer. The solvent was removed under reduced pressure, and the residue was extracted with dichloromethane. After filtration the solvent was removed, and the resulting polymer was dried under reduced pressure at 40 °C.

^{1}H NMR (300 MHz, CD_3OD, δ, ppm): 3.54 (m, N—CH_2), 3.08 (m, CH_3—N), 2.76 (NH—CH_2), 2.42 (m, C—CH_2—C), 1.11 (m, C—CH_3).

CONCLUSION

A cheap and easy method for the synthesis of the monomer HOx was developed, and its polymerization kinetics were investigated. The obtained PHOx was characterized by ^{1}H NMR, MALDI-TOF-MS, and ESI-Q-TOF-MS. The monomer (HOx) was further used to synthesize PEtOx-*b*-PHOx copolymers in a sequential monomer addition approach. During the reaction, the polymer precipitated, due to hydrogen bond formation between the formyl side chains. If the HOx block became too long the polymer was only soluble in water, making the characterization challenging. However, if an EtOx/HOx ratio of 4:1 is used, the copolymer was soluble in polar solvents like methanol, DMF, and DMAc. Block copolymers with two different block lengths and an EtOx/HOx ratio of 4:1 were synthesized and characterized by ^{1}H NMR spectroscopy, SEC, and MALDI-TOF MS, proving that the block copolymer was formed. Subsequently, the basic hydrolysis to PEtOx-*b*-LPEI was performed. ^{1}H NMR spectroscopy and MALDI-TOF-MS demonstrated that the HOx block was successfully hydrolyzed to LPEI, and SEC indicated the formation of a cationic species, due to a different column interaction of the product and educt. The obtained PEtOx-*b*-LPEI copolymers represent interesting materials for pharmaceutical studies, with promising features for a high transfection efficiency and a "stealth effect." Their potential is currently under investigation.

ACKNOWLEDGMENTS

The authors thank the Thuringian Ministry for Education, Science and Culture (grant no. B514-09051, B515-07008, and B715-08011) and the Dutch Polymer Institute (DPI, technology area HTE) for financial support of this study.

REFERENCES AND NOTES

1 Jäger, M.; Schubert, S.; Ochrimenko, S.; Fischer, D.; Schubert, U. S. *Chem. Soc. Rev.* **2012,** *41*, 4755–4767.

2 Neu, M.; Fischer, D.; Kissel, T. *J. Gene Med.* **2005,** *7*, 992–1009.

3 Knop, K.; Hoogenboom, R.; Fischer, D.; Schubert, U. S. *Angew. Chem. Int. Ed. Engl.* **2010,** *49*, 6288–6308.

4 Akiyama, Y.; Harada, A.; Nagasaki, Y.; Kataoka, K. *Macromolecules* **2000,** *33*, 5841–5845.

5 Wang, H.; Chen, X.; Pan, C. *J. Colloid Interface Sci.* **2008,** *320*, 62–69.

6 Zhong, Z.; Feijen, J.; Lok, M. C.; Hennink, W. E.; Christensen, L. V.; Yockman, J. W.; Kim, Y.-H.; Kim, S. W. *Biomacromolecules* **2005,** *6*, 3440–3448.

7 Adams, N.; Schubert, U. S. *Adv. Drug Deliv. Rev.* **2007,** *59*, 1504–1520.

8 Kronek, J.; Kroneková, Z.; Lustoň, J.; Paulovičová, E.; Paulovičová, L.; Mendrek, B. *J. Mater. Sci.: Mater. Med.* **2011,** *22*, 1725–1734.

9 Luxenhofer, R.; Schulz, A.; Roques, C.; Li, S.; Bronich, T. K.; Batrakova, E. V.; Jordan, R.; Kabanov, A. V. *Biomaterials* **2010,** *31*, 4972–4979.

10 Luxenhofer, R.; Sahay, G.; Schulz, A.; Alakhova, D.; Bronich, T. K.; Jordan, R.; Kabanov, A. V. *J. Control. Release* **2011,** *153*, 73–82.

11 Viegas, T. X.; Bentley, M. D.; Harris, J. M.; Fang, Z.; Yoon, K.; Dizman, B.; Weimer, R.; Mero, A.; Pasut, G.; Veronese, F. M. *Bioconjugate Chem.* **2011,** *22*, 976–986.

12 Zalipsky, S.; Hansen, C. B.; Oaks, J. M.; Allen, T. M. *J. Pharm. Sci.* **1996,** *85*, 133–137.

13 Bauer, M.; Lautenschlaeger, C.; Kempe, K.; Tauhardt, L.; Schubert, U. S.; Fischer, D. *Macromol. Biosci.* **2012,** *12*, 986–998.

14 Mero, A.; Pasut, G.; Via, L. D.; Fijten, M. W. M.; Schubert, U. S.; Hoogenboom, R.; Veronese, F. M. *J. Control. Release* **2008,** *125*, 87–95.

15 Schroeder, S.; Bauer, M.; Tauhardt, L.; Kempe, K.; Schubert, U. S.; Fischer, D., in preparation.

16 Konradi, R.; Pidhatika, B.; Muhlebach, A.; Textor, M. *Langmuir* **2008,** *24*, 613–616.

17 Jeong, J. H.; Song, S. H.; Lim, D. W.; Lee, H.; Park, T. G. *J. Control. Release* **2001,** *73*, 391–399.

18 Hsiue, G.-H.; Chiang, H.-Z.; Wang, C.-H.; Juang, T.-M. *Bioconjugate Chem.* **2006,** *17*, 781–786.

19 Lambermont-Thijs, H. M. L.; van der Woerdt, F. S.; Baumgaertel, A.; Bonami, L.; Du Prez, F. E.; Schubert, U. S.; Hoogenboom, R. *Macromolecules* **2009,** *43*, 927–933.

20 Tanaka, R.; Ueoka, I.; Takaki, Y.; Kataoka, K.; Saito, S. *Macromolecules* **1983,** *16*, 849–853.

21 Tauhardt, L.; Kempe, K.; Knop, K.; Altuntaş, E.; Jäger, M.; Schubert, S.; Fischer, D.; Schubert, U. S. *Macromol. Chem. Phys.* **2011,** *212*, 1918–1924.

22 Bartulín, J.; Rivas, B. L.; Rodríguez-Baeza, M.; Angne, U. *Makromol. Chem.* **1982,** *183*, 2935–2940.

23 Saegusa, T.; Ikeda, H.; Fujii, H. *Polym. J.* **1972,** *3*, 35–39.

24 Lambermont-Thijs, H. M. L.; Heuts, J. P. A.; Hoeppener, S.; Hoogenboom, R.; Schubert, U. S. *Polym. Chem.* **2011,** *2*, 313–322.

25 Litt, M. H.; Lin, C. S. *J. Polym. Sci. Part A: Polym. Chem.* **1992,** *30*, 779–786.

26 Wenker, H. *J. Am. Chem. Soc.* **1938,** *60*, 2152–2153.

27 Chu, V. P.; Overberger, C. G. *J. Polym. Sci.: Polym. Chem. Ed.* **1985,** *23*, 2385–2404.

28 Levine, M.; Kenesky, C. S.; Zheng, S.; Quinn, J.; Breslow, R. *Tetrahedron Lett.* **2008,** *49*, 5746–5750.

29 Smith, F. T.; Atigadda, R. V. *J. Heterocycl. Chem.* **1991,** *28*, 1813–1815.

30 Lee, J. W.; Park, B. S.; Kim, H. B. *Bull. Korean Chem. Soc.* **1993,** *14*, 436–436.

31 Franco, F.; Muchowski, J. M. *J. Heterocycl. Chem.* **1980,** *17*, 1613–1613.

32 Ito, Y.; Inubushi, Y.; Zenbayashi, M.; Tomita, S.; Saegusa, T. *J. Am. Chem. Soc.* **1973,** *95*, 4447–4448.

33 Ito, Y.; Ito, I.; Hirao, T.; Saegusa, T. *Synth. Commun.* **1974,** *4*, 97–103.

34 Bredereck, H.; Bangert, R. *Chem. Ber.* **1964,** *97*, 1414–1423.

35 Cornforth, J. W.; Cornforth, R. H. *J. Chem. Soc. (Resumed)* **1947**, 96–102.

36 Ito, K.; Miyajima, S. *J. Heterocycl. Chem.* **1997,** *34*, 501–503.

37 Mulder, R. J.; Shafer, C. M.; Molinski, T. F. *J. Org. Chem.* **1999,** *64*, 4995–4998.

38 Lee, J. C.; Cha, J. K. *Tetrahedron* **2000,** *56*, 10175–10184.

39 Hess, L. G. Union Carbide Corp., U.S. Patent 2,844,589, July 22, **1958.**

40 Kaiser, M. E. The Dow Chemical Company, Midland, MI, U.S.Patent 4,443,611, April 17, **1984.**

41 Saegusa, T.; Ikeda, H.; Fujii, H. *Polym. J.* **1972,** *3*, 176–180.

42 Saegusa, T.; Ikeda, H.; Fujii, H. *Polym. J.* **1973,** *4*, 87–92.

43 Saegusa, T.; Ikeda, H.; Fujii, H. *Macromolecules* **1973,** *6*, 315–319.

44 Saegusa, T. *Pure Appl. Chem.* **1974,** *39*, 81–97.

45 Baumgaertel, A.; Altuntaş, E.; Kempe, K.; Crecelius, A.; Schubert, U. S. *J. Polym. Sci. Part A: Polym. Chem.* **2010,** *48*, 5533–5540.

46 Baumgaertel, A.; Weber, C.; Fritz, N.; Festag, G.; Altuntaş, E.; Kempe, K.; Hoogenboom, R.; Schubert, U. S. *J. Chromatogr. A* **2011,** *1218*, 8370–8378.

Publication 9

"Dextran-*graft*-linear poly(ethylene imine)s for gene delivery: Importance of linking strategy"

S. Ochrimenko,[#] A. Vollrath,[#] K. Kempe, L. Tauhardt, S. Schubert, U. S. Schubert, D. Fischer
#Both authors contributed equally.

Carbohydr. Polym. **2014**, *113*, 597-606

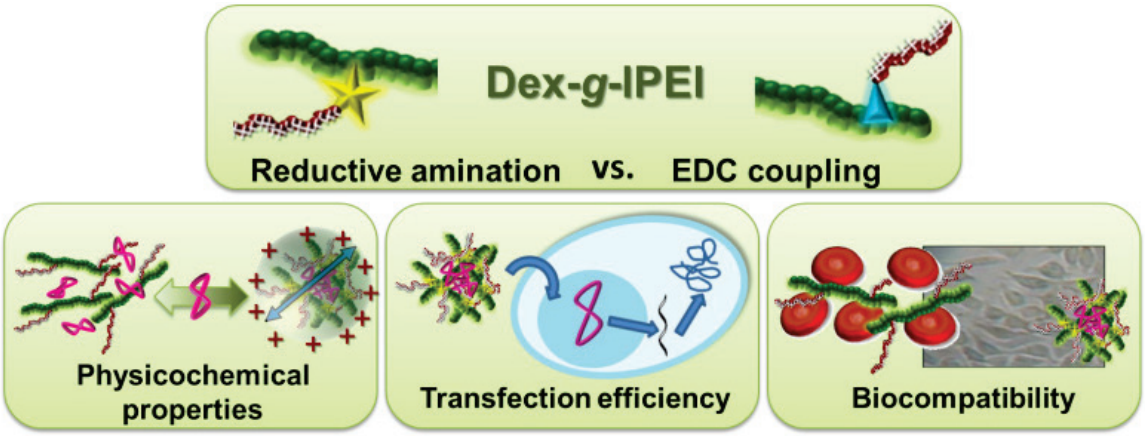

Carbohydrate Polymers 113 (2014) 597–606

Contents lists available at ScienceDirect

Carbohydrate Polymers

journal homepage: www.elsevier.com/locate/carbpol

Dextran-*graft*-linear poly(ethylene imine)s for gene delivery: Importance of the linking strategy

Sofia Ochrimenko[a,b,1], Antje Vollrath[b,1], Lutz Tauhardt[b], Kristian Kempe[b,2], Stephanie Schubert[a,c], Ulrich S. Schubert[b,c,**], Dagmar Fischer[a,c,*]

[a] Department of Pharmaceutical Technology, Institute of Pharmacy, Friedrich-Schiller-University Jena, Otto-Schott-Str. 41, 07745 Jena, Germany
[b] Laboratory of Organic and Macromolecular Chemistry (IOMC), Friedrich-Schiller-University Jena, Humboldtstr. 10, 07743 Jena, Germany
[c] Jena Center for Soft Matter (JCMS), Friedrich-Schiller-University Jena, Philosophenweg 7, 07743 Jena, Germany

ARTICLE INFO

Article history:
Received 21 March 2014
Received in revised form 11 July 2014
Accepted 15 July 2014
Available online 29 July 2014

Keywords:
Biocompatibility
Cationized dextran
Gene delivery
Poly(ethylene imine)
Structure-property relationship

ABSTRACT

Low molar mass linear poly(ethylene imine)s (lPEI) were grafted onto dextran *via* different synthesis routes aiming at the elucidation of structure-property relationships of dextran-*graft*-linear poly(ethylene imine) (dex-*g*-lPEI) conjugates for gene delivery applications. Beside the molar mass of well-defined lPEIs and the linker unit, also the amount of lPEI in the polymeric vectors was varied. The synthesized dextran modifications were characterized regarding their chemical structure and showed enhanced complexation and stabilization of DNA against enzymatic degradation. The transfection efficiency of dex-*g*-lPEIs was increased compared to unmodified lPEI and revealed a dependency of the used linking strategy. All complexes of DNA and dex-*g*-lPEIs were found to be nontoxic, but the synthesis route showed a strong influence on the aggregation of red blood cells. In conclusion, the linking strategy of lPEI to dextran has a significant impact on the physicochemical characteristics of DNA/polymer complexes, the biocompatibility as well as the transfection efficiency.

1. Introduction

Dextran, a natural hydrophilic, biodegradable polysaccharide mainly based on α-1-6-linked D-glucose units, has been widely used in medical, pharmaceutical, and drug delivery applications (Varshosaz, 2012). More than 50 years of clinical use provided an impressive proof of its safety in parenteral and oral administration, *e.g.* as lubricant in ophthalmic solutions, creams, and ointments or as coating material for diagnostic nanoparticles(Heinze, Liebert, Heublein, & Hornig, 2006; Mehvar, 2000). Additionally, several modern drug delivery systems containing dextran are under preclinical development, for instance nanoparticles, hydrogels or microspheres (Vlugt-Wensink et al., 2007). In the field of gene therapy, series of attempts have been made to selectively modify dextran with cationic moieties such as diethylaminoethyl (Eshita et al., 2009), spermine (Abdullah et al., 2010; Azzam et al., 2002; Cohen et al., 2011), protamine (Thomas, Rekha, & Sharma, 2010b), poly(L-lysine) (Maruyama et al., 1998), poly(ethylene imine) (PEI) (Jiang & Salem, 2012; Sun et al., 2011; Sun, Xiao, Cheng, Zhang, & Zhuo, 2008a; Sun, Zhang, Cheng, Cheng, & Zhuo, 2008b; Tseng & Jong, 2003), or 2,3-epoxypropyl-trimethylammonium chloride (Thomas, Rekha, & Sharma, 2010a) in order to make them suitable as non-viral vector system. PEI was thereby one of the most favored cationic polymers applied for conjugation to dextran owing to its excellent transfection efficiency.

Several studies have evaluated dextran-*graft*-poly(ethylene imine) (dex-*g*-PEI) conjugates as promising gene delivery systems in recent years. Three different strategies for conjugation were followed:

(i) Low molar mass dextran was covalently grafted onto high molar mass branched PEIs (bPEIs) or linear PEIs (lPEIs) to decrease its cytotoxicity, to enhance the complex stability and to decrease the charge effects of salts and proteins present

* Corresponding authors at: D. Fischer Department of Pharmaceutical Technology, Institute of Pharmacy, Friedrich Schiller University Jena, Otto-Schott-Str. 41, 07745 Jena, Germany. Tel.: +49 3641 949940/+49 3641 948200; fax: +49 3641 949942/+49 3641 948202.
** Corresponding authors at: Laboratory of Organic and Macromolecular Chemistry (IOMC), Friedrich-Schiller-University Jena, Humboldtstr. 10, 07743 Jena, Germany. Tel.: +49 3641 948200; fax: +49 3641 948202.
E-mail addresses: ulrich.schubert@uni-jena.de (U.S. Schubert), dagmar.fischer@uni-jena.de (D. Fischer).
[1] These authors contributed equally.
[2] Present address: Department of Chemical and Biomolecular Engineering, The University of Melbourne, Parkville 3010, VIC, Australia.

http://dx.doi.org/10.1016/j.carbpol.2014.07.048
0144-8617/

in the extracellular environment as also observed for stealth polymers like poly(ethylene glycol) (Knop, Hoogenboom, Fischer, & Schubert, 2010; Petersen et al., 2002; Tseng & Jong, 2003; Tseng, Tang, & Fang, 2004). Depending on the molar mass of dextran and the degree of grafting, transfection efficiencies of dex-*g*-PEI were reported to be comparable or lower than that of the unmodified PEI. This finding was ascribed to a steric hindrance of the PEI protonation causing a decreased buffering capacity dependent on the molar mass of the dextran (Tseng, Fang, Su, & Tang, 2005).

(ii) The grafting of low molar mass bPEI onto large dextran backbones was investigated. The cytotoxicity of the conjugate was lower compared to high molar mass bPEI. In addition, the transfection could be enhanced by increasing the degree of substitution (DS) of low molar mass bPEI conjugated to dextran or increasing the N/P ratio of DNA/dextran-*g*-bPEI complexes or by using serum containing media (Jiang & Salem, 2012; Sun et al., 2008a; Sun et al., 2008b). First *in vivo* studies with pEGFP were already performed in mice using *in vivo* fluorescent imaging (Chu et al., 2013).

(iii) Dextran nanoparticles were formed by crosslinking of dextran and grafted in different extents with bPEI by reductive amination. In this way, the steric hindrance of the dextran molecules to form stable complexes of PEI and plasmid could be decreased and the transgene expression as well as the cell viability were enhanced compared to unconjugated bPEI (Tripathi, Goyal, & Gupta, 2011).

Several linking strategies have been reported to covalently bind bPEI to dextran by commonly exploiting the primary amine groups. Reductive amination of oxidized dextran with bPEI results in improved complex stability, lower cytotoxicity, and higher or comparable transfection efficiency than the respective unmodified PEI dependent on the degree of grafting (Jiang & Salem, 2012; Tseng et al., 2004). The oxidation followed by conjugation represents a convenient method to form irreversible linkages in aqueous solution, but also yields adverse products with undefined chemical structures due to the occurrence of various chain scission reactions during the oxidation reaction of dextran. In another approach, dextran was functionalized with hexamethylene diisocyanate (HMDI) for subsequent reaction with PEI (Sun et al., 2008a; Xiao et al., 2010). The HMDI linkage was found to be advantageous since the functionalization reaction could be conducted fast and effectively without addition of any catalyst and by maintaining the original dextran backbone structure. However, crosslinking is an important parameter both inter- and intramolecular, which might result in non-defined structures, higher molar masses, and undesired solution properties. The functionalization of dextran with carboxymethyl groups and the subsequent amidation might also influence the original properties significantly due to the introduction of negatively charged carboxyl groups (Sun et al., 2008b).

So far, the influence of the different linker strategies has only received little attention, but might have a significant influence on the biocompatibility, transgene expression and DNA binding characteristics. Most studies also lack in systematic analysis of polymer characteristics such as molar mass, copolymer composition, but also the purity and structure of the original polymers. To gain a better insight into the structure-property relationships, a direct comparison of the effects of various linking strategies was performed. To this end, only well-defined and in depth characterized polymers were used. In contrast to previously published studies using bPEI, linear PEI (lPEI) was chosen because it can be synthesized in a controlled manner with narrow molar mass distributions and well-defined structures such as tailored end groups (Altuntaş et al., 2012; Tauhardt et al., 2011). Consequently, no intra- and intermolecular crosslinking can be expected in contrast to bPEI. lPEI with 20 ($lPEI_{20}$) and 40 repeating units ($lPEI_{40}$) were prepared and subsequently grafted onto different dextran-precursors, namely dextran aldehyde (CHO-dex), carboxymethylated dextran (CM-dex), and 4-nitrophenyl carbonate-substituted dextran (NPC-dex). The degree of the functional groups (CHO, COOH, NPC) per anhydroglucose unit (AGU) of dextran as well as the degree of substitution (DS) and the molar mass of conjugated lPEI were varied. Finally, the influence of the linker, the DS, and the molar mass of lPEI of the various dex-*g*-PEI conjugates were examined regarding the interaction with DNA, the complex formation, and the cell- and hemocompatibility as well as transgene expression.

2. Materials and methods

See supporting information.

3. Results and discussion

3.1. Synthesis of dextran-graft-poly(ethylene imine) polymers

Well-defined, proton initiated poly(2-ethyl-2-oxazoline)s (PEtOx) were initially synthesized and subsequently hydrolyzed to lPEI under acidic conditions (Scheme S1). LPEI with a theoretical molar mass of $M_n = 860\,g\,mol^{-1}$ (20 repeating units, $lPEI_{20}$) and $1720\,g\,mol^{-1}$ (40 repeating units, $lPEI_{40}$) were obtained, which both carried an active ω-primary amine end group for the subsequent conjugation to dextran (Table S1, Scheme S1). A detailed characterization of the utilized lPEI is published elsewhere (Altuntaş et al., 2012; Tauhardt et al., 2011). To evaluate the influence of the linker unit, but also of the DS and molar mass of lPEI, various lPEIs were allowed to react with different ratios with dextran-precursors. To this end, a library of various dextran-*graft*-linear poly(ethylene imine)s (dex-*g*-lPEI), was synthesized applying different dextran-precursors and degrees of functional groups. In detail, three synthesis strategies were utilized to graft lPEI to dextran: (i) reductive amination of aldehyde functionalized dextran (CHO-dex), (ii) EDC promoted coupling of lPEI to carboxymethylated dextran (CM-dex), and (iii) carbamate formation *via* activation of dextran to 4-nitrophenyl carbonate-substituted dextran (NPC-dex) followed by reaction with lPEI (Scheme 1) (Azzam et al., 2002; Sun et al., 2008b; Vandoorne, Bruneel, Vercauteren, & Schacht, 1991). In preliminary studies (data not shown), these synthesis routes were examined to enable a straightforward reaction of the primary amino functionality of lPEI with the respective active groups introduced to dextran. It was found that the reductive amination and the EDC coupling are well-suited techniques for the synthesis of various dex-*g*-lPEI. In contrast, the carbamate formation method was not qualified because significant crosslinking occurred during reaction of 4-nitrophenyl carbonate-activated dextran with lPEI, resulting in insoluble products for higher DS values (data not shown).

3.2. Reductive amination

Pharmaceutical grade dextran from *Leuconostoc mesenteroides* ($M_w = 65{,}900\,g\,mol^{-1}$, supplier information $60{,}000\,g\,mol^{-1}$) was oxidized in a low level with potassium periodate (KIO_4). This dextran sample is frequently applied in preclinical and clinical applications (Mehvar, 2000; Sun et al., 2008b). For the oxidation, two different ratios of KIO_4 per anhydroglucose unit (AGU) (1:3 and 1:10) were chosen to react with dextran. The final degree of oxidation (degree of aldehyde groups per AGU) of the products was found to be 0.51 (**CHO-dex$_{0.5}$**) and 1.09 (**CHO-dex$_{1.0}$**), as examined by hydroxylamine chloride titration, and correlates directly to the amount of KIO_4 applied per AGU (Table S2) (Zhao & Heindel, 1991). Further investigations by size exclusion chromatography

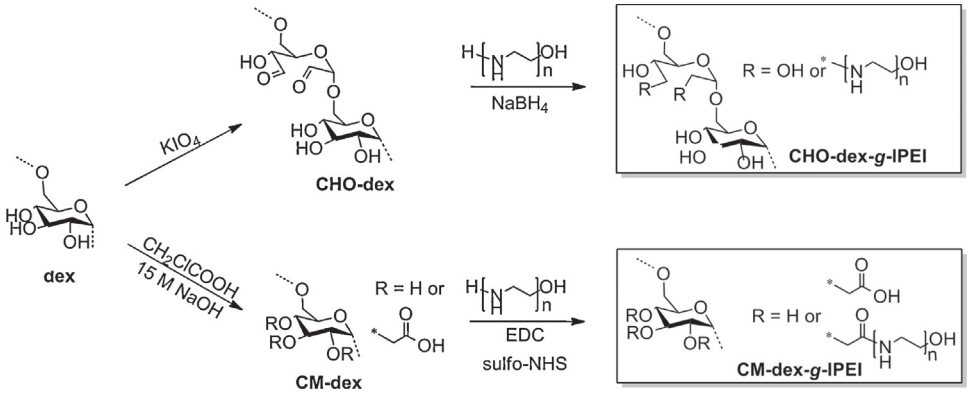

Scheme 1. Schematic representation of the functionalization of dextran by oxidation and carboxymethylation with subsequent reaction with lPEIs via reductive amination (**CHO-dex-*g*-lPEI**) and EDC coupling (**CM-dex-*g*-lPEI**), respectively.

(SEC) exhibited, as expected, a slight decrease in the molar mass due to chain degradation with increasing KIO_4-ratio (**CHO-dex$_{0.5}$**: M_w = 55,100 g mol^{-1}, **CHO-dex$_{1.1}$**: M_w = 52,500 g mol^{-1}, Table S2). The final products were further characterized by elemental analysis (EA) and ^{1}H NMR spectroscopy (Table S2, Fig. S3). In the ^{1}H NMR spectra, the signals at 3.4 ppm to 4.1 ppm can be assigned to the protons of the AGU, and the peak at 5.2 ppm to 5.3 ppm is attributed to the anomeric proton (Fig. S3). Additionally, the ^{1}H NMR spectra showed several distinctive signals in the region of 4.0 ppm to 6.0 ppm that were not present in the original dextran and give hints for different C—C bond breaking reactions as well as the formation of various hemiacetals (Jeanes & Wilham, 1950; Kent, 1949; Rankin & Jeanes, 1954).

Subsequently, the two dextran precursors were each converted with **lPEI$_{20}$** and **lPEI$_{40}$** by reductive amination in water at 60 °C (Scheme 1A). To reduce aminolysis side reactions caused by a fast conjugation rate, the pH value of the lPEI solution was adjusted to pH 6, which additionally improved the solubility of the lPEI. The DS of conjugated lPEIs per AGU was aimed to be highest 0.5, thus, the molar ratio of NH_2-lPEI to CHO was set to 1:2 for **CHO-dex$_{1.0}$** and 1:1 for **CHO-dex$_{0.5}$**. After subsequent reduction with $NaBH_4$, all dex-*g*-lPEIs (**CHO-dex-*g*-lPEIs**) were purified by extensive dialysis against water at 60 °C (for enhanced lPEI solubility), lyophilized, and investigated by ^{1}H NMR spectroscopy, EA as well as SEC measurements (Table S3, Fig. S4). In the ^{1}H NMR spectra, the signals of the CHO-dex samples are still detectable (AGU: 3.4 to 4.1 ppm; anomeric proton: 5.2 to 5.3 ppm). The additional peaks at 3.1 to 3.3 ppm correspond to the protons of the lPEI backbone and confirm the successful covalent conjugation of lPEI to CHO-dex. Various DS of lPEI per AGU were obtained (DS = 0.13 to 0.38) as calculated from the nitrogen content determined by EA (Table 1). The molar masses increase with DS from M_w = 24,000 g mol^{-1} for **CHO$_{0.5}$-dex-*g*-lPEI$_{20}$** to M_w = 36,500 g mol^{-1} for the **CHO$_{1.0}$-dex-*g*-lPEI$_{40}$** (Table S3). However, these results are not absolute values due to the fact that a dramatic rise in charge density of the polymers leads to a considerable change in the elution behavior from the column.

3.3. EDC coupling

For the second synthetic strategy, carboxylic moieties, which are able to react with the primary amino groups of the lPEIs, were introduced to the dextran backbone by carboxymethylation using monochloroacetic acid (MCA) under basic conditions (Sun et al., 2008b; Wotschadlo et al., 2009). The ratios of the reagents (dextran-AGU:MCA:NaOH = 2.2:1:1 or 1:5:10) as well as the reaction times (90 or 300 min) were altered in order to obtain different CM-dex precursors with varying DS. The lyophilized samples were characterized with regard to their content of the carboxymethyl groups according to a HPLC procedure (Heinze, Erler, Nehls, & Klemm, 1994; Liebert & Heinze, 1998). Three degrees of carboxymethyl functionalization per AGU were found, namely 0.32 (**CM$_{0.3}$-dex**), 0.54 (**CM$_{0.5}$-dex**), and 1.60 (**CM$_{1.6}$-dex**) (Table S4). The ^{1}H NMR spectra (600 MHz, D_2O) showed the expected methylene peak of the carboxymethyl group in the CM-dex at 4.1 to 4.3 ppm, and the proton signals of the AGU (3.4 to 4.1 ppm) as well as the anomeric proton peak at 5.2 to 5.3 ppm (Fig. S5). SEC data revealed increasing molar masses with increasing attachment of the carboxymethyl groups, ranging from M_w = 51,100 g mol^{-1} (**CM$_{0.3}$-dex**) up to 60,100 g mol^{-1} (**CM$_{1.6}$-dex**, Table S4).

The subsequent grafting of $lPEI_{20}$ and $lPEI_{40}$ to the various CM-dex samples was performed in water in the presence of *N*-hydroxysulfosuccinimide (sulfo-NHS) and 1-ethyl-3-(3-dimethylaminopropyl)-carbodiimide (EDC) (Sun et al., 2008b). Both **CM-dex$_{0.3}$** and **CM-dex$_{0.5}$** were allowed to react with a slight excess of lPEI (COOH:NH_2 = 1:1.2), whereas the COOH:NH_2 ratio was reduced to 3:1 for **CM-dex$_{1.6}$**. After extensive purification and lyophilization, the products (**CM-dex-*g*-lPEIs**) were characterized by ^{1}H NMR spectroscopy, SEC, and EA (Table S5). The chemical shifts of the protons of the lPEI backbone are detected at 3.1 to 3.3 ppm confirming the successful binding of the lPEIs to the CM-dextrans (Table S6) (Park et al., 2005; Sun et al., 2008b). The resulting DS of lPEI per AGU was again calculated from the nitrogen content obtained by EA and found to be in the range of 0.06 to 0.18 (Table 1). Furthermore, SEC analysis also revealed an increase of molar mass due to attachment of the lPEI to the CM-dex.

By comparing the strategies applied for the grafting of lPEI to dextran, it is apparent that both ways enabled the synthesis of various dex-*g*-lPEIs with different DS of lPEI in a straightforward manner. Although the reductive amination method reached considerably higher DS values, this technique has the drawback that the required oxidization of dextran led to ring opening reactions of the glucose, chain degradation, and other adverse side-reactions, which resulted in hardly predictable chemical structures and biophysicochemical characteristics. In contrast, during dextran activation *via* carboxymethylation the glucose units of the dextran kept their ring structure and no chain degradation occurred. However, dex-*g*-lPEIs prepared by EDC coupling additionally contained carboxylic acid functionalities (COOH) in the dextran backbone, which resulted in polyelectrolyte structures including both cationic and anionic charges that might influence the physicochemical and the biological properties as well.

3.4. Binding and protection of DNA

Nanoassemblies can be formed spontaneously by masking the anionic charge of the DNA based on electrostatic interactions

Table 1
Overview about the DS and nitrogen content of all synthesized dex-*g*-lPEI samples.

dex-*g*-lPEIs	CHO/COOH: NH_2 [mol]	DS [lPEI/AGU]	N [%]	Cationic charge/$M_{Monomer}$[a]	Anionic charge/$M_{Monomer}$[b]
Reductive amination (**CHO-dex-*g*-lPEI**)					
$CHO_{0.5}$-dex-*g*-lPEI$_{20}$	1:0.5	0.18	15.78	0.0114	–
$CHO_{0.5}$-dex-*g*-lPEI$_{40}$	1:0.5	0.13	19.12	0.0135	–
$CHO_{1.0}$-dex-*g*-lPEI$_{20}$	1:0.5	0.38	21.45	0.0156	–
$CHO_{1.0}$-dex-*g*-lPEI$_{40}$	1:0.5	0.19	21.73	0.0156	–
EDC coupling (**CM-dex-*g*-lPEI**)					
$CM_{0.3}$-dex-*g*-lPEI$_{20}$	1:1.2	0.06	6.73	0.0052	0.0013
$CM_{0.3}$-dex-*g*-lPEI$_{40}$	1:1.2	0.07	12.80	0.0093	0.0010
$CM_{0.5}$-dex-*g*-lPEI$_{20}$	1:1.2	0.07	7.96	0.0056	0.0020
$CM_{0.5}$-dex-*g*-lPEI$_{40}$	1:1.2	0.10	14.83	0.0110	0.0014
$CM_{1.6}$-dex-*g*-lPEI$_{20}$	3:1	0.11	8.16	0.0063	0.0046
$CM_{1.6}$-dex-*g*-lPEI$_{40}$	3:1	0.18	18.38	0.0127	0.0028

[a] Calculated cationic charge/molar mass of monomer unit.
[b] Calculated anionic charge/molar mass of monomer unit.

between the cationic carrier material and the anionic DNA. Complexes of lPEI modified dextran were formed with herring testes DNA as model DNA (Fischer, Dautzenberg, Kunath, & Kissel, 2004) applying different N/P ratios (0.5 to 40) and analyzed by agarose gel electrophoresis (Fig. S7 for N/P 0.5–10, for N/P ratio >10 to 40 data not shown). The complex parameters (N/P ratio) as well as the polymer characteristics (molar mass lPEI, DS and type of linker technology) were tested in a systematically modified way as they were expected to influence the interaction with DNA.

Depending on the N/P ratio, all cationic dextrans spontaneously formed interpolyelectrolyte complexes with the DNA as a result of cooperative electrostatic interactions. With increasing cationic dextran concentration, the amount of DNA migrating into the gel decreased indicating that the complexes were larger in size and/or less negatively charged than free DNA. It was explored that all **CHO-dex-*g*-lPEIs** fully complexed herring testes DNA already at an N/P ratio of 1 (Fig. S7) indicating charge balance. The complexation was found to be slightly increased with higher molar mass of lPEI coupled to CHO-dex. Other studies also showed that an increase of the molar mass of bPEI resulted in a higher binding capacity independent of the degree of grafting (Jiang & Salem, 2012). For comparison, both linear PEIs (20 and 40 monomers) also fully retarded the DNA at a N/P ratio 1 (Lungwitz, Breunig, Liebl, Blunk, & Goepferich, 2008). Furthermore, CM-dex-*g*-lPEIs were found to completely retard DNA migration into the gel at an N/P ratio firstly at 2, which indicates a weaker complexation ability compared to free lPEI and **CHO-dex-*g*-lPEI** samples. This may be attributed to the presence of the anionic charges that could interfere with lPEI and decrease the interaction with DNA. This assumption is supported by polymer **$CM_{1.6}$-dex-*g*-lPEI$_{20}$**, which contained the highest number of anionic charges and demonstrated the lowest interaction with DNA with a total complexation earliest at N/P ratio 5. The negative "charge effect" on DNA binding can be balanced by a higher DS and molar mass of lPEI grafted on the CM-dex backbone as demonstrated for sample **$CM_{1.6}$-dex-*g*-lPEI$_{40}$** (complexation at N/P ratio 1). A slight trend to higher compaction with increasing molar mass of lPEI can be found as already observed for dextran copolymers with bPEI (Sun et al., 2008b).

Compaction of plasmid DNA (pDNA) by cationized dextrans should substantially hinder the access of enzymes to the pDNA by physical or electrostatic barriers and, thus, increase the stability (Tripathi et al., 2011). To study the integrity of pDNA after enzymatic treatment by gel electrophoresis (Fig. 1), pDNA/cationized dextran complexes of different N/P ratios were treated with DNase I for 45 min. After inactivation of the enzyme by heating and release of the plasmid by dissociation of the complex using dextran sulfate, free pDNA was detected on agarose gels. Intact plasmid revealed two major fluorescent bands corresponding to the supercoiled and open circular form (Fig. 1a–c, lane 1, "untreated"). Free plasmid

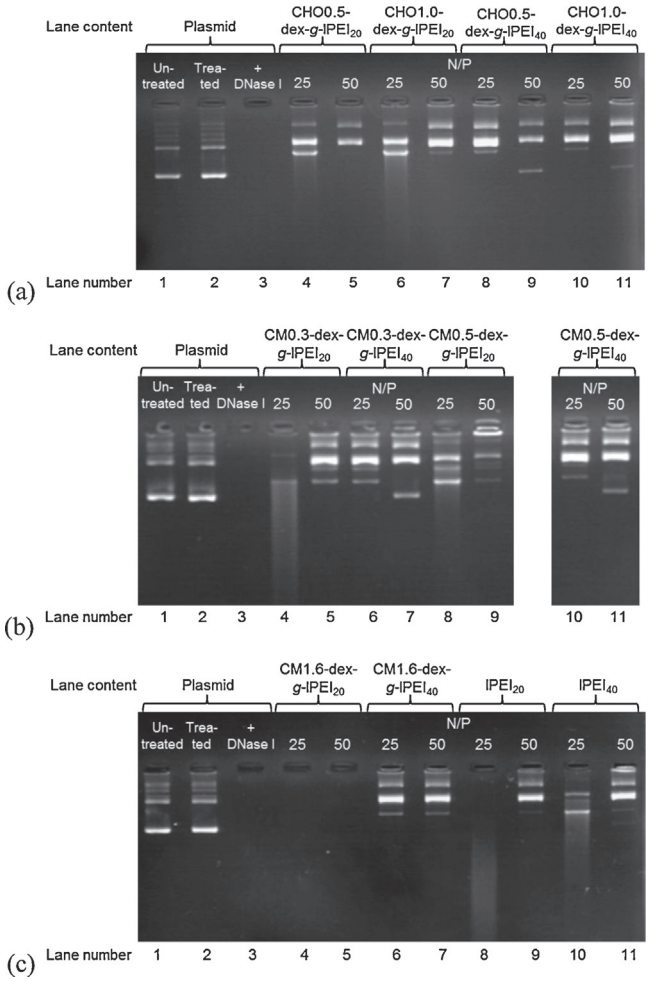

Fig. 1. Stability of dex-*g*-lPEI/plasmid complexes against enzymatic degradation (DNase I, 37 °C, 45 min) at N/P ratio 25 and 50: (a) C; (b) and (c) dex-*g*-lPEIs by EDC-coupling, (c) lPEIs. Controls: lane 1: untreated free plasmid; lane 2: free plasmid treated in the same way as complexes but without enzyme; lane 3: free plasmid treated with enzyme.

was rapidly degraded after DNase I incubation at 37 °C already after 5 min (data not shown). Thus, the characteristic bands disappeared due to degradation to lower molar mass products (Fig. 1a–c, lane 3, "DNase I"). Plasmid treated by the same procedure but without enzyme remained stable and served as control to exclude nonspecific degradation (Fig. 1a–c, lane 2, "treated").

Since in the binding studies a high N/P ratio, high molar lPEI mass and DS as well as a low number of COOH residues were identified

as parameters for an efficient interaction with DNA, they were suggested to correlate with a high enzymatic stability of the complexes. Although a full pDNA complexation by cationic dextrans already occurred at low N/P ratios, higher N/P ratios were selected for physicochemical analysis according to later transfection results. The results of the stability assay indicated that the efficiency to stabilize DNA was increased with increasing N/P ratio, higher molar masses of lPEI, and DS with lPEI independent of the type of linker. For free lPEI, a molar mass dependent interaction with pDNA could be observed (Fig. 1c, lanes 8 and 10). The higher the molar mass of free lPEI, the more efficient was the stabilizing effect of the complex. This effect could also be observed for the dex-*g*-lPEIs and was more pronounced for these than for the free lPEI. In particular, at N/P ratio 25 of dex-*g*-lPEI the stability increased with higher molar mass, which might be related to the increase in charge density within the macromolecules.

For **CHO-dex-*g*-lPEIs**, the stabilization effect was most obvious. **CHO-dex-*g*-lPEI$_{20}$** polymers revealed at N/P ratio 25 a different pattern of DNA bands compared to the **CHO-dex-*g*-lPEI$_{40}$** complexes. Changes in the topology of the plasmids are common as reported in many other studies (Fischer et al., 2004; Gebhart et al., 2002). **CHO$_{0.5}$-dex-*g*-lPEI$_{40}$** and **CHO$_{0.1}$-dex-*g*-lPEI$_{40}$** protected the plasmid better than their lPEI$_{20}$ counterparts, since at N/P ratio 25 no degradation product was visible and just a weak fluorescent band between the expected supercoiled and the open circular band appeared (Fig. 1a lanes 8 and 10). At N/P ratio 50 for both conjugates even a low fluorescent supercoiled plasmid band is still visible (Fig. 1a, lanes 9 and 11).

Likewise all **CM-dex-*g*-lPEI$_{20}$** conjugates were not able to protect the pDNA as good as their lPEI$_{40}$ counterparts. **CM$_{0.3}$-dex-*g*-lPEI$_{20}$** with the lowest DS of lPEI demonstrated at N/P ratio 25 a high plasmid damaging effect. In contrast, for **CM$_{0.3}$-dex-*g*-lPEI$_{40}$** and **CM$_{0.5}$-dex-*g*-lPEI$_{40}$**, a certain amount of supercoiled plasmid could be conserved. In accordance with the low DNA binding efficiency described above, **CM$_{1.6}$-dex-*g*-lPEI$_{20}$** was not able to stabilize plasmid DNA even at N/P ratio 50.

In summary, it could be demonstrated that improved binding and protection of DNA is basically reached with increased N/P ratio. Furthermore, the higher the molar mass of lPEI and DS with lPEIs the better the stabilization of pDNA by the conjugates due to the increase of positive charge. Thus, it is not surprising that in contrast to the **CHO-dex-*g*-lPEIs**, the **CM-dex-*g*-lPEIs** showed weaker DNA binding and less stabilization characteristics. Theses polymers are characterized by lower DS with lPEI and also by negative charges originating from the carboxymethyl (CM) functionalities within the polymer backbone that might decrease the interaction with negatively charged pDNA due to electrostatic repulsion.

3.5. Size and zeta potential of complexes

The efficiency of the dex-*g*-lPEI-mediated cellular DNA delivery will also be determined by the size and the surface charge of the complexes formed. A positive surface charge represents a prerequisite to stabilize the included nucleic acid against enzymatic degradation in small sized complexes, which are able to interact with the negatively charged cell membrane for an effective endocytosis into cellular compartments (Grund, Bauer, & Fischer, 2011). Complexes were prepared with two different N/P ratios (25 and 50) in bidistilled water to avoid any influence of the ionic strength of the solvent and were studied by light scattering with regard to the final size and surface charge. Based on the electrophoresis experiments, it was hypothesized that (i) all copolymers should be able to form small, positively charged nanoassemblies with DNA with (ii) **CHO-dex-*g*-lPEIs** being more effective than **CM-dex-*g*-lPEIs**.

In detail, all dex-*g*-lPEI/pDNA assemblies revealed sizes in the range of 70 to 113 nm with monomodal size distributions

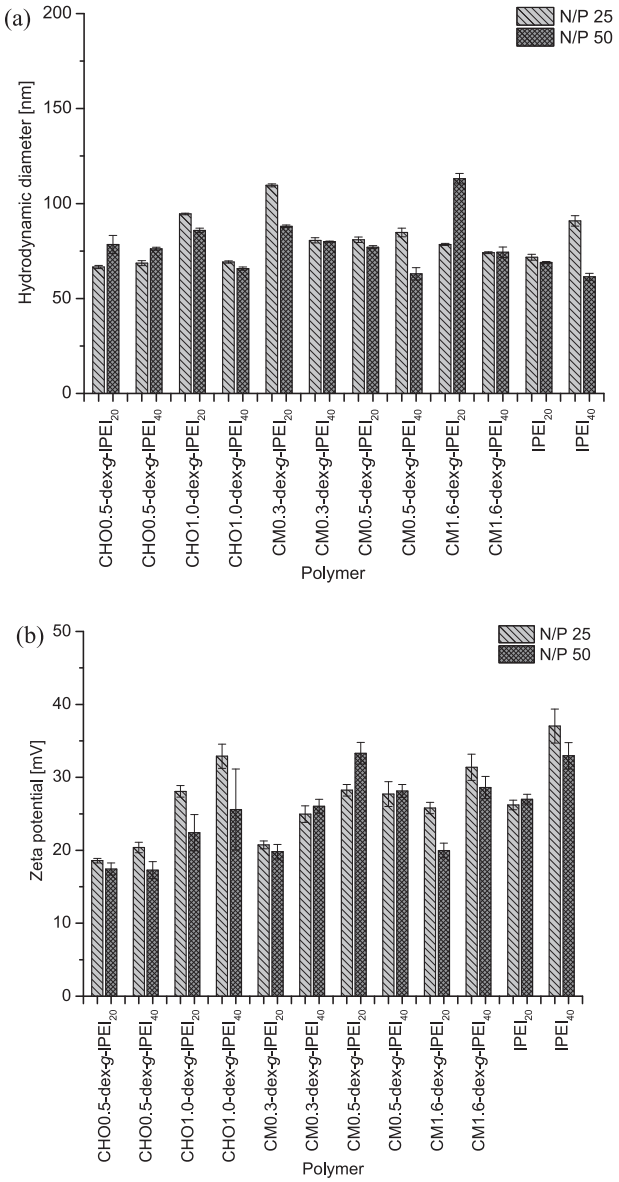

Fig. 2. (a) Hydrodynamic diameter and (b) zeta potential of dex-*g*-lPEI and lPEI complexes with plasmid DNA at N/P ratio 25 and 50 measured in water. Results are shown as mean of six measurements ± SD.

(polydispersity indices (PDI) 0.13 to 0.31, data not shown), which were comparable to the sizes obtained for the DNA complexes with lPEI$_{20}$ and lPEI$_{40}$ (Fig. 2a). Since an excess of polymer was used, no major differences could be observed between N/P ratio 25 and 50. For polymer **CM$_{1.6}$-dex-*g*-lPEI$_{20}$**, a relatively high hydrodynamic diameter of 113 nm was measured at N/P ratio 50. The insufficient DNA binding and stabilization of DNA by **CM$_{1.6}$-dex-*g*-lPEI$_{20}$** correlates with a lower DNA compaction and, consequently, a larger complex size. A similar trend was observed for **CM$_{0.3}$-dex-*g*-lPEI$_{20}$** at N/P ratio 25 (hydrodynamic diameter 110 nm). All complexes were positively charged with zeta potentials between +17 and +37 mV with comparable results for N/P ratios 25 and 50 due to the excess of the cationic component (Fig. 2b).

Additionally, complexes were prepared in 50 mM NaCl solution at pH 7.4 (data not shown). All complexes of **CHO-dex-*g*-lPEIs** prepared with N/P ratio 25 aggregated immediately. In contrast, by trend smaller sized complexes were obtained at N/P ratio 50 with diameters of about 170 to 320 nm due a more intense compaction of the plasmid by the modified dextrans, but again with a tendency to

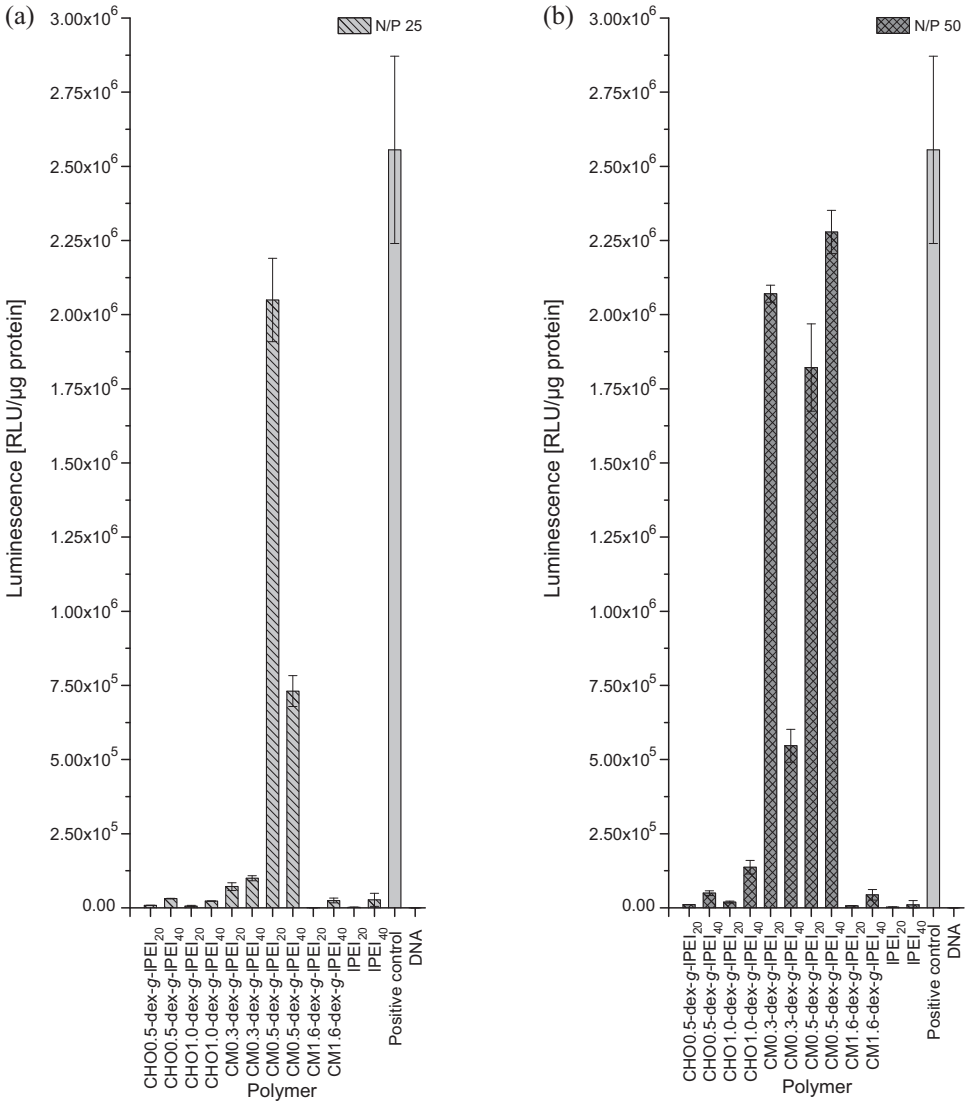

Fig. 3. Transfection efficiency of dex-*g*-lPEIs and free lPEIs complexed with plasmid pGL3 at (a) N/P ratio 25 and (b) N/P ratio 50 in CHO-K1 cells determined by luciferase assay; in comparison to the positive control 2.5 kDa lPEI at N/P ratio 25 and naked plasmid (DNA).

slowly agglomerate over time. Measurements of complexes of the CM-dex-*g*-lPEIs with pDNA in 50 mM NaCl did not lead to evaluable results due to strong aggregation, forming complexes larger than 1 μm with multimodal size distributions.

It is known that the complex formation can be strongly influenced by the medium used for preparation, since complexation is driven by electrostatic forces (van Gaal et al., 2011). Usually, the higher the ionic strength of the media the higher the impact on the complexation and the resulting complex size (Rinkenauer et al., 2013). 150 mM NaCl as iso-osmotic solution is often used for transfections, but can lead to a fast complex aggregation (Petersen et al., 2002). To reveal relevant information about the complex size for product characterization, many authors described therefore useful measurements under salt-free conditions (Cavallaro et al., 2008; Ogris, Brunner, Schuller, Kircheis, & Wagner, 1999; Ogris et al., 2003). Measurements of complexes in cell culture medium and serum supplemented cell culture medium are often misleading, since the proteins itself prevent a proper characterization by DLS. Several authors have mentioned this effect, and formation of complexes and their measurements under low salt conditions have been therefore widely described (van Gaal et al., 2011). Furthermore, in serum containing media the process of aggregation could often be avoided due to the stabilization of the complexes by the formation of a surrounding protein corona. For transfection experiments it has to be taken into consideration that possible aggregation is a time-dependent process. Consequently, complexes were freshly prepared before each biological experiment and used within 10 min. Ogris et al. (1998) hypothesized that the transfection efficacy *in vitro* might increase with larger complex sizes due to their faster sedimentation. Although we also observed aggregation for the pDNA complexes prepared from **CHO-dex-*g*-lPEIs**, they revealed a decrease in complex size demonstrating a positive impact of dextran on the complex formation in comparison to free $lPEI_{20/40}$.

However, the influence of complex aggregation on transfection, cytotoxicity and hemolysis results was not in the focus of this study and therefore, not further addressed. For future studies, a low ionic strength medium supplemented *e.g.* with glucose at iso-osmotic concentrations might be beneficial since it tolerates the characterization as well as the transfection (van Gaal et al., 2011).

3.6. Transfection mediated by pDNA/dex-g-lPEI complexes

CHO-K1 cells were transfected with complexes of the cationized dextrans and the plasmid pGL3 at different N/P ratios for 4 h. Based on preliminary experiments, N/P ratios 25 and 50 were found to be suitable for the following experiments. Luciferase expression was presented by normalizing the measured relative light units (RLU) to the total protein mass of the cells per culture well. For all tested samples, cytotoxicity-related effects as the reason for the declining transfection efficiencies were unlikely, since the protein concentrations in cell lysates (an indicator for cell growth, determined by a BCA assay) were very similar (data not shown). Free plasmid itself revealed only a limited ability to transfect cells. Unmodified dextran was tested in concentrations up to 25 $\mu g\,\mu g^{-1}$ pGL3 plasmid in a preliminary study and failed to produce any detectable level of transgene expression (data not shown). Also $lPEI_{20}$ and $lPEI_{40}$, were characterized by a low transgene expression.

The transfection experiments for the copolymers were designed to evaluate the importance of the structural polymer characteristics identified above, for the delivery of genes *in vitro*. Besides increasing N/P ratios, especially molar mass of lPEI and DS with lPEIs leading to smaller and more stable complexes, were found to be important factors for efficient DNA transfer. Furthermore, the influence of the carboxy groups of the **CM-dex-*g*-lPEIs**, which seemed to cause reduced interactions with DNA, on cellular processing of DNA has to be elucidated.

Interestingly, the transfection efficiency obtained for the **CHO-dex-*g*-lPEIs** was only slightly higher than for the corresponding free lPEIs, but cationized dextrans with negatively charged groups, prepared by EDC coupling, demonstrated a high activity (Fig. 3). For **CM-dex-*g*-lPEIs**, the transgene expression increased with higher molar mass of the lPEIs and N/P ratio, as already expected from the available physicochemical characterization data. For the **CM-dex-*g*-lPEIs**, the transfection rate increased in the range **$CM_{0.3}$-dex-*g*-$lPEI_{20}$**, **$CM_{0.3}$-dex-*g*-$lPEI_{40}$**, **$CM_{0.5}$-dex-*g*-$lPEI_{20}$** at N/P ratio 25, whereas for **$CM_{0.5}$-dex-*g*-$lPEI_{40}$** a decrease could be observed (Fig. 3a). It has to be highlighted that **$CM_{0.3}$-dex-*g*-$lPEI_{20}$**, **$CM_{0.5}$-dex-*g*-$lPEI_{20}$** and **$CM_{0.5}$-dex-*g*-$lPEI_{40}$** at N/P ratio 50 (1.8 to 2.3×10^6 RLU μg^{-1} protein, Fig. 3b) showed transfection efficiencies comparable to that of a commercially available linear 2,500 g mol^{-1} lPEI at N/P ratio 25 (2.55×10^6 RLU μg^{-1} protein, Fig. 3b). A similar effect could be observed earlier for CM-dex-PEIs (Sun et al., 2008b). **$CM_{0.3}$-dex-*g*-$lPEI_{40}$** and **$CM_{0.5}$-dex-*g*-$lPEI_{40}$** were expected to induce higher transfection rates than **$CM_{0.3}$-dex-*g*-$lPEI_{20}$** and **$CM_{0.5}$-dex-*g*-$lPEI_{20}$**, as it is known from the higher molar mass dex-*g*-bPEI conjugates(Jiang & Salem, 2012) and was also observed for the **CHO-dex-*g*-lPEIs**. However, a contrary effect was revealed for **$CM_{0.5}$-dex-*g*-$lPEI_{40}$** at N/P ratio 25 and **$CM_{0.3}$-dex-*g*-$lPEI_{40}$** at N/P ratio 50, since an approximately 1/3 lower transfection compared to their $lPEI_{20}$ counterparts was found. This is ascribed to stronger interactions between the longer lPEI chain with COOH groups of the CM-dex than with the pDNA.

In conclusion, **$CM_{0.5}$-dex-*g*-$lPEI_{20}$** provides the best gene delivery properties in this study at both N/P ratios, what might be related to the ratio of cationic charges to anionic charges per monomer (Table 1). Additionally, the low efficiency of the **CHO-dex-*g*-lPEIs** may be attributed to the higher DNA complexation efficiency of the polymer and, therefore, lower ability to release pDNA from the complexes compared to the polymers of the **CM-dex-*g*-lPEIs** as shown by the electrophoresis assays. Dissociation of DNA from the complexes is one of the critical steps in the biological process, since only released and intact DNA can be transcribed. The observed trends are in accordance with the results of the physicochemical experiments: As uptake of complexes into cells imposes certain size and stability requirements on the endocytosed material, it is necessary for a successful gene transfer that the cation in polyplexes not only binds DNA, but also compacts it. Since the condensation of DNA is also known to protect the genetic material from enzymatic degradation (Godbey, Barry, Saggau, Wu, & Mikos, 2000), the decrease of transfection ability of the complexes formed by polymers **$CM_{1.6}$-dex-*g*-$lPEI_{20}$** and **$CM_{1.6}$-dex-*g*-$lPEI_{40}$** may result from the insufficient interactions with pDNA based on the highest number of anionic charges.

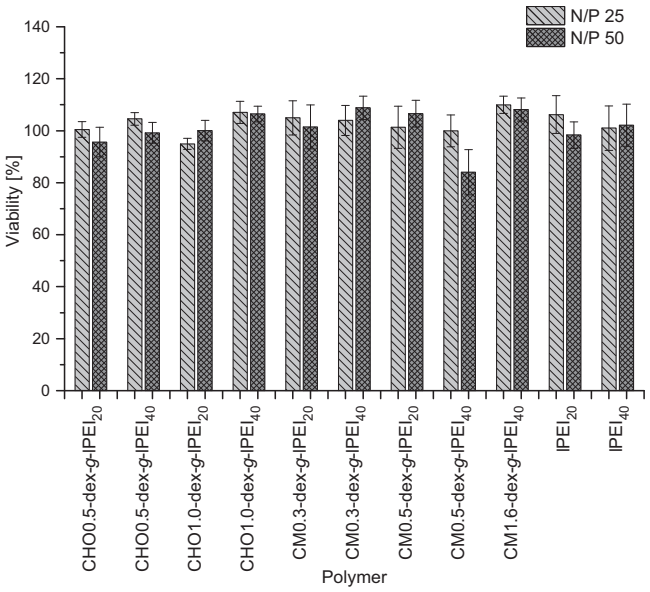

Fig. 4. Viability of L929 mouse fibroblasts treated with dex-*g*-lPEI/DNA and lPEI/DNA complexes at N/P ratio 25 and 50 for 24 h, determined by MTT assay. Complexes were formed with herring testes DNA as model DNA. Results are shown as mean of seven values ± SD.

3.7. In vitro biocompatibility testing

Biocompatibility testing has been performed with respect to cyto- and hemotoxicity. The *in vitro* cytotoxicity of the non-viral vectors was evaluated by the 3-(4,5-dimethylthiazol-2-yl)-2,5-diphenyltetrazolium bromide (MTT) assay representing the metabolic activity of cells (Fig. 4). The same conditions as in the transfection experiments were used. Independent of the N/P ratio, complexes with the two lPEIs did not cause any cytotoxic effect, which is supported by results from earlier studies demonstrating the low cytotoxicity of complexes formed with low molar mass lPEIs (Breunig et al., 2005; Thomas, Ge, Lu, Chen, & Klibanov, 2005; Yu et al., 2009). Taking the DIN ISO 10993-5 guideline (2009) into consideration which defines a reduction of cell viability lower than 70% as nontoxic, all tested dex-*g*-lPEI/DNA complexes were found to be highly compatible (84 to 110%) at N/P ratios 25 and 50. The compatibility was thereby independent of the linker technique, the DS and the selected N/P ratios (Fig. 4). For comparison, the positive control thiomersal solution (0.02%) reduced the mean cell viability to 0.6% (data not shown). The results of the MTT assay correlated well with the observation of the BCA assay (data not shown) in the transfection experiments. Similar results were reported in earlier studies as well (Jiang & Salem, 2012; Sun et al., 2008b).

Furthermore, the compatibility of non-viral vectors with blood indicates their suitability for administration directly into the systemic circulation. The hemolytic behavior of the free polymers was tested as worst case scenario and classified according to the ASTM F756-08 standard (data not shown) (2008). According to this standard, neither free lPEIs nor dex-*g*-lPEIs did show any detectable disturbance of the red blood cell membranes (hemolysis <2%) up to 1 mg mL^{-1}. The observed behavior can be attributed to the low

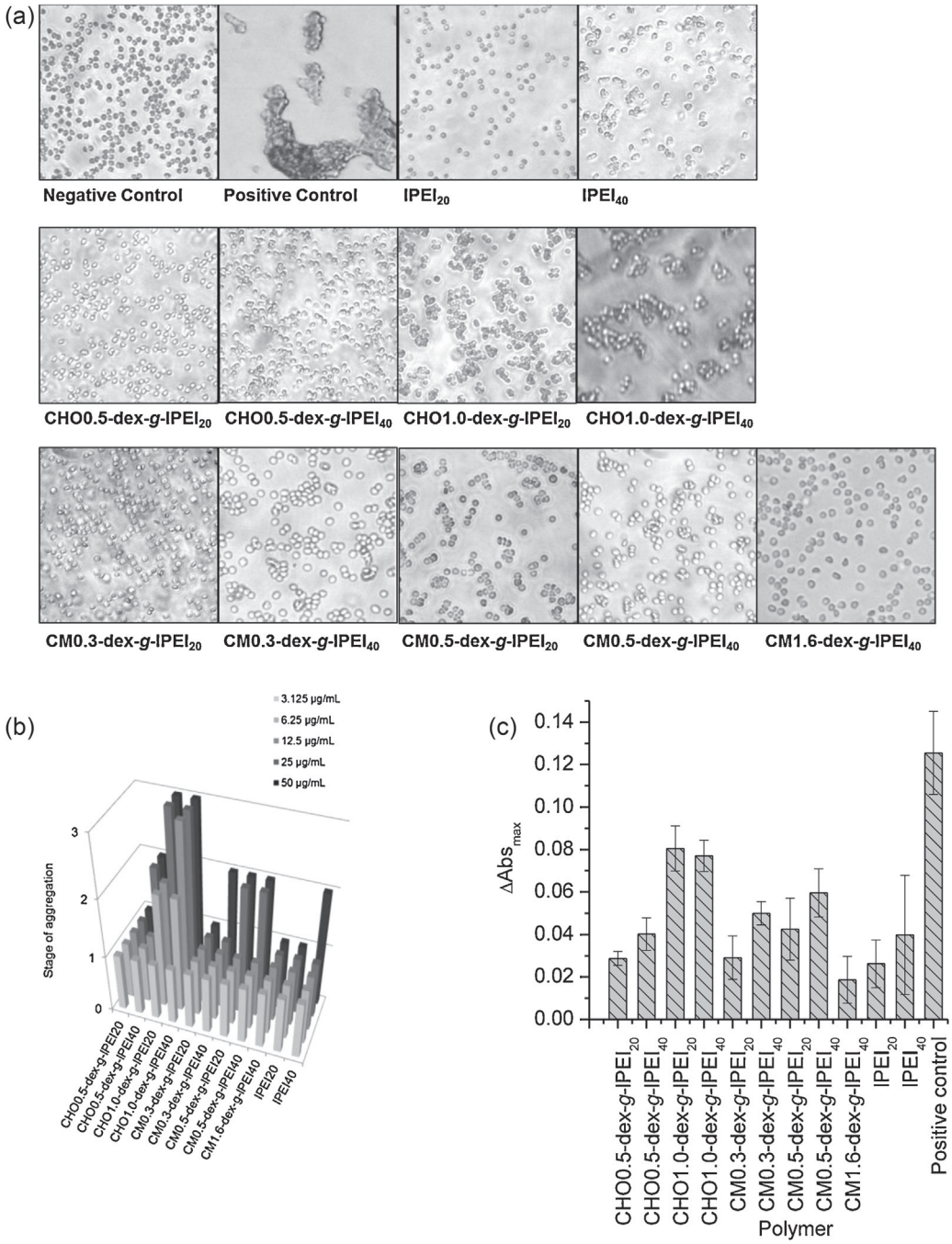

Fig. 5. Aggregation of sheep red blood cells after treatment with free dex-*g*-lPEI and lPEI polymers incubated at 37 °C for 2 h. (a) Representative pictures of microscopic observation at 50 μg mL^{-1} (negative control = PBS; positive control = 15 μg mL^{-1} bPEI 25,000 g mol^{-1}) with magnification 200×. (b) Stages of sheep blood erythrocyte aggregation of dex-*g*-lPEIs and lPEIs at concentrations up to 50 μg mL^{-1}. Classification: 1 = no aggregation of erythrocytes, 2 = moderate aggregation with rouleau formation, 3 = strong aggregation with cluster formation. (c) ΔAbs_{max} of polymers. The RBC aggregation experiments were performed with $n = 2$ and repeated once (mean ± SD).

DS and the low molar mass of the cationic polymers (Moreau, Domurado, Chapon, Vert, & Domurado, 2002). For comparison, dextran itself showed no erythrocyte membrane disturbance up to 16 mg mL^{-1} with 0.2% hemolytic activity (Yang et al., 2012).

To avoid clinical complications like thrombosis and embolism by systemic use of the dextran-based vectors, their potential to aggregate red blood cells was investigated by qualitative light microscopy (Fig. 5a and b) and classified into three stages (Fig. 5b) as well as quantitatively by UV–vis spectroscopy (Fig. 5c). Both methods gave comparable results and displayed a concentration-dependent red blood cell aggregation behavior of the polymers up to 50 μg mL^{-1}. In microscopic experiments, the negative control did not show any signs of cluster formation (stage 1), whereas the positive control (25,000 g mol^{-1} bPEI, 15 μg mL^{-1}) caused the formation of large aggregates (stage 3) as described before (Fig. 5a) (Bauer et al., 2012). Additionally, the ΔAbs_{max} value was introduced, meaning the difference of the reduction in absorbance to the negative control absorbance. In contrast to the positive control ($\Delta Abs_{max} = 0.12$), $lPEI_{20}$ was well tolerated and classified as stage 1 ($\Delta Abs_{max} = 0.026$), whereas an increase in molar mass ($lPEI_{40}$) initiated rouleaux formation only at the highest tested concentration of 50 μg mL^{-1} (stage 2, $\Delta Abs_{max} = 0.04$). The molar mass and concentration dependent effects of PEIs on red blood cell aggregation were described by several authors (Jeon, Yang, Lee, & Kim,

2008; Petersen et al., 2002). Correlated to the increasing number of charges with size, the interactions with negatively charged cell membranes increase as well.

In accordance to the results obtained for the free lPEIs, also for the dex-*g*-lPEIs an increase of red blood cell aggregation could be observed with higher molar mass of lPEI (Fig. 5). For the **CHO-dex-*g*-lPEIs** erythrocyte aggregation could be observed starting at concentrations of 6.25 and 25 mg mL^{-1} for **CHO$_{1.0}$-dex-*g*-lPEI$_{20}$**, CHO1.0-dex-*g*-lPEI40, and **CHO$_{0.5}$-dex-*g*-lPEI$_{40}$**, respectively. In contrast, **CHO$_{0.5}$-dex-*g*-lPEI$_{20}$** did not show any signs of interaction up to the highest tested concentration of 50 μg mL^{-1} (Fig. 5b). Therefore, interactions with negatively charged cell membranes of the red blood cells were found to increase with the molar mass of lPEI; this observation correlated well with the nitrogen content of the **CHO-dex-*g*-lPEIs**. In general, the conjugates synthesized by reductive amination demonstrated a higher red blood cell aggregation potential compared to the modified dextrans prepared by EDC-coupling. **CM$_{0.3}$-dex-*g*-lPEI$_{40}$**, **CM$_{0.5}$-dex-*g*-lPEI$_{20}$**, and **CM$_{0.5}$-dex-*g*-lPEI$_{40}$** reached only stage 2 with maximum Abs$_{max}$ values of 0.06, even at the highest concentration of 50 μg mL^{-1}. Again, for the lPEI40-containing polymers **CM$_{0.3}$-dex-*g*-lPEI$_{40}$** and **CM$_{0.5}$-dex-*g*-lPEI$_{40}$** the aggregation effects were more pronounced than for the lPEI20-based polymers (**CM$_{0.3}$-dex-*g*-lPEI$_{20}$** and **CM$_{0.5}$-dex-*g*-lPEI$_{20}$**). The higher compatibility of the **CM-dex-*g*-lPEIs** compared to the **CHO-dex-*g*-lPEIs** may be ascribed to the polyelectrolyte nature of the **CM-dex-*g*-lPEIs** since they contain both positive and negative charges. This was particularly demonstrated by the polymer **CM$_{1.6}$-dex-*g*-lPEI$_{40}$**, that possesses a higher number of anionic charges and revealed the lowest effects on red blood cells (stage 1 at 50 μg mL^{-1}, Abs$_{max}$ = 0.02). Hence, the high number of anionic charges within the **CM-dex-*g*-lPEI** polymers seems to interfere with the electrostatic interactions between the anionic cell membranes and the cationic polymers resulting in a decreased cell aggregation. De facto, for polyelectrolytes (*e.g.* zwitterionic polymers) a higher resistance to non-specific protein adsorption and blood cell interactions, which lead to a prolonged half life time in blood circulation, has been shown (Jiang & Cao, 2010).

4. Conclusion

With the objective to evaluate the influence of the linking strategy of lPEI to dextran, several dextran-*g*-lPEIs were prepared. For this purpose, different low molar mass lPEIs were synthesized and conjugated to dextran *via* two routes, namely reductive amination and EDC coupling. These linking strategies were already used in the past but mainly lack on a detailed characterization of the resulting molecules and a direct comparison of the different linking strategies (Jiang & Salem, 2012; Sun et al., 2008b). For a detailed comparative study of structure-activity relationships, the content of functional groups (CHO, COOH) within the dextran precursors and the DS with lPEI were varied as well. Subsequently, the final dex-*g*-lPEI samples were characterized in detail and investigated with regard to their physicochemical properties (DNA binding and stabilization, complex size and surface charge), transfection efficiency as well as biocompatibility. The investigations were performed in terms of dependency on the linking strategy, the molar mass of conjugated lPEIs, and the N/P ratio of the formed DNA/dex-*g*-lPEI complexes. Independent from the linking strategy, DS and molar mass of lPEI, it was observed that almost all conjugates formed with DNA were in the range of 100 nm (in water), stable against enzymatic degradation, and revealed a positive surface charge. Differences between the types of conjugation were visible when lPEI was conjugated with CM$_{1.6}$-dex (**CM$_{1.6}$-dex-*g*-lPEI$_{20}$**): The binding capacity was reduced, as well as the stability and the zeta potential, which was attributed to the higher content of COOH groups along the dextran backbone. Moreover, cell viability studies revealed a good cytocompatibility of the resulting dex-*g*-lPEI/DNA complexes with no crucial influence of the synthesis route or the DS and molar mass of lPEI. Instead, a remarkable effect of these parameters was observed regarding transfection efficiency, since the cationic dextrans prepared by EDC coupling showed a more than one order of magnitude increased transgene expression compared to the **CHO-dex-*g*-lPEIs** despite much lower lPEI content. For comparison, free lPEIs formed complexes that showed almost no transgene expression. The additional integration of COOH-groups seems to accomplish a positive to negative charge ratio within the **CM-dex-*g*-lPEI** conjugates that is advantageous for DNA release and transfection efficiency. Their transfection rates were found to be comparable with the positive control 2.5 kDa lPEI. It was also discovered that both polymer series induced higher red blood cell aggregation compared to unconjugated lPEIs, with **CM-dex-*g*-lPEI** showing a lower erythrocyte aggregation activity than **CHO-dex-*g*-lPEI**. This was again ascribed to the polyelectrolyte nature of the **CM-dex-*g*-lPEI**.

In conclusion, the variation of the linking strategy of cationic polymers to dextran affects the biological properties significantly, while the physicochemical properties were only marginally affected. The EDC coupling was more suitable as linking strategy compared to the polymers obtained by reductive amination, since the conjugates showed improved hemocompatibility and enhanced performance in the transfection experiments.

Acknowledgements

Financial support from the Thuringian Ministry for Education, Science and Culture (grant no. B514-09051, NanoConSens) and from the Carl-Zeiss Foundation (JCSM Strukturantrag) is gratefully acknowledged. The authors also thank Angela Herre, Ramona Brabetz and Maxi Prange for their excellent laboratory assistance.

Appendix A. Supplementary data

Supplementary material related to this article can be found, in the online version, at http://dx.doi.org/10.1016/j.carbpol.2014.07.048.

References

Abdullah, S., Wendy-Yeo, W. Y., Hosseinkhani, H., Hosseinkhani, M., Masrawa, E., Ramasamy, R., Rosli, R., Rahman, S. A., & Domb, A. J. (2010). Gene transfer into the lung by nanoparticle dextran-spermine/plasmid DNA complexes. *Journal Biomedical Biotechnology*, *2010*, 284840.

Altuntaş, E., Knop, K., Tauhardt, L., Kempe, K., Crecelius, A. C., Jäger, M., Hager, M. D., & Schubert, U. S. (2012). Tandem mass spectrometry of poly(ethylene imine)s by electrospray ionization (ESI) and matrix-assisted laser desorption/ionization (MALDI). *Journal of Mass Spectrometry*, *47*(1), 105–114.

ASTM. (2008). *Standard practice for assessment of hemolytic properties of materials. Annual book of ASTM standards* (vol. 13) Philadelphia, PA: ASTM. ASTM F756-13

Azzam, T., Eliyahu, H., Shapira, L., Linial, M., Barenholz, Y., & Domb, A. J. (2002). Polysaccharide-oligoamine based conjugates for gene delivery. *Journal of Medicinal Chemistry*, *45*(9), 1817–1824.

Bauer, M., Lautenschlaeger, C., Kempe, K., Tauhardt, L., Schubert, U. S., & Fischer, D. (2012). Poly(2-ethyl-2-oxazoline) as alternative for the stealth polymer poly(ethylene glycol): Comparison of in vitro cytotoxicity and hemocompatibility. *Macromolecular Bioscience*, *12*(7), 986–998.

Breunig, M., Lungwitz, U., Liebl, R., Fontanari, C., Klar, J., Kurtz, A., Blunk, T., & Goepferich, A. (2005). Gene delivery with low molecular weight linear polyethylenimines. *Journal of Gene Medicine*, *7*(10), 1287–1298.

Cavallaro, G., Scirè, S., Licciardi, M., Ogris, M., Wagner, E., & Giammona, G. (2008). Polyhydroxyethylaspartamide-spermine copolymers: Efficient vectors for gene delivery. *Journal of Controlled Release*, *131*(1), 54–63.

Chu, M., Dong, C., Zhu, H., Cai, X., Dong, H., Ren, T., Su, J., & Li, Y. (2013). Biocompatible polyethylenimine-graft-dextran catiomer for highly efficient gene delivery assisted by a nuclear targeting ligand. *Polymer Chemistry*, *4*(8), 2528–2539.

Cohen, J. L., Schubert, S., Wich, P. R., Cui, L., Cohen, J. A., Mynar, J. L., & Frećhet, J. M. J. (2011). Acid-degradable cationic dextran particles for the delivery of siRNA therapeutics. *Bioconjugate Chemistry*, *22*(6), 1056–1065.

Eshita, Y., Higashihara, J., Onishi, M., Mizuno, M., Yoshida, J., Takasaki, T., Kubota, N., & Onishi, Y. (2009). Mechanism of introduction of exogenous genes into cultured cells using DEAE-dextran-MMA graft copolymer as non-viral gene carrier. *Molecules*, *14*(7), 2669–2683.

Fischer, D., Dautzenberg, H., Kunath, K., & Kissel, T. (2004). Poly(diallyldimethylammonium chlorides) and their *N*-methyl-*N*-vinylacetamide copolymer-based DNA-polyplexes: Role of molecular weight and charge density in complex formation, stability, and in vitro activity. *International Journal of Pharmaceutics*, *280*(1–2), 253–269.

Gebhart, C. L., Sriadibhatla, S., Vinogradov, S., Lemieux, P., Alakhov, V., & Kabanov, A. V. (2002). Design and formulation of polyplexes based on pluronic-polyethyleneimine conjugates for gene transfer. *Bioconjugate Chemistry*, *13*(5), 937–944.

Godbey, W. T., Barry, M. A., Saggau, P., Wu, K. K., & Mikos, A. G. (2000). Poly(ethylenimine)-mediated transfection: A new paradigm for gene delivery. *Journal of Biomedical Materials Research*, *51*(3), 321–328.

Grund, S., Bauer, M., & Fischer, D. (2011). Polymers in drug delivery—State of the art and future trends. *Advanced Engineering Materials*, *13*(3), B61–B87.

Heinze, T., Erler, U., Nehls, I., & Klemm, D. (1994). Determination of the substituent pattern of heterogeneously and homogeneously synthesized carboxymethyl cellulose by using high-performance liquid chromatography. *Angewandte Makromolekulare Chemie*, *215*(1), 93–106.

Heinze, T., Liebert, T., Heublein, B., & Hornig, S. (2006). Functional polymers based on dextran. *Advances in Polymer Science*, *205*, 199–291.

International Organization for Standardization/ANSI. (2009). Biological evaluation of medical devices Part 5: Tests for in vitro cytotoxicity. In *ISO 10993-5* (2nd ed.). Geneva, Switzerland: International Organization for Standardization/ANSI.

Jeanes, A., & Wilham, C. A. (1950). Periodate oxidation of dextran. *Journal of the American Chemical Society*, *72*(6), 2655–2657.

Jeon, O., Yang, H. S., Lee, T.-J., & Kim, B.-S. (2008). Heparin-conjugated polyethylenimine for gene delivery. *Journal of Controlled Release*, *132*(3), 236–242.

Jiang, D., & Salem, A. K. (2012). Optimized dextran-polyethylenimine conjugates are efficient non-viral vectors with reduced cytotoxicity when used in serum containing environments. *International Journal of Pharmaceutics*, *427*(1), 71–79.

Jiang, S., & Cao, Z. (2010). Ultralow-fouling, functionalizable, and hydrolyzable zwitterionic materials and their derivatives for biological applications. *Advanced Materials*, *22*(9), 920–932.

Kent, P. W. (1949). Periodate oxidation in the study of the structure of dextrans. *Science*, *110*(2869), 689–690.

Knop, K., Hoogenboom, R., Fischer, D., & Schubert, U. S. (2010). Poly(ethylene glycol) in drug delivery: Pros and cons as well as potential alternatives. *Angewandte Chemie International Edition*, *49*(36), 6288–6308.

Liebert T., Heinze T. (1998). Induced phase separation: A new synthesis concept in cellulose chemistry, In: Cellulose derivatives: Synthesis, characterization and nansotructures. ACS Symposium Series No. 688, W.G. Glaser and T. Heinze (eds.), American Chemical Society, Washington DC, pp. 1-72.

Lungwitz, U., Breunig, M., Liebl, R., Blunk, T., & Goepferich, A. (2008). Methoxy poly(ethylene glycol)—Low molecular weight linear polyethylenimine-derived copolymers enable polyplex shielding. *European Journal of Pharmaceutics and Biopharmaceutics*, *69*(1), 134–148.

Maruyama, A., Watanabe, H., Ferdous, A., Katoh, M., Ishihara, T., & Akaike, T. (1998). Characterization of interpolyelectrolyte complexes between double-stranded DNA and polylysine comb-type copolymers having hydrophilic side chains. *Bioconjugate Chemistry*, *9*(2), 292–299.

Mehvar, R. (2000). Dextrans for targeted and sustained delivery of therapeutic and imaging agents. *Journal of Controlled Release*, *69*(1), 1–25.

Moreau, E., Domurado, M., Chapon, P., Vert, M., & Domurado, D. (2002). Biocompatibility of polycations: In vitro agglutination and lysis of red blood cells and in vivo toxicity. *Journal of Drug Targeting*, *10*(2), 161–173.

Ogris, M., Brunner, S., Schuller, S., Kircheis, R., & Wagner, E. (1999). PEGylated DNA/transferrin-PEI complexes: Reduced interaction with blood components, extended circulation in blood and potential for systemic gene delivery. *Gene Therapy*, *6*(4), 595–605.

Ogris, M., Steinlein, P., Kursa, M., Mechtler, K., Kircheis, R., & Wagner, E. (1998). The size of DNA/transferrin-PEI complexes is an important factor for gene expression in cultured cells. *Gene Therapy*, *5*(10), 1425–1433.

Ogris, M., Walker, G., Blessing, T., Kircheis, R., Wolschek, M., & Wagner, E. (2003). Tumor-targeted gene therapy: strategies for the preparation of ligand-polyethylene glycol-polyethylenimine/DNA complexes. *Journal of Controlled Release*, *91*(1–2), 173–181 (Proceedings of the Second International Symposium on Tumor Targeted Delivery Systems).

Park, M. R., Han, K. O., Han, I. K., Cho, M. H., Nah, J. W., Choi, Y. J., & Cho, C. S. (2005). Degradable polyethylenimine-alt-poly(ethylene glycol) copolymers as novel gene carriers. *Journal of Controlled Release*, *105*(3), 367–380.

Petersen, H., Fechner, P. M., Martin, A. L., Kunath, K., Stolnik, S., Roberts, C. J., Fischer, D., Davies, M. C., & Kissel, T. (2002). Polyethylenimine-graft-poly(ethylene glycol) copolymers: Influence of copolymer block structure on DNA complexation and biological activities as gene delivery system. *Bioconjugate Chemistry*, *13*(4), 845–854.

Rankin, J. C., & Jeanes, A. (1954). Evaluation of the periodate oxidation method for structural analysis of dextrans. *Journal of the American Chemical Society*, *76*(17), 4435–4441.

Rinkenauer, A. C., Vollrath, A., Schallon, A., Tauhardt, L., Kempe, K., Schubert, S., Fischer, D., & Schubert, U. S. (2013). Parallel high-throughput screening of polymer vectors for nonviral gene delivery: Evaluation of structure–property relationships of transfection. *ACS Combinatorial Science*, *15*(9), 475–482.

Sun, K., Wang, J., Zhang, J., Hua, M., Liu, C., & Chen, T. (2011). Dextran-*g*-PEI nanoparticles as a carrier for co-delivery of adriamycin and plasmid into osteosarcoma cells. *International Journal of Biological Macromolecules*, *49*(2), 173–180.

Sun, Y.-X., Xiao, W., Cheng, S.-X., Zhang, X.-Z., & Zhuo, R.-X. (2008). Synthesis of (dex-HMDI)-*g*-PEIs as effective and low cytotoxic nonviral gene vectors. *Journal of Controlled Release*, *128*(2), 171–178.

Sun, Y.-X., Zhang, X.-Z., Cheng, H., Cheng, S.-X., & Zhuo, R.-X. (2008). A low-toxic and efficient gene vector: Carboxymethyl dextran-graft-polyethylenimine. *Journal of Biomedical Materials Research A*, *84A*(4), 1102–1110.

Tauhardt, L., Kempe, K., Knop, K., Altuntaş, E., Jäger, M., Schubert, S., Fischer, D., & Schubert, U. S. (2011). Linear polyethyleneimine: Optimized synthesis and characterization—On the way to "Pharmagrade" batches. *Macromolecular Chemistry and Physics*, *212*(17), 1918–1924.

Thomas, J. J., Rekha, M. R., & Sharma, C. P. (2010a). Dextran-glycidyltrimethylammonium chloride conjugate/DNA nanoplex: A potential non-viral and haemocompatible gene delivery system. *International Journal of Pharmaceutics*, *389*(1–2), 195–206.

Thomas, J. J., Rekha, M. R., & Sharma, C. P. (2010b). Dextran-protamine polycation: An efficient nonviral and haemocompatible gene delivery system. *Colloids and Surfaces B: Biointerfaces*, *81*(1), 195–205.

Thomas, M., Ge, Q., Lu, J. J., Chen, J., & Klibanov, A. (2005). Cross-linked small polyethylenimines: While still nontoxic, deliver DNA efficiently to mammalian cells in vitro and in vivo. *Pharmaceutical Research*, *22*(3), 373–380.

Tripathi, S. K., Goyal, R., & Gupta, K. C. (2011). Surface modification of crosslinked dextran nanoparticles influences transfection efficiency of dextran-polyethylenimine nanocomposites. *Soft Matter*, *7*(24), 11360–11371.

Tseng, W.-C., Fang, T.-Y., Su, L.-Y., & Tang, C.-H. (2005). Dependence of transgene expression and the relative buffering capacity of dextran-grafted polyethylenimine. *Molecular Pharmaceutics*, *2*(3), 224–232.

Tseng, W.-C., & Jong, C.-M. (2003). Improved stability of polycationic vector by dextran-grafted branched polyethylenimine. *Biomacromolecules*, *4*(5), 1277–1284.

Tseng, W.-C., Tang, C.-H., & Fang, T.-Y. (2004). The role of dextran conjugation in transfection mediated by dextran-grafted polyethylenimine. *Journal of Gene Medicine*, *6*(8), 895–905.

van Gaal, E. V. B., van Eijk, R., Oosting, R. S., Kok, R. J., Hennink, W. E., Crommelin, D. J. A., & Mastrobattista, E. (2011). How to screen non-viral gene delivery systems in vitro? *Journal of Controlled Release*, *154*(3), 218–232.

Vandoorne, F., Bruneel, D., Vercauteren, R., & Schacht, E. (1991). New approach to dextran derivatives containing primary amino functions. *Makromolekulare Chemie*, *192*(3), 673–677.

Varshosaz, J. (2012). Dextran conjugates in drug delivery. *Expert Opinion on Drug Discovery*, *9*(5), 509–523.

Vlugt-Wensink, K. D. F., Vrueh, R., Gresnigt, M. G., Hoogerbrugge, C. M., Buul-Offers, S. C., Leede, L. G. J., Sterkman, L. G. W., Crommelin, D. J. A., Hennink, W. E., & Verrijk, R. (2007). Preclinical and clinical in vitro in vivo correlation of an hGH dextran microsphere formulation. *Pharmaceutical Research*, *24*(12), 2239–2248.

Wotschadlo, J., Liebert, T., Heinze, T., Wagner, K., Schnabelrauch, M., Dutz, S., Mueller, R., Steiniger, F., Schwalbe, M., Kroll, T. C., Hoeffken, K., Buske, N., & Clement, J. H. (2009). Magnetic nanoparticles coated with carboxymethylated polysaccharide shells—Interaction with human cells. *Journal of Magnetism and Magnetic Materials*, *321*(10), 1469–1473.

Xiao, W., Sun, Y.-X., Cheng, H., Zeng, X., Zhang, X.-Z., & Zhuo, R.-X. (2010). Inhibition of enhanced green fluorescent protein expression by (dextran-hexamethylenediisocyanate)-*g*-polyethylenimine/siRNA complexes. *Journal of Microencapsulation*, *27*(5), 447–452.

Yang, J., Liu, Y., Wang, H., Liu, L., Wang, W., Wang, C., Wang, Q., & Liu, W. (2012). The biocompatibility of fatty acid modified dextran-agmatine bioconjugate gene delivery vector. *Biomaterials*, *33*(2), 604–613.

Yu, J.-H., Quan, J.-S., Kwon, J.-T., Xu, C.-X., Sun, B., Jiang, H.-L., Nah, J.-W., Kim, E.-M., Jeong, H.-J., Cho, M.-H., & Cho, C.-S. (2009). Fabrication of a novel core-shell gene delivery system based on a brush-like polycation of α, β-poly (L-aspartate-graft-PEI). *Pharmaceutical Research*, *26*(9), 2152–2163.

Zhao, H., & Heindel, N. D. (1991). Determination of degree of substitution of formyl groups in polyaldehyde dextran by the hydroxylamine hydrochloride method. *Pharmaceutical Research*, *8*(3), 400–402.

Supplementary data for

Dextran-graft-linear poly(ethylene imine)s for gene delivery: Importance of the linking strategy

Sofia Ochrimenko,[a,b,#] Antje Vollrath,[b,#] Lutz Tauhardt,[b] Kristian Kempe,[b,1] Stephanie Schubert,[a,c] Ulrich S. Schubert,[b,c,*] Dagmar Fischer[a,c,*]

[#]Equal Contributors
*Corresponding Authors

[a]Department of Pharmaceutical Technology, Institute of Pharmacy, Friedrich Schiller University Jena, Otto-Schott-Str. 41, 07745 Jena, Germany

[b]Laboratory of Organic and Macromolecular Chemistry (IOMC), Friedrich Schiller University Jena, Humboldtstr. 10, 07743 Jena, Germany

[c]Jena Center for Soft Matter (JCMS), Friedrich Schiller University Jena, Philosophenweg 7, 07743 Jena, Germany

[1]Present address: Department of Chemical and Biomolecular Engineering, The University of Melbourne, Victoria 3010 VIC, Australia

Material and Methods

1. Instrumentation

Size exclusion chromatograms (SEC) of poly(2-ethyloxazoline) were measured on an Agilent Technologies 1200 Series gel permeation chromatography system equipped with a G1310A isocratic pump, a G1329A autosampler, a G1362A refractive index detector, and both a PSS Gram 30 and a PSS Gram 1000 column placed in series. A 0.21% lithium chloride (LiCl, ACROS Organic, New Jersey, USA) solution in *N,N*-dimethylacetamide (DMA, HiPerSolv CHROMANORM, VWR Prolabo, Darmstadt, Germany) was used as eluent at 1 mL · min^{-1} flow rate and a column oven temperature of 40 °C. The molar masses were calculated against poly(ethylene glycol) (PEG, Polymer Standards Service, Mainz, Germany).
The dextran aldehyde and carboxymethylated dextran were investigated on a Jasco SEC system composed of a DG-2080-53 degasser, a PU-980 pump and a RI-930 refractive index detector running in dimethyl sulfoxide (DMSO, ROTIPURAN 99.8%, Carl-Roth GmbH, Karlsruhe, Germany) containing 0.5% lithium bromide (LiBr, Riedel-de Haën, Seelze, Germany) at 0.5 mL · min^{-1} at 65 °C. The samples were separated on PSS NOVEMA 3000 and 300 Å columns and their molar masses calculated against narrow distributed dextran standards (Polymer Standards Service, Mainz, Germany).
Moreover, all dextran-*graft*-linear poly(ethylene imine)s were measured on a Jasco SEC system equipped with a PU-980 pump, a AS-1555 autosampler, a DG-980-50 degasser, a RI-930 refractive index detector, and a PSS SUPREMA-MAX column. As eluent, a solution of 0.1% trifluoroacetic acid (TFA, Uvasol, MERCK, Darmstadt, Germany) and 0.05 M NaCl (Sigma Aldrich, Deisenhofen, Germany) in water (pH 2), running at a flow rate of 1 mL · min^{-1} and a column oven temperature of 60 °C, was used. The molar masses were calculated against pullulan (Polymer Standards Service, Mainz, Germany).

^{1}H NMR and ^{13}C NMR spectra were recorded in deuterated water (D_2O, Eurisotop, Gif sur Yvette Cedex, France) or deuterated dichlormethane (CD_2Cl_2, Eurisotop, Gif sur Yvette Cedex, France) on a Bruker Avance 250 MHz or 300 MHz spectrometer. Chemical shifts are given in ppm relative to signals from the NMR solvents. Conversions were calculated from ^{1}H spectra using anisole as an internal standard.

Elemental analysis (EA) was carried using an Elementaranalysator Vario EL III CHNS from Elementar Analysensysteme GmbH, Hanau.

2. Synthesis

Synthesis of poly(2-oxazolines)
The poly(2-ethyl-2-oxazoline)s (pEtOx) used in this study as starting materials for the preparation of linear poly(ethylene imine)s (lPEIs) were synthesized according to literature procedures.(Hoogenboom, Paulus, Pilotti & Schubert, 2006; Tauhardt et al., 2011) Briefly, pEtOx with monomer-to-initiator ratios of 20 and 40 were synthesized under microwave

irradiation. In order to obtain solely proton initiated chains *p*-toluene sulfonic acid (Sigma Aldrich) was used as initiator for the cationic ring-opening polymerization (Scheme S1). Polymerization kinetics revealed a linear increase of $\ln([M]_0/[M]_t)$ with time demonstrating a constant concentration of propagating species indicative of a living polymerization mechanism. The resulting first-order kinetic plot is shown in Figure S1, left. The linear increase in the molar mass with conversion as well as low polydispersity index (PDI) values (< 1.3) further support the living character of the polymerization (Figure S1, right). Based on these results two large batches of $pEtOx_{20}$ and $pEtOx_{40}$ were synthesized. The molar mass determined by ^{1}H NMR spectroscopy was in accordance with the feed ratio ($pEtOx_{20}$: 2,000 g · mol^{-1}, $pEtOx_{40}$: 4,000 g · mol^{-1}) and SEC measurements revealed reasonable molar mass distributions with low PDI values ($PEtOx_{20}$: 3,530 g · mol^{-1}, PDI = 1.14; $PEtOx_{40}$: 5,900 g · mol^{-1}, PDI = 1.2) (Figure S2).

Synthesis of linear poly(ethylene imines)

The lPEI synthesis was performed according to a modified procedure described in literature.(Tauhardt et al., 2011) Briefly, corresponding pEtOx (30 g) was dissolved in 6 M HCl (400 mL, Sigma Aldrich) and heated for 24 h at 150 °C. The solvent was removed under reduced pressure. The residue was dissolved in water (500 mL) and 3 M NaOH (Sigma Aldrich) was added until precipitation occurred. The precipitate was filtered off and recrystallized from water (600 mL). After filtration the lPEI was dissolved in methanol (200 mL, Mineralöl Albert, Jena, Germany) and precipitated into ice-cold diethyl ether (1,300 mL, Mineralöl Albert). The white precipitate was filtered off and dried under reduced pressure at 40 °C for 5 d. The purity and degree of hydrolysis of the resulting lPEI were determined by ^{1}H NMR spectroscopy.(Altuntaş et al., 2012; Tauhardt et al., 2011)

Table S1. Analytical data of pEtOx and the resulting lPEIs.

	M_n [a] [g · mol^{-1}]	PDI
$PEtOx_{20}$	3,550 [a]	1.14 [a]
$PEtOx_{40}$	5,900 [a]	1.20 [a]
$lPEI_{20}$	860[b]	-
$lPEI_{40}$	1,720[b]	-

[a] SEC were performed in DMA containing 0.21% LiCl using PEG as standard.
[b] Theoretical values calculated from the pEtOx precursor.

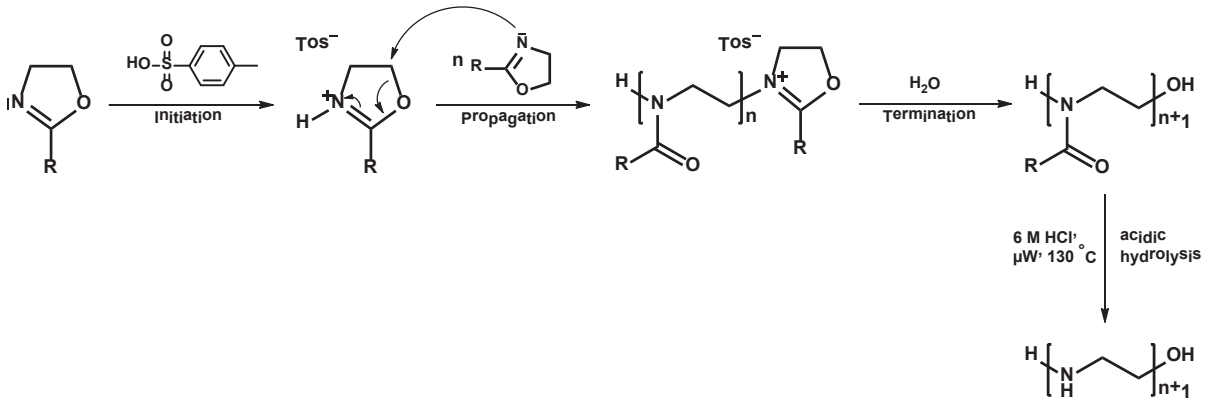

Scheme S1. Schematic representation of the cationic ring-opening polymerization of pEtOxs followed by the subsequent acidic hydrolysis to lPEI.

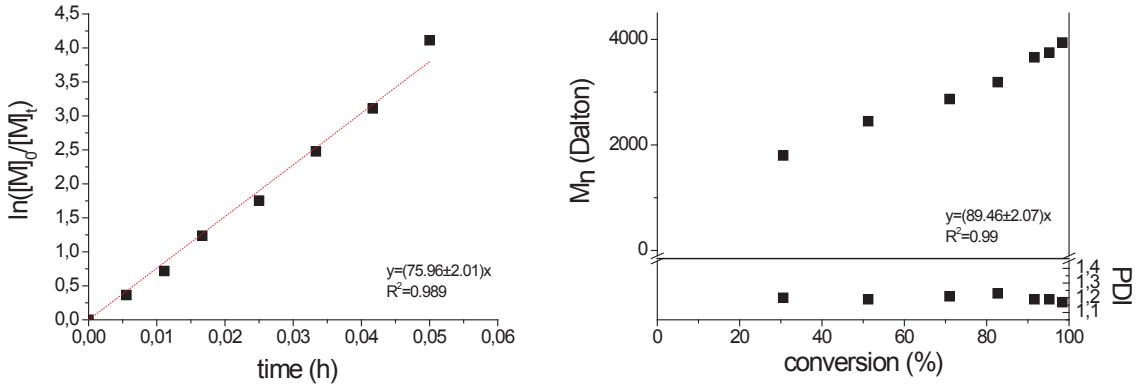

Figure S1. Kinetics of the cationic ring-opening polymerization of pEtOx: Resulting first-order kinetic plot of $\ln([M]_0/[M]_t)$ (left) linear increase in the molar mass with conversion as well as low polydispersity index (PDI) values (right).

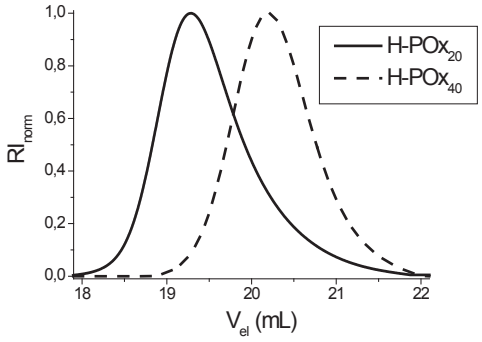

Figure S2. SEC traces of $pEtOx_{20}$ and $pEtOx_{40}$ using DMA as eluent.

Synthesis of dextran aldehyde (CHO-dex)

Pharmaceutical grade dextran with an average molar mass of 65,900 $g \cdot mol^{-1}$ (Pharmacosmos, Holbaek, Denmark) (5 g, 0.0136 mol per anhydroglucose unit (AGU)) was dissolved in 20 mL distilled water, and the adequate amount (0.0045 or 0.00136 mol) of potassium periodate (KIO_4, Sigma Aldrich) was added. After stirring in the dark at room temperature for 24 h, the products were dialyzed for 5 days (10 times exchange of water) and were transferred into tare glass vials and lyophilized in an Alpha 1-2/LD Plus freeze dryer (Martin Christ, Osterode Germany) at a pressure of 0.006 mbar for 72 h (yield 90%). The final CHO-dextrans were characterized by elemental analysis, SEC (Table S2) as well as ^{1}H NMR spectroscopy (Figure S3). The degree of oxidation in the CHO-dex was determined according to the hydroxylamine chloride titration after Zhao *et al.* in distilled water.(Zhao & Heindel, 1991) CHO-dex samples (100 mg) were dissolved in 25 mL of 0.25 M hydroxylamine hydrochloride solution (Sigma Aldrich). After 2 h incubation at room temperature, the solution was titrated against 1 N NaOH solution. Thereby, the degree of substitution (DS) of CHO was calculated based on the sample weights (formula) and subscripted as CHO_X-dex.

$$DS\,[CHO_X - dex] = \frac{V_{mL} \times 10^{-3}(L) \times M_{NaOH}\,(mol \times L^{-1})}{\frac{m_{dex}\,(g)}{M_{dex}(g \times mol^{-1})}}$$

Table S2. Overview of analytical data of the oxidation of dextran with KIO_4.

	KIO_4:AGU [mol]	**[CHO/AGU][a]**	**M_w [g · mol^{-1}][b]**	**PDI[b]**	**C [%]**	**H [%]**	**N [%]**
Dextran	-	-	65,900	1.86	40.49	6.79	-
$CHO_{0.5}$-dex	1:10	0.51	55,100	2.51	42.34	6.39	-
$CHO_{1.0}$-dex	1:3	1.09	52,500	2.35	41.43	6.25	-

[a] Determined by hydroxylamine chloride titration.

[b] SEC were performed in DMSO containing 0.5 % LiBr using pullulan as standard.

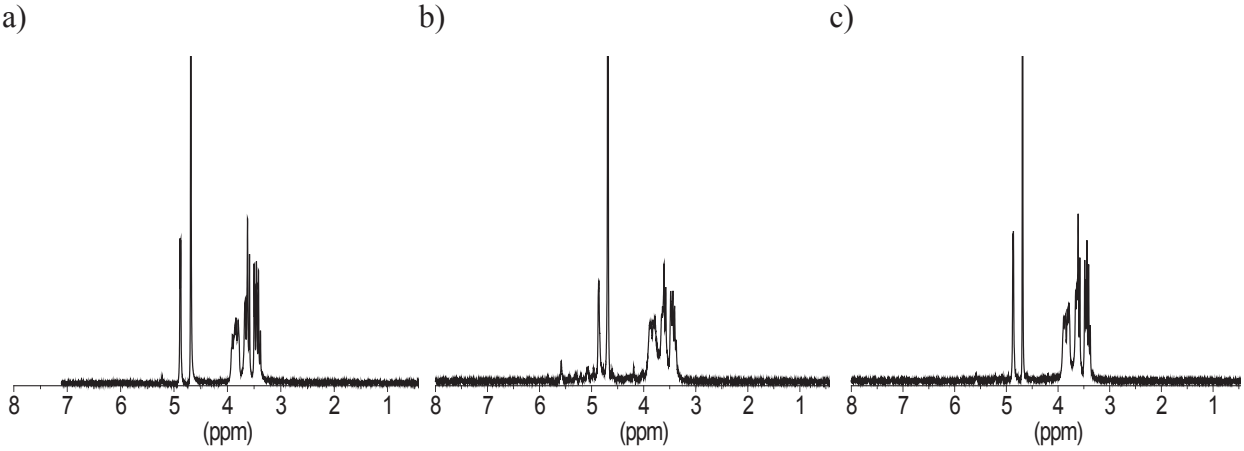

Figure S3. ^{1}H NMR spectra of (a) dextran, (b) $CHO_{0.5}$-dex and (c) $CHO_{1.0}$-dex prepared by oxidation with KIO_4. The ^{1}H NMR spectra were measured at 25 °C in D_2O.

Synthesis of CHO-dex-*g*-lPEI

For the synthesis of various dextran conjugated lPEIs, 200 mg (0.0012 mol AGU) $CHO_{0.5}$-dex and $CHO_{1.0}$-dex as well as the desired amount of lPEI (CHO:NH_2-PEI ratio = 1:1 or 1:0.5) were dissolved in water at 60 °C. After mixing both solutions, the color turned to yellow indicating an imine bond formation. The mixture was stirred for 24 h at 60 °C following the slow addition of a 5 times excess of sodium borohydride ($NaBH_4$, Sigma Aldrich). The solutions became colorless due to the reduction of the imine bond to an amine formation and were stirred for 2 days at room temperature. Subsequently, the product was purified from uncoupled lPEI and $NaBH_4$ residues by extensive dialysis against water at 60 °C. The water was exchanged at least 10 times within 5 days until the pH of the dialysis water was neutral (pH 6-7). The product was lyophilized in an Alpha 1-2/LD Plus freeze dryer (Martin Christ) at a pressure of 0.006 mbar for 72 h reaching 30 to 40% overall yield. The absence of unbound lPEI was proven by ^{1}H NMR measurement (600 MHz, D_2O, 60 °C) of the collected dialysis water and the final DS of lPEI was calculated by the nitrogen content obtained from elemental analysis (Table S3). The polymers were further characterized by SEC measurements (in H_2O, 0.1% TFA) and ^{1}H NMR spectroscopy (600 MHz, D_2O, 60 °C) (Figure S4).

Table S3. Overview of analytical data of the CHO-dex-*g*-lPEI samples obtained by reductive amination.

Products	CHO: NH_2-lPEI [mol]	DS[a] [lPEI/ AGU]	C [%]	H [%]	N [%]	M_w [g · mol^{-1}][b]	PDI[b]
$CHO_{0.5}$-dex-*g*-$lPEI_{20}$	1:1	0.18	41.95	9.75	15.78	24,000	1.21
$CHO_{0.5}$-dex-*g*-$lPEI_{40}$	1:1	0.13	43.00	10.38	19.12	27,600	1.26
$CHO_{1.0}$-dex-*g*-$lPEI_{20}$	2:1	0.38	43.74	10.58	21.45	31,300	1.20
$CHO_{1.0}$-dex-*g*-$lPEI_{40}$	2:1	0.19	43.62	10.45	21.73	36,500	1.20

[a] Calculated from the nitrogen content N [%] of the elemental analysis.

[b] SEC measurements were performed in H_2O containing 0.1% TFA and 0.05 M NaCl (pH 2) using pullulan as standard.

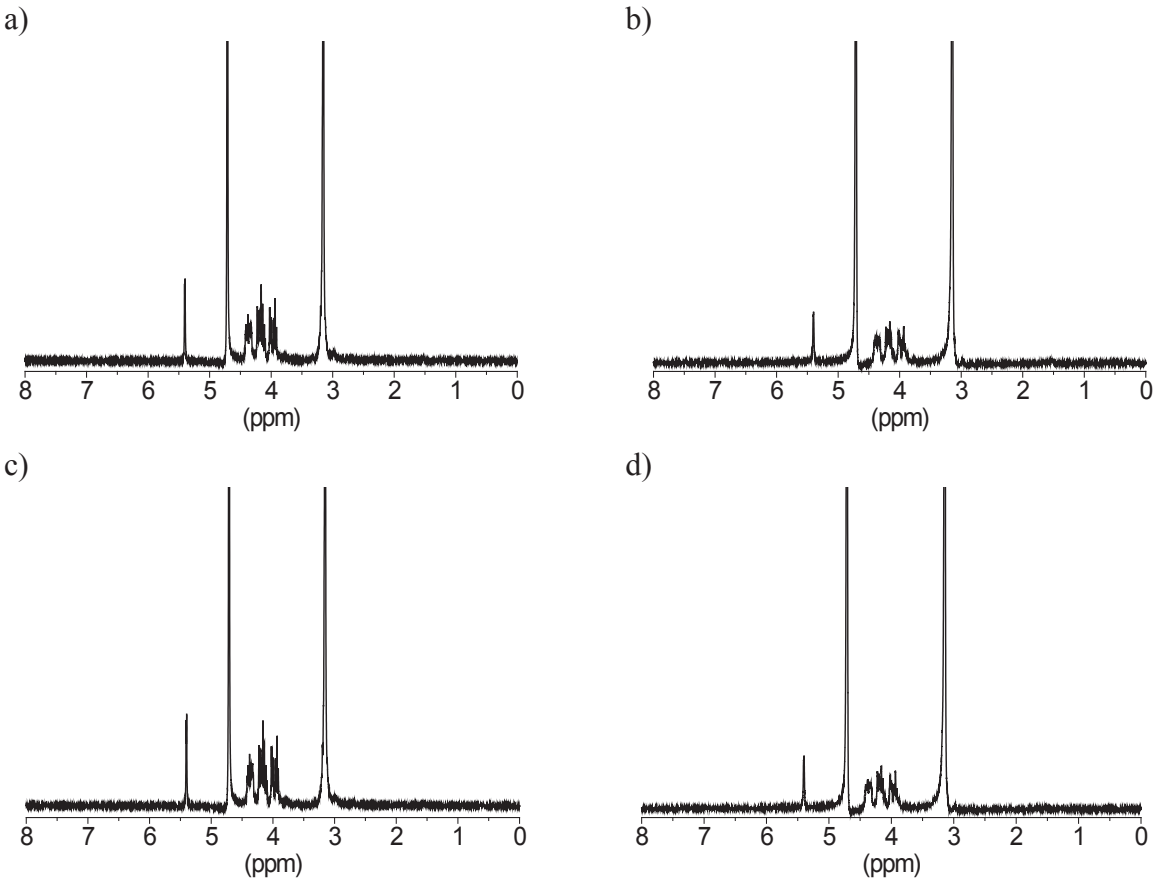

Figure S4. ^{1}H NMR spectra of dex-*g*-lPEI samples obtained by reductive amination. The ^{1}H NMR spectra were measured at 60 °C in D_2O. (a) $CHO_{0.5}$-dex-*g*-$lPEI_{20,}$ (b) $CHO_{0.5}$-dex-*g*-$lPEI_{40}$ (c) $CHO_{1.0}$-dex-*g*-$lPEI_{20}$, (d) $CHO_{1.0}$-dex-*g*-$lPEI_{40.}$

Synthesis of carboxymethyl dextran (CM-dex)

Pharmaceutical grade dextran with an average molar mass (M_n)of 65,900 $g \cdot mol^{-1}$ (Pharmacosmos) (5 g, 0.0136 mol per AGU) was dissolved in 50 mL water and stirred for 20 minutes at room temperature. The desired amount of 15 M NaOH was added dropwise, and the reaction mixture stirred for further 60 minutes. Subsequently, the desired amount of monochloracetic acid (Sigma Aldrich) was added dropwise and the temperature was increased to 60 °C. The reaction was stopped after 90 minutes or 300 minutes by neutralization with acetic acid (pH 6-7, Sigma Aldrich). After precipitation in 1.5 L of cold methanol (Mineralöl Albert), the solid product was filtered off over a G3 frit and washed (at least 3 times) with methanol. After dialysis (5 times exchange of water, 3 days) the products were obtained in 80% yield by lyophilization in an Alpha 1-2/LD Plus freeze dryer (Martin Christ) at a pressure of 0.006 mbar for 72 h. The DS of carboxymethyl groups was determined according to the HPLC procedure described by Wotschadlo *et al.*(Wotschadlo et al., 2009) Furthermore, the products were characterized by ^{1}H NMR spectroscopy (600 MHz, D_2O), SEC (in DMSO) and EA measurements (Table S4).

Table S4. Overview of analytical data of the CM-dex samples obtained by carboxymethylation.

	AGU:ClCH$_2$COOH :NaOH [mol]	**DS[a] [CH$_2$COOH /AGU]**	**M_w [g · mol^{-1}][b]**	**PDI[b]**
$CM_{0.3}$-dex	2.2:1:1 (90 minutes)	0.32	51,100	2.36
$CM_{0.5}$-dex	2.2:1:1 (300 minutes)	0.54	54,400	2.37
$CM_{1.6}$-dex	1:5:10 (300 minutes)	1.6	60,100	2.04

[a] Determined by HPLC measurement.

[b] SEC were performed in DMSO containing 0.5% LiBr using pullulan as standard.

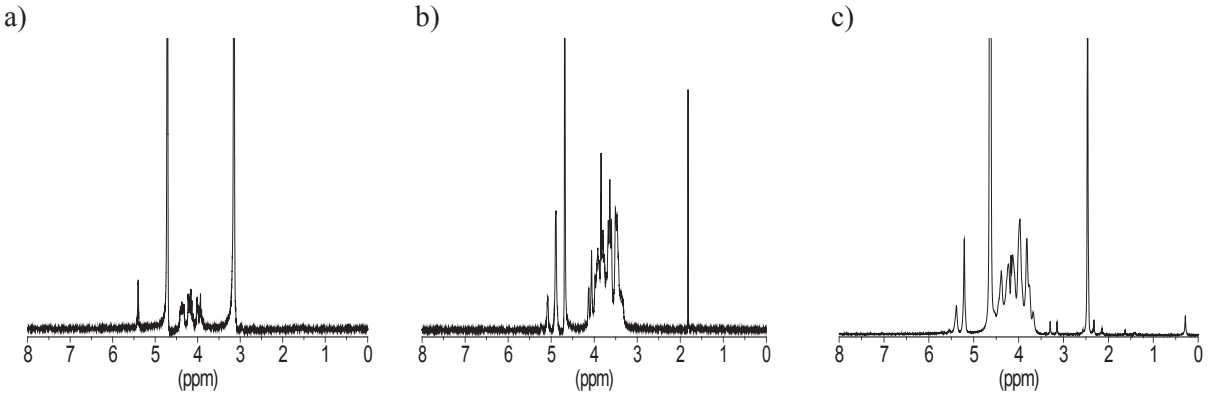

Figure S5. ^{1}H NMR spectra of (a) $CM_{0.3}$-dex, (b) $CM_{0.5}$-dex and (c) $CM_{1.6}$-dex obtained by carboxymethylation with monochloroacetic acid. The ^{1}H NMR spectra were measured at 25 °C in D_2O.

Synthesis of CM-dex-*g*-lPEI

The reactions of the CM-dex with the lPEIs were performed using 1-ethyl-3-(3-dimethylaminopropyl)carbodiimide (EDC, Sigma-Aldrich) as coupling reagent. Firstly, 300 mg of each CM-dex and the desired amount of lPEI (NH_2:COOH = 1.2:1) were dissolved in distilled water at 60 °C to ensure complete dissolution of the lPEIs. Subsequently, the pH value of the solution was adjusted to 6.0 by 1 M HCl solution. After 20 minutes stirring at 60 °C EDC (COOH:EDC = 1:1) and *N*-hydroxysulfosuccinimide (sulfo-NHS, Sigma Aldrich) (EDC:sulfo-NHS = 1:1) were added. The reaction mixture was stirred for 24 h at 60 °C, and the product was purified by extensive dialysis (at least 10 times exchange of water within 5 days) at 60 °C. The products were obtained by lyophilization (Alpha 1-2/LD Plus freeze dryer, Martin Christ) at a pressure of 0.006 mbar for 72 h in 30 to 40% overall yield. The absence of free unbound lPEI was proven by ^{1}H NMR (600 MHz, D_2O) measurement of the collected dialysis water. Furthermore, SEC analyses (in H_2O, 0.1% TFA) as well as ^{1}H NMR spectroscopy (600 MHz, D_2O, 60 °C) and elemental analysis investigations of the products were performed. The final DS of lPEI was calculated by the nitrogen content obtained from elemental analysis (Table S5).

Table S5. Overview of analytical data of the dex-*g*-lPEI samples obtained by EDC coupling.

Products	COOH:EDC :NH_2-lPEI	DS[a] [lPEI /AGU][b]	M_w [g · mol^{-1}][b]	PDI[b]	C [%]	H [%]	N [%]
$CM_{0.3}$-dex-*g*-$lPEI_{20}$	1:1.2	0.06	22,900	1.06	40.91	7.35	6.73
$CM_{0.3}$-dex-*g*-$lPEI_{40}$	1:1.2	0.07	36,500	1.09	38.91	8.07	12.80
$CM_{0.5}$-dex-*g*-$lPEI_{20}$	1:1.2	0.07	25,000	1.07	40.55	7.11	7.96
$CM_{0.5}$-dex-*g*-$lPEI_{40}$	1:1.2	0.1	36,000	1.09	37.89	8.51	14.83
$CM_{1.6}$-dex-*g*-$lPEI_{20}$	3:1	0.11	15,600	1.14	43.29	7.09	8.16
$CM_{1.6}$-dex-*g*-$lPEI_{40}$	3:1	0.18	17,200	1.18	33.91	8.57	18.38

[a] Calculated from the nitrogen content N [%] of the elemental analysis.

[b] SEC measurements were performed in H_2O containing 0.1% TFA and 0.05 M NaCl (pH 2) using pullulan as standard.

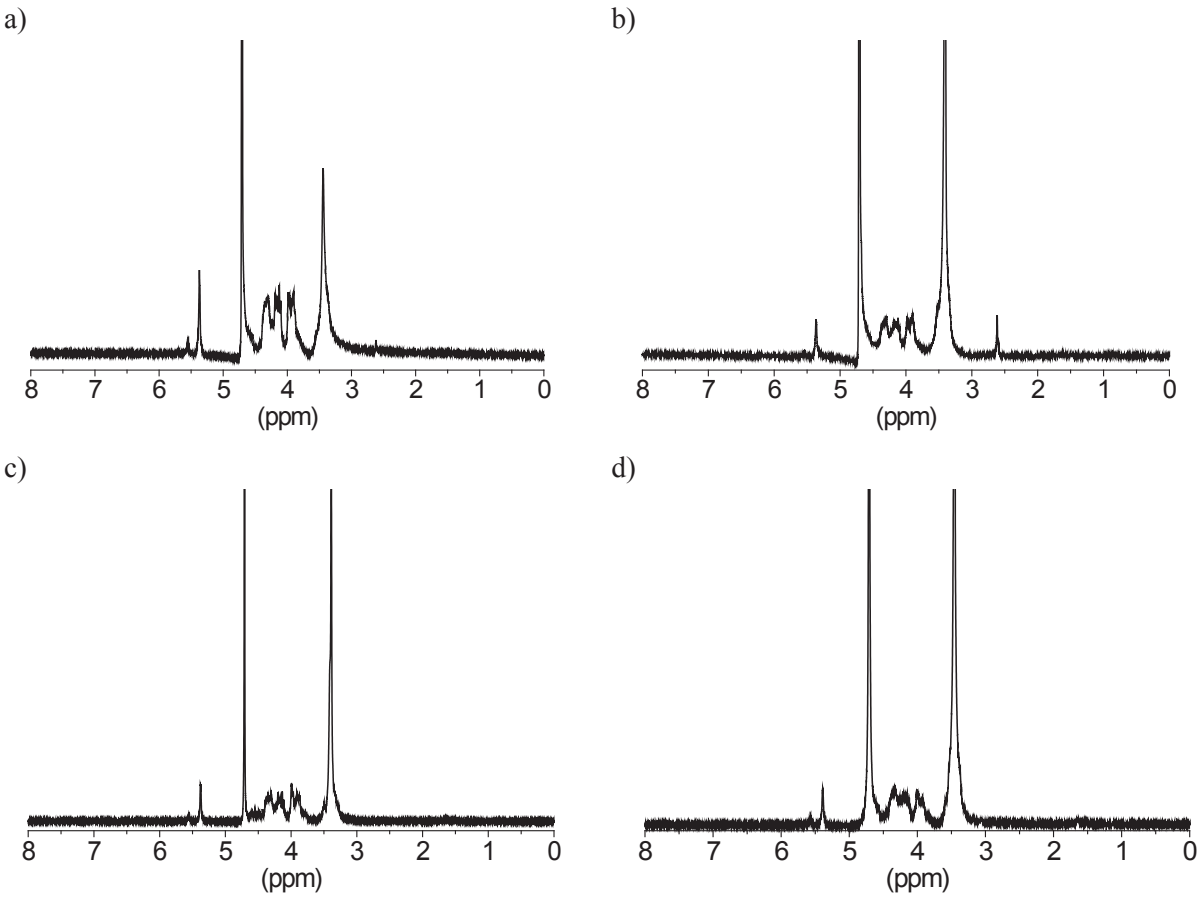

Figure S6. Representative ^1H NMR spectra of dex-*g*-PEI samples obtained by EDC coupling of CM-dex and lPEI: (a) $CM_{0.3}$-dex-*g*-$lPEI_{20}$ (b) $CM_{0.3}$-dex-*g*-$lPEI_{40}$ (c) $CM_{0.5}$-dex-*g*-$lPEI_{20}$ (d) $CM_{0.5}$-dex-*g*-$lPEI_{40}$. The ^1H NMR spectra were measured at 60 °C in D_2O.

3. Biological studies

DNA preparation

Luciferase reporter gene encoding plasmid pGL3 (Promega, Madison, WI, USA) was transferred to competent E. coli TG1 (kind gift of Hans-Knoell-Institute, Jena) and isolated with the plasmid Maxi kit according to manufacturer's protocol (E.Z.N.A®, OMEGA bio-tek, Norcross, GA, USA). Herring testes DNA Type XIV (Sigma Aldrich) was used as model DNA.

Preparation of polymer/DNA complexes

Stock solutions of dextran derivatives and lPEIs were prepared in highly purified water at a concentration of 1 mg · mL^{-1}, and the pH was adjusted to 7.4. The solutions were sterile filtered (0.2 µm, VWR international, Darmstadt, Germany). Polymer concentrations after filtration were quantified as copper(II) (Cu^{2+}) complexes according to Perrine *et al.*(Perrine & Landis, 1967) by measurement of the absorbance at 645 nm in 96-well plates (Greiner Bio-One, Frickenhausen, Germany) with a microplate reader (Fluostar OPTIMA, BMG Labtech, Offenburg, Germany) using a calibration curve of the corresponding derivatives. The complexes were formed according to Fischer *et al.* (Fischer, Bieber, Li, Elsasser & Kissel, 1999) and Tseng *et al.*(Tseng & Jong, 2003) The N/P ratio was calculated by the molar ratio of the nitrogen (N) (determined by elemental analyses) of each dex-*g*-lPEI sample to phosphorus (P) in the DNA. Five µg DNA and the appropriate amount of polymer solution were each diluted in 125 µL 150 mM NaCl (Roth, Karlsruhe, Germany) pH 7.4 and vortexed for 10 minutes. Afterwards, the polymer solution was added to the DNA solution, vortexed for 10 seconds and incubated at room temperature for 10 minutes.

Horizontal gel retardation assay

A 50 µL aliquot (containing 1 µg herring testes DNA type XIV) of the complex dilution was mixed with 5 µL loading buffer (40 mM Tris, 50% (*v/v*) glycerol 85%, 1 mM EDTA, pH 7.4, all from Roth). Subsequently, 5 µL dilution was applied on a 1% agarose gel (PeqGold Universal agarose, Peqlab Biotechnology GmbH, Erlangen, Germany). Electrophoretic separation was carried out in TAE running buffer (40 mM Tris, 1% acetic acid, 1 mM EDTA, all from Roth) in a horizontal electrophoresis chamber (Biometra, Goettingen, Germany) at 80 V for 1 h. For DNA detection, the fluorescence of intercalated ethidium bromide (Roth) was determined using a UV transilluminator (Intas GmbH, Goettingen, Germany) at 312 nm. Photographs were taken with a gel documentation system (Digit Store UNO, Intas GmbH).

The analysis of the free DNA as control (left lane of each gel), which was detected by ethidium bromide intercalation, revealed a broad fluorescent band corresponding to its broad molar mass distribution. Free polymers were used as controls (data not shown) to exclude unspecific interactions between polymer and dye and exhibited no signal. Free 60,000 g · mol^{-1} dextran was not able to interact with DNA due to the missing charge since the bands showed the same signal as the DNA control (data not shown).

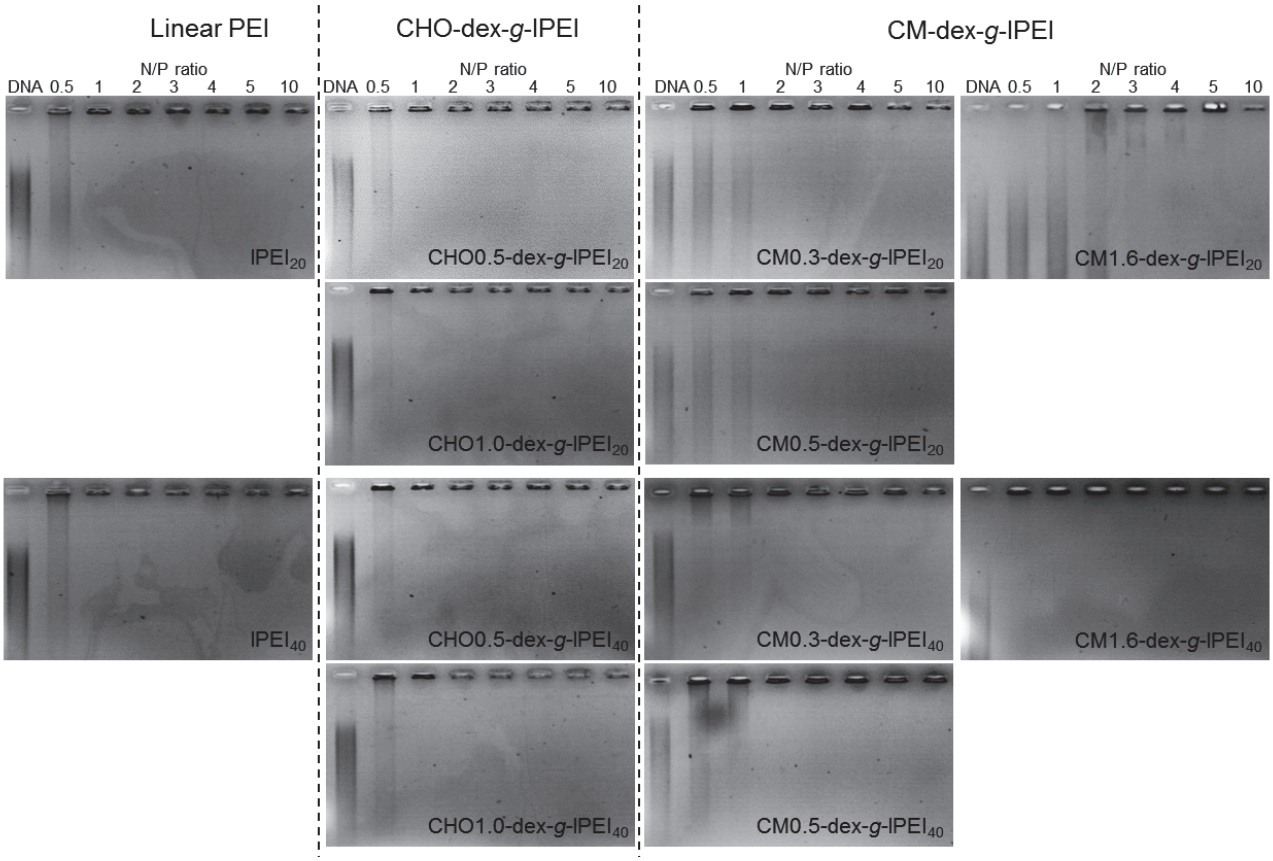

Figure S7. DNA binding capacity of $lPEI_{20/40}$ and dex-*g*-lPEIs at different N/P ratios in comparison to free DNA, determined by agarose gel electrophoresis.

Complex stability against enzymatic degradation

Complexes were prepared as described above with 4 µg pGL3 plasmid in a total volume of 200 µL 150 mM NaCl solution. DNase I (2.5 Kunitz units/µL, Applichem, Darmstadt, Germany) diluted in 150 mM NaCl and 20 mM $MgCl_2$ pH 7.4 with an activity of 1.5 Kunitz units/µg plasmid was added to the complex solution, gently mixed and incubated for 45 minutes in a water bath at 37 °C. The enzyme was inactivated in a water bath at 70 °C for 30 minutes. Subsequently, plasmid was released from the complexes by incubation with 10 µL dextran sulfate solution (5,000 $g \cdot mol^{-1}$, 10 $mg \cdot mL^{-1}$, Sigma) per µg plasmid at 37 °C for 20 minutes. Naked plasmid treated with DNase I, untreated plasmid, as well as plasmid incubated in the same way like complexes but without enzyme were used as controls. An aliquot of 50 µL complex solution (containing 1 µg plasmid) of each sample were mixed with 5 µL TAE loading buffer and electrophoresed as described above.

Complex size measurement and zeta potential

Size and zeta potential of complexes with N/P ratios of 25 and 50 with 2 µg plasmid were measured with the Zetasizer Nano ZS (Malvern Instruments, Herrenberg, Germany) in 50 mM NaCl and highly purified water. Photon correlation spectroscopy was carried out in a minimal volume cuvette ZEN 0040 (BRAND GmbH, Wertheim, Germany) with a laser beam at 633 nm and a scattering angle of 173° at 25 °C. The viscosity (0.89 mPa · s) and refractive index (1.33) of purified water at 25 °C were used for data analysis. Results are shown as the mean of Z-average of 6 runs ± standard deviation (SD) and calculated with the "General purpose" (normal resolution) algorithm using the Malvern software 6.20. Zeta potential of the complexes was performed in a zetasizer cuvette (DTS1060, Malvern Instruments) by measuring the electrophoretic mobility at 25 °C. The results were calculated with the Malvern software 6.20 and shown as the mean of 6 runs ± SD. All measurements were repeated once.

Cell culture

L929 mouse fibroblasts (German Collection of Microorganisms and Cell Cultures, DSMZ, Braunschweig, Germany) were cultured in Roswell Park Memorial Institute 1640 (RPMI 1640) culture medium supplemented with 2 mM L-glutamine and 10% fetal bovine serum gold (FBS) (all PAA, Pasching, Austria). CHO-K1 (Chinese hamster ovary cells, DSMZ) cells were cultured in Ham's F12 (PAA) supplemented with 1 mM L-alanyl-L-glutamine and 10% FBS (PAA). Cells were subcultured once a week and incubated at 37 °C, 5% CO_2 and 95% relative humidity. To test the absence of squirrel monkey retrovirus, DNA of the cells was isolated (QIAamp® DNA Mini kit, Qiagen, Hilden, Germany) and regularly screened by PCR (polymerase chain reaction). Absence of mycoplasma in the cells was periodically tested with a standard test kit (Venor® GeM, Minerva Biolabs, Berlin, Germany).

Cytotoxicity of complexes

In vitro cytotoxicity of complexes was tested by the 3-(4,5-dimethylthiazol-2-yl)-2,5-diphenyltetrazolium bromide (MTT) assay as described by Mosman(Mosmann, 1983) and Fischer *et al.*.(Fischer, Li, Ahlemeyer, Krieglstein & Kissel, 2003) Briefly, complexes were prepared as described above with 3.2 µg herring testes DNA (in 10 mM Tris buffer) and the appropriate amount of polymer to receive N/P ratios of 25 and 50. Afterwards, RPMI 1640

culture medium was added to each complex solution up to 1,210 µL. L929 mouse fibroblasts were selected since they were recommended as target cells for *in vitro* toxicity testing by many standard institutions.(2009) The cells (8500/well) were seeded in 96-well plates (Greiner Bio-One, Frickenhausen, Germany) and incubated for 24 h. The culture medium was then replaced by 110 µL complex dilution/well. Cells were incubated with the complexes for 4 h. Afterwards, the test solution was removed and replaced by 200 µL RPMI 1640 medium followed by incubation for further 20 h. The following MTT assay procedure was performed as described before. Absorbance (A) of the samples was measured in a microplate reader (Fluostar OPTIMA) at 570 nm. As blank control culture medium without cells was used. Negative control (100% viability) was determined using cells treated only with culture medium. The positive control (0% viability) was obtained by treatment of the cells with 0.02% thiomersal solution (Synopharm, Barsbüttel, Germany). Relative cell viability was calculated as follows:

$$Relative\ viability\ [\%] = \frac{A_{sample} - A_{blank}}{A_{negative\ control} - A_{blank}} \times 100$$

Relative cell viability < 70% was regarded as cytotoxic according to DIN ISO 10993-5.(2009) All experiments were run with n = 7 and repeated once.

Aggregation of erythrocytes

To investigate the erythrocyte aggregation of the polymers a modified method of Ogris *et al.*(Ogris, Brunner, Schuller, Kircheis & Wagner, 1999) was applied. Polymers were tested in phosphate buffered saline (PBS) [8 mM disodium hydrogen phosphate, 1.5 mM potassium dihydrogen phosphate, 137 mM sodium chloride and 2.7 mM potassium chloride (all from Roth)] pH 7.4 at concentrations of 0.024 to 50 µg · mL^{-1}. Sheep blood was collected in heparinized tubes and the serum was removed by centrifugation at 2,880 *g* for 7 minutes (Eppendorf Centrifuge 5804R, Eppendorf, Hamburg, Germany). The pellet was washed three times with PBS by centrifugation at 2,880 *g* for 7 minutes and was resuspended in PBS to the initial volume. The red blood cell suspensions were used within 24 h after collection. Erythrocyte suspension (100 µL) containing 20 × 10^6 erythrocytes/mL was mixed with 100 µL test compound in a 96-well plate (Greiner Bio-One). The plates were incubated under vigorous shaking at 37 °C for 2 h. Afterwards, erythrocyte aggregation was evaluated by microscopic observations (Leica DM IL, Achromat 10/0.20 Phaco 1a objective, 200fold magnifications, Wetzlar, Germany) and the results were classified in three stages. In stage 1 the erythrocytes stay discrete in suspension, no aggregation is detectable. At stage 2 the majority of red blood cells stays separate and shows only a moderate aggregation with rouleau formation. In stage 3 almost all erythrocytes are aggregated in clusters. As negative control for the determination of stage 1, erythrocytes were treated with PBS. As stage 3 (positive control), erythrocytes were treated with a 15 µg · mL^{-1} solution of 25,000 g · mol^{-1} branched poly(ethylene imine) (bPEI, a kind gift of BASF corporation, Ludwigshafen, Germany). Additionally, the aggregation of erythrocytes was analyzed by quantitative measurement of total absorbance at 645 nm with a microplate reader (Fluostar OPTIMA) according to Bauer

et al.(Bauer, Lautenschlaeger, Kempe, Tauhardt, Schubert & Fischer, 2012) To quantify the erythrocyte aggregation the calculation of ΔAbs_{max} was established by using the following equation according to Florian Schlenk (personal communication)*:*

$$\Delta Abs_{max} = \left(A_{negative\ control} - A_{blank}\right) - \left(A_{sample\ min} - A_{blank}\right)$$

The experiments were run in duplicate and repeated once. The results are shown as the mean of two experiments (n = 4) ± SD.

Hemolysis of erythrocytes

According to Bauer *et al.*(Bauer, Lautenschlaeger, Kempe, Tauhardt, Schubert & Fischer, 2012) the hemolytic activity of the dex-*g*-lPEIs was determined. The erythrocytes were isolated as described in the previous section. Polymers were tested in PBS buffer with concentrations of 0.125 to 1 mg · mL^{-1}. They were mixed with the erythrocyte dilution and incubated on a shaker (Heidolph Instruments Titrimax 100, Schwabach, Germany) at 450 rpm at 37 °C for 1 h. Hemoglobin release was determined by spectrophotometric analysis of 100 µL supernatant at 544 nm with a microplate reader (Infinite® M200 PRO, Tecan, Maennedorf, Switzerland) after centrifugation at 2,250*g* for 5 min (Eppendorf Centrifuge 5804R). As positive control 0.05% Triton X-100 solution (Ferak, Berlin, Germany) was used. Erythrocytes treated with PBS provided the negative control. Percentage hemolysis was calculated according to the following equation:

$$Hemolysis\ [\%] = \frac{\left(A_{sample} - A_{blank}\right) - \left(A_{negative\ control} - A_{blank}\right)}{A_{positive\ control} - A_{blank}} \times 100$$

Hemolytic activity of the polymers was evaluated with the limit values of the ASTM F756-08 standard.(2008) A hemoglobin release of 0% to 2%, 2% to 5%, or >5% of the total hemoglobin release was classified as non-hemolytic, slightly hemolytic, or hemolytic, respectively. Experiments were run in duplicate and repeated once. The results are shown as the mean of the two experiments ± SD.

Transfection

CHO-K1 cells (50,000/well) were seeded in 12-well plates (Greiner bio one) and incubated for 24 h. Afterwards, culture medium and complex solution (200 µL/well) prepared as described above containing 4 µg pGL3 plasmid at N/P ratios 25 and 50 were added to the wells. Cells were incubated with complexes for 4 h. As controls were used cells treated with 200 µL physiological saline, free plasmid as well as complexes formed with 2,500 g · mol^{-1} lPEI (Polysciences Europe GmbH, Eppelheim, Germany) N/P 25. Culture medium was changed, and the cells were incubated for further 44 h. Cells were washed twice with PBS buffer. Lysis of cells and luciferase assay were carried out according to manufacturer's protocol (Luciferase assay system, Promega). Protein mass was quantified with a standard BCA assay kit (Thermo Scientific, Rockford, USA) according to manufacturer's protocol with minor modifications: cell lysate (25 µL) was incubated with

10 µL 0.05 M iodacetamide solution (Applichem) to inactivate dithiothreitol (DTT) of the lysis reagent at 37 °C for 20 minutes. The transfection efficiency was calculated as RLU/µg protein and presented as the mean of a duplicate testing ± SD. The experiment was repeated twice.

4. References

ASTM F756, 2008, "Standard practice for assessment of hemolytic properties of materials". *Annual Book of ASTM Standards, Vol. 13. 01, ASTM, Philadelphia*.

"Biological evaluation of medical devices part 5: Tests for in vitro cytotoxicity". *2nd edition, International Organization for Standardization/ANSI; ISO ISO 10993-5, Geneva, Switzerland* (2009).

Altuntaş, E., Knop, K., Tauhardt, L., Kempe, K., Crecelius, A. C., Jäger, M., Hager, M. D., & Schubert, U. S. (2012). Tandem mass spectrometry of poly(ethylene imine)s by electrospray ionization (ESI) and matrix-assisted laser desorption/ionization (MALDI). *Journal of Mass Spectrometry, 47*(1), 105-114.

Bauer, M., Lautenschlaeger, C., Kempe, K., Tauhardt, L., Schubert, U. S., & Fischer, D. (2012). Poly(2-ethyl-2-oxazoline) as alternative for the stealth polymer poly(ethylene glycol): Comparison of in vitro cytotoxicity and hemocompatibility. *Macromolecular Bioscience*, 986–998.

Fischer, D., Bieber, T., Li, Y. X., Elsasser, H. P., & Kissel, T. (1999). A novel non-viral vector for DNA delivery based on low molecular weight, branched polyethylenimine: Effect of molecular weight on transfection efficiency and cytotoxicity. *Pharmaceutical Research, 16*(8), 1273-1279.

Fischer, D., Li, Y. X., Ahlemeyer, B., Krieglstein, J., & Kissel, T. (2003). In vitro cytotoxicity testing of polycations: influence of polymer structure on cell viability and hemolysis. *Biomaterials, 24*(7), 1121-1131.

Hoogenboom, R., Paulus, R. M., Pilotti, A., & Schubert, U. S. (2006). Scale-up of microwave-assisted polymerizations in batch mode: The cationic ring-opening polymerization of 2-ethyl-2-oxazoline. *Macromolecular Rapid Communications, 27*(18), 1556-1560.

Mosmann, T. (1983). Rapid colorimetric assay for cellular growth and survival: Application to proliferation and cytotoxicity assays. *Journal of Immunological Methods, 65*(1–2), 55-63.

Ogris, M., Brunner, S., Schuller, S., Kircheis, R., & Wagner, E. (1999). PEGylated DNA/transferrin-PEI complexes: Reduced interaction with blood components, extended circulation in blood and potential for systemic gene delivery. *Gene Therapy, 6*(4), 595-605.

Perrine, T. D., & Landis, W. R. (1967). Analysis of polyethylenimine by spectrophotometry of its copper chelate. *Journal of Polymer Science Part A-1: Polymer Chemistry, 5*(8), 1993-2003.

Tauhardt, L., Kempe, K., Knop, K., Altuntaş, E., Jäger, M., Schubert, S., Fischer, D., & Schubert, U. S. (2011). Linear polyethyleneimine: Optimized synthesis and characterization – on the way to "Pharmagrade" batches. *Macromolecular Chemistry and Physics, 212*(17), 1918-1924.

Tseng, W.-C., & Jong, C.-M. (2003). Improved stability of polycationic vector by dextran-grafted branched polyethylenimine. *Biomacromolecules, 4*(5), 1277-1284.

Wotschadlo, J., Liebert, T., Heinze, T., Wagner, K., Schnabelrauch, M., Dutz, S., Mueller, R., Steiniger, F., Schwalbe, M., Kroll, T. C., Hoeffken, K., Buske, N., & Clement, J. H. (2009). Magnetic nanoparticles coated with carboxymethylated polysaccharide shells – Interaction with human cells. *Journal of Magnetism and Magnetic Materials, 321*(10), 1469-1473.

Zhao, H., & Heindel, N. D. (1991). Determination of degree of substitution of formyl groups in polyaldehyde dextran by the hydroxylamine hydrochloride method. *Pharmaceutical Research, 8*(3), 400-402.

Publication 10

“A cationic poly(2-oxazoline) with high *in vitro* transfection efficiency identified by a library approach “

C. Rinkenauer,[#] L. Tauhardt,[#] F. Wendler, K. Kempe, M. Gottschaldt,
A. Träger, U. S. Schubert
#Both authors contributed equally.

Macromolecular Bioscience, accepted 07.10.2014

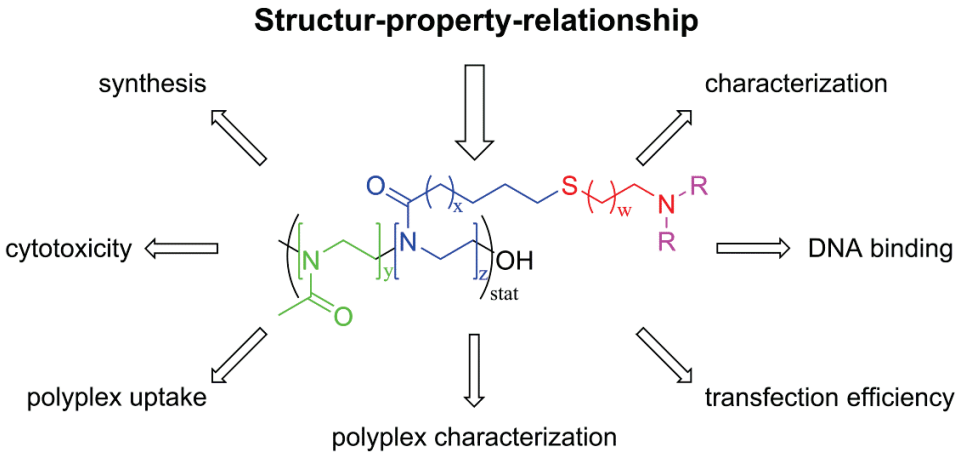

A cationic poly(2-oxazoline) with high *in vitro* transfection efficiency identified by a library approach

Alexandra C. Rinkenauer,[1,2‡] Lutz Tauhardt,[1,2‡] Felix Wendler,[1,2] Kristian Kempe,[1,2 †] Michael Gottschaldt,[1,2] Anja Träger,[1,2] Ulrich S. Schubert [1,2,3]**

[‡] *both authors contributed equally*

[1]Laboratory of Organic and Macromolecular Chemistry (IOMC), Friedrich Schiller University Jena, Humboldtstrasse 10, 07743 Jena, Germany

[2]Jena Center for Soft Matter (JCSM), Friedrich Schiller University Jena, Philosophenweg 7, 07743 Jena, Germany

[3]Dutch Polymer Institute (DPI), John F. Kennedylaan 2, 5612 AB Eindhoven, The Netherlands.

[†]Current address: Department of Chemical and Biomolecular Engineering, The University of Melbourne, Victoria 3010, Australia

*Address correspondence to: ulrich.schubert@uni-jena.de; anja.traeger@uni-jena.de

KEYWORDS. Gene delivery, viability, poly(2-oxazoline)s, hydrophobic side chain, structure property relationship, primary amine, tertiary amine

ABSTRACT. To date, cationic polymers with high transfection efficiencies often have a high cytotoxicity. By screening an 18-membered library of cationic polymers based on 2-methyl-2-oxazoline and 2-(9-decenyl)-2-oxazoline or 2-(3-butenyl)-2-oxazoline, respectively, a polymer could be identified that is superior to linear poly(ethylene imine), since it has a similar transfection efficiency but no detectable cytotoxicity at the investigated concentrations. The library was investigated regarding the influence of different polymer parameters, namely the polymer side chain hydrophobicity and the type and content of amino groups, on the pDNA condensation, the transfection efficiency, the cytotoxicity, and cellular membrane interaction as well as the size, charge and stability of the polyplexes. First structure-property relationships revealing that for the presented polymer class, primary amines and an amine content of at least 40% were required for an efficient polyplex formation. While short hydrophobic polymer side chains were non-toxic up to an amine content of 40%, long hydrophobic side chains revealed a high cytotoxicity.

Introduction

Nanomaterials and their applications are of great interest for scientists of different disciplines such as biology, pharmacy, chemistry, biotechnology, physics, and medicine.[1] Within the field of nanomedicine, non-viral gene delivery has a high potential for the treatment of a large variety of diseases.[2, 3] Although many problems have been solved during the last three decades, the ideal delivery agent, i.e. vector, still has to be found.[4] To design successful non-viral vectors for genetic materials, several bottlenecks have to be overcome.[5, 6]

Non-viral vectors, in particular synthetic polymers, offer the advantage of being tailor-made systems, which can be produced in large scale and stored without further complications. Due to their good interaction with negatively charged genetic material such as plasmid DNA (pDNA) or small interfering RNA (siRNA), cationic polymers play an important role within the field of gene delivery.[1, 7-12] Prominent examples of this polymer class are poly(ethylene imine) (PEI),[13-16] poly(L-lysine) (PLL),[17] and poly(methacrylate)s (*e.g.* PDMAEMA)[18-20] in which PEI represent the "gold standard" for *in vitro* transfections. Previous studies on structure-property relationships revealed the influence of molar mass, pK_a value, polymer end groups, side chain substitution and polyplex size on the transfection efficiency (TE).[21-23] However, comprehensive structure-property relationships are rare[24] and the results of the different studies often cannot be transferred to other polymer classes leading to the necessity to perform detailed analyses for every material.

The main requirement for transfection agents is an efficient delivery, combined with a low cytotoxicity. However, most cationic polymers are either efficient in delivering the genetic material but cytotoxic or they are non-toxic and fail in their delivery potential.[25, 26] An often used method to overcome this drawback is the functionalization with non-toxic and biocompatible compounds such as carbohydrates or non-ionic polymers, e.g. poly(ethylene glycol) (PEG) and poly(2-oxazoline)s (POx).[27-35] Due to the so called "stealth effect", the polymers reduce the nonspecific interactions with blood components, *e.g.* by shielding of positive charges. Moreover, a prolonged blood circulation time leading to an enhanced permeability and retention (EPR) effect as well as a reduced cytotoxicity can be observed and the water solubility is increased.[31] POx, in particular poly(2-ethyl-2-oxazoline) (PEtOx) and poly(2-methyl-2-oxazoline) (PMeOx), have been intensively investigated as PEG alternative.[36-46] Compared to

PEG, the synthesis of POx by a living cationic ring-opening polymerization (CROP) is rather undemanding, but also leads to well-defined polymers.[47-50] The preparation of cationic PEtOx copolymers with primary amine units,[51] and their usage in DNA binding hydrogels has been reported earlier.[52] However, the 2-(4-aminobutyl)-2-oxazoline/EtOx copolymers showed no transfection efficiencies (TE) (unpublished data). In addition, it was reported that partially hydrolyzed POxs, *i.e.* P(Ox-*stat*-EI), show less cytotoxicity but also less TE with increasing POx concentrations.[32, 34] Further studies described a correlation between the polyplex stability and the amount of positive charges. Often, a decrease of the positive charge goes along with a reduction of the polyplex stability and, hence, leads to an inefficient cellular uptake and endosomal release. Moreover, the functionalization with PEG or hydrophilic POx (*e.g.* PMeOx, PEtOx) can result in an inefficient delivery, due to a reduced interaction with the genetic material and the cellular membranes caused by the cell- and protein-repellent character of the polymers, the so called PEG dilemma.[53-58] To solve this problem, additional polymer features have to be considered. Besides modifying polycations with "stealth" polymers,[31, 37] the introduction of more neutral or hydrophobic characteristics have been discussed for gene delivery applications.[59, 60] It is known from the development of antimicrobial POx that the introduction of long alkyl spacers leads to an enhanced membrane interaction.[61] Hence, it is assumed that the cellular uptake of modified cationic polymers, which is often reduced to the "stealth effect", can be improved by introducing hydrophobic moieties.

In this study, the influence of hydrophobicity, type of amine, and amine content of 2-oxazoline based polymers on the transfection behavior was systematically investigated. In detail, copolymers of alkene containing 2-oxazolines, namely 2-(9-decenyl)-2-oxazoline (DecEnOx) or 2-(3-butenyl)-2-oxazoline (ButEnOx), and 2-methyl-2-oxazoline (MeOx) were synthesized and

further functionalized by thiol-ene photoaddition.[62-66] MeOx was chosen as comonomer to improve the water-solubility which is limited for P(EtOx-*co*-ButEnOx) and P(EtOx-*co*-DecEnOx) due to the LCST behavior of PEtOx.[67] These copolymers were further systematically investigated with regard to: 1) their ability to interact with pDNA and the cellular membrane, 2) their cellular uptake, 3) cytotoxicity, and 4) the transfection efficiency.

Experimental Part

See supporting information.

Results and discussion

Synthesis of a cationic poly(2-oxazoline) library

To investigate the influence of the type of amine (primary or tertiary), the amine content, and the side chain hydrophobicity, a library of 18 new cationic POx copolymers has been synthesized (Scheme 1). Starting from MeOx and ButEnOx as well as DecEnOx, a series of copolymers containing up to 50 mol% of the double bond bearing comonomer has been prepared. In a straightforward approach these double bonds have been functionalized with different amines (primary or tertiary) using the thiol-ene photoaddition procedure. For clarity, the final products have been labeled according to the following pattern: **s**, for all copolymers based on a "short" side chain of ButEnOx; **l**, for all polymers based on a "long" side chain of DecEnOx; the amine content is given as number in mol%; **p** or **t**, characterize the type of amine, namely primary (**p**) or tertiary amine (**t**) (Scheme 1). If not stated otherwise, there is a C_2H_4 spacer between the sulfur and the final amine group. In case of a hexamethylene spacer the term **h** is added to the compound abbreviation.

Scheme 1. Schematic representation of the synthesis of cationic poly(2-oxazoline)s. Reaction conditions: a) 140 °C, microwave reactor, acetonitrile, b) room temperature, overnight, methanol, catalyst: 0.1 mol% 2,2-dimethoxy-2-phenylacetophenone with respect to contained double bonds, c) room temperature, overnight, dichloromethane/trifluroacetic acid. Product terms: **s** = short butyl side chain, **l** = long decenyl side chain, N = amine content in mol%, **h** = hexamethylene spacer, **p** = primary amine, **t** = tertiary amine.

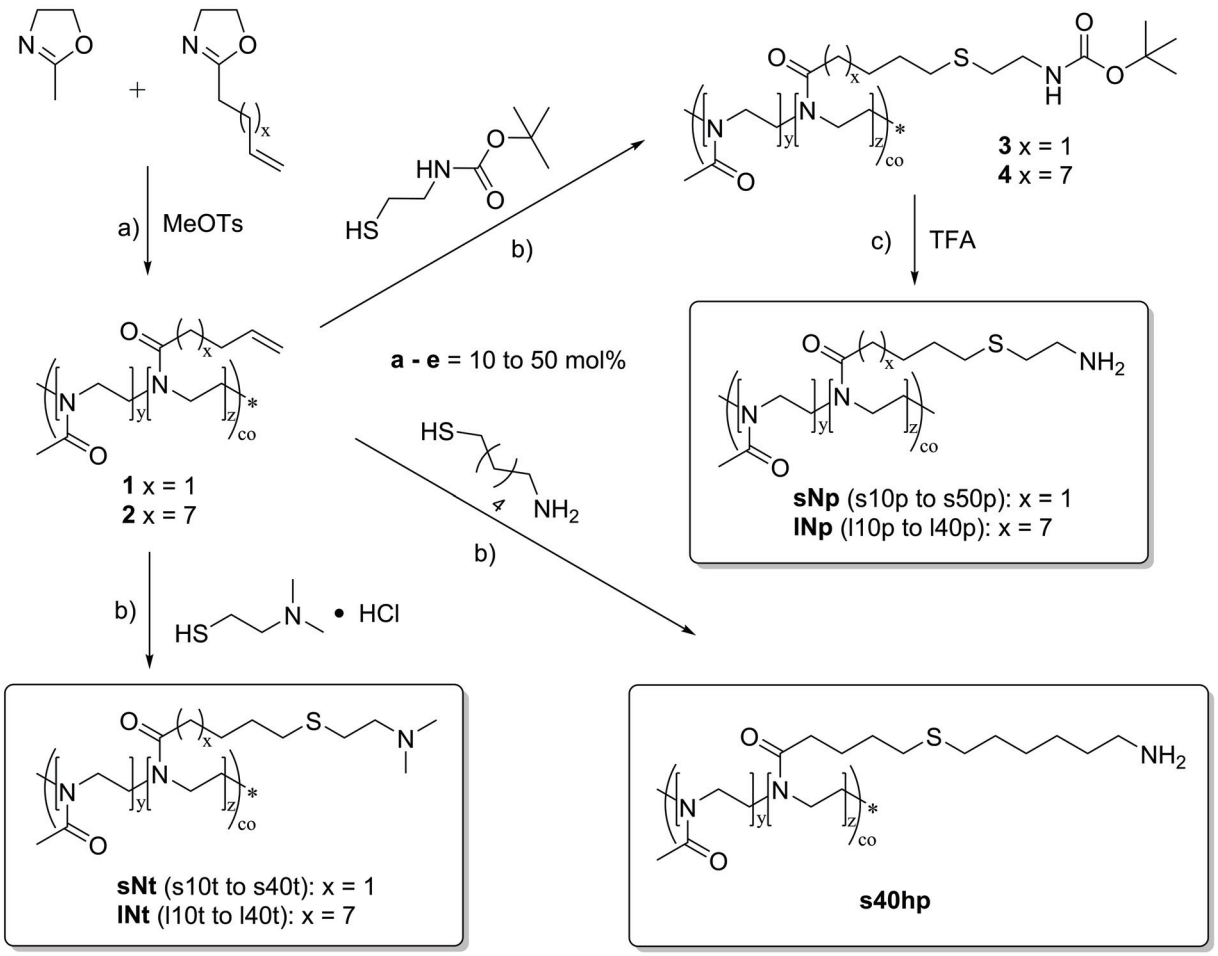

Synthesis of P(MeOx-*co*-ButEnOx) and P(MeOx-*co*-DecEnOx)

In order to synthesize well-defined P(MeOx-*co*-ButEnOx), a kinetic study was performed for this copolymer system. The linearity of the first-order kinetic plots shows the living character of the copolymerization (Figure S1). Having a higher polymerization rate, MeOx (k_p = 0.097 L mol^{-1} s^{-1}) is incorporated faster into the polymer chain than ButEnOx (k_p = 0.052 L mol^{-1} s^{-1}) indicative for the formation of a gradient copolymer. Characterization by size exclusion chromatography (SEC) showed an increasing molar mass with increasing conversion (Table S1). Similar results were obtained for P(MeOx-*co*-DecEnOx), as reported elsewhere.[68]

To achieve a sufficient binding with the genetic material and a low cytotoxicity, an overall degree of polymerization (DP) of 200 was chosen. The ButEnOx/DecEnOx content was varied between 10, 20, 30, and 40 mol%. Full conversion of the monomers was proven by ^{1}H NMR investigations. Copolymers with dispersity ($Đ_M$) values between 1.43 and 1.63 (Table S2) were obtained. The rather high $Đ_M$ values for a living cationic polymerization can be attributed to two aspects: 1) The different hydrodynamic volumes and column interactions of the polymers compared to the used poly(styrene) standard and 2) the occurrence of chain-transfer,[69, 70] commonly observed for PMeOx systems with DP values higher than 100.[50] Due to the monomodality of the obtained SEC curves (exemplarily shown for the P(MeOx-*co*-ButEnOx) copolymer in Figure S2), it is assumed that no chain coupling or "long chain branching"[70] reactions occurred, since those would lead to a shoulder at lower elution volumes, i.e. higher molar masses. Instead tailing of the SEC curves is observed, indicating the existence of low molar mass polymer chains, originating from chain-transfer and termination reactions. The extent of chain transfer reactions might have been reduced using EtOx as comonomer (more controlled

reaction up to a DP of 200). However, to avoid low critical solution temperature (LCST) behavior known of PEtOx containing copolymers, MeOx was chosen as comonomer.[62, 67, 71]

The ^{1}H NMR spectra showed that both monomers are incorporated (Figure 1, Figure S3). In each case, two signals for the double bonds are visible around 5.86 and 5.00 ppm. The polymer backbone signal is found around 3.52 ppm. The signals of the side chain protons occur between 1.00 and 2.60 ppm. By correlating the proton signal of the double bond at 5.86 ppm with the backbone signal, the monomer ratios within the polymer could be calculated. They were found to be in agreement with the ratios aimed for.

In general two different end groups are possible, namely a hydroxyl or an ester end group.[72] Unfortunately, the end group analysis, e.g. by ESI- or MALDI-TOF-MS, is not possible due to the high DP. However, at this high molar mass the influence of the end group should be only marginal or even negligible.

Thiol-ene functionalization of P(MeOx-*co*-ButEnOx) and P(MeOx-*co*-DecEnOx) with different amines

To obtain a cationic character, required for DNA-binding, primary and tertiary amino groups were introduced into the copolymers by thiol-ene photoaddition reaction (Scheme 1). The primary amines were obtained by reaction of the copolymers with 2-(boc-amino)ethanethiol under UV irradiation (λ = 365 nm) and subsequent deprotection with trifluoroacetic acid. Characterization by ^{1}H NMR spectrometry showed that for both copolymer types (**3** and **4**) the double bond signals of the starting materials at 5.86 and 5.00 ppm disappeared after the photoaddition, indicating the complete functionalization with the thiol (Figure 1, Figure S3). Moreover, a singlet of the boc protecting group at 1.44 ppm was obtained. For both **3** and **4**, the

signals of the CH_2 next to the boc protected nitrogen can be found around 3.21 ppm. The protons signals at 2.60 ppm can be assigned to the CH_2 groups adjacent to the sulfur atom. After treatment with TFA and precipitation into ice-cold diethyl ether, the singlet of the boc protecting group disappeared, indicating the successful deprotection. SEC characterization of the MeOx/ButEnOx systems revealed a growing molar mass (lower elution volume) after the photoaddition of 2-(boc-amino)ethanethiol (Figure 2, Table S2). After deprotection, the molar mass decreases further. For the MeOx/DecEnOx systems, SEC measurements were performed for the starting materials **2**and the final products **lNp**. A growing molar mass of the end products **lNp** compared to the starting materials **2** was observed. This is in accordance with the MeOx/ButEnOx systems. In all cases the $Đ_M$ values changed only slightly.

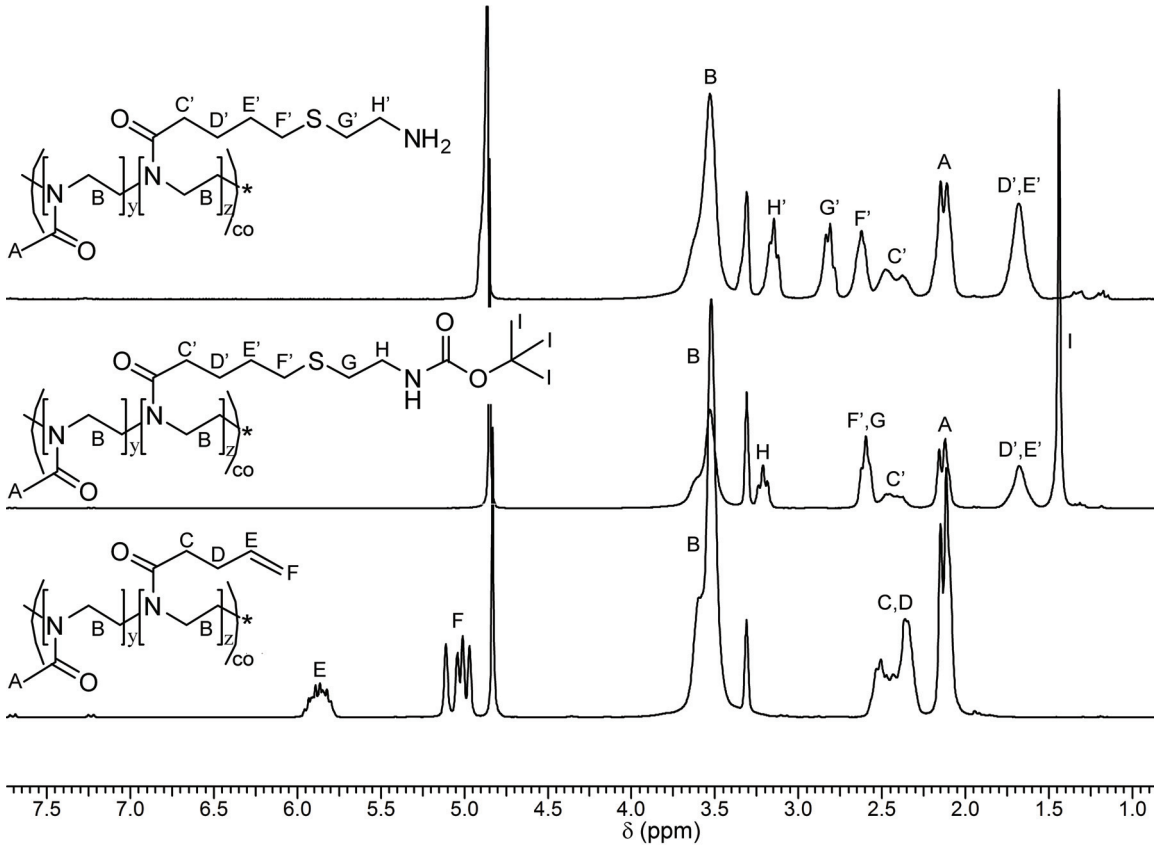

Figure 1. ^{1}H NMR spectra of **1d** (bottom), **3d** (middle), **s40p** (top) (250 MHz, solvent: CD_3OD).

In addition, copolymers with a tertiary amino group were prepared form **1** and **2** by UV-initiated thiol-ene reaction with dimethylaminoethanethiol hydrochloride. The ^{1}H NMR spectra of **sNt** and **lNt** showed a broad peak around 2.92 ppm belonging to the two CH_3 groups of the amino thiol (Figure S3). The double bond signals of the starting materials disappeared, indicating a complete conversion. Although in theory the molar mass should increase after thiol-addition, analysis by SEC revealed lower molar masses of the cationic **sNt** polymers compared to the neutral starting material (Table S2). Depending on the particular compound the **lNt** polymers showed both increasing and decreasing molar masses. This is ascribed to the different hydrodynamic volumes of the cationic polymers in DMAc, but also to the different column interactions compared to the neutral PS standards used for calibration. It also explains the large variation in the molar masses and $Đ_M$ values, e.g. of **s40p** (M_n = 29,100 g/mol, $Đ_M$ = 1.52) and **s40t** (M_n = 20,180, $Đ_M$ = 1.35), which are both synthesized from the same starting material and only differ by the type of amine.

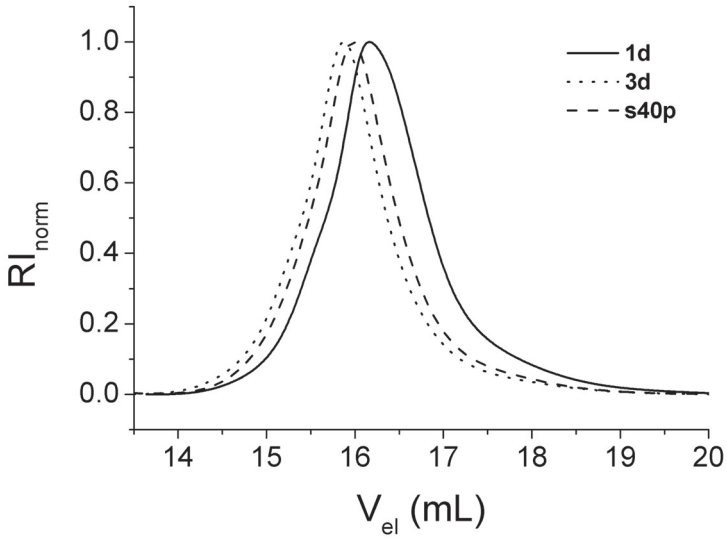

Figure 2. SEC curves of the copolymers **1d** (straight), **3d** (dashed), and **s40p** (dotted) (eluent: DMAc + 0.21% LiCl; calibration: PS).

Binding of genetic material

An essential requirement for non-viral vectors is their interaction with negatively charged nucleic acids, resulting in the formation of interelectrolyte complexes, also known as polyplexes. The resulting plasmid DNA (pDNA) condensation caused by the interaction with the polymers was analyzed using the ethidium bromide quenching assay (EBA). Due to electrostatic and hydrophobic interactions between polymer and pDNA, ethidium bromide (EB) is excluded from a preformed pDNA/EB complex and the decrease in the EB fluorescence intensity can be detected. All 16 polymers (**sNp**, **sNt**, **lNp**, l**Nt**) led to a decrease in the fluorescence intensity of EB and, thus, showed interaction with the pDNA (Figure S6). As positive control, linear PEI (lPEI) with a DP of 200 was used, decreasing the fluorescence intensity to 44.9 ± 3.1% (Figure S7). Higher relative fluorescence intensities of 65 to 80% were observed for the **sNp** polymers without significant differences concerning their amine content.

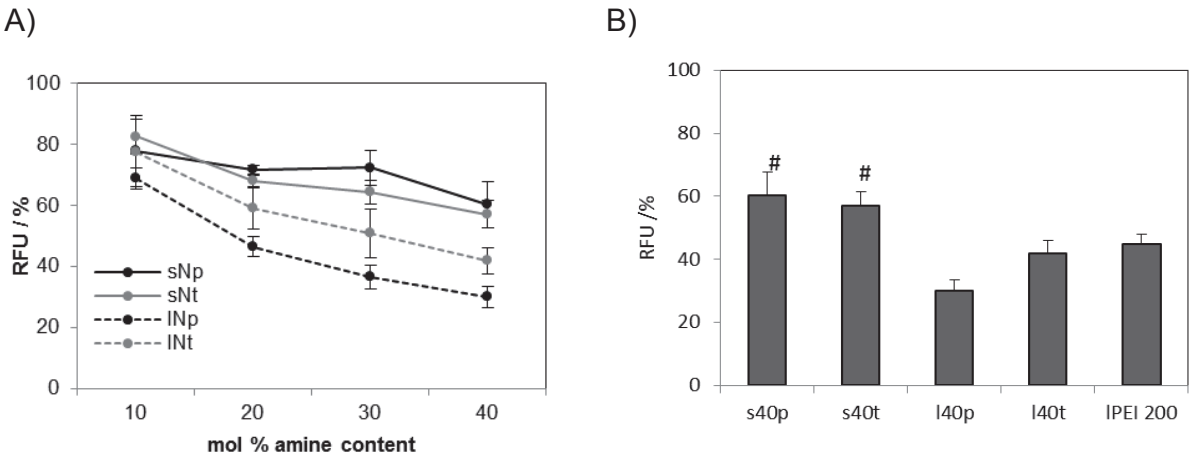

Figure 3. Ethidium bromide quenching assay of all 16 polymers with pDNA measured at physiological pH via EBA. A) Comparison at N/P ratio 40. B) Comparison of 40 mol% amine content (N/P 40) polymers. Values represent the mean ± S.D (n=3); # represents a significant difference ($p < 0.05$) to **l40p**.

For the investigated copolymers three tendencies can be observed: 1) In the case of the polymers with long side chains, primary amines bind better than tertiary, 2) the amine content correlates with the pDNA condensation, and 3) the pDNA condensation increases with the side chain length (Figure 3A and B). The latter can be probably ascribed to stronger hydrophobic interaction with the pDNA, caused by the higher number of CH_2 groups in the side chains.[49] However, based on the obtained data it is evident that the influence of the type of alky side chain (long *vs.* short) is more pronounced. In detail, up to 30% difference in the relative fluorescence intensity of **s40p** and **l40p** compared to 10% of **l40p** and **l40t** were found (Figure 3 B). This observation emphasizes the importance of understanding the physicochemical interactions between the polymer and the genetic material, and not only the influence of electrostatic interactions for the polyplex formation mainly discussed in literature.[73, 74]

Transfection efficiency

Since an interaction with the pDNA could be observed, the polymer library was analyzed regarding the transfection efficiency. To this end, human embryonic kidney cells (HEK) and pDNA, encoding the reporter gene EGFP, were used. As transfection outcome, the percentage of cells successfully expressing EGFP was identified using flow cytometry. Interestingly, one polymer, the **s40p**, showed a TE (30.5 ± 7.6%) comparable to that of lPEI (31.2 ± 1.7%) (Figure 4, S18 and Table S3, S6), whereas all other polymers showed lower TEs (below 10%). The comparable TE of **s40p** and lPEI is surprising, since the same DP was used and, hence, **s40p** exhibits a much lower amine content (only 80 of 200 repeating units bear an amino group).

The observed differences in TE of 2-oxazoline-based polymers lead to the assumption that primary amino groups in the side chain in combination with small spacers to the backbone are beneficial. These results were not expected and highlight the influence of the polymer

constitution for the biological properties. Only slight changes in the amine type, the amine content, or the side chain length can have a great impact on the TE. To gain a deeper insight into the structure-property relationship and find an answer to the question, why the other comparable polymers are less efficient, further investigations were performed. Subsequently, the polymers were studied concerning their polyplex properties, their cytotoxicity, and their membrane interaction.

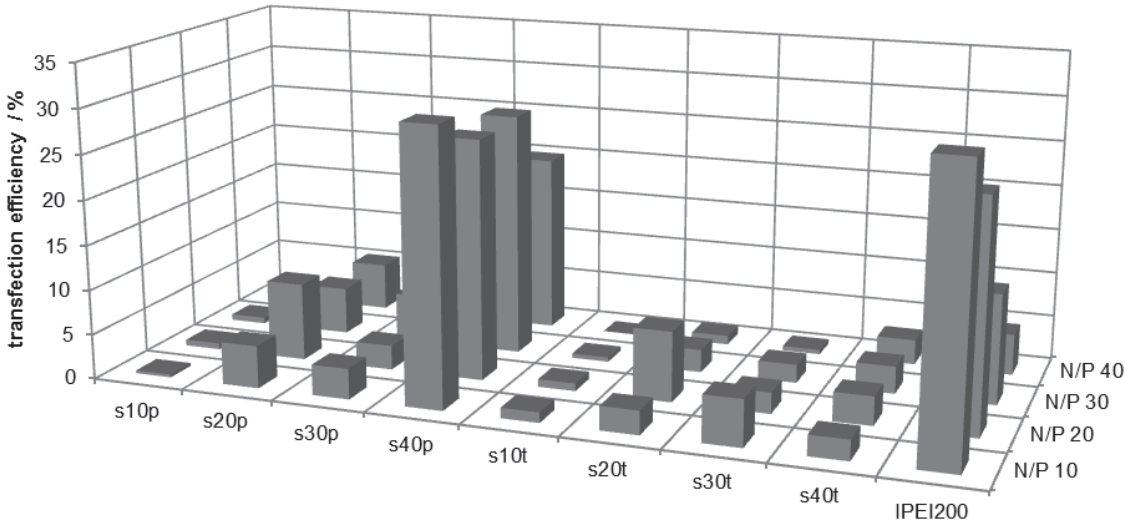

Figure 4. Transfection efficiency of all polymers with short side chains (**sNp** and **sNt**) and $lPEI_{200}$ for adherent HEK cells in serum reduced media at different N/P ratios. Values represent the mean (n=3), SD can be found in the Supporting Information.

Size and charge of polyplexes

For a fast and efficient internalization by endocytosis, polyplexe sizes between 100 and 200 nm and positive surface charge are beneficial.[6, 75] It was found that all polymers, except **s10p**, form

polyplexes with diameters below 200 nm (Table 1). Moreover, with increasing amine content a tendency to form smaller polyplexes was observed. The polyplexes prepared from the four 10 mol% amine containing polymers exhibited a negative zeta potential, indicating an insufficient polyplex formation and, thus, explaining the insufficient TE (Figure 4). All other polymers formed polyplexes with a positive zeta potential (Table 1).

Table 1: Polyplex properties and hemolysis assay: Polyplexes of indicated polymers and pDNA were formed at N/P ratio 20 in HBG buffer at pH 7.4 (PDI^P see Figure S8). Hemolysis assay of the whole polymer library using blood of three different donors (n=3). 1% Triton X-100 was used as positive control and values were set to 100% hemolysis. Values represent the mean (n=3) (SD can be found in the Supporting Information).

			Polyplex properties		**Hemolysis / %**		
			zeta potential / mV	diameter / nm	concentration		
					10 µg/mL	50 µg/mL	100 µg/mL
Short hydrophobic side chain	primary amines	**s10p**	-4.3 ± 2.1	255 ± 57	0.09	0.05	0.2
		s20p	22 ± 2.7	178 ± 2.6	0.4	1.5	2.6
		s30p	40 ± 1.6	110 ± 11	0.09	0.2	0.2
		s40p	23 ± 2.7	94 ± 3.4	0.6	1.6	2.9
	teriary amines	**s10t**	-5.5 ± 2.5	151 ± 14.7	0.5	0.6	0.7
		s20t	19 ± 1.7	158 ± 0.4	0.8	0.6	0.5
		s30t	29 ± 4.7	124 ± 3.5	0.6	0.6	0.7
		s40t	29 ± 1.7	105 ± 1.2	0.8	0.7	0.8
Long hydrophobic side chain	primary amines	**l10p**	-17 ± 1.1	152 ± 3.1	0.9	18	17
		l20p	28 ± 1.8	105 ± 3.2	83	107	107
		l30p	29 ± 1.3	84 ± 0.5	105	124	102
		l40p	34 ± 1	97 ± 3	106	104	108
	teriary amines	**l10t**	-9 ± 1.2	152 ± 3.5	0.7	0.6	0.7
		l20t	26 ± 0.7	113 ± 3.6	10	50	86
		l30t	30 ± 2.7	84 ± 0.5	62	101	95
		l40t	27 ± 3	67 ± 1.8	102	100	100

Furthermore, neither the hydrophobicity of the side chain nor the amine type showed an influence on the size and zeta potential of the investigated polyplexes. In conclusion, a critical amine content of 20 mol% is necessary for an efficient polyplex formation, indicated by a positive zeta potential.

Cytotoxicity of polymers and interaction with cellular membranes

In a next step, the biocompatibility of the polymers was investigated. To study the interactions between polymers and cellular membranes a hemolysis assay was performed. It was found that the polymers with short side chains (**sNp** and **sNt**) exhibit a hemolysis below 3%, indicative of no hemolytic activity (Table 1). In contrast, the polymers with long side chains (**lNp** and **lNt**) showed high hemolytic activity even at low concentrations (Table 1). This finding can be ascribed to strong membrane interaction of the more hydrophobic side chain leading to membrane destruction, as also reported elsewhere.[61] Moreover, the **lNp** polymers are more hemolytic compared to **lNt**, which also indicates an enhanced interaction of primary amines with the negative cellular membrane or their proteins. Due to their low amine chain content and insufficient polyplex formation, **l10p** and **l10t** did not cause any hemolytic effect (1.8%) (Table 1). The results show that the interaction between the polymers and membranes is much more influenced by the hydrophobic nature of the polymers than by the amine type and content. This is in accordance with the results of the pDNA condensation (EBA) study (Figure 3).

Besides the hemolytic activity, the cytotoxicity was investigated. It is a well-known problem that cationic polymers, such as high molar mass PEI or PDMAEMA, lead to low cell viabilities.[19, 76] Both, PMeOx and PEtOx were postulated to decrease the cytotoxicity. Hence, the cytotoxicity of the 16 PMeOx containing copolymers was analyzed using the AlamarBlue assay (Figure 5). This assay is based on a non-fluorescent indicator dye (resazurin) that is

converted into a fluorescent dye by metabolically active cells. While the **sNp** and **sNt** polymers caused no cytotoxicity at concentrations up to 200 µg mL^{-1} (Figure 5 A), lPEI showed an IC_{50} (concentration where 50% of cells are viable) at 3.6 µg mL^{-1} (data not shown). In this context, it has to be noted that **s40p** shows the same TE as lPEI but without any cytotoxic effects. In contrast, higher cytotoxicities were observed for polymers with long side chains (**lNp** and **lNt**), showing furthermore a dependency on the amine content, amine type, and the used concentration (Figure 5 B). IC_{50} values of 4 to 14 µg mL^{-1} were obtained, meaning they have a cytotoxicity comparable to lPEI. In contrast to the **lNp** polymers, where **l40p** showed a lower cytotoxicity than **l30p**, an increasing cytotoxicity with increasing amine content was observed for the **lNt** polymers. The decreased toxicity of **l40p** might be caused by (electrostatic) interactions with serum components and will be investigated in further studies. In summary, the alkyl content and the hydrophobicity of the side chains showed again a high impact on the interaction of the polymers with cellular membranes.

To further investigate the reason for the different cytotoxicity of the polymers, in particular **s40p** and **s40t** or **l40p**, a lactate dehydrogenase (LDH) assay was performed with all four 40 mol% amine containing polymers (Figure 6). Due to the possibility to determine the released cellular LDH in a sensitive way, the LDH assay is used to detect membrane destruction.[77]

A)

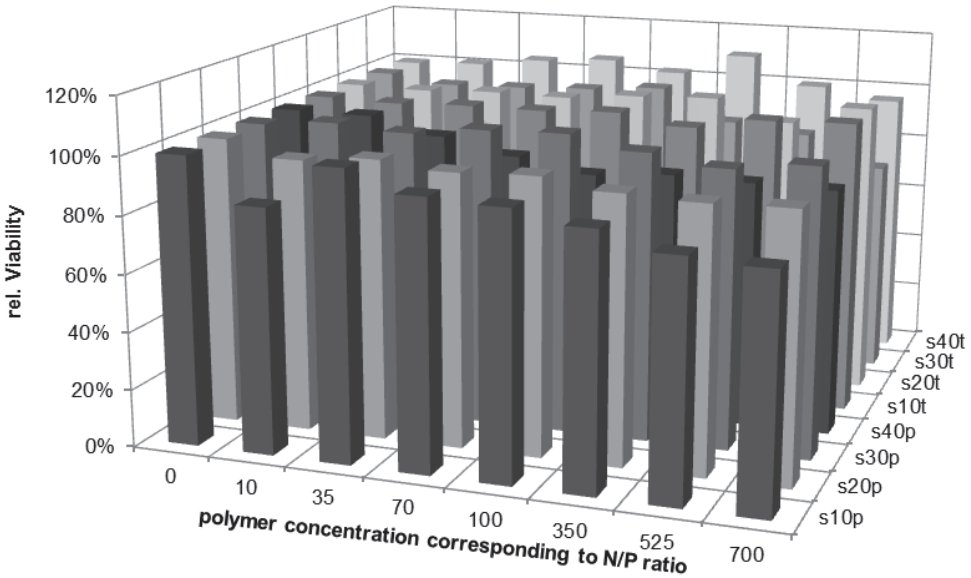

B)

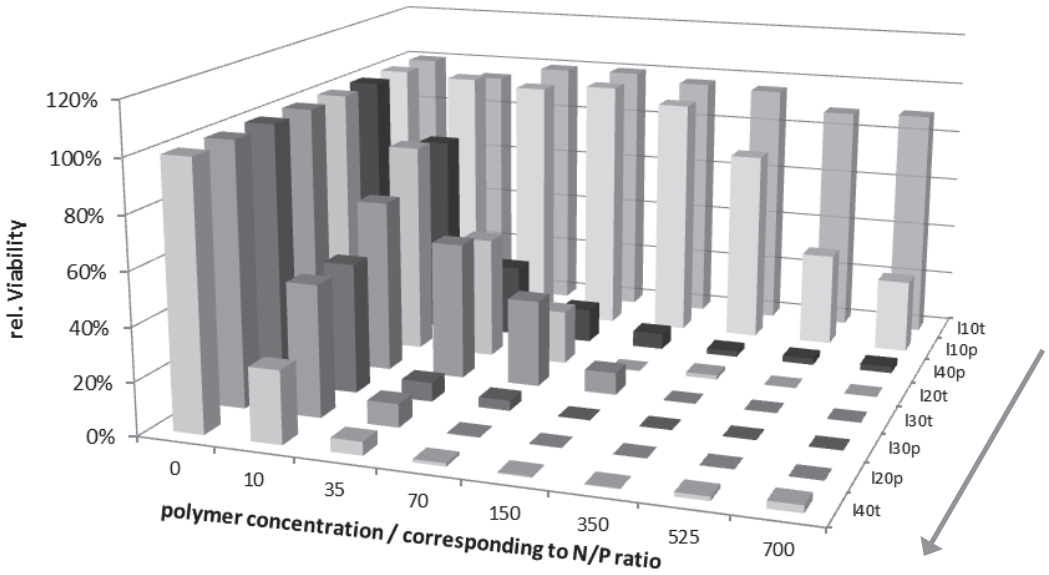

Figure 5. Cytotoxicity of indicated polymers (A, short side chains; B, long side chains) using AlamarBlue and L929 cells. A, Cells treated with **sNp** polymers and **sNt** polymers. B, Cells treated with **lNp** polymers and with **lNp** polymers. Arrow represents the increased cytotoxicity of **lNp** polymers. Values represent the mean (n=3), SD can be found in the Supporting Information.

In contrast to the hemolysis assay, the LDH assay can be performed with HEK cells which are also used for transfection studies. Consequently, the membrane destruction ability of both, the polymers and the polyplexes, can be analyzed. It was observed that the polymers **s40p** and **s40t** as well as their polyplexes showed no membrane destruction, at an N/P ratio of 20. In case of **l40p** the polyplex is less toxic than the corresponding polymer, which was also observed for PEI. This was already reported in literature and was ascribed to the shielding of the cationic charges of PEI by interactions with the genetic material.[78] It is assumed that this is also valid for **l40p**, since this polymer strongly interacts with the pDNA (Figure 3). Interestingly, the polyplexes of **l40t** showed a slightly higher membrane destruction activity compared to the non-complexed polymers. A possible explanation can be an enhanced internalization of polyplexes compared to the polymers resulting in high intracellular cytotoxicity.

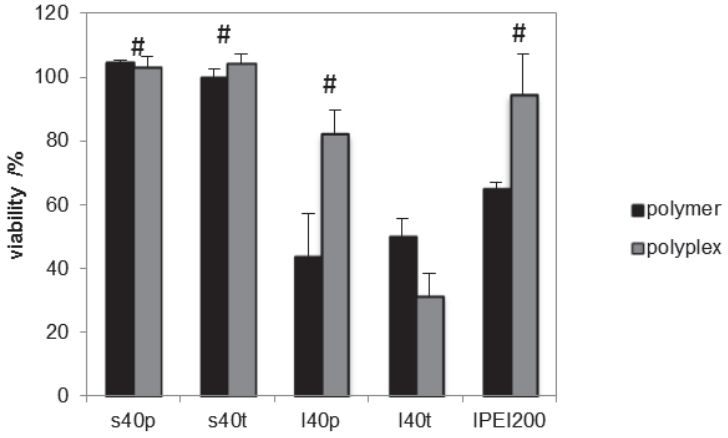

Figure 6. LDH assay of HEK cell. Cells were incubated with polyplexes of indicated polymers for 1 h at N/P 20. Values represent the mean (n=3), SD can be found in the Supporting Information; # represents a significant difference ($p < 0.05$) compared to **l40t**.

A possible reason for the higher cytotoxicity of **l40t** compared to **l40p** is the more hydrophobic character of the tertiary amine compared to the primary counterpart. In addition, the sterically demanding methyl groups of the tertiary amine possibly reduce the pDNA binding (Figure 3) and shield the cationic charges, as observed for **l40t** Thus, the LDH assay confirms the assumption that an increased side chain hydrophobicity enhances the interaction with the membrane. In the case of **s40p** an optimum between the amount of "stealth" (MeOx) units for high biocompatibility, the amount and type of cationic groups for pDNA interaction, and the ideal length of the hydrophobic segment for membrane interactions was found, making **s40p** the best performing polymer.

Uptake of polyplexes

Hitherto, the performed experiments could not explain the differences between the good performer **s40p** and the bad performer **s40t** regarding its transfection mechanism. Therefore, the uptake behavior was investigated using YOYO-1 labeled pDNA. The uptake of the fluorescent polyplexes was determined by flow cytometry.[79] To focus on the influence of amine type and hydrophobicity, only the 40 mol% polymers were studied (Figure 7). Polyplexes based on **l40p** showed a time dependent uptake, similar to that of lPEI. Compared to this, the **s40p** based polyplexes, which showed the highest TE, were taken up much faster and more efficiently. 70% of the HEK cells internalized **s40p** polyplexes already after one hour of incubation (LPEI: 34%). In contrast to the **s40p** polyplexes, its corresponding polymer with tertiary amines (**s40t**) showed the lowest polyplex internalization. Only 60% of the cells internalized polyplexes, even after 4 h. For **l40t** polyplexes, no analysis was possible since the cytotoxicity was too high to obtain any reliable data, as also observed by the AlamarBlue and the LDH assay (Figure 5 and Figure 6).

The reduced uptake of polymers with tertiary amine side chains (**s40t)** and/or their high cytotoxicity (**l40t**) can explain their insufficient TE, compared to **s40p**. The bad TE of polymers with tertiary amines coupled to long hydrophobic side chains is in contrast to the poly(amine-*co*-ester) terpolymers systems reported by Zhou *et al*., where polymers with long hydrophobic domains and tertiary amines in the main chain revealed an excellent transfection behavior and low cytotoxicity.[80] This once more highlights the importance of the polymer hydrophobicity for gene delivery applications. However, it also shows that results from different studies cannot easily be transferred to other polymer classes. Therefore, it is necessary to perform detailed analyses for each compound.

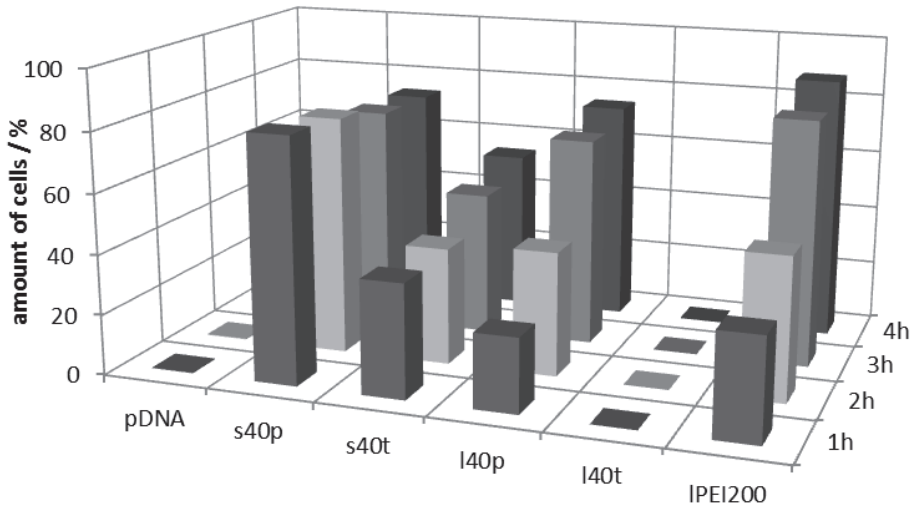

Figure 7. Uptake study: Amount of cells transfected with YOYO-1 labeled pDNA for indicated time points using the polymers with 40 mol % amine content and pDNA and $lPEI_{200}$ (NP ratio 20) as controls. Values represent the mean (n=3), SD can be found in the Supporting Information.

Polyplex stability

To understand, why some polymers perform better than others, different bottlenecks were analyzed, starting from the polyplex itself to the cellular mechanisms. Another critical parameter is the polyplex stability. On one hand the pDNA has to be protected against digestion, on the other hand it has to be released inside cells. Hence, an optimum between strong and weak binding has to be found. The polyplex stability was analyzed using the heparin assay, in which negatively charged heparin competes with the pDNA. In Figure 8 the heparin concentration necessary for complete polyplex dissociation is presented (Data of all compound see Figure S9). Compared to the polyplexes formed from polymers with short side chains (**sNp** and **sNt**), the ones of long side chain (**lNp** and **lNt**) are more stable, as indicated by higher heparin concentrations required to release the pDNA. This is particularly the case for **l40p**, where 50 U mL^{-1} heparin are required for the polyplex dissociation, which is in good correlation with the strong pDNA condensation (Figure 3). In contrast, the **s40p** polyplexes release the pDNA already at heparin concentration of 10 U mL^{-1}. This indicates a stronger binding of **l40p** and could result in an inefficient release of pDNA in the cytoplasm and, hence, a low TE (Figure 4 and Figure 7). For the **sNt** and **lNt** polyplexes only a small amount of heparin leads to dissociation. This is another indication that tertiary amines interact less strongly with genetic material and, hence, are not able to protect the pDNA at physiological pH 7 (Figure 3). As a consequence, the pDNA could be degraded due to the polyplex instability during the incubation in the transfection media or inside the cell (pH 7). The latter could also explain their inefficient uptake and the low amount of internalized pDNA.

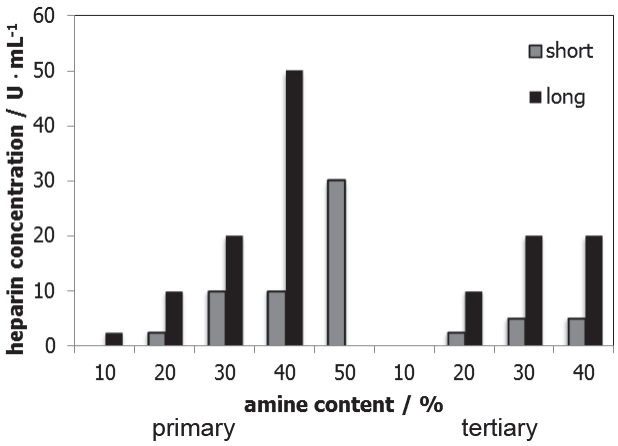

Figure 8. Polyplex stability: Dissociation assay of polyplexes formed at N/P 20. The bars represent the heparin concentration at which the polyplexes are dissociated.

Influence of the thioether position and higher amine content

The type of polymer side chain showed a high impact on the cytotoxicity and the TE. To test whether the location of the sulfur within the side chain has an influence on the properties another polymer (**s40hp**, Scheme 1), having a hexamethylene spacer between the sulfur and the amine, was prepared by thiol-ene photoaddition. The polymer exhibits the same total number of CH_2 groups in the side chain but a different position of the thioether group. Analysis of the TE (data not shown) and the cytotoxicity (Figure 9 A) yielded similar results as for the analogous **l40p** polymer. In detail, no TE and high cytotoxicity was observed. This proves that the cytotoxicity and TE is influenced by the side chain length and not by the location of the thioether group in the side chain.

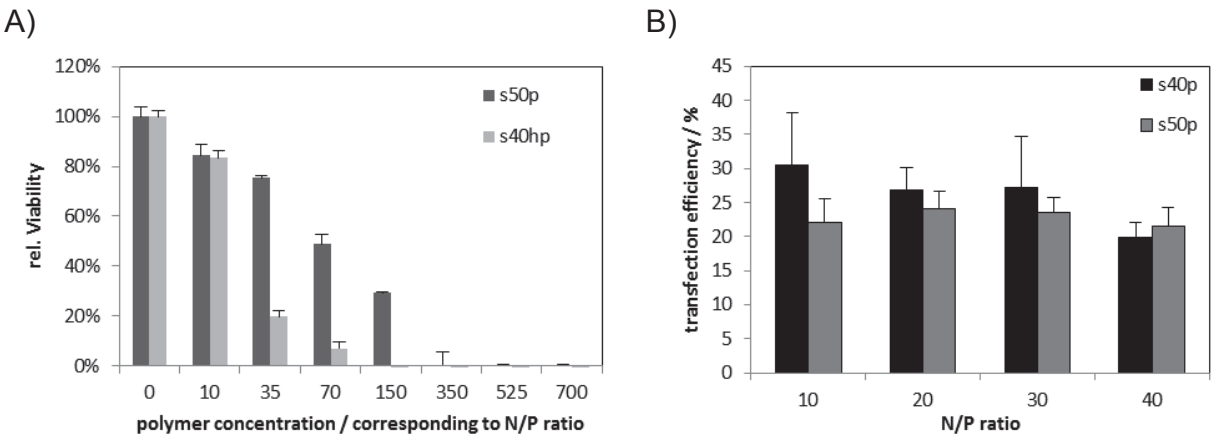

Figure 9. (A) Cytotoxicity of indicated polymers (s50p and s40hp) using AlamarBlue and L929 cells (n=3) and (B) transfection efficiency of indicated polymers for adherent HEK cells in serum reduced media at different N/P ratios.

Another question that arises is, if a higher amine content will lead to a further increased TE. Thus, a polymer with a short side chain and 50 mol% of primary amines was synthesized (**s50p**) according to the procedure described for the other **sNp** polymers (Scheme 1). Again, the TE and the cytotoxicity were investigated. For this polymer (**s50p**), the TE was slightly lower but showed no significant differences to the **s40p** polymer (Figure **9** B). However, it was cytotoxic at higher concentration (Figure **9** A), whereas for **s40p** no cytotoxicity was observed up to N/P ratio 700 (Figure **5** A). Since a higher amine content showed no advantage for the transfection process and an increased cytotoxity, the **s50p** was not investigated further. Obviously, the polymer **s40p** represents an optimal combination of cationic charges, hydrophobicity and biocompatible monomers for enhanced cellular interaction and transfection efficiency as well as reduced cytotoxicity.

Conclusion

Understanding the interplay between different parameters represents an important prerequisite for the development of non-toxic cationic polymers used as non-viral vectors in gene delivery applications. Here, we presented the synthesis and biological screening of an 18-membered 2-oxazoline-based copolymer library. Different parameters, such as the polymer side chain hydrophobicity, the type and content of amine groups were systematically varied. 2-Methyl-2-oxazoline as biocompatible "stealth" comonomer and 2-(9-decenyl)-2-oxazoline or 2-(3-butenyl)-2-oxazoline, respectively, have been copolymerized with varying ratios. Subsequent functionalization of the double bonds by thiol-ene photoaddition yielded cationic polymers with primary and tertiary amine groups. The influence of the different parameters on the pDNA condensation, the transfection efficiency, the cytotoxicity and cellular membrane interaction as well as the size, charge and stability of the polyplexes was investigated (Table 1).

It was found that independent of the amine content, long hydrophobic side chains enhance the pDNA condensation to the genetic material but interrupt the cellular membranes, leading to a higher cytotoxicity, hemolysis, and LDH release. Poly(2-oxazoline)s with short side chains and an amine content below 50 mol% were found to be biocompatible at all studied concentrations.

In addition, it was observed that primary amines are more suitable for an efficient binding and protection of pDNA. Here, an amine content of at least 40 mol% is necessary, since lower amine mol% revealed a decreased pDNA condensation. In case of tertiary amines the binding with pDNA was too weak for all investigated polymers. Hence, the pDNA was released into the transfection media or inside the endosomes, which resulted in a reduced TE.

In the end, we could identify one polymer, namely **s40p**, which showed superior properties over lPEI. High transfection efficiencies similar to that of lPEI and a faster internalization were

found. Most importantly, no cytotoxicity was observed in the tested concentration range. The presented study demonstrates the high potential of cationic poly(2-oxazoline)s for gene delivery and shows that it is possible to design cationic polymers having a high transfection efficiency while being non-toxic. Further investigations will be executed, in particular on the best performing polymer, to gain a deeper insight into the transfection mechanism.

Table 2. Overview of all polymers regarding their characteristics and bottlenecks for the transfection process. Probable reasons for transfection failure or drawbacks are described as comments. Toxicity (AlamarBlue), hemolysis and LDH were classified with 0 for no effect, 0.5 for middle occurrence, and 1 for high occurrence.

			EBA [%]	Size [nm]	ZP [mV]	Toxicity	Hemolysis	LDH	Uptake [%]	Heparin [U mg^{-1}]	TE [%]	Comments
Short hydrophobic side chain	primary amines	10	80	255	-4	0	0	-	-	0	0	no polyplex formation
		20	72	178	22	0	0	-	-	3	8	labile polyplex
		30	72	110	40	0	0	-	-	10	6	?
		40	60	94	23	0	0	0	90	10	31	best performer!
		50	60	51	47	1	-	-	-	30	24	increased toxicity
	teriary amines	10	82	151	-6	0	0	-	-	0	1	no polyplex formation
		20	68	158	19	0	0	-	-	3	8	labile polyplex
		30	64	124	29	0	0	-	-	5	5	?
		40	57	105	29	0	0	0	60	5	3	inefficient uptake
Long hydrophobic side chain	primary amines	10	69	152	-17	1	0	-	-	3	0	no polyplex formation
		20	46	105	28	1	1	-	-	10	6	toxic
		30	36	84	29	1	1	-	-	20	4	toxic
		40	30	97	34	1	1	1	80	50	6	toxic
	teriary amines	10	76	152	-9	0	0	-	-	0	0	no polyplex formation
		20	60	113	26	1	1	-	-	10	3	toxic
		30	50	84	30	1	1	-	-	20	6	toxic
		40	41	67	27	1	1	1	-	20	2	toxic
LPEI200			45	-	-	1	-	0	90	-	31	good performer but toxic

Supporting Information. Includes synthetic details, mass spectrometric and NMR characterization data of polymers, experimental descriptions, mean value and standard deviations

of the presented values. Supporting Information is available from the Wiley Online Library or from the author.

Acknowledgment

The authors want to thank the Dutch Polymer Institute (DPI, Technology area HTE). The Carl-Zeiss Foundation (JCSM Strukturantrag) are gratefully acknowledged. We like to thank Cornelia Bader and Anette Kuse for the scale-up synthesis of ButEnOx and DecEnOx. Furthermore, Carolin Fritzsche is gratefully acknowledged for the performance of the hemolysis, AlamarBlue, and EBA assays. Dr. Kristian Kempe is grateful to the Alexander von Humboldt-foundation for financial support.

References

[1] R. Duncan, R. Gaspar, *Mol. Pharm.* **2011**, *8*, 2101.

[2] K. Itaka, K. Kataoka, *Eur. J. Pharm. Biopharm.* **2009**, *71*, 475.

[3] R. J. Christie, N. Nishiyama, K. Kataoka, *Endocrinology* **2010**, *151*, 466.

[4] K. Miyata, N. Nishiyama, K. Kataoka, *Chem. Soc. Rev.* **2012**, *41*, 2562.

[5] K. A. Whitehead, R. Langer, D. G. Anderson, *Nat. Rev. Drug Discov.* **2009**, *8*, 129.

[6] A. Aied, U. Greiser, A. Pandit, W. Wang, *Drug Discov. Today* **2013**, *18*, 1090.

[7] S. Barua, J. Ramos, T. Potta, D. Taylor, H. C. Huang, G. Montanez, K. Rege, *Comb. Chem. High Throughput Screening* **2011**, *14*, 908.

[8] A. Basarkar, J. Singh, *Int. J. Nanomedicine* **2007**, *2*, 353.

[9] S. C. De Smedt, J. Demeester, W. E. Hennink, *Pharm. Res.* **2000**, *17*, 113.

[10] D. W. Pack, A. S. Hoffman, S. Pun, P. S. Stayton, *Nat. Rev. Drug Discov.* **2005**, *4*, 581.

[11] R. Duncan, *Nat. Rev. Drug Discov.* **2003**, *2*, 347.

[12] M. A. Mintzer, E. E. Simanek, *Chem. Rev.* **2008**, *109*, 259.

[13] M. Breunig, U. Lungwitz, R. Liebl, J. Klar, B. Obermayer, T. Blunk, A. Goepferich, *Biochimica et Biophysica Acta (BBA) - General Subjects* **2007**, *1770*, 196.

[14] W. T. Godbey, K. K. Wu, A. G. Mikos, *J. Control. Release* **1999**, *60*, 149.

[15] M. Jäger, S. Schubert, S. Ochrimenko, D. Fischer, U. S. Schubert, *Chem. Soc. Rev.* **2012**, *41*, 4755.

[16] O. M. Merkel, D. Librizzi, A. Pfestroff, T. Schurrat, K. Buyens, N. N. Sanders, S. C. De Smedt, M. Béhé, T. Kissel, *J. Control. Release* **2009**, *138*, 148.

[17] R. J. Christie, K. Miyata, Y. Matsumoto, T. Nomoto, D. Menasco, T. C. Lai, M. Pennisi, K. Osada, S. Fukushima, N. Nishiyama, Y. Yamasaki, K. Kataoka, *Biomacromolecules* **2011**, *12*, 3174.

[18] P. van de Wetering, J. Y. Cherng, H. Talsma, D. J. A. Crommelin, W. E. Hennink, *J. Control. Release* **1998**, *53*, 145.

[19] C. V. Synatschke, A. Schallon, V. Jerome, R. Freitag, A. H. E. Muller, *Biomacromolecules* **2011**, *12*, 4247.

[20] S. Agarwal, Y. Zhang, S. Maji, A. Greiner, *Materials Today* **2012**, *15*, 388.

[21] D. G. Anderson, A. Akinc, N. Hossain, R. Langer, *Mol. Ther.* **2005**, *11*, 426.

[22] P. van de Wetering, E. E. Moret, N. M. E. Schuurmans-Nieuwenbroek, M. J. van Steenbergen, W. E. Hennink, *Bioconjugate Chemistry* **1999**, *10*, 589.

[23] D. J. Chen, B. S. Majors, A. Zelikin, D. Putnam, *Journal of Controlled Release* **2005**, *103*, 273.

[24] Y. Yue, C. Wu, *Biomater. Sci.* **2013**, *1*, 152.

[25] S. Choksakulnimitr, S. Masuda, H. Tokuda, Y. Takakura, M. Hashida, *J. Control. Release* **1995**, *34*, 233.

[26] H. Lv, S. Zhang, B. Wang, S. Cui, J. Yan, *J. Control. Release* **2006**, *114*, 100.

[27] M. Lee, S. W. Kim, *Pharm. Res.* **2005**, *22*, 1.

[28] T. G. Park, J. H. Jeong, S. W. Kim, *Adv. Drug Deliver. Rev.* **2006**, *58*, 467.

[29] J. Dai, S. Zou, Y. Pei, D. Cheng, H. Ai, X. Shuai, *Biomaterials* **2011**, *32*, 1694.

[30] A. Mathew, H. Cao, E. Collin, W. Wang, A. Pandit, *Int. J. Pharm.* **2012**, *434*, 99.

[31] K. Knop, R. Hoogenboom, D. Fischer, U. S. Schubert, *Angew. Chem. Int. Ed.* **2010**, *49*, 6288.

[32] J. C. Fernandes, X. P. Qiu, F. M. Winnik, M. Benderdour, X. L. Zhang, K. R. Dai, Q. Shi, *Int. J. Nanomedicine* **2013**, *8*, 4091.

[33] G.-H. Hsiue, H.-Z. Chiang, C.-H. Wang, T.-M. Juang, *Bioconjugate Chem.* **2006**, *17*, 781.

[34] J. H. Jeong, S. H. Song, D. W. Lim, H. Lee, T. G. Park, *Journal of Controlled Release* **2001**, *73*, 391.

[35] Z. Zhong, J. Feijen, M. C. Lok, W. E. Hennink, L. V. Christensen, J. W. Yockman, Y.-H. Kim, S. W. Kim, *Biomacromolecules* **2005**, *6*, 3440.

[36] N. Adams, U. S. Schubert, *Adv. Drug Deliv. Rev.* **2007**, *59*, 1504.

[37] M. Bauer, C. Lautenschlaeger, K. Kempe, L. Tauhardt, U. S. Schubert, D. Fischer, *Macromol. Biosci.* **2012**, *12*, 986.

[38] J. Kronek, Z. Kroneková, J. Lustoň, E. Paulovičová, L. Paulovičová, B. Mendrek, *J. Mater. Sci.: Mater. Med.* **2011**, *22*, 1725.

[39] R. Luxenhofer, G. Sahay, A. Schulz, D. Alakhova, T. K. Bronich, R. Jordan, A. V. Kabanov, *J. Control. Release* **2011**, *153*, 73.

[40] A. Mero, G. Pasut, L. D. Via, M. W. M. Fijten, U. S. Schubert, R. Hoogenboom, F. M. Veronese, *J. Control. Release* **2008**, *125*, 87.

[41] T. X. Viegas, M. D. Bentley, J. M. Harris, Z. Fang, K. Yoon, B. Dizman, R. Weimer, A. Mero, G. Pasut, F. M. Veronese, *Bioconjugate Chem.* **2011**, *22*, 976.

[42] S. Zalipsky, C. B. Hansen, J. M. Oaks, T. M. Allen, *J. Pharm. Sci.* **1996**, *85*, 133.

[43] M. Bauer, S. Schroeder, L. Tauhardt, K. Kempe, U. S. Schubert, D. Fischer, *J. Polym. Sci., Part A: Polym. Chem.* **2013**, *51*, 1816.

[44] R. Hoogenboom, *Angew. Chem. Int. Ed.* **2009**, *48*, 7978.

[45] H. Schlaad, C. Diehl, A. Gress, M. Meyer, A. L. Demirel, Y. Nur, A. Bertin, *Macromol. Rapid Commun.* **2010**, *31*, 511.

[46] J. Ulbricht, R. Jordan, R. Luxenhofer, *Biomaterials* **2014**, *35*, 4848.

[47] R. Hoogenboom, M. W. M. Fijten, H. M. L. Thijs, B. M. van Lankvelt, U. S. Schubert, *Des. Monomers Polym.* **2005**, *8*, 659.

[48] R. Hoogenboom, R. M. Paulus, Å. Pilotti, U. S. Schubert, *Macromol. Rapid Commun.* **2006**, *27*, 1556.

[49] F. Wiesbrock, R. Hoogenboom, M. Leenen, S. F. G. M. van Nispen, M. van der Loop, C. H. Abeln, A. M. J. van den Berg, U. S. Schubert, *Macromolecules* **2005**, *38*, 7957.

[50] F. Wiesbrock, R. Hoogenboom, M. A. M. Leenen, M. A. R. Meier, U. S. Schubert, *Macromolecules* **2005**, *38*, 5025.

[51] S. Cesana, J. Auernheimer, R. Jordan, H. Kessler, O. Nuyken, *Macromol. Chem. Phys.* **2006**, *207*, 183.

[52] M. Hartlieb, D. Pretzel, K. Kempe, C. Fritzsche, R. M. Paulus, M. Gottschaldt, U. S. Schubert, *Soft Matter* **2013**, *9*, 4693.

[53] R. Konradi, B. Pidhatika, A. Muhlebach, M. Textor, *Langmuir* **2008**, *24*, 613.

[54] L. Tauhardt, K. Kempe, M. Gottschaldt, U. S. Schubert, *Chem. Soc. Rev.* **2013**, *42*, 7998.

[55] I. Banerjee, R. C. Pangule, R. S. Kane, *Adv. Mater.* **2011**, *23*, 690.

[56] J. Blümmel, N. Perschmann, D. Aydin, J. Drinjakovic, T. Surrey, M. Lopez-Garcia, H. Kessler, J. P. Spatz, *Biomaterials* **2007**, *28*, 4739.

[57] H. Hatakeyama, H. Akita, H. Harashima, *Adv. Drug Deliv. Rev.* **2011**, *63*, 152.

[58] Y. Ikeda, Y. Nagasaki, *J. Appl. Polym. Sci.* **2014**, *131*.

[59] J. A. Fortune, T. I. Novobrantseva, A. M. Klibanov, *J. Drug Deliv.* **2011**, *2011*, 204058.

[60] S. T. Kim, K. Saha, C. Kim, V. M. Rotello, *Acc. Chem. Res.* **2013**, *46*, 681.

[61] C. J. Waschinski, V. Herdes, F. Schueler, J. C. Tiller, *Macromol. Biosci.* **2005**, *5*, 149.

[62] A. Gress, A. Völkel, H. Schlaad, *Macromolecules* **2007**, *40*, 7928.

[63] K. Kempe, A. Vollrath, H. W. Schaefer, T. G. Poehlmann, C. Biskup, R. Hoogenboom, S. Hornig, U. S. Schubert, *Macromol. Rapid Commun.* **2010**, *31*, 1869.

[64] C. Diehl, H. Schlaad, *Macromol. Biosci.* **2009**, *9*, 157.

[65] K. Kempe, R. Hoogenboom, M. Jaeger, U. S. Schubert, *Macromolecules* **2011**, *44*, 6424.

[66] K. Kempe, R. Hoogenboom, U. S. Schubert, *Macromol. Rapid Commun.* **2011**, *32*, 1484.

[67] K. Kempe, T. Neuwirth, J. Czaplewska, M. Gottschaldt, R. Hoogenboom, U. S. Schubert, *Polym. Chem.* **2011**, *2*, 1737.

[68] T. R. Dargaville, R. Forster, B. L. Farrugia, K. Kempe, L. Voorhaar, U. S. Schubert, R. Hoogenboom, *Macromol. Rapid Commun.* **2012**, *33*, 1695.

[69] M. Litt, A. Levy, J. Herz, *J. Macromol. Sci., Part A: Pure Appl. Chem.* **1975**, *9*, 703.

[70] J. M. Warakomski, B. P. Thill, *J. Polym. Sci., Part A: Polym. Chem.* **1990**, *28*, 3551.

[71] K. Kempe, C. Weber, K. Babiuch, M. Gottschaldt, R. Hoogenboom, U. S. Schubert, *Biomacromolecules* **2011**, *12*, 2591.

[72] A. Baumgaertel, E. Altuntaş, K. Kempe, A. Crecelius, U. S. Schubert, *J. Polym. Sci., Part A: Polym. Chem.* **2010**, *48*, 5533.

[73] K. A. Howard, *Adv. Drug Deliv. Rev.* **2009**, *61*, 710.

[74] J. Ziebarth, Y. M. Wang, *Biophys. J.* **2009**, *97*, 1971.

[75] J. Rejman, V. Oberle, I. S. Zuhorn, D. Hoekstra, *Biochem. J.* **2004**, *377*, 159.

[76] D. Fischer, T. Bieber, Y. Li, H. P. Elsasser, T. Kissel, *Pharm. Res.* **1999**, *16*, 1273.

[77] H. Kim, S. C. Yoon, T. Y. Lee, D. Jeong, *Toxicol. Lett.* **2009**, *184*, 13.

[78] A. Schallon, V. Jérôme, A. Walther, C. V. Synatschke, A. H. E. Müller, R. Freitag, *React. Funct. Polym.* **2010**, *70*, 1.

[79] M. Ogris, E. Wagner, P. Steinlein, *Bba-Gen Subjects* **2000**, *1474*, 237.

[80] J. Zhou, J. Liu, C. J. Cheng, T. R. Patel, C. E. Weller, J. M. Piepmeier, Z. Jiang, W. M. Saltzman, *Nat. Mater.* **2012**, *11*, 82.

Supporting Information

A cationic poly(2-oxazoline) with high *in vitro* transfection efficiency identified by a library approach

Alexandra C. Rinkenauer,[1,2‡] Lutz Tauhardt,[1,2‡] Felix Wendler,[1,2] Kristian Kempe,[1,2 †] Michael Gottschaldt,[1,2] Anja Träger,[1,2] Ulrich S. Schubert [1,2,3]**

[‡] *both authors contributed equally*

[1]Laboratory of Organic and Macromolecular Chemistry (IOMC), Friedrich Schiller University Jena, Humboldtstrasse 10, 07743 Jena, Germany

[2]Jena Center for Soft Matter (JCSM), Friedrich Schiller University Jena, Philosophenweg 7, 07743 Jena, Germany

[3]Dutch Polymer Institute (DPI), John F. Kennedylaan 2, 5612 AB Eindhoven, The Netherlands.

[†]Current address: Department of Chemical and Biomolecular Engineering, The University of Melbourne, Victoria 3010, Australia

*Address correspondence to: ulrich.schubert@uni-jena.de; anja.traeger@uni-jena.de

Results Section

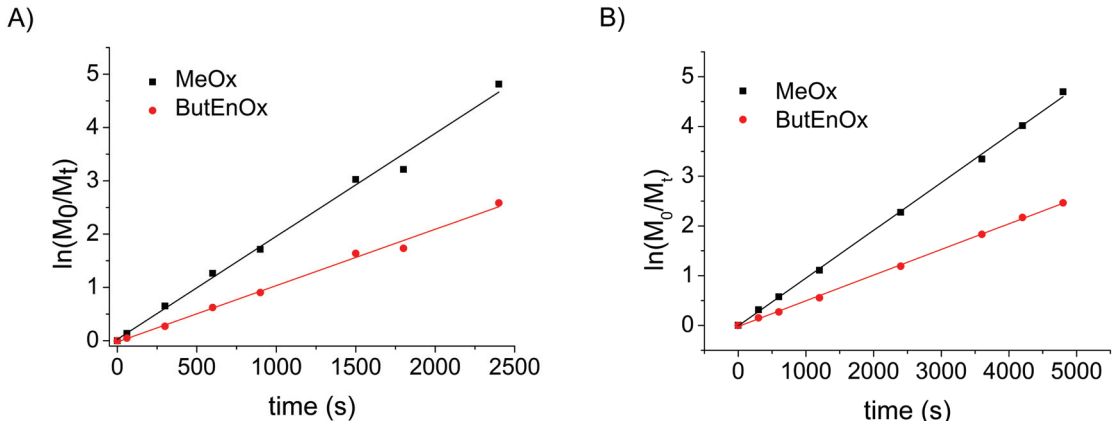

Figure S1. First-order kinetic plots of the copolymerization of MeOx and ButEnOx in acetonitrile at 140 °C for A) MeOx : ButEnOx = 90 : 10(kp_{MeOx} = 0.095 L mol^{-1} s^{-1}; $kp_{ButEnOx}$ = 0.052 L mol^{-1} s^{-1}) and for B) MeOx : ButEnOx = 180 : 20 (kp_{MeOx} = 0.097 L mol^{-1} s^{-1}; $kp_{ButEnOx}$ = 0.052 L mol^{-1} s^{-1}). The conversion was determined by gas chromatography.

Table S1. Kinetic and SEC Data for the copolymerization of MeOx and ButEnOx.

$MeOx_{90}$-*co*-$ButEnOx_{10}$				$MeOx_{180}$-*co*-$ButEnOx_{20}$			
Time [s]	MeOx : ButEnOx [%][a)]	M_n [g mol^{-1}][b)]	$Đ_M$[b)]	Time [s]	MeOx : ButEnOx [%][a)]	M_n [g mol^{-1}][b)]	$Đ_M$[b)]
60	13 : 5	2,200	1.10	1	1 : 0	-	-
300	48 : 24	5,780	1.11	300	27 : 14	6,510	1.20
600	72 : 46	7,400	1.13	600	44 : 24	8,690	1.28
900	82 : 59	8,310	1.14	1200	67 : 43	11,560	1.34
1500	95 : 80	9,190	1.15	2400	90 : 70	14,690	1.39
1800	96 : 82	9,470	1.16	3600	96 : 84	15,650	1.43
2400	99 : 92	9,550	1.16	4200	98 : 89	16,470	1.43
				4800	99 : 91	16,140	1.40

[a)]Conversion determined by gas chromatography. [b)]Determined by SEC.

Table S2. SEC Data of the different copolymers.

MeOx-*co*-ButEnOx				MeOx-*co*-DecEnOx			
Sample	MeOx : ButEnOx	M_n (g/mol)	$Đ_M$	Sample	MeOx : DecEnOx	M_n (g/mol)	$Đ_M$
1a	180 : 20	22,800	1.43	**2a**	180 : 20	19,800	1.47
1b	160 : 40	23,300	1.46	**2b**	160 : 40	25,500	1.47
1c	140 : 60	23,300	1.49	**2c**	140 : 60	19,800	1.45
1d	120 : 80	22,200	1.56	**2d**	120 : 80	22,900	1.63
1e	100 : 100	20,300	1.48				
3a	180 : 20	26,000	1.43	**4a**	180 : 20	-	-
3b	160 : 40	29,000	1.46	**4b**	160 : 40	-	-
3c	140 : 60	29,500	1.47	**4c**	140 : 60	-	-
3d	120 : 80	32,000	1.50	**4d**	120 : 80	-	-
3e	100 : 100	27,700	1.47				
s10p	180 : 20	24,100	1.44	**l10p**	180 : 20	23,600	1.51
s20p	160 : 40	23,200	1.40	**l20p**	160 : 40	31,600	1.43
s30p	140 : 60	27,400	1.40	**l30p**	140 : 60	30,500	1.54
s40p	120 : 80	29,100	1.52	**l40p**	120 : 80	38,100	1.62
s50p	100 : 100	28,500	1.26				
s10t	180 : 20	20,440	1.43	**l10t**	180 : 20	20,300	1.49
s20t	160 : 40	19,560	1.43	**l20t**	160 : 40	28,100	1.47
s30t	140 : 60	18,120	1.45	**l30t**	140 : 60	23,900	1.37
s40t	120 : 80	20,180	1.35	**l40t**	120 : 80	30,300	1.57
s40hp	120 : 80	34,200	1.31				

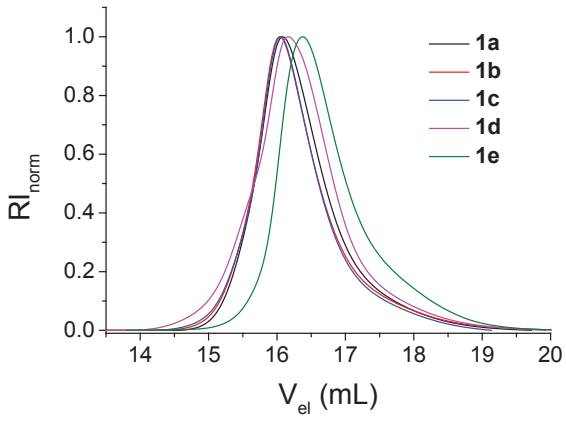

Figure S2. SEC curves of the P(MeOx-*grad*-ButEnOx).

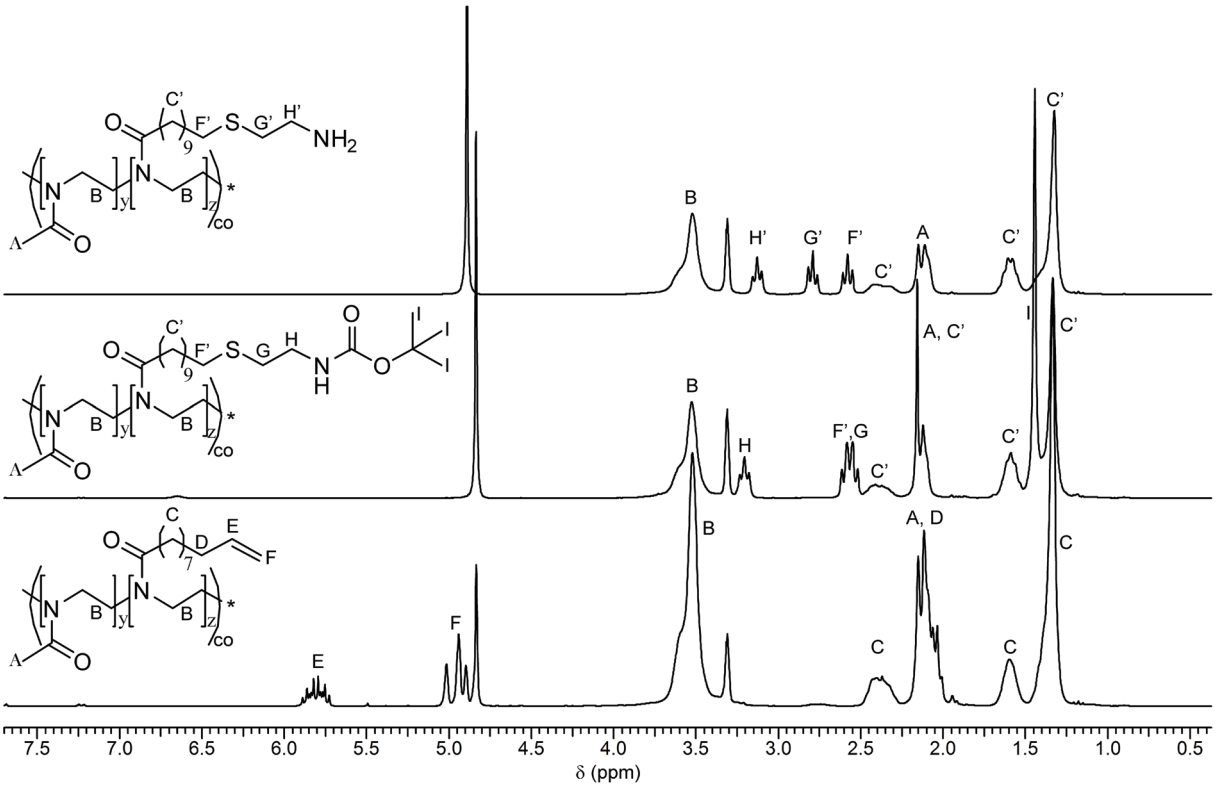

Figure S3. ^{1}H NMR spectra of **2d** (bottom), **4d** (middle), and **l40p** (top) (250 MHz, solvent: CD_3OD).

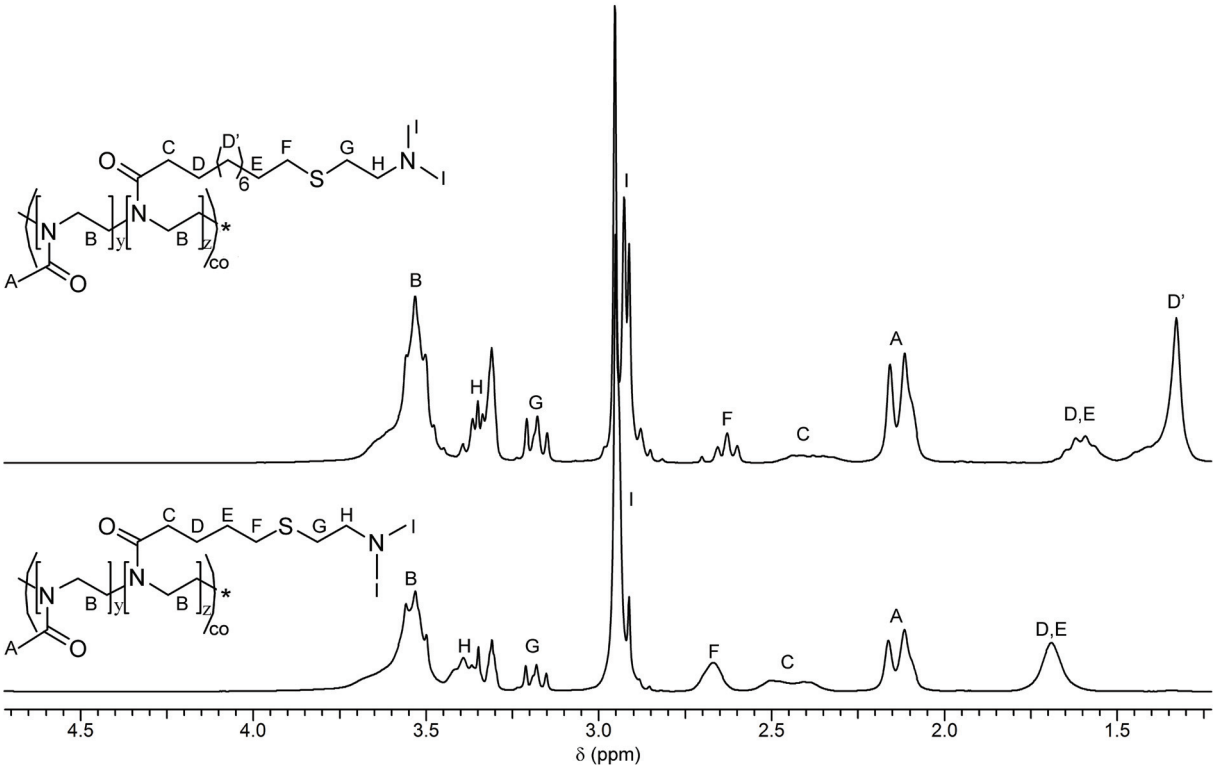

Figure S4. ^{1}H NMR spectra of **s40t** (bottom) and **l40t** (top) (250 MHz, solvent: CD_3OD).

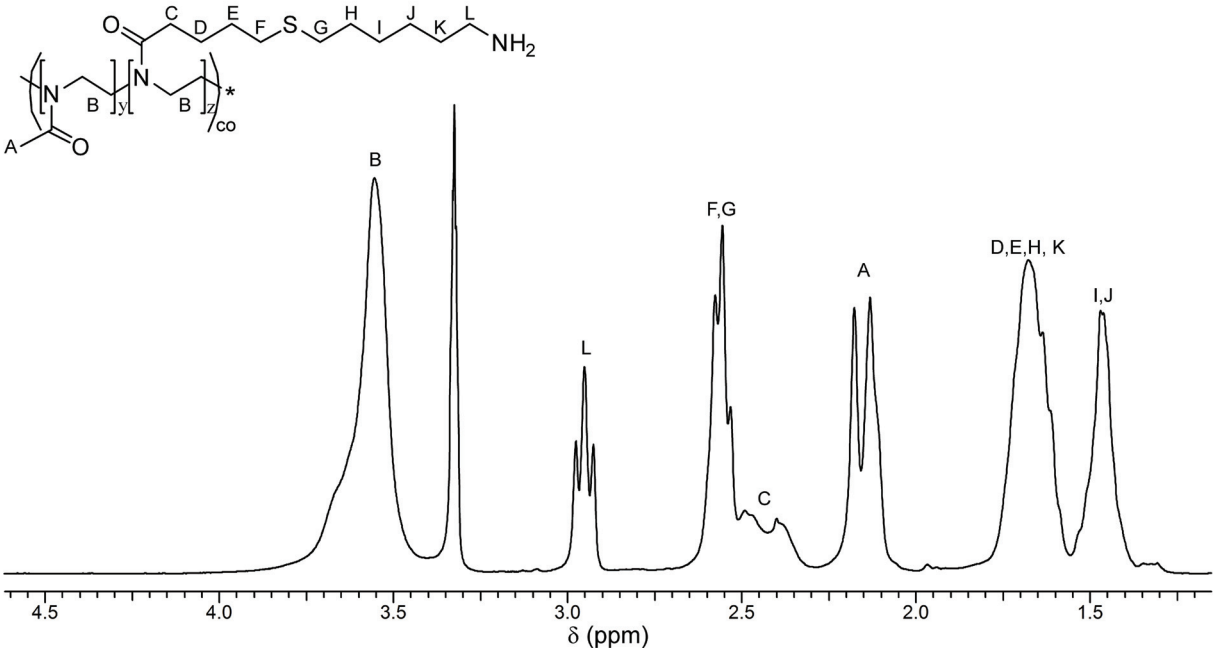

Figure S5. ^{1}H NMR spectrum of **s40hp** (300 MHz, solvent: CD_3OD).

Ethidium bromide binding assay

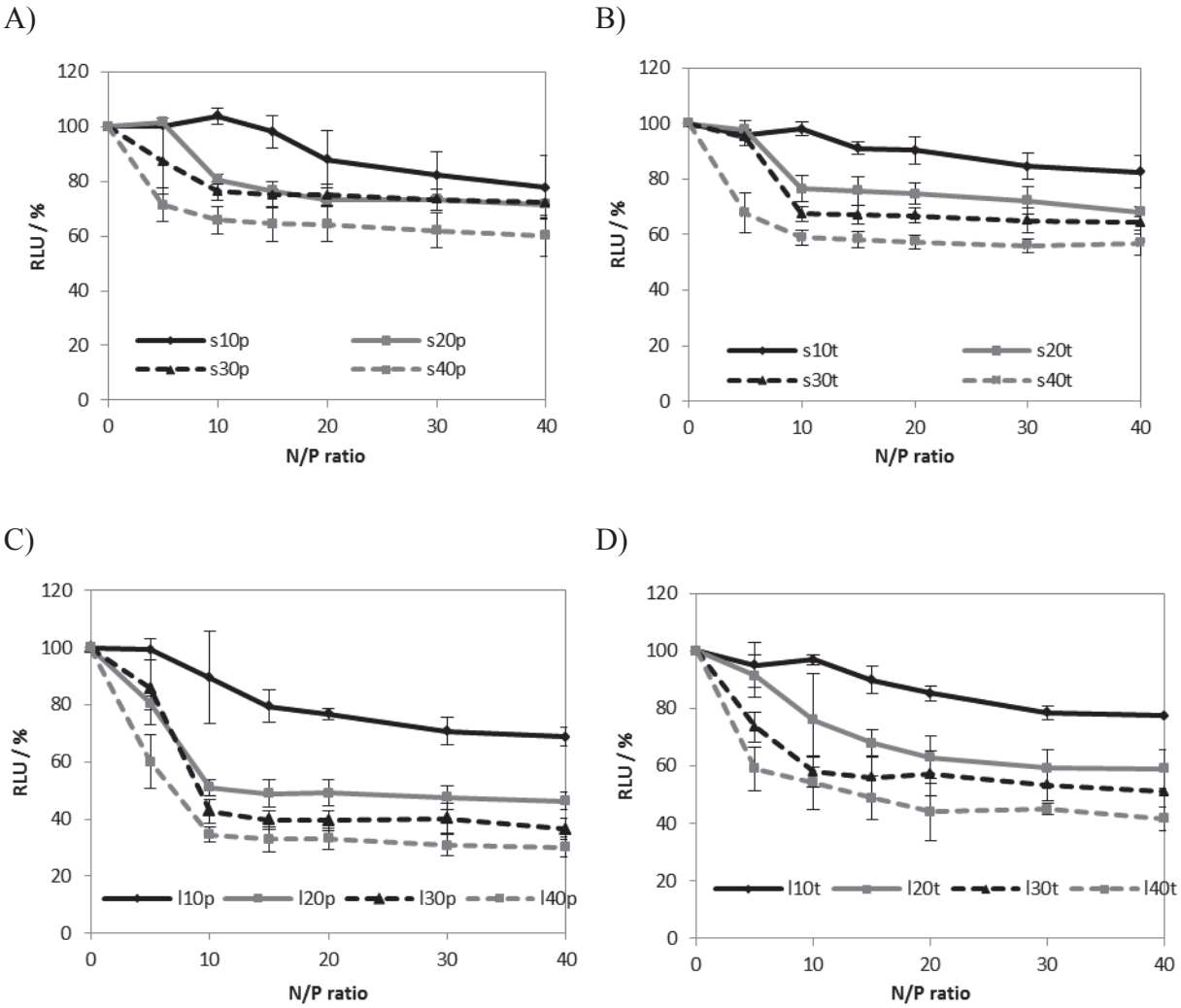

Figure S6. pDNA condensation of all 16 polymers with pDNA measured at physiological pH *via* EBA at indicated N/P ratios (n = 3).

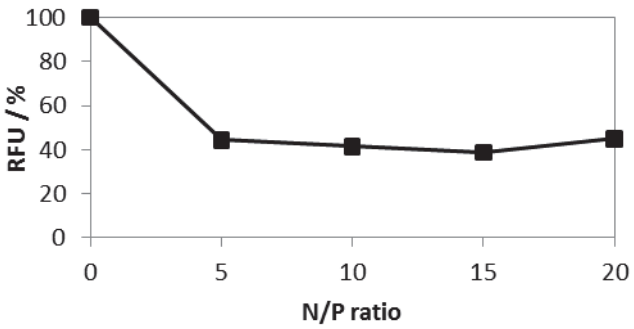

Figure S7. pDNA condensation of lPEI (DP = 200) with pDNA measured at physiological pH *via* EBA (n = 3).

Transfection efficiency

Table S3. Transfection efficiency: Raw data and standard derivation of all polymer at the indicated N/P ratio (n = 3).

N/P ratio	Sample	TE / %	SD	Sample	TE / %	SD	Sample	TE / %	SD	Sample	TE / %	SD
10	**s10p**	0.33	0.57	**s10t**	1.15	1.63	**l10p**	0	0	**l10t**	0.33	0.58
20		0.67	0.57		0.85	1.2		0	0		0	0
30		0.67	0.57		0.5	0.71		0	0		0.17	0.29
40		0	0		0	0		0	0		0.77	0.40
10	**s20p**	4.73	3.59	**s20t**	2.65	3.75	**l20p**	3.65	3.89	**l20t**	0.43	0.35
20		8.7	8.16		7.8	0.99		4.2	4.53		2.1	1.51
30		5.27	2.34		2.55	0.07		3.75	0.21		1.37	0.49
40		5.33	1.38		1	0		6.1	0		2.52	1.35
10	**s30p**	3.4	0.2	**s30t**	5.15	4.31	**l30p**	2.4	2.26	**l30t**	6.48	3.76
20		2.73	1.16		2.35	1.91		3.95	3.04		2.98	2.4
30		5.33	2.97		2.05	1.77		2.65	1.63		1	0
40		5.77	2.91		0.5	0		2.7	2.97		1	0
10	**s40p**	30.5	7.64	**s40t**	2.25	1.77	**l40p**	2.7	0.85	**l40t**	1.33	0.58
20		26.77	3.30		3.2	1.56		5.85	3.89		1	0
30		27.17	7.51		3.05	2.19		7.4	3.25		0.67	0.58
40		19.93	2.15		2.8	0		8.8	5.52		0.33	0.58
10	**s50p**	22.1	3.55	**lPEI200**	31.27	1.75						
20		24.07	2.54		25.23	8.81						
30		23.63	2.17		12.17	11.6						
40		21.6	2.63		4.57	6.18						

Polyplex properties PDI^P

Besides size and zeta potential, also the PDI^P was measured.

A)

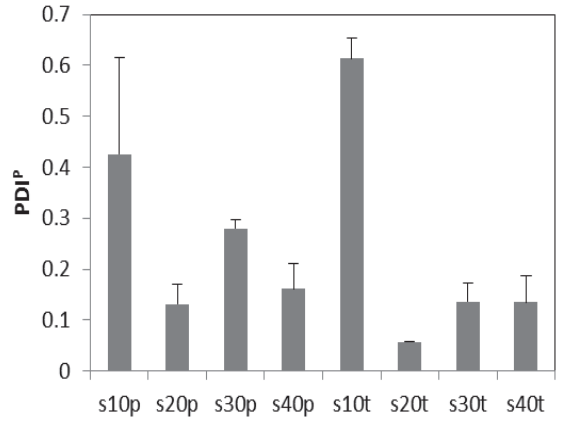

B)

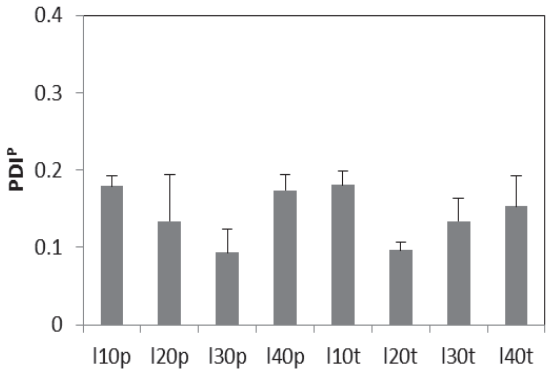

Figure S8. PDIs of the polyplexes prepared at NP ratio of 20.

Cytotoxicity and hemolysis assay

Table S4. Raw data with standard derivation for cytotoxicity (IC50) and hemolysis assay at the indicated polymer concentration.

			Toxicity		**Hemolysis**					
					raw data			STAB		
			IC_{50}	STAB	**10 µg/mL**	**50 µg/mL**	**100 µg/mL**	**10 µg/mL**	**50 µg/mL**	**100 µg/mL**
Short hydrophobic side chain	**primary amines**	**10**	0	-	0.0999	0.0544	0.1872	0.0269	0.0059	0.0642
		20	0	-	0.402	1.5459	2.5634	0.144	0.2172	0.4657
		30	0	-	0.0938	0.1925	0.188	0.0143	0.0291	0.0539
		40	0	-	0.5647	1.6672	2.8517	0.1148	0.0924	0.3764
		50	1	-	-	-	-	-	-	-
	teriary amines	**10**	0	-	0.47	0.57	0.71	3E-05	1E-07	3E-07
		20	0	-	0.76	0.56	0.47	4E-07	2E-07	7E-08
		30	0	-	0.55	0.57	0.69	0.5488	0.572	0.6938
		40	0	-	0.80	0.68	0.80	0.7989	0.6844	0.796
Long hydrophobic side chain	**primary amines**	**10**	0	0	0.8589	1.802	1.6973	0.1767	0.544	0.6171
		20	5	0.0794	83.206	107.42	107.07	27.032	44.606	45.089
		30	4.7127	0.0157	105	124.21	102.13	40.686	43.969	41.632
		40	34.853	0.0619	106.8	104.16	108.75	44.857	43.014	43.779
	teriary amines	**10**	0	0	0.6555	0.6133	0.7276	0.0616	0.0185	0.045
		20	13.795	0.059	10.204	50.688	85.833	0.4399	3.4895	3.3771
		30	13.795	0.0393	62.046	101.21	94.963	5.8019	5.557	17.997
		40	4.5983	0.1263	102.47	100.68	99.833	1.0602	3.8171	2.8269

Uptake studies

Table S5. Raw data and standard derivation of time dependent uptake kinetic.

	1 h		2 h		3 h		4 h	
	amount of cells / %	STAB	amount of cells / %	STAB	amount of cells / %	STAB	amount of cells / %	STAB
pDNA	0.3	0.2646	0.25	0.2121	0.65	0.495	0.4666667	0.1155
s40p	81.233333	7.9223	70	19	74.2	4.3841	73.4	3.2512
s40t	37.85	2.6163	38.9	0	48.05	16.9	53.7	4.1328
l40p	24.666667	6.8712	41.25	6.1518	69.65	16.051	74	14.47
l40t	0	0	0	0	0	0	0	0
lPEI200	33.8	0.8485	47.45	0.2121	81.85	13.647	88.033333	6.3058

Dissociation assay

A)

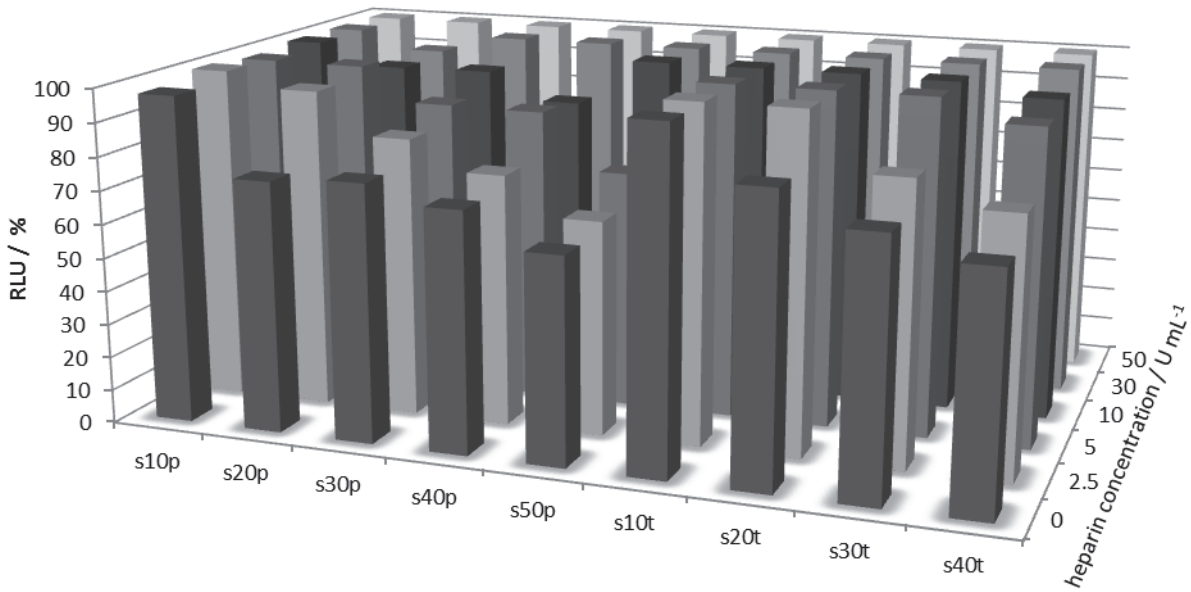

B)

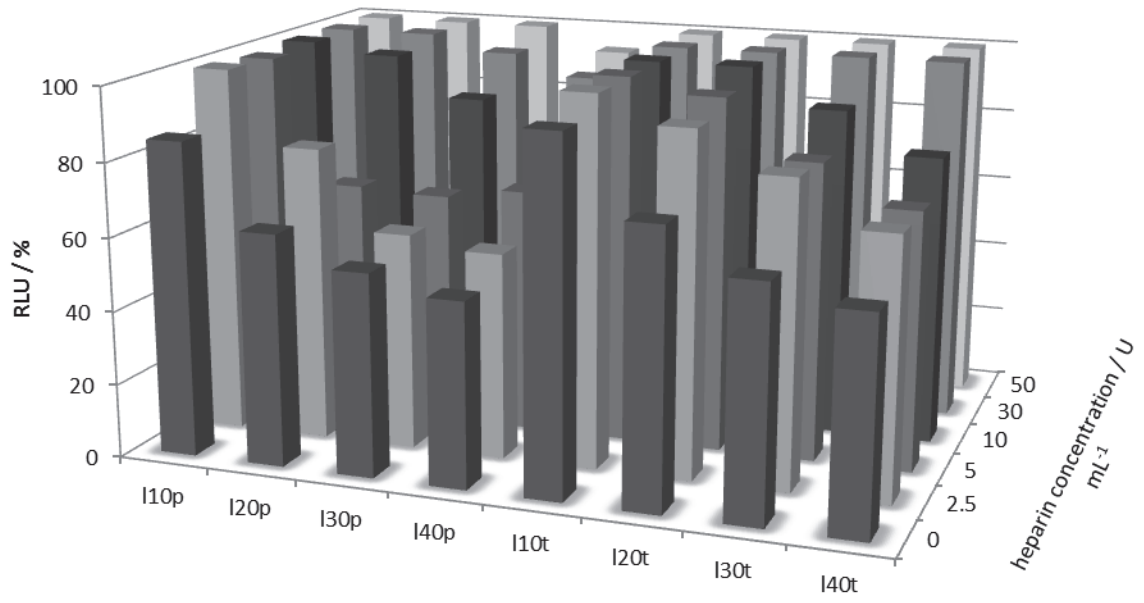

Figure S9. Dissociation assay with the indicated heparin concentration.

Experimental Section

Chemicals and instrumentation

Dry acetonitrile, MeOx and methyl tosylate (MeOTs) were obtained from Acros Organics. ButEnOx[1] and DecEnOx[2] were prepared according to literature procedure. All compounds were distilled to dryness over barium oxide (BaO), and stored under nitrogen. 2-(Boc-amino)ethanethiol and 2-dimethylaminoethanethiol hydrochloride were purchased from Sigma Aldrich.

Ethidium bromide solution 1% was purchased from Carl Roth (Karlsruhe, Germany). AlamarBlue and YOYO-1 was obtained from Life Technologies (Darmstadt, Germany). If not stated otherwise, cell culture materials, cell culture media, and solutions were obtained from PAA (Pasching, Austria). Plasmid pEGFP-N1 (4.7 kb, Clontech, USA) was isolated using Qiagen Giga plasmid Kit (Hilden, Germany). The CytoTox-One homogenous membrane integrity assay (LDH) was purchased from Promega (Mannheim, Germany) All other chemicals were purchased from Sigma Aldrich (Steinhausen, Germany) and are of analytical grade or better and used without further purification.

The Initiator Sixty single-mode microwave synthesizer from Biotage, equipped with a noninvasive IR sensor (accuracy: ±2%), was used for polymerizations microwave irradiation. Prior to use, the microwave vials were heated to 110 °C overnight and allowed to cool to room temperature under a nitrogen atmosphere. Proton (^{1}H) nuclear magnetic resonance (NMR) spectra were recorded on a Bruker AC 250 MHz at 298 K. Chemical shifts are reported in parts per million (ppm, δ scale) relative to the residual signal of the deuterated solvent. Size exclusion chromatographies (SEC) were measured on an Agilent Technologies 1200 Series gel permeation chromatography system equipped with a G1329A autosampler, a G131A isocratic pump, a G1362A refractive index detector, and both a PSS Gram 30 and a PSS Gram 1000 column placed in series. As eluent a 0.21% LiCl solution in *N,N*-

dimethylacetamide (DMAc) was used at 1 mL min-1 flow rate and a column oven temperature of 40 °C. Molar masses were calculated against poly(styrene).

Gas chromatography (GC) was measured on a Shimadzu GC-2010 VP equipped with an AOC-20s autosampler, an AOC-20i injector, a FID detector, a Restek Rtx-5 column (30 m length, 0.25 mm inner diameter, 0.25 μm film thickness, stationary phase: 5% diphenyl/95% dimethyl polysiloxane), and chloroform as solvent.

Kinetic investigation of the synthesis of P(MeOx-*co*-ButEnOx)

For the kinetic studies, a stock solution containing initiator (MeOTs), monomer (MeOx and ButEnOx), and solvent (acetonitrile) was prepared. The total monomer concentration was adjusted to 2 M with a total monomer to initiator ratio ([M]/[I]) = 100 with 10 mol% of ButEnOx. The stock solution was divided over seven microwave vials and capped under argon. For the calculation of the conversion a t_0 samples was taken. The vials were heated in the microwave synthesizer at 140 °C for different times. After cooling, the reaction was quenched. The monomer conversion was determined GC using the polymerization solvent as internal standard.

Synthesis of P(MeOx-*co*-ButEnOx) (1a-d) and P(MeOx-*co*-DecEnOx) (2a-d)

A solution of initiator (MeOTs), monomers (MeOx, and ButEnOx or DecEnOx), and solvent (acetonitrile) was prepared. The total monomer to initiator ratio was [M]/[I] = 200, with a ButEnOx/DecEnOx amount of 10, 20, 30, and 40 mol%, respectively (corresponding to 20, 40, 60, and 80 repeating units). For MeOx/ButEnOx also a 50 mol% solution was prepared (corresponding to 100 ButEnOx repeating units). The total monomer concentration was adjusted to of 4 M. The solution was heated in a microwave synthesizer for a predetermined time at 140 °C. After cooling to room temperature a sample was taken and the conversion was determined by ^{1}H NMR. The solvent was removed under reduced pressure.

The residue was dissolved in dichloromethane and precipitated into ice-cold diethyl ether. After filtration the polymer was dried at 40 °C for 3 days under reduced pressure.

Thiol-ene functionalization of P(MeOx-*co*-ButEnOx) with 2-(boc-amino)ethanethiol (3a-d)

A 5% solution of P(MeOx-*stat*-ButEnOx), 0.1 mol% 2,2-dimethoxy-2-phenylacetophenone (DMPA) per double bond, and a 10-fold excess per double bond of 2-(boc-amino)ethanethiol in ethanol was prepared. After degassing with nitrogen for 30 min, the reaction mixture was stirred in a UV chamber (λ = 365 nm) overnight, and the polymer was precipitated in ice-cold diethyl ether. After filtration the polymer was dried under reduced pressure for 3 days at 40 °C.

Thiol-ene funtionalization of P(MeOx-*co*-DecEnOx) with 2-(boc-amino)ethanethiol (4a-d)

A 5% solution of P(MeOx-*stat*-DecEnOx), 0.1 mol% 2,2-dimethoxy-2-phenylacetophenone (DMPA) per double bond, and a 10-fold excess per double bond of 2-(boc-amino)ethanethiol in tetrahydrofurane was prepared. After degassing with nitrogen for 30 min, the reaction mixture was stirred in a UV chamber (λ = 365 nm) overnight, and the polymer was precipitated in ice-cold diethyl ether. After filtration the polymer was dried under reduced pressure for 3 days at 40 °C.

Deprotection of P(MeOx-*co*-bocAmButEnOx) (sNp) and P(MeOx-*co*-bocAmDecEnOx) (lNp)

The polymer dissolved in dichloromethane (3 mL). Trifluoracetic acid was added (5 mL) and the reaction mixture was stirred overnight at room temperature. After the addition of methanol, the polymer was precipitated in ice-cold diethyl ether. The precipitate was filtered,

dissolved in methanol and stirred over night with Amberlyst® A21 (free base). The solvent was removed and polymer dried at 40 °C under reduced pressure for 3 days.

Thiol-ene funtionalization of P(MeOx-*co*-ButEnOx) (sNt) and P(MeOx-*co*-DecEnOx) (lNt) with 2-dimethylaminoethanethiol hydrochloride

A 5% solution of P(MeOx-*stat*-ButEnOx) or P(MeOx-*stat*-DecEnOx), respectively, 0.1 mol% 2,2-dimethoxy-2-phenylacetophenone (DMPA) per double bond, and a 10-fold excess per double bond of 2-dimethylaminoethanethiol hydrochloride in methanol was prepared. After degassing with nitrogen for 30 min, the reaction mixture was stirred in a UV chamber (λ = 365 nm) overnight. The reaction mixture was concentrated and purified by size exclusion chromatography using Sephadex® LH-20 running with methanol. The product was dried at 40 °C for 3 days.

Thiol-ene funtionalization of P(MeOx-co-ButEnOx) with 6-amino-1-hexanethiol hydrochloride (s40hp)

A 5% solution of P(MeOx-*stat*-ButEnOx) (**1d**), 0.1 mol% 2,2-dimethoxy-2-phenylacetophenone (DMPA) per double bond, and a 2-fold excess per double bond in methanol was prepared. After degassing with nitrogen for 30 min, the reaction mixture was stirred in a UV chamber (λ = 365 nm) overnight. The reaction mixture was concentrated and purified by size exclusion chromatography using Sephadex® LH-20 running with methanol. The product was dried at 40 °C for 3 days.

Polyplex preparation

Polyplexes of pDNA and polymers were prepared by mixing stock solutions of pDNA and polymers at a certain N/P ratio (nitrogen of polymer to phosphate of pDNA ratio) with 15 µg mL^{-1} pDNA solution in HBG buffer (20 mM 4-(2-hydroxethyl) piperazine-1-ethanesulfonic

acid (HEPES) and 5% (w/v) glucose, pH 7.2). Subsequently, the solutions were vortexed for 10 sec at maximal speed, and incubated at room temperature for 20 min.

Ethidium bromide quenching assay

The polyplex formation of pDNA and polymers was detected by quenching of the ethidium bromide (EB) fluorescence as described previously.[3] Briefly, 15 µg mL^{-1} pDNA in a total volume of 100 µL HBG (hepes buffered glucose) were incubated with EB (0.4 µg mL^{-1}) for 10 min at room temperature. Then, polyplexes with increasing amounts of indicated polymers were prepared in black 96-well plates (Nunc, Langenselbold, Germany). The samples were equilibrated for 10 min before the fluorescence was measured using a Tecan Genios Pro fluorescence microplate reader (Tecan, Crailsheim, Germany); the excitation and emission wavelength were 525 and 605 nm, respectively. A sample containing only pDNA and EB was used to calibrate the device to 100% fluorescence against a background of 0.4 µg mL^{-1} of EB in HBG solution. The percentage of dye displaced upon polyplex formation was calculated using equation (1):

$$\mathrm{RFU}\ [\%] = \frac{F_{sample} - F_0}{F_{pDNA} - F_0} \qquad (1)$$

Here, RFU is the relative fluorescence and F_{sample}, F_0, and F_{pDNA} are the fluorescence intensities of a given sample, the EB in HBG alone, and the EB intercalated into pDNA alone.

Cytotoxicity

The cytotoxicity was tested with L929 cells, as this sensitive cell line is recommended by ISO10993-5. In detail, cells were seeded at 10^4 cells per well in a 96-well plate and incubated for 24 h. No cells were seeded in the outer wells. After exchanging the media with fresh one and 30 min incubation, polymers at the indicated end concentrations were added, and the cells

were incubated at 37 °C for further 24 h. Subsequently, the medium was replaced by fresh media and AlamarBlue as recommended by the supplier. After incubation for 4 h, the fluorescence was measured at Ex 570/Em 610 nm, with untreated cells on the same well plate serving as controls. The experiments were performed independently three times.

Dynamic and electrophoretic light scattering

Dynamic light scattering (DLS) was performed on an ALV-CGS-3 system (ALV, Langen, Germany) equipped with a He-Ne laser operating at a wavelength of $\lambda = 633$ nm. The counts were detected at an angle of 90°. All measurements were carried out at 25 °C after an equilibration time of 120 sec. For analyzing the autocorrelation function (ACF), the CONTIN algorithm[4] was applied. Apparent hydrodynamic radii were calculated according to the Stokes–Einstein equation.

Electrophoretic light scattering was used to measure the electrokinetic potential, also known as zeta potential. The measurements were performed on a Zetasizer Nano ZS (Malvern Instruments, Herrenberg, Germany) by applying laser Doppler velocimetry.[5] For each measurement, 20 runs were carried out using the slow-field reversal and fast-field reversal mode at 150 V. Each experiment was performed in triplicate at 25 °C. The zeta potential (ζ) was calculated from the electrophoretic mobility (μ) according to the Henry Equation. Henry coefficient f(ka) was calculated according to Oshima.[6]

Transfection of adherent cells

HEK-293 cells (CRL-1573, ATCC) cells were maintained in RPMI 1640 culture medium, L929 cells (CCL-1, ATCC) in DMEM culture medium. Both media were supplemented with 10% fetal calf serum (FCS), 100 $\mu g\ mL^{-1}$ streptomycin, 100 IU mL^{-1} penicillin, and 2 mM L-glutamine. Cells were cultivated at 37 °C in a humidified 5% CO_2 atmosphere.

For transfection of the adherent cell lines, cells were seeded at a density of 10^4 cells per well in 24-well plates one day before transfection. One hour prior to transfection, cells were rinsed with PBS and supplemented with 1 mL OptiMEM (Life Technologies) or fresh serum containing growth media (without antibiotics). After polyplexes formation (as described above "polyplexes formation"), the polyplexes (100 µL) were added to the cells and the plates were incubated for 4 h in the incubator. Afterwards, the supernatant was replaced by1 mL of fresh growth medium, and the cells were further incubated for 20 h. For analysis, adherent cells were harvested by trypsinization.

For determination of the viability during flow cytometry, dead cells were identified via counterstaining with propidium iodide. The relative expression of EGFP fluorescence of 10^4 cells was quantified via flow cytometry using a Cytomics FC 500 (Beckman Coulter). For determination of the transfection efficiency viable cells expressing EGFP were gated. The experiments were performed independently three times.

Hemolysis assay

The membrane damaging properties of the polymers were quantified by analyzing the release of hemoglobin from human erythrocytes. The hemolysis assay was performed as described before.[7] Briefly, blood from sheep was centrifuged at 4.500 × g for 5 min and the pellet was washed three times with cold DPBS. The stock solutions were diluted in HBG of indicated pH, and polymer solutions were prepared in HBG buffer as well. 100 µL of each solution were mixed and further incubated for 60 min at 37 °C. The release of hemoglobin in the supernatant was determined at 580 nm after centrifugation (2,400 g for 5 min). The absorbance was measured using a plate reader (Genios Pro, Tecan, Germany). For comparison, collected erythrocytes were washed with DPBS and either lysed with 1% Triton X-100 yielding the 100% lysis control value (A_{100}) or resuspended in DPBS as reference (A_0).

The analysis was repeated with blood from at least six independent donors. The hemolytic activity of the polycations was calculated as follow (2):

$$\% \text{ Hemolysis} = 100 * \frac{(A_{sample} - A_0)}{(A_{100} - A_0)} \quad (2)$$

Here, A_{sample}, A_0, and A_{100} are the absorbance intensities of a given sample, erythrocytes incubated with DPBS, and erythrocytes lysed with Titon X-100.

Lactate dehydrogenase (LDH) assay

For the LDH assay the CytoTox-ONE homogenouse membrane integrity assay was used. The assay was performed as recommended by the supplier. The samples (polymer as well as polyplexes) were incubated for 1 h with adHEK cells.

Plasmid DNA labeling

For labeling of a 1 µg pDNA, 0.026 µL of 1M YOYO-1 solution was mixed with pDNA in 20 µL of pure water. The solution was incubated for 1 h at room temperature protected from light, before HBG was added to the used pDNA concentration described before. Polymers were added at the indicated N/P ratio, and the polyplex solution was treated as described before and added to the cells. After the indicated time points of incubation, the cells were harvested and 10% trypan blue was added to quench the outer fluorescence of cells and identify only those cells, which have taken up the genetic material. To determine the relative uptake of NPs, 10,000 cells were measured by flow cytometry and the amount of viable cells showing YOYO-1 signal were gated. For measuring the mean fluorescence intensity, all viable cells were measured.

Heparin dissociation assay

To investigate the release of pDNA from polyplexes, the heparin dissociation assay was used. For this purpose, 15 µg mL^{-1} pDNA were incubated for 10 min with EB (0.4 µg mL^{-1}) in a total volume of 100 µL HBG before polyplexes at N/P 20 were formed. After 15 min in the dark the polyplexes were transferred into black 96-well plates, and heparin was added at the indicated concentrations. The solution was mixed and incubated for further 30 min at 37 °C in the dark. The fluorescence of EB (Ex 525 nm / Em 605 nm) was measured, and the percentage of intercalated EB was calculated as described before (1).

Statistical analysis

The values represent the mean ± SD. For the calculation of the standard derivation of two different groups the two sample t-test (student's t-test) was used. Statistical significant was defined with p-values of < 0,05.

References

[1] A. Gress, A. Völkel, H. Schlaad, *Macromolecules* **2007**, *40*, 7928.

[2] K. Kempe, A. Vollrath, H. W. Schaefer, T. G. Poehlmann, C. Biskup, R. Hoogenboom, S. Hornig, U. S. Schubert, *Macromol. Rapid Commun.* **2010**, *31*, 1869.

[3] A. Schallon, C. V. Synatschke, D. V. Pergushov, V. Jerome, A. H. E. Müller, R. Freitag, *Langmuir* **2011**, *27*, 12042.

[4] S. W. Provencher, *Comput. Phys. Commun.* **1982**, *27*, 229.

[5] A. V. Delgado, F. Gonzalez-Caballero, R. J. Hunter, L. K. Koopal, J. Lyklema, *J. Colloid Interface Sci.* **2007**, *309*, 194.

[6] H. Ohshima, *J. Colloid Interf. Sci.* **1994**, *168*, 269.

[7] A. Vollrath, D. Pretzel, C. Pietsch, I. Perevyazko, S. Schubert, G. M. Pavlov, U. S. Schubert, *Macromol. Rapid Commun.* **2012**.

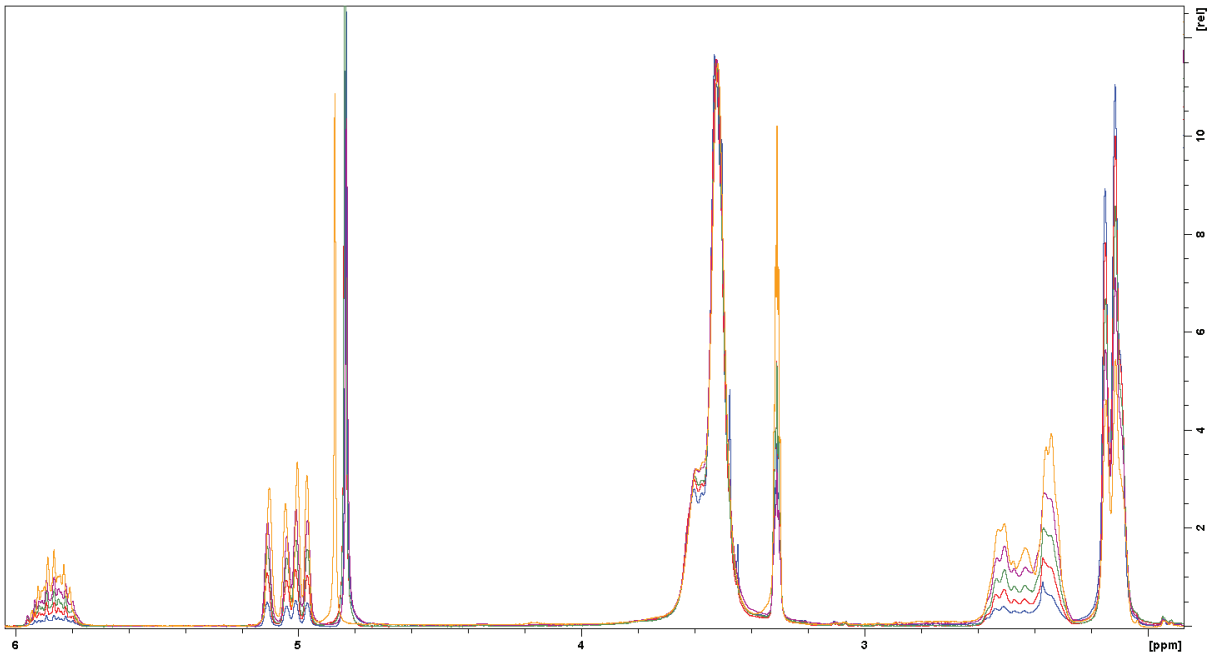

Figure S10. Overlay of the ^{1}H NMR spectra of **1a** (blue), **1b** (red), **1c** (green), **1d** (purple), and **1e** (orange). The signal intensities of the spectra were normalized to the peak of the polymer backbone signal at around 3.5 ppm (250 MHz, solvent: CD_3OD).

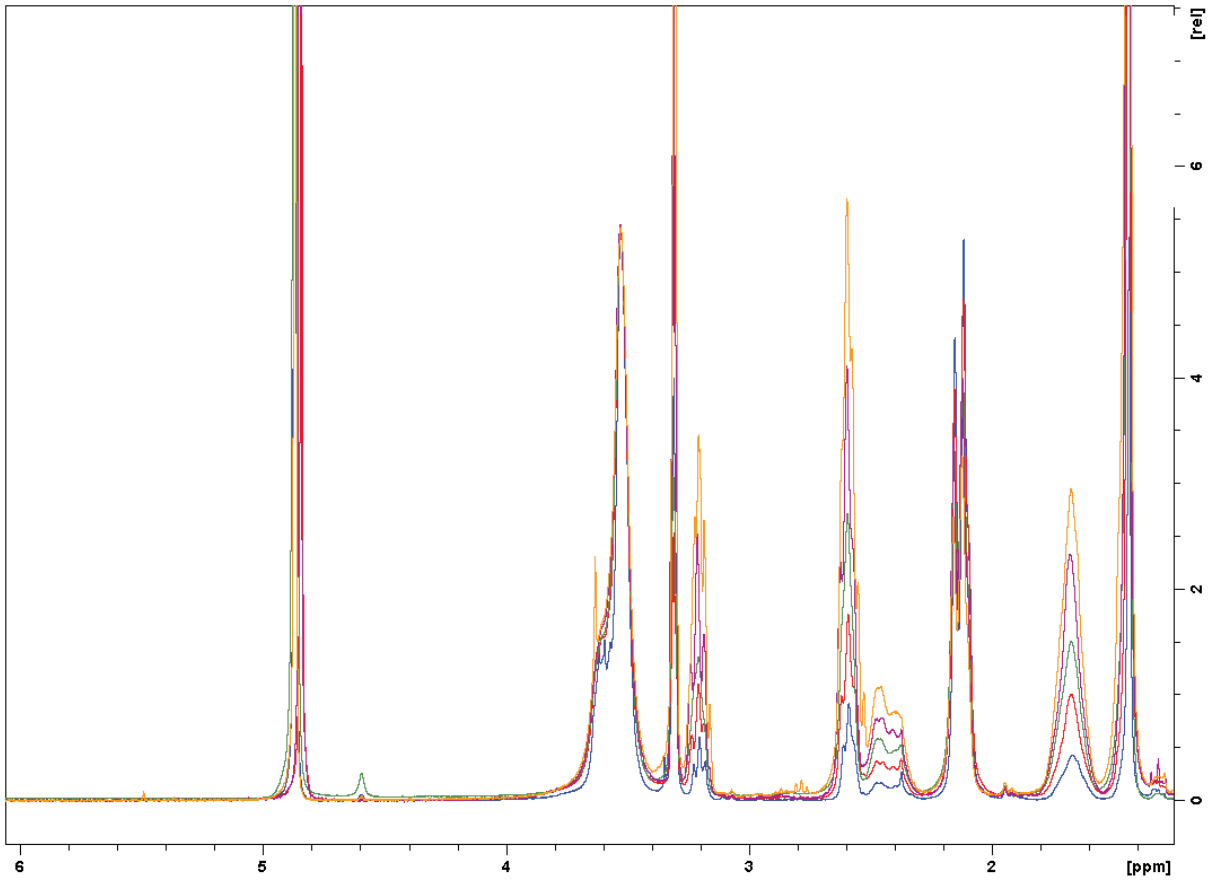

Figure S11. Overlay of the ^{1}H NMR spectra of **3a** (blue), **3b** (red), **3c** (green), **3d** (purple), and **3e** (orange). The signal intensities of the spectra were normalized to the peak of the polymer backbone signal at around 3.5 ppm (250 MHz, solvent: CD_3OD).

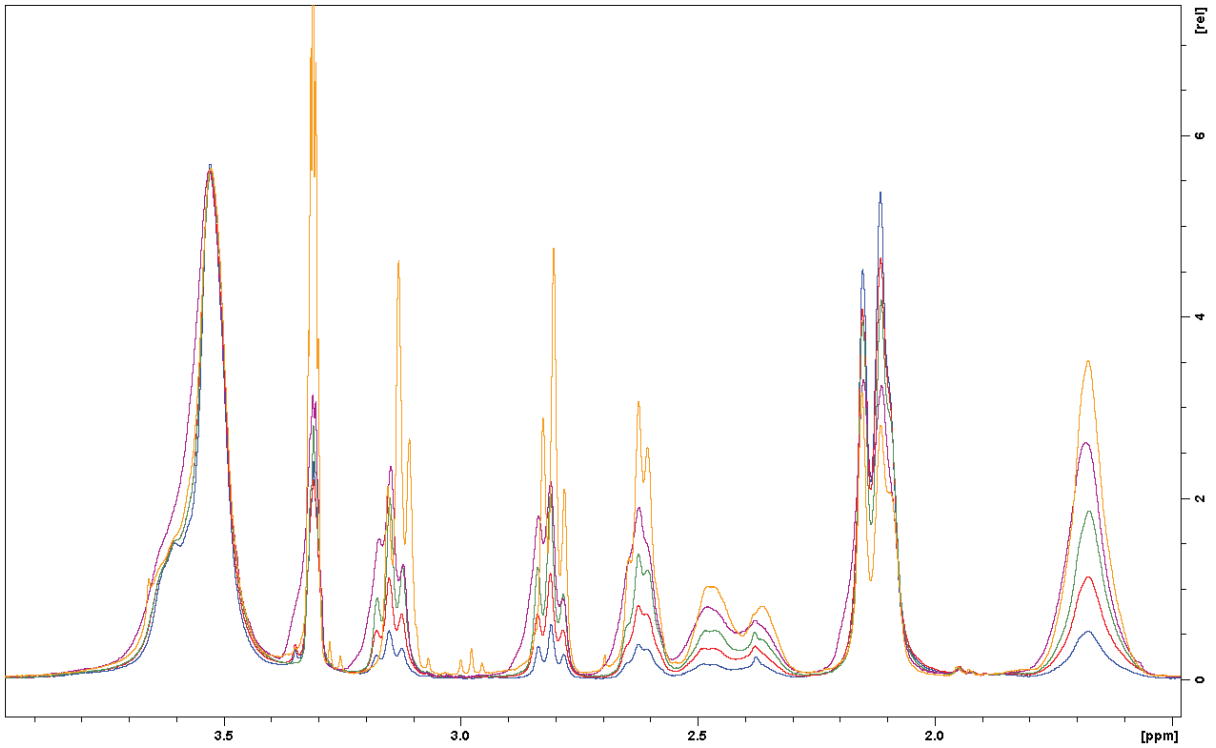

Figure S12. Overlay of the ^{1}H NMR spectra of **s10p** (blue), **s20p** (red), **s30p** (green), **s40p** (purple), and **s50p** (orange). The signal intensities of the spectra were normalized to the peak of the polymer backbone signal at around 3.5 ppm (250 MHz, solvent: CD_3OD).

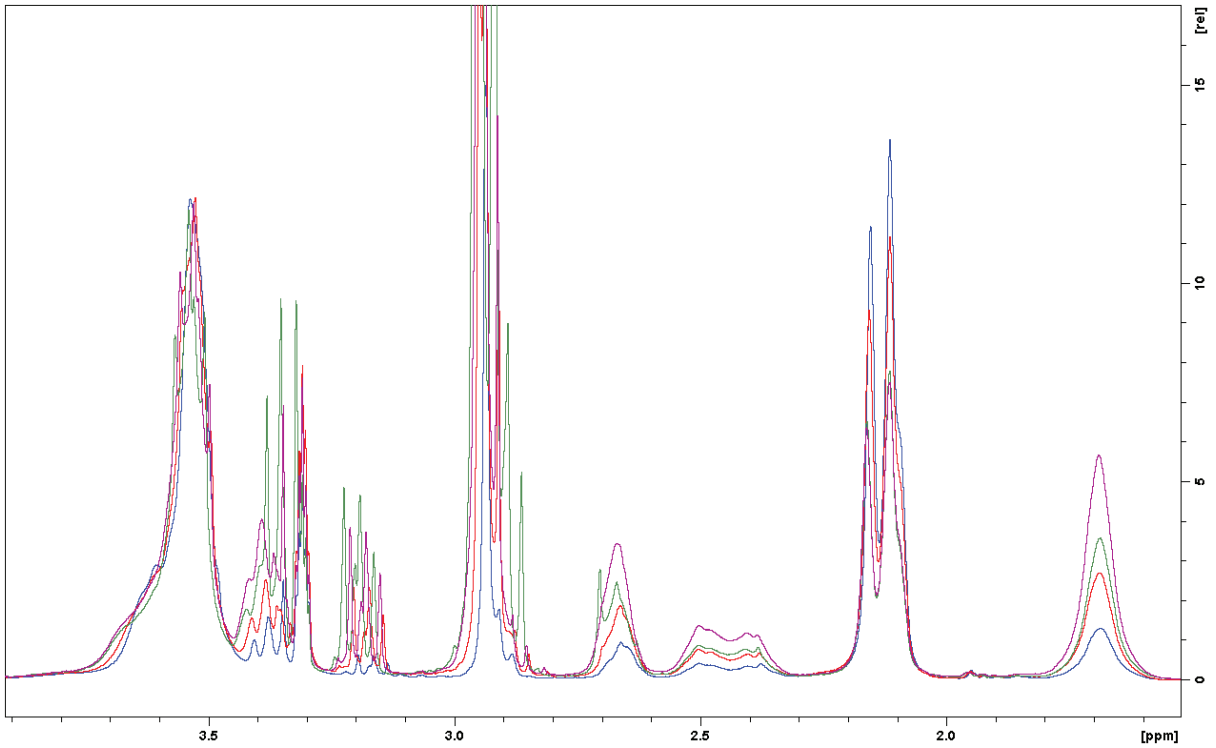

Figure S13. Overlay of the ^{1}H NMR spectra of **s10t** (blue), **s20tp** (red), **s30t** (green), and **s40t** (purple). The signal intensities of the spectra were normalized to the peak of the polymer backbone signal at around 3.5 ppm (250 MHz, solvent: CD_3OD).

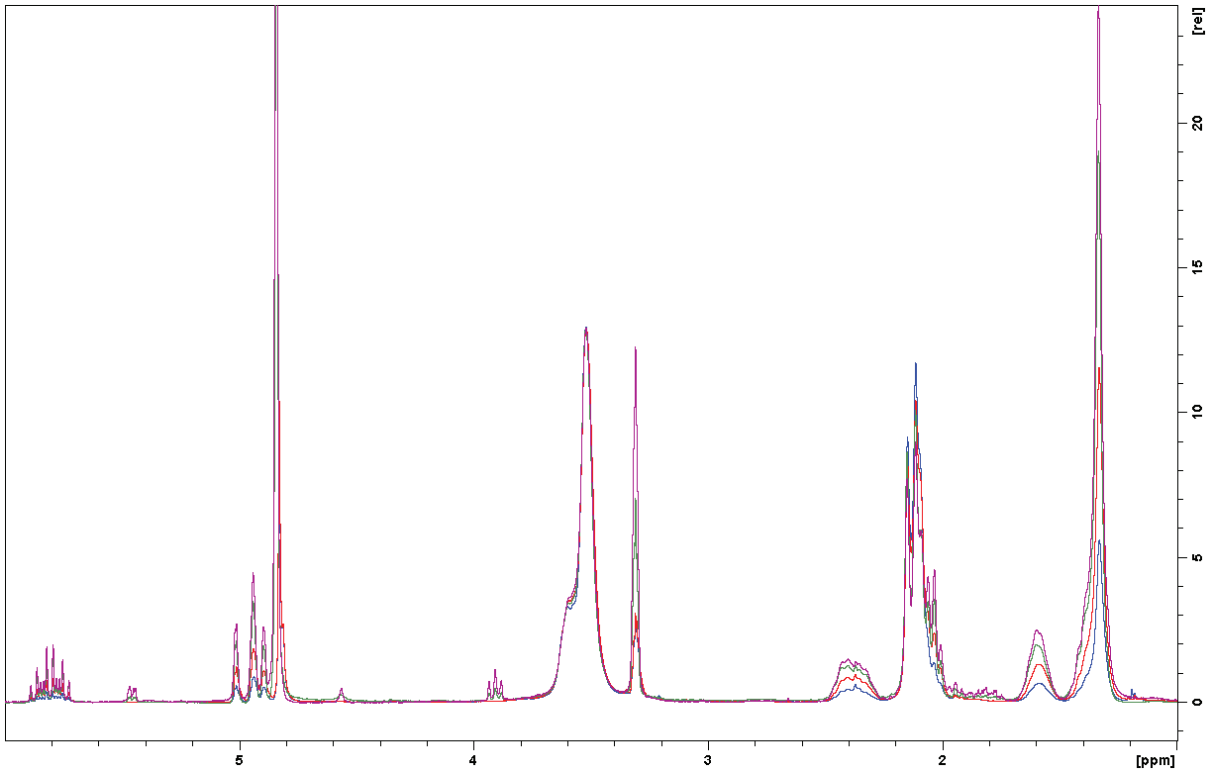

Figure S14. Overlay of the ^{1}H NMR spectra of **2a** (blue), **2b** (red), **2c** (green), and **2d** (purple). The signal intensities of the spectra were normalized to the peak of the polymer backbone signal at around 3.5 ppm (250 MHz, solvent: CD_3OD).

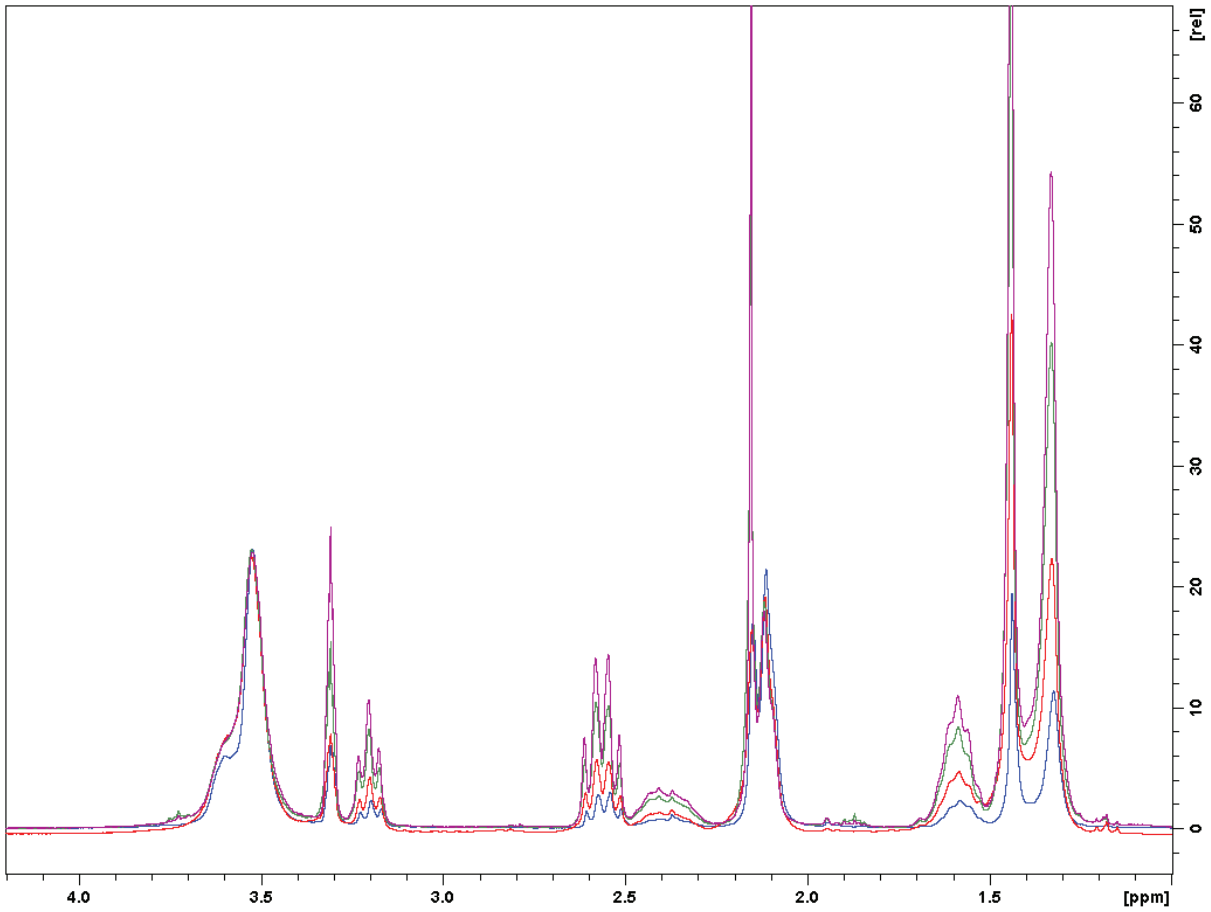

Figure S15. Overlay of the ^{1}H NMR spectra of **4a** (blue), **4b** (red), **2c** (green), and **4d** (purple). The signal intensities of the spectra were normalized to the peak of the polymer backbone signal at around 3.5 ppm (250 MHz, solvent: CD_3OD).

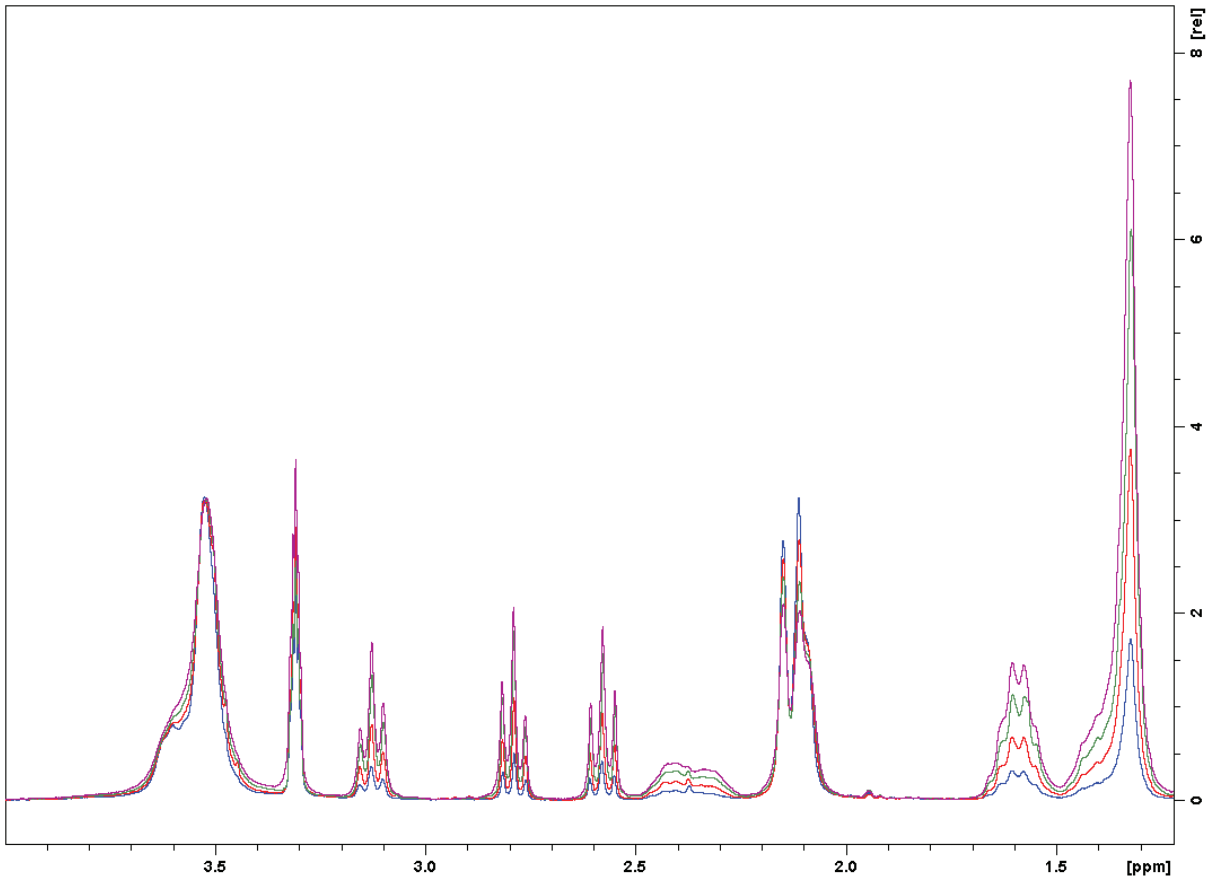

Figure S16. Overlay of the ^{1}H NMR spectra of **l10p** (blue), **l20p** (red), **l30p** (green), and **l40p** (purple). The signal intensities of the spectra were normalized to the peak of the polymer backbone signal at around 3.5 ppm (250 MHz, solvent: CD_3OD).

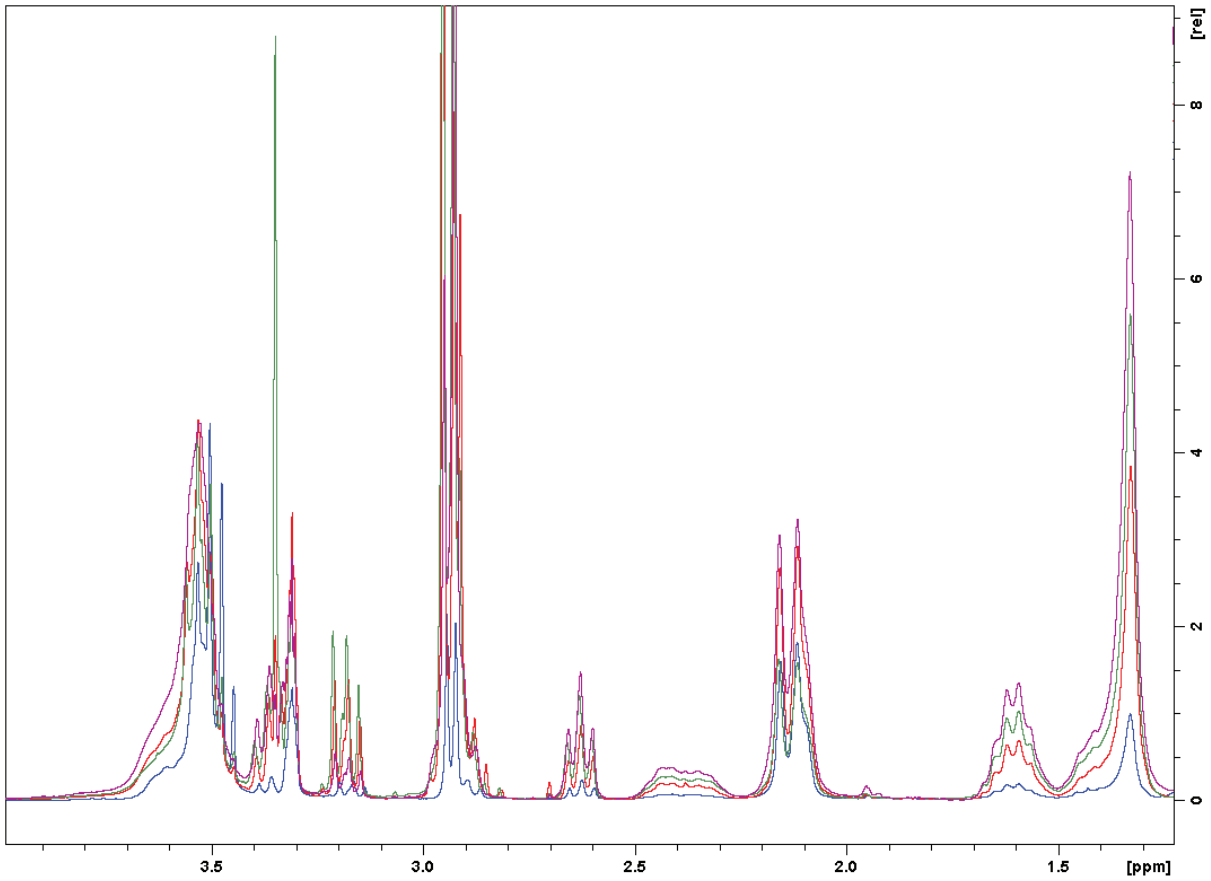

Figure S17. Overlay of the ^{1}H NMR spectra of **l10t** (blue), **l20t** (red), **l30t** (green), and **l40t** (purple). The signal intensities of the spectra were normalized to the peak of the polymer backbone signal at around 3.5 ppm (250 MHz, solvent: CD_3OD).

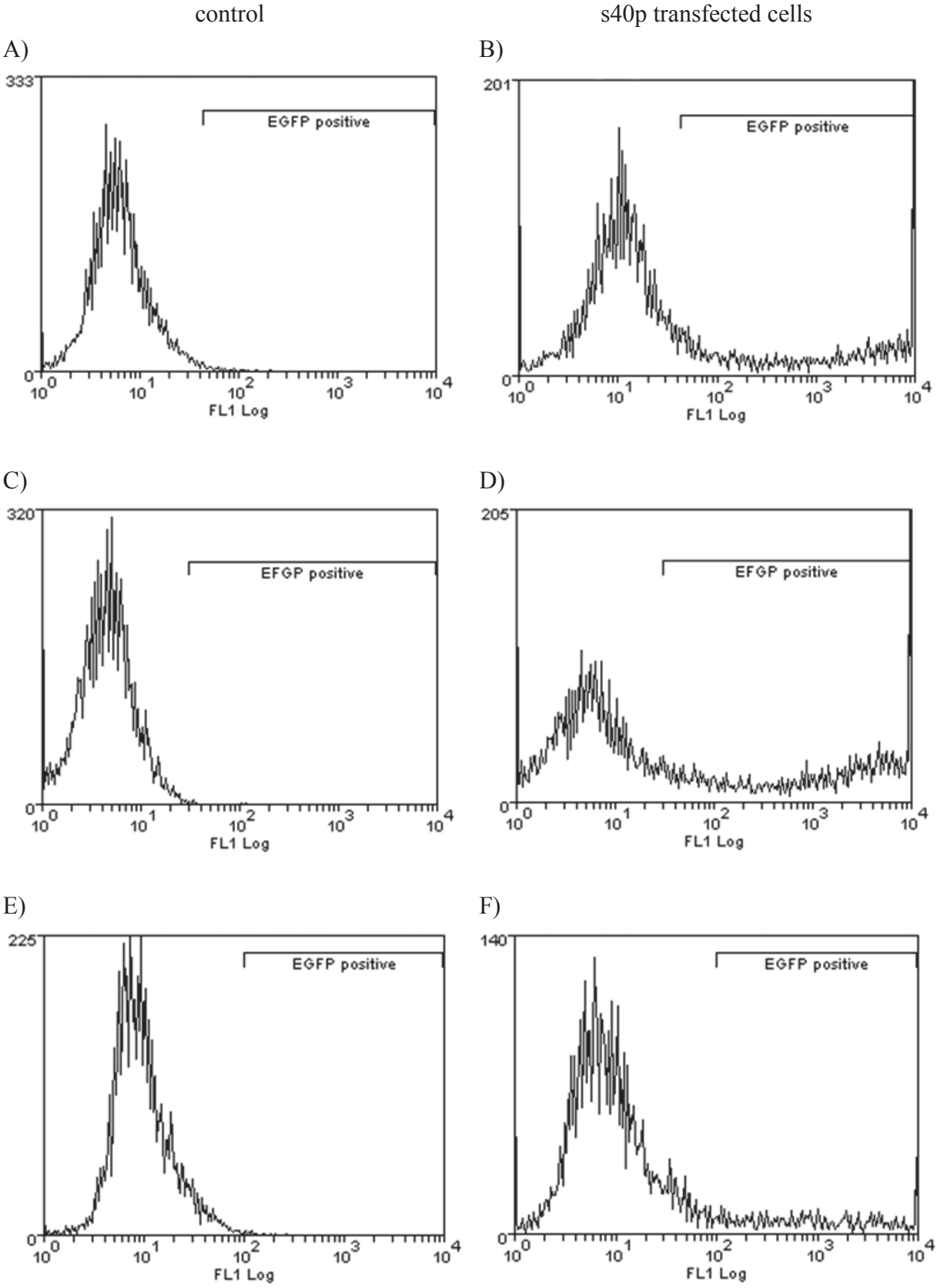

Figure S18. Histograms of non-transfected cells (A, C, E) and the corresponding HEK cell transfected with s40p (B, D, F) (NP 20). FL1 represents green fluorescence by EGFP expression.

Table S6. Mean fluorescence intensities (MFI) of non-transfected cells (control cells) and corresponding HEK cells transfected with s40p or lPEI (NP20). The values represent the MFI of the gated EGFP positive area (s. figure S18).

	MFI control cells	MFI transfected cells s40p	MFI transfected cells lPEI
Sample A, B	0,682	381	389
Sample C, D	4,37	317	297
Sample D, E	11,3	226	257

Publication 11

“Parallel high-throughput screening of polymer vectors for nonviral gene delivery: Evaluation of structure–property relationships of transfection”

C. Rinkenauer,[#] A. Vollrath,[#] A. Schallon, L. Tauhardt, K. Kempe,

S. Schubert, D. Fischer, U. S. Schubert

#Both authors contributed equally.

ACS Comb. Sci. **2013**, *15*, 475-482

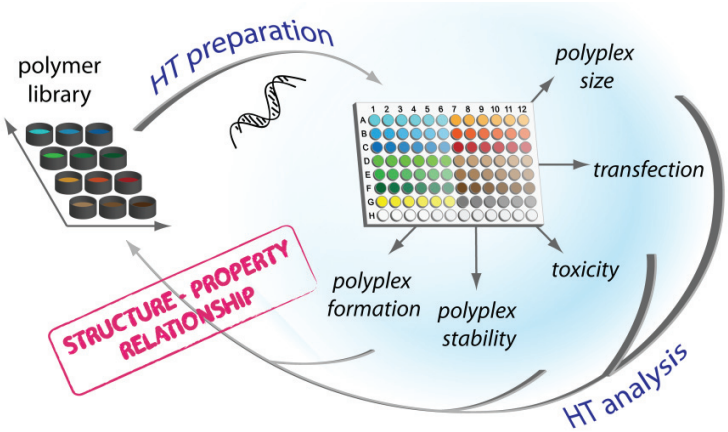

ACS Combinatorial Science

Research Article

pubs.acs.org/acscombsci

Parallel High-Throughput Screening of Polymer Vectors for Nonviral Gene Delivery: Evaluation of Structure–Property Relationships of Transfection

Alexandra C. Rinkenauer,[†,‡] Antje Vollrath,[†,‡] Anja Schallon,[†,‡] Lutz Tauhardt,[†,‡] Kristian Kempe,[†,‡] Stephanie Schubert,[‡,§] Dagmar Fischer,[§] and Ulrich S. Schubert*[,†,‡,∥]

[†]Laboratory of Organic and Macromolecular Chemistry (IOMC), Friedrich Schiller University Jena, Humboldtstraße 10, 07743 Jena, Germany

[‡]Jena Center for Soft Matter (JCSM), Friedrich Schiller University Jena, Philosophenweg 7, 07743 Jena, Germany

[§]Institute of Pharmacy, Department of Pharmaceutical Technology, Friedrich Schiller University Jena, Otto-Schott-Straße 41, 07745 Jena, Germany

[∥]Dutch Polymer Institute, P.O. Box 902, 5600 AX Eindhoven, the Netherlands

Supporting Information

ABSTRACT: In recent years, "high-throughput" (HT) has turned into a keyword in polymer research. In this study, we present a novel HT workflow for the investigation of cationic polymers for gene delivery applications. For this purpose, various poly(ethylene imine)s (PEI) were used as representative vectors and investigated via HT-assays in a 96-well plate format, starting from polyplex preparation up to the examination of the transfection process. In detail, automated polyplex preparation, complex size determination, DNA binding affinity, polyplex stability, cytotoxicity, and transfection efficiency were performed in the well plate format. With standard techniques, investigation of the biological properties of polymers is quite time-consuming, so only a limited number of materials and conditions (such as pH, buffer composition, and concentration) can be examined. The approach described here allows many different polymers and parameters to be tested for transfection properties and cytotoxicity, giving faster insights into structure–activity relationships for biological activity.

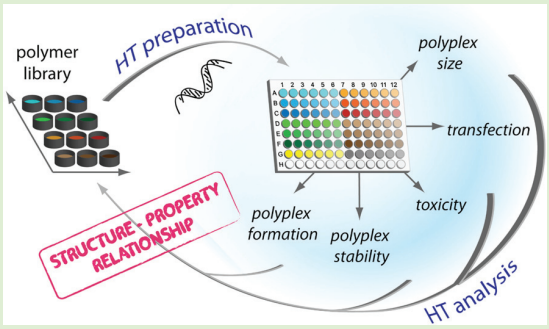

KEYWORDS: *high-throughput screening, transfection, nonviral gene delivery, polyplex stability, poly(ethylene imine), heparin, combinatorial workflow*

INTRODUCTION

Nonviral gene delivery (transfection) methods are of great interest for research and clinical applications. The use of cationic polymers as nonviral vectors to form complexes (polyplexes) with negatively charged plasmid DNA (pDNA) has long been explored as a safer and more controllable alternative to the use of possible infectious viral vectors.[1,2] For the evaluation of polymers as transfection agents, two main aspects must be considered: the efficiency of gene delivery with subsequent reporter gene expression and cytotoxicity.[3] Biophysical properties, such as polyplex size, surface charge, and binding affinity between the polymer and the genetic material play crucial roles in the required cellular uptake.[4,5] The binding within the interelectrolyte complex of polymer and pDNA has to be strong enough to protect the pDNA but must be reversible to release the pDNA inside the cells.[6,7] While much progress has been made, there is still an insufficient knowledge of how polymers should be constructed to be highly efficient and safe gene delivery vectors.[8,9]

This lack of predictability results in part from the great diversity of polymer classes and methods reported in the literature, which are difficult to compare to each other. For instance, transfection protocols differ notably for different cells and media, and different polymer solutions and buffers are used in the preparation of polyplexes.[10,11] While some examples have been used for in vitro applications and biotechnology research for decades, no polymer-based transfection agent has been approved for clinical use.[12−14]

The development of robotic techniques for the preparation of polymeric materials provides an opportunity for the high-throughput (HT) synthesis and characterization of cationic polymers in this context.[15−20] Using this synthetic approach, polymer properties such as molar mass, functional groups, architecture, and the combination of different monomers in

Received: February 21, 2013
Revised: June 20, 2013
Published: July 25, 2013

Scheme 1. Workflow of the High-Throughput Transfection Studies for Structure−Property Evaluations Concerning Molar Ratio, Size, Polyplex Formation, Polyplex Stability, Release, Transfection Efficiency, and Cytotoxicity

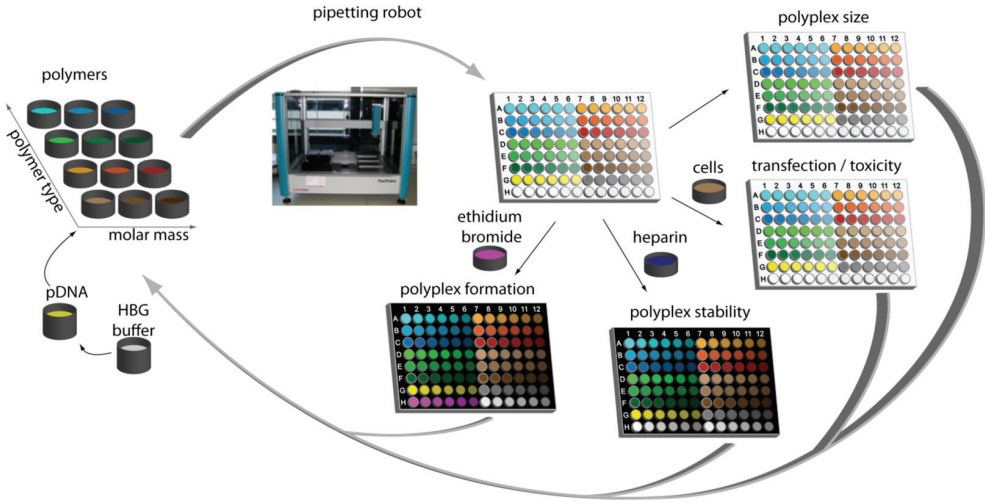

statistic or block copolymers can be altered, yielding systematic polymer libraries, which enable the elucidation of structure−property relationships.[15−23] Unfortunately, rapid methods for biological evaluation have not been hyphenated with efficient automated synthesis to construct a combinatorial HT workflow.[24−27] For example, binding affinity and polyplex stability have commonly been assessed by agarose gel electrophoresis, which is not well suited to HT screening. The use of an intercalating dye to establish binding affinities can provide an alternative compatible with a microtiter plate format.[28] Transfection and cytotoxicity assays can be similarly performed in multiwell plates with repeating samples to reduce measurement mistakes. Pioneers in this type of HT screening of a wide range of polymers as transfection agents have been Langer and co-workers (synthesis and transfection efficiency)[29] and Massing and co-workers (lipofection transfection efficiency and toxicity).[30]

We describe here a simple and powerful combinatorial high-throughput workflow that combines polyplex formation and biological screening (Scheme 1). It starts with the automated polyplex preparation via pipetting robots and continues with a parallel and HT analysis of analytical and biological properties of size, binding affinity, stability, transfection efficiency, and toxicity. We show that the novel workflow is applicable to a variety of polymer systems and conditions, allowing for fast and efficient screening of important vector parameters, such as polyplex formation, pDNA release, cytotoxicity, and transfection.

RESULTS AND DISCUSSION

Poly(ethylene imine) (PEI), the most prominent cationic polymer and most efficient transfection agent for pDNA in vitro, was used to validate the method.[31,14] Linear PEI (LPEI), obtained from poly(2-ethyl-2-oxazoline)s of different molar masses, was prepared.[32,33] By application of automated microwave synthesizers, poly(2-ethyl-2-oxazoline)s can be obtained within 10 min and converted into PEI within 1 h by acidic hydrolysis.[32] These cationic PEI polymers offer the advantage to be molecularly designed in a highly reproducible manner for specific applications in pharmacy or biotechnology. Commercially available branched PEI (BPEI) materials were also used in this study.

Evaluation of an Appropriate Buffer System. The formation of polyplexes from cationic polymers and anionic genetic material is driven by electrostatic interactions and a gain of entropy.[34] Thus, ionic strength, pH, and the final polyplex concentration have a major impact on the complexation behavior and the resulting polyplex size.[35,36] For the ex cellular characterization, polyplexes are often prepared in high ionic strength buffers, such as 150 mM sodium chloride (NaCl) or buffer systems using phosphate (PBS) or TRIS (TBS). Such high ionic strength media can have a negative impact on particle size and stability and lead to fast polyplex aggregation.[36,37] Thus, a low ionic strength 20 mM HEPES buffer with 5% glucose for physiological osmolarity (HBG buffer) was examined for polyplex preparation in a HT manner, as has been previously done for transfection.[37] Preliminary studies with linear PEI_{600} revealed that smaller polyplexes were formed in HBG.[35] A lower tendency to aggregate over time compared to physiological salt solutions (150 mM NaCl) was observed if the polyplexes were prepared in HBG.[38−40] Our measurements showed $LPEI_{600}$ polyplexes to exhibit no aggregation over 2 h in HBG (see Supporting Information), no aggregation or particle growth before and after the addition to serum containing culture media.[36−38] Furthermore, HBG buffer can be used for zeta potential measurements[41] in this concentration range as well as for electron microscopic evaluations, where salts cause electrophoresis or artifacts, respectively. Consequently, HBG was selected as most appropriate buffer system for HT studies and was used here for all polyplex preparations and analytical investigations.

Polyplex Preparation Using Pipetting Robots. A standard liquid handling robot was used for automated preparation of polyplexes from cationic polymers and DNA, similar to reports of robotic production of polymeric nanoparticles.[42] The benefit of such pipetting systems is the ability to systematically alter different parameters, such as polymer concentration, pH, or buffer composition.[43] Automated deposition of a buffered pDNA solution into wells containing various buffered cationic polymer solutions at desired concentrations was performed. While the reverse

dx.doi.org/10.1021/co400025u | ACS Comb. Sci. 2013, 15, 475−482

addition (pipetting polymer to DNA solution, vortexing after polymer addition) is the more conventional method,[1] giving better transfection results,[44] we observed similar outcomes in preliminary experiments using $LPEI_{600}$ and $BPEI_{600}$ (see Supporting Information) and in scattered tests of the HT method (data not shown). This may be due to more reversible interelectrolyte formation in the low ionic strength HBG buffer compared to high ionic strength buffers used previously.

To evaluate the dependence of polyplex properties on the nature of the polymers and preparation conditions, various cationic LPEI and BEI with varied degree of polymerization (DP = 20, 200, and 600) were used to form polyplexes with pDNA. Besides the molar mass and architecture, several nitrogen (polymer) to phosphate (DNA) ratios (N/P = 2.5, 5, 10, and 20) were applied. To this end, pDNA solution was added to a dilution series of polymer solutions, and the resulting suspensions were directly mixed by repetitive suction and release. After polyplex formation, the prepared suspensions were distributed automatically into different well plates for parallel analysis studies.

Investigation of Polyplex Size and Stability. The polyplex size allows a first hint of the polymer's capability to be used as a transfection agent, since polyplexes larger than 500 nm are known to show relatively poor uptake.[45] For this purpose, the polyplexes were first analyzed on a dynamic light scattering (DLS) plate reader.[46] As shown in Figure 1, all

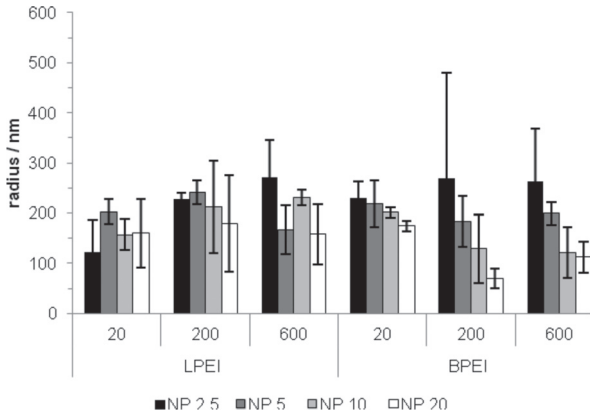

Figure 1. Hydrodynamic radii of polyplexes prepared using the pipetting robot. The values represent the mean ($n \geq 3$) of each polymer at different N/P ratios. PDI^{P} values of 0.09 to 0.5 were found.

polyplexes exhibited an average radius of less than 270 nm, with materials mixed at N/P ratios above 5 showing smaller radii. The smallest size (70 nm radius) was obtained for $BPEI_{200}$. It should be noted that the HT-DLS analysis data tended to report larger radii than measurements performed with a single-beam DLS instrument (see Supporting Information). HT-DLS results should be always considered with care, and we consider them informative only in a relative sense, to establish the potential of polymers to form nanoscaled polyplexes and gain information about their stability in comparison to standard polymer controls. Our data revealed three tendencies, also described in the literature: (i) increasing N/P ratios gave rise to smaller polyplexes, (ii) BPEI with higher DPs showed a stronger size dependency compared to LPEI, and (iii) BPEI condensed DNA into smaller particles compared to LPEI.[31] Interestingly, no systematic influence of the degree of polymerization or the molar mass on polyplex size was observed under the chosen conditions.

Fluorescence Displacement Assay. Considering the interpretation of transfection results the determination of the binding affinity of the polymers to the genetic material is of vital importance. As previously mentioned, the binding of a polyplex is at its optimal state when having a strong and reversible interaction. The required N/P ratio to form polyplexes were either done by usage of gel retardation assays or by fluorescence measurement of intercalating dyes, such as ethidium bromide (EB) or Pico Green. For an HT screening application, the gel retardation method is not suitable in a 96-well plate format, thus, the fluorescence displacement assay with EB (EBA) was chosen. Commonly, the binding of EB with pure pDNA leads to a high fluorescence signal. However, provided that the pDNA forms interelectrolyte complexes with the polymers, the displacement of dyes leads to a decrease of fluorescence signals. In Figure 2, the fluorescence signals

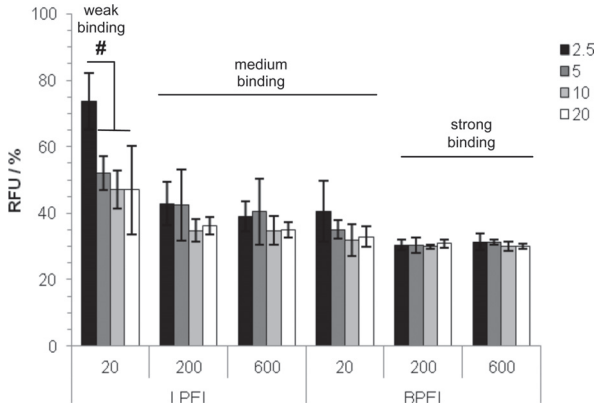

Figure 2. Fluorescence displacement assay using LPEI and BPEI with varying DP. The RFU of pure pDNA represent 100% RFU. N/P ratios of 2.5 up to 20 were studied using EB as intercalating agent. The values represent the mean ± S.D., $n \geq 3$, # indicate significant statistical difference (ANOVA, $p < 0.05$).

(RFU) of all PEI polymers with increasing N/P ratio are illustrated. It was found that $BPEI_{200}$ and $BPEI_{600}$ reached a comparable RFU of around 30.5 ± 1.4% ($p > 0.5$) indicating a strong DNA binding. Furthermore, the higher molar mass LPEIs ($LPEI_{200}$ and $LPEI_{600}$) along with $BPEI_{20}$ revealed comparable RFUs in the range of 37.1 ± 6.2% ($p > 0.1$). The weakest binding was obtained with $LPEI_{20}$ also showing the strong dependence of N/P. In particular, polyplexes formed at N/P 20 revealed a mediate RFU of 48.7 ± 8% ($p > 0.5$) in comparison to 73.8 ± 8.5% at N/P 5. The findings accredit that the binding affinity depends on the molar mass and the architecture of the polymer as well as on the N/P ratio applied. The relationship between the binding affinity and the molar mass of the polymer increases in a proportional manner. In addition, a higher binding affinity of branched structures (BPEI) was detected in comparison to linear architectures.[8,31] The literature[47,48] reports similar trends and confirms the possible analysis of polyplexes by this HT assay. Moreover, identical tendencies were obtained for this particular handmade assay using polyplexes of linear PEIs (see Supporting Information). At this point of the workflow, one should note that after performing size measurements and binding affinity assays, it is possible to exclude nonsuitable polymers as

dx.doi.org/10.1021/co400025u | ACS Comb. Sci. 2013, 15, 475−482

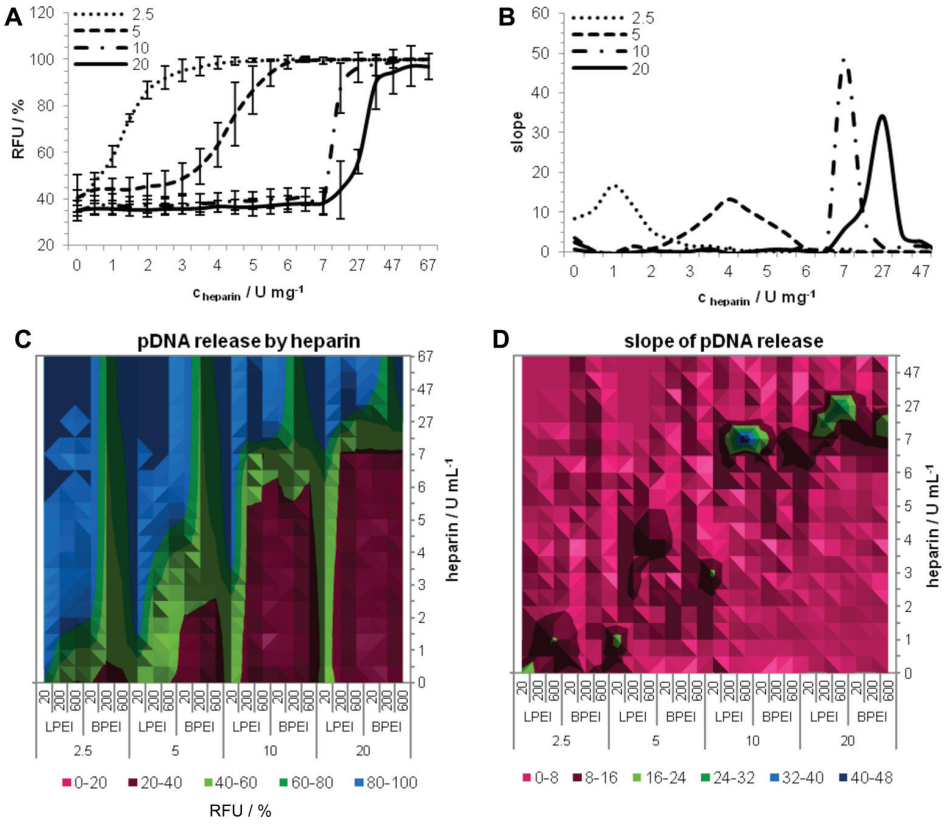

Figure 3. pDNA release of polyplexes after titration with heparin. Release of pDNA was measured by incubation of polyplexes with increasing heparin concentrations. (A) RFU of polyplexes prepared from $LPEI_{600}$ at different N/P ratios and increasing heparin concentrations. (B) Slope of RFU of $LPEI_{600}$ polyplexes at different N/P ratios. (C) RFU of all polyplexes at different N/P ratios and increasing heparin concentrations. Color represents the RFU. (D) Slope of RFU of all polyplexes at different N/P ratios. Color represents the slope. The values represent the mean ± S.D., $n \geq 3$.

transfection agents, which showed undesired interaction such as aggregation or no polyplex formation.

DNA Release. Subsequent to the determination of binding affinity, the release of pDNA from the polyplexes was investigated using the heparin assay. Heparin is a polyanion and it was reported to be a good competitor to negatively charged pDNA.[48] As a result of the polymer-heparin interaction, the pDNA is released and EB is repeatedly intercalating into pDNA leading to increased fluorescence intensities. Studies using heparin are often quantified via gel retardation assays or applying only one N/P ratio, which would potentially lead to misinterpretations. In particular for in vitro cultivations of adherent cells, the polyplex concentration at the cell membrane at the beginning of the transfection and after incubation differs. The explanation for this behavior could be justified by the polyplex sedimentation process.[8,49,50] For a more trustworthy outcome, all polyplex suspensions were titrated automatically against two heparin stock solutions to determine the critical heparin concentration at different N/P ratios. Using this approach, a wide range of heparin concentrations (n = 20) could be tested for one sample. The results obtained from the performed assay are displayed in detail for $LPEI_{600}$ (Figure 3A) and for all polymers and N/P ratios in (Figure 3C). As expected, the release of pDNA detected by RFU was dependent on the heparin concentration. Moreover, it was explored that for the release of total pDNA at higher N/P ratios, an increased amount of heparin was required. This can be explained by the fact that the amount of noncomplexed free polymer was increased at high N/P ratios, whereas the amount of complexed polymer remained constant.[51] Thus, by the addition of heparin to polyplex suspensions at high N/P ratios, first the free polymers complex with the heparin and no pDNA was released. Unless the critical concentration of heparin was met, the pDNA was not released. For an improved comparability, the inflection point of the titration curves in Figure 3A and C was defined as the critical heparin concentration (HC_{50}) and implemented as a representative value of the concentration at which 50% of the complexed pDNA was released (Figure 3B and D). The correlation between the N/P ratio and the heparin concentration was an apparent observation and confirmed already published trends.[48] However, our findings underline the relation between the architecture of PEI and the ability to release pDNA.

Polyplexes prepared from BPEIs showed higher HC_{50} values in comparison to the LPEIs (indicated by larger purple areas in particular at N/P 2.5 and 5, Figure 3C and D). Furthermore, the polyplexes prepared with the $LPEI_{20}$ exhibited an early release of the pDNA at low heparin concentration in contrast to its branched analog ($BPEI_{20}$) and the linear PEIs with higher molar masses ($LPEI_{200}$ and $LPEI_{600}$). A flagrant correlation could be made of these with the weak binding affinity (Figure 2).

dx.doi.org/10.1021/co400025u | ACS Comb. Sci. 2013, 15, 475−482

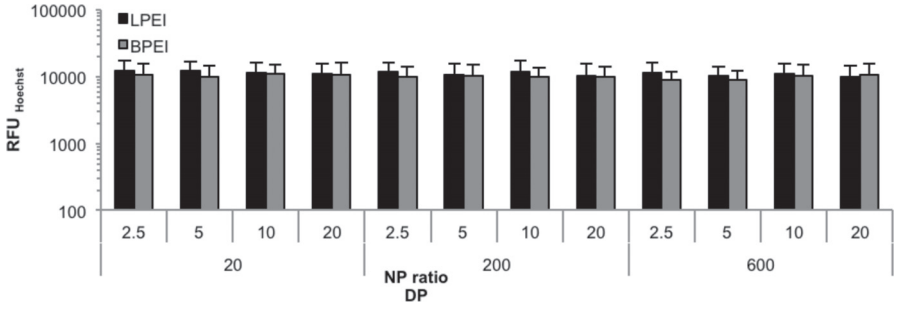

Figure 4. Investigation of cytotoxicity. The viability of cells after incubation of the polyplexes up to N/P 20. Nontreated cells served as controls and gave comparable results. The bottom of 96-well plates were measured at Em_{350}/Ex_{461} (Hoechst 33324).

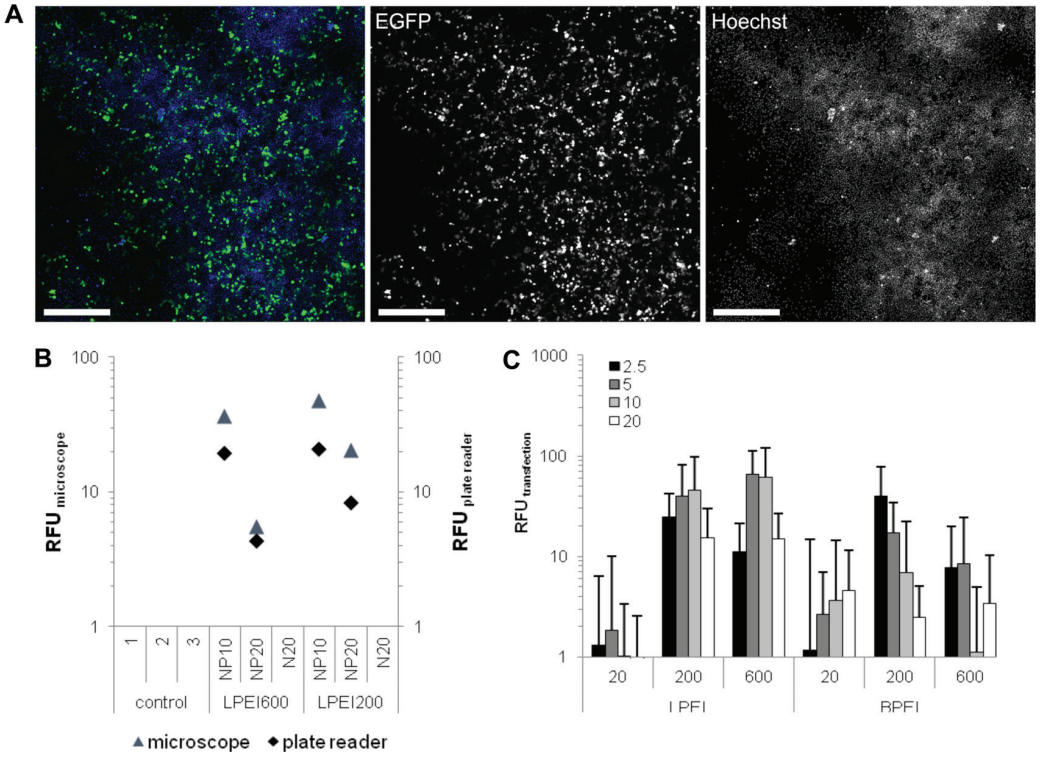

Figure 5. Transfection efficiency by microscopic evaluation and fluorescence intensity measurements. (A) HEK cells transfected with EGFP coding pDNA and $LPEI_{600}$ at N/P 10. Cell nuclei were stained with Hoechst 33324 (blue). Scale bare indicates 500 μm. (B) Correlation of the microscopic evaluation of EGFP content determined ($RFU_{microscope}$) and bottom measurements using a plate reader ($RFU_{plate\ reader}$). Three control wells, where cells were not transfected, as well as cells only incubated with the polymer at concentrations correspond N/P 20 (N20) showed no RFU. (C) Transfection efficiency and number of cells transfected with a pipetting robot in a 96-well plate. Values represent the mean ± S.D., $n \geq 3$.

Cytotoxicity. To study the cytotoxicity of the polyplexes, HEK cells used as for transfection experiments, were seeded in 96-well plates and incubated for 24 h with the prepared polyplex suspensions. Afterward, the viability of the cells was detected by staining with Hoechst 33324. This dye crosses of the cell membrane and stains the chromosomal DNA of attached cells. Subsequently, the fluorescence was measured utilizing the fluorescence plate reader. The obtained RFU signals of Hoechst of all treated cells are presented in Figure 4. No indication for cytotoxic effects of the polyplexes was found considering the fact that the obtained values were comparable to nontreated cells (ANOVA, $p > 0.05$).

As the polyplexes exhibited a lower cytotoxicity than the single polymers, due to neutralized cationic groups, the toxicity of these polyplexes at N/P 20 would be a criterion for knock out. However, for a comprehensive analysis, the polymers were also screened with concentrations up to 72 μg mL^{-1}, correlating to N/P 500 (DP 20 and 600, see Supporting Information). A relationship was elucidated between the increasing DP of the cationic polymers and the higher cytotoxicity level, which is in accordance to literature where no significant difference between linear and branched PEI was observed.[3,31] Interestingly, the polymers with the lowest DP showed no cytotoxicity at all investigated concentrations (see Supporting Information).

Transfection Efficiency. The transfection efficiency of the polyplexes was quantified using EGFP as reporter protein. For HT screening, the studies regarding the transfection efficiency were performed with a fluorescence plate reader by automatic scanning of the bottom area of the wells and complemented by

dx.doi.org/10.1021/co400025u | ACS Comb. Sci. 2013, 15, 475−482

microscope analysis. In Figure 5A, a representative overview of the cells (blue) transfected with $LPEI_{600}$ (green) is portrayed. Microscopic analysis and, in particular, subsequent data processing is not appropriate and efficient enough for a rapid HT screening, thus the quantification of EGFP using a fluorescence plate reader were compared to the mean fluorescence in each picture (Figure 5B). Thereby, a good correlation between the microscopic analysis and the fluorescence plate reader results was demonstrated, proving the capability to screen the EGFP amount in a fast and facile manner, in contrast to flow cytometry or microscopy. In general, it can be stated that there are some decent advantages of a fluorescence screening with a plate reader compared to luciferase or galactose based assays, namely, (i) an easy and cheap detection, (ii) the possibility to perform afterward single cell analysis by flow cytometry or microscopy of the same cells, and (iii) the fact that EGFP is a stable reporter protein.

The EGFP expression for all investigated PEI polymers are shown in Figure 5C. The polymers can be ranked from high to low transfection efficiency: $LPEI_{600}$ > $LPEI_{200}$ > $BPEI_{200}$ > $BPEI_{600}$ > $BPEI_{20}$ > $LPEI_{20}$, whereby the obvious increase in the standard deviation compared to flow cytometry measurements (see Supporting Information) must be taken into account. However, the HT investigation showed clear trends confirming a suitable approach to spot high potential candidates and to be subsequently investigated in depth. Thus, $LPEI_{20}$ revealed no transfection efficiency, while $LPEI_{600}$ shows the highest one, also confirmed by handmade polyplexes and the detection of EGFP by flow cytometry (see Supporting Information). This observation further verifies the potential of such a HT screening using a fluorescent plate reader for determination of the transfection efficiencies of polymers.

CONCLUSION

Since HT synthesis and characterization of polymers could be managed by synthetic robots and microwave synthesizers combined with subsequent automated characterization of the molecular properties, polymer libraries for biological applications can be prepared in a rapid manner.[15−20] So far, an efficient and fast HT screening of these polymers for gene delivery purposes regarding structure−property relationship was not possible. Herein, a solution for the biological screening for gene delivery applications has been presented. The discussed HT workflow enables a rapid analysis of polymer vectors in an automated way with respect to important polymer characteristics, such as molar mass, architecture, and N/P ratio. This supports the identification and evaluation of polymers with regard to their capability of efficient complexation, protection, and transfection efficiency. For instance, the described heparin assay can be used for 23 polymers at four different N/P ratios resulting in 92 samples plus controls (n = 1). Furthermore, the HT approach was applied and demonstrated the possible screening of the cytotoxicity and the transfection efficiency of the polyplexes. As expected, the study of the different PEI model polymers revealed that linear and branched PEI are noncytotoxic at the investigated concentrations, but with rising molar mass and polymer concentration the cytotoxic effect was increasing.[31] The polymeric architecture itself showed thereby no influence on the cell viability.[3] As per literature, at low molar masses the DNA binding affinity is influenced by the polymeric architecture, since $BPEI_{20}$ revealed a stronger pDNA binding than $LPEI_{20}$.[15,26] The obtained results indicated that PEIs with branched architectures and small molar masses have the highest potential to be used as gene vectors in vitro, as they offer the advantage of low cytotoxicity combined with high pDNA binding affinity. Beyond, the best transfection results were obtained for $LPEI_{600}$ and the $BPEI_{200}$.

In comparison with literature and handmade performances proof was established that the developed workflow is applicable for polymer systems. Furthermore, conditions enabling a fast and efficient screening in terms of important vector parameters, such as polyplex formation, transfection, and release were found. The possible screening of polymer libraries for the best transfection candidate will help to elucidate main polymer characteristics and to understand why some polymers are high performers and others not. Thus, an enhanced development of more efficient polymers and polyplexes can be realized.

EXPERIMENTAL PROCEDURES

Material. Ethidium bromide solution 1% was purchased from Carl Roth (Karlsruhe, Germany). AlamarBlue was obtained from Life Technologies (Darmstadt, Germany). If not otherwise stated, cell culture materials, cell culture media, and solutions were obtained from PAA (Pasching, Austria). Plasmid pEGFP-N1 (4.7 kb, Clontech, Mountain View, CA, U.S.A.) was isolated using Qiagen Giga plasmid Kit (Hilden, Germany). All other chemicals were purchased from Sigma Aldrich (Steinhausen, Germany) and are of analytical grade or better and used without further purification. Linear PEI was synthesized according to procedure described in literature.[32]

Polyplex Preparation Using Pipetting Robot. For an automated polyplex preparation, 100 μL buffered DNA solution (c = 15 μg mL^{-1}) were injected into wells that contain 300 μL of the desired polymer solution. As cationic polymers, linear PEI with a DP of 20, 200, and 600, as well as branched PEI with a DP of 20, 200, and 600 were applied. To achieve different polymer to DNA ratios (N/P ratios), a dilution series in HBG of four different polymer concentrations (N/P ratio 2.5, 5, 10, 20) was prepared using a pipetting robot from a polymer stock solution of c = 72 μg mL^{-1}. After addition of the DNA solution, the polyplex suspension was mixed five times by suction and release using 200 μL tips and incubated at least 20 min. Subsequently, 100 μL of each polyplex suspension were transferred into three different well plates for a detailed analysis studies. The following assays were performed up to 2 h after polyplex preparation.

ASSOCIATED CONTENT

Supporting Information

Additional experimental details, tables of SEC data and hydrodynamic radii of polyplexes, comparison of the conventional handmade ployplexes and HT polyplexes, figures showing transfection efficiency, fluorescence displacement and cytotoxicity, and hydrodynamic radii and PDI^{p}, and additional references. This material is available free of charge via the Internet at http://pubs.acs.org.

AUTHOR INFORMATION

Corresponding Author

*E-mail: ulrich.schubert@uni-jena.de.

Present Address

Kristian Kempe: Department of Chemical and Biomolecular Engineering, The University of Melbourne, Victoria 3010, Australia

Author Contributions

A.C.R. and A.V. contributed equally.

Funding

The financial support from the Thuringian Ministry for Education, Science and Culture (Grant B514-09051, NanoConSens), the Dutch Polymer Institute (DPI, technology area HTE, project 729), and the Carl-Zeiss Foundation (JCSM Strukturantrag) are gratefully acknowledged.

Notes

The authors declare no competing financial interest.

■ ACKNOWLEDGMENTS

We express our gratitude to Caroline Fritzsche for assistance in the cell culture, Dr. David Pretzel for assistance at the microscope, Michael Wagner for helpful discussions, and Sarah Crotty for corrections of the manuscript.

■ REFERENCES

(1) Schlenk, F.; Grund, S.; Fischer, D. Recent developments and perspectives on gene therapy using synthetic vectors. *Ther. Delivery* **2013**, *4* (1), 95−113.

(2) Pezzoli, D.; Chiesa, R.; De Nardo, L.; Candiani, G. We still have a long way to go to effectively deliver genes! *J. Appl. Biomater. Funct. Mater.* **2012**, *10* (2), e82−91.

(3) Breunig, M.; Lungwitz, U.; Liebl, R.; Goepferich, A. Breaking up the correlation between efficacy and toxicity for nonviral gene delivery. *Proc. Natl. Acad. Sci. U. S. A.* **2007**, *104* (36), 14454−9.

(4) Kunath, K.; von Harpe, A.; Fischer, D.; Petersen, H.; Bickel, U.; Voigt, K.; Kissel, T. Low-molecular-weight polyethylenimine as a non-viral vector for DNA delivery: comparison of physicochemical properties, transfection efficiency and in vivo distribution with high-molecular-weight polyethylenimine. *J. Controlled Release* **2003**, *89* (1), 113−125.

(5) Pereira, P.; Jorge, A. F.; Martins, R.; Pais, A. A.; Sousa, F.; Figueiras, A. Characterization of polyplexes involving small RNA. *J. Colloid Interface Sci.* **2012**, *387* (1), 84−94.

(6) Dai, Z.; Wu, C. How does DNA complex with polyethylenimine with different chain lengths and topologies in their aqueous solution mixtures? *Macromolecules* **2012**, *45* (10), 4346−4353.

(7) Itaka, K.; Harada, A.; Yamasaki, Y.; Nakamura, K.; Kawaguchi, H.; Kataoka, K. In situ single cell observation by fluorescence resonance energy transfer reveals fast intra-cytoplasmic delivery and easy release of plasmid DNA complexed with linear polyethylenimine. *J. Gene Med.* **2004**, *6* (1), 76−84.

(8) Neu, M.; Fischer, D.; Kissel, T. Recent advances in rational gene transfer vector design based on poly(ethylene imine) and its derivatives. *J. Gene Med.* **2005**, *7* (8), 992−1009.

(9) Patil, S. D.; Rhodes, D. G.; Burgess, D. J. DNA-based therapeutics and DNA delivery systems: a comprehensive review. *AAPS J.* **2005**, *7* (1), E61−77.

(10) Jiang, X.; Qu, W.; Pan, D.; Ren, Y.; Williford, J. M.; Cui, H.; Luijten, E.; Mao, H. Q. Plasmid-templated shape control of condensed DNA-block copolymer nanoparticles. *Adv. Mater.* **2013**, *25* (2), 227−32.

(11) Iwai, R.; Haruki, R.; Nemoto, Y.; Nakayama, Y. Enhanced transfection efficiency of poly(*N*,*N*-dimethylaminoethyl methacrylate)-based deposition transfection by combination with tris-(hydroxylmethyl)aminoethane. *Bioconjugate Chem.* **2013**, *29*, 29.

(12) Derouazi, M.; Girard, P.; Van Tilborgh, F.; Iglesias, K.; Muller, N.; Bertschinger, M.; Wurm, F. M. Serum-free large-scale transient transfection of CHO cells. *Biotechnol. Bioeng.* **2004**, *87* (4), 537−45.

(13) Florian, M. W. Production of recombinant protein therapeutics in cultivated mammalian cells. *Nat. Biotechnol.* **2004**, No. 22, 1393−1398.

(14) Boussif, O.; Lezoualch, F.; Zanta, M. A.; Mergny, M. D.; Scherman, D.; Demeneix, B.; Behr, J. P. A versatile vector for gene and oligonucleotide transfer into cells in culture and in-vivo—Polyethylenimine. *Proc. Natl. Acad. Sci. U. S. A.* **1995**, *92* (16), 7297−7301.

(15) Hoogenboom, R.; Fijten, M. W. M.; Thijs, H. M. L.; Van Lankvelt, B. M.; Schubert, U. S. Microwave-assisted synthesis and properties of a series of poly(2-alkyl-2-oxazoline)s. *Des. Monomers Polym.* **2005**, *8* (6), 659−671.

(16) Hoogenboom, R.; Schubert, U. S. Microwave-assisted polymer synthesis: Recent developments in a rapidly expanding field of research. *Macromol. Rapid Commun.* **2007**, *28* (4), 368−386.

(17) Hoogenboom, R.; Wiesbrock, F.; Huang, H. Y.; Leenen, M. A. M.; Thijs, H. M. L.; van Nispen, S. F. G. M.; Van der Loop, M.; Fustin, C. A.; Jonas, A. M.; Gohy, J. F.; Schubert, U. S. Microwave-assisted cationic ring-opening polymerization of 2-oxazolines: A powerful method for the synthesis of amphiphilic triblock copolymers. *Macromolecules* **2006**, *39* (14), 4719−4725.

(18) Wiesbrock, F.; Hoogenboom, R.; Abeln, C. H.; Schubert, U. S. Single-mode microwave ovens as new reaction devices: Accelerating the living polymerization of 2-ethyl-2-oxazoline. *Macromol. Rapid Commun.* **2004**, *25* (22), 1895−1899.

(19) Wiesbrock, F.; Hoogenboom, R.; Leenen, M.; van Nispen, S. F. G. M.; van der Loop, M.; Abeln, C. H.; van den Berg, A. M. J.; Schubert, U. S. Microwave-assisted synthesis of a 4(2)-membered library of diblock copoly(2-oxazoline)s and chain-extended homo poly(2-oxazoline)s and their thermal characterization. *Macromolecules* **2005**, *38* (19), 7957−7966.

(20) Wiesbrock, F.; Hoogenboom, R.; Leenen, M. A. M.; Meier, M. A. R.; Schubert, U. S. Investigation of the living cationic ring-opening polymerization of 2-methyl-, 2-ethyl-, 2-nonyl-, and 2-phenyl-2-oxazoline in a single-mode microwave reactor. *Macromolecules* **2005**, *38* (12), 5025−5034.

(21) Meier, M. A. R.; Hoogenboom, R.; Schubert, U. S. Combinatorial methods, automated synthesis and high-throughput screening in polymer research: The evolution continues. *Macromol. Rapid Commun.* **2004**, *25* (1), 21−33.

(22) Hoogenboom, R.; Meier, M. A. R.; Schubert, U. S. Combinatorial methods, automated synthesis and high-throughput screening in polymer research: Past and present. *Macromol. Rapid Commun.* **2003**, *24* (1), 16−32.

(23) Potyrailo, R.; Rajan, K.; Stoewe, K.; Takeuchi, I.; Chisholm, B.; Lam, H. Combinatorial and high-throughput screening of materials libraries: Review of state of the art. *ACS Comb. Sci.* **2011**, *13* (6), 579−633.

(24) Abeylath, S. C.; Ganta, S.; Iyer, A. K.; Amiji, M. Combinatorial-designed multifunctional polymeric nanosystems for tumor-targeted therapeutic delivery. *Acc. Chem. Res.* **2011**, *44* (10), 1009−1017.

(25) Akinc, A.; Lynn, D. M.; Anderson, D. G.; Langer, R. Parallel synthesis and biophysical characterization of a degradable polymer library for gene delivery. *J. Am. Chem. Soc.* **2003**, *125* (18), 5316−5323.

(26) Peters, A.; Brey, D. M.; Burdick, J. A. High-throughput and combinatorial technologies for tissue engineering applications. *Tissue Eng., Part B* **2009**, *15* (3), 225−239.

(27) Hook, A. L.; Chang, C. Y.; Yang, J.; Luckett, J.; Cockayne, A.; Atkinson, S.; Mei, Y.; Bayston, R.; Irvine, D. J.; Langer, R.; Anderson, D. G.; Williams, P.; Davies, M. C.; Alexander, M. R. Combinatorial discovery of polymers resistant to bacterial attachment. *Nat. Biotechnol.* **2012**, *30* (9), 868−U99.

(28) Batchelor, R.; Hagen, D.; Johnson, I.; Beechem, J. A fluorescent high-throughput assay for double-stranded DNA: the RediPlate PicoGreen assay. *Comb. Chem. High Throughput Screen.* **2003**, *6* (4), 287−291.

(29) Anderson, D. G.; Lynn, D. M.; Langer, R. Semi-automated synthesis and screening of a large library of degradable cationic polymers for gene delivery. *Angew. Chem., Int. Ed.* **2003**, *42* (27), 3153−3158.

(30) Regelin, A. E.; Fernholz, E.; Krug, H. F.; Massing, U. High throughput screening method for identification of new lipofection reagents. *J. Biomol. Screen* **2001**, *6* (4), 245−54.

(31) Parhamifar, L.; Larsen, A. K.; Hunter, A. C.; Andresen, T. L.; Moghimi, S. M. Polycation cytotoxicity: a delicate matter for nucleic acid therapy-focus on polyethylenimine. *Soft Matter* **2010**, *6* (17), 4001−4009.
(32) Tauhardt, L.; Kempe, K.; Knop, K.; Altuntas, E.; Jager, M.; Schubert, S.; Fischer, D.; Schubert, U. S. Linear polyethyleneimine: Optimized synthesis and characterization—On the way to "pharma-grade" batches. *Macromol. Chem. Phys.* **2011**, *212* (17), 1918−1924.
(33) Adams, N.; Schubert, U. S. Poly(2-oxazolines) in biological and biomedical application contexts. *Adv. Drug Delivery Rev.* **2007**, *59* (15), 1504−1520.
(34) Schallon, A.; Synatschke, C. V.; Pergushov, D. V.; Jerome, V.; Müller, A. H. E.; Freitag, R. DNA melting temperature assay for assessing the stability of DNA polyplexes intended for nonviral gene delivery. *Langmuir* **2011**, *27* (19), 12042−12051.
(35) van Gaal, E. V. B.; Spierenburg, G.; Hennink, W. E.; Crommelin, D. J. A.; Mastrobattista, E. Flow cytometry for rapid size determination and sorting of nucleic acid containing nanoparticles in biological fluids. *J. Controlled Release* **2010**, *141* (3), 328−338.
(36) van Gaal, E. V. B.; van Eijk, R.; Oosting, R. S.; Kok, R. J.; Hennink, W. E.; Crommelin, D. J. A.; Mastrobattista, E. How to screen non-viral gene delivery systems in vitro? *J. Controlled Release* **2011**, *154* (3), 218−232.
(37) Wightman, L.; Kircheis, R.; Rossler, V.; Carotta, S.; Ruzicka, R.; Kursa, M.; Wagner, E. Different behavior of branched and linear polyethylenimine for gene delivery in vitro and in vivo. *J. Gene Med.* **2001**, *3* (4), 362−72.
(38) Breunig, M.; Lungwitz, U.; Liebl, R.; Klar, J.; Obermayer, B.; Blunk, T.; Goepferich, A. Mechanistic insights into linear polyethylenimine-mediated gene transfer. *Biochim. Biophys. Acta, Gen. Subj.* **2007**, *1770* (2), 196−205.
(39) Goula, D.; Remy, J. S.; Erbacher, P.; Wasowicz, M.; Levi, G.; Abdallah, B.; Demeneix, B. A. Size, diffusibility and transfection performance of linear PEI/DNA complexes in the mouse central nervous system. *Gene Ther.* **1998**, *5* (5), 712−7.
(40) Wightman, L.; Kircheis, R.; Rossler, V.; Carotta, S.; Ruzicka, R.; Kursa, M.; Wagner, E. Different behavior of branched and linear polyethylenimine for gene delivery in vitro and in vivo. *J. Gene Med.* **2001**, *3* (4), 362−72.
(41) Wagner, M.; Rinkenauer, A. C.; Schallon, A.; Schubert, U. S. Opposites attract: Influence of the molar mass of branched poly(ethylene imine) on biophysical characteristics of siRNA-based polyplexese. *RSC Adv.* **2013**, *3*, 12774−12785.
(42) Perevyazko, I.; Vollrath, A.; Hornig, S.; Pavlov, G. M.; Schubert, U. S. Characterization of poly(methyl methacrylate) nanoparticles prepared by nanoprecipitation using analytical ultracentrifugation, dynamic light scattering, and scanning electron microscopy. *J. Polym. Sci., Part A: Polym. Chem.* **2010**, *48* (18), 3924−3931.
(43) Perevyazko, I. Y.; Delaney, J. T.; Vollrath, A.; Pavlov, G. M.; Schubert, S.; Schubert, U. S. Examination and optimization of the self-assembly of biocompatible, polymeric nanoparticles by high-throughput nanoprecipitation. *Soft Matter* **2011**, *7* (10), 5030−5035.
(44) Gebhart, C. L.; Kabanov, A. V. Evaluation of polyplexes as gene transfer agents. *J. Controlled Release* **2001**, *73* (2−3), 401−416.
(45) Rejman, J.; Bragonzi, A.; Conese, M. Role of clathrin- and caveolae-mediated endocytosis in gene transfer mediated by lipo- and polyplexes. *Mol. Ther.* **2005**, *12* (3), 468−474.
(46) Rejman, J.; Oberle, V.; Zuhorn, I. S.; Hoekstra, D. Size-dependent internalization of particles via the pathways of clathrin-and caveolae-mediated endocytosis. *Biochem. J.* **2004**, *377*, 159−169.
(47) Grayson, A. C.; Doody, A. M.; Putnam, D. Biophysical and structural characterization of polyethylenimine-mediated siRNA delivery in vitro. *Pharm. Res.* **2006**, *23* (8), 1868−76.
(48) Kwok, A.; Hart, S. L. Comparative structural and functional studies of nanoparticle formulations for DNA and siRNA delivery. *Nanomedicine* **2011**, *7* (2), 210−9.
(49) Luo, D.; Saltzman, W. M. Enhancement of transfection by physical concentration of DNA at the cell surface. *Nat. Biotechnol.* **2000**, *18* (8), 893−895.
(50) Tros de Ilarduya, C.; Sun, Y.; Duzgunes, N. Gene delivery by lipoplexes and polyplexes. *Eur. J. Pharm. Sci.* **2010**, *40* (3), 159−70.
(51) Perevyazko, I. Y.; Bauer, M.; Pavlov, G. M.; Hoeppener, S.; Schubert, S.; Fischer, D.; Schubert, U. S. Polyelectrolyte complexes of DNA and linear PEI: Formation, composition and properties. *Langmuir* **2012**, *28* (46), 16167−16176.

Supporting information:

Parallel high-throughput screening of polymer vectors for non-viral gene delivery: Evaluation of structure-property-relationships of transfection

Alexandra C. Rinkenauer,[+,§,#] *Antje Vollrath,*[+,§,#] *Anja Schallon,*[+,§] *Lutz Tauhardt,*[+,§] *Kristian Kempe,*[+,§,∫] *Stephanie Schubert,*[§,&] *Dagmar Fischer,*[&] *Ulrich S. Schubert*[+,§,‡,]*

[#]equal contribution

[+]Laboratory of Organic and Macromolecular Chemistry (IOMC), Friedrich Schiller University Jena, Humboldtstraße 10, 07743 Jena, Germany

[§]Jena Center for Soft Matter (JCSM), Friedrich Schiller University Jena, Philosophenweg 7, 07743 Jena, Germany

[&]Institute of Pharmacy, Department of Pharmaceutical Technology, Friedrich Schiller University Jena, Otto-Schott-Str. 41, 07745 Jena, Germany

[‡]Dutch Polymer Institute, P.O. Box 902, 5600 AX Eindhoven, The Netherlands

[∫] Current address: Department of Chemical and Biomolecular Engineering, The University of Melbourne, Victoria 3010, Australia

* Address correspondence to: ulrich.schubert@uni-jena.de

1. Experimental section

Synthesis of LPEI

LPEIs were synthesized from the corresponding poly(2-ethyl-2-oxazoline)s (PEtOx) by acidic hydrolysis as described in literature.[1] Briefly, PEtOx (2 g) was dissolved in 6 M aqueous hydrochloric acid (15 mL) and heated at 130 °C for 1 h in a Initiator Sixty single-mode microwave synthesizer from Biotage, equipped with a noninvasive IR sensor (accuracy: ± 2%). The acid was removed under reduced pressure. The residue was dissolved in water and 3 M aqueous NaOH was added until precipitation occurred. The precipitate was filtered off, recrystallized from water, filtered, dissolved in methanol, and precipitated into ice-cold diethyl ether. Subsequently, the LPEI was dried for 3 day at 40 °C. The degrees of hydrolysis were determined by ^{1}H NMR spectroscopy and found to be 99% for all LPEIs. A detailed characterization of the short $LPEI_{20}$ can be found elsewhere.[1-2] ^{1}H NMR (300 MHz, CD_3OD): δ = 3.65 (t, CH_2-OH), 2.73 (br., N-CH_2), 2.39 (s, CH_3-N). IR (FT-IR): ν = 3217 (NH), 2 873 (CH_3), 2804 (CH), 1 446 (CH_2/CH_3), 1330 (C-N), 1134 (C-N), 1103 (C-N) cm^{-1}.

Table S1. SEC-Data of the PEtOx precursors.

PEtOx precursor	Repeating units[a)]	M_n (g/mol)[b)]	PDI[b)]
$PEtOx_{20}$	20	3,600	1.11
$PEtOx_{200}$	200	58,200	1.14
$PEtOx_{600}$	600	40,600	1.79

[a)]Calculated from ^{1}H NMR; [b)]Determined by size exclusion chromatography (solvent: chloroform/triethylamine/ iso-propanol [94/4/2]; calibration standard: PS)

Investigation of polyplex size and stability

For first studies, the polyplex sizes were studied by utilization of a Zetasizer Nano ZS (Malvern Instruments, Herrenberg, Germany). The measurements were carried out in a minimal volume cuvette ZEN 0040 (BRAND GmbH, Wertheim, Germany) with a laser beam at 633 nm and a

scattering angle of 173° at 25 °C. The viscosity (0.89 mPa s) and refractive index (1.33) of purified water at 25 °C were used for data analysis. 40 µL of polyplex suspensions were measured five times for 20 sec. The mean particle size was approximated as the effective (Z average) diameter and calculated with the General purpose (normal resolution) algorithm using the Malvern software 6.20. For the polyplex size analysis by dynamic light scattering, a DynaPro Plate Reader Plus (Wyatt Technology Corporation, Santa Barbara, CA) equipped with a 60 mV linearly polarized gallium arsenide (GaAs) laser of $\lambda = 832.5$ nm and operating at an angle of 156° was utilized. Again, the viscosity (0.89 mPa s) and refractive index (1.33) of purified water at 25 °C were used for data analysis. The data were analyzed with the Dynamics software ver. 6.10 by the method of cumulants as previously described for nanoparticle analysis.[3] The measurement time was set to 10 seconds per run and 10 acquisitions were collected five times per well and repeated 3 times in independent experiments.

Polyplex preparation: conventional methode

Polyplexes of pDNA and polymer were prepared by adding polymers at a certain N/P ratio to stock solutions of pDNA with 15 µg mL^{-1} in HBG buffer (20 mM 4-(2-hydroxethyl) piperazine-1-ethanesulfonic acid (HEPES) and 5% (w/v) glucose, pH 7.2). Subsequently, the solutions were vortexed for 10 sec at maximal speed, and incubated at room temperature for 10 min.

Binding affinity

The polyplex formation and binding affinity responsible for complexation of pDNA and polymers were detected by quenching of the ethidium bromide (EB) fluorescence as described previously.[4] After the polyplex preparation via pipetting robot or per hand, 100 µL of the polyplex solution were incubated with EB (0.4 µg mL^{-1}) for 10 min at room temperature in black 96-well plates (Nunc, Langenselbold, Germany). The fluorescence was measured using a Tecan

Genios Pro fluorescence microplate reader (Tecan, Crailsheim, Germany) with excitation and emission wavelength at 525 and 605 nm, respectively. A sample containing only pDNA and EB was used to calibrate the device to 100% fluorescence. The percentage of dye displaced upon polyplex formation was calculated using equation (1):

$$\text{RFU}\ [\%] = \frac{F_{\text{sample}}}{F_{\text{pDNA}}} \qquad (1)$$

Here, RFU represent the relative fluorescence. F_{sample} and F_{siRNA} indicate the fluorescence intensities of a given sample and the EB intercalated into pDNA alone, respectively.

DNA release by heparin

To investigate the release of pDNA from polyplexes, the heparin dissociation assay was used. For this purpose, 100 µL of polyplex solution were incubated for 10 min with EB (0.4 µg mL^{-1}) in a black 96-well plate. After transferring into the Tecan Genios Pro fluorescence microplate reader, heparin solutions were automatically added at the indicated concentrations. Therefore, 20 cycles of the following procedure were used: 5 µL of heparin stock solutions (10 U mL^{-1} or 200 U mL^{-1}) were dropped to each well. Afterwards the plate was shaked (orbital, 10 sec, 2 mm) and incubated for 5 min at 37 °C. After each cycle, the fluorescence of EB was measured, and the percentage of intercalated EB was calculated as described before (1).

Cell Culture

HEK-293 (CRL-1573, ATCC) cells were maintained in RPMI 1640 culture medium, L929 (CCL-1, ATCC) in DMEM culture medium. Both media were supplemented with 10% fetal calf serum (FCS), 100 µg/mL streptomycin, 100 IU mL^{-1} penicillin, and 2 mM L-glutamine. Cells were cultivated at 37 °C in a humidified 5% CO_2 atmosphere.

Cytotoxicity

The cytotoxicity of the single polymers was tested with L929 cells, as this cell line is recommended by ISO10993-5. In detail, cells were seeded at 10^4 cells per well in a 96-well plate and incubated for 24 h. No cells were seeded in the outer wells. Afterwards, polymers at the indicated endconcentrations were added, the plates were slued, and incubated at 37 °C for further 24 h. Subsequently, the medium was replaced by PBS and AlamarBlue as recommended by the supplier. After incubation for 4 h, the fluorescence was measured at Ex 570 / Em 610 nm, with untreated cells on the same well plate serving as controls (2).

$$\text{viability [\%]} = \frac{F_{sample} - F_0}{F_{control} - F_0} \quad (2)$$

Here, viability is the relative fluorescence and F_{sample}, F_0, and $F_{control}$ are the fluorescence intensities of a given sample, the blank wells without cells, and the control cells without polymer treatment.

Transfection of cells: HT manner

HEK 293 cells were maintained in RPMI 1640 culture medium, supplemented with 10% fetal calf serum (FCS), 100 µg mL^{-1} streptomycin, 100 IU mL^{-1} penicillin, and 2 mM L-glutamine. Cells were cultivated at 37 °C in a humidified 5% CO_2 atmosphere.

For transfection experiments, HEK cells were seeded at a density of 10^4 cells per well in 96-well plates 24 h before transfection. In order to avoid any misleading measurement results and to prevent a systematic mistake, the polyplexes were always placed and measured at different positions in the 96-well plate to avoid alterations due to differences in the gas exchange between outer and inner wells and 25 measuring points per well were taken. One hour prior transfection, cells were washed with PBS and supplemented with 100 µL OptiMEM (Life Technologies). Polyplex solutions were added (10 µL) to the cells and the plates were slued and incubated for 4 h at 37 °C. Afterwards, the supernatant was replaced by 100 µL of fresh growth medium (RPMI1640 based), and the cells were further incubated for 20 h. Before analysis, the cells were

incubated with 1 µg mL^{-1} Hoechst 33324 for 10 min at 37 °C, washed twice with PBS, and the plates were transferred to the plate reader. The expression of EGFP fluorescence (Ex 475 nm / Em 509 nm) and viability (Hoechst, Em 350 nm / Ex 461 nm) was quantified by using the fluorescence measured from the bottom of the plates. The transfection efficiency was calculated relative to cell number and control cells using the following equation (3), where and $EGFP_{sample}$, $EGFP_{control}$, $Hoechst_{sample}$, $Hoechst_{control}$ are the fluorescence signal of EGFP and Hoechst of treated (sample) and non treated (control) cells, respectively. Experiments were repeated 3 times independently.

$$\text{transfection efficiency} = \frac{EGFP_{sample} - EGFP_{control}}{Hoechst_{sample}/Hoechst_{control}} \quad (3)$$

Transfection of cells: conventional method

For transfection of the HEK 293 cell lines, cells were seeded at a density of 10^5 cell mL^{-1} in 12-well plates one day before transfection. One hour prior to transfection, cells were rinsed with PBS and supplemented with 1 mL OptiMEM (Life Technologies). Polyplexes (100 µL) were added to the cells and the plates were incubated for 4 h in the incubator. Afterwards, the supernatant was replaced by1 mL of fresh growth medium, and the cells were further incubated for 20 h. For analysis, adherent cells were harvested by trypsinization.

For determination of, dead cells, they were counterstained with propidium iodide. The relative expression of EGFP fluorescence of 10^4 cells was quantified via flow cytometry using a Cytomics FC 500 (Beckman Coulter). For determination of the transfection efficiency viable cells expressing EGFP were gated using non-treated cells as negative control. Experiments were repeated ≥ 3 times independently.

2. Results and Discussions

2.1 Comparison of conventional handmade polyplexes and polyplexes prepared by HT workflow

For examination of the presented HT screening workflow, selected experiments were performed with conventional methods, also called handmade.

2.1.1 Investigations of polyplex size and stability

In order to compare the preparation of the polyplexes *via* pipetting robot with the conventional vortexing method, $lPEI_{600}$ and $bPEI_{600}$ polymers were chosen for polyplex formation with DNA applying both techniques, pipetting and vortexing. As shown in Table S2, similar polyplex sizes and polydispersities were observed proving that the pipetting approach is suitable for the preparation of polyplexes.

Table S2. Hydrodynamic radii of polyplexes prepared by conventional preparation (vortexed for 10 sec, incubated for at least 15 min) and pipetting. Radii were measured with Zetasizer Nano ZS (Malvern Instruments, Herrenberg, Germany).

	METHOD	PEI (μL)	DNA (µL)	HB (µL)	Z Average (r, nm)	PDI
$lPEI_{600}$	pipetted 3x mix	100	50	50	80	0.40
	vortexed 10s	100	50	50	79	0.38
$bPEI_{600}$	pipetted 3x mix	100	50	50	68	0.23
	vortexed 10s	100	50	50	75	0.43

2.1.2 Transfection efficiency and binding affinity

Exemplary the transfection efficiency of the linear PEIs were performed handmade and analyzed with flow cytometer. The same tendencies obtained as with the platereader can be observed: enhanced transfection efficiencies with increased molar mass. This demonstrates the potential of using the platereader in a HT screening manner

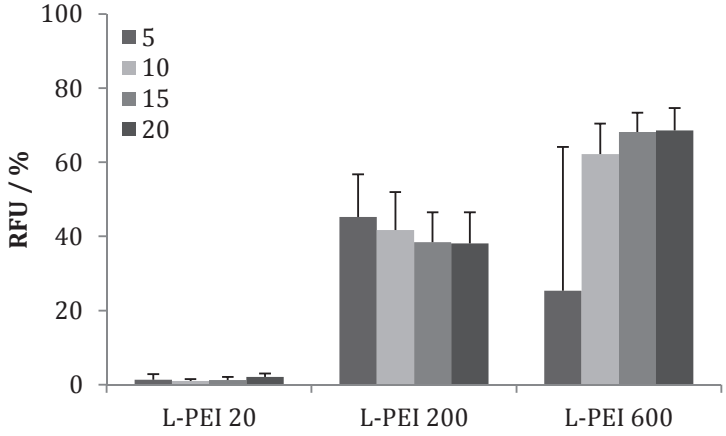

Figure S1. Transfection efficiency of linear PEIs: Polyplexes were formed handmade and analyzed via flow cytometer (n=3).

Moreover the binding affinity was analyzed. In this case the polyplexes were formed per hand and afterwards measured like in HT manner.

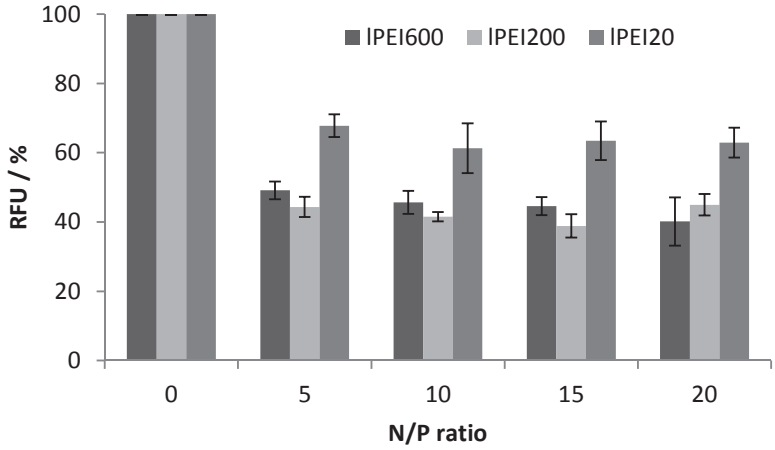

Figure S2. Fluorescence displacement assay of linear PEIs. EBA were performed handmade (n=3).

2.1.4 Cytotoxicity

Moreover the proof of the AlamarBlue as cytotoxicity test system was proven. Thus the high and low molecular weight PEIs were exemplary used. As shown in figure S3 the high molecular weight PEIs show the excepted cytotoxicity in contrast to the low molecular weight one. Demonstrating the possibility to use the AlamarBlue assay as test sytem.

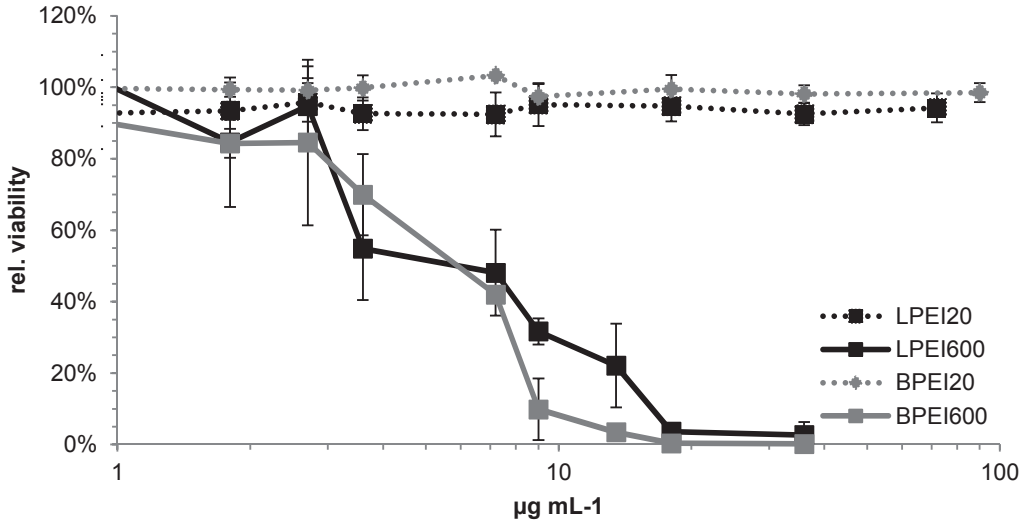

Figure S3. Cytotoxicity of the high and low molecular PEIs using the AlamarBlue assay (n=3)

2.2 Time-dependent stability of polyplexes

Additionally, selected polyplexes were studied over 2 h and revealed no occurance of aggregation (Table S3), which further confirmed the formation of stable polyplexes by utilization of the pipetting robot.

Table S3. Hydrodynamic radii of polyplexes prepared from $lPEI_{600}$ at NP 20 measured with Zetasizer Nano ZS (Malvern Instruments, Herrenberg, Germany).

Time [min]	Radius [nm]	PDI^P
30	82	0.400
60	58	0.325
120	59	0.395

2.3 Comparison of HT-DLS investigations with conventional single DLS measurements using NanoZetasizer, Malvern

To evaluate the reliability of the HT-DLS instrument, the polyplex sizes were measured manually using the Zetasizer (Malvern) (Figure S4). Polyplexes for all N/P ratios and all PEIs revealed thereby radii between 33 to 100 nm with PDI^Ps in a range of 0.2 to 0.6. Throughout this study, the values obtained by the Zetasizer were smaller compared to the ones measured by HT-DLS

reader. This could be due to the different measurement procedures, in particular in the case of the HT-DLS reader, where aggregates, often sediment during measurements, are taken much more into account. In the Zetasizer the laser beam passes the solution from one side in a defined height, where as the laser beam in the HT-DLS reader passes from the bottom.

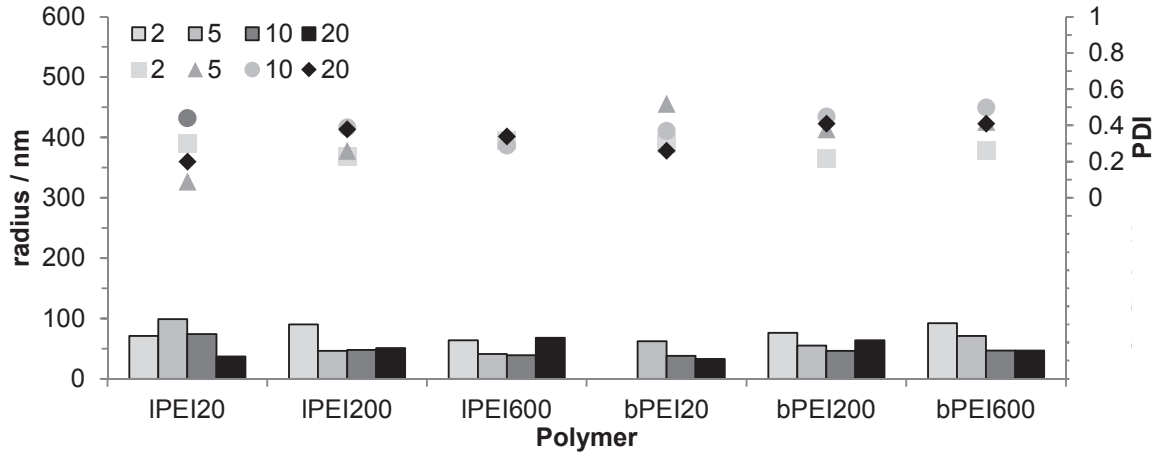

Figure S4. Hydrodynamic radii and PDI^P of polyplexes prepared from various linear and branched PEIs (number indicate the DP) at indicated NP ratios (2, 5, 10, 20) prepared by pipetting robot and measured with Zetasizer Nano ZS.

1. Tauhardt, L.; Kempe, K.; Knop, K.; Altuntaş, E.; Jäger, M.; Schubert, S.; Fischer, D.; Schubert, U. S., Linear Polyethyleneimine: Optimized Synthesis and Characterization – On the Way to "Pharmagrade" Batches. *Macromol. Chem. Phys.* **2011,** *212* (17), 1918-1924.
2. Altuntaş, E.; Knop, K.; Tauhardt, L.; Kempe, K.; Crecelius, A. C.; Jäger, M.; Hager, M. D.; Schubert, U. S., Tandem mass spectrometry of poly(ethylene imine)s by electrospray ionization (ESI) and matrix-assisted laser desorption/ionization (MALDI). *J. Mass Spec.* **2012,** *47* (1), 105-114.
3. Perevyazko, I. Y.; Delaney, J. T.; Vollrath, A.; Pavlov, G. M.; Schubert, S.; Schubert, U. S., Examination and optimization of the self-assembly of biocompatible, polymeric nanoparticles by high-throughput nanoprecipitation. *Soft Matter* **2011,** *7* (10), 5030-5035.
4. Tang, M. X.; Szoka, F. C., The influence of polymer structure on the interactions of cationic polymers with DNA and morphology of the resulting complexes. *Gene Ther.* **1997,** *4* (8), 823-832.

Publication 12

"Characterization of cationic polymers by asymmetric flow field-flow fractionation and multi-angle light scattering – A comparison with traditional techniques"

M. Wagner, C. Pietsch, L. Tauhardt, A. Schallon, U. S. Schubert

J. Chromatogr. A **2014***, 1325,* 195-203

Journal of Chromatography A, 1325 (2014) 195–203

Contents lists available at ScienceDirect

Journal of Chromatography A

journal homepage: www.elsevier.com/locate/chroma

Characterization of cationic polymers by asymmetric flow field-flow fractionation and multi-angle light scattering—A comparison with traditional techniques

Michael Wagner[a,b], Christian Pietsch[a,b], Lutz Tauhardt[a,b], Anja Schallon[a,b], Ulrich S. Schubert[a,b,*]

[a] Laboratory of Organic and Macromolecular Chemistry (IOMC), Friedrich Schiller University Jena, Humboldtstraße 10, 07743 Jena, Germany
[b] Jena Center for Soft Matter (JCSM), Friedrich Schiller University Jena, Philosophenweg 7, 07743 Jena, Germany

ARTICLE INFO

Article history:
Received 18 April 2013
Received in revised form
10 September 2013
Accepted 26 November 2013
Available online 7 December 2013

Keywords:
Cationic polymers
Field flow fractionation
Gene delivery
PEI
PDMAEMA
PLL

ABSTRACT

In the field of nanomedicine, cationic polymers are the subject of intensive research and represent promising carriers for genetic material. The detailed characterization of these carriers is essential since the efficiency of gene delivery strongly depends on the properties of the used polymer. Common characterization methods such as size exclusion chromatography (SEC) or mass spectrometry (MS) suffer from problems, *e.g.* missing standards, or even failed for cationic polymers. As an alternative, asymmetrical flow field-flow fractionation (AF4) was investigated. Additionally, analytical ultracentrifugation (AUC) and ^{1}H NMR spectroscopy, as well-established techniques, were applied to evaluate the results obtained by AF4. In this study, different polymers of molar masses between 10 and 120 kg mol^{-1} with varying amine functionalities in the side chain or in the polymer backbone were investigated. To this end, some of the most successful gene delivery agents, namely linear poly(ethylene imine) (LPEI) (only secondary amines in the backbone), branched poly(ethylene imine) (B-PEI) (secondary and tertiary amino groups in the backbone, primary amine end groups), and poly(L-lysine) (amide backbone and primary amine side chains), were characterized. Moreover, poly(2-(dimethylamino)ethyl methacrylate) (PDMAEMA), poly(2-(amino)ethyl methacrylate) (PAEMA), and poly(2-(*tert*-butylamino)ethyl methacrylate) (P*t*BAEMA) as polymers with primary, secondary, and tertiary amines in the side chain, have been investigated. Reliable results were obtained for all investigated polymers by AF4. In addition, important factors for all methods were evaluated, *e.g.* the influence of different elution buffers and AF4 membranes. Besides this, the correct determination of the partial specific volume and the suppression of the polyelectrolyte effect are the most critical issues for AUC investigations.

1. Introduction

Polyelectrolytes, in particular cationic polymers, are a highly promising class of compounds in biological, pharmaceutical, and medical research. They represent promising carriers for genetic material like DNA or RNA into cells [1–3]. The efficiency of gene delivery strongly depends on different parameters, such as the molar mass and architecture of the used polymer, since they influence the cytotoxicity, the cellular uptake, and transfection efficiency, or in the case of siRNA the protein knockdown. To investigate these structure–property relationships, a detailed molecular characterization of the polymers with respect to their physico-chemical properties is essential. In particular, key parameters such as molar mass, radius, architecture, intermolecular interactions, and conformation strongly influence the resulting macroscopic properties. For the determination of the molar mass, a large range of techniques are available in modern analytical and bioanalytical chemistry. Unfortunately, common methods like size exclusion chromatography (SEC) or mass spectrometry (MS) suffer problems or failed for polyelectrolytes, in particular for cationic ones [4,5]. While results from MS (MALDI–TOF MS or ESI–TOF MS) are difficult to achieve and the interpretation becomes more complex due to the probable multiply charged species in the polymer chain [6], SEC results should be regarded carefully, due to strong interactions of the polyelectrolytes with the column material and the lack of suitable standards for most of the cationic polymers [7]. Here, the development of modern stationary phases and the coupling of a multi-angle light scattering (MALS)

* Corresponding author at: Laboratory of Organic and Macromolecular Chemistry (IOMC), Friedrich Schiller University Jena, Humboldtstraße 10, 07743 Jena, Germany. Tel.: +49 3641948201.
E-mail addresses: ulrich.schubert@uni-jena.de, u.s.schubert@tue.nl (U.S. Schubert).

0021-9673/$ – see front matter © 2013 Elsevier B.V. All rights reserved.
http://dx.doi.org/10.1016/j.chroma.2013.11.049

detector to SEC can circumvent some of these limitations [8]. Other methods like viscosimetry or techniques based on colligative phenomena are applicable, but suffer the drawback that the constants in the Kuhn–Mark–Houwink–Sakurada equation are not available for most of these polymers, moreover, the determination of the degree of protonation of the polymer in water and the degree of dissociation are problematic. As a consequence, in solution the amount of species having counterions is not known. Further, important methods for characterization are NMR spectroscopy, static light scattering (SLS), and analytical ultracentrifugation (AUC). However, just average values and no or limited information about the polydispersity index (PDI) of the sample can be obtained. Having knowledge of the PDI is important from a synthetical and applicational point of view, particularly when structure–property relationships are investigated.

Due to intrinsic limitations described for the other analytical methods, asymmetric flow field-flow fractionation (AF4) coupled to a UV/RI and a MALS detector was investigated in this study as an alternative characterization method for cationic polyelectrolytes. AF4 was firstly introduced in 1966 by J. Calvin Giddings. It is an emerging technique and nowadays widely applied for colloids, *e.g.* nanoparticles or proteins [9]. Although preferred for the analysis of high molar mass samples, only rarely studies were performed using synthetic macromolecules, in particular polyelectrolytes of lower molar mass [10–13]. With AF4, the polymers are separated in a trapezoidal channel without any porous packing material according to their diffusion coefficient [14]. The separation of the sample is achieved by application of a cross-flow perpendicular to the direction of the sample flow through a semipermeable membrane with a defined molar mass cut-off (MWCO). A detailed description and theoretical consideration for the calculation of the diffusion coefficient based on the retention time was given by Wahlund and Giddings [15]. In comparison to classic chromatography techniques such as HPLC or SEC, AF4 contains no stationary phase, which reduces disturbing interactions and adsorption effects in the most cases. Moreover, the flow is less tortuous for the sample, due to the decreased shear forces in an empty channel. This is advantageous for sensitive biological samples [16]. Nowadays, in most cases, a MALS detector is used for the analysis after the fractionation process [17]. The calculation of molar mass or radius of gyration is based on the same principle as classic static light scattering. A common way to treat the data uses the well-known Zimm-plot. In contrast to classical SLS, the second virial coefficient A_2 can be neglected due to the high dilution during the fractionation process.

In contrast to AF4, analytical ultracentrifugation (AUC) and ^{1}H NMR spectroscopy are well-established techniques, which are used for many years for the characterization of biological and synthetic macromolecules [18–20]. It should be noted that both methods yield different molar mass averages. While ^{1}H NMR spectroscopy gives the number average molar mass (M_n), in AUC the sedimentation diffusion average molar mass (M_{sD}) is obtained from sedimentation velocity experiments and the Svedberg equation (1). These methods can be used for the comparison of the results and to show the potentials and possible limitations of AF4 with regard to the characterization of (cationic) polymers.

In this study, cationic polymers of different molar masses with varying amine functionalities in the side chain or the polymer backbone (Fig. 1) were investigated for the first time by AF4. As the most successful gene delivery agents, a tailor-made linear, and commercially available linear and branched poly(ethylene imine)s (L-PEI, B-PEI) were characterized [21]. Moreover, poly(2-(dimethylamino)ethyl methacrylate) (PDMAEMA), poly(2-(amino)ethyl methacrylate) (PAEMA), and poly(2-(*tert*-butylamino)ethyl methacrylate) (P*tBAEMA*) as polymers with primary, secondary, and tertiary amines in the side chain were studied. Additionally, two samples of different molar masses of commercially available poly(L-lysine) (PLL), a prominent polyamino acid in gene delivery research [22], are analyzed by AF4. As AF4-MALS is typically not applied to low molar mass ($M < 100\,kg\,mol^{-1}$) polymers, this study focuses on the evaluation of AF4 as a potential alternative for characterization of these cationic polyelectrolytes. Therefore, the results obtained from the synthesized methacrylate based cationic polymers are compared to well-established methods like ^{1}H NMR spectroscopy, SEC and AUC. Beside the determination of the molar masses and the polydispersity index values, different types of membranes and eluents were evaluated to identify optimal conditions for the analysis. This should also reveal potential interactions with the membrane and show how far it affects the retention behavior and the obtained results. PDMAEMA was studied in more detail by AF4 to gain deeper insight into the conformation as well as the influence of ionic strength and pH value on the retention behavior. This study shows that AF4 allows fast and reliable characterization of cationic polymers. Moreover, the limitations concerning molar mass limits and membrane interactions for different classes of cationic polymers are discussed in detail.

2. Experimental

2.1. Materials

Poly(L-lysine) (PLL) and branched poly(ethylene imine) (B-PEI$_{com}$) were purchased from Sigma Aldrich (Steinhausen, Germany). Linear poly(ethylene imine) (L-PEI$_{com}$) was purchased from Polysciences (Eppelheim, Germany). Methyl tosylate and 2-ethyl-2-oxazoline (EtOx) were purchased from Acros Organics (Geel, Belgium), distilled to dryness over barium oxide (BaO), and stored under argon. A second linear poly(ethylene imine) (L-PEI$_{600}$) was synthesized by acidic hydrolysis of poly(2-ethyl-2-oxazoline) (PEtOx) in a microwave synthesizer (Biotage) as described recently (see supporting info SI-I) [6].

2-(Dimethylamino)ethyl methacrylate (DMAEMA), 2-aminoethyl methacrylate hydrochloride (AEMA) and 2-(*tert*-butylamino)ethyl methacrylate (*tBAEMA*) were purchased from Sigma–Aldrich and purified by stirring in the presence of inhibitor-remover for hydroquinone or hydroquinone monomethyl ether (Aldrich) for 30 min prior to use. The initiators 4,4′-azo*bis*(4-cyanopentanoic acid) (ACVA), 1,1′-azo*bis*(cyclohexane carbonitrile) and 4-cyano-4-(phenylcarbonothioylthio)pentanoic acid as well as 4-cyano-4-[(dodecylsulfanylthiocarbonyl) sulfanyl] pentanoic acid RAFT agents were purchased from

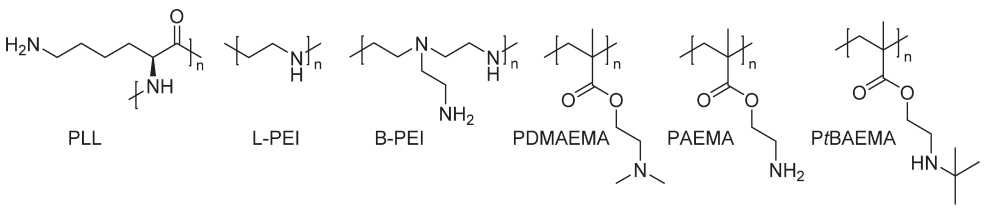

Fig. 1. Schematic representation of the structure of the polymers used in this study.

Sigma–Aldrich. Poly(2-(dimethylamino)ethyl methacrylate) (PDMAEMA), poly(2-(amino)ethyl methacrylate) (PAEMA), and poly(2-(*tert*-butylamino)ethyl methacrylate) (P*tBAEMA*) were synthesized using the RAFT polymerization technique (see supporting info SI-II) [23,24]. All solvents, salts and other chemicals used in this study were of analytical grade or better.

2.2. Analytical ultracentrifugation (AUC)

AUC was performed using a Beckman XL-I analytical ultracentrifuge (ProteomeLab XLI Protein Characterization System). Experiments were carried out in double-sector epon or aluminum centerpieces, depending on the solvent, with optical path length of 12 mm in a four holes rotor setup. Each cell was filled with 0.44 mL of solvent and 0.42 mL of sample. A rotor speed of 40,000 rpm was used for all samples. The system was equilibrated for 40 min at 25 °C in the centrifuge. Sedimentation data were recorded by absorbance optics. Data analysis was done by the Sedfit software [25]. For c(s) analysis of sedimentation data, the partial specific volume of the polymers was determined *via* AUC using the "density variation method" as described by Mächtle [26]. For calculating the molar mass the Svedberg equation (1) was used:

$$M_{sD} = \frac{s_0 RT}{D_0(1-\bar{\nu}\rho)} \quad (1)$$

Here, R is the universal gas constant, T is the temperature, s_0 is the sedimentation coefficient, D_0 is the translational diffusion coefficient, $\bar{\nu}$ is the partial specific volume and ρ is the density of the solvent. Solvent density and viscosity measurements were performed on a DMA 02 density meter (Anton Paar, Graz, Austria) and an AMVn falling sphere viscometer (Anton Paar). s_0 was obtained by measurement of at least three concentrations and extrapolation to zero concentration using the Gralen relations [27].

2.3. Dynamic light scattering

Dynamic light scattering (DLS) was performed using an ALV-CGS-3 system (ALV, Langen, Germany) equipped with a He–Ne laser operating at a wavelength of $\lambda = 633$ nm. The counts were detected at angles θ of 30°, 60°, 90°, 120°, and 150°. All measurements were carried out at 25 °C after an equilibration time of 120 s. All polymers were measured at three different concentrations. For analyzing the autocorrelation function, the CONTIN algorithm [28] was applied. The diffusion coefficient was obtained by linear extrapolation of the apparent diffusion coefficient to zero concentration and $\theta = 0°$. Hydrodynamic radii were calculated according to the Stokes–Einstein equation (2):

$$R_H = \frac{kT}{6\pi\eta D_0} \quad (2)$$

Here, R_H is the hydrodynamic radius, k is the Boltzmann constant, T is the absolute temperature, η is the viscosity of the sample, and D_0 is the translational diffusion coefficient.

2.4. Asymmetric flow field-flow fractionation (AF4)

Asymmetric flow field-flow fractionation (AF4) was performed on an AF2000 MT System (Postnova Analytics, Landsberg, Germany) coupled to an UV (PN3211, 260 nm), RI (PN3150) and MALS (PN3070, 633 nm) detector. The eluent is delivered by three different pumps (tip, focus, cross-flow) and the sample is injected by an autosampler (PN5300) into the channel. The channel has a trapezoidal geometry and an overall area of 31.6 cm^2. The nominal height of the spacer was 500 μm and a regenerated cellulose membrane (Z-MEM-AQU-670, PostNova Analytics) with a MWCO of 10 kg mol^{-1} was used as accumulation wall, if not stated otherwise. All experiments were carried out at 25 °C. For each measurement 20 μL of the sample were injected with an injection flow rate of 0.2 mL min^{-1} for 7 min. For PLL and L/B-PEI the detector flow rate was set to 0.6 mL min^{-1} and 0.8 mL min^{-1} for PDMAEMA, PAEMA and P*tBAEMA*. The cross-flow rate was set to 5 mL min^{-1} for PLL, 4.5 mL min^{-1} for L-PEI and 4 mL min^{-1} for B-PEI_{com} as well as the methacrylate based polymers. After the focusing step, the cross-flow rate was kept constant for 5 min and then reduced under an exponential gradient (0.5) within 20 min to 0.1 mL min^{-1}. Afterwards, the cross-flow rate was reduced under a linear gradient to zero within 5 min and then kept constant for 20 min to ensure complete elution. For calculation of the molar mass and the radius of gyration from the MALS signal, the Zimm plot, according to Eq. (3), was used [29]. All measurements were repeated five times

$$\frac{Kc}{R(\theta)} = \frac{1}{M}\left(1 + \frac{2}{3!}\langle R_g^2\rangle\left[\frac{4\pi\eta_0}{\lambda}\sin\frac{\theta}{2}\right]^2\right) \quad (3)$$

$$K = \frac{(2\pi n_0(dn/dc))^2}{\lambda^4 N_A} \quad (4)$$

Here, K is a constant factor according to Eq. (4), c is the concentration, R is the excess Rayleigh ratio, M is the molar mass, R_g is the radius of gyration, λ is the laser wavelength, θ is the scattering angle, n_0 is the refractive index of the solvent, N_A is the Avogadro's number and dn/dc is the refractive index increment.

2.5. Refractive index increment

The refractive index increment of the samples was measured by manual injection of a known concentration directly into the AF4 channel without any focusing or cross-flow. Integration of the RI signal and comparison with the injected mass gives the dn/dc value. All measurements were repeated five times. To increase the accuracy, all polymers were dissolved in the eluent of the corresponding AF4 run.

2.6. ^1H NMR spectroscopy

Proton nuclear magnetic resonance (^{1}H NMR) spectra were recorded on a Bruker AC 300 (300 MHz) spectrometer at 298 K. The chemical shifts are reported in parts per million (ppm, δ scale) relative to the signals from the NMR solvents. The standard deviations were calculated using the individual —CH_2— signals of the polymer.

2.7. Size-exclusion chromatography

Size-exclusion chromatography (SEC) of the PEtOx precursor, PDMAEMA and PAEMA was performed on a system using an Agilent1200 series system, a G1310A pump, G1329A autosampler, a G1362A refractive index detector and both a PSS Gram 30 and a PSS Gram 1000 column in series, whereby *N*,*N*-dimethylacetamide (DMAc) with 50 mM lithium chloride was used as an eluent at 1 mL min^{-1} flow rate and the column oven was set to 40 °C. The system was calibrated against polystyrene (M_n from 374 g mol^{-1} to 1,040,000 g mol^{-1}) standards. Additional SEC experiments of P*tBAEMA* were performed on a JASCO system equipped with a PU-980 pump, a RI-930 refractive index detector and a PSS SUPREMA-MAX guard/300 Å column using water with 0.1% trichloracetic acid (pH 2.3) and 0.05 M NaCl as eluent and the column oven was set to 30 °C. A calibration with low PDI pullulan standards was used.

3. Results and discussion

In principle, AF4 coupled to a UV/RI-MALS detector allows a detailed characterization of biological and synthetic macromolecules or nanoparticles by combination of a gentle separation with the broad molar mass and size range of SLS. Nevertheless, AF4-MALS was, to the best of our knowledge, never applied on these kinds of polymers. Therefore, the results have to be compared to already well-established methods. On the one hand, data from the supplier were used for the commercially available polymers (PLL, B-PEI$_{com}$, L-PEI$_{com}$) that are often obtained by classic light scattering, SEC, or viscosity. On the other hand, polymers synthesized in our lab (polymethacrylates, L-PEI$_{600}$) were characterized using AUC, SEC, and end group analysis by ^{1}H NMR.

3.1. AF4 – choice of eluent and membrane

For AF4, several types of membranes with different MWCOs and different eluents can be used to influence the retention of the sample. Besides the limitations of the MALS detector, the MWCO of the membrane predefines the lowest molar mass, which can be studied. All samples with a molar mass below the MWCO will, in theory, pass through the membrane and, hence, cannot be analyzed. Another important parameter, with regard to the used solvent and the potential interactions between the sample and the membrane surface, is the chemical nature of the membrane. The available membranes have different surface charges as well as varying degrees of hydrophilicity and hydrophobicity. In the case of aqueous eluents, the interactions with the sample can be affected by adjusting the pH, addition of surfactants or increasing the ionic strength, *e.g.* for screening of charges. Also the adsorption of ions or the addition of chaotropic or kosmotropic agents, which influence the hydration of the sample, can alter the interactions and the resulting retention behavior [30]. Since the investigated polymers show a high positive charge density and in the case of the methacrylate based polymers a hydrophobic backbone, several eluent compositions and three different membranes were evaluated, namely: a regenerated cellulose (RC), a cellulose triacetate (CTA), and a polyvinylidenedifluoride (PVDF) membrane. As eluents water with different amounts of sodium chloride, sodium azide, sodium hydroxide, and solutions containing urea as chaotropic agent were investigated. Additionally, an acetate as well as an ammonia buffer at different pH values and ionic strength were studied. On PVDF and CTA based membranes, strong sample interactions were observed, leading to peak deformation and broadening (SI-III). This behavior was independent of the ionic strength, which was varied from 0 to 150 mM NaCl. In particular, CTA membranes with a MWCO < 10 kg mol^{-1} and PVDF membranes (MWCO 30 kg mol^{-1}) showed large deviations between different batches. These findings can probably be attributed to a non-uniform pore size distribution. The best results were obtained using a RC membrane with a MWCO of 10 kg mol^{-1} and water containing 0.02% NaN_3, to avoid bacterial growth, as eluent. The isoeletric point of this membrane is around 3.4, so that it is negatively charged at pH > 3.4 and positively charged at pH < 3.4 [31]. At neutral pH, this causes attractive electrostatic interactions between the negative surface of the membrane and the positive charges in the polymer, and consequently leads to the adsorption of polymer chains onto the surface of a fresh RC membrane after the first injection. During further injections repulsive forces occur between the now positively charged membrane surface and the sample, leading to reduced interactions and fast retention [32]. Taking this into account, the polyelectrolyte saturated RC membrane was used to determine the molar mass of all polymers investigated in this study.

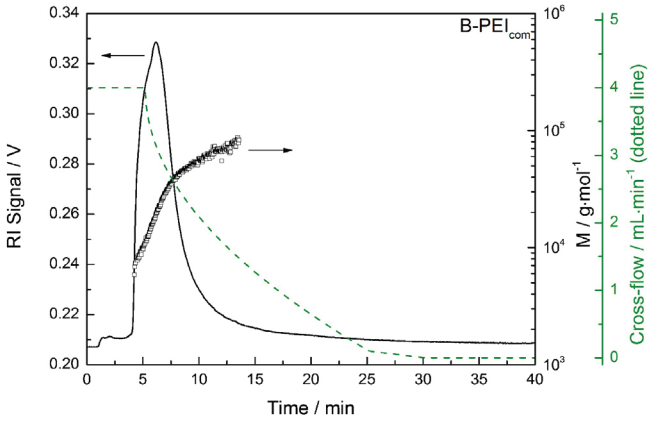

Fig. 2. AF4 fractogram with the corresponding cross-flow rate and molar masses of B-PEIcom.

3.2. Poly(ethylene imine) (PEI)

PEI is a well-known cationic polymer and used in several applications, *e.g.* for waste water treatment [33], as flocculant in paper industry [34], and it is of high interest in the field of gene delivery [35]. PEI is widely applied for the delivery of plasmid DNA as well as mRNA or siRNA [36–38]. Different architectures and molar masses are available, but typically, linear or hyperbranched structures with molar masses of around 25 kg mol^{-1} were used [39,40]. Here, two commercially available PEIs, a linear (L-PEI$_{com}$) and a branched (B-PEI$_{com}$), with a given molar mass (M_w) of around 25 kg mol^{-1} as well as a tailor-made linear PEI (L-PEI$_{600}$) with a theoretical molar mass (M_n) of around 26 kg mol^{-1} were characterized. The results obtained by AF4-MALS and the Zimm-plot are shown in Table 1. A representative AF4 fractogram of B-PEI$_{com}$ is shown in Fig. 2 (for L-PEIs see SI-IV). In the case of B-PEI$_{com}$ a complete separation between the void peak and the main peak was observed, whereas for both L-PEIs no full baseline separation was possible. This was also the case at higher cross-flows (data not shown). The measured values agree well to the data provided by the manufacturers and the PDI values are in the known range for hyperbranched and linear PEIs [6]. For B-PEI$_{com}$ the M_n obtained by AF4 (13.4 kg mol^{-1}) is higher compared to the value given by the manufacturer (10 kg mol^{-1}). This deviation is probably due to the MWCO of the RC membrane (10 kg mol^{-1}), which can lead to a loss of low molar mass species through the membrane. For the L-PEI$_{600}$ the M_n (24.3 kg mol^{-1}) obtained by AF4-MALS differs only slightly

Table 1
Molar masses given by the manufacturers and values obtained by AF4 for PEI.

Sample	Molar mass/kg mol^{-1}	M_n (AF4)/kg mol^{-1}	M_w (AF4)/kg mol^{-1}	PDI (AF4)
B-PEI$_{com}$	10.0 (M_n)[a], 25.0 (M_w)[b]	13.4 ± 1.4	25.4 ± 1.2	1.91
L-PEI$_{com}$	25.0 (M_w)[b]	19.9 ± 1.5	26.1 ± 1.3	1.31
L-PEI$_{600}$	26.0 (theoretical M_n)[c]	24.3 ± 2.7	32.0 ± 2.7	1.32

[a] Obtained by SEC as specified by the manufacturer.
[b] Obtained by light scattering as specified by the manufacturer.
[c] Calculated from the M/I ratio used for the synthesis of the PEtOx precursor.

Table 2
Molar masses given by the manufacturers and values obtained by AF4 of PLL.

Sample	Molar mass/kg mol^{-1}	M_n (AF4)/kg mol^{-1}	M_w (AF4)/kg mol^{-1}	PDI (AF4)
PLL-1	15–30 (M_η)[a]	16.8 ± 0.7	20.9 ± 0.8	1.25
PLL-2	30–70 (M_η)[a]	23.4 ± 1.86	30.8 ± 2.9	1.32

[a] Obtained by viscosity as specified by the manufacturer.

from the theoretical M_n (26 kg mol^{-1}), which is calculated from the monomer to initiator ratio (M/I) used for the synthesis of the poly(2-ethyl-2-oxazoline) (PEtOx) precursor. This slight difference probably derives from difficulties in adjusting the M/I ratio. For high molar masses only a very small amount of initiator is required in comparison to the monomer, which results in an increased weighing error. Taking the refractive index increment into account, the studied PEIs reached the lower detection limit of the MALS detector (low signal to noise ratio) for calculation of molar masses from the Zimm plot. In particular, linear PEIs with lower molar masses (<10 kg mol^{-1}) did not show a reliable light scattering signal, which can be distinguished from the baseline (data not shown). A molar mass of 15–20 kg mol^{-1} was found to be the acceptable minimum for L-PEI. For these low molar mass polymers the radius of gyration could not be obtained. Here, the minimum is around 8–10 nm [41].

3.3. Poly(L-lysine) (PLL)

Another class of polymers with high importance for industrial and research applications is the polyamino acid poly(L-lysine) (PLL). It is widely used for the preparation of surfaces for cell attachment, as preservative in food products, and also as polyplex forming carrier in the field of gene delivery [3,42–44]. In this study, PLLs of two different molar masses were investigated. The results obtained by AF4-MALS are shown in Table 2. Fractograms of PLL-1 and PLL-2 are shown in Fig. 3 and SI-V, respectively. While the values obtained for PLL-1 are in accordance with the data provided by the supplier (15–30 kg mol^{-1}, measured by viscosity), the molar masses by AF4 for PLL-2 are lower (M_n 23.4 kg mol^{-1}), compared to the given specification (30–70 kg mol^{-1}, measured by viscosity). Two explanations are conceivable. First, the data obtained by viscosity are limited to the accurate determination of the constants in the Kuhn-Mark–Houwink–Sakurada equation (5) and, second, some kind of polymer degradation could occur. It should also be noted that the lower detection limit of the light scattering signal for accurate measurement of the molar mass is reached for PLL-1, resulting in a low signal to noise ratio. However, the data show that AF4 is still applicable for the analysis of this kind of biodegradable polymers even if they have a low molar mass.

3.4. Methacrylate based polymers

The third class of polymers, investigated in this study, is based on polymethacrylates. Within this class, polymers with primary, secondary and tertiary amino groups in the side chain were investigated, namely PAEMA, P*tBAEMA*, and PDMAEMA (Fig. 1). In particular, PDMAEMA is well-known for gene delivery applications [45,46] and was, therefore, further investigated at four different molar masses. All methacrylate based polymers were successfully characterized by AF4. A representative fractogram of PDMAEMA$_{500}$ is shown in Fig. 4 (for PAEMA, P*tBAEMA* and the other PDMAEMAs see SI-VI). Reliable molar masses and, even more importantly, PDI values were obtained (Table 3). For comparison with traditional chromatography methods, analysis was additionally performed on a common SEC-RI system with DMAc/LiCl as eluent and polystyrene as calibration standard. It was found that the obtained molar mass (SI-II) differs significantly from the results obtained by AF4. This finding is ascribed to the lack of a suitable standard and the use of a MALS detector similar as for AF4 would circumvent this problem. However, this does not solve the problem of polymer-column interactions which can occur for this kind of polymers, as shown for P*tBAEMA*$_{170}$ in SI-VII. Since interactions were present at both, AF4 and SEC, the general statement that AF4 shows less interactions than SEC cannot be abiden for these cationic polyelectrolytes. To verify the AF4 data, ^{1}H NMR and AUC were applied (Table 3). As a standard method to determine M_n, end group analysis by ^{1}H NMR was performed by comparison of the integral, in this case the aromatic RAFT end group and the integrals from the repeating units in the polymer. Unfortunately, this method is limited to relatively low molar masses, as the integral volumes of the end group decreases with increasing degree of polymerization. A typical ^{1}H NMR spectrum for PDMAEMA$_{320}$ synthesized *via* RAFT is shown in SI-VIII. In addition to ^{1}H NMR spectroscopy, AUC was applied. It is as a powerful technique for characterization of macromolecules and

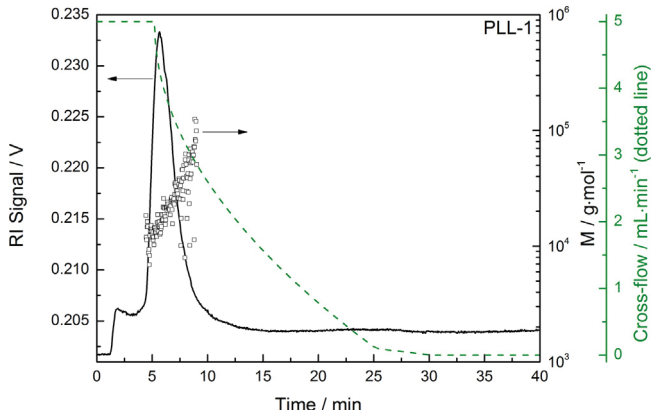

Fig. 3. AF4 fractogram with the corresponding cross-flow rate and molar masses of PLL-1.

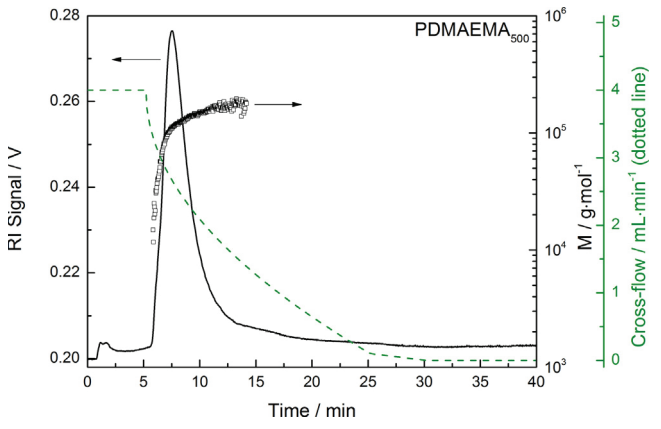

Fig. 4. AF4 fractogram with the corresponding cross-flow rate and molar masses of PDMAEMA$_{500}$.

Table 3
Molar masses and PDI values of the methacrylate based cationic polymers obtained by ^{1}H NMR spectroscopy, AUC, and AF4.

Sample	M_n (NMR)/kg mol^{-1} [a]	M_{sD} (AUC)/kg mol^{-1}	M_n (AF4)/kg mol^{-1}	M_w (AF4)/kg mol^{-1}	PDI (AF4)
PDMAEMA$_{90}$	14.5 ± 0.2	16.3 ± 0.3	14.7 ± 0.7	16.8 ± 0.4	1.14
PDMAEMA$_{230}$	36.3 ± 3.3	42.5 ± 0.2	36.1 ± 0.61	41.1 ± 0.72	1.14
PDMAEMA$_{320}$	42.6 ± 1.9	65.8 ± 1.7	51.2 ± 1.9	67.3 ± 1.2	1.31
PDMAEMA$_{500}$	72.3 ± 1.6	112.0 ± 2.6	80.2 ± 2.1	113.1 ± 1.0	1.41
PAEMA$_{150}$	25.0 ± 0.2	27.2 ± 1.4	24.9 ± 1.2	29.1 ± 1.2	1.17
P*tBAEMA*$_{170}$	31.2 ± 2.8	36.0 ± 0.6	29.9 ± 2.3	37.3 ± 1.3	1.25

[a] Measured in CD_2Cl_2 or D_2O.

nanomedicines, such as nanoparticles or polyplexes [47]. The molar mass (M_{sD}), obtained by sedimentation velocity experiments and the Svedberg equation (1), is a weight-average molar mass comparable to M_w [48]. Here, the translational diffusion coefficient, which is measured by DLS, is required for calculations. For an accurate determination of the molar mass by AUC the suppression of the polyelectrolyte effect is of the utmost importance [48]. Therefore, an aqueous solution of 150 mM NaCl and 1 mM NaOH was used to guaranty that the polymers are in the unionized state [49]. For P*tBAEMA*$_{170}$, which is not soluble under these conditions, methanol containing 1 mM NaOH was used as solvent. The suppression of the polyelectrolyte effect can be proven by the measurement of the reduced viscosity as shown exemplarily for PDMEAMA$_{500}$ in SI-IX. A linear positive slope at low concentrations indicates the absence of any polyelectrolyte specific behavior. An overview of the molar mass obtained by AUC can be found in Table 3. For PAEMA$_{150}$, P*tBAEMA*$_{170}$, PDMAEMA$_{90}$, and PDMAEMA$_{230}$ the molar masses obtained by AF4-MALS are in good accordance with the molar masses from ^{1}H NMR spectroscopy, AUC, and the theoretical molar masses. For the two polymers with higher molar mass (PDMAEMA$_{320/500}$), the results from AF4 correlate well to those by AUC, whereas larger deviations to the molar masses obtained by ^{1}H NMR were observed. These differences are probably caused by limitations of ^{1}H NMR spectroscopy for high molar mass polymers, as the signal integral of the used RAFT agents decreases with increasing molar mass (M/I), resulting in a lower signal to noise ratio. This results in the calculation of lower molar masses. In case of the synthesis of high molar mass polymers by RAFT, also the probability of side reactions, *e.g.* chain termination reaction, increases, affecting the end group fidelity (not each chain has the specific RAFT end group). Here, AF4-MALS is more reliable since the accuracy in light scattering increases with increasing size and molar mass. An advantage of AF4 over AUC is the reduced measurement time. Moreover, less material is required for the measurements and information about the polydispersity can easily be obtained.

Since the molar masses of the investigated PDMAEMA polymers ranges from around 15 to 80 kg mol^{-1}, larger differences between the retention times of the different polymers were expected, as their diffusion coefficients differ remarkably. However, this was not the case. All polymers show similar retention times or just slight changes (Fig. 4 and SI-VI). This indicates that the elution is highly influenced by other forces, than cross-flow and diffusion, leading to a certain equilibrium height in the channel. Probably the repulsive electrostatic forces between the positive charges on the surface and the sample in solution govern the retention. This leads to a larger equilibrium height of the polymer and results in a faster elution due to the higher flow velocity in the center of the channel. This assumption is supported by the observation that a change of the cross-flow rate (up to 6 mL min^{-1}) only slightly influenced the retention time (data not shown). To gain further information on the interactions and the conformation of PDMAEMA, the high molar mass PDMAEMA$_{500}$ was investigated in more detail.

3.5. Influence of sample concentration and ionic strength

As already mentioned, the choice of eluent and its composition essentially influences the retention behavior in AF4. In particular, for charged samples, like polyelectrolytes, the ionic strength of the solvent plays an important role for the interactions in the separation channel. An increase of ionic strength results in a reduction of the range of attractive or repulsive electrostatic forces (Debye length) and can, therefore, be used to adjust the interactions between the polymer or colloid itself and the interactions between the polymer and the membrane surface. To investigate this effect on the retention behavior, PDMAEMA$_{500}$ was studied at different concentrations of NaCl (5–150 mM) by AF4 (Fig. 5). The applied separation method was the same as for molar mass determination of all methacrylate based polymers. It was found that the retention time is shifted to higher values with increasing concentration of NaCl or ionic strength, respectively. The recovery rate increased slightly from around 80% at 5 mM to 84% at 150 mM NaCl. Additionally, a peak broadening with a shoulder in the beginning and at the end was observed. At salt concentrations higher than 50 mM NaCl, the retention time and the peak shape does not change significantly, except small alterations of the shoulder at the end. This can probably be attributed to the switch-off of the cross-flow at 25 min and was a general observation for different polymers and methods. The molar masses obtained at different concentrations of NaCl are identical and show no deviations therefore, excluding the possibility of the degradation or alteration of the sample. The shift in the retention time is a further indication of the dominating effect of electrostatic interactions at low ionic strength. As mentioned above (3.1), the fresh membrane surface is saturated with cationic PDMAEMA$_{500}$ after the first run, as indicated by a lower recovery rate of 70% in contrast to around 80% for subsequent runs. The repulsive long-ranged electrostatic interactions between

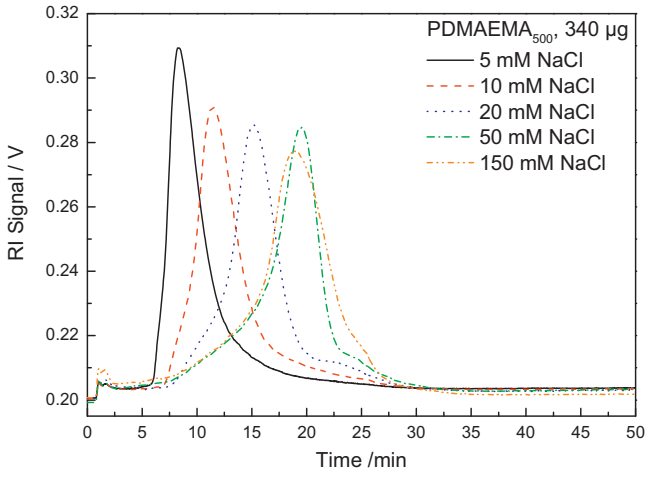

Fig. 5. AF4 fractograms (RI) of PDMAEMA$_{500}$ at different concentrations of NaCl present in the eluent.

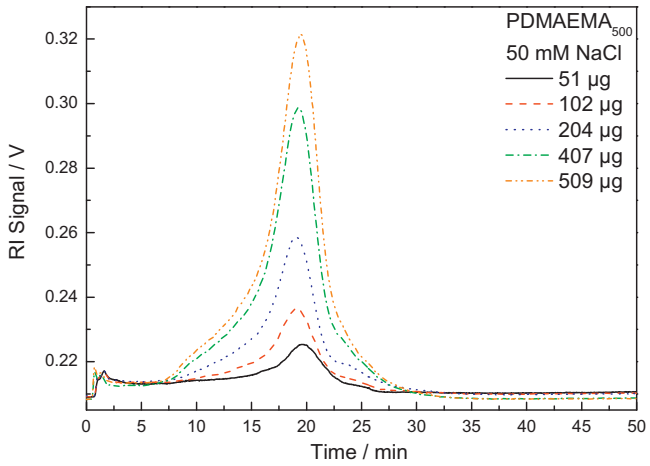

Fig. 6. AF4 fractograms (RI) of $PDMAEMA_{500}$ and different amounts of injected polymer mass.

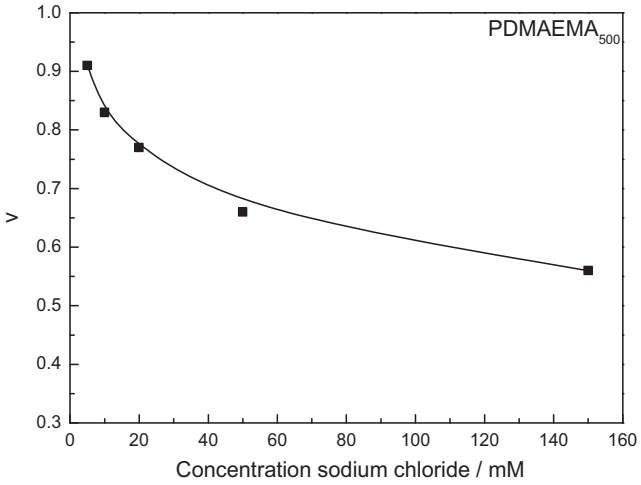

Fig. 7. Mark–Houwink exponent of $PDMAEMA_{500}$ at different concentrations of NaCl obtained by AF4.

the positive formulated surface and the cationic polymer lead to a movement of the sample in a certain distance to the membrane, resulting in a faster elution, caused by a higher flow velocity in the center of the channel compared to the accumulation wall. With increasing ionic strength, the long-ranged electrostatic forces are more shielded and the sample could move closer to the membrane [50], facilitating other short-ranged interactions such as Van-der-Waals or hydrophobic interactions. In particular, the hydrophobic backbone of PDMAEMA chains on the membrane surface and in the sample, lead to attractive interactions and can explain the late elution at high ionic strength and the peak broadening/tailing.

The amount of the polymer sample was altered to evaluate in detail the possible limitations of the determination of the molar masses by AF4. It is known that the volume injected into the channel can influence the retention time and the peak shape, if overloading occurs [4]. In general, the overloading depends on the focusing of the sample zone. If the concentration of the sample in the zone becomes too high some molecules are excluded, which leads to the broadening of peaks. Also intermolecular interactions will increase and can start to affect the elution. In general, the overloading starts to take place at a certain critical concentration which decreases with increasing molar mass. Also for low molar mass samples, where a relative high amount of sample is necessary for a reliable light scattering signal, this effect has to be taken into account. In general, it could be observed that polyelectrolytes elute earlier with increasing sample load, whereas neutral polymers in aqueous solution show an increase of retention time [4,51]. Additionally, a peak distortion and zone broadening is widely described in literature [14,52]. For polyelectrolytes, overloading is mainly influenced by electrostatic repulsion, both, inter/intra-molecular and between sample and membrane. With increasing charge the critical concentration is reduced and the sample is repelled from the accumulation wall. Overloading is also influenced by the ionic strength. An increase of the ionic strength suppresses electrostatic forces and, therefore, reduces the excluded volume of the chains, the chain expansion, and the electrostatic repulsion from the membrane. To see if any effect of the peak distortion was caused by sample overloading [52], the AF4 experiment with $PDMAEMA_{500}$ in 50 mM NaCl was repeated with different amounts of injected polymer mass. As shown in Fig. 6, a slightly higher retention time was found for the lowest amount of $PDMAEMA_{500}$, which is typically observed for charged polymers and in accordance with other studies mentioned above. It also indicates that polyelectrolyte effects are still present. This is in agreement with measurements of reduced viscosity (SI-IX), showing the presence of such effects even at 150 mM NaCl. However, the peak shape does not depend on the injected amount of sample for the investigated range. The recovery rate for all amounts of sample is constant at 83%, a value, which is also typically observed for polyelectrolytes [53]. Molar masses obtained from the light scattering signal are similar for all amounts of injected masses. Taking all results into account, overloading seems to be slightly present, but does not affect the characterization of the polymers.

3.6. Conformational investigations using AF4

It was expected that not only the interactions between different polymer chains (intermolecular) and between the polymer and the membrane, but also the intramolecular interactions vary with the ionic strength and, therefore, influence the conformation of the macromolecule [53]. The conformation of a macromolecule can be described by the exponent of the Kuhn–Mark–Houwink–Sakurada equation or the so called power-law-relationships (5), where the molar mass (M) is combined, *e.g.* with the radius of gyration (R_g), the sedimentation coefficient (s_0), the diffusion coefficient (D_0) or the intrinsic viscosity (η).

$$X = KM^{\nu} \tag{5}$$

$$\log X = \log K + \nu * \log M \tag{6}$$

Here, $X = R_g$, s_0, D_0 or $[\eta]$. In AF4-MALS, the exponent (ν) is calculated as the slope in a log–log plot of the radius against the molar mass of each slice, as illustrated in SI-X for $PDMAEMA_{500}$ in 150 mM NaCl. A slope of 0.56 was found, which fits well to the typical range for a linear chain (0.5–0.7). The dependency of the slope (ν), or the conformation of the polymer chain is related to the ionic strength as shown in Fig. 7. At low ionic strength (5 mM) a value of around 0.91 is obtained, which decreases to 0.56 at 150 mM NaCl. Moreover, it can be observed that even above a NaCl concentration of 50 mM the conformation still changes. In contrast, the ionic strength dependent fractograms (Fig. 5) showed a constant retention time and peak shape above 50 mM NaCl. This indicates that no relevant (detectable) changes in hydrodynamic radius (R_H) or interactions with the membrane occurred. This observation clearly illustrates the differences between inter/intra-molecular interactions of the polymer chains and interactions with the membrane. While an exponent ν of 1 describes a rod like structure and a value of 0.33 a sphere, a value of 0.9 was typically observed for elongated structures [54,55]. It is assumed that this is caused by the

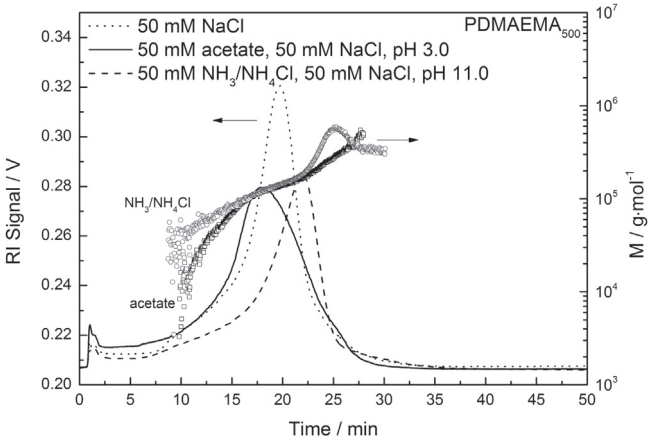

Fig. 8. AF4 fractograms of $PDMAEMA_{500}$ in different buffers: 50 mM acetate, 50 mM NaCl, pH 3.0, 50 mM NH_3/NH_4Cl, 50 mM NaCl, pH 11.0 and 50 mM NaCl.

electrostatic repulsion of the positive charges present in the side chain. With increasing ionic strength, the charges are screened and the range of the electrostatic forces is diminished. This reduces the repulsion between the side chains and leads to a conformation similar to a Gaussian chain, as indicated by an exponent of around 0.56.

The power-law-relationships were also applied to the data of the sedimentation and diffusion coefficients for all PDMAEMAs (SI-XI). Here, a value of 0.39 for the sedimentation and value of −0.62 for the diffusion coefficient was obtained. Both exponents are in the limits for a Gaussian chain (0.35–0.5 for s and −0.5 to −0.7 for D). Since the sedimentation velocity is more sensitive to the polyelectrolyte effect (molar mass obtained by Eq. (3)), the polymers should be in the unionized state [48]. For this reason, the sedimentation velocity and dynamic light scattering experiments were conducted in 150 mM NaCl + 1 mM NaOH. The polyelectrolyte effect is even present at neutral pH and 150 mM NaCl, as shown by measurements of the reduced viscosity (SI-IX). Fortunately, this does not seem to affect the determination of the molar mass by AF4-MALS. Moreover, a separation before the light scattering measurement has a time-related advantage, in particular for the characterization of polymers using AF4. Providing that the sample polydispersity is not too low, information about the conformation of the macromolecule can be obtained from a single experiment. In contrast, traditional techniques (*e.g.* sedimentation, diffusion or viscosity) to study the conformation require synthesis and analysis of a variety of polymers of different molar masses.

3.7. Influence of the pH value

For charged colloids, *e.g.* proteins, with positive and negative charges or polyelectrolytes with just one type of charge, the pH value of the solvent dramatically influences the structure of the sample. The pH primarily affects the protonation of the functional groups and, therefore, the appearance of charges, in a synthetic or biological macromolecule. For the characterization of $PDMAEMA_{500}$ by AF4 two other pH regions, an acidic and a basic, were investigated. First, a pH value of 3.0 was chosen (50 mM acetic acid/sodium acetate and 50 mM NaCl). As the isoelectric point (IEP) of a fresh RC membrane is around 3.4, the cellulose is expected to be positively charged at pH 3 [31]. The second region of interest was pH 11, where PDMAEMA is nearly unionized (50 mM ammonia/ammonium chloride buffer and 50 mM NaCl). The results obtained at pH 3.0 show a molar mass distribution similar to previous results (Fig. 8). In addition, a small shift in the retention time and a peak deformation was observed. By comparing both fractograms (neutral pH and pH 3) at 50 mM NaCl, it is obvious that the retention behavior seems not to be influenced by the pH value. Probably the repulsive electrostatic forces at this ionic strength are shielded and short-ranged interactions, caused by the hydrophobic backbone or van-der-Waals interactions, dominate the retention, even at pH 3.

The situation is more complex at pH 11, where PDMAEMA is in the unionized state. The retention time is slightly shifted to higher values but the progression of molar mass shows an irregular behavior at 26 min (Fig. 8). This might be caused by massive interactions of the hydrophobic backbone with the membrane or the tubes of the AF4 system, since the molecule is uncharged at pH 11 and no repulsive electrostatic interactions are present. An aminolysis of the ester groups in the PDMAEMA polymer seems to be unlikely for the applied NH_3 concentration (50 mM) and temperature. From a practical point of view, the observed effect of decreasing molar mass just appears at the end of the peak where the concentration is rather low and does not influence the molar mass distribution noticeably. Nevertheless, further experiments are necessary to elucidate the origin of this effect and to exclude that it is caused by irregular changes of the membrane surface by the buffer used in the experiment.

4. Conclusion

In this study, the characterization of cationic polymers, which are of great interest for gene delivery and numerous industrial applications, by asymmetric flow field-flow fractionation (AF4) was presented for the first time. It could be shown that AF4 coupled to multi-angle light scattering enables a fast and reliable determination of molar masses and PDI values of polymers such as poly(ethylene imine), poly(L-lysine) and poly(2-(dimethylamino)ethyl methacrylate) and its derivatives. For the validation of the results, ^{1}H NMR spectroscopy and AUC were applied. It was found that the lower molar mass limit, which yields a reliable light scattering signal, was around 15 kg mol^{-1}, depending on the refractive index increment. For polymers with a lower molar mass ^{1}H NMR spectroscopy or AUC is recommended. With increasing molar mass the accuracy of AF4-MALS increases and becomes more adequate, due to the fact that information about polydispersity, different mass averages and conformation can be obtained from a single measurement.

Furthermore, different membranes and eluents were evaluated for AF4 and the influence of ionic strength, injected mass of the analyte, and pH value was investigated. It could be shown that the retention behavior at low ionic strength is probably dominated by repulsive electrostatic forces between the polymer, adsorbed on the membrane surface, and the sample. In contrast, hydrophobic or other short-ranged interactions are important at higher ionic strength. Both diminish the advantage of AF4 to show less interaction with the sample than column based techniques. Up to now, no ideal membrane material was found for these cationic polyelectrolytes. Additionally, the conformation of PDMAEMA was studied by power-law-relationships in dependence of the ionic strength. It was found that the exponent, ν, decreases from 0.91 at 5 mM NaCl to 0.56 at 150 mM NaCl, which probably describes the conformational change from a stretched chain to a linear Gaussian chain. The recovery rate of around 80% was in the typical range for cationic polymers. In summary, we could successfully present that AF4 is a well-suitable method for the characterization of cationic polymers, with respect to their molar masses, PDI values, and conformational information within short time and requiring only low amounts of samples. This enables a more detailed investigation of cationic

polymers used for further applications, *e.g.* for the formation of polyplexes in gene delivery.

Acknowledgements

This project was funded by the Carl-Zeiss Foundation (Strukturantrag JCSM). Furthermore, the authors would like to thank Nicole Fritz for technical assistance at the AF4, and Kristian Kempe for the synthesis of the poly(2-ethyl-2-oxazoline) precursor.

Appendix A. Supplementary data

Supplementary data associated with this article can be found, in the online version, at http://dx.doi.org/10.1016/j.chroma.2013.11.049.

References

[1] O. Boussif, F. Lezoualch, M.A. Zanta, M.D. Mergny, D. Scherman, B. Demeneix, J.P. Behr, Proc. Natl. Acad. Sci. U.S.A. 92 (1995) 7297.
[2] A. Fire, S.Q. Xu, M.K. Montgomery, S.A. Kostas, S.E. Driver, C.C. Mello, Nature 391 (1998) 806.
[3] A. Akinc, M. Thomas, A.M. Klibanov, R. Langer, J. Gene Med. 7 (2005) 657.
[4] M.A. Benincasa, J.C. Giddings, J. Microcolumn Sep. 9 (1997) 479.
[5] C. Augsten, K. Mäder, Int. J. Pharm. 351 (2008) 23.
[6] L. Tauhardt, K. Kempe, K. Knop, E. Altuntas, M. Jäger, S. Schubert, D. Fischer, U.S. Schubert, Macromol. Chem. Phys. 212 (2011) 1918.
[7] Y. Guillaneuf, P. Castignolles, J. Polym. Sci. Part A: Polym. Chem. 46 (2008) 897.
[8] X.-L. Jiang, Y.-F. Chu, J. Liu, G.-Y. Zhang, R.-X. Zhuo, Chin. J. Polym. Sci. 29 (2011) 421.
[9] J.C. Giddings, J. Sep. Sci. 1 (1966) 123.
[10] W. Fraunhofer, G. Winter, Eur. J. Pharm. Biopharm. 58 (2004) 369.
[11] G. Yohannes, M. Jussila, K. Hartonen, M.-L. Riekkola, J. Chromatogr. A 1218 (2011) 4104.
[12] F.A. Messaud, R.D. Sanderson, J.R. Runyon, T. Otte, H. Pasch, S.K.R. Williams, Prog. Polym. Sci. 34 (2009) 351.
[13] A.C. Makan, T. Otte, H. Pasch, Macromolecules 45 (2012) 5247.
[14] A. Litzén, K.G. Wahlund, J. Chromatogr. 548 (1991) 393.
[15] K.G. Wahlund, J.C. Giddings, Anal. Chem. 59 (1987) 1332.
[16] H. Cölfen, M. Antonietti, Adv. Polym. Sci. 150 (2000) 67.
[17] L. Nilsson, M. Leeman, K.G. Wahlund, B. Bergenstahl, Biomacromolecules 7 (2006) 2671.
[18] P. Schuck, M.A. Perugini, N.R. Gonzales, G.J. Howlett, D. Schubert, Biophys. J. 82 (2002) 1096.
[19] B. Schulze, C. Friebe, S. Höppener, G.M. Pavlov, A. Winter, M.D. Hager, U.S. Schubert, Macromol. Rapid Commun. 33 (2012) 597.
[20] G.M. Pavlov, A.M. Breul, M.D. Hager, U.S. Schubert, Macromol. Chem. Phys. 213 (2012) 904.
[21] J.P. Behr, Acc. Chem. Res. 45 (2012) 980.
[22] R.J. Christie, N. Nishiyama, K. Kataoka, Endocrinology 151 (2009) 466.
[23] J. Chiefari, Y.K. Chong, F. Ercole, J. Krstina, J. Jeffery, T.P.T. Le, R.T.A. Mayadunne, G.F. Meijs, C.L. Moad, G. Moad, E. Rizzardo, S.H. Thang, Macromolecules 31 (1998) 5559.
[24] C. Pietsch, U. Mansfeld, C. Guerrero-Sanchez, S. Höppener, A. Vollrath, M. Wagner, R. Hoogenboom, S. Saubern, S.H. Thang, C.R. Becer, J. Chiefari, U.S. Schubert, Macromolecules 45 (2012) 9292.
[25] P. Schuck, Biophys. J. 78 (2000) 1606.
[26] W. Mächtle, Macromol. Chem. Phys. 185 (1984) 1025.
[27] T. Pauck, H. Cölfen, Anal. Chem. 70 (1998) 3886.
[28] S.W. Provencher, Comput. Phys. Commun. 27 (1982) 229.
[29] M. Andersson, B. Wittgren, K.G. Wahlund, Anal. Chem. 75 (2003) 4279.
[30] T. Lang, K.A. Eslahian, M. Maskos, Macromol. Chem. Phys. 213 (2012) 2353.
[31] S. Lee, H.D. Kwen, S.K. Lee, S.V. Nehete, Anal. Bioanal. Chem. 396 (2010) 1581.
[32] A. Ulrich, S. Losert, N. Bendixen, A. Al-Kattan, H. Hagendorfer, B. Nowack, C. Adlhart, J. Ebert, M. Lattuada, K. Hungerbuhler, J. Anal. At. Spectrom. 27 (2012) 1120.
[33] K. Matsumoto, A. Suganuma, D. Kunui, Powder Technol. 25 (1980) 1.
[34] A. von Harpe, H. Petersen, Y.X. Li, T. Kissel, J. Control. Release 69 (2000) 309.
[35] E. Wagner, Acc. Chem. Res. 45 (2012) 1005.
[36] A. Kwok, S.L. Hart, Nanomed. Nanotechnol. Biol. Med. 7 (2011) 210.
[37] O.M. Merkel, D. Librizzi, A. Pfestroff, T. Schurrat, K. Buyens, N.N. Sanders, S.C. De Smedt, M. Béhé, T. Kissel, J. Control. Release 138 (2009) 148.
[38] C. Scholz, E. Wagner, J. Control. Release 161 (2012) 554.
[39] M.-E. Bonnet, P. Erbacher, A.-L. Bolcato-Bellemin, Pharm. Res. 25 (2008) 2972.
[40] S.M. Zou, P. Erbacher, J.S. Remy, J.P. Behr, J. Gene Med. 2 (2000) 128.
[41] A. Zattoni, D.C. Rambaldi, P. Reschiglian, M. Melucci, S. Krol, A.M.C. Garcia, A. Sanz-Medel, D. Roessner, C. Johann, J. Chromatogr. A 1216 (2009) 9106.
[42] D.T. Curiel, S. Agarwal, E. Wagner, M. Cotten, Proc. Natl. Acad. Sci. U.S.A. 88 (1991) 8850.
[43] C. Plank, K. Mechtler, F.C. Szoka, E. Wagner Jr., Hum. Gene Ther. 7 (1996) 1437.
[44] M. Sanjoh, S. Hiki, Y. Lee, M. Oba, K. Miyata, T. Ishii, K. Kataoka, Macromol. Rapid Commun. 31 (2010) 1181.
[45] C.V. Synatschke, A. Schallon, V. Jerome, R. Freitag, A.H.E. Müller, Biomacromolecules 12 (2011) 4247.
[46] P. van de Wetering, J.Y. Cherng, H. Talsma, D.J.A. Crommelin, W.E. Hennink, J. Control. Release 53 (1998) 145.
[47] I.Y. Perevyazko, M. Bauer, G.M. Pavlov, S. Höppener, S. Schubert, D. Fischer, U.S. Schubert, Langmuir 28 (2012) 16167.
[48] K.L. Planken, H. Cölfen, Nanoscale 2 (2010) 1849.
[49] L.N. Andreeva, S.V. Bushin, M.A. Bezrukova, T.N. Nekrasova, R.T. Imanbaev, V.D. Pautov, O.V. Nazarova, Y.I. Zolotova, E.F. Panarin, Russ. J. Appl. Chem. 85 (2012) 417.
[50] S. Lee, P.O. Nilsson, G.S. Nilsson, K.G. Wahlund, J. Chromatogr. A 1011 (2003) 111.
[51] M.A. Benincasa, C. Delle Fratte, J. Chromatogr. A 1046 (2004) 175.
[52] A. Litzén, K.G. Wahlund, Anal. Chem. 63 (1991) 1001.
[53] E. Alasonati, M.A. Benincasa, V.I. Slaveykova, J. Sep. Sci. 30 (2007) 2332.
[54] W. Burchard, Adv. Polym. Sci. 143 (1999) 113.
[55] H. Thielking, W.M. Kulicke, Anal. Chem. 68 (1996) 1169.

Supporting information

Characterization of Cationic Polymers by Asymmetric Flow Field-Flow Fractionation and multi-angle light scattering – A Comparison with Traditional Techniques

Michael Wagner,[1,2] Christian Pietsch,[1,2] Lutz Tauhardt,[1,2] Anja Schallon,[1,2] Ulrich. S. Schubert[1,2]*

[1] *Laboratory of Organic and Macromolecular Chemistry (IOMC), Friedrich Schiller University Jena, Humboldtstraße 10, 07743 Jena, Germany*

[2] *Jena Center for Soft Matter (JCSM), Friedrich Schiller University Jena, Philosophenweg 7, 07743 Jena, Germany*

ulrich.schubert@uni-jena.de; www.schubert-group.com

SI-I: Synthesis L-PEI$_{600}$

A solution of dry acetonitrile (Acros Organics, Geel Belgium), 2-ethyl-2-oxazoline (monomer), and methyl tosylate (initiator) was prepared with a total monomer concentration of 4 M and a total monomer-to-initiator ratio of 600 as recently published.[1] The mixture was heated in a microwave synthesizer at 140 °C for a pre-determined time. A sample was taken and full monomer conversion was confirmed by ^{1}H NMR spectroscopy. Subsequently, the solvent was removed. The resulting PEtOx (M_n = 40.6 kg·mol^{-1}, PDI = 1.79, 3.8 g) was dissolved in 6 M aqueous hydrochloric acid (15 mL) and heated at 130 °C for 1 h in the microwave synthesizer. After removing the acid under reduced pressure, the residue was dissolved in water and 3 M aqueous NaOH was added until precipitation occurred. The precipitate was filtered off, recrystallized from water, filtered, dissolved in methanol, and precipitated into ice-cold diethyl ether. Subsequently, the L-PEI$_{600}$ was dried for 3 day at 40 °C. The degree of hydrolysis was 99% as determined by ^{1}H NMR spectroscopy.

^{1}H NMR (300 MHz, CD_3OD): δ = 3.65 (t, CH_2-OH), 2.73 (br., N-CH_2), 2.39 (s, CH_3-N).

SI-II: Synthesis PDMAEMA, PAEMA and P*t*BAEMA via RAFT

In a typical polymerization experiment, 1.258 g of DMAEMA (8.0×10^{-3} mol), 2.8 mg of 4,4′-azo*bis*(4-cyanopentanoic acid), ACVA, initiator (1.0×10^{-5} mol), 11.18 mg of 4-cyano-4-(phenylcarbonothioylthio) pentanoic acid (used as a CTA) RAFT agent (4.0×10^{-5} mol) and ethanol/water (in total 50/50 vol%) were mixed together in a 10 mL glass vial as follows DMAEMA

monomer, followed by individual stock solutions of initiator and RAFT agent dissolved in ethanol and filled with water up to a ratio of 50/50 vol%. The ratio between [CTA] and [AIBN] was 1:0.25. Before closing the vial, the reaction solutions were degassed by sparging argon for at least 30 min prior to use. Subsequently, the reaction was performed in an oil bath at 70 °C for 12 h keeping a total monomer concentration of 2.0 M or 3.0 M. After the polymerization, acetone was added to the final mixtures, and the polymers were subsequently precipitated into cold diethyl ether. The utilized reaction conditions, monomer concentration and [M]/[CTA] ratios are summarize in Table 1. In the case of PDMAEMA-90 the 1,1'-azo*bis*(cyclohexane carbonitrile) initiator and as RAFT agent the 4-cyano-4-[(dodecylsulfanylthiocarbonyl) sulfanyl]pentanoic acid were used.

Table 1: Overview of the selected reaction conditions and SEC data of methacrylate based polymers.

Sample	amine	[M]/[CTA]	*c* / M	M_n (SEC) / kg·mol^{-1}	PDI (SEC)
PDMAEMA$_{90}$	*tert.*	100/1	3.0	15.2[a]	1.21
PDMAEMA$_{230}$	*tert.*	200/1	2.0	25.7[a]	1.34
PDMAEMA$_{320}$	*tert.*	600/1	3.0	47.2[a]	1.35
PDMAEMA$_{500}$	*tert.*	1200/1	3.0	66.9[a]	1.37
PAEMA$_{150}$	*prim.*	200/1	2.0	77.8[b]	1.15
P*t*BAEMA$_{170}$	*sec.*	200/1	2.0	37.8[a]	1.25

[a] Calculated from SEC (DMAc) using PS calibration. [b] Calculated from aqueous SEC (CF_3COOH/NaCl/pH 2.3) using Pullulan calibration.

SI-III: AF4 fractogram of PDMAEMA$_{500}$ on a 10 kg·mol^{-1} CTA and 30 kg·mol^{-1} PVDF membrane and 150 mM NaCl as eluent.

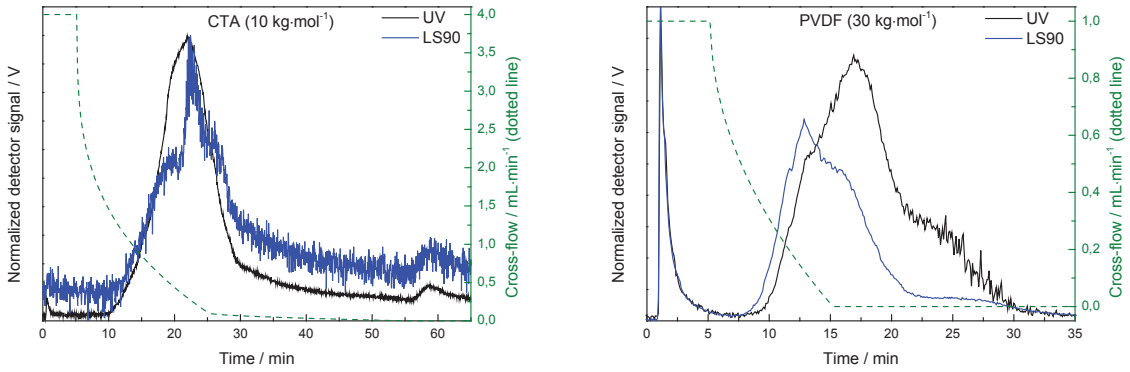

SI-IV: AF4 fractograms with the corresponding cross-flow rates and molar masses of (A) L-PEI$_{com}$, and (B) L-PEI$_{600}$.

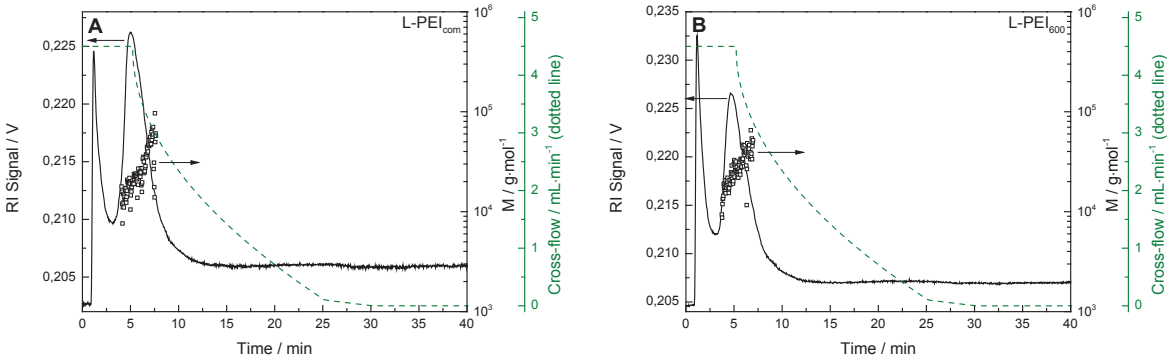

SI-V: AF4 fractograms with the corresponding cross-flow rates and molar masses of PLL-2.

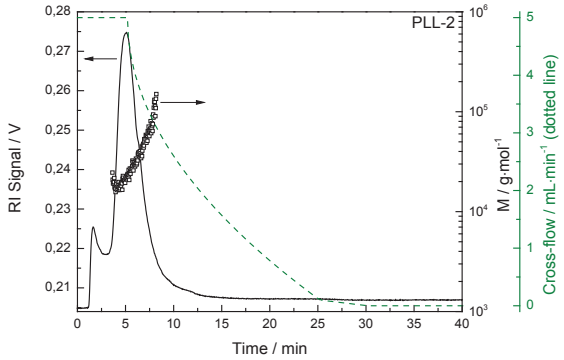

SI-VI: AF4 fractograms with the corresponding cross-flow rates and molar masses of (A) $PAEMA_{150}$, (B) $PtBAEMA_{170}$, (C) $PDMAEMA_{90}$, (D) $PDMAEMA_{230}$, and (E) $PDMAEMA_{320}$.

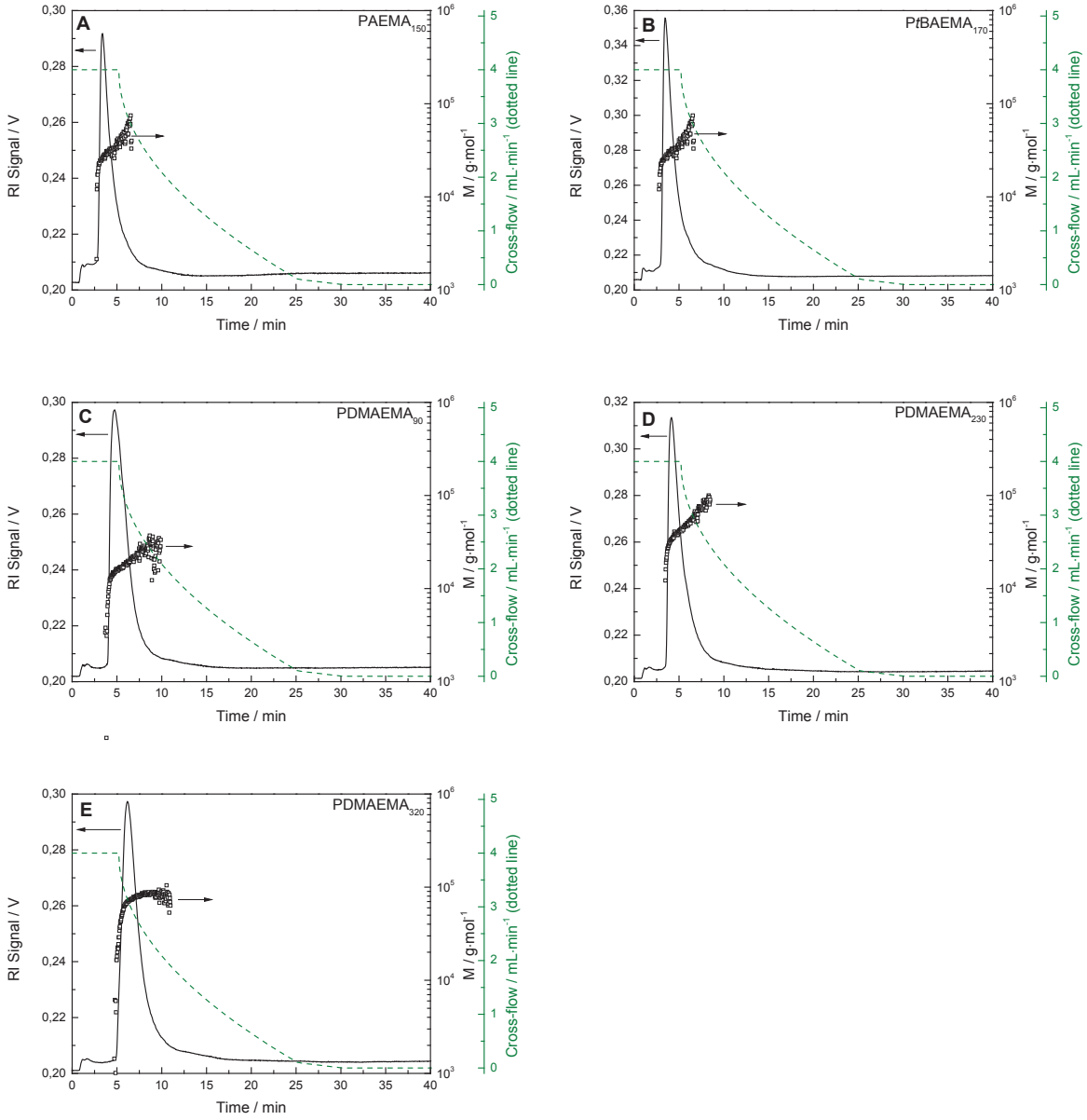

SI-VII: SEC results of P*t*BAEAMA$_{170}$ with DMAc/LiCl as eluent and polystyrene as calibration standard.

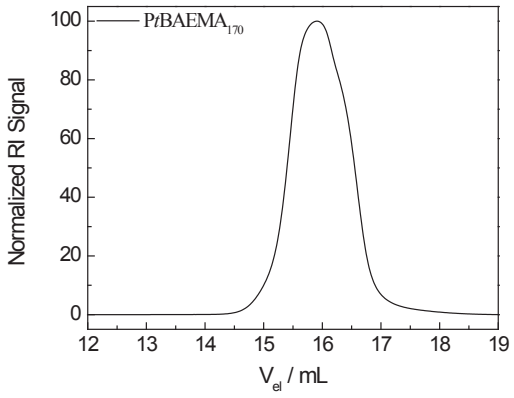

SI-VIII: ^{1}H NMR of PDMAEMA$_{320}$ in CD_2Cl_2

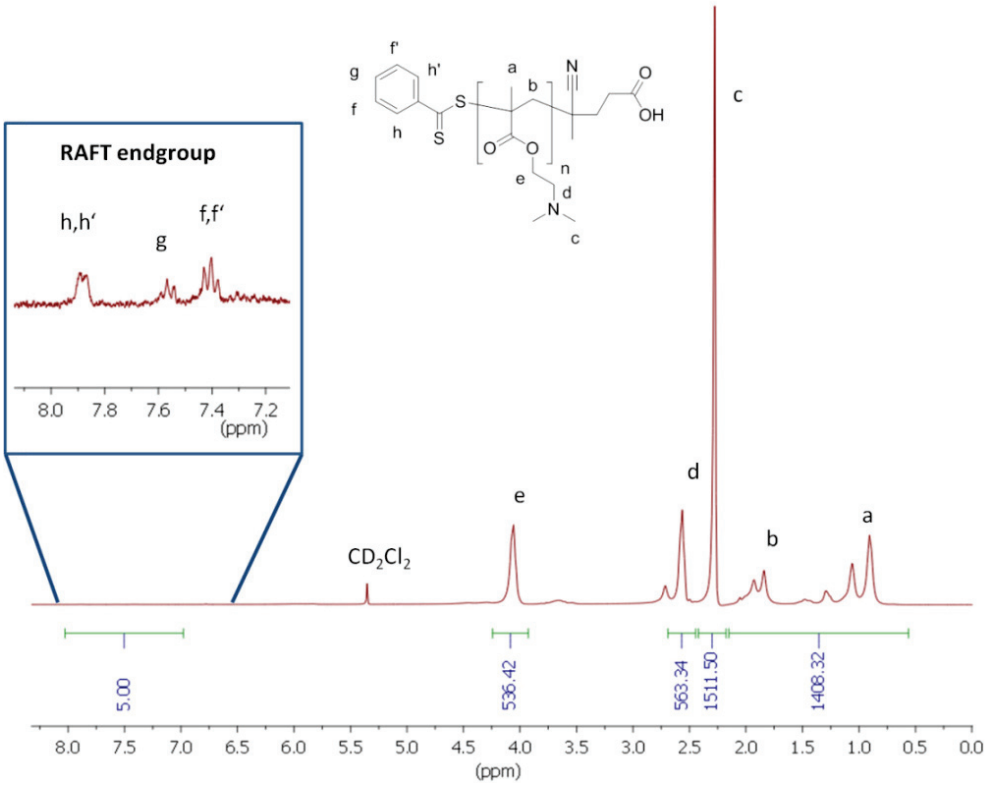

SI-IX: Measurement of reduced viscosity for $PDMAEMA_{500}$

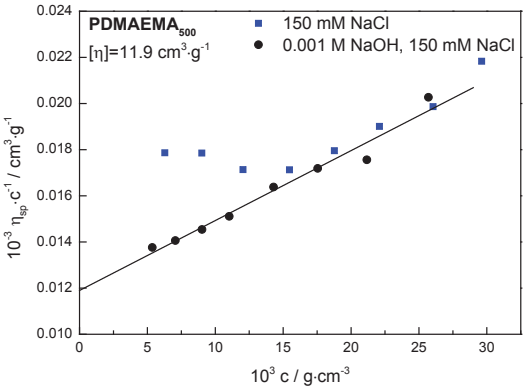

SI-X: Conformation plot of $PDMAEMA_{500}$ in 150 mM NaCl obtained by AF4-MALS.

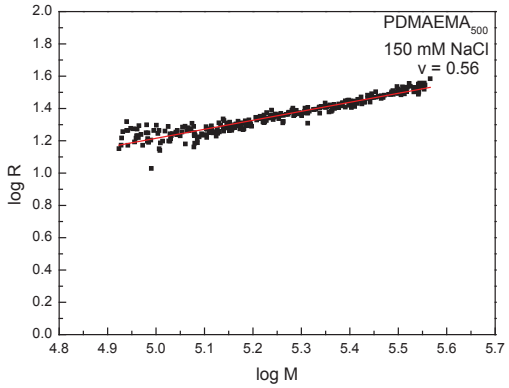

SI-XI: Log-log plots of (A) s_0 and (B) D_0 against the different molar masses of PDMAEMA in 150 mM NaCl + 1 mM NaOH.

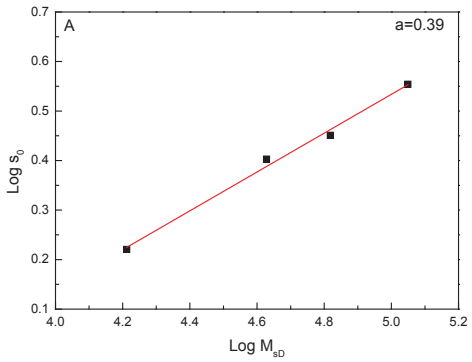

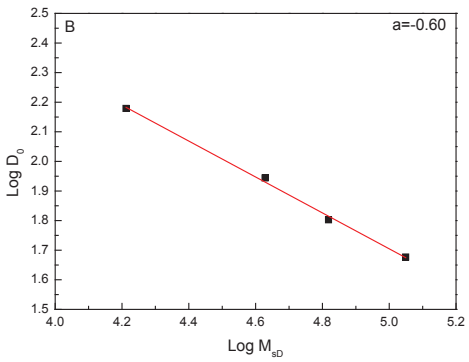

References

[1] L. Tauhardt, K. Kempe, K. Knop, E. Altuntas, M. Jäger, S. Schubert, D. Fischer, U.S. Schubert, Macromol. Chem. Phys. 212 (2011) 1918.

Publication 13

“Linear poly(ethylene imine)-based hydrogels for effective binding and release of DNA”

C. Englert, L. Tauhardt, M. Hartlieb, K. Kempe, M. Gottschaldt, U. S. Schubert,

Biomacromolecules **2014**, *15*, 1124–1131

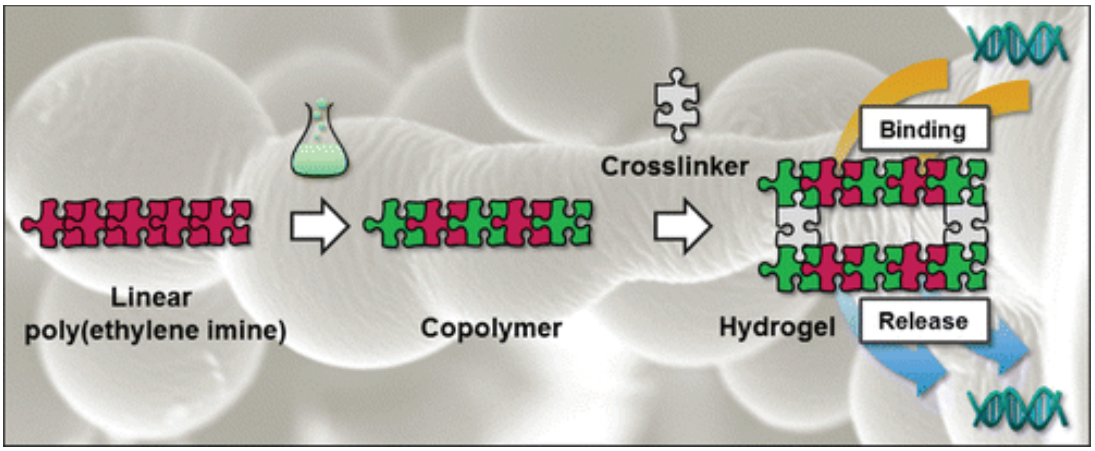

Article

pubs.acs.org/Biomac

Linear Poly(ethylene imine)-Based Hydrogels for Effective Binding and Release of DNA

Christoph Englert,[†,‡] Lutz Tauhardt,[†,‡] Matthias Hartlieb,[†,‡] Kristian Kempe,[†,‡,§] Michael Gottschaldt,[†,‡] and Ulrich S. Schubert*[,†,‡]

[†]Laboratory of Organic and Macromolecular Chemistry (IOMC), Friedrich Schiller University Jena, Humboldtstr. 10, 07743 Jena, Germany

[‡]Jena Center for Soft Matter (JCSM), Friedrich Schiller University Jena, Philosophenweg 7, 07743, Jena, Germany

Supporting Information

ABSTRACT: A series of copolymers containing both amine groups of linear poly(ethylene imine) (LPEI) and double bonds of poly(2-(3-butenyl)-2-oxazoline) (PButEnOx) was prepared. To this end, a poly(2-ethyl-2-oxazoline) (PEtOx) precursor was hydrolyzed to the respective LPEI and functionalized in an amidation reaction with butenyl groups resulting in the double bond containing poly(2-(3-butenyl-2-oxazoline)-*co*-ethylene imine) (P(ButEnOx-*co*-EI)). Hydrogels were obtained by cross-linking with dithiols under UV-irradiation resulting in networks with different properties in dependence of the content of double bonds. The developed method allows the exact control of the amount of ethylene imine units within the copolymer and, thus, within the resulting hydrogels. The gel structures were characterized by solid state NMR and infrared spectroscopy. In addition the water uptake behavior from the liquid and the gas phase was investigated. It was shown by an ethidium bromide assay (EBA) that the copolymers and the respective hydrogels were able to bind and release DNA. Furthermore, the influence of the ethylene imine content on this interaction was investigated.

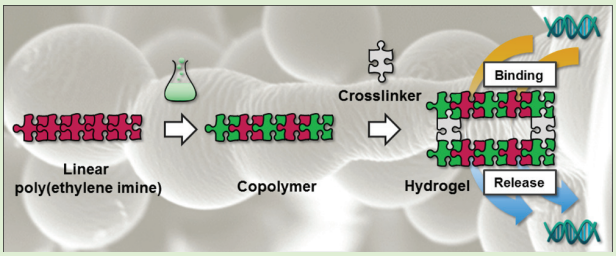

INTRODUCTION

The fast and efficient detection of pathogenes is of tremendous interest nowadays, ranging from applications in agriculture to medicine. Each species of pathogen carries a unique set of DNA and RNA sequences, which can be potentially detected by hybridization with another DNA strand containing complementary nucleic acid sequences. This approach is exploited by DNA biochips that consist of DNA sequences covalently bound/attached to solid substrates like glass,[1,2] silicon, gold,[3] or polymers such as poly(methyl methacrylate).[4] However, an essential prerequisite for a successful detection is the isolation and purification of nucleic acids from highly complex samples, such as blood and feces.[5] For this purpose, materials that can specifically and reversibly bind genetic materials are of significant interest. In this context, the interaction between DNA and cationic polymers has been investigated intensely. In particular, poly(ethylene imine) (PEI) has been widely studied, since its amine groups interact effectively with the DNA/RNA phosphate groups, forming a so-called polyplex.[6−11]

The major drawbacks of two-dimensional DNA chips are the limited loading capacity of surface materials and the restricted hybridization efficiency.[12,13] An alternative approach, overcoming these issues, is the reversible binding of genetic materials within a three-dimensional network. In this way a considerable increase of the loading capacity compared to a two-dimensional system can be achieved.[14,15] A special class of three-dimensional networks are the so-called hydrogels. Although insoluble in any solvents, they can incorporate water up to a multitude of their own mass. This property allows the encapsulation and rapid diffusion of DNA molecules inside the network. The immobilization of DNA and other biomolecules within hydrogel-like structures has been recently the topic of intensive research.[16−19]

In this contribution we focus on the synthesis of three-dimensional networks based on linear poly(ethylene imine) (LPEI). The most common method for the formation of PEI-based hydrogels is the cross-linking of the amine groups using difunctional compounds like diglycidyl ethers or diisocyanates.[20−26] However, due to the insolubility of the network, it is not possible to determine the amount of amine groups that remain after the cross-linking process. For the binding and release of genetic material, it is essential to know the exact amount of amine groups. Hence, it is desirable to perform the cross-linking without decreasing the amine binding sides. To this end, a second functionality needs to be incorporated into the hydrogel precursor, which can be exploited for cross-linking. Possible candidates could be partially hydrolyzed double bond bearing poly(2-oxazoline)-based homo- and copolymers.[27] However, the double bonds of poly(2-(3-butenyl)-2-oxazoline) (PButEnOx)[28−30] and poly(2-(9-decen-

Received: October 7, 2013
Revised: January 20, 2014
Published: January 26, 2014

   dx.doi.org/10.1021/bm4017572 | *Biomacromolecules* 2014, 15, 1124−1131

yl)-2-oxazoline) (PDecEnOx)[31−33] based polymers do not stand the harsh hydrolysis conditions required to cleave of the oxazoline side chains. To overcome this problem, the alkene functionalities have to be introduced subsequently to hydrolysis.

This report introduces a new route to obtain LPEI-hydrogels with an adjustable amount of amine groups. To this end, we have synthesized an eight-membered library of poly(2-(3-butenyl)-2-oxazoline-*co*-ethylene imine) (P(ButEnOx-*co*-EI) copolymers by reaction of LPEI with *N*-succinimidyl-4-pentenate. Subsequent cross-linking via thiol−ene photoaddition leads to the formation of LPEI-containing hydrogels with a predetermined amount of amine groups.

Both the copolymers and the hydrogels are characterized by means of NMR and IR spectroscopies. The synthesized systems are investigated regarding their structure and swelling ability. The DNA interaction of the copolymers and the hydrogels is studied using the ethidium bromide assay (EBA; DNA binding) and a heparin assay (DNA release).

EXPERIMENTAL SECTION

Materials. PEtOx (50,000 g/mol), pyridine, 4-*N*,*N*-dimethylaminopyridine (DMAP), ethanol, 3,6-dioxaoctane-1,8-dithiol, and 2,2-dimethoxy-2-phenylacetophenone (DMPA), and genomic DNA sodium salt from herring testes (gDNA) were obtained from Sigma Aldrich. Ethidium bromide solution (1%) was purchased from Carl Roth (Karlsruhe, Germany). *N*-Succinimidyl-4-pentenate was prepared according to literature procedures.[28]

General Methods and Instrumentation. The hydrolysis of PEtOx was performed under microwave irradiation in an Initiator Sixty single-mode microwave synthesizer from Biotage, equipped with a noninvasive IR sensor (accuracy 2%). ^{1}H NMR spectra were recorded at room temperature using a Bruker AC 300 MHz spectrometer or a Bruker AC 250 MHz spectrometer, respectively. ^{13}C NMR was recorded at 100 MHz. Chemical shifts are reported in parts per million (ppm, δ scale) relative to the residual signal of the deuterated methanol. Solid state NMR measurements were performed on a Bruker Avance 400 spectrometer. The dry hydrogels were measured with 4 mm zircon-oxid rotors at 12.5 kHz. Swollen samples (12 h in D_2O) were measured using Kel-F rotors from Bruker-Biospin at 6.5 kHz. Tetrakis-trimethylsilylsilan (^{1}H) and adamantan (^{13}C) were used as standards. ^{1}H NMR was measured for 6 s, for ^{13}C NMR 70000 scans were carried out. Size exclusion chromatographies (SEC) were performed on an Agilent Technologies 1200 Series gel permeation chromatography system equipped with a G1329A autosampler, a G131A isocratic pump, a G1362A refractive index detector, and both a PSS Gram 30 and a PSS Gram 1000 column placed in series. As eluent a 0.21% LiCl solution in *N*,*N*-dimethylacetamide (DMAc) was used at 1 mL min^{-1} flow rate and a column oven temperature of 40 °C. Molar masses were calculated using poly(styrene) as standard. Fourier transform infrared (FT-IR) spectra were recorded on a FT-IR spectrometer IRAffinity-1 (Shimadzu) using the reflection method.

The water uptake measurements from the gas phase were performed using a TGA Q5000 SA thermogravimetric analyzer from TA Instruments Eschborn, Germany. For the data evaluation the "Universal Analysis" software was used. The water uptake of the hydrogels from the liquid state was measured gravimetrically. The used filter tubes were centrifuged with a Multifuge 1S-R from Thermo Scientific, and the swelling values (Q_{eq}) were calculated according to literature.[34] The fluorescence measurements were recorded on the microplate reader Infinite M200 PRO. The samples were excited at 525 nm and the emission was measured at a wavelength of 605 nm in a temperature range between 25 and 30 °C. Well plates were obtained from Sigma-Aldrich (NunclonTM Surface, 96 well, F-bottom) and centrifuge filter tubes from Costar (Spin-X, cellulose acetate membrane, 0.45 μm).

Microscopic detection of the DNA binding of hydrogels was performed using a fluorescence microscope (Cell Observer Z1, Carl Zeiss, Jena, Germany) equipped with a mercury arc UV lamp and the appropriate filter combinations for excitation and detection of emission. The fluorescence signal was captured directly in the wells. Images of a series (11 × 11 pictures per well) were captured with a 10× objective using identical instrument settings (e.g., UV lamp power, integration time, and camera gain) and spots of the 12-well plate were addressed using an automated XY table.

Linear Poly(ethylene imine). Poly(2-ethyl-2-oxazoline) (50,000 g/mol, PDI = 2.0; 5.0 g) was treated with an excess of 6 M aqueous hydrochloric acid (30 mL) for 1 h at 130 °C in a microwave synthesizer.[35] The excess of HCl and the resulting propionic acid were removed under reduced pressure and the obtained LPEI hydrochloride was dissolved in water. After addition of 3 M NaOH up to a pH value of 9, precipitation occurred. The LPEI was filtered off, recrystallized from water, dissolved in methanol, and precipitated into 650 mL of ice-cold diethyl ether. The white solid was dried at 85 °C under high vacuum and the degree of hydrolysis was determined by ^{1}H NMR by correlating the integrals of the PEI backbone and the remaining methyl group of the PEtOx side chain (yield: 3.0 g). ^{1}H NMR (250 MHz, MeOD): δ 2.95−2.52 (N-CH_2), 1.45−0.81 (CH_3 EtOx) ppm. FT-IR (ATR): 3175 (OH, NH), 2866 (CH asym/sym str), 1485 (C−H def), 1281, 1134 (C−N str), 1045 (C−N) cm^{-1}.

***N*-Succinimidyl-4-pentenate.** The synthesis of *N*-succinimidyl-4-pentenate was performed with minor changes according to a procedure described earlier by Gress et al.[28] 4-Pentenoic acid (30.738 g, 307 mmol) and *N*-hydroxysuccinimide (56.401 g, 490 mmol) were dissolved in 800 mL of dichloromethane. To the solution, *N*,*N*′-dicyclcohexylcarbodiimide (74.334 g, 360 mmol) was added. After stirring for 23 h at room temperature, the white precipitate was filtered off and the filtrate was evaporated to dryness under reduced pressure. The residue was dissolved in 450 mL of diethyl ether and 150 mL of water. After separation, the organic phase was washed five times with water. The organic layer was dried over sodium sulfate and the solvent was removed. The high viscous product was dried in high vacuum (5 × 10^{-2} mbar) at room temperature for three days and crystallized in the freezer at −18 °C for two days. The activated acid, *N*-succinimidyl-4-pentenate, was obtained as a white solid (yield: 54.9 g, 91%). ^{1}H NMR (250 MHz, $CDCl_3$): δ 5.82 (*H*C═CH$_2$), 5.03 (HC═C*H*$_2$), 2.82 (C*H*$_2$ NHS), 2.70 (CH$_2$-C*H*$_2$-CO), 2.48 (C*H*$_2$-CH$_2$-CO) ppm. FT-IR (ATR): 2932 (CH asym/sym str), 1802 (CH═CH), 1728 (C═O), 1643, 1528 (C−H def), 1369, 1204 (C−N str), 1065 (C−N str) cm^{-1}.

Poly(2-(3-butenyl)-2-oxazoline-*co*-ethylene imine). The synthesis is exemplified by the copolymer with a 50% PEI content. LPEI (0.475 g) and the catalyst 4-*N*,*N*-dimethylamino-pyridine (DMAP, 0.117 g, 1.0 mmol) were dissolved in a microwave vial in pyridine at 80 °C. In a second vial, a defined quantity of *N*-succinimidyl-4-pentenate (1 equiv per EI unit, 1.015 g, 5.2 mmol for 50% PEI) was dissolved in the same solvent. The two solutions were combined to a 4 wt % mixture of LPEI and stirred for 20 h at 80 °C. Afterward, the mixture was added dropwise into 500 mL of cold diethyl ether. The precipitated copolymer was filtered off and washed with 40 mL of diethyl ether. The residue was dried under reduced pressure to constant weight. The side product *N*-hydroxysuccinimide (NHS) was removed by dialysis in a regenerated cellulose membrane (Spectra/Por, Rancho Dominguez, CA, molar mass cutoff 3500 g/mol) against water. ^{1}H NMR (250 MHz, MeOD): δ 6.00−5.74 (*H*C═CH$_2$), 5.18−4.93 (HC═C*H*$_2$), 3.79−3.36 (NR-C*H*$_2$-CH$_2$), 3.12−2.61 (NH-C*H*$_2$-CH$_2$), 2.63−2.59 (NHS), 2.60−2.17 (C*H*$_2$ ButEnOx), 1.41−0.80 (C*H*$_3$ EtOx) ppm, PEI = 50%. SEC (DMAc, LiCl): M_n = 10700 g·mol^{-1}, PDI = 1.44. FT-IR (ATR): 3280 (OH, NH), 2870 (CH asym/sym str), 1640 (C═O), 1420 (C−H def), 1240 (C−N str), 1080 (C−N str) cm^{-1}.

Poly(2-(3-butenyl)-2-oxazoline-*co*-ethylene imine)-Based Hydrogel. The synthesis is exemplified by the gel starting from the 50% PEI containing copolymer described above. In a microwave vial, poly(2-(3-butenyl)-2-oxazoline-*co*-ethylene imine) with 50% PEI content (0.103 g) was dissolved in ethanol. In a second vial, the

Scheme 1. Schematic Representation of the Synthesis of (a) Linear Poly(ethylene imine) by Acidic Hydrolysis of Poly(2-ethyl-2-oxazoline); (b) Copolymer Poly(2-(3-butenyl)-2-oxazoline-*co*-ethylene imine) Starting from Linear Poly(ethylene imine); and (c) Hydrogel by Cross-Linking the Copolymer via Thiol−Ene Photoaddition

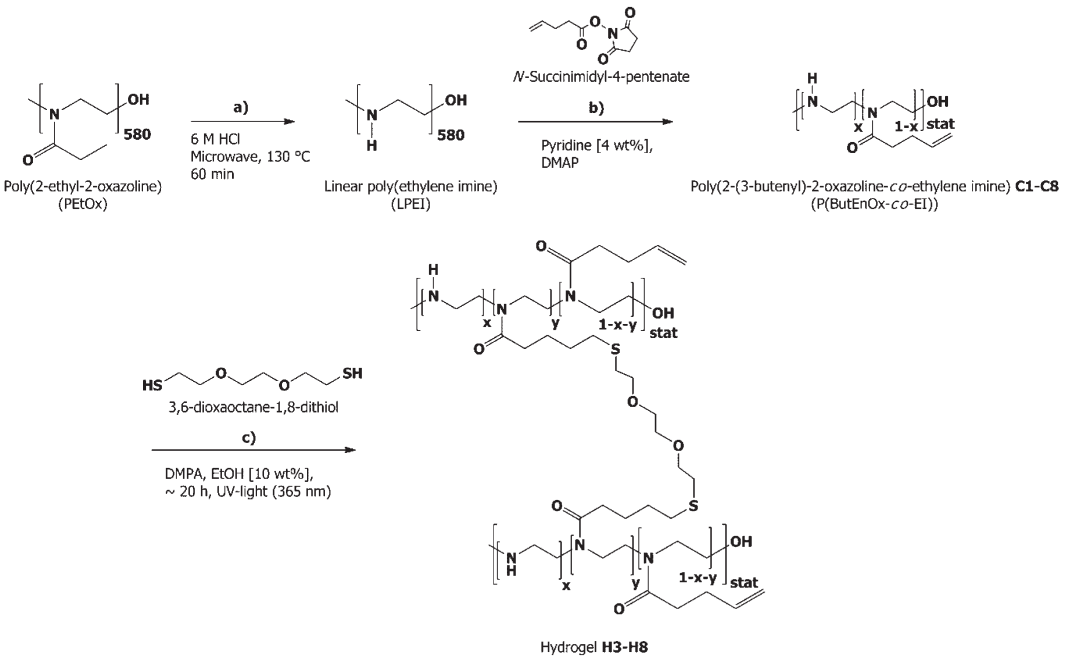

photoinitiator 2,2-dimethoxy-2-phenylacetophenone (0.013 g, 0.05 mmol) and the *bis*-functional thiol, 3,6-dioxaoctane-1,8-dithiol (45 μL, 0.28 mmol), were dissolved in ethanol (0.9:1.0 thiol/double bond). The combined solutions (10 wt %) were degassed with nitrogen for 30 min. Afterward, the clear solution was exposed to UV light (365 nm) for 24 h. The occurring gelation announced the successful synthesis of a three-dimensional network. Subsequently, the obtained gel was washed several times with ethanol (150 mL) and water (150 mL) for 20 min, respectively, and dried by lyophilization.[27,32]

Swelling Value. Q_{eq} 74%. Solid state ^{13}C NMR (100 MHz): δ 173.5, 138.6, 116.4, 71.1, 47.7, 39.4, 32.3 ppm. Solid state ^{1}H NMR (400 MHz, swollen state): δ 5.94 (*H*C═CH$_2$), 5.12 (HC═C*H*$_2$), 4.37−3.25 (N-C*H*$_2$, C*H*$_2$ EDDET), 3.30−2.07 (C*H*$_2$ ButEnOx, C*H*$_2$-S-C*H*$_2$), 2.02−1.22 (RS-CH$_2$-C*H*$_2$-C*H*$_2$) ppm. FT-IR (ATR): 3294 (OH, NH), 2886 (CH asym/sym str), 1636 (C═O), 1421 (C−H def), 1367, 1292, 1234, 1103 (C−N str), 1038 (C−N str) cm^{-1}.

Ethidium Bromide Assay (EBA) of P(ButEnOx-*co*-EI) and Release Studies. The interaction between genomic DNA (gDNA) and cationic copolymers was detected by fluorescence measurements. The EBA was carried out by a procedure adapted from literature.[19] gDNA (7.5 mg mL^{-1}) and EB (0.4 mg mL^{-1}) were dissolved in HBG-buffer (HEPES buffered glucose, pH 7) and incubated for 10 min at room temperature. A total of 100 μL of the gDNA-EB solution were transferred to the wells of a black 96-well plate containing copolymers at defined concentrations (N/P ratios) with different PEI contents. Fluorescence was measured after 15 min of incubation in a repeat determination. A mixture containing only gDNA, EB, and HBG buffer served as calibration standard.

For release studies, 100 μL of the gDNA-EB solution were transferred to a well-plate as described above and the copolymers (3.6 μL of a 1 mg mL^{-1} stock solution, respectively) were added. After incubation, the fluorescence was measured and defined as start value. Subsequently, 10 μL of a heparin stock solution (3 mg mL^{-1}) was added to each of the samples and the fluorescence was measured at defined times.

EBA of P(ButEnOx-*co*-EI)-Based Hydrogels and Release Studies. The hydrogels (1.7 to 2.0 mg) were swollen for 19 h in 250 mL of HBG buffer (pH 7). Subsequently, 1 mL of gDNA-EB solution (containing 7.5 mg gDNA per mL and 0.4 mg EB per mL) was added. The sample aliquot of 50 μL was taken at defined times and returned after fluorescence measurement. Microscopic detection of the resulting fluorescence signal was performed at different time points (0, 1.5, and 18 h).

The release studies were performed by adding 1 mL of a mixture of heparin (6 mg mL^{-1}) and EB (0.4 mg mL^{-1}), dissolved in HBG buffer, to the swollen and loaded hydrogel samples. In addition, the temperature was increased up to 90 °C. Aliquots of 50 μL were taken at defined times and returned after fluorescence measurement.

RESULTS AND DISCUSSION

Synthesis and Characterization of a Copolymer Library of P(ButEnOx-*co*-EI)s. Starting from commercially available poly(2-ethyl-2-oxazoline) (PEtOx, 50,000 g/mol), LPEI was prepared by acidic hydrolysis (degree of hydrolysis > 99%) using a microwave synthesizer (Scheme 1a).[35] Subsequently, LPEI was reacted in an amidation reaction with *N*-succinimidyl-4-pentenate to introduce alkene functionalities into the polymer (Scheme 1b). To this end, LPEI and the catalyst 4-(dimethylamino)-pyridine (DMAP) were dissolved in pyridine at 80 °C and mixed with the activated acid. Due to the negligible effect of the side product *N*-hydroxysuccinimide on the formation of hydrogels, the step of dialysis (performed for 71% PEI containing copolymer) was skipped for further reactions.

Using this method, an eight-membered library of P(ButEnOx-*co*-EI)s (**C1−C8**) with varying amounts of secondary amine groups was synthesized (Table 1).

^{1}H NMR spectroscopy showed the successful conversion of LPEI to the copolymers. The percentage of remaining LPEI units in the copolymer was determined by correlating the integrals of the single proton signal of the double bond (δ = 5.9 ppm, *H*C═CH$_2$, E) to the ones of the LPEI backbone (δ = 3.0 to 2.6 ppm, HN-C*H*$_2$-C*H*$_2$, B; Figure 1). Moreover, the appearance of the signals of the 4-pentenate protons (δ = 2.6 to

dx.doi.org/10.1021/bm4017572 | *Biomacromolecules* 2014, 15, 1124−1131

Table 1. Summary of the Characterization Data for the P(ButEnOx-*co*-EI)s (C1−C8): PEI Content and SEC Data

	C1	C2	C3	C4	C5	C6	C7	C8
PEI [%][a]	85	82	71	62	50	44	36	5
M_n' (NMR) [g·mol^{-1}][b]	32,100	33,500	38,700	43,000	48,700	51,600	55,400	70,100
PDI[b]	-*	-*	1.35	1.37	1.44	1.38	1.64	1.48
M_n (SEC) [g·mol^{-1}][c]	-*	-*	9,400	9,900	10,700	13,700	14,800	14,400

[a]Percentage of remaining LPEI units determined by ^{1}H NMR spectroscopy. [b]Determined by ^{1}H NMR (calculated from LPEI: 25,000 g/mol, PEI content). [c]Determined by SEC (eluent: DMAc + 0.21% LiCl, calibration against polystyrene). *Not soluble in SEC eluent DMAc.

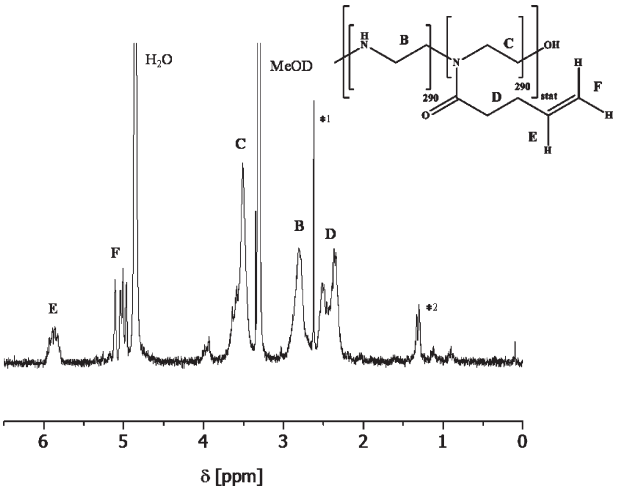

Figure 1. ^{1}H NMR spectrum (MeOD, 250 MHz) of **C5** (50% PEI) produced from linear poly(ethylene imine) (580 units; *1 side-product *N*-hydroxysuccinimide, *2 remaining 2-ethyl-2-oxazoline side chains ~1%).

2.2 ppm, CH_2 ButEnOx, D), the protons of the double bond (δ = 5.0 ppm, HC═CH_2, F) and the oxazoline backbone (δ = 3.8 to 3.4 ppm, RN-CH_2-CH_2, C) prove the proposed structure of the synthesized polymers. The successful conversion was also shown by infrared spectroscopy (IR). After the reaction, a carbonyl vibration of the oxazoline units appears at 1,636 cm^{-1} ($\nu_{C=O}$; Figure 2).

Mass spectrometry (MS) of the copolymers is not possible due to the high molar masses (>32,000 g/mol), which are difficult to transfer to the gas phase. However, using MALDI-TOF-MS, we could obtain a complex isotopic pattern of a low molar mass copolymer (45% PEI content, M_n ~ 1,650 g/mol, ^{1}H NMR: M_n' = 1,800 g/mol). The results are shown in the Supporting Information (Figure S1). Clearly the repeating units of the copolymer can be seen, but due to the complexity of the spectrum, a further assignment is nearly impossible.

Up to a content of 82% PEI, the copolymers are soluble in water. It is known that above a PEI content of 85% the copolymers only dissolve at elevated temperatures.[36] However, all the copolymers showed good solubility in organic solvents such as alcohols (e.g. methanol).

Characterization by size exclusion chromatography (SEC) revealed the formation of polymers with polydispersity indices

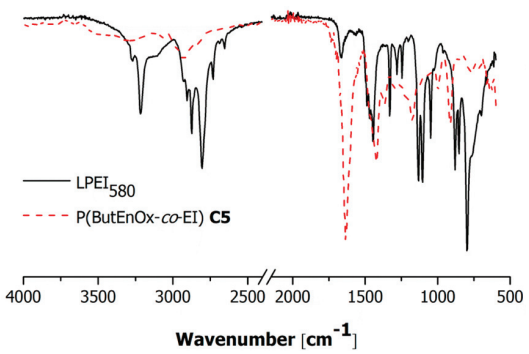

Figure 2. IR spectra of the starting linear poly(ethylene imine) homopolymer and the synthesized copolymer **C5** (50% PEI; determined by ^{1}H NMR spectroscopy of the precursor copolymers).

(PDI values) between 1.35 and 1.64 (Table 1). The molar masses obtained by SEC differ from the molar masses calculated from ^{1}H NMR (M_n'), which are based on the molar mass data of the poly(2-ethyl-2-oxazoline) precursor provided by the supplier. Possible cross-linking or other side reactions are not taken into account. The low molar mass values measured by SEC can be explained considering the different physicochemical properties, that is, the different hydrodynamic volumes of the copolymers and the used PS calibration standard.

Hydrogel Synthesis and Characterization. LPEI-based hydrogels were formed by the reaction of the precursor copolymers P(ButEnOx-*co*-EI)s (**C3−C8**) with 3,6-dioxaoctane-1,8-dithiol (EDDET; Scheme 1c) in a thiol−ene photoaddition reaction. It was performed under UV light using 2,2-dimethoxy-2-phenylacetophenone (DMPA) as initiator. In this way, a library of six hydrogels (**H3−H8**) was synthesized (Figure 3). Due to an insufficient amount of double bonds for cross-linking, copolymers with a PEI content above 82% (**C1**, **C2**) did not form hydrogels at a polymer concentration of 10 wt %, which was adapted from literature.[27] Gelation occurred

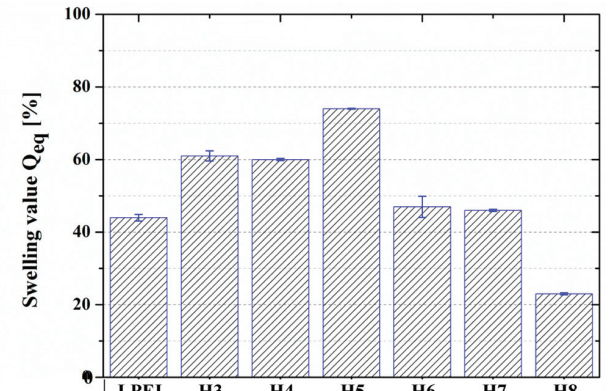

	LPEI	H3	H4	H5	H6	H7	H8
PEI [%][a]	100	71	62	50	44	36	5
Q_{eq} [%][b]	*44*	61	60	74	47	46	23

Figure 3. Swelling values Q_{eq} depending on the amount of poly(ethylene imine) units in formed hydrogels **H3−H8** (T = 25.5 °C). Linear poly(ethylene imine) was added as reference (repeated determination).

dx.doi.org/10.1021/bm4017572 | *Biomacromolecules* 2014, 15, 1124−1131

after an irradiation time between 150 min for **H3** and 5 min for **H8**. Moreover, an effect of concentration of the prepolymer could be observed. Further information can be found in the Supporting Information (Table S1).

When the reaction was performed under the same conditions but without the dithiol, neither cross-linking nor gelation was observed.

The swelling behavior of the synthesized hydrogels was investigated gravimetrically using centrifuge filter tubes.[19] The filter tubes were saturated with water and the excess water was removed by centrifugation (3,000 rpm, 10 min). The determined mass of the tube was set to m_0. After addition of the hydrogel ($m_{0,gel}$), the sample weight could be determined by eq 1.

$$m_{gel} = m_{0,gel} - m_0 \quad (1)$$

Subsequently, the hydrogel sample was swollen in water for 24 h. The filter tube was centrifuged again (3,000 rpm, 10 min) and weighted (m_{wet}) to determine the mass of the swollen gel (m_{sw}) using eq 2.

$$m_{sw} = m_{wet} - m_0 \quad (2)$$

The swelling value Q_{eq} was calculated according to literature (eq 3).[34]

$$Q_{eq} = \frac{m_{sw} - m_{gel}}{m_{sw}} \times 100\% \quad (3)$$

The formed hydrogels revealed a water uptake up to a multitude of their own mass (Q_{eq} = 23−74%) from the liquid phase. The ability of the formed networks to absorb water is ascribed to the hydrophilic parts of the cross-linker and the oxazoline units. But also the LPEI segments have hygroscopic properties and can exhibit different hydrated states.[37−39] As a reference, pure LPEI (which is insoluble in cold water) was investigated regarding its swelling value (Q_{eq} = 44%).

A maximum of the swelling values of the investigated hydrogels was reached for a PEI content of 50% (**H5**, Figure 3) with 74%. This behavior can be explained with two competing trends. Starting from pure LPEI as reference, a decreasing PEI content, accompanied with an increasing amount of water-soluble gel components, leads to higher swelling values. The decreasing swelling values at LPEI contents lower than 50% can be ascribed to a higher network density, caused by a higher degree of cross-linking for these polymers. The increased linking density and the associated decrease of the degrees of freedom of the polymer chains limit the amount of water, which can be incorporated within the polymer network. This causes the low swelling of the 5% PEI containing gel. Compared to PEtOx-containing hydrogels with similar degrees of cross-linking (Q_{eq} = 97−98%[19]), the swelling values are significantly decreased, which is caused by the lower hydrophilicity of the LPEI systems.

The water uptake behavior from the gas phase was analyzed for **H5** (50% PEI content) at varying humidity levels using a thermogravimetric analysis (TGA) setup, which was already described for the investigation of hydrophilic polymers.[40] The TGA diagram showed the adsorption of water molecules to the hydrogel network as a function of the weight change (%) and the relative humidity (%) at a constant temperature (25 °C). Before starting the measurement, the sample was heated to 60 °C at 0% humidity to completely dry the sample. After the weight of the gel was constant, its mass was set as m_{gel} (compare to eq 1). Subsequently, the relative humidity was gradually increased to 90%, whereupon a weight change of up to 30% (m_{sw}, eq 2) could be observed (equates to Q_{eq} = 23%), with an exponential increase. This value is identical to the swelling behavior of the 5% PEI containing hydrogel determined from the liquid phase. By decreasing the relative humidity in the same way, the desorption curve showed an identical trend, stating a reversibility of the swelling process. In comparison to the swelling studies from the liquid phase (for PEI content >5%), water uptake from the gas phase is much less efficient (about 10×), as depicted in Figure 3.

To confirm the structure of hydrogel **H5** (50% PEI content), solid state NMR measurements were performed. In Figure 4, a comparison of the ^{13}C NMR spectrum of the copolymer **C5** and the solid state ^{13}C NMR spectrum of the resulting purified hydrogel **H5** is depicted. An important evidence for a successful synthesis is the appearance of the signal of the cross-linker (D) at 71.0 ppm. In addition, a solid state ^{1}H NMR spectrum was recorded (Figure 5). To improve the resolution, a special method for the sample preparation was used. The gel was swollen for 16 h inside a Kel-F rotor in D_2O to increase the degrees of freedom of the polymer chains, which was placed into the spinning tube. Signals between 2.0 and 1.2 ppm (RS-CH_2-CH_2-CH_2) belonging to the EDDET cross-linker further demonstrated the success of the reaction. Both ^{13}C and ^{1}H NMR spectra revealed an incomplete conversion of the double bonds that, hence, can be used for further functionalization.

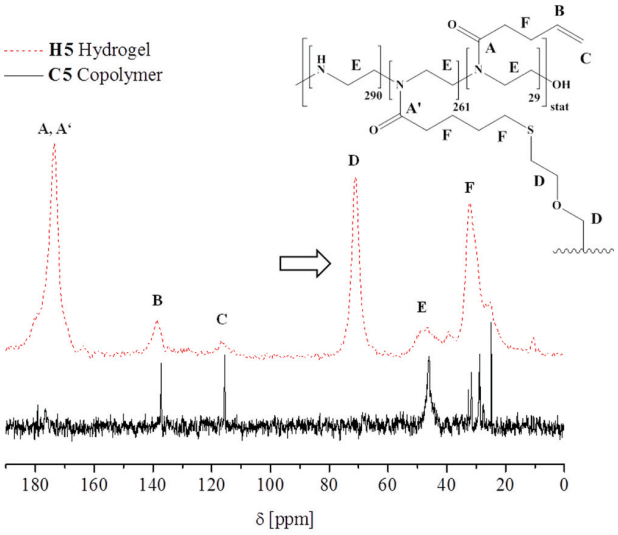

Figure 4. Solid state ^{13}C NMR spectrum of the 50% PEI containing copolymer **C5** (D_2O, 63 MHz) and the resulting hydrogel **H5** (100 MHz).

DNA Binding Studies. After the successful synthesis of copolymers and hydrogels with well-defined LPEI contents, their ability to bind and release DNA was investigated using an ethidium bromide assay (EBA). Genomic herring DNA was treated with ethidium bromide (EB) resulting in a fluorescent DNA-EB complex, which could be detected using a fluorescence microscope. The assay allowed to monitor the interaction between DNA and polymer/hydrogel by a displacement of EB resulting in a decrease of the fluorescence intensity.[41]

The results of the EBA for the chosen copolymers P(ButEnOx-*co*-EI)s (**C3**−**C5**, **C7**) are depicted in Figure 6a.

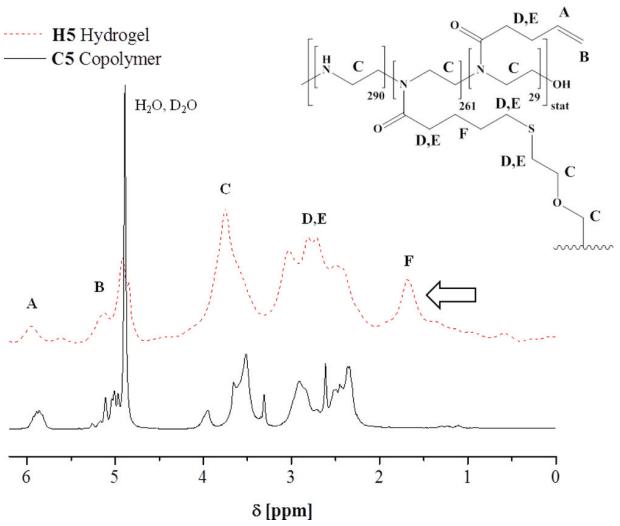

Figure 5. Comparison of the ^{1}H NMR spectrum of the 50% PEI containing copolymer **C5** (MeOD, 250 MHz) and the solid state ^{1}H NMR of the resulting hydrogel **H5** (swollen in D_2O, 400 MHz).

As expected, the system with a high content of LPEI showed an increased binding capacity and, hence, a decreased fluorescence intensity. At a nitrogen$_{polymer}$ to phosphate$_{DNA}$ (N/P) ratio higher than 2, a constant fluorescence level was reached, meaning that further excess of positively charged copolymers was not able to replace more EB. The copolymer with the highest charge density (71% PEI content) showed the highest complexation efficiency of all investigated copolymers, with a decrease in fluorescence intensity of 70%. As reference the LPEI precursor was used, which led to a fluorescence intensity decrease of about 90%.

Three hydrogels with different PEI contents, namely, **H4** (62%), **H5** (50%), and **H7** (36%), were chosen to study their DNA binding and release capability. Due to the high molar masses and the large network structures, low N/P ratios, as used for the copolymers, were not suitable. Hence, the EBA procedure had to be adjusted and N/P ratios between 250 and 500 were investigated (Figure 6b). To obtain comparable results for hydrogels, similar masses were used (1.7−2.0 mg). Prior to the EBA measurements, the hydrogel samples were swollen for 19 h in a 96-well plate in 250 μL of HBG buffer solution, respectively. The large excess of buffer allowed a complete swelling of the hydrogels independent of the PEI content and swelling value. Moreover, the concentration after the addition of 1 mL stock solution to each swollen sample was nearly identical. For each measurement an aliquot of 50 μL of each sample was taken at defined times and returned afterward. A mixture of 250 μL of HBG buffer and 1 mL of stock solution served as reference for each measuring point. To exclude the decrease of fluorescence intensity due to the degradation of the DNA-EB complex, the reference sample was treated and stored exactly as the other samples.

A similar behavior as for the copolymers was observed for the corresponding hydrogels. Besides the decrease in fluorescence intensity over time, a trend dependent on the PEI content was observed. The gel **H4** with the highest amount of PEI units (62%) showed the highest binding capacity with a fluorescence level of 20%, which was significantly lower than the value of the corresponding copolymer. For the 50% PEI containing gel, similar results to the corresponding copolymer were obtained. The hydrogel **H7** with 36% of LPEI showed no DNA binding. A possible explanation is the dense structure of the hydrogel due to the high amount of cross-linking sites hindering the access of DNA to the hydrogel network. This fact also causes the long time required for a complete DNA binding (95 h). Furthermore, the low swelling values and, thus, the inflexibility of the network, led to a time-consuming complexation process. These long adsorption periods might indicate a diffusion controlled process. To sum up, a high PEI content seems to be the predominant factor for high binding capacities of the hydrogels studied as demonstrated by the remarkable value of **H4**. However, the amount of amine groups is limited by the number of functional sides (here alkene groups) necessary for the formation of stable hydrogels. In addition, the DNA binding of the hydrogel sample **H4** was monitored using a fluorescence microscope (Figure 7). The photometric measurements showed the decrease of the fluorescence intensity of the DNA-EB complex over time after the addition of the hydrogel. A DNA-EB solution of the same concentration served as reference and showed no indications of degradation of the dye. In contrast to the DNA investigations of the supernatant of the P(ButEnOx-*co*-EI) copolymers and the corresponding hydrogels, the microscopic study was performed with the complete

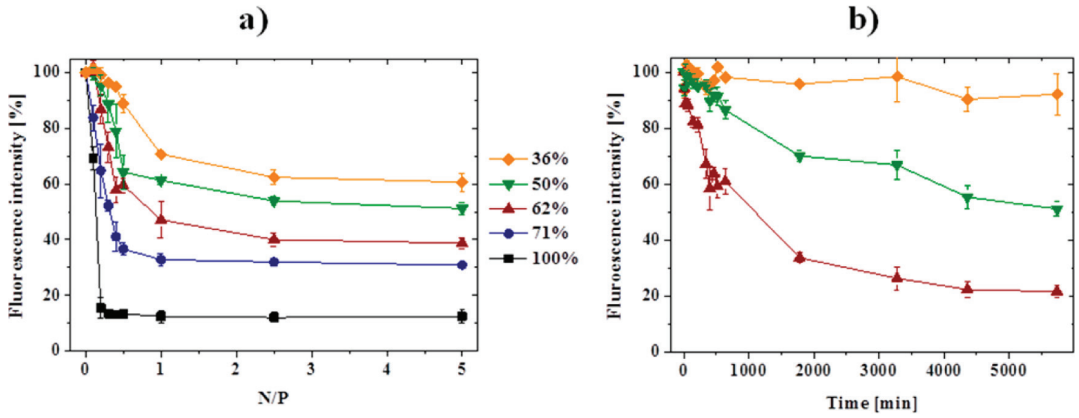

Figure 6. Binding of DNA (ethidium bromide assay)[41] to (a) copolymers **C3**−**C5** and **C7** at increasing nitrogen/phosphate ratios (triple determination) and (b) hydrogel samples **H4**, **H5**, and **H7** at nitrogen/phosphate ratios above 250 (repeated determination) with different PEI content via fluorescence measurements.

dx.doi.org/10.1021/bm4017572 | *Biomacromolecules* 2014, 15, 1124−1131

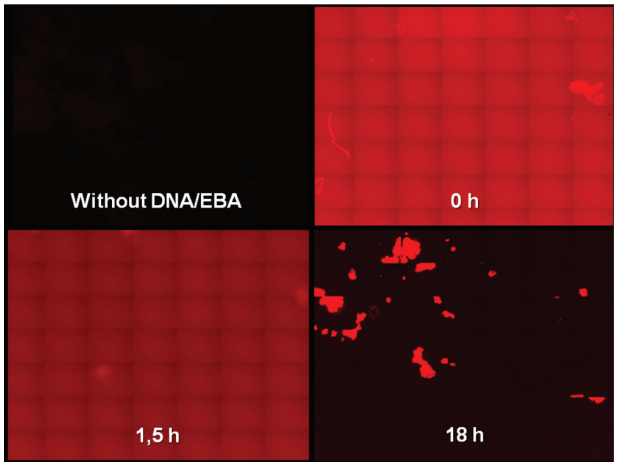

Figure 7. Microscopic pictures of DNA binding to hydrogel **H4** (62% PEI) measured by fluorescence microscopy without DNA/EBA and after addition of DNA/EBA at defined times.

sample including the hydrogel. Since the bound DNA still has free coordination sides for EB, a fluorescence signal is detectable in the area of the hydrogel.

Besides an effective DNA binding, its release from the hydrogel and the copolymer, respectively, represents an essential step for further applications. The DNA release was studied using a heparin assay. Heparin is a polyanion with multiple negative charges per repeating unit, which can effectively bind to the positively charged hydrogel or copolymer, causing the release of the DNA. Thus, the latter can intercalate again with free EB, which was added in the same concentrations as before. The formation of the DNA-EB complex led to an increase of the fluorescence intensity. For the copolymers, the DNA was released very fast. Within 4 min, the fluorescence intensity increased rapidly up to a constant level of nearly 90% (Figure 8a). As reference, a mixture of 250 μL of HBG buffer and 1 mL of DNA-EB stock solution was chosen. It was treated with heparin in the same way as the copolymers, and the resulting fluorescence intensity was set to 100%.

The hydrogels showed a different behavior. Here, neither the addition of heparin (5% release) nor an increase of temperature (up to 90 °C, 10%) resulted in an efficient release. However, a combination of both led to a detachment of nearly 50% of the bound DNA within 80 min (Figure 8b). This behavior could be associated with the PEI segments of the synthesized hydrogels. LPEI is not soluble in cold water and the PEI components of the hydrogels could form clusters within the network that inhibit an efficient release due to sterical reasons. At higher temperatures, the PEI segments melt and a replacement of DNA with heparin becomes possible.

CONCLUSION

In summary, a new and efficient method to obtain hydrogels for the binding and release of DNA with a controlled amount of amine binding sides was developed. To this end, a new class of copolymer containing 2-butenyl-2-oxazoline and ethylene imine units was synthesized by partial functionalization of LPEI with *N*-succinimidyl-4-pentenate. An eight-membered library of P(ButEnOx-*co*-EI)s was prepared, and subsequently, the double bonds were exploited for cross-linking via thiol−ene photoaddition using *bis*-functional 3,6-dioxaoctane-1,8-dithiol. Compared to the formation of PEI hydrogels by cross-linking the free amines, the presented approach allows the exact adjustment of the amount of free amines in the copolymer and, thus, within the hydrogel. Both copolymers and hydrogels were characterized by means of NMR spectroscopy and FT-IR spectroscopy. Furthermore, the swelling and deswelling behavior of the hydrogels from liquid and gas phase was investigated, showing that the water uptake from the liquid phase is 10× more efficient. Swelling values up to 74% were observed.

The DNA studies showed that copolymers and hydrogels are able to bind and release DNA reversibly via the secondary amine groups with binding capacities strongly depending on the PEI content. The copolymers bound up to 70% of the initial DNA. Because of their large three-dimensional networks, the hydrogels exhibited a much higher binding capacity for the appropriate PEI contents. However, due to the low swelling values compared to POx-based hydrogels and, thus, the inflexibility of the network, the DNA uptake was rather slow, probably indicating a diffusion-controlled process.

The DNA release studies were performed using a heparin assay. While the copolymers at room temperature rapidly

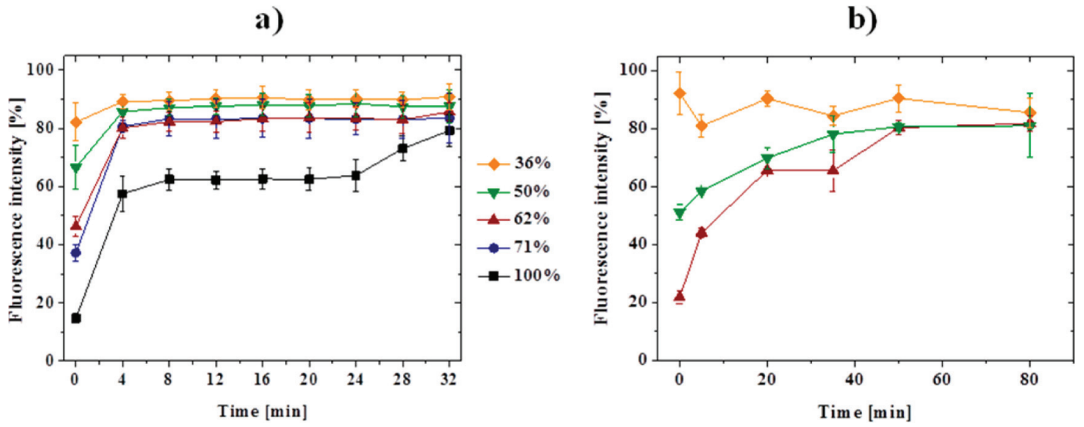

Figure 8. Time-dependent release of DNA from (a) copolymers **C3**−**C5** and **C7** (heparin, triple determination) at a nitrogen/phosphate ratio of 2 and (b) hydrogel samples **H4**, **H5**, and **H7** at nitrogen/phosphate ratios above 250 (heparin, 90 °C, repeat determination) with different PEI content via fluorescence measurements.

dx.doi.org/10.1021/bm4017572 | *Biomacromolecules* 2014, 15, 1124−1131

released up to 90% of the initial DNA quantity after heparin addition, the hydrogels released 50% at elevated temperatures.

To accelerate the binding and release of genetic material, further studies, dealing with the improvement of the swelling behavior of the hydrogels, have to be performed. Hence, hydrogels starting from a precursor poly(2-ethyl-2-oxazoline-*co*-ethylene imine) instead of linear poly(ethylene imine) should be investigated. This will be part of a follow-up study.

In addition, solid NMR spectroscopy revealed the presence of unreacted alkene groups, which could be used for further functionalizations like surface attachment. The treated surfaces are available for DNA binding and release studies in terms of chip-based point-of-care diagnostics.

Besides its use in hydrogel synthesis, the copolymer P(ButEnOx-*co*-EI) represents an interesting molecule for other applications, such as gene delivery or gene silencing.

■ ASSOCIATED CONTENT

Ⓢ Supporting Information

Supporting Figure S1 and Table S1. This material is available free of charge via the Internet at http://pubs.acs.org.

■ AUTHOR INFORMATION

Corresponding Author

*Fax: +49 3641 948 202. E-mail: ulrich.schubert@uni-jena.de.

Present Address

[§]Department of Chemical and Biomolecular Engineering, The University of Melbourne, Victoria 3010, Australia (K.K.).

Notes

The authors declare no competing financial interest.

■ ACKNOWLEDGMENTS

C.E. is grateful to the Stiftung Industrieforschung for financial support. We thank Dr. Andreas Seifert from TU Chemnitz for the solid NMR measurements. Grateful thanks to Dr. Jürgen Vitz for water uptake measurements from the gas phase and Dr. David Pretzel for the fluorescence microscopy investigations.

■ REFERENCES

(1) Joos, B.; Kuster, H.; Cone, R. *Anal. Biochem.* **1997**, *247*, 96−101.

(2) Rogers, Y.-H.; Jiang-Baucom, P.; Huang, Z.-J.; Bogdanov, V.; Anderson, S.; Boyce-Jacino, M. T. *Anal. Biochem.* **1999**, *266*, 23−30.

(3) Steel, A. B.; Levicky, R. L.; Herne, T. M.; Tarlov, M. J. *Biophys. J.* **2000**, *79*, 975−981.

(4) Fixe, F.; Dufva, M.; Telleman, P.; Christensen, C. B. V. *Nucleic Acids Res.* **2004**, *32*, e9.

(5) Wink, M. *An Introduction to Molecular Biotechnology: Molecular Fundamentals, Methods and Applications in Modern Biotechnology*; Wiley-VCH: Weinheim, Germany, 2006.

(6) Brissault, B.; Kichler, A.; Guis, C.; Leborgne, C.; Danos, O.; Cheradame, H. *Bioconjugate Chem.* **2003**, *14*, 581−587.

(7) Boussif, O.; Lezoualch, F.; Zanta, M. A.; Mergny, M. D.; Scherman, D.; Demeneix, B.; Behr, J. P. *Proc. Natl. Acad. Sci. U.S.A.* **1995**, *92*, 7297−7301.

(8) Zhou, Y.-l.; Li, Y.-z. *Spectrochim. Acta, Part A* **2004**, *60*, 377−384.

(9) Hellweg, T.; Henry-Toulmé, N.; Chambon, M.; Roux, D. *Colloids Surf., A* **2000**, *163*, 71−80.

(10) Sharma, V. K.; Thomas, M.; Klibanov, A. M. *Biotechnol. Bioeng.* **2005**, *90*, 614−620.

(11) Godbey, W. T.; Wu, K. K.; Mikos, A. G. *J. Controlled Release* **1999**, *60*, 149−160.

(12) Peterson, A. W.; Heaton, R. J.; Georgiadis, R. M. *Nucleic Acids Res.* **2001**, *29*, 5163−5168.

(13) Rampal, J. B. *Microarrays: Synthesis Methods*; Humana Press: Totowa, NJ, 2001.

(14) Anzenbacher, P.; Liu, Y.-l.; Kozelkova, M. E. *Curr. Opin. Chem. Biol.* **2010**, *14*, 693−704.

(15) Guschin, D.; Yershov, G.; Zaslavsky, A.; Gemmell, A.; Shick, V.; Proudnikov, D.; Arenkov, P.; Mirzabekov, A. *Anal. Biochem.* **1997**, *250*, 203−211.

(16) Okay, O. *J. Polym. Sci., Part B: Polym. Phys.* **2011**, *49*, 551−556.

(17) Kivlehan, F.; Paolucci, M.; Brennan, D.; Ragoussis, I.; Galvin, P. *Anal. Biochem.* **2012**, *421*, 1−8.

(18) Liu, J. *Soft Matter* **2011**, *7*, 6757−6767.

(19) Hartlieb, M.; Pretzel, D.; Kempe, K.; Fritzsche, C.; Paulus, R. M.; Gottschaldt, M.; Schubert, U. S. *Soft Matter* **2013**, *9*, 4693−4704.

(20) Chujo, Y.; Sada, K.; Saegusa, T. *Polym. J.* **1993**, *25*, 599−608.

(21) Chujo, Y.; Sada, K.; Saegusa, T. *Macromolecules* **1993**, *26*, 6315−6319.

(22) Chujo, Y.; Sada, K.; Saegusa, T. *Macromolecules* **1993**, *26*, 6320−6323.

(23) Chujo, Y.; Yoshifuji, Y.; Sada, K.; Saegusa, T. *Macromolecules* **1989**, *22*, 1074−1077.

(24) Chujo, Y.; Sada, K.; Saegusa, T. *Macromolecules* **1990**, *23*, 2636−2641.

(25) Wiesbrock, F.; Hoogenboom, R.; Leenen, M.; van Nispen, S. F. G. M.; van der Loop, M.; Abeln, C. H.; van den Berg, A. M. J.; Schubert, U. S. *Macromolecules* **2005**, *38*, 7957−7966.

(26) Goyal, R.; Tripathi, S. K.; Tyagi, S.; Sharma, A.; Ram, K. R.; Chowdhuri, D. K.; Shukla, Y.; Kumar, P.; Gupta, K. C. *Nanomed. Nanotechnol. Biol. Med.* **2012**, *8*, 167−175.

(27) Dargaville, T. R.; Forster, R.; Farrugia, B. L.; Kempe, K.; Voorhaar, L.; Schubert, U. S.; Hoogenboom, R. *Macromol. Rapid Commun.* **2012**, *33*, 1695−1700.

(28) Gress, A.; Volkel, A.; Schlaad, H. *Macromolecules* **2007**, *40*, 7928−7933.

(29) Diehl, C.; Schlaad, H. *Macromol. Biosci.* **2009**, *9*, 157−161.

(30) Diehl, C.; Schlaad, H. *Chem.—Eur. J.* **2009**, *15*, 11469−11472.

(31) Kempe, K.; Vollrath, A.; Schaefer, H. W.; Poehlmann, T. G.; Biskup, C.; Hoogenboom, R.; Hornig, S.; Schubert, U. S. *Macromol. Rapid Commun.* **2010**, *31*, 1869−1873.

(32) Kempe, K.; Hoogenboom, R.; Jaeger, M.; Schubert, U. S. *Macromolecules* **2011**, *44*, 6424−6432.

(33) Kempe, K.; Hoogenboom, R.; Schubert, U. S. *Macromol. Rapid Commun.* **2011**, *32*, 1484−1489.

(34) Koschella, A.; Hartlieb, M.; Heinze, T. *Carbohydr. Polym.* **2011**, *86*, 154−161.

(35) Tauhardt, L.; Kempe, K.; Knop, K.; Altuntas, E.; Jäger, M.; Schubert, S.; Fischer, D.; Schubert, U. S. *Macromol. Chem. Phys.* **2011**, *212*, 1918−1924.

(36) Lambermont-Thijs, H. M. L.; van der Woerdt, F. S.; Baumgaertel, A.; Bonami, L.; Du Prez, F. E.; Schubert, U. S.; Hoogenboom, R. *Macromolecules* **2010**, *43*, 927−933.

(37) Chatani, Y.; Tadokoro, H.; Saegusa, T.; Ikeda, H. *Macromolecules* **1981**, *14*, 315−321.

(38) Chatani, Y.; Kobatake, T.; Tadokoro, H.; Tanaka, R. *Macromolecules* **1982**, *15*, 170−176.

(39) Chatani, Y.; Kobatake, T.; Tadokoro, H. *Macromolecules* **1983**, *16*, 199−204.

(40) Thijs, H. M. L.; Becer, C. R.; Guerrero-Sanchez, C.; Fournier, D.; Hoogenboom, R.; Schubert, U. S. *J. Mater. Chem.* **2007**, *17*, 4864−4871.

(41) Wagner, M.; Rinkenauer, A. C.; Schallon, A.; Schubert, U. S. *RSC Adv.* **2013**, *3*, 12774−12785.

SUPPORTING INFORMATION

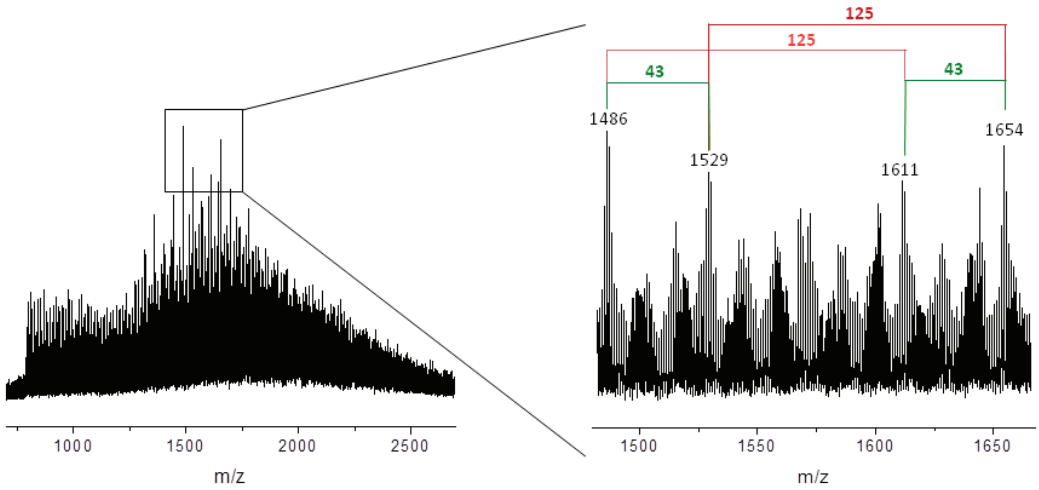

Figure S1. MALDI-TOF-MS spectrum (matrix: DHB, solvent: methanol) of a 45% PEI containing copolymer (20 units, M_n ~ 1,650 g/mol, ^{1}H NMR: Mn' = 1,800 g/mol) with a detailed analysis of a selected part of the spectrum.

Table S1. Effect of concentration of the prepolymer for sample C5 (50% PEI content) and C3 (71% PEI content).

	P(ButEnOx-*co*-EI$_{71\%}$)			**P(ButEnOx-*co*-EI$_{50\%}$)**		
Polymer concentration [wt%]	5.8	9.4	16.9	5.0	9.7	14.8
Swelling value Q_{eq} [%]	-*	62	64	68	74	70

* No hydrogel was obtained.